National Research Council Canada

Conseil national de recherches Canada

NRC · CNRC

Canadian Journal of Fisheries and Aquatic Sciences

Journal canadien des sciences halieutiques et aquatiques

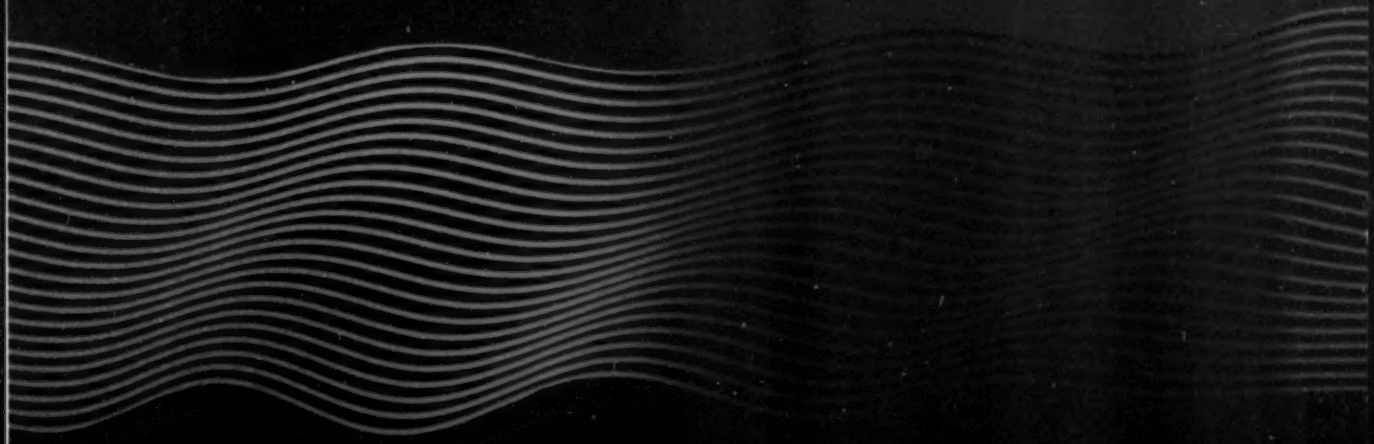

http://cjfas.nrc.ca

http://jcsha.cnrc.ca

ISSN 0706-652X / CJFSDX 61(5) 673–856 (2004)

The *Canadian Journal of Fisheries and Aquatic Sciences*, previously published as *Contributions to Canadian Biology* 1901–1925, *Contributions to Canadian Biology and Fisheries* 1926–1934, *Journal of the Biological Board of Canada* 1934–1937, and *Journal of the Fisheries Research Board of Canada* 1938–1979, is issued monthly to form annual volumes of 12 numbers plus supplements.

Editorial policy. The Journal publishes original research articles, perspectives (syntheses, critiques, re-evaluations), discussions (comment and reply), and rapid communications. Manuscripts may concern cells, organisms, populations, communities, ecosystems, or processes that affect aquatic systems. They may cover a range of disciplines including biology and ecology of marine and freshwater organisms, limnology, oceanography, physiology, toxicology, genetics, economics, disease, and management. Preference will be given to manuscripts that emphasize understanding of observed phenomena and interpretation of experimental results. The Journal encourages papers that lead from clearly stated purpose or rationale and from testable hypotheses, concepts, or questions to identifiable conclusions or syntheses. Such papers may amplify, modify, question, or redirect accumulated knowledge embodied in contemporary perceptions of a particular state of aquatic sciences. The Journal discourages papers that are essentially descriptive, except in emerging disciplines; have only site-specific or local applications (a certain year, place, taxon, chemical compound, etc.); only confirm previously established principles; or apply standard techniques without breaking new methodological ground.

Manuscripts for publication should be submitted to the Senior Editor, *Canadian Journal of Fisheries and Aquatic Sciences*, Department of Zoology, University of Guelph, Guelph, ON N1G 2W1, Canada (519-824-4120 ext. 52646; fax: 519-767-9798; e-mail: cjfas@uoguelph.ca).

Submissions in either English or French are acceptable. The information must be original, that is, not copyrighted, published, or submitted elsewhere except in abstract form or unless by written consent of the Editor.

Correspondence concerning accepted manuscripts and corrected proofs should be sent to NRC Research Press, National Research Council of Canada, Ottawa, ON K1A 0R6, Canada (fax: 613-952-7656; e-mail: pubs@nrc-cnrc.gc.ca).

Instructions to Authors are published once a year in the first issue of each volume. Copies are available from NRC Research Press or at http://cjfas.nrc.ca. The **Publication Policy** of NRC Research Press is available at http://pubs.nrc-cnrc.gc.ca.

Microfilm. Issues from 1934 through the current volume can be purchased on 16- or 35-mm microfilm. Photocopies of individual articles or issues can be purchased from University Microfilms International, 330 North Zeeb Road, Ann Arbor, MI 48106, U.S.A.

U.S. periodical postage paid at Champlain, N.Y., and at additional mailing offices. Attention U.S. POSTMASTER: Send address changes to **Canadian Journal of Fisheries and Aquatic Sciences**, c/o USACAN Media Distribution Center, P.O. Box 2888, Plattsburg, NY 12901, U.S.A.

Publié sans interruption depuis 1901, le *Journal canadien des sciences halieutiques et aquatiques* a paru sous plusieurs titres : *Contributions to Canadian Biology* 1901–1925, *Contributions to Canadian Biology and Fisheries* 1926–1934, *Journal of the Biological Board of Canada* 1934–1937, et *Journal of the Fisheries Research Board of Canada* 1938–1979. Le Journal paraît tous les mois, formant ainsi un volume de 12 numéros, et offre en plus jusqu'à deux suppléments par année.

Politique éditoriale. On publie, dans le Journal, des articles rendant compte de recherche originale, des perspectives (synthèses, critiques et réévaluations), des discussions (commentaires et réponses) et des communications rapides. Les documents peuvent porter sur les cellules, organismes, populations, communautés, écosystèmes ou processus qui affectent les systèmes aquatiques. Ils peuvent relever de divers domaines y compris la biologie et l'écologie des organismes marins et d'eau douce, la limnologie, l'océanographie, la physiologie, la toxicologie, la génétique, l'économie, la pathologie et la gestion. On accorde la préséance aux articles qui contribuent à la compréhension de phénomènes observés et à l'interprétation de résultats expérimentaux. On invite les auteurs à soumettre des articles ayant des objectifs précis ou relevant d'hypothèses, de concepts ou de questions vérifiables et se terminant par de solides conclusions ou d'utiles synthèses. Ces articles enrichissent, changent, mettent en question ou réorientent les connaissances acquises sur divers aspects des sciences aquatiques. On décourage toutefois la soumission d'articles simplement descriptifs (à moins qu'il ne s'agisse de nouvelles disciplines), d'application très limitée (applicables à une seule année, une seule région ou un seul taxon, portant sur un unique composé chimique, etc.); d'articles qui ne font que reprendre les principes énoncés dans des articles précédents; et d'articles rendant compte de l'application de normes sans gain de méthodologie.

Les auteurs voudront adresser leurs **manuscrits** à la directrice scientifique principale, *Journal canadien des sciences halieutiques et aquatiques*, Department of Zoology, University of Guelph, Guelph, ON N1G 2W1, Canada (519-824-4120 poste 52646; télécopieur : 519-767-9798; courriel : cjfas@uoguelph.ca).

Les contributions peuvent être en anglais ou en français. Elles doivent être originales, c.-à.-d. qu'elles ne doivent pas avoir fait l'objet d'un copyright, avoir été publiées ou soumises ailleurs, sauf sous forme abrégée ou avec le consentement du rédacteur. Le CNRC ne se tient en aucune façon responsable des opinions exprimées par un collaborateur ou des déclarations qui pourrait faire ce dernier.

La correspondance ayant trait aux manuscrits acceptés et les **épreuves corrigés** doivent être envoyées aux Presses scientifiques du CNRC, Conseil national de recherches du Canada, Ottawa, ON K1A 0R6, Canada (télécopieur : 613-952-7656; courriel : pubs@nrc-cnrc.gc.ca).

Les Recommandations aux auteurs sont publiées une fois par année dans le premier numéro de chaque volume. Des copies sont disponibles auprès du Bureau de la rédaction aux Presses scientifiques du CNRC ou au http://jcsha.cnrc.ca. **La Politique de publication** est disponible auprès des Presses scientifiques du CNRC ou au http://pubs.nrc-cnrc.gc.ca.

Microfilms. On peut acheter sur microfilms de 16 ou 35 mm tous les numéros depuis 1934. Des photocopies d'articles ou de numéros individuels sont aussi en vente auprès de University Microfilms International, 330 North Zeeb Road, Ann Arbor, MI 48106, É.-U.

This Journal is indexed or abstracted in / Cette revue est signalée ou résumée dans

ABSEARCH, Applied Science and Technology Index and Abstracts, Aquatic Sciences and Fisheries Abstracts, Biological Abstracts, Biological and Agricultural Abstracts, CAB Abstracts, Chemical Abstracts, Current Contents, Elsevier BIOBASE, Environmental Abstracts, ETDE Energy Database, General Science Index and Abstracts, GEOBASE, GeoRef, Life Sciences Collection, Meteorological and Geoastrophysical Abstracts, Oceanic Abstracts, PASCAL Database, and Science Citation Index.

Volume 61, Number 5, May 2004

Canadian Journal of Fisheries and Aquatic Sciences

Published by the National Research Council of Canada

Volume 61, numéro 5, mai 2004

Journal canadien des sciences halieutiques et aquatiques

Publié par le Conseil national de recherches du Canada

Senior Editor / Directrice scientifique principale **Moira M. Ferguson**

Editors / Directeurs

Jeffrey A. Hutchings, *Dalhousie University, Halifax*
Pierre Pepin, *Northwest Atlantic Fisheries Centre, DFO/MPO, St. John's, Newfoundland*
W. Gary Sprules, *University of Toronto at Mississauga*
Assistant to the Editors / Adjointe aux directeurs scientifiques **Holly Foster**

Associate Editors / Directeurs scientifiques associés

D. Boisclair, *Université de Montréal*
U. Borgmann, *Environment Canada, Burlington*
M.J. Bradford, *DFO/MPO and Simon Fraser University*
S.E. Campana, *DFO/MPO, Dartmouth*
R. Carignan, *Université de Montréal*
J.J. Dodson, *Université Laval*
G.T. Evans, *DFO/MPO, St. John's, Newfoundland*
K.T. Frank, *DFO/MPO, Dartmouth*
J.W.A. Grant, *Concordia University*
M.M. Hansen, *Danish Institute for Fisheries Research, Silkeborg, Denmark*
R. Hilborn, *University of Washington*
A. Hontela, *Université du Québec à Montréal*
D.F. Houlihan, *University of Aberdeen*
F.A. Huntingford, *University of Glasgow*
G.S. Jamieson, *DFO/MPO, Nanaimo*
J.M. Jech, *NFSC/NOAA, Woods Hole, Mass.*
B. Jonsson, *Norwegian Institute for Nature Research, Oslo, Norway*
D.L. MacLatchy, *University of New Brunswick, St. John*
P. Magnan, *Université du Québec à Trois Rivières*
C.T. Marshall, *University of Aberdeen*
R.B. Millar, *University of Auckland, New Zealand*
W.P. Patterson, *University of Saskatchewan*
Y.T. Prairie, *Université du Québec à Montréal*
T.J. Quinn II, *University of Alaska–Fairbanks, Juneau, Alaska*
T.P. Quinn, *University of Washington*
C.W. Ramcharan, *Laurentian University*
R.D. Robarts, *Environment Canada, Saskatoon*
B. Sainte-Marie, *DFO/MPO, Mont-Joli*
D.W. Schindler, *University of Alberta*
R.E.H. Smith, *University of Waterloo*
S.J. Smith, *DFO/MPO, Dartmouth*
W.F. Vincent, *Université Laval*
R.D. Vinebrooke, *University of Alberta*
C.J. Walters, *University of British Columbia*
R.D. Ward, *CSIRO Marine Research, Australia*
B. de Young, *Memorial University of Newfoundland*

NRC Research Press / Presses scientifiques du CNRC

Editor-in-Chief / Directeur général **Bruce P. Dancik**
Assistant Editor-in-Chief / Directeur général adjoint **Iain E.P. Taylor**

Journals Program / Programme des revues

Fax / Télécopieur : 613-952-7656; e-mail / courriel : pubs@nrc-cnrc.gc.ca; URL / URL : pubs.nrc-cnrc.gc.ca
Director / Directeur **Cameron D. Macdonald**
Acting Business Manager / Gestionnaire des affaires par intérim **Mike Boroczki**
Manager, Journals Program / Gestionnaire, Programme des revues **Carolyn Brown**
Managing Editor / Rédactrice administrative **Cecily M. Pearson** (613-993-9099)
Publication Officers / Agentes de publication **Jennifer McColl**
Advertising / Annonces publicitaires **Judy Gorman** (613-993-0151)
Reprints / Tirés à part **Roxanne Landriault** (613-990-2254)
Subscriptions / Abonnements **Eileen Evans-Nantais** (613-990-7873)

The National Research Council of Canada accepts no responsibility for statements or opinions expressed by a contributor. Acceptance of an advertisement, announcement, or other material does not imply endorsement by either the Journal's Senior Editor or the National Research Council.

© National Research Council of Canada 2004. All rights reserved.

No part of this publication may be reproduced, stored, or transmitted in any form or by any means, without the written permission of the publisher, except as stated below.

The National Research Council of Canada grants **permission*** to individuals to make single copies of articles for personal use. Any person may reproduce short excerpts from articles in the journal for any purpose that respects the moral rights of authors, provided that the source is fully acknowledged. As a courtesy, the consent of authors of such material should be obtained directly from the author.

Authorization to reproduce items for other than personal use, as stated above, is granted by the National Research Council of Canada provided that the copyright fee of $7.00 per copy is paid directly to CANCOPY, One Yonge Street, Suite 1900, Toronto, ON M5E 1E5, Canada.

*The above permission does not extend to other kinds of copying, such as copying for general distribution, for advertising, or promotional purposes, for creating new collective works, or for resale. For such copying, arrangements must be made with the publisher, National Research Council of Canada, Ottawa, ON K1A 0R6, Canada.

Subscription information

The *Canadian Journal of Fisheries and Aquatic Sciences* (ISSN 0706-652X) is published monthly by the National Research Council of Canada. The 2004 annual subscription rates (second class postage) for Canada are $830CAN institutional and $257CAN personal, for US & foreign $830US institutional and $257US personal. For air mail add $175US to foreign rate. Canadian customers please include 7% GST (business no. 12149 1807 RT 0275). Subscriptions are entered for the calendar year. Remittances should be made payable to the Receiver General for Canada, credit NRC. Price for regular single issues: institutional, $105.00; personal, $35.00. Supplements will be priced separately. Special rates apply to members of Canadian scientific and engineering societies if they subscribe through their respective societies.

There are no refunds on cancelled subscriptions once delivery has begun. Claims for missing issues should be made within four months (N. America) or six months (outside N. America) following the date of publication. The publisher expects to supply missing issues only when losses have occurred in transit and when the reserve stock will permit. For change of address and subscription enquiries: Subscription Office, NRC Research Press, National Research Council of Canada, Ottawa, ON K1A 0R6, Canada; tel.: 613-993-9084; fax: 613-952-7656; e-mail: pubs@nrc-cnrc.gc.ca.

Microform backfiles are available from UMI, P.O. Box 1346, Ann Arbor, MI 48106-1346, U.S.A., and Micromedia Ltd., 20 Victoria St., Toronto, ON M5C 2N8, Canada.

All issues of the *Canadian Journal of Fisheries and Aquatic Sciences* since 1996 are available on the Web. Pricing information can be found at http://pubs.nrc-cnrc.gc.ca.

Le Conseil national de recherches du Canada ne se tient en aucune façon responsable des opinions exprimées par un collaborateur ou des déclarations que pourrait faire ce dernier. La publication d'annonces publicitaires, d'avis et autres n'implique pas l'endossement de leur contenu par la directrice principale de la Revue ou le CNRC.

© Conseil national de recherches du Canada 2004. Tous droits réservés.

Il est interdit de reproduire, de sauvegarder ou de transmettre quelque partie de la présente publication dans quelque format ou de quelque façon sans le consentement écrit de l'éditeur, à l'exception des conditions suivantes.

Le Conseil national de recherches du Canada accorde aux particuliers le droit de faire des copies individuelles pour leur usage personnel. Toute personne peut reproduire de courts extraits des articles de la Revue pour autant que les droits moraux de l'auteur soient respectés et que la mention de provenance soit clairement indiquée. Il est de convenance de demander le consentement de l'auteur avant de faire mention de son travail.

On obtiendra l'autorisation de reproduire des articles à d'autres fins que l'usage personnel (tel qu'on l'a décrit ci-dessus) auprès du Conseil national de recherches du Canada pour autant que des redevances de droits d'auteurs de 7,00 $/copie soient versées au CANCOPY, 1, rue Yonge, bureau 1900, Toronto, ON M5E 1E5, Canada.

*La permission ci-dessus ne s'applique pas à la reproduction à grande échelle, telle que la reproduction aux fins de distribution générale, publicitaire ou promotionnelle, de compilation de nouveaux ouvrages collectifs ou de revente. Dans de tels cas, il faudra ratifier une entente particulière avec l'éditeur, le Conseil national de recherches du Canada, Ottawa, ON K1A 0R6, Canada.

Renseignements sur l'abonnement

Journal canadien des sciences halieutiques et aquatiques (ISSN 0706-652X) est une publication mensuelle du Conseil national de recherches du Canada. Le prix de l'abonnement annuel en 2004 au Canada (courrier de deuxième classe) est de 830 $CAN pour les organismes et de 257 $CAN pour les particuliers. À l'étranger (y compris les É.-U.), le prix de l'abonnement est de 830 $US pour les organismes et de 257 $US pour les particuliers. L'expédition par avion exige des frais de 175 $US en sus du prix d'abonnement à l'étranger. Les clients du Canada doivent ajouter la TPS de 7% (numéro d'entreprise 12149 1807 RT 0275). Les abonnements sont pour l'année civile. Tout paiement doit être adressé au Receveur général du Canada, crédit du CNRC. Le prix par numéro est de 105 $ pour les organismes et de 35 $ pour les particuliers. Le prix des hors-série varie. Les membres des sociétés canadiennes de sciences et de génie bénéficient de taux préférentiels en s'abonnant via leurs sociétés respectives.

Aucun remboursement ne sera accordé ni aucune annulation acceptée une fois que les livraisons auront commencé. Les réclamations de numéros manquants devront être soumises dans les quatre mois (Amérique du Nord) ou dans les six mois (à l'extérieur de l'Amérique du Nord) suivant la date de publication. L'éditeur ne fournira de numéros manquants que si le document a été perdu pendant l'expédition et que si le stock le permet. Adressez tout changement d'adresse ou toute question quant à l'abonnement au : Bureau des abonnements, Presses scientifiques du CNRC, Conseil national de recherches Canada, Ottawa, ON K1A 0R6, Canada; téléphone : 613-993-9084; télécopieur : 613-952-7656; courriel : pubs@nrc-cnrc.gc.ca.

On peut obtenir les fichiers rétrospectifs sur **microforme** auprès de UMI, P.O. Box 1346, Ann Arbor, MI 48106-1346, É.-U., et auprès de Micromedia Ltée, 20, rue Victoria, Toronto, ON M5C 2N8, Canada.

À partir de 1996, tous les numéros de *Journal canadien des sciences halieutiques et aquatiques* sont accessibles sur le Web. On trouvera des renseignements sur les tarifs à http://pubs.nrc-cnrc.gc.ca.

Third International Symposium on Biological and Environmental Chemistry of DMS(P) and Related Compounds

Rimouski, Quebec, Canada
26–28 September 2002

[Troisième symposium international sur la biochimie et la chimie environnementale du DMS(P) et des composés apparentés]

Rimouski (Québec) Canada
26–28 septembre 2002

Guest Editor

Maurice Levasseur
Maurice Lamontagne Institute
Fisheries and Oceans Canada
Mont-Joli, Quebec

Directeur scientifique invité

Maurice Levasseur
Institut Maurice-Lamontagne
Pêches et Océans Canada
Mont-Joli (Québec)

Left to right, bottom to top / De gauche à droite, de bas en haut : Maurice Levasseur, Chi Shing Wong, Sonia Michaud, Clara Deal, Claire Evans, Louise Darroch, Naoaki Uzuka, Martine Lizotte, René-Christian Bouillon, Moire Wadleigh, Mtinkheni Van Himbergen-Gondwe, Giacomo DiTullio, Michael Steinke, John W.H. Dacey, Jacqueline Stefels, Sarah F. Riseman, Nobue Kasamatsu, Richard W. Hill, Winfried W.C. Gieskes, Ippei Nagao, Alain Vézina, Peter Lee, Hiroyuki Fuse, Peter Burkill, Gill Malin, Dierdre A. Toole, Doris Slezak, Maria Vila, David Kieber, Stephen Archer, Guy Cantin, Rafel Simó, Patricia A. Matrai, Michel Gosselin, Ronald Kiene, Anissa Merzouk, Michael Scarratt, Sauveur Belviso, Francis Gilbert, Hyakubun Harada, Huixiang Xie, Joseph D. Husband, Emmy Wong, Yvonnick Le Clainche, Jean-Pierre Blanchet (Missing / Absents : Susanne Kadner, Juliette Fauchot, Tsuneo Odate, Henk Zemmelink).

INTRODUCTION / INTRODUCTION

This special issue offers a suite of papers presented at the Third International Symposium on Biological and Environmental Chemistry of DMS(P) and Related Compounds, which was held in Rimouski, Québec, Canada, on 26–28 September 2002. The first two symposia were held in Mobile, Ala., U.S.A., in June 1995 (R.P. Kiene, P.T. Visscher, M.D. Keller, and G.O. Kirst (*Editors*). 1996. Biological and environmental chemistry of DMSP and related sulfonium compounds. Plenum Press, New York and London) and in Groningen, the Netherlands, in August 1999 (J. Stefels, M. van Rijssel, T.A. Hansen, L. Dijkhuizen, and W.W.C. Gieskes (*Editors*). 2000. Biological and environmental Chemistry of DMS(P) and the role of *Phaeocystis* in marine biogeochemical cycles. J. Sea Res. **43**: 179–390). Over 50 scientists from eight countries attended the three-day symposium. All major institutes active in this research field were represented, and the papers and posters covered most aspects of the current research effort.

The articles present recent findings on the biological production of the volatile sulfur compound dimethylsulfide (DMS) and its roles (*i*) in the regulation of global climate and (*ii*) in algal physiology and food web processes. In addition to the articles, the reader will find three perspective papers providing, to both experts and nonexperts alike, a stimulating overview of this expanding multidisciplinary research field. The perspective by Rafel Simó presents a particularly insightful introduction to the field for newcomers.

The climatic role of the dimethylsulfoniopropionate (DMSP) degradation product, DMS, still holds the attention of many researchers, and because the climate issue is global in essence, there is an obvious trend toward the development of a global understanding and modelling of DMSP and DMS production. However, there are also fascinating new avenues. There is increasing evidence that DMSP may represent a major source of sulfur and carbon for marine bacteria. In addition, information is accumulating on the role of DMSP and its degradation products DMS and dimethylsulfoxide (DMSO) as antioxidants. Other papers address basic questions such as which organisms are responsible for producing and consuming DMSP and DMS, why do algae and other plants produce DMSP, and why do some release DMS? Finding answers to these questions is crucial as one of the major impediments to the development of biogeochemical models of ocean DMS production is our lack of understanding of the physiological role of this molecule.

Some papers cross the sea-to-air interface and explore the atmospheric side of the DMS–climate connection, which is unusual for the *Canadian Journal of Fisheries and Aquatic Sciences*. Such multidisciplinary approaches are essential to a full understanding of the feedbacks between the ocean and the atmosphere. This diversity is one ingredient that makes this research field so fascinating and challenging. You will find a flavour of that in this issue.

The organization of the symposium was a real team effort. I first wish to thank the members of the local organizing committee, namely Michel Gosselin, Sonia Michaud, Michael Scarratt and Paule Maranda, and acknowledge the assistance provided by the following members of my laboratory: Anissa Merzouk, Martine Lizotte, Juliette Fauchot, and Yvonnick Le Clainche. They are truly responsible for the success of the symposium. I also wish to thank the members of

Ce numéro spécial contient une série d'articles qui ont été présentés dans le cadre du troisième symposium international sur la biologie et la chimie environnementale du DMS(P) et des composés apparentés tenu à Rimouski, Québec, Canada, les 26–28 septembre 2002. Les deux premiers symposiums ont eu lieu à Mobile, Ala., É.-U., en juin 1995 (R.P. Kiene, P.T. Visscher, M.D. Keller, and G.O. Kirst (*Directeurs de la rédaction*). 1996. Biological and environmental chemistry of DMSP and related sulfonium compounds. Plenum Press, New York and London) et à Groningen, Pays-Bas, en août 1999 (J. Stefels, M. van Rijssel, T.A. Hansen, L. Dijkhuisen, and W.W.C. Gieskes (*Directeurs de la rédaction*). 2000. Biological and environmental chemistry of DMS(P) and the role of *Phaeocystis* in marine biogeochemical cycles. J. Sea Res. **43**: 179–390). Plus de 50 chercheurs de huit pays ont participé à la réunion de trois jours. Tous les laboratoires actifs dans le domaine y étaient représentés et les présentations orales et les affiches couvrent la plupart des aspects de la recherche actuelle sur le sujet.

Les articles traitent des découvertes récentes sur la production biologique du composé sulfuré volatil, le sulfure de diméthyle (DMS), et de ses rôles (*i*) dans le contrôle du climat global et (*ii*) dans la physiologie des algues et le fonctionnement des réseaux trophiques. En plus des articles scientifiques, on trouvera trois perspectives qui fourniront aux initiés et aux novices une synthèse stimulante de ce champ de recherche pluridisciplinaire en pleine expansion. La perspective de Rafel Simó contient une introduction au domaine particulièrement éclairée pour les débutants.

Les effets du DMS, produit de dégradation du diméthylsulfoniopropionate (DMSP), sur le climat continue de susciter l'intérêt de nombreux chercheurs. Comme le climat est essentiellement global, il y a naturellement une tendance à essayer de comprendre et à modéliser la production de DMSP et de DMS à l'échelle planétaire. Il y a, par ailleurs, de nouvelles pistes excitantes de recherche. Des études récentes indiquent que le DMSP peut être une source majeure de soufre et de carbone pour les bactéries marines. D'autres travaux semblent confirmer le rôle d'antioxydant du DMSP et de ses produits de dégradation, le DMS et le DMSO (sulfoxyde de diméthyle). D'autres articles traitent de questions fondamentales, telles que les organismes responsables de la production et de la consommation de DMSP et de DMS ou la raison pour laquelle les algues et d'autres plantes produisent du DMSP, alors que certaines autres libèrent du DMS. Les réponses à ces questions sont très importantes, car la compréhension insuffisante du rôle physiologique du DMS est un des obstacles majeurs à la mise au point de modèles biogéochimiques de la production de cette molécule dans l'océan.

Quelques travaux franchissent l'interface mer–atmosphère et explorent l'aspect atmosphérique du lien entre le DMS et le climat, ce qui se fait rarement dans le *Journal canadien des sciences halieutiques et aquatiques*. Une telle approche pluridisciplinaire est essentielle pour comprendre les rétroactions entre l'océan et l'atmosphère. Cette diversité d'approches est une des raisons qui rendent ce champ de recherche si fascinant et stimulant. Le numéro actuel de la revue reflète bien cette ambiance.

L'organisation du symposium est le fruit d'un véritable travail d'équipe. Je veux d'abord remercier les membres du

© 2004 NRC Canada

the Scientific Advisory Board for their guidance: Jacqueline Stefels (University of Groningen, the Netherlands), Gill Malin (University of East Anglia, U.K.), Winfried W.C. Gieskes (University of Groningen, the Netherlands), Ronald Kiene (University of South Alabama, U.S.A.), Rafel Simó (Institut de Ciències del Mar, Spain), and Gordon Wolfe (California State University, U.S.A.).

Financial support for the symposium was provided by Le programme de soutien à la tenue de congrès scientifiques du ministère de la Recherche, de la Science et de la Technologie du Québec, Maurice Lamontagne Institute of the Department of Fisheries and Oceans Canada, l'Institut des Sciences de la mer de Rimouski, Varian Canada Inc., and VWR International. I also wish to thank the editorial staff of the Journal for agreeing to publish the Proceedings and for their professional support during the publishing process.

I hope that you will enjoy this issue.

Maurice Levasseur
Guest Editor

comité local d'organisation, soit Michel Gosselin, Sonia Michaud, Michael Scarratt et Paule Maranda et souligner le soutien du personnel de mon laboratoire, en particulier d'Anissa Merzouk, de Martine Lizotte, de Juliette Fauchot et d'Yvonnick Le Clainche. Ce sont eux les véritables responsables du succès du symposium. Je veux aussi exprimer ma reconnaissance aux membres du comité-conseil scientifique pour leurs recommandations, soit Jacqueline Stefels (Université de Groningen, Pays-Bas), Gill Malin (University of East Anglia, Royaume-Uni), Winfried W.C. Gieskes (Université de Groningen, Pays-Bas), Ronald Kiene (University of South Alabama, É.-U.), Rafel Simó (Institut de Ciències del Mar, Espagne) et Gordon Wolfe (California State University, É.-U.).

Le programme de soutien à la tenue de congrès scientifiques du Ministère de la Recherche, de la Science et de la Technologie du Québec, l'Institut Maurice-Lamontagne de Pêches et Océans Canada, l'Institut des Sciences de la mer de Rimouski, et les compagnies Varian Canada Inc. et VWR International nous ont fourni leur appui financier. Je veux finalement remercier le bureau de rédaction et de l'édition du Journal d'avoir accepté de publier les actes du symposium et d'avoir fourni leur soutien professionnel lors de la publication.

Bonne et fructueuse lecture.

Maurice Levasseur
Directeur scientifique invité

© 2004 NRC Canada

PERSPECTIVE / PERSPECTIVE

From cells to globe: approaching the dynamics of DMS(P) in the ocean at multiple scales[1]

Rafel Simó

Abstract: Major advances in dimethylated sulfur research are being made by approaching its dynamics at multiple scales. At the molecular to cellular level, single-cell techniques in molecular biology allow us to identify the microbes involved in cycling of dimethylated sulfur. Also, we find that dimethylsulfoxide (DMSO) is as ubiquitous as dimethylsulfoniopropionate (DMSP) in marine plankton, which supports the recent suggestion that both compounds are involved in coping with oxidative stress. At the community level, there is recent evidence for the role of DMSP as a major carrier in organic sulfur transfer and cycling through trophic levels, from phytoplankton to bacteria and to zooplankton through herbivore protozoans. As a consequence, the food web dynamics drive the oceanic emission of atmospheric sulfur. At the ecosystem level, the diverse and intricate effects of the physicochemical setting (light, wind, nutrients) on the oceanic cycling of dimethylated sulfur are being uncovered. A proposed shortcut to detailed understanding of the individual processes presents the depth of the surface mixed layer as the variable that integrates most of the environmental effects and serves for predicting dimethylsulfide (DMS) concentrations, even at the global ocean level. This opens the door to assessing the strength of the DMS biogeophysical system as a climate regulator.

Résumé : Des progrès importants dans la recherche sur la dynamique du soufre diméthylé se réalisent actuellement grâce à une approche à plusieurs échelles. À l'échelle moléculaire à cellulaire, des techniques utilisant une seule cellule en biologie moléculaire ont permis d'identifier les microorganismes impliqués dans le recyclage du soufre diméthylé. DE plus, le sulfoxyde de diméthyle (DMSO) est aussi omniprésent que le diméthylsulfoniopropionate (DMSP) dans le plancton marin, ce qui appuie les suggestions récentes selon lesquelles les deux composés sont impliqués dans la gestion du stress oxydatif. À l'échelle de la communauté, il y a des indications récentes que le DMSP joue un rôle comme porteur important de soufre organique dans les transferts et le recyclage à travers les différents niveaux trophiques, du phytoplancton aux bactéries et au zooplancton par l'intermédiaire des protozoaires herbivores. En conséquence, la dynamique des réseaux alimentaires contrôle l'émission du soufre atmosphérique par l'océan. À l'échelle de l'écosystème, le cadre physicochimique (lumière, vent, nutriments) a des effets divers et complexes sur le recyclage du soufre diméthylé dans l'océan. Une méthode simplifiée proposée pour la compréhension détaillée des processus individuels utilise la profondeur de la couche de mélange de surface comme la variable qui intègre le mieux la plupart des effets de l'environnement et qui sert à prédire les concentrations de sulfure de diméthyle (DMS), même à l'échelle globale de l'océan. Cela mène à une évaluation de l'importance du système biogéophysique du DMS dans le contrôle du climat.

[Traduit par la Rédaction]

Introduction

In their seminal paper in 1987, Charlson, Lovelock, Andreae, and Warren suggested that marine phytoplankton might participate in climate regulation by the emission of volatile sulfur to the atmosphere. Such a suggestion, known as the CLAW hypothesis after the initials of the authors, was built upon the observation that the great majority of the oceanic exhalation of sulfur is in the form of dimethylsulfide (DMS). DMS is produced by degradation of the cellular component dimethylsulfoniopropionate (DMSP), which occurs in phytoplankton to fulfil important physiological functions (Kiene et al. 1996). DMSP is produced in the algal cell as a response to multiple environmental forcings and is released and degraded with involvement of the whole planktonic food web. Most of the evolved DMS, in turn, is

Received 1 February 2003. Accepted 5 November 2003. Published on the NRC Research Press Web site at http://cjfas.nrc.ca on 22 June 2004.
J17363

R. Simó. Department of Marine Biology and Oceanography, Institut de Ciències del Mar (CMIMA-CSIC), Pg Marítim de la Barceloneta 37-49, 08003 Barcelona, Catalonia, Spain (e-mail: rsimo@icm.csic.es).

[1]This paper is part of the proceedings of the Third International Symposium on Biological and Environmental Chemistry of DMS(P) and Related Compounds, held in Rimouski (Québec), 26–28 September 2002.

 doi: 10.1139/F04-030 © 2004 NRC Canada

degraded within the water column by microorganisms and solar radiation, and only a fraction escapes transformation to get vented into the atmosphere and become climatically active (Simó 2001).

Fifteen years after the appearance of the CLAW hypothesis, the biogeophysical–biogeochemical DMS system still draws such scientific interest that great research efforts are invested in the study of DMS and DMSP to the extent that these two tiny molecules are perhaps the organic substances for which distribution and cycling in the ocean are the best known (Simó 2001). Owing to its transversal nature across disciplines, DMS(P) research is stimulating important advances in marine science fields as diverse as the physiology and elemental composition of microorganisms, chemosensory strategies, enzymology, sulfur fluxes in food webs, photochemistry and photobiology, and air–sea exchange. Each of these research fields has its own relevant scale in time and space.

DMS(P) research reminds me of expanding circular ripples on the surface of a pond after having thrown a stone into the water: one will hardly understand the behavior of the outer rings unless one turns the sight onto the core rings and links their formation with the external forcing, the thrown stone. Likewise, we will hardly understand the global-scale dynamics of DMS and its influence on, and response to, climate unless we understand how DMSP is produced and degraded at the level of the individual cell in response to physicochemical forcing. In my opinion, the most stimulating as well as productive way of approaching DMS(P) research today is by observing how cellular controls on DMS(P) production and cycling propagate to larger scales by inclusion into community, ecosystem, and mesoscale ocean dynamics. Associated with this is the need for multidisciplinary research teams working in collaboration to address multiple scales, from molecular reactions in the cell up to the global view from satellites.

Here, I highlight several examples of recent progress in the knowledge of dimethylated sulfur dynamics at different scales. I will mainly (but not exclusively) focus on the advances made in our laboratory in collaboration with colleagues from around the world. Note that by DMS(P), I refer to DMSP and DMS together. This is not equal to referring to the dynamics of the DMSP and DMS pools summed in a single pool but to both the DMSP and DMS dynamics and their coupling. In most cases, dimethylsulfoxide (DMSO) should be included as well, but its dynamics are still too poorly known.

Cell and population scales (micrometres to centimetres and minutes to hours)

Unveiling the abundance and identity of DMSP-utilizing bacteria

The deeper we go into our knowledge of the many processes that comprise the biogeochemical cycle of DMS(P) in the pelagic ocean, the more complicated it appears. Some features that can be highlighted are that phytoplankton DMSP release occurs mostly through cell autolysis, viral attack, and grazing (in the latter case, a fraction of the DMSP is assimilated by the grazer). Some of the released DMSP is then converted into DMS by algal and (or) bacterial DMSP lyases, with the substrate either free in solution, attached to particles, or in the guts and vacuoles of the grazers. Exudation of DMSP or DMS by living algae is generally thought to play a minor role, though it has been suggested recently that oxidative stress may cause phytoplankton release of intracellularly produced DMS (Sunda et al. 2002). A large fraction of DMSP is utilized by bacteria through non-DMS-producing pathways as a source of reduced sulfur (Kiene et al. 2000) (Fig. 1).

Fig. 1. Simplified view of the fate of phytoplanktonic DMSP. The diagram is designed to stress the role of bacteria in switching between DMS- and non-DMS-producing DMSP degradation pathways. A fraction of phytoplanktonic DMSP is cleaved to DMS by algal DMSP lyases (in either healthy cells or upon lysis or grazing), as well as by bacterial DMSP lyases after release. Another (generally larger) fraction is utilized by bacteria, partly as a source of reduced sulfur. Therefore, there is a clear need to identify which bacteria do what and ask what controls their specific activity and sulfur demands.

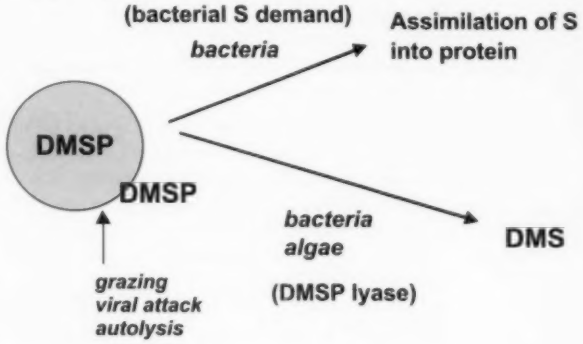

As stated by Simó (2001), a key to understand the dynamics of DMS(P) is to find out whether DMSP utilization is widespread among bacterioplankton or is a characteristic of only a few phylotypes. At present, the answer to this question is within reach thanks to the use of both classical and newly developed single-cell methods. These methods rely on the interrogation of individual cells for their activity and identity rather than measuring solely bulk activities and diversities.

We have recently applied microautoradiography (Pedrós-Alió and Newell 1989) with [^{35}S]DMSP to seawater samples from the coastal Gulf of Mexico enriched with inorganic nutrients (M. Vila, R. Simó, R. Kiene, J. Pinhassi, J.M. González, M.A. Moran, and C. Pedrós-Alió, unpublished data). This has allowed us to discriminate and count DMSP-assimilating cells. As many as 40–50% of the total heterotrophic bacteria associated with a DMSP-producing algal assemblage (particulate DMSP ($DMSP_p$) = 50–100 nmol·L^{-1}) were taking up sulfur from DMSP (Fig. 2). If these numbers are compared with those obtained simultaneously by use of a universal substrate like [^{3}H]leucine (60–65%), DMSP appears to be indeed an important substrate for marine bacteria.

We combined microautoradiography with fluorescent in situ RNA hybridization in a MICROFISH protocol (Lee et al. 1999) to find out the identity of those many DMSP-utilizing bacteria. Preliminary results showed that many of the cells that had taken up [^{35}S]DMSP belonged in the

© 2004 NRC Canada

Fig. 2. Epifluorescence microscopy image of marine bacteria showing the result of a microautoradiography test with [^{35}S]DMSP. Seawater from the coastal Gulf of Mexico was artificially enriched with inorganic nutrients to induce an algal bloom. The associated bacteria were incubated for 10 h with added [^{35}S]DMSP, filtered, and transferred onto a photographic emulsion. The white dots are 4′,6-diamidino-2-phenylindole stained bacterial cells. Black crowns are the marks left by the radioactive ^{35}S on the emulsion. Thus, white dots with and without crowns are bacteria that have and have not incorporated, respectively, ^{35}S from [^{35}S]DMSP (Vila et al. 2004).

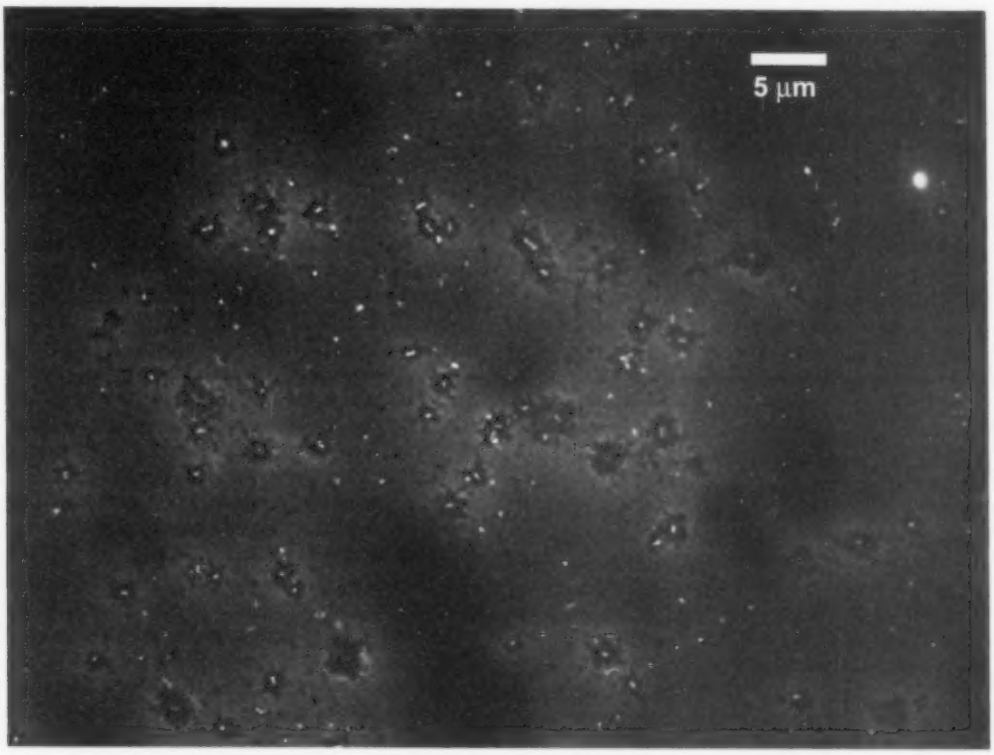

Roseobacter phylogenetic cluster. And most of the *Roseobacter* individuals stained with the RNA probe had taken up [^{35}S]DMSP (Vila et al. 2004). In previous works, several lines of circumstantial evidence had pointed to *Roseobacter* (a lineage of α-*Proteobacteria* very abundant in the marine environment) as potential major players in DMSP turnover (González et al. 1999, 2000; Zubkov et al. 2001). Now, thanks to techniques such as MICROFISH, for the first time we are able to actually look for coincidence of activity and identity in every single cell. Our very preliminary results indicate that *Roseobacter* may indeed be important, but not the only, players in DMSP cycling.

DMSO: a forgotten intracellular sulfur pool in phytoplankton

DMSO is ubiquitous in seawater, where it contributes to the pool of dissolved organic sulfur with concentrations of the same order as those of DMS and DMSP, in some cases even higher (compilations in Simó 1998; Lee and de Mora 1999*a*). At present, the role, origins, and fate of this compound in seawater are unclear. In representations of the biogeochemical DMS(P) cycle, DMSO generally appears as a dissolved substance that acts both as a product of DMS oxidation, either photochemical (Kieber et al. 1996) or microbiological (Taylor and Kiene 1989), and as a potential biological source for DMS (Taylor and Kiene 1989). Yet, these processes have not been reliably and systematically quantified in natural samples, except for the phochemical source of DMSO, for which very few estimates exist (Kieber et al. 1996; Hatton 2002).

Simó et al. (1998) measured a pool of $DMSO_p$ in marine seston and cells of cultured phytoplankton. These results, together with the later observation of increases in dissolved DMSO ($DMSO_d$) concentration in dark seawater incubations (Simó et al. 2000), strongly suggested that eukaryotic microorganisms, mainly phytoplankton, are involved in DMSO bioproduction and release. Those preliminary reports of intracellular DMSO were accompanied with speculation about its physiological role in phytoplankton. Simó et al. (1998) and Lee and de Mora (1999*b*) suggested that DMSO could be involved in protecting the cell against photogenerated oxidants and cryogenic damage or serve as a carrier for exudation of excess sulfur and carbon through membranes.

All aerobic organisms have developed mechanisms to deal with reactive oxygen species that are produced as by-products of photosynthesis, photooxidative stress, and respiration. In a recent paper, Sunda et al. (2002) have shown that DMSO is an effective scavenger of reactive oxygen species and suggested that this compound may join DMSP, DMS, and methane sulfinic acid in a cascade reaction system against oxidative stress. According to this hypothesis, DMSO

© 2004 NRC Canada

Fig. 3. Relationship between DMSP and DMSO in marine particles (GF/F retained) from the Norwegian Arctic, subpolar North Atlantic, coastal North Sea, Gulf of Maine, Sargasso Sea, subtropical Northeast Atlantic, western Mediterranean, Black Sea, and Weddel Sea (Antarctica). The mean $DMSP_p$-to-$DMSO_p$ ratio, as given by the slope of the linear regression line intercepting the 0:0 line, is 4.5 (R. Simó and M. Vila, unpublished data).

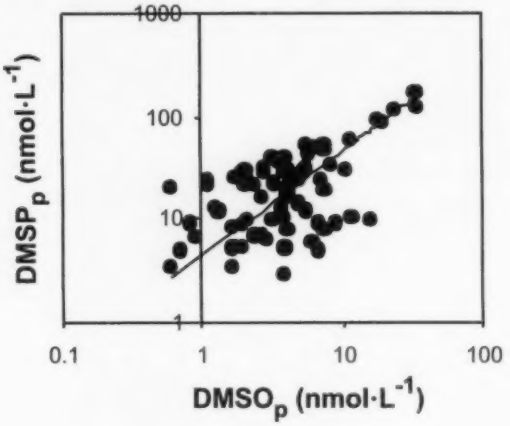

would be produced from ·OH oxidation of DMS or DMSP and, because of its hydrophilic nature, it would accumulate in the cell at the observed millimolar concentrations. Then, because of its high reactivity toward ·OH, DMSO itself would act as an efficient oxidant scavenger.

Now, we have expanded the particulate DMSO ($DMSO_p$) data set by carrying out analyses of GF/F-retained particles from a wide variety of Atlantic, Arctic, Antarctic, North Sea, Mediterranean, and Black seawaters (R. Simó and M. Vila, unpublished data). The results show that $DMSO_p$ is as ubiquitous as $DMSP_p$ in surface seawater. There is a significant positive correlation between both compounds throughout the different regions (Fig. 3), a general indication that both have a common phytoplanktonic origin.

In most of the samples, the ratio $DMSP_p$ to $DMSO_p$ falls within a range between 1 and 20, with a mean value of 4.5 (as indicated by the slope of the plot in Fig. 3). In other words, DMSO accounts for about 20% of the algal dimethylated sulfur pool (which is the far largest sulfur pool in many unicellular algae). We suggest, therefore, that $DMSO_p$ occurrence and $DMSO_d$ release have to be included in any representation of the DMS(P) cycle, and DMSO has to be considered when quantifying the fluxes of organic sulfur from phytoplankton through food chains. Both suggestions bring us to the next level, that of the whole plankton community.

Community scale (centimetres to metres and hours to days)

Tracking DMSP through the food web

Over the years since DMSP was discovered to occur in many phytoplankton species, the major foci for the study of this compound in the marine environment have been its role as the precursor of DMS and its physiological function in the algal cell (Kiene et al. 1996). Although some authors had observed that DMSP alone can make up >10% of intracellular carbon and >50% of intracellular sulfur in high DMSP producers (e.g., Matrai and Keller 1994), a quantitative role in the fluxes of organic matter had not been recognized, and DMSP has been regarded as a minor substance of high interest for osmoregulation and potential influence on climate. Only recently has DMSP been shown to contribute a large fraction of sulfur for heterotrophic bacterial production (Kiene et al. 1999, 2000). The mechanistic basis is the incorporation of the CH_3S moiety into protein in the bacterial cell (Fig. 1). Associated with this finding was the suggestion that a large fraction of algal DMSP sulfur would be returned up the food web by means of the microbial loop through bacterial biomass (Kiene et al. 2000).

In the last 5 years, two open-sea experiments have addressed the quantitative role of DMSP in carbon and sulfur fluxes through whole microbial food webs (Simó and Pedrós-Alió 1999*a*; Burkill et al. 2002). These experiments had the common characteristics of a Lagrangian approach and the gathering of comprehensive teams. For the first time, the contributions of phytoplankton, bacteria, and grazers to DMS(P) cycling were measured simultaneously (Burkill et al. 2002; Simó et al. 2002). Both studies happened to pick up similar food webs dominated by high DMSP producing algae, and both studies showed that the contribution of DMSP and derivatives to carbon and sulfur demands was significant for all three trophic levels.

In subpolar North Atlantic waters dominated by the coccolithophore *Emiliania huxleyi* in the month of June, Simó et al. (2002) estimated that DMSP was the fate for 7% of carbon fixation through photosynthesis in phytoplankton >5 μm and accounted for 8–15% of the bacterial carbon demand and 5% of the net microzooplankton carbon production. The numbers were much higher for sulfur: DMSP and derivatives constituted 71% of algal organic sulfur, provided enough reduced sulfur to sustain all bacterial sulfur demand, and supplied 48% of the sulfur demand of microzooplankton. I show plots of the estimated contribution of DMS(P) to carbon and sulfur fluxes through the microbial food web as encountered in this Lagrangian study (Fig. 4). Values are normalized to every 100 mol of carbon and sulfur assimilated in primary production.

In the northern North Sea in June, with the phytoplankton assemblage dominated by high DMSP producers like dinoflagellates and *E. huxleyi*, Burkill et al. (2002) obtained similar results to those of the North Atlantic study. Potential $DMSP_p$ production in terms of algal carbon amounted to 7% of the ^{14}C production (Archer et al. 2002*a*), microzooplankton played a major role in mobilizing algal DMSP, and this compound satisfied a large fraction (30–120%) of bacterial sulfur demand (Zubkov et al. 2002).

All in all, recent investigations clearly indicate that DMSP is a prominent player in pelagic sulfur and carbon biogeochemical pumps. From the perspective of sulfur biogeochemistry and food web functioning, DMSP stands out particularly as a major carrier in organic sulfur transference and cycling through trophic levels. From the perspective of the oceanic emission of atmospheric sulfur, experimental results keep showing that DMS production cannot be understood by considering phytoplankton biomass or activity alone. Although DMSP production can be proportional to

© 2004 NRC Canada

Fig. 4. Diagrams of the contribution of DMSP to C and S fluxes through a microbial food web in the subpolar North Atlantic. All are normalized to a C and S photosynthetic assimilation of 100 nmol·L^{-1}·day^{-1} by phytoplankton. Within each data pair, the top number is the measured or estimated flux of total C or S and the bottom number is the measured or estimated contribution of DMSP and derivatives to that flux, all in nmol·L^{-1}·day^{-1}. Assumptions have been made to provide estimates of those fluxes that were not measured, such as direct release to the dissolved pool by phytoplankton (Phyto), bacterial growth efficiency, or bacterial S assimilation. See details in Simó et al. (2002). DOC, dissolved organic C; Zoo, zooplankton; Het, heterotrophic; DOS, dissolved organic S.

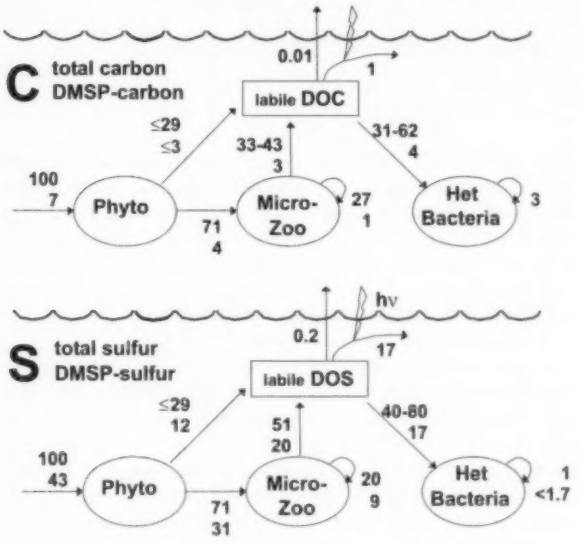

primary production in phytoplankton assemblages dominated by high DMSP producers (Simó et al. 2002), grazers and heterotrophic bacteria utilize a large fraction of DMSP on its way to DMS, and DMS itself is utilized and photooxidized, too. Eventually, the DMS that escapes the tight couplings existing between autotrophs and heterotrophs and vents to the atmosphere represents just a tiny fraction of algal DMSP production.

Emerging role of microzooplankton in DMS(P) cycling

The observations described above and others (e.g., Wakeham and Dacey 1989; Belviso et al. 1990; Bates et al. 1994) confirm that it is the community structure and the food web dynamics that drive the DMS(P) cycle (Simó 2001). In particular, recent field and laboratory studies show that grazers play a major role in the initial loss of phytoplanktonic DMSP (Table 1). Protozoans and other microzooplankton are major grazers in the ocean (e.g., Burkill et al. 1993). In the subpolar North Atlantic, microzooplankton ingested on average 44% of the DMSPp standing stock per day, accounting for 63% of the algal DMSP loss rates, during an *E. huxleyi* bloom (Simó et al. 2002). In the northern North Sea, 57% of the DMSP standing stock loss was ingested by microzooplankton, and as much as 91% of the phytoplankton DMSP loss was mediated by micrograzers (Archer et al. 2002*a*).

Because this dominant role of microzooplankton in channeling the loss of DMSP from the algal cell, the fate of the ingested DMSP will be a key factor in DMSP dynamics. As stated by Tang and Simó (2003), the micrograzers can either strengthen or weaken the coupling between algal DMSP and DMS production. The micrograzers may act mainly by causing the release of phytoplankton DMSP into the dissolved phase (by disruption of the algal cell, ejestion, or other unknown mechanisms) and making it available to bacteria. It can also facilitate DMSP cleavage into DMS by mixing algal DMSP lyases with DMS during cell disruption or digestion (Christaki et al. 1996; Wolfe and Steinke 1996). In both cases, microzooplankton will accelerate the coupling between phytoplankton DMSP and its transformation products such as DMS. Conversely, if DMSP accumulates in the micrograzers' biomass, it can be further transferred to higher trophic levels and the coupling between DMSP and DMS productions will be weakened.

During fieldwork, Simó et al. (2002) found that 67% of the ingested DMSP was released as $DMSP_d$ and DMS_d, and the other 33% was assumed to be retained in the microzooplankton biomass. Burkill et al. (2002) estimated that 70% of the phytoplankton DMSP ingested by microzooplankton was released as $DMSP_d$, only a small fraction (<7%) was converted to DMS, and the fate of the remaining fraction (>23%) was unknown.

Whether protozoans accumulate ingested DMSP is uncertain, and only indirect evidence was available until the recent laboratory experiments of Tang and Simó (2003). In multitrophic level experiments with two phytoplankters (*Phaeocystis globolosa* and *Isochrysis galbana*), a dinoflagellate micrograzer (*Gyrodinium dominans*), and a copepod (*Acartia tonsa*), we observed that although much of the algal DMSP was destroyed or released during the micrograzing process, a significant portion (32–44%) was accumulated in the protozoan biomass and transferred to the higher predator (Table 1). It is likely that the DMSP uptake efficiencies reported for *G. dominans* were a transient phenomenon; however, they were enough for the algal DMSP to pass on to the next trophic level. Selective feeding of the copepod on the protozoan when offered a protozoan–alga mixture still enhanced the role of microzooplankton in transferring DMSP up the food chain (Tang and Simó 2003).

Ecosystem scale (metres to kilometres and hours to months)

Physicochemical forcing on DMS(P) cycling: a case of complexity

Here, I differentiate the ecosystem from the community by including in the former the geophysical context. I am particularly interested in the role that physicochemical forcing of different kinds play in controlling the dynamics of DMS(P). A number of short-term effects of meteorological (total solar radiation, UV spectrum and intensity, wind speed) and chemical (inorganic nutrients, colored dissolved organic matter) forcing on DMS-producing communities and processes have been described (see some of them in Table 2). To mention several examples, solar irradiance affects cellular DMSP levels in algae, wind speed affects the air–sea exchange of DMS, nitrogen availability might affect DMSP

© 2004 NRC Canada

Table 1. Recent experimental studies of the role of microzooplankton in releasing and assimilating algal DMSP.

Herbivore protozoan	DMSP-containing phytoplankton prey	DMSP retention efficiency (%)[a]
Gyrodinium dominans	*Phaeocystis globolosa*	44
Gyrodinium dominans	*Isochrysis galbana*	32
Microzooplankton action	**Northeast Atlantic[b]**	**Northern North Sea[c]**
Algal DMSP standing stock ingested per day (%)	43	57
Contribution to algal DMSP loss rate (%)	63	91
DMSP uptake efficiency (%)	33	30[d]

[a]Calculated by budgeting DMSP in tritrophic (phytoplankter plus protozoan plus copepod) experiments in the laboratory. This retention value might be contributed by transient DMSP from the residence of the algal prey in the vacuole. After Tang and Simó (2003).

[b]Measured by dilution experiments plus budgeting over a Lagrangian time series in the field. After Simó et al. (2002).

[c]Similar approach. After Archer et al. (2002*a*) and Burkill et al. (2002).

[d]Assumed, not measured (see Burkill et al. 2002).

biosynthesis and accumulation in phytoplankton, and colored dissolved organic matter acts as a photosensitizer for the photochemical destruction of DMS.

Physicochemical forcing factors potentially operate at all stages of the DMS(P) cycle and, unfortunately for the researchers studying them, some act in opposite ways. For instance, bacterial DNA damage by UV-B may reduce both DMS production and consumption. Hence, the influence of the environmental setting on the oceanic cycling of DMS(P) stands as a nice case of "complexity in biogeochemical systems", although this hampers our ability to represent the plankton – DMS – sulfur emission chain in the form of a simple mechanistic, quantitative, and predictive model.

DMS losses: does biological consumption always dominate?

A good example of this complexity is given by aqueous DMS losses. DMS is lost from the mixed layer principally through three different processes: (*i*) microbial transformation, (*ii*) photolysis, and (*iii*) air–sea exchange (ventilation). Depending on the time scale considered, there is still a fourth, poorly quantified sink: vertical export by mixing events. In their pioneering study in the equatorial Pacific, Kiene and Bates (1990) observed that microbial utilization was much faster than ventilation and probably also much faster than photolysis. After that work, and in the absence of reliable field measurements of the photochemical sink, the notion that bacterial consumption far controlled DMS loss held for most of the decade of the 1990s.

In 1996, Kieber et al. reported UV photooxidation in low latitudes of the Pacific, and they showed that it could be an important sink for DMS (almost as fast as bacterial utilization and significantly faster than ventilation) at the very surface waters. Because of UV attenuation within the water, the relative strength of the photochemical sink would decrease when a thicker water column was considered. Three years later, Simó and Pedrós-Alió (1999*a*) estimated average DMS photolysis rates in the mixing layer of the subpolar North Atlantic and compared them with microbial consumption and ventilation rates. The depth criterion used for such comparison was the depth of the surface mixing layer. The results obtained showed that the three major loss processes were significant and their relative intensity was variable with time in the short term (within 2 weeks). Thus, photooxidation dominated DMS sinks under conditions of high irradiance (clear skies) and very shallow mixing, whereas bacterial consumption dominated under deeper mixing and (or) cloudy skies. Even ventilation, generally considered a minor sink, became comparable with bacterial consumption in a windstorm (Simó and Pedrós-Alió 1999*a*).

Another way of looking at the several contributions to DMS loss is by budgeting measurements of DMS production rates with DMS consumption rates. Only microbial consumption rates have been systematically measured along with production rates, so that the existence or absence of a balance between both rates will illustrate the potential role of microbes as major controllers of DMS concentrations. I show a log–log plot of 65 concurrent biological DMS production and consumption rates from different authors (Fig. 5). The majority of the data points fall below the 1:1 line, i.e., DMS production generally exceeds bacterial DMS consumption. Unless we were systematically sampling under conditions of net DMS production (there is no apparent reason to think that this is the case), the plot demonstrates that the microbial sink only accounts for a fraction of the total DMS loss. The average production:consumption ratio for all data pairs is 1.9 ± 1.4, and the slope of the linear correlation is 1.3 ± 0.18 ($r^2 = 0.46$). That is, although more data need to be compiled, so far we can say that bacterial consumption amounts to on average 50–80% of DMS production, and therefore, the remaining 20–50% required to close the balance must be accounted for by the other losses (mostly photolysis and ventilation) altogether.

Vertical mixing: integrating complexity

Several of the many individual processes that constitute the DMS(P) cycle have been and are still being studied in isolation. This provides an essential knowledge of, for example, what are the most active wavelengths for DMS photooxidation or what is the pH optimum for a DMSP lyase or what are the major products of bacterial DMSP utilization. This allows us to explore how each of these processes responds to external forcing or perturbation, e.g., how the intracellular DMSP concentration changes with changes in

© 2004 NRC Canada

Table 2. Potential shorter- and longer-term effects of surface vertical mixing on different parts of the DMS(P) cycle.

Time scale	Physicochemical forcing	Agent	Receptor of the effect	Chemical– biochemical–biological–ecological effect	Effect on the DMS(P) cycle	Sign[a]	Reference(s)[b]
Short term (minutes to days)	Light exposure	UV–PAR	Phytoplankton	Inhibition of photosynthesis	Inhibition of DMSP biosynthesis	NL?	1, 2, 3
				Photooxidative stress	Cellular DMSP, DMS, and DMSO contents, DMS exudation	+	4, 5
			Bacteria	DNA damage repair, inhibition	S and C demands, DMSP assimilation, DMS utilization	–	6, 7, 8, 9
				Exoenzyme damage	Bacterial exo-DMSP lyase activity (DLA)	–?	10
			Phytoplankton and bacteria	Combination of all of the above	DMS yield from DMSP consumption	NL, +	11
		UV – low visible	Dissolved	Potential quantum yields	DMS photolysis or photooxidation	+	12, 13
	Nutrient pulses	N, Fe (P?)	Phytoplankton	Acclimation to N availability	Switch from DMSP to N analogs	–?	14, 15
				Oxidative stress	Cellular DMSP and DMS contents and DLA	+	4
				Unbalanced growth	DMSP overflow (DLA-mediated exudation)	+	16
Longer term (days to months)	Light exposure	UV	CDOM	Production, photobleaching	DMS photolysis/photooxidation	±[c]	17, 18
	Nutrient regime	N, P	Phytoplankton	Succession of species and sizes	Cellular DMSP content	+	11, 19
			Bacteria	Succession	DMSP and DMS consumption	?	20, 21
			Whole food web	Succession	DMSP fluxes within the mixed layer, turnover	+?	2, 19

Note: The physicochemical forcings associated with the depth of the surface mixed layer, as well as the receptors and the non-sulfur-specific effects, are identified. The derived effects on parts of the DMS(P) cycle are either empirically observed or hypothetical. The direction of the effect with a shoaling mixed layer is also estimated. UV–PAR, UV – photosynthetically active radiation; CDOM, colored disolved organic matter.

[a]The sign estimates the direction of the effect on the DMS(P) process as forced by a shoaling in the surface MLD. +, increase; –, reduction; NL, nonlinear (sign changes with mixing depth); ?, highly uncertain because of lack of data or contradictory observations.

[b]Example references chosen to support or illustrate the suggested effect. 1, Neale et al. (1998); 2, Simó et al. (2002); 3, Archer et al. (2002*a*); 4, Sunda et al. (2002); 5, Slezak and Herndl (2003); 6, Herndl et al. (1993); 7, Jeffrey et al. (1996); 8, Kiene et al. (2000); 9, Slezak et al. (2001); 10, Yoch et al. (1997); 11, Simó and Pedrós-Alió (1999*b*); 12, Kieber et al. (1996); 13, Toole et al. (2003); 14, Andreae (1986); 15, Keller et al. (1999); 16, Stefels (2000); 17, Dacey et al. (1998); 18, Brugger et al. (1998); 19, Simó (2001); 20, Schauer et al. (2003); 21, González et al. (2000).

[c]Higher irradiances and shallower MLD in spring and summer cause both higher CDOM production and higher CDOM photobleaching. As DMS photolysis is photosensitized by CDOM, the net effect is uncertain.

© 2004 NRC Canada

Fig. 5. Relationship between microbial DMS consumption and production rates in 65 surface waters from the subpolar Northeast Atlantic (Simó and Pedrós-Alió 1999*a*), Barents Sea (Matrai and Vernet 1997), Labrador Sea (Wolfe et al. 1999), Gulf of Maine and Sargasso Sea (Ledyard and Dacey 1996; R. Simó et al. unpublished data), Northwest Mediterranean and coastal North Sea (van Duyl et al. 1998; Simó et al. 2000), equatorial and Northwest Pacific (Kiene and Bates 1990; Bates et al. 1994), and coastal Japan (Yang et al. 2001). All were obtained by dark seawater incubations for concurrent measurements of production and consumption, and in most of the cases, an inhibitor of DMS metabolism was used. The 1:1 line is plotted as a reference.

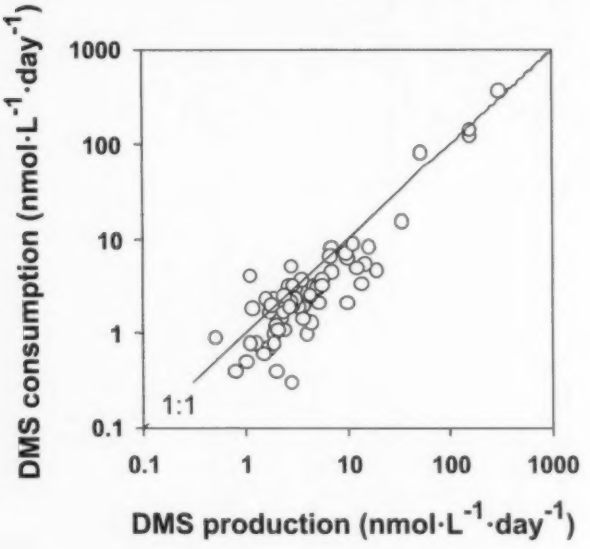

solar radiation intensity and spectrum. However, most of these processes are tightly interconnected, and for the purpose of gaining predictability in DMS distribution and dynamics, this complicated web of individual processes and responses becomes a maze that is hard to resolve by measurement and mechanistic modeling (Gabric et al. 2001*a*).

For this sole purpose of being able to predict surface DMS distribution under any biogeophysical conditions, we have suggested that the depth of the mixed layer (MLD) can be used as the variable that integrates most of the environmental effects, either on its own or in combination with chlorophyll *a* (Chl) concentration. The first intuition of a relationship between DMS and MLD arose a few years ago from the observation of the "summer DMS paradox": In large regions of the ocean, highest surface DMS concentrations are found in summer, when surface Chl levels are at their annual minimum and the MLD is shallowest (Simó and Pedrós-Alió 1999*b*). More recently, we have empirically found a numerical expression of this inverse relationship between DMS and MLD (see below) (Simó and Dachs 2002).

The underlying mechanistic reasons are to be found in the fact that vertical mixing/stratification controls the exposure of dissolved substances, nonliving particles, and buoyant organisms to solar radiation. It also affects phytoplankton succession and food web structure in the uppermost waters via turbulence and setting the entrainment of nutrient-rich waters. All of these effects are influential in parts of the DMS(P) cycle, as collected and summarized in Table 2. As a consequence, vertical mixing plays a key role in controlling the net production of DMS, and its quantitative expression (MLD) can therefore be used as a good predictor for surface DMS concentration.

Global ocean scale (kilometres to global and months to decades)

Towards global DMS prediction

If a major aim of DMS research is unraveling its link with climate, there is the unavoidable need to go global, i.e., to capture the DMS dynamics and its response to physicochemical forcing on a global scale and over months to decadal or even longer time scales (Gabric et al. 2001*a*). Like "regular" ecological models, mechanistic DMS models developed for regional studies cannot be expected to perform well at the global level.

A few semi-empirical shortcuts to global DMS prediction have been proposed. All of them have their origin in the knowledge of parts of the DMS(P) cycle but overcome a detailed understanding of the processes. Anderson et al. (2001) identified high DMS production regions as those with high light, not severe nutrient limitation, and enough decoupling between primary production and grazing. Accordingly, these authors related DMS to a proxy of the algal growth rate to produce monthly global maps of surface DMS concentration, where regions of high DMS concentration where much better represented than regions of low DMS concentration. Aumont et al. (2002) and Belviso et al. (2004) proposed a nonlinear parameterization that uses Chl concentrations and a community structure – trophic state index for DMS prediction. Underlying their relationship are the observations that DMSP occurs mostly in nano- and picophytoplankton and that DMSP is converted more efficiently into DMS when the fraction of phytoplankton contributed by the smaller algae is either very high or very low. Conceptually, this latter parameterization differs from the former in that the structure of the food web, and not only total phytoplankton growth, is taken into account. A critical evaluation of these parameterizations is given elsewhere in this issue (Vézina 2004).

A third parameterization has recently been suggested by Simó and Dachs (2002). We have derived empirical equations that relate surface DMS concentrations to Chl and the MLD as follows:

$$\mathrm{DMS} = -\ln(\mathrm{MLD}) + 5.7 \text{ if } \mathrm{Chl/MLD} < 0.02$$

$$\mathrm{DMS} = 55.8(\mathrm{Chl/MLD}) + 0.6 \text{ if } \mathrm{Chl/MLD} \geq 0.02.$$

These equations have been successfully used to predict the monthly distribution and flux of DMS in the global ocean (Fig. 6). Thus, we have found a simple empirical relationship that permits DMS concentration to be computed from measurable variables only, in particular from a combination of remotely sensed biospheric data (Chl) and climatological geophysical data (MLD).

The explanation for the good performance of this double algorithm is to be found in the "summer DMS paradox" mentioned above (Simó and Pedrós-Alió 1999*b*). An inverse

© 2004 NRC Canada

Fig. 6. (*a*) Monthly latitudinal averages of surface DMS concentrations in the global ocean, as predicted by the Simó and Dachs (2002) algorithm by use of climatological MLDs and satellite-derived Chl concentrations. (*b*) Monthly latitudinal averages of the sea to air emission flux of DMS, as estimated from the predicted concentrations and satellite-derived sea surface temperature and wind speed, by use of the Nightingale et al. (2000) parameterization of the air–sea exchange constant. See details in Simó and Dachs (2002). Shaded broken line, January; black line, April; black broken line, July; shaded line, October.

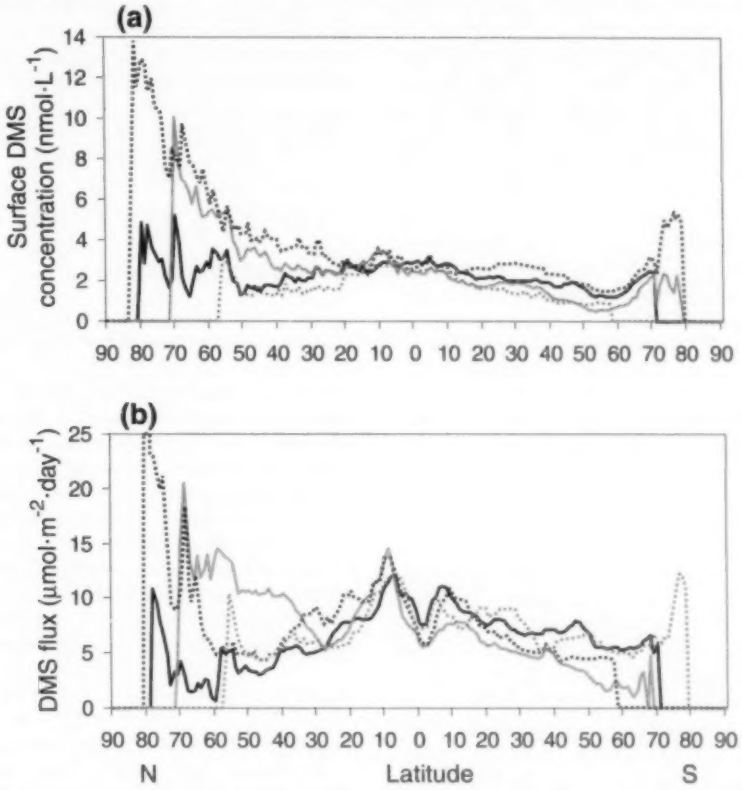

relationship between DMS concentration and MLD or Chl is apparent in a variety of oligotrophic regions. In more productive regions, however, high DMS levels generally accompany local high Chl levels, yet true proportionality is found only in blooms of high-DMSP-producing algae. The two equations of the Simó and Dachs (2002) algorithm indicate that high DMS concentrations occur associated not only with very high Chl concentrations but also with moderate to low Chl concentrations in shallow mixed waters, whereas deeply mixed waters exhibit low DMS concentrations. This is because shallow mixing favors blooms of DMSP-producing taxa, highly efficient DMS-producing food webs, and an array of photochemical and photobiological effects that all lead to DMS accumulation (see Table 2) (also Dacey et al. 1998; Simó and Pedrós-Alió 1999*b*; Simó et al. 2002; Simó and Dachs 2002).

Towards linking DMS and climate

The parameterizations mentioned in the previous section allow for the desired synopticity in the global DMS distribution. They add to the climatology of existing field measurements (Kettle et al. 1999) by filling the gaps left by undersampled regions and times of the year. Moreover, these parameterizations offer predictability for projections into changing environmental conditions so that the door is open towards assessing the strength of the ocean to atmosphere sulfur flux in climate regulation.

The finding that there is an inverse relationship between DMS concentration and the MLD that holds for large regions of the global ocean surface (Simó and Dachs 2002) can be regarded as an argument in support of the CLAW hypothesis (Charlson et al. 1987), for which mechanistic explanations are still lacking. In the hypothesis, DMS emission and subsequent atmospheric oxidation affect the cloud albedo, i.e., the amount of top of atmosphere irradiance that is reflected and prevented from passing through toward ocean surface, thus affecting solar heating and probably surface wind speed as well. Since solar radiation and wind friction are the primary forcing factors that set the MLD by in-water downward fluxes of heat and turbulent energy, respectively, then a closed loop of chained effects from DMS emission to aqueous DMS through albedo and vertical mixing can be envisaged (Simó 2001).

Nonetheless, the eventual links between the DMS flux, the cloud albedo, and the MLD will not be straightforward and will depend on the time scale considered. Any change in wind speed caused by a change in albedo, for instance, will have a time-depending effect on the DMS flux. Thus, an in-

© 2004 NRC Canada

creasing wind speed increases the air–sea flux in a matter of minutes to hours, but it also deepens the mixed layer and reduces the DMS concentration and flux in the longer term (hours to days). Persistent (days to months) strong winds provide a high air–sea exchange constant but do not allow for a DMS buildup in surface waters, so that they are associated with persistent low fluxes.

Over time scales much longer than short-term wind variability (months to seasons), higher DMS fluxes will be associated with shallower MLD. If the hypothesized subsequent increase in the albedo and reduction of the heat flux occur, these should prevent MLD from further shoaling and DMS concentrations from further rising, thus closing a negative feedback loop á la CLAW. At time scales of years to decades to centuries, a persistent forcing such as the radiative effect of rising atmospheric CO_2 will generate a persistent response in the DMS-emitting system, which so far we have not been able to anticipate reliably. For DMS research to meet societal interests, it is crucial that we use all that we have learned in the past 15 years to predict if global warming will result in an increase or a decrease of DMS emissions, i.e., if DMS will attenuate or amplify global warming.

As DMS and its oxidation products are short-lived substances in the atmosphere, any significant influence of oceanic sulfur emission on global climate, and vice versa, has to build upon the sum of local (mesoscale) effects. Diagnostic modeling with existing or newly generated comprehensive data sets (e.g., Archer et al. 2002*b*) should help define the feasibility and proper time scale of any double-way link between DMS flux and geophysical (meteorological) perturbation on the mesoscale. However, getting beyond the mesoscale in both time and space requires the great effort of coupling biogeochemical prognostic DMS models of regional applicability (e.g., Gabric et al. 1993) to coupled general circulation models for the global ocean (CGCMs) (Grassl 2000). The problem with this is that the representation of oceanic biogeochemistry (including plankton ecology) in CGCMs is still in its low developmental stages.

While awaiting, and working towards, the evolution of prognostic models (e.g., Gabric et al. 2001*b*) applicable to the global ocean, the coupling of semi-empirical parameterizations with CGCMs (e.g., Bopp et al. 2004) is a very useful tool for assessing the role of the DMS system in past climate and foreseeing its evolution in response to global warming.

Conclusions

After many years of fragmented research that has provided the foundations, several international teams are currently making efforts to integrate the many aspects of DMS(P) research through multiple scales. I anticipate that these efforts will be greatly rewarded. Firstly, the understanding of the complexity of this fascinating biosphere-driven ocean–atmosphere gear is now within reach. And, equally important, DMS(P) research is getting better embedded in marine and environmental sciences as it benefits from, and at the same time provides advances for, the state-of-the-art study of, e.g., food webs, theoretical ecology, physiology and phylogeny, biogeochemical cycles, aerosol chemistry, or remote sensing.

Back to the metaphor of expanding circular ripples, we understand the behavior of the outer ripples thanks to having asked the proper questions at the core ripples and vice versa. We are beginning to capture the global dynamics of DMS(P) and their role in climate because we are gaining understanding of their dynamics at smaller scales, as small as the unicellular microbe and its food web partners. Likewise, the over the years observation of the meso- and macroscale distribution of DMS(P) has allowed us to ask the right questions at the cellular level, which are yielding important advances in the knowledge of the physiology, phenology, and dynamics of marine plankton.

Acknowledgements

I am grateful to all who provided data, assistance, and fruitful discussions, particularly Carlos Pedrós-Alió, Maria Vila, and Jordi Dachs, but also Steve Archer, Evilio del Rio, Al Gabric, Pep Gasol, Linda Gilpin, Jose M. González, Watson Gregg, Jamie Kettle, Ron Kiene, Laura Linn, Ramon Massana, Mary Ann Moran, Jarone Pinhassi, Kam Tang, and Claire Widdicombe. I also thank Maurice Levasseur and the organizing committee of the Third DMSP Symposium for inviting me to present this overview paper. Multiple sources of funding are acknowledged: the Spanish Ministerio de Ciencia y Tecnología through projects AMIGOS (REN2001-3562/CLI), MicroDiFF (REN2001-2120/MAR), and REN2000-2457-E and the European Commission through project BASICS (EVK3-CT-2002-00078).

References

Anderson, T.R., Spall, S.A., Yool, A., Cipollini, P., Challenor, P.G., and Fasham, M.J.R. 2001. Global fields of sea surface dimethylsulfide predicted from chlorophyll, nutrients and light. J. Mar. Syst. **30**: 1–20.

Andreae, M.O. 1986. The ocean as a source of atmospheric sulfur compounds. *In* The role of sea–air exchange in geochemical cycling. *Edited by* P. Buat-Menard. Reidel, Dordrecht, the Netherlands. pp. 331–362.

Archer, S.D., Smith, G.C., Nightingale, P.D., Widdicombe, C.E., Tarran, G.A., Rees, A.P., and Burkill, P.H. 2002*a*. Dynamics of particulate dimethylsulphoniopropionate during a Lagrangian experiment in the northern North Sea. Deep-Sea Res. II, **49**: 2979–2999.

Archer, S.D., Gilbert, F.J., Nightingale, P.D., Zubkov, M.V., Taylor, A.H., Smith, G.C., and Burkill, P.H. 2002*b*. Transformation of dimethylsulphoniopropionate to dimethylsulphide during summer in the North Sea with an examination of key processes via a modelling approach. Deep-Sea Res. II, **49**: 3067–3101.

Aumont, O., Belviso, S., and Monfray, P. 2002. Dimethylsulfoniopropionate (DMSP) and dimethylsulfide (DMS) sea surface distributions simulated from a global 3-D ocean carbon cycle model. J. Geophys. Res. **107** (doi: 10.1029/1999JC000111).

Bates, T.S., Kiene, R.P., Wolfe, G.V., Matrai, P.A., Chavez, F.P., Buck, K.R., Blomquist, B.W., and Cuhel, R.L. 1994. The cycling of sulfur in surface seawater of the northeast Pacific. J. Geophys. Res. **99**: 7835–7843.

Belviso, S., Kim, S.-K., Rassoulzadegan, F., Krajka, B., Nguyen, B.C., Mihalopoulos, N., and Buat-Menard, P. 1990. Production of

© 2004 NRC Canada

dimethylsulfonium propionate (DMSP) and dimethylsulfide (DMS) by a microbial food web. Limnol. Oceanogr. **35**: 1810–1821.

Belviso, S., Moulin, C., Bopp, L., and Stefels, J. 2004. Assessment of a global climatology of oceanic dimethylsulfide (DMS) concentrations based on SeaWiFS imagery (1998–2001). Can. J. Fish. Aquat. Sci. **61**(5). This issue.

Bopp, L., Boucher, O., Aumont, O., Belviso, S., Dufresne, J.-L., Pham, M., and Monfray, P. 2004. Will marine dimethylsulfide emissions amplify or alleviate global warming? A model study. Can. J. Fish. Aquat. Sci. **61**(5). This issue.

Brugger, A., Slezak, D., Obernosterer, I., and Herndl, G.J. 1998. Photolysis of dimethylsulfide in the northern Adriatic Sea: dependence on substrate concentration, irradiance and DOC concentration. Mar. Chem. **59**: 321–331.

Burkill, P.H., Edwards, E.S., John, A.W.G., and Sleigh, M.A. 1993. Microzooplankton and their herbivorous activity in the northeastern Atlantic Ocean. Deep-Sea Res. II, **40**: 479–493.

Burkill, P.H., Archer, S.D., Robinson, C., Nightingale, P.D., Groom, S.B., Tarran, G.A., and Zubkov, M.V. 2002. Dimethyl sulphide biogeochemistry within a coccolithophore bloom (DISCO): an overview. Deep-Sea Res. II, **49**: 2863–2885.

Charlson, R.J., Lovelock, J.E., Andreae, M.O., and Warren, S.G. 1987. Oceanic phytoplankton, atmospheric sulphur, cloud albedo and climate. Nature (Lond.), **326**: 655–661.

Christaki, U., Belviso, S., Dolan, J.R., and Corn, M. 1996. Assessment of the role of copepods and ciliates in the release to solution of particulate DMSP. Mar. Ecol. Prog. Ser. **141**: 119–127.

Dacey, J.W.H., Howse, F.A., Michaels, A.F., and Wakeham, S.G. 1998. Temporal variability of dimethylsulfoniopropionate in the Sargasso Sea. Deep-Sea Res. **45**: 2085–2104.

Gabric, A.J., Murray, C.N., Stone, L., and Kohl, M. 1993. Modeling the production of dimethylsulphide during a phytoplankton bloom. J. Geophys. Res. **98**: 22 805 – 22 816.

Gabric, A., Gregg, W., Najjar, R., Erickson, D., and Matrai, P. 2001*a*. Modelling the biogeochemical cycle of dimethylsulfide in the upper ocean: a review. Chemosphere–Global Change Sci. **3**: 377–392.

Gabric, A.J., Whetton, P.H., and Cropp, R. 2001*b*. Dimethylsulphide production in the subantarctic Southern Ocean under enhanced greenhouse conditions. Tellus Ser. B Chem. Phys. Meteorol. **53**: 273–287.

González, J.M., Kiene, R.P., and Moran, M.A. 1999. Transformation of sulfur compounds by an abundant lineage of marine bacteria in the alpha-subclass of the class *Proteobacteria*. Appl. Environ. Microbiol. **65**: 3810–3819.

González, J.M., Simó, R., Massana, R., Covert, J.S., Casamayor, E.O., Pedrós-Alió, C., and Moran, M.A. 2000. Bacterial community structure associated to a DMSP-producing North Atlantic algal bloom. Appl. Environ. Microbiol. **66**: 4237–4246.

Grassl, H. 2000. Status and improvements of coupled general circulation models. Science (Wash., D.C.), **288**: 1991–1997.

Hatton, A.D. 2002. Influence of photochemistry on the marine biogeochemical cycle of dimethylsulphide in the northern North Sea. Deep-Sea Res. II, **49**: 3039–3052.

Herndl, G.J., Müller-Niklas, G., and Frick, J. 1993. Major role of ultraviolet-B in controlling bacterioplankton growth in the surface layer of the ocean. Nature (Lond.), **361**: 717–719.

Jeffrey, W.H., Pledger, R.J., Aas, P., Hager, S., Coffin, R.B., Von Haven, R., and Mitchell, D.L. 1996. Diel and depth profiles of DNA photodamage in bacterioplankton exposed to ambient solar ultraviolet radiation. Mar. Ecol. Prog. Ser. **137**: 283–291.

Keller, M.D., Kiene, R.P., Matrai, P.A., and Belows, W.K. 1999. Production of glycine betaine and dimethylsulfoniopropionate in marine phytoplankton. I. Batch cultures. II. N-limited chemostat cultures. Mar. Biol. **135**: 237–257.

Kettle, A.J. et al. 1999. A global database of sea surface dimethylsulfide (DMS) measurements and a procedure to predict sea surface DMS as a function of latitude, longitude, and month. Global Biogeochem. Cycles, **13**: 399–444.

Kieber, D.J., Jiao, J., Kiene, R.P., and Bates, T.S. 1996. Impact of dimethylsulfide photochemistry on methyl sulfur cycling in the equatorial Pacific Ocean. J. Geophys. Res. **101**: 3715–3722.

Kiene, R.P., and Bates, T.S. 1990. Biological removal of dimethyl sulphide from sea water. Nature (Lond.), **345**: 702–705.

Kiene, R.P., Visscher, P.T., Keller, M.D., and Kirst, G.O. (*Editors*). 1996. Biological and environmental chemistry of DMSP and related sulfonium compounds. Plenum Press, New York.

Kiene, R.P., Linn, L., Gonzalez, J., Moran, M.A., and Bruton, J. 1999. Dimethylsulfoniopropionate and methanethiol are important precursors of methionine and protein-sulfur in marine bacterioplankton. Appl. Environ. Microbiol. **65**: 4549–4558.

Kiene, R.P., Linn, L.J., and Bruton, J.A. 2000. New and important roles for DMSP in marine microbial communities. J. Sea Res. **43**: 209–224.

Ledyard, K.M., and Dacey, J.W.H. 1996. Microbial cycling of DMSP and DMS in coastal and oligotrophic seawater. Limnol. Oceanogr. **41**: 33–40.

Lee, N., Nielsen, P.H., Andreasen, H., Juretschko, S., Nielsen, J.L., Schleifer, K.-H., and Wagner, M. 1999. Combination of fluorescent in situ hybridization and microautoradiography — a new tool for structure–function analyses in microbial ecology. Appl. Environ. Microbiol. **65**: 1289–1297.

Lee, P.A., and de Mora, S.J. 1999*a*. A review of dimethylsulfoxide in aquatic environments. Atmos. Ocean, **37**: 439–456.

Lee, P.A., and de Mora, S.J. 1999*b*. Intracellular dimethylsulfoxide (DMSO) in unicellular marine algae: speculations on its origin and possible biological role. J. Phycol. **35**: 8–18.

Matrai, P.A., and Keller, M.D. 1994. Total organic sulfur and dimethylsulfonio-propionate in marine phytoplankton: intracellular variations. Mar. Biol. **119**: 61–68.

Matrai, P.A., and Vernet, M. 1997. Dynamics of the vernal bloom in the marginal ice zone of the Barents Sea: dimethyl sulfide and dimethylsulfoniopropionate budgets. J. Geophys. Res. **102**: 22 965 – 22 979.

Neale, P.J., Davis, R.F., and Cullen, J.J. 1998. Interactive effects of ozone depletion and vertical mixing on photosynthesis of Antarctic phytoplankton. Nature (Lond.), **392**: 585–589.

Nightingale, P.D., Liss, P.S., and Schlosser, P. 2000. Measurements of air–sea gas transfer during an open ocean algal bloom. Geophys. Res. Lett. **27**: 2117–2120.

Pedrós-Alió, C., and Newell, S.Y. 1989. Microautoradiographic study of thymidine uptake in brackish waters around Sapelo Island, Georgia, USA. Mar. Ecol. Prog. Ser. **55**: 83–94.

Schauer, M., Balagué, V., Pedrós-Alió, C., and Massana, R. 2003. Seasonal changes in the taxonomic composition of the bacterioplankton in a coastal oligotrophic system. Aquat. Microb. Ecol. **31**: 175–182.

Simó, R. 1998. Trace chromatographic analysis of dimethyl sulfoxide and related methylated sulfur compounds in natural waters (review). J. Chromatogr. A, **807**: 151–164.

Simó, R. 2001. Production of atmospheric sulfur by oceanic plankton: biogeochemical, ecological and evolutionary links. Trends Ecol. Evol. **16**: 287–294.

Simó, R., and Dachs, J. 2002. Global ocean emission of dimethylsulfide predicted from biogeophysical data. Global Biogeochem. Cycles, **16**(4): 1078 (doi: 10.1029/2001GB001829).

© 2004 NRC Canada

Simó, R., and Pedrós-Alió, C. 1999*a*. Short-term variability in the open ocean cycle of dimethylsulfide. Global Biogeochem. Cycles, **13**: 1173–1181.

Simó, R., and Pedrós-Alió, C. 1999*b*. Role of vertical mixing in controlling the oceanic production of dimethyl sulphide. Nature (Lond.), **402**: 396–399.

Simó, R., Hatton, A.D., Malin, G., and Liss, P.S. 1998. Particulate dimethyl sulphoxide in sea water: production by microplankton. Mar. Ecol. Prog. Ser. **167**: 291–295.

Simó, R., Pedrós-Alió, C., Malin, G., and Grimalt, J.O. 2000. Biological turnover of DMS, DMSP and DMSO in contrasting open-sea waters. Mar. Ecol. Prog. Ser. **203**: 1–11.

Simó, R., Archer, S.D., Pedrós-Alió, C., Gilpin, L., and Stelfox-Widdicombe, C.E. 2002. Coupled dynamics of dimethylsulfoniopropionate and dimethylsulfide cycling and the microbial food web in surface waters of the North Atlantic. Limnol. Oceanogr. **47**: 53–61.

Slezak, D., and Herndl, G.J. 2003. Effects of ultraviolet and visible radiation on the cellular content of dimethylsulfoniopropionate (DMSP) in *Emiliania huxleyi* (strain L). Mar. Ecol. Prog. Ser. **246**: 61–71.

Slezak, D., Brugger, A., and Herndl, G.J. 2001. Impact of solar radiation on the biological removal of dimethylsulfoniopropionate and dimethylsulfide in marine surface waters. Aquat. Microb. Ecol. **25**: 87–97.

Stefels, J. 2000. Physiological aspects of the production and conversion of DMSP in marine algae and higher plants. J. Sea Res. **43**: 183–197.

Sunda, W., Kieber, D.J., Kiene, R.P., and Huntsman, S. 2002. An antioxidant function for DMSP and DMS in marine algae. Nature (Lond.), **418**: 317–320.

Tang, K.W., and Simó, R. 2003. Trophic uptake and transfer of dimethylsulfoniopropionate (DMSP) in simple planktonic food chains. Aquat. Microb. Ecol. **31**: 193–202.

Taylor, B.F., and Kiene, R.P. 1989. Microbial metabolism of dimethyl sulfide. *In* Biogenic sulfur in the environment. *Edited by* E. Saltzman and W.J. Cooper. American Chemical Society, Washington, D.C. pp. 202–221.

Toole, D.A., Kieber, D.J., Kiene, R.P., Siegel, D.A., and Nelson, N.B. 2003. Photolysis and the dimetylsulfide (DMS) summer paradox in the Sargasso Sea. Limnol. Oceanogr. **48**: 1088–1100.

van Duyl, F.C., Gieskes, W.W.C., Kop, A.J., and Lewis, W.E. 1998. Biological control of short-term variations in the concentration of DMSP and DMS during a *Phaeocystis* spring bloom. J. Sea Res. **40**: 221–231.

Vila, M., Simó, R., Kiene, R.P., Pinhassi, J., González, J.M., Moran, M.A., and Pedrós-Alió, C. 2004. Use of microautoradiography combined with fluorescence in situ hybridization to determine dimethylsulfoniopropionate incorporation by marine bacterioplankton taxa. Appl. Environ. Microbiol. **70**. In press.

Vézina, A.F. 2004. Towards modelling marine DMS production and emissions over regional and global scales. Can. J. Fish. Aquat. Sci. **61**(5). This issue.

Wakeham, S.G., and Dacey, J.W.H. 1989. Biogeochemical cycling of dimethyl sulfide in marine environments. *In* Biogenic sulfur in the environment. *Edited by* E. Saltzman and W.J. Cooper. American Chemical Society, Washington, D.C. pp. 152–166.

Wolfe, G.V., and Steinke, M. 1996. Grazing-activated production of dimethyl sulfide (DMS) by two clone of *Emiliania huxleyi*. Limnol. Oceanogr. **41**: 1151–1160.

Wolfe, G.V., Levasseur, M., Cantin, G., and Michaud, S. 1999. Microbial consumption and production of dimethyl sulfide (DMS) in the Labrador Sea. Aquat. Microb. Ecol. **18**: 197–205.

Yang, G.-P., Watanabe, S., and Tsunogai, S. 2001. Distribution and cycling of dimethylsulfide in surface microlayer and subsurface seawater. Mar. Chem. **76**: 137–153.

Yoch, D.C., Ansede, J.H., and Rabinowitz, K.S. 1997. Evidence for intracellular and extracellular dimethylsulfoniopropionate (DMSP) lyases and DMSP uptake site in two species of marine bacteria. Appl. Environ. Microbiol. **63**: 3182–3188.

Zubkov, M.V., Fuchs, B.M., Archer, S.D., Kiene, R.P., Amann, R., and Burkill, P.H. 2001. Linking the composition of bacterioplankton to rapid turnover of dissolved dimethylsulphoniopropionate in an algal bloom in the North Sea. Environ. Microbiol. **3**: 304–311.

Zubkov, M.V., Fuchs, B.M., Archer, S.D., Kiene, R.P., Amann, R., and Burkill, P.H. 2002. Rapid turnover of dissolved DMS and DMSP by defined bacterioplankton communities in the stratified euphotic zone of the North Sea. Deep-Sea Res. II, **49**: 3017–338.

© 2004 NRC Canada

Responses of coastal phytoplankton populations to nitrogen additions: dynamics of cell-associated dimethylsulfoniopropionate (DMSP), glycine betaine (GBT), and homarine[1]

Maureen D. Keller, Patricia A. Matrai, Ronald P. Kiene, and Wendy K. Bellows

Abstract: Dimethylsulfoniopropionate (DMSP) and glycine betaine (GBT) are organic osmolytes abundant in many marine phytoplankton. Herein, we field tested for the first time the hypothesis that GBT production might be favored over DMSP in natural phytoplankton populations growing in high-N environments or when N is added to a system. Concentrations of particulate DMSP ($DMSP_p$; 15–45 nmol·L^{-1}) were equal to, or greater than, concentrations of particulate GBT (GBT_p; 0–15 nmol·L^{-1}) in the upper water column. Homarine, another N-containing osmolyte, was detected at lower levels in all samples. These are the first reported values of GBT_p, and homarine in seawater. During N enrichment experiments, no consistent pattern of response in the DMSP pool resulted. Under N stress, nitrate addition either caused DMSP to be released but without an equivalent increase in GBT or DMSP dynamics were not affected but GBT increased. In populations under less N stress, GBT levels were similar to those of $DMSP_p$ throughout the experiments. Homarine levels remained low at all times. We conclude that no simple switch between DMSP and GBT occurs as a function of N availability in natural populations. Variable responses to N supply probably resulted from differences in species composition and physiological state of the populations present.

Résumé : Le démethylsulfoniopropionate (DMSP) et la glycine bétaïne (GBT) sont des osmolytes organiques abondants dans plusieurs organismes phytoplanctoniques marins. Nous évaluons ici pour la première fois en nature l'hypothèse selon laquelle la production de GBT est favorisée au détriment de celle de DMSP dans les populations naturelles de phytoplancton qui se développent dans des milieux riches en azote ou dans des systèmes où il y a eu addition d'azote. Les concentrations de DMSP particulaire ($DMSP_p$; 15–45 nmol·L^{-1}) sont semblables ou supérieures aux concentrations de GBT particulaire (GBT_p; 0–15 nmol·L^{-1}) dans la partie supérieure de la colonne d'eau. La homarine, un autre osmolyte contenant de l'azote, peut être décelée à concentration plus faible dans tous les échantillons. C'est la première fois que l'on rapporte des valeurs de concentrations de GBT_p et de homarine dans l'eau de mer. Au cours d'expériences d'enrichissement à l'azote, il ne se produit pas de réaction uniforme dans le pool de DMSP. Lorsqu'il y a un stress azoté, l'addition de nitrate ou bien entraîne une libération de DMSP, mais sans accroissement équivalent de GBT, ou alors elle reste sans effet sur la dynamique du DMSP, mais avec un accroissement de GBT. Chez les populations soumises à un stress azoté, les concentrations de GBT sont semblables à celles de $DMSP_p$ dans toutes les expériences. Les concentrations de homarine restent faibles à tout moment. En conclusion, il n'existe pas de simple substitution du DMSP et de la GBT en fonction de la disponibilité de l'azote dans les populations naturelles. Les réactions variables à l'apport d'azote résultent probablement de différences dans la composition spécifique et l'état physiologique des peuplements planctoniques présents.

[Traduit par la Rédaction]

Introduction

Marine algae produce a variety of organic N- and S-containing osmolytes including the quaternary ammonium compound glycine betaine (GBT) and the tertiary sulfonium compound dimethylsulfoniopropionate (DMSP) (White 1982; Roch et al. 1985; Blunden and Gordon 1986). DMSP in marine phytoplankton is the primary source of dimethylsulfide (DMS), the most significant and abundant biogenic sulfur gas in the environment. Oceanic flux of DMS is cur-

Received 12 February 2003. Accepted 13 February 2004. Published on the NRC Research Press Web site at http://cjfas.nrc.ca on 22 June 2004.
J17369

M.D. Keller,[2] P.A. Matrai,[3] and W.K. Bellows. Bigelow Laboratory for Ocean Sciences, McKown Point, W. Boothbay Harbor, ME 04575, U.S.A.
R.P. Kiene. Department of Marine Sciences, University of South Alabama, LSCB 25, Mobile, AL 36688, U.S.A.

[1]This paper is part of the proceedings of the Third International Symposium on Biological and Environmental Chemistry of DMS(P) and Related Compounds, held in Rimouski (Québec), 26–28 September 2002.
[2]M.D. Keller (1954–1999) passed away unexpectedly. This manuscript, written by her, is submitted posthumously by her co-authors.
[3]Corresponding author (e-mail: pmatrai@bigelow.org).

 doi: 10.1139/F04-058 © 2004 NRC Canada

rently estimated at 0.6–1.7 Tmol S·year^{-1} (1 Tmol = 32 × 10^{12} g of S) and accounts for a significant fraction (30–50%) of natural global S emissions (Andreae 1990; Bates et al. 1992; Kettle and Andreae 2000). Direct attempts to correlate DMS production with phytoplankton biomass (chlorophyll (Chl)) have been only moderately successful (e.g., Barnard et al. 1982; Matrai et al. 1995; but see Simó and Dachs 2002). This lack of correlation can be at least partially attributed to the fact that not all phytoplankton produce DMSP. The classes Dinophyceae and Prymnesiophyceae and some other chromophyte microalgae contain the highest intracellular levels of DMSP (Keller et al. 1989). In addition, the release of DMSP and its conversion to DMS is accomplished by a number of biologically mediated processes, including phytoplankton internal and (or) external enzymatic degradation (e.g., Stefels 2000), oxidative stress (Sunda et al. 2002), phytoplankton cell lysis (e.g., Matrai and Keller 1993), grazing by zooplankton (e.g., Dacey and Wakeham 1986), and bacterial degradation (e.g., Kiene and Bates 1990).

Because of the known structural similarity between DMSP and GBT, Andreae (1986) suggested that a reciprocal relationship between these compounds might exist, with DMSP production being favored over that of GBT in N-limited populations. Andreae (1986) argued that the overwhelming abundance of sulfate in seawater (~28 mmol·L^{-1}) as compared with combined N (1–10 μmol·L^{-1}) might result in the selective production of S-containing compounds that serve similar functions. When N is not limiting, cells may begin to produce GBT and other nitrogenous compounds and replace DMSP. It is known that some marine algal species produce both GBT and DMSP (Dickson and Kirst 1987*a*, 1987*b*; Keller et al. 1999*a*) and that the relative proportions of GBT and DMSP are not constant, as was observed in cells of *Platymonas subcordiformis* grown at different salinities (Dickson and Kirst 1986) or different temperatures (Sheets et al. 1996). There is also evidence to support the idea of an inverse relationship between DMSP and available N in phytoplankton. Turner et al. (1988) reported that in cultures of *Emiliania huxleyi* supplemented with 15 mg nitrate·L^{-1}, the per-cell DMSP levels were lower than in cultures with low nitrate. Similarly, Gröne and Kirst (1992) observed that DMSP levels in *Tetraselmis subcordiformis* were 75% higher in N-limited batch cultures. Likewise, Keller and Bellows (1996) reported increases of 30–90% in intracellular DMSP concentrations in several species of phytoplankton grown in N-limited versus N-replete batch cultures.

Recently, Keller et al. (1999*a*, 1999*b*) reported on the distribution of cell-associated DMSP and GBT in batch and chemostat cultures of several marine phytoplankton. They found that each of the six species examined in batch mode produced DMSP, while three produced GBT at lower levels. In one species, levels of GBT were higher than DMSP during the exponential phase of growth but declined sharply as the culture approached stationary phase, a change that appeared to coincide with the onset of N limitation. Other nitrogenous osmolytes were produced in five of the six clones but in lower quantities. Based on these experiments, there does not appear to be a strict reciprocal relationship between DMSP and GBT production, although GBT production does appear to be related to N availability. Additionally, this relationship was examined in three axenic clones of phytoplankton in chemostat cultures at three N-limited growth rates (Keller et al. 1999*b*). Levels of GBT and homarine, another nitrogenous osmolyte, were inversely related to DMSP in the diatom *Thalassiosira pseudonana*, with GBT and homarine preferentially produced at the highest growth rate when cells would be most N replete (Parsons et al. 1977). DMSP concentrations did not change in the prymnesiophyte *E. huxleyi*, although GBT and homarine levels did increase at the highest growth rate. In *Amphidinium carterae*, a dinoflagellate, neither DMSP nor GBT varied in any systematic way with growth rate. However, in all three algae, additions of N to N-limited cultures resulted in short-term increases in GBT production. Additionally, phytoplankton appeared to be capable of directly assimilating extracellular GBT (Keller et al. 1999*b*), although it was not determined if they eliminated equivalent amounts of DMSP in the process.

Although GBT production by marine phytoplankton has been known for some time, very little is known about the role that GBT plays in the N economy of marine phytoplankton or of marine systems in general (King 1988). There are no reports, to our knowledge, of GBT concentrations in seawater, and as such, GBT may represent a substantial unknown pool of organic N. Our initial hypothesis was that production of GBT over DMSP, or the selection of species that produce GBT, may be favored in high-N environments or when N is supplied to a population. We tested these hypotheses in the stratified, low-nutrient basins of the Gulf of Maine by conducting N enrichment experiments where nitrate, GBT or deep water containing nitrate was added to surface water samples. Variations in particulate DMSP and GBT concentrations, in relation to phytoplankton population dynamics, were examined.

Materials and methods

The study was conducted aboard the R/V *Cape Hatteras* in the Gulf of Maine during the period of 15–25 June 1995. We surveyed the hydrography using a conductivity–temperature–depth meter and rosette water sampler equipped with Niskin bottles. At each station, samples were taken from at least three depths, surface, Chl maximum, and 1% light level, for analysis of dissolved DMSP ($DMSP_d$) and particulate DMSP ($DMSP_p$), DMS, particulate GBT (GBT_p), particulate organic C (POC), particulate organic N (PON), particulate organic S (POS), protein, amino acids, Chl, inorganic nutrients, and samples for microscopic cell counts and identifications.

At selected stations (Fig. 1), we conducted a series of enrichment experiments. Four experimental treatments, in duplicate, were tested using acid-washed 20-L polycarbonate carboys and water collected from surface (5 m) depths. The four treatments were (*i*) unamended (controls), (*ii*) supplemented with filtered deep water (from the vicinity of the deep Chl maximum and presumptive nitracline: 75 m for the first incubation and 100 m for the subsequent three incubations), (*iii*) supplemented with nitrate (10 μmol·L^{-1}), or (*iv*) supplemented with GBT (10 μmol·L^{-1}). Controls consisted of 10 L of "whole" surface seawater plus 10 L of 0.2-μm-filtered surface seawater. The nitrate addition treatments were set up the same way as the controls and then the nitrate was added. The

© 2004 NRC Canada

Fig. 1. Map of the Gulf of Maine noting locations of incubation stations. Incubation station 1 was located in Stellwagen Basin (42°20.17′N, 70°22.77′W), station 2 was located in Georges Basin (42°23.45′N, 67°26.44′W), station 3 was located in Wilkinson Basin (42°44.02′N, 69°40.32′W), and station 4 was located in Jordan Basin (43°33.27′N, 67°53.27′W).

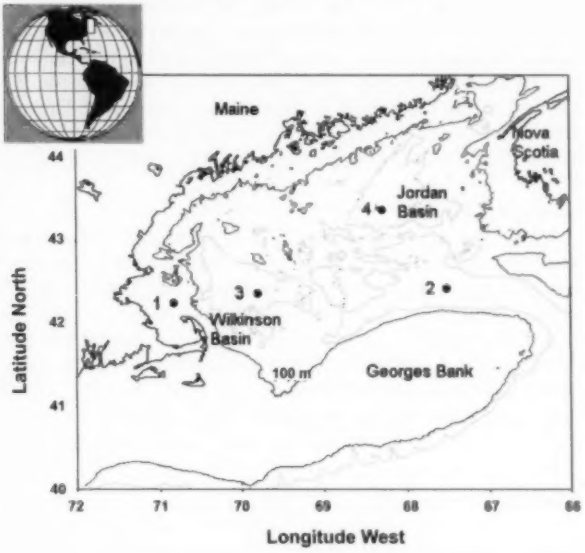

GBT treatments were identical, with the GBT subsequently added, and the deepwater treatments were 10 L of whole surface water plus 10 L of 0.2-μm-filtered deep water. Deep and surface water to be used for the dilutions was collected several hours before the incubations, prefiltered through 20-μm Nitex, and then gravity filtered through a 0.2-μm filter cartridge into polycarbonate carboys. Whole water was collected at 5 m immediately before the start of the experiment and prefiltered through 100-μm Nitex into a 208-L polyethylene container that had been acid washed and presoaked with seawater. This water was gently but well mixed before dispensing appropriate volumes into a smaller (57 L) similarly washed container to mix the duplicate treatments and make the additions. Initial samples (T_0) were taken from this mixing container and then the treatments were dispensed to duplicate carboys. The carboys were incubated in an on-deck incubator with flowing seawater and screened to the appropriate light level (approximately 10%). They were sampled at 24 and 45 h for all parameters to observe longer term physiological responses of the initial phytoplankton population present while avoiding the species replacement characteristic of longer nutrient enrichment bottle experiments (Cullen 1991). In addition, water from the nitrate addition (+10 μmol·L^{-1}) treatment was placed in triplicate acid washed 2.5-L polycarbonate bottles and incubated in an on-deck incubator as above. These 2.5-L bottles were sacrificed at 2, 6, and 12 h and sampled for GBT, $DMSP_p$, $DMSP_d$, DMS, Chl, POC, and PON.

DMS and DMSP concentrations

Particulate and dissolved concentrations of DMSP and free DMS were analyzed on a Varian 3300 gas chromatograph with flame photometric detection and a Chromosil 330 Teflon column. DMS was measured immediately upon sample collection, after sparging and cryotrapping. Whole water samples and the filtrates from samples gently filtered (<4 psi (1 psi = 6.895 kPa)) through glass fiber filters (GF/F) were collected in glass vials (15 mL, triplicate samples), base (1 mL of 5 mol/L^{-1} KOH) was added, and the vials were sealed. Samples were incubated for 24 h in the dark at room temperature and then sonicated before sparging. DMS was collected and analyzed via the cryogenic trap method (Keller et al. 1999*a*). DMS measured in these samples includes the free DMS and the total and dissolved fractions of the DMSP pool. $DMSP_p$ concentrations were determined by difference. Extensive preliminary tests were run comparing values from filters and filtrates with total DMSP values using both cultures and field samples. Filter values for DMSP tended to be variable, though replicates averaged to calculated concentrations. Total DMSP and $DMSP_d$ replicates were consistent and hence were preferred for this work. DMSP was obtained from Research Plus, Inc., and standards were prepared in DMSP-free filtered seawater.

GBT and other nitrogenous osmolytes

GBT_p and other nitrogenous compounds were measured by the high-performance liquid chromatography – ion chromatography method of Gorham (1984) and King (1988). Water samples (1000 mL, duplicate samples) were filtered gently (<4 psi) onto a glass fiber filter (GF/F) to capture cells and extracted with a methanol–chloroform–water (12:5:1) mixture for >24 h. The extract was evaporated to dryness under a stream of N and reconstituted in 0.5 mL of deionized water. The samples were then filtered through a 0.45-μm Teflon filter before injection. The high-performance liquid chromatography consisted of a Rheodyne injector equipped with a 100-μL loop, Knauer pump, and ISCO V4 variable-wavelength detector. Data were collected by E-lab chromatography software (OMS Tech.). Mixtures were separated on a strong cation-exchange column (4 mm × 250 mm) (Whatman Partisil SCX) using 0.05 mol KH_2PO_4·L^{-1} buffer and 2.5% methanol, flow rate 1 mL·min^{-1}, with detection by UV absorbance at 190 nm. Sensitivity was modest; the minimum detectable amount of GBT was ~0.4 nmol·100 μL injection^{-1}, corresponding to 2.0 nmol GBT·L filtered water^{-1} (nanomoles of GBT_p per litre). GBT standards were prepared from reagents obtained from Sigma Chemicals. GBT peak identities were confirmed by standard addition to samples and cochromatography. Homarine standards were not available at the time that this study was carried out. Homarine was identified and quantified by relative retention time and response factors given in Gorham (1984). Identity was later confirmed with authentic homarine obtained from D. Rhodes (Department of Horticulture and Landscape Architecture, Purdue University, West Lafayette, IN 47907, U.S.A.). Identification of homarine peaks was aided by its strong absorbance at 272 nm and by its separation from trigonelline. Based on 1000 mL of water filtered, the detection limit for particulate homarine was 0.06 nmol·L^{-1}.

POS concentration

Samples were gently filtered (<4 psi) (500 mL, duplicate samples) onto precombusted quartz fiber QM/A filters and

© 2004 NRC Canada

rinsed with 3% isotonic ammonium formate to remove sulfate salts and frozen. Before analysis, the filters were dried at 60 °C. Analyses were carried out with an Antek 771 pyroreactor unit coupled to an Antek 701C S detector (Matrai 1989). Methionine was used as a standard. The limit of detection was 0.01 μg of S and the precision of the method was within 5%.

POC and PON concentrations

Samples (500 mL, duplicate samples) for POC and PON were gently filtered (<4 psi) onto precombusted Whatman GF/F filters, stored at –20 °C in baked foil envelopes, and dried for 24 h at 50 °C immediately before analysis. POC concentrations may include a contribution from particulate inorganic C, usually less than 5% of POC content in the Gulf of Maine (W. Balch, Bigelow Laboratory for Ocean Sciences, W. Boothbay Harbor, ME 04575, U.S.A., personal communication). Analysis was on a Control Equipment Corp. CHN analyzer. Acetanilide was used as a standard.

Total protein and amino acid concentrations

Samples (500 mL, duplicate samples) were gently filtered (<4 psi) onto glass fiber filters (Whatman GF/F), which were then ground in cold 10% trichloroacetic acid. The sample was then centrifuged and the pellet analyzed for protein by the Lowry method (Lowry et al. 1951), as modified by Dortch et al. (1984). Bovine serum albumin was used as the standard for protein measurements. Amino acids were analyzed in the supernatant using the fluorescamine method (Packard and Dortch 1975). Glutamate was used as the standard for the amino acid analyses. Fluorescence was measured at 480 nm using a spectrofluorometer with excitation at 390 nm. This method was determined to be the best in terms of recovery and sensitivity for marine phytoplankton samples (Clayton et al. 1988).

Chl *a* concentration and cell counts

Samples for Chl *a* analysis (250 mL, triplicate samples) were gently filtered (<4 psi) onto Whatman GF/F filters, extracted for at least 24 h in 90% acetone at –20 °C in the dark, and concentrations determined fluorometrically with a Turner-Designs 10-005R fluorometer (Parsons et al. 1984). Samples (250 mL) for quantitative phytoplankton analyses were preserved immediately with 50% glutaraldehyde to a final concentration of 0.5% and refrigerated for at least 1 h. One hundred to two hundred millilitres were filtered onto a 3-μm Nuclepore filter and the filter placed on a slide and frozen until enumeration (Murphy and Haugen 1985). Samples were examined using a Zeiss Axiomat epifluorescence microscope. In addition, vertical net tows (25-μm mesh) were made and additional whole water samples (250 mL) were collected; both of these were fixed with Lugol's iodine solution to provide a qualitative estimate of larger phytoplankton. These samples were examined using settling chambers and a Zeiss inverted microscope. Chl-containing cells were counted using epifluorescence microscopy and cells identified, when possible, into major taxa or pigment groups. Larger cells comprising greater than 1% of the population were identified to genera or species, if possible, on the inverted microscope. A minimum of 100 cells was counted in each sample.

Inorganic nutrient concentrations

Samples (50 mL, unfiltered) for inorganic nutrient concentrations were frozen and subsequently analyzed for inorganic nutrients using standard autoanalyzer techniques (T. Loder, Earth and Ocean Sciences, University of New Hampshire, Durham, NH 03824, U.S.A.). Although there is some controversy over the validity of ammonium levels derived from frozen seawater samples, extensive results from direct comparisons done during the 1990s show that the ammonium concentrations presented here are realistic for the Gulf of Maine (L. Codispoti, Horn Point Laboratory, University of Maryland Center for Environmental Science, Cambridge, MD 21613, U.S.A., personal communication).

Statistical analysis

Error bars represent the range of experimental or sampling replicates. Statistical significance of rates of change for various parameters was tested by evaluating whether slopes deviated from zero using a two-tailed *t* test, as well as regression analysis, for each incubation; no autocorrelation correction was applied. ANOVAs were completed for comparisons among and within means of $DMSP_p$ or GBT_p of all four incubations (Sokal and Rohlf 1981) for nutrient (control, + nitrate, + deep) or GBT (control, + GBT) treatments.

Results

In situ conditions and depth profiles of $DMSP_p$, GBT_p, and homarine

Station locations where incubation experiments were conducted are shown in Fig. 1. Vertical distributions of DMSP and GBT at the time that water was collected for the experiments are also presented (Fig. 2). At each station, nitrate was depleted in surface waters and high levels were present at the depth where water for the deepwater treatment was collected (Tables 1–4). In all cases, $DMSP_p$ was the dominant fraction of DMSP, although at incubation stations 2 and 3, the dissolved fraction was significant in surface waters (Tables 1–4). $DMSP_p$ concentrations ranged from 15 to 45 $nmol \cdot L^{-1}$, were maximal in surface waters, and decreased to very low or undetectable levels at depth. GBT_p concentrations ranged from undetectable to approximately 15 $nmol \cdot L^{-1}$ and displayed no typical distribution pattern, i.e., the maximum was at the surface at one station, while it increased with depth at another (Fig. 2). Highest levels of $DMSP_p$ and minimal levels of GBT_p were seen at incubation station 1; $DMSP_p$ and GBT_p were equivalent (approximately 20 $nmol \cdot L^{-1}$) in surface waters at incubation station 2. At incubation station 3, GBT_p was undetectable in surface waters but increased to approximately 15 $nmol \cdot L^{-1}$ at depth, while $DMSP_p$ was present at 18 $nmol \cdot L^{-1}$ in surface waters. Incubation station 4 had the lowest observed levels of $DMSP_p$ in surface waters and approximately 5 nmol $GBT_p \cdot L^{-1}$ at 5 m.

Particulate homarine concentrations ranged from 1.8 to 5.4 $nmol \cdot L^{-1}$ and were about 10-fold lower than $DMSP_p$ concentrations in water samples from above 30 m depth (Fig. 2). Homarine concentrations were, however, equivalent to those of GBT_p in the upper 30 m (e.g., incubation stations 1 and 3). At the deeper depths of 75–100 m, homarine was very low, as were $DMSP_p$ and GBT_p in general.

© 2004 NRC Canada

Fig. 2. Vertical profiles of $DMSP_p$ (●, nmol·L^{-1}), GBT (□, nmol·L^{-1}), and homarine (▼, nmol·L^{-1}) at cruise stations where water samples for incubation experiments were collected. Profiles were obtained immediately before collection of water for (*a*) incubation station 1 in Stellwagen Basin, (*b*) station 2 in Georges Basin, (*c*) station 3 in Wilkinson Basin, and (*d*) station 4 in Jordan Basin.

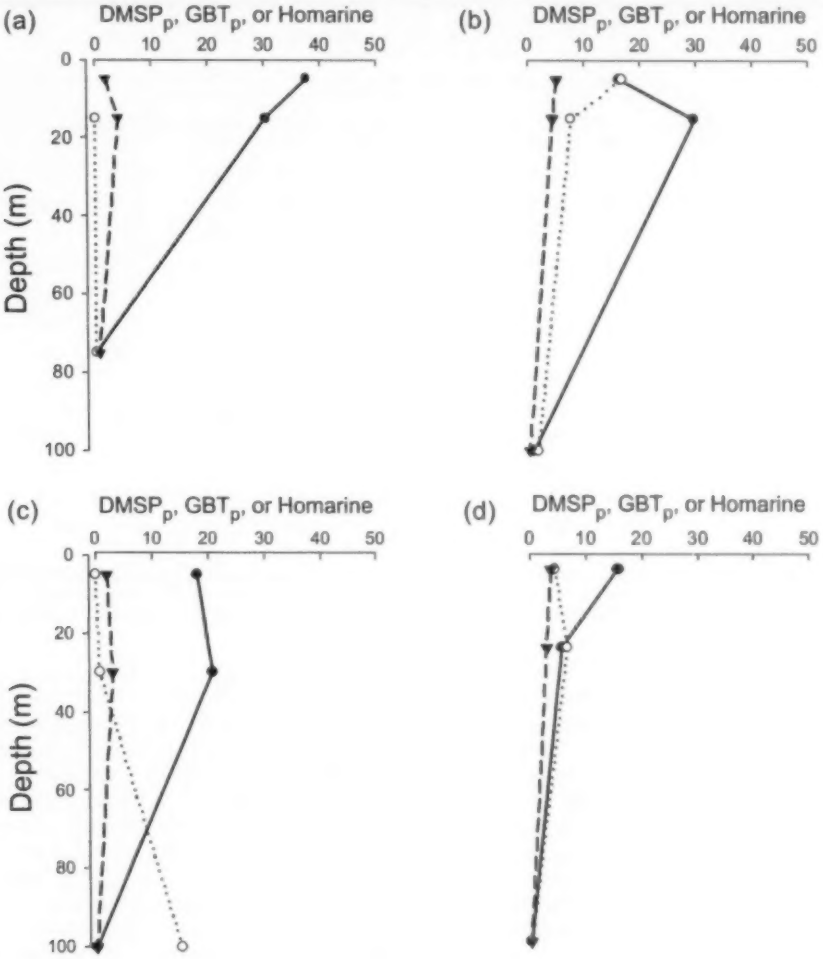

Incubation experiments

In incubation 1, combined levels of nitrate and ammonia were 0.6 µmol·L^{-1} and initial Chl levels were low (0.41 µg·L^{-1}) (Table 1). The initial C:N and C:Chl ratios were both high and suggest N stress (Goldman 1980). The deepwater addition contained 3.0 µmol nitrate·L^{-1}, which was less than the nitrate addition treatment (10.0 µmol·L^{-1}). In neither case did the populations use much of the added nitrate (<2%) during the incubation. Levels of POC and amino acids remained stationary and low. However, in all treatments, including the controls, the C:N and C:Chl ratios dropped. Furthermore, concentrations of Chl, protein, and POS increased three- to five-fold from T_0 concentrations under all conditions, especially in the nitrate and deep treatments.

$DMSP_p$ levels were twice as high as those of GBT_p at the onset of experiment 1 and increased over 45 h under all treatment conditions (Table 1). No significant differences in $DMSP_p$ concentrations were observed among the different treatments ($p < 0.05$) (Table 1). GBT_p concentrations remained lower than $DMSP_p$ in the control, nitrate, and deepwater additions. In the GBT addition treatment, the GBT_p concentrations increased significantly (two- to four-fold) ($p < 0.01$), up to 32 nmol·L^{-1} at 45 h, and approached the concentrations of $DMSP_p$, suggesting uptake of the added substrate (Table 1). After 45 h of incubation, GBT_p concentrations were two- to five-fold higher in the nitrate treatment (5.1 nmol·L^{-1}) than in the control (1.1 nmol·L^{-1}) or deep treatment (2.0 nmol·L^{-1}). Homarine increased, but not significantly ($p > 0.05$), in all treatments except for the deepwater addition and remained lower than GBT_p (Table 1). There were no significant differences in DMS over time and between treatments ($p < 0.05$) (Table 1). $DMSP_d$ levels doubled in the nitrate addition treatment with respect to the control in the first 12 h but declined by a factor of 5 after 24 h in both treatments (Table 1). On the other hand, $DMSP_d$ remained stationary in the GBT and deep treatments.

During incubation 2, combined levels of nitrate and ammonia were approximately 1 µmol·L^{-1} and initial Chl levels

© 2004 NRC Canada

Table 1. Time course of changes in organic pools of DMS, DMSP, GBT, homarine, POC, POS, protein, and amino acids, as well as concentrations of Chl, DIN, and various cellular ratios at incubation station 1 in response to N additions or addition of deep water (collected at 75 m).

	Treatment and time									
	Control (no addition)			+ 10 μmol $NO_3 \cdot L^{-1}$		+ 10 μmol GBT·L^{-1}		+ deep water		
Compound	T_0	T_{24}	T_{45}	T_{24}	T_{45}	T_{24}	T_{45}	T_0	T_{24}	T_{45}
DMS (nmol·L^{-1})	0.9	1.3	1.5	1.5	1.1	1.2	1.1	0.4	0.9	0.8
$DMSP_d$ (nmol·L^{-1})	13.9	7.0	2.9	4.1	2.9	15.6	12.8	9.2	2.4	11.8
$DMSP_p$ (nmol·L^{-1})	14.0	22.8	40.1	34.6	45.8	24.3	33.9	15.6	35.4	40.9
GBT_p (nmol·L^{-1})	7.4	3.3	<2.0	2.1	5.6	16.1	32.0	4.1	2.4	<2.0
Particulate homarine (nmol·L^{-1})	1.0	1.0	1.6	1.2	1.9	0.7	1.0	0.8	0.9	2.5
Chl (μg·L^{-1})	0.4	1.0	1.3	1.0	1.8	0.9	1.1	0.4	1.2	2.1
DIN-NO_3 (μmol·L^{-1})	0.2	0.1	0.03	10.6	11.2	0.1	0.1	3.0	3.1	3.5
DIN-NH_4 (μmol·L^{-1})	0.4	0.3	0.2	0.4	0.2	0.7	0.9	1.4	1.0	0.8
POS (μg·L^{-1})	0.5	0.6	0.6	0.2	1.0	0.6	0.8	0.5	0.6	1.6
Protein (μg·L^{-1})	69.2	69.6	105.4	80.6	103.8	76.0	85.6	61.2	84.6	140.1
Amino acids (μg·L^{-1})	0.1	0.03	0.04	0.01	0.1	0.01	0.1	0.03	0.2	0.2
POC (mg·L^{-1})	0.2	0.2	0.2	0.1	0.2	0.2	0.2	0.1	0.2	0.2
C:N	9.7	6.6	6.4	6.3	6.0	6.8	7.4	8.2	7.1	5.9
C:Chl	397	149	148	133	115	160	196	347	151	105
DMSP:Chl	35	23	31	35	26	32	31	41	29	19

Note: $DMSP_p$, GBT_p, and particulate homarine all represent intracellular levels of these compounds. The T_0 concentrations are the same for the control and first two treatments and are representative of levels at 5 m; the T_0 concentrations for the deep treatment are representative of levels at 75 m.

were 1.1 μg·L^{-1} (Table 2). The initial C:N and C:Chl ratios from surface samples were both low and suggest that the population was not N stressed. The deepwater addition contained 5.6 μmol nitrate·L^{-1}, although not as much as the nitrate addition (10.0 μmol·L^{-1}) treatment. In both cases, and unlike incubation 1, the populations used 14% and 88% of the nitrate in the nitrate and deepwater additions, respectively, during incubation. This was reflected in the C:N ratio, which did not change over 45 h in the nitrate treatment, while it decreased by almost half in the deep treatment. The C:Chl ratios also decreased 27–47% in the nitrate and deep treatments. On the other hand, concentrations of Chl, protein, and POS increased in all treatments, with Chl and POS tripling in the nitrate and deep treatments and protein doubling in the deep treatment only. Levels of amino acids and POC remained stationary and low (Table 2).

During incubation 2, $DMSP_p$ levels were comparable with those of GBT_p, showed short-term variability, and again increased steadily over 45 h under all conditions (Fig. 3). During this incubation, GBT_p levels were also very variable in the short term but increased in the nitrate and deep treatments (Table 2). The GBT treatment caused a fivefold increase in GBT_p up to 54.9 nmol·L^{-1} (Table 2), suggesting uptake of the added substrate. Homarine increased in all treatments, most notably in the nitrate and deepwater treatments, but remained lower than GBT_p in all cases (Table 2). There were no significant changes ($p > 0.05$) in DMS over time and between treatments, except for a doubling in the GBT treatment (Table 2). $DMSP_d$ levels were twice as high in the nitrate addition treatment as in the control after 12 h but declined over 45 h in all treatments (Table 2).

Incubation 3 showed low initial nutrient (0.6 μmol·L^{-1}) and Chl levels (0.2 μg·L^{-1}), similar to those observed in incubation 1 (Table 3). Again, the initial C:N and C:Chl ratios from surface samples were higher and suggestive of N stress. The added nitrate appeared to be unutilized over 45 h, while the populations in the deep treatment (5.7 μmol nitrate·L^{-1}) used 60% of the N present. This apparent lack of activity was also reflected by the DMSP and GBT pools, which remained constant during the 2-day incubation (Fig. 3). GBT_p was undetectable (<2 nmol·L^{-1}) in the control and nitrate treatments but was 3.9 nmol·L^{-1} in the deepwater treatment after 45 h. In the GBT treatment, GBT_p was 20-fold higher (40 nmol·L^{-1}) in the 24-h sample and declined sharply to 21 nmol·L^{-1} by 45 h, still 10-fold higher than at T_0 (Table 3). DMS levels remained lower in the control than in the nitrate addition samples and unchanged in the other treatments (Table 3). After 45 h, $DMSP_d$ levels were higher in the nitrate and deep treatments than in the control and GBT treatments. Other indicators of phytoplankton biomass and physiology remained stationary, with short-term variability observed in some but with no consistent pattern (Table 3).

Incubation 4 was the only one in which GBT_p levels increased significantly ($p < 0.05$) in the nitrate addition (Fig. 3), but transient increases were seen in the control (Fig. 3) and deep treatments as well (Table 4). Highest GBT_p concentrations were observed at 24 h in all treatments, dropping to initial levels in the 45-h samples in all but the GBT enrichment where it continued to increase (Table 4). Homarine remained within a narrow range (1.3–2 nmol·L^{-1}) in all treatments (Table 4). $DMSP_p$ concentrations were low and remained unchanged in all treatments over 45 h (Table 4).

© 2004 NRC Canada

Table 2. Time course of changes in organic pools of DMS, DMSP, GBT, homarine, POC, POS, protein, and amino acids, as well as concentrations of Chl, DIN, and various cellular ratios at incubation station 2 in response to N additions or addition of deep water (collected at 100 m).

	Treatment and time									
	Control (no addition)			+ 10 μmol $NO_3 \cdot L^{-1}$		+ 10 μmol $GBT \cdot L^{-1}$		+ deep water		
Compound	T_0	T_{24}	T_{45}	T_{24}	T_{45}	T_{24}	T_{45}	T_0	T_{24}	T_{45}
DMS ($nmol \cdot L^{-1}$)	1.3	2.0	1.4	2.3	1.9	2.5	2.5	0.4	0.9	0.9
$DMSP_d$ ($nmol \cdot L^{-1}$)	10.0	2.7	2.2	5.2	2.2	8.9	7.1	9.5	1.8	0.8
$DMSP_p$ ($nmol \cdot L^{-1}$)	21.3	22.1	35.1	20.8	32.6	26.5	31.7	19.2	21.7	39.4
GBT_p ($nmol \cdot L^{-1}$)	11.4	11.1	6.5	10.6	13.3	29.4	54.9	14.0	4.0	20.0
Particulate homarine ($nmol \cdot L^{-1}$)	1.8	2.7	2.9	2.8	4.5	1.6	2.4	1.8	3.9	4.2
Chl ($\mu g \cdot L^{-1}$)	1.1	1.5	1.7	1.8	3.4	1.6	2.0	1.0	1.1	3.0
DIN-NO_3 ($\mu mol \cdot L^{-1}$)	0.3	0.1	0.02	10.0	7.9	0.1	0.1	5.6	4.5	0.03
DIN-NH_4 ($\mu mol \cdot L^{-1}$)	0.6	0.2	0.1	0.6	0.7	0.2	0.8	0.2	0.2	0.6
POS ($\mu g \cdot L^{-1}$)	0.4	1.0	0.9	0.8	1.3	1.1	2.0	0.9	0.9	2.1
Protein ($\mu g \cdot L^{-1}$)	103.5	141.2	159.8	158.7	156.9	151.8	198.2	83.8	190.2	252.8
Amino acids ($\mu g \cdot L^{-1}$)	0.1	0.01	0.1	0.02	0.1	0.02	0.03	0.1	0.01	0.1
POC ($mg \cdot L^{-1}$)	0.2	0.3	0.3	0.2	0.3	0.2	0.3	0.2	0.2	0.5
C:N	6.9	6.5	6.7	5.6	5.6	5.7	5.2	8.1	5.8	4.8
C:Chl	183	170	187	108	86	140	173	241	120	176
DMSP:Chl	20	16	21	12	10	17	16	19	24	14

Note: $DMSP_p$, GBT_p, and particulate homarine all represent intracellular levels of these compounds. The T_0 concentrations are the same for the control and first two treatments and are representative of levels at 5 m; the T_0 concentrations for the deep treatment are representative of levels at 100 m.

DMS and $DMSP_d$ levels were very low and showed no significant differences over time or between treatments ($p > 0.05$) (Table 4). This incubation had combined levels of nitrate and ammonia of less than 1 $\mu mol \cdot L^{-1}$ and low initial Chl levels (0.4 $\mu g \cdot L^{-1}$) (Table 4). The initial C:N and C:Chl ratios from surface samples were intermediate to the levels observed at the previous stations. In neither the nitrate addition (10.0 $\mu mol \cdot L^{-1}$) nor the deepwater (6.8 $\mu mol \cdot L^{-1}$) treatments did the populations use more than 8% of the added nitrate during the incubation. This was reflected in an unchanging C:N ratio in the control, nitrate, and deep treatments, while in the GBT treatment, it decreased by a third. The C:Chl ratios dropped in the control, nitrate, and deep treatments but increased in the GBT treatments. Concentrations of Chl, protein, and POS increased in all of the treatments, with the protein and POS levels increasing fourfold in the GBT treatments. Levels of amino acids and POC remained stationary and low (Table 4).

Changes in phytoplankton species composition were also evaluated (Tables 5–8). In broad terms, incubations 1 and 2 were initially dominated by or had diatoms, whereas incubations 3 and 4 had no diatoms early on and the population was dominated by dinoflagellates. During incubation 1, over 45 h, the phytoplankton assemblage increased significantly (20-fold in cell number) in the control, especially the numbers of the dinoflagellate *Katodinium rotundatum* (Table 5). In addition, there was a clear increase in the photosynthetic flagellate group and the heterotrophic population, especially in the deep treatment. However, in the nitrate addition, the diatoms and flagellates actually decreased, whereas the dinoflagellates doubled in number. In incubation 2, the population was dominated initially by dinoflagellates and cryptomonads, with diatoms being less abundant. At the end of the time course in all treatments, there had been a population shift to an increase in the proportion of diatoms and euglenids (Table 6).

In contrast with the previously described incubations, at incubation station 3, diatoms and cryptomonads were initially absent, whereas photosynthetic dinoflagellates were clearly dominant (Table 7). This remained the case in the controls but not in the other three treatments, in which diatoms became important with no changes in other taxa. Again, during incubation 4, diatoms were not observed, and dinoflagellates and cryptomonads were the dominant forms (Table 8). Both of these categories continued to increase in the controls, as well as in the nitrate and GBT addition samples.

Discussion

There is some evidence in the literature that an inverse relationship exists in phytoplankton between DMSP and N availability (Andreae 1986; Turner et al. 1988; Gröne and Kirst 1992). It also appears that some phytoplankton will preferentially synthesize the N analog of DMSP, GBT, when N is available (Keller et al. 1999*a*, 1999*b*). Thus, when N is limiting to phytoplankton, i.e., during the summer months in temperate waters, DMSP may be higher intracellularly than when N is abundant. This idea has been explored previously by comparing the distributions of DMSP versus dissolved inorganic N pools (Turner et al. 1988; Leck et al. 1990; Townsend and Keller 1996). No correlation between DMS or DMSP and external N levels has been found, although this is not surprising, as it is well established that external

© 2004 NRC Canada

Fig. 3. Variations in (*a*, *c*, and *e*) $DMSP_p$ and (*b*, *d*, and *f*) GBT concentrations during incubations 1, 2, and 4 in response to a nitrate addition (10 μmol·L^{-1} at T_0) (◇). Control (◆) = no addition. Net production of DMSP or GBT corresponds to the difference between the slopes of the treatment and control lines across time.

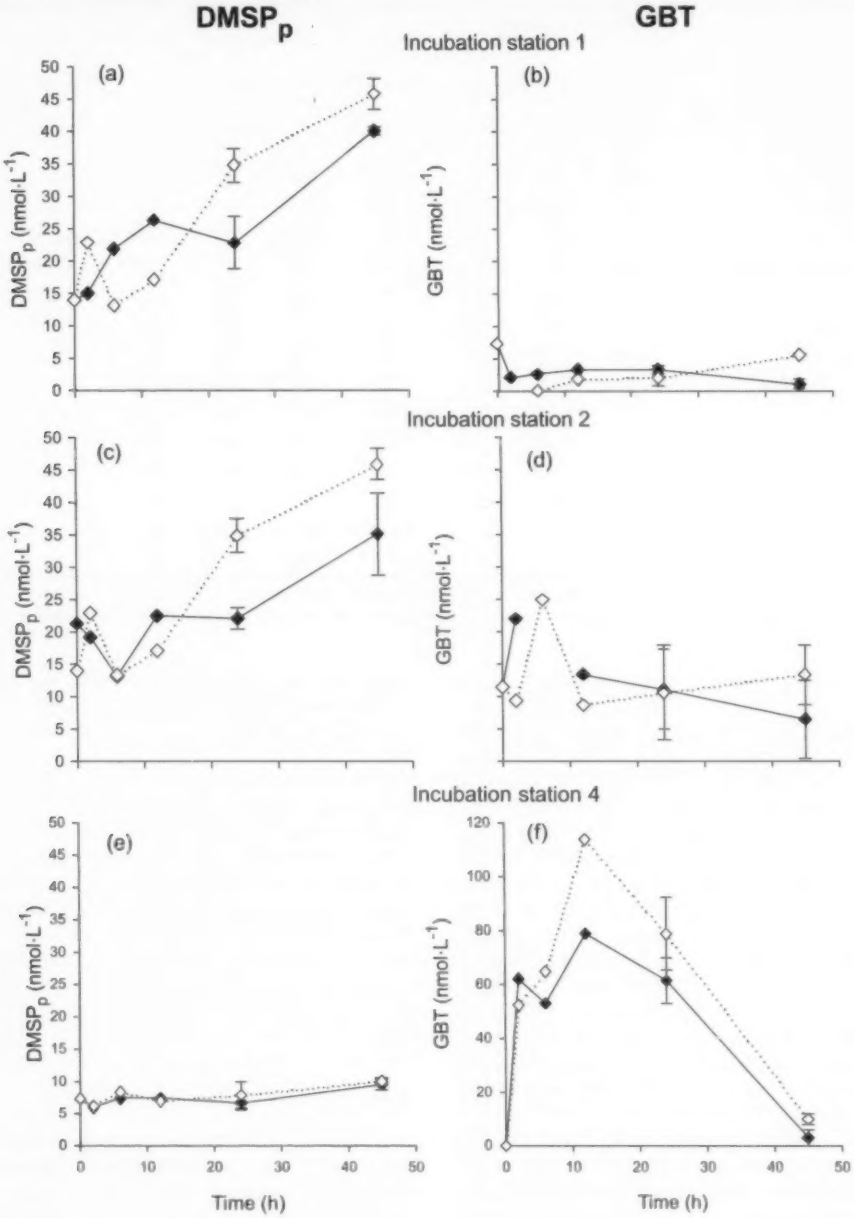

nutrient levels are not reliable indicators of intracellular nutrient physiology (Cullen et al. 1992). A relationship may exist between intracellular DMSP and N, a concept that has been explored in laboratory cultures (e.g., Keller et al. 1999*a*, 1999*b*) but never, to our knowledge, in the field. We hypothesized that if a relationship between DMSP, GBT, and N availability exists, then intracellular levels of DMSP should drop when N is incorporated into the cells. We further hypothesized that increased N availability might result in a release of $DMSP_d$ or DMS_d. At the same time, intracellular levels of GBT or other nitrogenous compounds would increase.

Based on our observations of external nutrients, biomass, and biochemical indicators of cellular nutrient status, there appeared to be a range of conditions, from N limitation to N repletion, at the incubation stations. However, the net production (i.e., the difference between treatment and control across time) of $DMSP_p$ and GBT was not statistically differ-

© 2004 NRC Canada

Table 3. Time course of changes in organic pools of DMS, DMSP, GBT homarine, POC, POS, protein, and amino acids, as well as concentrations of Chl, DIN, and various cellular ratios at incubation station 3 in response to N additions or addition of deep water (collected at 100 m).

	Treatment and time									
	Control (no addition)			+ 10 μmol $NO_3 \cdot L^{-1}$		+ 10 μmol $GBT \cdot L^{-1}$		+ deep water		
Compound	T_0	T_{24}	T_{45}	T_{24}	T_{45}	T_{24}	T_{45}	T_0	T_{24}	T_{45}
DMS ($nmol \cdot L^{-1}$)	1.4	1.6	1.6	2.8	3.1	1.5	2.4	0.2	0.2	0.8
$DMSP_d$ ($nmol \cdot L^{-1}$)	3.8	2.8	2.7	3.4	5.9	3.4	2.1	2.0	3.6	3.8
$DMSP_p$ ($nmol \cdot L^{-1}$)	19.7	17.0	17.8	18.4	18.4	14.9	20.4	20.5	13.2	20.0
GBT_p ($nmol \cdot L^{-1}$)	<2.0	<2.0	<2.0	nd	<2.0	40.0	21.0	3.9	nd	3.1
Particulate homarine ($nmol \cdot L^{-1}$)	0.7	1.2	1.1	1.4	2.1	0.8	1.4	0.7	1.4	2.4
Chl ($\mu g \cdot L^{-1}$)	0.2	0.5	0.3	0.5	0.9	0.5	0.7	0.2	0.5	0.9
DIN-NO_3 ($\mu mol \cdot L^{-1}$)	0.1	0.03	0.03	11.0	11.2	0.1	0.1	5.7	4.8	2.2
DIN-NH_4 ($\mu mol \cdot L^{-1}$)	0.3	0.1	0.0	0.7	0.3	5.0	5.2	1.7	0.3	0.2
POS ($\mu g \cdot L^{-1}$)	0.1	0.1	0.2	0.2	1.0	1.7	2.1	0.7	0.9	1.4
Protein ($\mu g \cdot L^{-1}$)	67.7	65.2	68.8	71.4	58.6	217.9	225.6	44.4	100.3	166.4
Amino acids ($\mu g \cdot L^{-1}$)	0.03	0.1	0.1	0.1	0.1	0.1	0.1	0.1	0.1	0.1
POC ($mg \cdot L^{-1}$)	0.1	0.1	0.2	0.1	0.2	0.3	0.3	0.1	0.1	0.3
C:N	7.2	6.1	7.2	5.4	6.3	4.0	4.3	7.4	5.0	5.1
C:Chl	580	228	474	187	172	690	451	652	313	322
DMSP:Chl	106	38	57	35	21	33	28	118	30	23

Note: $DMSP_p$, GBT_p, and particulate homarine all represent intracellular levels of these compounds. The T_0 concentrations are the same for the control and first two treatments and are representative of levels at 5 m; the T_0 concentrations for the deep treatment are representative of levels at 100 m. nd, no data.

Table 4. Time course of changes in organic pools of DMS, DMSP, GBT, homarine, POC, POS, protein, and amino acids, as well as concentrations of Chl, DIN, and various cellular ratios at incubation station 4 in response to N additions or addition of deep water (collected at 100 m).

	Treatment and time									
	Control (no addition)			+ 10 μmol $NO_3 \cdot L^{-1}$		+ 10 μmol $GBT \cdot L^{-1}$		+ deep water		
Compound	T_0	T_{24}	T_{45}	T_{24}	T_{45}	T_{24}	T_{45}	T_0	T_{24}	T_{45}
DMS ($nmol \cdot L^{-1}$)	1.1	1.3	1.5	1.3	1.2	1.3	1.5	0.5	0.8	0.6
$DMSP_d$ ($nmol \cdot L^{-1}$)	2.2	5.1	1.9	2.4	1.5	3.1	1.5	1.5	1.1	1.0
$DMSP_p$ ($nmol \cdot L^{-1}$)	8.4	8.7	9.6	7.9	10.0	8.0	7.9	5.7	8.4	11.4
GBT_p ($nmol \cdot L^{-1}$)	<2.0	61.3	3.0	62.8	9.9	53.9	74.7	<2.0	23.0	<2.0
Particulate homarine ($nmol \cdot L^{-1}$)	1.7	2.0	2.0	1.6	1.7	1.3	1.5	1.7	1.4	1.2
Chl ($\mu g \cdot L^{-1}$)	0.4	0.5	1.0	0.6	0.9	0.5	0.8	0.4	0.5	0.9
DIN-NO_3 ($\mu mol \cdot L^{-1}$)	0.1	0.1	0.1	10.9	11.2	0.1	0.1	6.8	6.6	6.5
DIN-NH_4 ($\mu mol \cdot L^{-1}$)	0.8	0.7	0.4	0.7	0.1	0.6	4.8	0.3	0.02	0.04
POS ($\mu g \cdot L^{-1}$)	0.7	0.9	1.0	0.7	0.8	0.8	2.8	0.7	0.3	1.1
Protein ($\mu g \cdot L^{-1}$)	65.6	71.8	113.0	135.7	67.0	90.4	256.6	42.9	87.1	85.3
Amino acids ($\mu g \cdot L^{-1}$)	0.1	0.01	0.01	0.1	0.03	0.02	0.01	0.1	0.04	0.02
POC ($mg \cdot L^{-1}$)	0.1	0.2	0.2	0.2	0.2	0.2	0.4	0.1	0.2	0.2
C:N	6.2	6.7	6.1	6.7	6.2	6.9	4.2	6.5	6.4	5.9
C:Chl	341	321	168	247	190	351	441	361	273	186
DMSP:Chl	20	13	10	14	11	16	10	16	16	13

Note: $DMSP_p$, GBT_p, and particulate homarine all represent intracellular levels of these compounds. The T_0 concentrations are the same for the control and first two treatments and are representative of levels at 5 m; the T_0 concentrations for the deep treatment are representative of levels at 100 m.

© 2004 NRC Canada

Table 5. Changes in phytoplankton species composition over time in different treatments at incubation station 1.

	Treatment and time					
	Control (no addition)		+ 10 μmol $NO_3 \cdot L^{-1}$	+ 10 μmol GBT·L^{-1}	+ deep water	
Cell type	T_0	T_{45}	T_{45}	T_{45}	T_0	T_{45}
Diatoms						
Centric[a]	2.6×10^3	4.4×10^4	9.7×10^2	4.0×10^1	4.0×10^1	5.0×10^2
Pennate[b]	1.5×10^3	4.4×10^4	1.7×10^3	8.2×10^2	2.0×10^1	3.5×10^3
Dinoflagellates						
Photosynthetic[c]	2.8×10^3	5.6×10^4	6.8×10^3	3.7×10^3	2.0×10^1	1.4×10^4
Heterotrophic[d]	3.0×10^2	3.0×10^1	4.0×10^1	6.0×10^1	1.8×10^2	0
Cryptomonads	8.9×10^3	7.5×10^4	1.3×10^4	1.8×10^3	1.7×10^3	2.1×10^4
Euglenids	2.2×10^2	5.2×10^3	4.0×10^1	2.0×10^1	1.8×10^2	0
Plastidic flagellates[e]	1.4×10^2	4.1×10^3	5.2×10^1	1.6×10^2	2.3×10^3	1.7×10^4
Ciliates[f]	4.8×10^2	1.7×10^3	5.0×10^1	4.0×10^2	2.4×10^2	4.0×10^2
Silicoflagellates	4.2×10^2	8.1×10^2	2.0×10^3	1.0×10^2	1.6×10^2	3.0×10^2
Aplastidic flagellates[g]	5.6×10^2	2.3×10^3	1.6×10^3	8.4×10^3	1.6×10^2	1.0×10^3

Note: The T_0 concentrations are the same for the control and first two treatments and are representative of cell numbers at 5 m; the T_0 concentrations for the deep treatment are representative of cell numbers at 75 m. Values are in cells·L^{-1}.

[a]Dominated by *Chaetoceros* spp. and *Thalassiosira* spp.

[b]Dominated by *Navicula* spp., *Cylindrotheca* spp., and *Nitzchia* spp.

[c]Dominated by *Gymnodinium* spp. at T_0; dominated by *Katodinium* spp. and *Gymnodinium* spp. at T_{45}.

[d]Dominated by *Gyrodinium* spp.

[e]Photosynthetic flagellates of diverse taxonomy (5–10 μm in size).

[f]Dominated by tintinnids.

[g]Heterotrophic flagellates of diverse taxonomy (5–10 μm in size).

Table 6. Changes in phytoplankton species composition over time in different treatments at incubation station 2.

	Treatment and time					
	Control (no addition)		+ 10 μmol $NO_3 \cdot L^{-1}$	+ 10 μmol GBT·L^{-1}	+ deep water	
Cell type	T_0	T_{44}	T_{44}	T_{44}	T_0	T_{44}
Diatoms						
Centric[a]	1.2×10^2	8.3×10^3	4.2×10^4	1.8×10^3	1.2×10^2	2.4×10^4
Pennate[b]	5.6×10^2	0	0	6.6×10^1	5.6×10^2	0
Dinoflagellates						
Photosynthetic[c]	1.9×10^4	7.7×10^3	1.0×10^4	1.2×10^4	1.6×10^4	1.5×10^4
Heterotrophic[d]	2.8×10^2	0	4.9×10^2	6.6×10^1	2.8×10^2	3.2×10^2
Cryptomonads	9.0×10^3	1.0×10^4	1.7×10^4	3.1×10^3	9.0×10^3	1.5×10^4
Euglenids	0	1.67×10^3	2.16×10^3	1.9×10^3	0	2.0×10^3
Ciliates[e]	8.1×10^1	2.1×10^3	2.1×10^3	5.3×10^2	8.1×10^1	2.2×10^3
Silicoflagellates	2.8×10^2	4.9×10^2	7.9×10^2	9.8×10^2	2.8×10^2	7.9×10^2
Aplastidic flagellates[f]	7.6×10^3	2.0×10^2	4.9×10^2	1.1×10^3	7.6×10^3	1.9×10^3

Note: The T_0 concentrations are the same for the control and first two treatments and are representative of cell numbers at 5 m; the T_0 concentrations for the deep treatment are representative of cell numbers at 100 m. Values are in cells·L^{-1}.

[a]Dominated by *Eucampia* spp., *Chaetoceros* spp., and *Thalassiosira* spp.

[b]Dominated by *Cylindrotheca* spp. and *Nitzchia* spp.

[c]Dominated by *Heterocapsa* spp., *Scrippsiella* spp., *Amphidinium* spp., and *Prorocentrum minimum*.

[d]Dominated by *Gyrodinium* spp.

[e]Dominated by *Mesodinium rubrum*.

[f]Heterotrophic flagellates of diverse taxonomy (5–10 μm in size).

ent from zero (two-tailed t test, t_{sDMSP} = 0.24–0.82, t_{sGBT} = 0.21–0.42, df = 7, ns, $p < 0.05$) in any of the four sites sampled, regardless of apparent N stress, when either nitrate or deep water with nitrate was added. No significant effect of nutrient addition (+ nitrate or deep water) with respect to the control was seen when all four sites were grouped (ANOVA, $p < 0.05$).

The incubations (experiments and treatments) showed unique trends at each site. Although dissolved inorganic N (DIN) levels were depleted at incubation stations 1 and 3 (approximately 0.5 μmol·L^{-1}) and were twice as high at incubation stations 2 and 4 (approximately 1 μmol·L^{-1}), the uptake of added N and intracellular responses to N supply were quite different. Three responses can be seen in Fig. 3. Nitro-

© 2004 NRC Canada

Table 7. Changes in phytoplankton species composition over time in different treatments at incubation station 3.

	Treatment and time					
	Control (no addition)		+ 10 μmol $NO_3 \cdot L^{-1}$	+ 10 μmol GBT·L^{-1}	+ deep water	
Cell type	T_0	T_{45}	T_{45}	T_{45}	T_0	T_{45}
Diatoms						
Centric	0	6.0×10^1	1.9×10^3	3.6×10^2	3.9×10^2	1.2×10^3
Pennate	0	0	4.0×10^1	3.3×10^3	0	1.0×10^1
Dinoflagellates						
Photosynthetic[a]	3.0×10^3	5.8×10^2	2.1×10^3	4.6×10^3	4.4×10^3	2.1×10^3
Heterotrophic[b]	1.2×10^2	2.0×10^1	0	2.0×10^2	2.6×10^2	6.0×10^1
Cryptomonads	0	2.3×10^2	2.3×10^3	1.7×10^3	3.3×10^3	2.6×10^3
Plastidic flagellates[c]	0	4.9×10^2	1.9×10^2	8.3×10^3	0	0
Ciliates	8.0×10^1	2.7×10^2	6.1×10^2	4.4×10^2	5.5×10^2	7.9×10^2
Silicoflagellates	0	0	2.4×10^2	1.6×102	6.6×10^2	3.3×10^2
Aplastidic flagellates[d]	1.2×10^2	0	1.4×10^2	3.5×10^3	3.9×10^2	8.9×10^2

Note: The T_0 concentrations are the same for the control and first two treatments and are representative of cell numbers at 5 m; the T_0 concentrations for the deep treatment are representative of cell numbers at 100 m. Values are in cells·L^{-1}.

[a]Dominated by *Gymnodinium* spp.

[b]Dominated by *Dinophysis* spp. and *Gyrodinium* spp.

[c]Photosynthetic flagellates of diverse taxonomy (5–10 μm in size).

[d]Heterotrophic flagellates of diverse taxonomy (5–10 μm in size).

Table 8. Changes in phytoplankton species composition over time in different treatments at incubation station 4.

	Treatment and time					
	Control (no addition)		+ 10 μmol $NO_3 \cdot L^{-1}$	+ 10 μmol GBT·L^{-1}	+ deep water	
Cell type	T_0	T_{45}	T_{45}	T_{45}	T_0	T_{45}
Diatoms						
Centric	0	0	0	2.0×10^2	0	2.0×10^1
Pennate	0	0	0	6.6×10^1	1.3×10^2	0
Dinoflagellates						
Photosynthetic[a]	1.3×10^3	8.6×10^3	5.6×10^3	1.1×10^4	5.1×10^3	5.4×10^3
Heterotrophic[b]	4.0×10^1	2.0×10^2	1.6×10^2	1.3×10^2	0	2.0×10^1
Cryptomonads	1.2×10^3	2.6×10^3	3.3×10^3	2.8×10^3	2.8×10^3	1.7×10^3
Ciliates[c]	4.4×10^2	2.7×10^3	3.1×10^3	1.8×10^3	1.7×10^3	1.7×10^3
Silicoflagellates	0	3.9×10^2	3.9×10^2	5.2×10^2	2.6×10^2	1.0×10^2
Aplastidic flagellates[d]	3.2×10^2	3.5×10^3	3.5×10^3	1.8×10^3	2.0×10^3	2.5×10^3

Note: The T_0 concentrations are the same for the control and first two treatments and are representative of cell numbers at 5 m; the T_0 concentrations for the deep treatment are representative of cell numbers at 100 m. Values are in cells·L^{-1}.

[a]Dominated by *Heterocapsa* spp.

[b]Dominated by *Oxyphysis* spp.

[c]Dominated by *M. rubrum*.

[d]Heterotrophic flagellates of diverse taxonomy (5–10 μm in size).

gen stress, as indicated by initially low DIN and high C:N and C:Chl ratios, may have led to the two- to six-fold higher $DMSP_p$ than GBT_p concentrations observed in incubation 1. The addition of nitrate led to $DMSP_p$ increases, without concomitant GBT_p changes. However, it should be noted that this response was also seen in the control, which when taken jointly with a drop in the C:N and C:Chl ratios in all treatments suggests that something other than N limitation may have been a controlling factor in this population. An addition of N to the similarly N-stressed samples during incubation 3 resulted in net $DMSP_p$ and GBT_p levels remaining unchanged in a pattern much like the response seen in incubation 4.

A lack of N stress, as indicated in incubation 2 by low initial C:N and C:Chl ratios, resulted in a decrease in the C:N ratio in all the treatments except the controls, suggesting further N uptake (also shown by decreased DIN levels) and assimilation. Here, the pools of $DMSP_p$ and GBT_p were of similar magnitude (6–20 nmol·L^{-1}). This pattern contrasts with that in experiments 1 and 3 where, as indicated above, GBT_p concentrations were low or undetectable when starting DIN levels were low.

An intermediate scenario of moderate N stress resulted in the highest increase of GBT_p upon nitrate addition (two orders of magnitude), as seen in incubation 4. In accord with the added nitrate being virtually untouched in this experiment, C:N ratios remained stationary in all but the GBT treatment, where it declined. The C:Chl ratios in this treatment increased, however, suggesting that there was an in-

© 2004 NRC Canada

crease in something other than phytoplankton C. It should be noted that $DMSP_p$ remained invariant in all treatments, except the deepwater addition where it doubled. During five coastal cruises from early spring to summer in Dabob Bay, Washington, Dortch et al. (1985) observed that populations never became extremely N deficient, as indicated by high amino acid to protein ratios, even though nitrate and ammonium became depleted in surface waters. They speculated that the resupply of N to these populations was either frequent or recent. The response of a population to a nutrient addition may be more a reflection of the time scale of the nutrient supply rather than any real limitation. If the nutrient has been supplied recently, there may be no response; if it was supplied distantly, the response may be strong. Neither response indicates nutrient deficiency or sufficiency per se (Harris 1986). Cells are rarely in balanced growth in situ because of frequent changes in nutrient supply and light regimes among other factors (Eppley 1981). The cells themselves are inherently unbalanced, as the synthesis of individual cellular components occurs at discrete intervals over the growth cycle. The addition of a limiting nutrient may result in a depression of the uptake of other elements as cells shift their energy to the assimilation of the depleted nutrient. In addition, within an algal cell, the major pathways of nutrient metabolism are interconnected, as C, N, P, and S are required for biosynthesis and as a source of energy (Harris 1986). Co-limitation can be a problem and if incubations are not long enough, the eventual positive response to a nutrient addition may not be observed. Likewise, if the incubations are too long, there are all of the problems associated with container effects and other loss processes: respiration, cells lysis, grazing, etc. The length of our incubations (45 h) was chosen to enhance the former while minimizing the latter.

There were population shifts among the various locations and treatments, nonetheless. All of the samples were prefiltered through a 100-μm screen before the incubations began, and thus, metazooplankton and the larger microzooplankton were removed. This fractionation, coupled with the 50% dilution with 0.2-μm-filtered water, undoubtedly resulted in a significant relaxation of grazing pressure. During incubation 1, this effect appears to have been especially important, as even in the controls, phytoplankton biomass, particularly dinoflagellates, increased. Many authors have demonstrated that dinoflagellates are selectively grazed by microzooplankton and smaller copepods (e.g., Stoecker et al. 1986; Gifford and Dagg 1988). Diatoms increased especially in the nitrate and deep enrichments at incubation stations 2 and 3. The deepwater enrichments in particular appeared to have a stimulatory effect at these locations. It is entirely possible that other growth factors besides nitrate were present in the deep waters, including trace metals such as iron or chelators. Diatoms in particular are known to be responsive to iron additions (e.g., Coale 1991).

Particulate, cell-associated levels of GBT and homarine, another nitrogenous osmolyte, exhibited significant increases (4- to 35-fold) ($p < 0.05$) in all of the GBT enrichment carboys, higher than observed in the other treatments. It is likely that these increases were due to active uptake of the GBT from solution rather than the synthesis of GBT, as appears to be the case in the nitrate and deepwater enrichments. Active uptake of GBT by marine phytoplankton (Hoffmann 1996; Keller et al. 1999*a*, 1999*b*) and bacterioplankton (Kiene and Hoffmann Williams 1998) has been observed previously. Although GBT appears to be readily assimilated into the cells, it does not appear to be an effective N source for phytoplankton metabolism. In experiments 2 and 3, Chl levels increased least in the controls and GBT treatments. The exception to this was experiment 4, where biomass increase was greatest in the GBT treatments. GBT may have been used as a general N source in this population. During incubations 3 and 4, there was also a large increase (6- to 16-fold) in the DIN ammonium pool in the GBT enrichments. GBT is a precursor of the methylamines (King 1988) and ammonium is a possible by-product of methylamine metabolism.

Both the in situ depth profiles and the incubation experiments showed that there was no consistent reciprocal response in the DMS or DMSP pools to GBT uptake or synthesis and that the net response (nitrate treatment – control) over 24 h was not significantly different from zero, as indicated earlier. Although short-term variability was frequently observed in the first 12 h, $DMSP_p$ increased in all treatments over the course of the incubations, including the controls, which is undoubtedly a reflection of the increase in biomass in all treatments. During incubation 4, despite the high levels of GBT_p, both fractions of DMSP and DMS remained low and stationary in all treatments. In most cases, $DMSP_d$ remained high in the GBT treatments. It is unclear whether DMSP was being released as $DMSP_d$ in these enrichments or if the normal metabolism of $DMSP_d$ had been inhibited. Kiene and Gerard (1995) added GBT (up to 50 $\mu mol \cdot L^{-1}$) to estuarine seawater samples and found that it consistently inhibited bacterial consumption of $DMSP_d$, although its effectiveness diminished after 6–8 h of incubation. In the other enrichments and the controls in the present study, there were sometimes no differences in the levels of $DMSP_d$ or DMS, whereas in some experiments, DMS and $DMSP_d$ levels were elevated in the nitrate and deepwater enrichments. These observations are difficult to attribute to a single cause. In those cases where there was no change in the $DMSP_d$ and DMS pools, there may have been high rates of microbial consumption that kept concentrations in steady state (Kiene and Bates 1990; Kiene and Service 1993).

Work with phytoplankton cultures has shown that intracellular levels of DMSP and GBT do appear to be related to N availability in the short term (Keller et al. 1999*b*). The first 12 h of these field incubations indicated that GBT and homarine were produced when N was introduced to cells, as it was in the diatom *T. pseudonana* grown in continuous culture (Keller et al. 1999*b*). However, over the full term of our 2-day incubation, the GBT and homarine pools showed a variable response. As far as we are aware, ours is the first study to measure homarine in marine particulate matter, although it is known to be produced by some phytoplankton (e.g., *T. subcordiformis*; Dickson and Kirst 1986), soft corals (Slattery et al. 1997), and marine shrimp (Netherton and Gurin 1982). Homarine comprised a lesser pool of organic osmolyte relative to both DMSP and GBT, but in some cases, it was present at levels similar to those of GBT. It is possible that the N additions in the present study affected

© 2004 NRC Canada

not only GBT and homarine but also other N-containing osmolytes that were not measured (e.g., proline). Clearly, further work on the distribution and production of N-containing osmolytes needs to be conducted.

There were no differences in DMSP:Chl ratios among treatments. The DMSP:Chl ratios were quite low and decreased over time in most of the experiments and treatments. If there was a physiological change that resulted in a shift from DMSP to nitrogenous compounds, the Chl-specific DMSP values should have dropped. However, because DMSP production is so dependent on the species composition of the population, species shifts in the populations might mask any physiological shift. In experiment 1, there was a large increase (one to three orders of magnitude) in the autotrophic dinoflagellate population, especially in the control and deep treatments. The dominant species in these increases was *K. rotundatum*, which has been observed to produce large amounts of DMSP (Keller et al. 1989; Townsend and Keller 1996). DMSP:Chl ratios might be expected to increase dramatically in these treatments, but that was not observed. Diatoms and cryptomonads increased especially in the nitrate and deep enrichments in experiment 2 and 3. These classes tend to be minor sources of DMSP unless their biomass is very high (Keller et al. 1989; Keller and Bellows 1996); thus, in these cases, a drop in the DMSP:Chl ratio might be expected. In addition, it has been demonstrated that protozoan grazers can sequester DMSP for considerable periods of time (Belviso et al. 1990; Wolfe et al. 1994) and this can confound the relationship between DMSP and Chl. Microheterotroph populations in the incubation experiments were quite diverse and sometimes abundant. These potentially confounding factors suggest that caution should be applied in the use of DMSP:Chl ratios to describe specific phytoplankton populations. We also did not completely characterize the phytoplankton community, choosing to ignore the picoalgae and smaller nanoalgae in our samples. We have previously determined that picoalgae (<2 μm) are not a significant source of DMSP (Keller et al. 1989; Keller 1991) but acknowledge that the smaller nanoalgae (<5 μm) can be significant producers and may have contributed to the DMSP pool in this study.

To our knowledge, these are the first recorded values of particulate, cell-associated GBT in seawater. GBT was present in surface seawater at concentrations up to 15 nmol·L^{-1}. As such, it represents a previously unaccounted for pool of organic N in coastal seawater. GBT is thought to be a primary source of methylamines in seawater (King 1988; Gibb et al. 1999) and potentially of methane. Phytoplankton and bacterioplankton are readily capable of taking up GBT from solution (Hoffmann 1996; Kiene and Hoffmann Williams 1998). It is not clear whether GBT is metabolized and used as an N source by the phytoplankton or whether it remains intact for use as a compatible solute. There is some evidence to suggest that the latter occurs (Hoffmann 1996), and its accumulation in particulate material after addition of 10 μmol GBT_d·L^{-1} supports this. The role of GBT in algal N metabolism, osmoregulation, and the production of volatile compounds deserves further attention.

The refinement of estimates and prediction of DMS fluxes in the world's oceans remain an elusive goal. An understanding of the physiology of production of its precursor, DMSP, continues to be problematic and new physiological and ecological roles have recently been proposed (Simó 2001). The taxonomic composition of phytoplankton populations remains as one of the best proxies for estimation of DMS concentrations, although the reliability of these predictions is diminished by a host of other factors (e.g., Simó and Dachs 2002). Clearly, the physiology and nutrient status of these populations also play a role. The hypothesis originally suggested by Andreae (1986) that variations in DMSP in phytoplankton may be due to the selective production of GBT when N is available does not appear to be strictly valid at either the physiological or the community level. Our assays, the first of this kind to be performed in the field, were designed to determine the influence of the N status of the algae on their synthesis of DMSP versus N-containing osmolytes and showed that the N status of cells and populations does affect DMSP and DMS dynamics, but in ways not easily resolved.

Acknowledgements

This work was supported by the U.S. National Science Foundation (OCE-9218511 to M.D.K., R.P.K., and P.A.M.). This work was done in partial satisfaction of M.D.K.'s Ph. D. degree at the University of Maine. We acknowledge the invaluable support of the R/V *Cape Hatteras* crew, as well as Brian Yocis and the late Amy Jennings for their help with laboratory and field analyses. We also thank Gordon Wolfe for invaluable discussions on various aspects of this work.

References

Andreae, M.O. 1986. The ocean as a source of atmospheric sulphur compounds. *In* The role of air–sea exchange in geochemical cycling. *Edited by* P. Buat-Merard. Reidel, New York. pp. 331–362.

Andreae, M.O. 1990. Ocean–atmosphere interactions in the global biogeochemical sulfur cycle. Mar. Chem. **30**: 1–29.

Barnard, W.R., Andreae, M.O., Watkins, W.E., Bingemer, H., and Georgii, H.W. 1982. The flux of dimethylsulfide from the oceans to the atmosphere. J. Geophys. Res. **87**: 8787–8793.

Bates, T.S., Lamb, B.K., Guenther, A., Dignon, J., and Stoiber, R.E. 1992. Sulfur emissions to the atmosphere from natural sources. J. Atmos. Chem. **14**: 315–337.

Belviso, S., Kim, S.K., Rassoulzadegan, F., Krajka, B., Nguyen, B.C., Mihalopoulos, N., and Buat-Menard, P. 1990. Production of dimethylsulfonium propionate (DMSP) and dimethyl sulfide (DMS) by a microbial food web. Limnol. Oceanogr. **35**: 1810–1821.

Blunden, G., and Gordon, S.M. 1986. Betaines and their suphonio analogues in marine algae. *In* Progress in phycological research. *Edited by* F. Round and D. Chapman. Biopress Ltd., Bristol. pp. 39–80.

Clayton, J.R., Jr., Dortch, Q., Thoresen, S.S., and Ahmed, S.I. 1988. Evaluation of methods for the separation and analysis of proteins and free amino acids in phytoplankton samples. J. Plankton Res. **10**: 341–358.

Coale, K.H. 1991. Effects of iron, manganese, copper, and zinc enrichments on productivity and biomass in the subarctic Pacific. Limnol. Oceanogr. **36**: 1851–1864.

Cullen, J.J. 1991. Hypotheses to explain high-nutrient conditions in the open sea. Limnol. Oceanogr. **36**: 1578–1599.

© 2004 NRC Canada

Cullen, J.J., Yang, X., and MacIntyre, H.L. 1992. Nutrient limitation of marine photosynthesis. *In* Primary productivity and biogeochemical cycles in the sea. *Edited by* P.G. Falkowski and A.D. Woodhead. Plenum Press, New York.

Dacey, J.W.H., and Wakeham, S.G. 1986. Oceanic dimethylsulfide: production during zooplankton grazing on phytoplankton. Science (Wash., D.C.), **233**: 1314–1316.

Dickson, D.M.J., and Kirst, G.O. 1986. The role of β-dimethylsulfoniopropionate, glycine betaine and homarine in the osmoacclimation of *Platymonas subcordiformis*. Planta, **167**: 536–543.

Dickson, D.M.J., and Kirst, G.O. 1987*a*. Osmotic adjustment in marine eukaryotic algae: the role of inorganic ions, quaternary ammonium, teriary sulphonium and carbohydrate solutes. I. Diatoms and a rhodophyte. New Phytol. **106**: 645–655.

Dickson, D.M.J., and Kirst, G.O. 1987*b*. Osmotic adjustment in marine eukaryotic algae: the role of inorganic ions, quaternary ammonium, teriary sulphonium and carbohydrate solutes. II. Prasinophytes and haptophytes. New Phytol. **106**: 657–666.

Dortch, Q., Clayton, J.R., Jr., Thoresen, S.S., and Ahmed, S.I. 1984. Species differences in accumulation of nitrogen pools in phytoplankton. Mar. Biol. **81**: 237–250.

Dortch, Q., Clayton, J.R., Jr., Thoresen, S.S., Cleveland, J.S., Bressler, S.L., and Ahmed, S.I. 1985. Nitrogen storage and use of biochemical indices to assess nitrogen deficiency and growth rate in natural phytoplankton populations. J. Mar. Res. **43**: 437–464.

Eppley, R.W. 1981. Relations between nutrient assimilation and growth in phytoplankton with a brief review of estimates of growth rate in the ocean. *In* Physiological bases of phytoplankton ecology. *Edited by* T. Platt. Can. Bull. Fish. Aquat. Sci. No. 210. pp. 251–263.

Gibb, S.W., Mantoura, R.F.C., Liss, P.S., and Barlow, R.G. 1999. Distributions and biogeochemistries of methylamines and ammonium in the Arabian Sea. Deep Sea Res. II, **46**: 593–615.

Gifford, D.J., and Dagg, M.J. 1988. Feeding of the estuarine copepod *Acartia tonsa* Dana: carnivory vs. herbivory in natural microplankton assemblages. Bull. Mar. Sci. **43**: 458–468.

Goldman, J.C. 1980. Physiological processes, nutrient availability, and concept of relative growth in marine phytoplankton ecology. *In* Primary productivity in the sea. *Edited by* P.G. Falkowski. Plenum Press, New York. pp. 179–194.

Gorham, J. 1984. Separation of plant betaines and their sulfur analogues by cation-exchange high-performance liquid chromotography. J. Chromatogr. **287**: 345–351.

Gröne, T., and Kirst, G.O. 1992. The effect of nitrogen deficiency, methionine and inhibitors of methionine metabolism on the DMSP content of *Tetraselmis subcordiformis* (Stein). Mar. Biol. **112**: 497–503.

Harris, G.P. 1986. Phytoplankton ecology. Structure, function and fluctuation. Chapman and Hall, London, U.K.

Hoffmann, L. 1996. Characterization of uptake and use of glycine betaine by marine phytoplankton and natural microbial assemblages. M.S. thesis, University of South Alabama, Mobile, Ala.

Keller, M.D. 1991. Dimethyl sulfide production and marine phytoplankton: the importance of species composition and cell size. Biol. Oceanogr. **6**: 375–382.

Keller, M.D., and Bellows, W.K. 1996. Physiological aspects of the production of dimethylsulfoniopropionate (DMS) by marine phytoplankton. *In* Biological and environmental chemistry of DMSP and related sulfonium compounds. *Edited by* R.P. Kiene, P.T. Visscher, M.D. Keller, and G.O. Kirst. Plenum Press, New York. pp. 131–142.

Keller, M.D., Bellows, W.K., and Guillard, R.R.L. 1989. Dimethyl sulfide production in marine phytoplankton. *In* Biogenic sulfur in the environment. *Edited by* E. Saltzman and W.J. Cooper. American Chemical Society, Washington, D.C. pp. 167–182.

Keller, M.D., Kiene, R.P., Matrai, P.A., and Bellows, W.K. 1999*a*. Production of glycine betaine and dimethylsulfoniopropionate in marine phytoplankton. I. Batch cultures. Mar. Biol. **135**: 237–248.

Keller, M.D., Kiene, R.P., Matrai, P.A., and Bellows, W.K. 1999*b*. Production of glycine betaine and dimethylsulfoniopropionate in marine phytoplankton. II. Nitrogen-limited chemostat cultures. Mar. Biol. **135**: 249–257.

Kettle, A.J., and Andreae, M.O. 2000. Flux of dimethylsulfide from the oceans: a comparison of updated data sets and flux models. J. Geophys. Res. **105**: 26 793 – 26 808.

Kiene, R.P., and Bates, T.S. 1990. Biological removal of dimethyl sulfide from seawater. Nature (Lond.), **345**: 702–705.

Kiene, R.P., and Gerard, G. 1995. Evaluation of glycine betaine as an inhibitor of dissolved dimethylsulfoniopropionate degradation in coastal waters. Mar. Ecol. Prog. Ser. **128**: 121–131.

Kiene, R.P., and Hoffmann Williams, L.P. 1998. Glycine betaine uptake, retention and degradation by microorganisms in seawater. Limnol. Oceanogr. **43**: 1592–1603.

Kiene, R.P., and Service, S.K. 1993. The influence of glycine betaine on dimethyl sulfide and dimethylsulfoniopropionate concentrations in seawater. *In* The biogeochemistry of global change: radiatively important trace gases. *Edited by* R.S. Oremland. Chapman and Hall, New York. pp. 654–671.

King, G. 1988. Distribution and metabolism of quaternary amines in marine sediments. *In* Nitrogen cycling in coastal marine environments. *Edited by* R. Blackburn and J. Sorensen. John Wiley, New York. pp. 143–173.

Leck, C., Larsson, U., Bagander, L.-E., Johansson, L., and Hajdu, S. 1990. DMS in the Baltic Sea — annual variability in relation to biological activity. J. Geophys. Res. **95**: 3353–3363.

Lowry, O.H., Rosenbrough, N.J., Farr, A.L., and Randall, R.J. 1951. Protein measurement with Folin-phenol reagent. J. Biol. Chem. **193**: 265–275.

Matrai, P.A. 1989. Determination of sulfur in ocean particulates by combustion-fluorescence. Mar. Chem. **26**: 227–238.

Matrai, P.A., and Keller, M.D. 1993. Dimethyl sulfide in a large-scale coccolithophore bloom in the Gulf of Maine. Continental Shelf Res. **13**: 831–843.

Matrai, P.A., Vernet, M., Hood, R., Jennings, A., Brody, E., and Saemundsdottir, S. 1995. Light-dependence of carbon and sulfur production by polar clones in the genus *Phaeocystis*. Mar. Biol. **124**: 157–167.

Murphy, L.S., and Haugen, E.M. 1985. The distribution and abundance of phototrophic ultraplankton in the North Atlantic. Limnol. Oceanogr. **30**: 47–58.

Netherton, J., and Gurin, S. 1982. Biosynthesis and phsiological role of homarine in marine shrimp. J. Biol. Chem. **257**: 11 971 – 11 975.

Packard, T.T., and Dortch, Q. 1975. Particulate protein-nitrogen in North Atlantic surface waters. Mar. Biol. **33**: 347–354.

Parsons, T.R., Takahashi, M., and Hargraves, B. 1977. Biological oceanographic processes. Pergamon Press, Oxford and New York.

Parsons, T.R., Maita, Y., and Lalli, C.M. 1984. Manual of chemical and biological methods for seawater analysis. Pergamon Press, New York.

Roch, O., Crabb, T.A., Blunden, G., and Gordon, S.M. 1985. Quarternary ammonium and tertiary sulfonium compounds in phytoplankton. Br. Phycol. J. **20**: 190–191.

Sheets, E.B., and Rhodes, D. 1996. Determination of DMSP and other onium compounds in *Tetraselmis subcordiformis* by plasma desorption mass spectrometry. *In* Biological and environmental chemistry of DMSP and related sulfonium compounds. *Edited by*

© 2004 NRC Canada

R.P. Kiene, P.T. Visscher, M.D. Keller, and G.O. Kirst. Plenum Press, New York. pp. 55–64.

Simó, R. 2001. Production of atmospheric sulfur by oceanic plankton: biogeochemical, ecological and evolutionary links. Trends Ecol. Evol. **16**: 287–294.

Simó, R., and Dachs, J. 2002. Global ocean emission of dimethylsulfide predicted from biogeophysical data. Global Biogeochem. Cycles, **16** (doi: 10.1029/2001GB001829).

Slattery, M., Hamman, M.T., McClintock, J.B., Perry, T.L., Puglisi, M.P., and Yoshida, W.Y. 1997. Ecological roles for water-borne metabolites from Antartic soft corals. Mar. Ecol. Prog. Ser. **161**: 133–144.

Sokal, R.R., and Rohlf, F.J. 1981. Biometry. W.H. Freeman and Co., San Francisco, Calif.

Stefels, J. 2000. Physiological aspects of the production and conversion of DMSP in marine algae and higher plants. J. Sea Res. **43**: 183–197.

Stoecker, D.K., Cucci, T.L., Hulburt, E.M., and Yentsch, C.M. 1986. Selective feeding by *Balanion* sp. (Ciliata: Balanionidae) on phytoplankton that best support its growth. J. Exp. Mar. Biol. Ecol. **95**: 113–130.

Sunda, W., Kieber, D.J., Kiene, R.P., and Huntsman, S. 2002. An antioxidant function for DMSP and DMS in marine algae. Nature (Lond.), **418**: 317–320.

Townsend, D.W., and Keller, M.D. 1996. Dimethyl sulfide (DMS) and dimethylsulfoniopropionate (DMSP) in relation to phytoplankton in the Gulf of Maine. Mar. Ecol. Prog. Ser. **137**: 229–241.

Turner, S.M., Malin, G., Liss, P.S., Harbour, D.S., and Holligan, P.M. 1988. The seasonal variation of dimethylsuphide and dimethylsulphoniopropionate concentrations in near-shore waters. Limnol. Oceanogr. **33**: 364–375.

White, R.H. 1982. Analysis of dimethyl sulfonium compounds in marine algae. J. Mar. Res. **40**: 529–536.

Wolfe, G.V., Sherr, E.B., and Sherr, B.F. 1994. Release and consumption of DMSP from *Emiliania huxleyi* during grazing by *Oxyrrhis marina*. Mar. Ecol. Prog. Ser. **111**: 111–119.

© 2004 NRC Canada

Latitudinal and vertical distributions of particle-associated dimethylsulfoniopropionate (DMSP) lyase activity in the western North Atlantic Ocean[1]

Hyakubun Harada, Mary-Anne Rouse, William Sunda, and Ronald P. Kiene

Abstract: Dimethylsulfoniopropionate (DMSP) lyase enzymes cleave phytoplankton-derived DMSP into dimethylsulfide (DMS) and acrylate. We measured particle-associated (>0.7 μm) DMSP lyase activity (DLA) in diverse waters from the Gulf of Maine to the Sargasso Sea. DLA fell within a relatively narrow range (0.63–5.4 nmol DMS·L^{-1}·min^{-1}), with no significant geographic trend. DLA was, however, generally highest near the surface and decreased with depth within the euphotic zone. When normalized to chlorophyll *a* (Chl *a*), DLA was significantly higher in oligotrophic surface waters of the Sargasso Sea (DLA:Chl *a* = 33–53 nmol DMS·min^{-1}·μg Chl a^{-1}) compared with more productive Gulf of Maine waters (DLA:Chl *a* = 0.5–7.9 nmol DMS·min^{-1}·μg Chl a^{-1}). In optically clear waters of the Sargasso Sea, DLA:Chl *a* was generally highest near the surface and decreased with depth, following a similar trend to that of the photoprotective pigment diadinoxanthin. When ammonium and phosphate were added to oligotrophic water from the Sargasso Sea, Chl *a* increased exponentially, whereas DLA:Chl *a* decreased by 83%. Our results suggest that Chl *a* specific DLA is highest when plankton are exposed to high solar radiation and low nutrients, consistent with the idea that DMSP lyases may be involved in oxidative stress protection.

Résumé : Les DMSP lyases sont des enzymes qui scindent le diméthylsulfoniopropionate (DMSP) provenant du phytoplancton en sulfure de diméthyle (DMS) et en acrylate. Nous avons mesuré l'activité de la DMSP lyase (DLA) associée aux particules (>0,7 μm) dans diverses eaux depuis le golfe du Maine jusqu'à la mer des Sargasses. Les valeurs de DLA se situent dans une gamme relativement étroite (0,63–5,4 nmol DMS·L^{-1}·min^{-1}), sans tendance géographique marquée. Cependant, la DLA est généralement plus grande près de la surface et elle décroît avec la profondeur dans la zone euphotique. Une fois la normalisation faite en fonction de la Chl *a*, la DLA est significativement plus élevée dans les eaux de surface oligotrophes de la mer des Sargasses (DLA:Chl *a* 33–53 nmol DMS·min^{-1}·μg Chl a^{-1}) que dans celles plus productives du golfe du Maine (DLA:Chl *a* 0,5–7,9 nmol DMS·min^{-1}·μg Chl a^{-1}). Dans les eaux optiquement claires de la mer des Sargasses, le rapport DLA:Chl *a* est généralement maximal près de la surface pour ensuite décroître en fonction de la profondeur, une répartition parallèle à celle de la diadinoxanthine, un pigment photoprotecteur. L'addition d'ammonium et de phosphate aux eaux oligotrophes de la mer des Sargasses entraîne une augmentation exponentielle de Chl *a*, mais un baisse de 83 % du rapport DLA:Chl *a*. Nos résultats indiquent que la DLA spécifique à la chlorophylle est maximale lorsque le plancton est exposé à une forte radiation solaire et à des concentrations faibles de nutriments, ce qui s'accorde avec le fait que les DMSP lyases sont peut-être impliquées dans la protection contre le stress oxydatif.

[Traduit par la Rédaction]

Introduction

Many marine phytoplankton species produce dimethylsulfoniopropionate (DMSP) and both phytoplankton and bacteria are able to cleave DMSP into dimethylsulfide (DMS) and acrylate with DMSP lyase enzymes (Stefels and VanBoekel 1993; Ledyard and Dacey 1994; Niki et al. 2000). DMS is an important volatile organic sulfur compound, contributing approximately 50% of the global biological sulfur flux to the atmosphere (Bates et al. 1992). The emission of DMS from the ocean to the atmosphere leads to the formation of non-sea-salt sulfate aerosols, which act as

Received 1 February 2003. Accepted 20 November 2003. Published on the NRC Research Press Web site at http://cjfas.nrc.ca on 22 June 2004.
J17360

H. Harada,[2] M.-A. Rouse, and R.P. Kiene. Department of Marine Sciences, University of South Alabama, Mobile AL, 36688, U.S.A., and Dauphin Island Sea Lab,101 Bienville Boulevard, Dauphin Island, AL 36528, U.S.A.
W. Sunda. CCFHR, National Ocean Service, National Oceanic and Atmospheric Administration, 101 Pivers Island Road, Beaufort, NC 28516, U.S.A.

[1]This paper is part of the proceedings of the Third International Symposium on Biological and Environmental Chemistry of DMS(P) and Related Compounds, held in Rimouski (Québec), 26–28 September 2002.
[2]Corresponding author (e-mail: bharada@yahoo.com).

 doi: 10.1139/F04-046 © 2004 NRC Canada

cloud condensation nuclei and thereby influence the radiative properties of the atmosphere (Bates et al. 1987; Charlson et al. 1987). Hence, production of DMSP and subsequent formation of DMS by plankton communities may affect the global heat budget and climate.

DMSP lyase activity (DLA) has been detected in a number of marine phytoplankton species (Stefels and VanBoekel 1993; Steinke et al. 1996; Wolfe et al. 2002). In vitro assays have been developed to determined the maximum potential DMSP cleavage rates in lysed or permeabilized cells under a given set of conditions (Steinke et al. 2000). Some species of dinoflagellates and prymnesiophytes were found to have high DLA, yet the enzymatic activity did not correlate with the intracellular concentration of DMSP, and not all DMSP-producing algae showed detectable lyase activity (Steinke et al. 1996; Niki et al. 2000).

DMSP functions as an osmolyte in many phytoplankton species, but the physiological and biogeochemical roles of algal DMSP cleavage are poorly understood (Stefels 2000). Wolfe et al. (1997) proposed that phytoplankton might use DMSP lyases to initiate a chemical defense against grazing. They observed that grazers appeared to prefer algal strains with low lyase enzyme activity. They suggested that nontoxic DMSP reacts with DMSP lyase when phytoplankton are grazed to produce potentially toxic acrylate, which could deter grazing. Stefels (2000) recently suggested that cellular synthesis of DMSP and its enzymatic lysis to DMS and acrylate may constitute a photosynthetic energy overflow mechanism in algal cells. Sunda et al. (2002) suggested that DMSP lyases may be involved in algal oxidative stress protection, since DMSP and its breakdown products (acrylate, DMS, dimethylsulphoxide, and methane sulphinic acid) are scavengers of oxygen radicals, particularly highly toxic OH radicals. These authors found that DMSP production and its cleavage were increased when phytoplankton cultures were exposed to oxidative stressors, such as solar UV radiation, hydrogen peroxide, and CO_2 or iron limitation.

Despite the potential importance of DMSP lyases to algal physiology and production of DMS, relatively little is known about the distribution of these enzymes in the ocean. Steinke et al. (2002*a*) recently reported potential rates of DLA ranging from 0.17 to 2.37 nmol DMS·L^{-1}·min^{-1} in a North Atlantic bloom dominated by coccolithophores and dinoflagellates, groups of algae known to have high levels of cellular DLA. Using an in vitro assay with lysed plankton samples, they found a correlation between peridinin, a chemotaxonomic pigment marker for dinoflagellates, and DLA. In another study by Steinke et al. (2002*b*), DLA to chlorophyll *a* (Chl *a*) ratios were highest in the upper part of the euphotic zone and exhibited a depth-dependent pattern similar to that of the ratio of the photoprotective pigment diadinoxanthin to Chl *a*.

In the present study, vertical profiles of planktonic DLA were measured at selected stations during a cruise from the Gulf of Maine to the subtropical Sargasso Sea during April 2002. DLA is operationally defined as the in vitro rate of DMS production in lysed or permeabilized plankton cells at a rate-saturating DMSP concentration (5 mmol·L^{-1}) at pH 8.0 and at 30 °C. Additional measurements included concentrations of DMS, particulate DMSP ($DMSP_p$), and phytoplankton pigments as well as ambient DMS production rates.

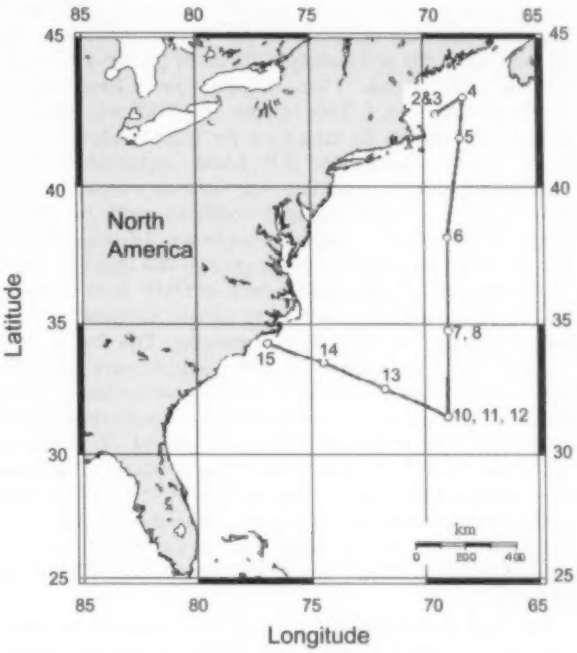

Fig. 1. Map of the western North Atlantic Ocean showing the cruise track and the sampling stations in the Gulf of Maine (Stations 2–4), the Georges Bank (Station 5), various areas of the Sargasso Sea (Stations 7–14), and the North Carolina shelf (Station 15).

Our goal was to describe vertical and latitudinal variations of DLA and test whether DLA correlated with DMS, DMSP, or other environmental factors. Additionally, the effects of nutrient enrichment on DMS, DMSP, and DLA were examined in oligotrophic water from the Sargasso Sea. Our observations provide some of the first measurements of lyase activity from oligotrophic regions, a major oceanic biome that is important in global flux of sulfur to the atmosphere.

Methods

Samples were collected aboard the R/V *Oceanus* from the Gulf of Maine, the Sargasso Sea, and the North Carolina shelf during 6–19 April 2002. The cruise track and sampling locations are shown in Fig. 1. Water samples from discrete depths were collected between 0600 and 0700 local time using a CTD (conductivity–temperature–depth) rosette equipped with 10-L Niskin bottles. Water samples were processed within 1 h of collection for various measurements as described below.

DLA

Particle-associated DLA was determined in plankton samples from all stations using a standardized in vitro assay that measured the production rate of DMS under saturating DMSP concentrations in cells lysed or permeabilized by chemical treatment. The assay that we used was based on that described by Steinke et al. (2000), with some modifications. For each sample assay, plankton from a known volume of seawater (100–200 mL) were filtered onto a 25-mm-

© 2004 NRC Canada

diameter Whatman GF/F filter (0.7 μm nominal pore size). The filter was subsequently placed in a 14-mL serum vial. One millilitre of Tris buffer (200 mmol·L^{-1}) prepared in 500 mmol NaCl·L^{-1} (pH 8.0) was added to lyse or permeabilize cells. The vials with filter and Tris buffer were sealed with a Teflon-coated gray butyl stopper (Wheaton), vortexed, and then incubated at 30 °C in a water bath for 20 min. After this preincubation, 20 μL of DMSP–HCl stock solution (250 mmol·L^{-1}) was added to give a final concentration of 5 mmol·L^{-1}. This amount of DMSP was found in preliminary tests to be saturating for lyase-catalyzed DMS production (H. Harada and R.P. Kiene, unpublished data). Immediately prior to sampling, the vial was vortexed vigorously for 3 s to equilibrate the headspace with the liquid phase, and a 100-μL headspace sample was subsequently removed with a Hamilton gas-tight syringe and injected into a gas chromatograph for quantification of DMS. Two replicate vials were prepared for each water sample. In addition, controls consisting of two vials containing Tris buffer and 5 mmol DMSP·L^{-1} without filtered particles were also prepared. At least three headspace samples were measured for each vial to yield a rate of DMS increase with time; DMS production was linear over the time period of sampling (<2 h after DMSP addition). The DLAs in plankton samples were corrected for abiotic cleavage of DMSP by subtraction of the DMS production rates measured in the control vials. The measured DLA was normalized to the volume of seawater filtered and algal-associated parameters (Chl *a* or $DMSP_p$).

The high concentrations of added Tris appeared to either lyse or permeablize plankton cells, allowing most, if not all, of the cellular lyase to contact the substrate. Tests showed that other means of cell disruption (0.1% Triton X-100 or sonication) did not increase DLA compared with the Tris buffer alone (H. Harada and R.P. Kiene, unpublished data). We used a pH 8.0 Tris buffer because preliminary tests showed that this pH yielded DLA that was equal to or greater than that in buffers with lower pH (range tested pH 6.5–8.0). As recommended by Steinke et al. (2000), all assays were conducted at 30 °C so that enzyme-based activities could be compared among samples and studies.

Sulfur compound determination

DMS in headspace subsamples from lyase assays was measured by direct injection into a Shimadzu GC-9A gas chromatograph equipped with a sulfur-selective flame photometric detector and a Carbopak B 1.5% XE-60 – 1% H_3PO_4 (60/80 mesh) column (Supelco, Belfonte, Pa.). The carrier gas was helium with a flow rate of 40 mL·min^{-1}, and the oven temperature was set at 70 °C. Standard curves for DMS produced in lyase assays were prepared in 14-mL serum vials by adding microlitre volumes of DMSP–HCl stock solutions and cleaving the DMSP with 1 mol·L^{-1} NaOH. The liquid volume in standard vials (~1 mL) was the same as that in assay vials, and the ionic strength of solution phases was also similar so that headspace DMS concentrations were comparable between standards and assay samples. Standard vials were held at 30 °C, the same temperature as the samples.

Concentrations of DMS in seawater samples collected at each station were measured with the purge and trap technique as described in Kiene and Service (1991). Concentrations of $DMSP_p$ were measured after alkaline hydrolysis to DMS. Briefly, a known volume of seawater was filtered by gravity onto a GF/F filter, which was immediately placed into a 14-mL serum vial with a Teflon-coated gray butyl stopper. $DMSP_p$ was cleaved to DMS by adding 2 mL of 5 mol·L^{-1} NaOH to the vials. The vials were incubated in the dark at room temperature, normally 25 °C, for at least 10 h to complete the reaction. Headspace subsamples were injected into the gas chromatograph and compared with standards prepared with DMSP–HCl stock solutions.

Nutrient enrichment experiment

Oligotrophic surface water was collected in the Sargasso Sea at 32.5765°N, 71.7795°W (Station 13) on 17 April 2002. Water from the Niskin bottles was transferred into a series of 1-L polycarbonate bottles. Two bottles were sacrificed for time zero measurements. Eight other bottles were used for incubation. Four unamended bottles served as controls and four were treated with 1 μmol $NH_4Cl·L^{-1}$ and 62.5 nmol $KH_2PO_4·L^{-1}$ (N:P = 16:1). These bottles were put in a black mesh bag, which blocked approximately 50% of the incident solar radiation. The bag containing the bottles was placed in an incubator fixed on the deck with flowing seawater to maintain ambient temperature. Two bottles for each treatment were sacrificed after 24 and 48 h for measurements of Chl *a*, DMS, $DMSP_p$, and DLA. These measurements were made between 0700 and 0800 local time.

Pigment measurements

Chl *a* concentrations were measured fluorometrically according to Strickland and Parsons (1968). Briefly, a known volume of water (0.5–1.0 L) was filtered through Whatman GF/F (0.7 μm pore size) glass-fiber filters and extracted in 90% acetone for 24 h at 4 °C. Chl *a* fluorescence was measured before and after acidification with two drops of 1 mol·L^{-1} HCl. Fluorescence was measured with a Turner Designs TD-700 fluorometer with a daylight white lamp (P/N 10-045) and chlorophyll optical kit (P/N 7000-961). Pigment biomarkers and diadinoxanthin were measured by HPLC at the Center for Hydro-Optics and Remote Sensing, San Diego State University, using the procedures outlined in Wright et al. (1991) and Bidigare and Trees (2000).

Hydrographic data

Depth profiles of temperature, salinity, and underwater photosynthetically active radiation (PAR) were obtained at each station with a SeaBird CTD package deployed with the Niskin bottle rosette.

Results

Characterization of sampling areas

Samples were collected from different regions and associated water types ranging from the Gulf of Maine (as far north as 43°03′N, 68°17′W) to the Sargasso Sea (as far south as 31°03′N, 69°00′W) (Fig. 1). Sea surface temperatures varied from 4.6 °C at Station 4 up to 22.5 °C at Station 14. Temperature profiles for each station are shown in Figs. 2 and 3. Stations 2–5 were in or near the Gulf of Maine and were characterized by nutrient-rich, productive surface waters

© 2004 NRC Canada

Fig. 2. Depth profiles of Chl *a* (△), DLA (●), and temperature (—) at coastal and shelf stations in the Gulf of Maine (Stations 2–4), the Georges Bank (Station 5), south of the Gulf Stream (Station 6), and the North Carolina shelf (Station 15).

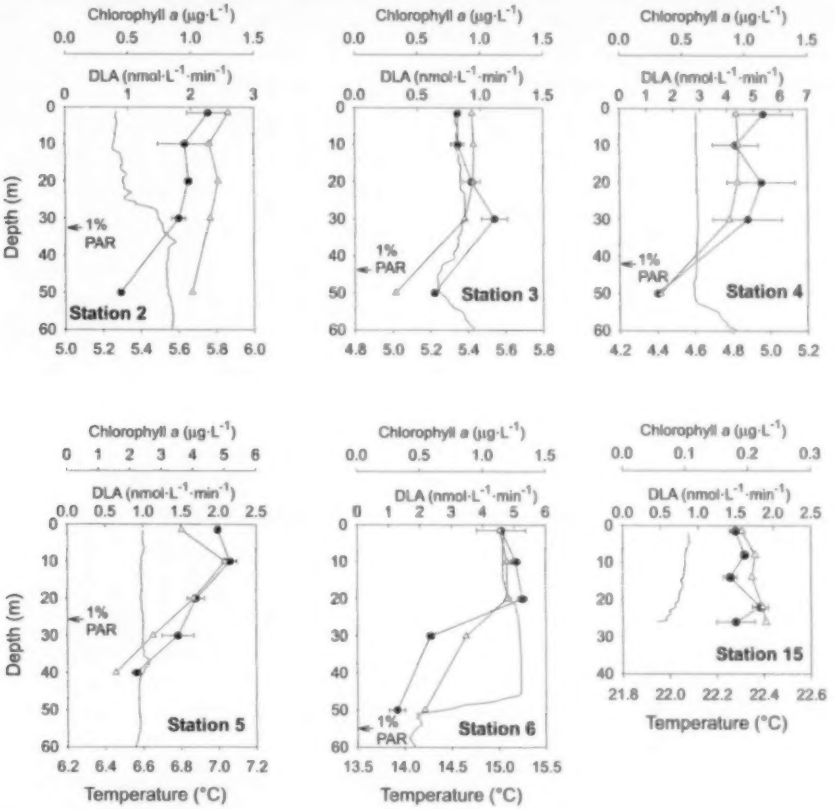

(2.6–7.9 μmol nitrate·L^{-1} and 0.93–3.6 μg Chl *a*·L^{-1}). The waters had relatively low light penetration, and PAR was attenuated to 1% of surface values at depths of 26–43 m. Stations 6–8 were located south of the Gulf Stream and were considered transitional (0.1–0.62 μmol nitrate·L^{-1}, 0.22–1.1 μg Chl *a*·L^{-1}, and 1% PAR depths of 47–75 m). Stations 10–14, located in the Sargasso Sea, had surface water characteristics opposite to those in the Gulf of Maine. Sargasso surface waters were warm and oligotrophic (<0.2 μmol nitrate·L^{-1}, <0.1 μg Chl *a*·L^{-1}) and had a high light penetration (1% PAR depths of 80–113 m). Station 15, located on the North Carolina shelf (30 m total depth), had surface temperatures similar to those in the Sargasso Sea but high light attenuation and an intermediate Chl *a* concentration (0.2 μg·L^{-1}). The lowest Chl *a* concentration (0.04 μg·L^{-1}) was observed at the surface of Station 12 in the Sargasso Sea, and the highest Chl *a* (5.0 μg·L^{-1}) occurred at 10 m depth at Station 5 on Georges Bank. Chl *a* tended to decrease with depth at higher latitude stations (Fig. 2), whereas it increased with depth at the Sargasso Sea stations (Fig. 3).

$DMSP_p$:Chl *a*, DMS:Chl *a*, and pigment biomarkers

The ratios of $DMSP_p$ concentration to Chl *a* ($DMSP_p$:Chl *a*) were low (8–34 nmol·μg^{-1}) in surface waters from the Gulf of Maine (Stations 2–5) but high (180–231 nmol·μg^{-1}) in surface waters from oligotrophic stations (Stations 10–14) (Fig. 4*a*). Transitional stations and North Carolina shelf water (Stations 6–8 and 15) showed intermediate values of $DMSP_p$:Chl *a* (62–196 nmol·μg^{-1}). DMS:Chl *a* also showed similar trends to that of $DMSP_p$:Chl *a*, with low values in the Gulf of Maine (0.52–0.74 nmol·μg^{-1}), high values in the Sargasso Sea (18–82 nmol·μg^{-1}), and intermediate values at the transitional stations and in North Carolina shelf water (DMS:Chl *a* = 4.4–10 nmol·μg^{-1}).

There was a phytoplankton bloom at Station 5 (Georges Bank) where surface water Chl *a* was 3.5 μg·L^{-1} and $DMSP_p$:Chl *a* was the lowest observed (8 nmol·μg^{-1}). The concentration of fucoxanthin (1.0 μg·L^{-1}) and the fucoxanthin:Chl *a* ratio (0.29, g:g) were the highest at this station (Fig. 5), suggesting that diatoms dominated the phytoplankton community. Based on the ratio of biomarker pigments to Chl *a* in surface waters, cryptophytes and diatoms were generally abundant in the high-latitude stations (Stations 2–6), and the relative abundance of prochlorophytes and prymnesiophytes was higher in the low-latitude stations (Fig. 5). Dinoflagellate abundance (based on peridinin:Chl *a*) was variable and showed no trend among stations (Fig. 5). The highest ratios of peridinin to Chl *a* (0.029, g:g) and 19′-hexanoyloxyfucoxanthin to Chl *a* (0.27, g:g) were observed in the transitional area (Stations 6 and 8, respectively); however, the values of $DMSP_p$:Chl *a* at these stations were intermediate between those of the Gulf of Maine and Sargasso Sea (Fig. 4). The fucoxanthin:Chl *a* values at the Sargasso Sea stations were low relative to other

© 2004 NRC Canada

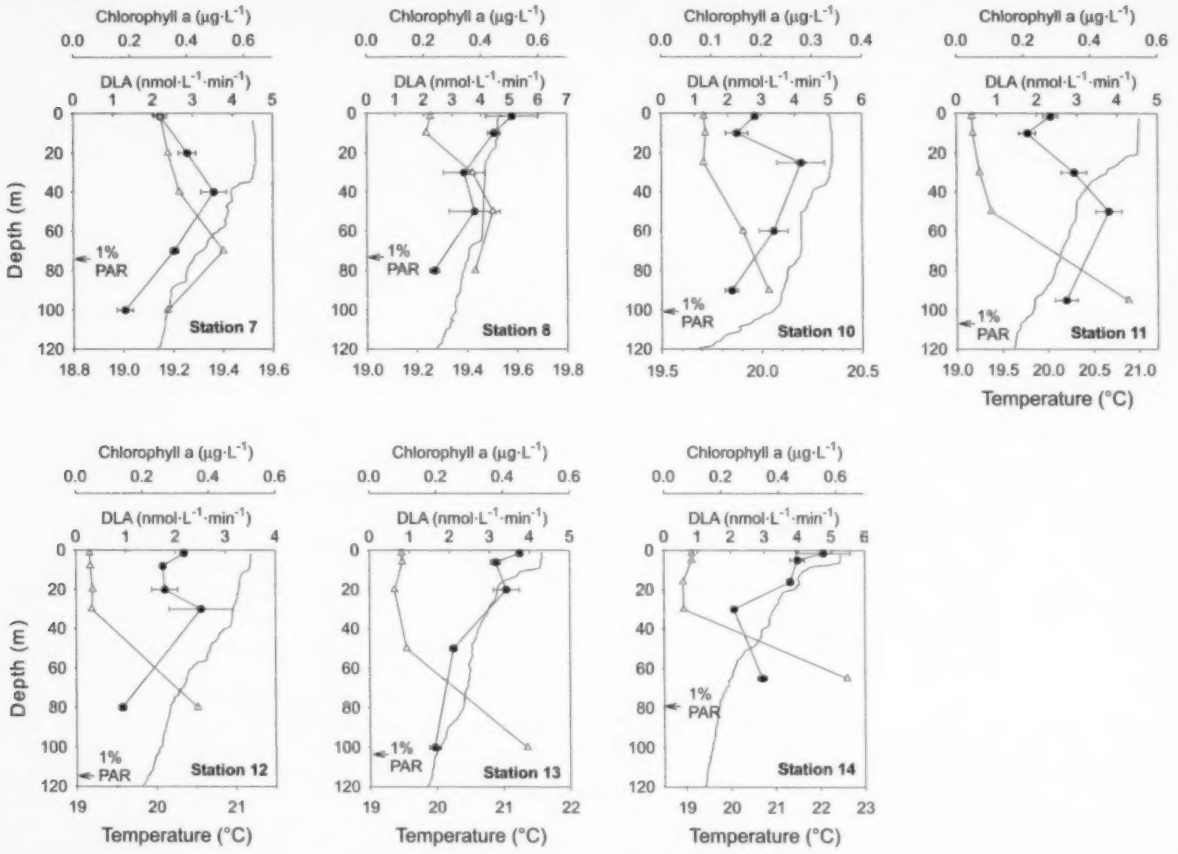

stations, indicating a relatively low abundance of diatoms. Some of the fucoxanthin that might otherwise be attributed to diatoms at the Sargasso Sea stations could have been derived from prymnesiophytes, which contain low levels of this pigment (Mackey et al. 1996).

DLA distributions

Despite a wide range of water mass characteristics, the DLA per litre of water filtered fell within a relatively narrow range (0.6–5.4 nmol·L^{-1}·min^{-1}) and the enzyme activity did not show apparent trends with respect to station location (Figs. 2 and 3). Additionally, DLA did not correlate with water temperature ($r^2 = 0.029$, $P = 0.17$, $n = 65$). DLA rates were, however, generally highest in the upper euphotic zone and were lower near or below the 1% PAR irradiance depths (Figs. 2 and 3). When normalized to Chl *a*, DLA was substantially higher in warm, oligotrophic waters of the Sargasso Sea compared with waters from the Gulf of Maine (Figs. 4*b* and 6). The average DLA:Chl *a* value was 2.2 nmol DMS·min^{-1}·μg Chl *a*$^{-1}$ in the surface water of high-latitude stations (Stations 2–5) and 45 nmol DMS·min^{-1}·μg Chl *a*$^{-1}$ at the low-latitude, oligotrophic stations (Stations 10–14) (Fig. 4*b*). The lowest value was 0.55 nmol DMS·min^{-1}·μg Chl *a*$^{-1}$ at Station 5 within a diatom bloom, and the highest value was 53 nmol DMS·min^{-1}·μg^{-1} Chl *a* at the oligotrophic Station 12 where prymnesiophytes and dinoflagellates predominated. Ratios of DLA to $DMSP_p$ in oligotrophic waters (0.14–0.32 nmol DMS·min^{-1}·nmol $DMSP_p^{-1}$ at Stations 10–14) also were higher than those in more productive waters (0.03–0.21 nmol DMS·min^{-1}·nmol $DMSP_p^{-1}$ at Stations 2–5). This trend is particularly evident in surface samples (Fig. 4*b*).

In addition to the differences among stations, DLA:Chl *a* decreased with depth at the Sargasso Sea stations (Fig. 6). The mean value in the upper 40 m was 43.9 ± 13.3 nmol DMS·min^{-1}·μg Chl *a*$^{-1}$ and values decreased substantially below that depth to as low as 2.5 nmol DMS·min^{-1}·μg Chl *a*$^{-1}$ at 100 m at Station 12. No such trend with depth was observed at the high-latitude stations where DLA:Chl *a* was much lower (Fig. 6). For the oligotrophic and transitional stations (Stations 6–14), the depth trends for DLA:Chl *a* were generally similar to those of the ratio of the photoprotective pigment diadinoxanthin to Chl *a*, with both values being highest in surface waters and decreasing with depth. By contrast, at the Gulf of Maine and North Carolina Shelf stations (Stations 2–5 and 15), the diadinoxanthin:Chl *a* ratios varied over a narrow range and showed no distinct patterns with depth (Fig. 6).

© 2004 NRC Canada

Fig. 4. (*a*) Concentrations of Chl *a* (●) and the ratios DMS:Chl *a* (□) and $DMSP_p$:Chl *a* (vertical shaded bars) at the surface (1–2 m depth) of each station. (*b*) DLA:Chl *a* (vertical shaded bars) and DLA:$DMSP_p$ (△) at the surface (1–2 m depth) of each station. No data were available for Station 9.

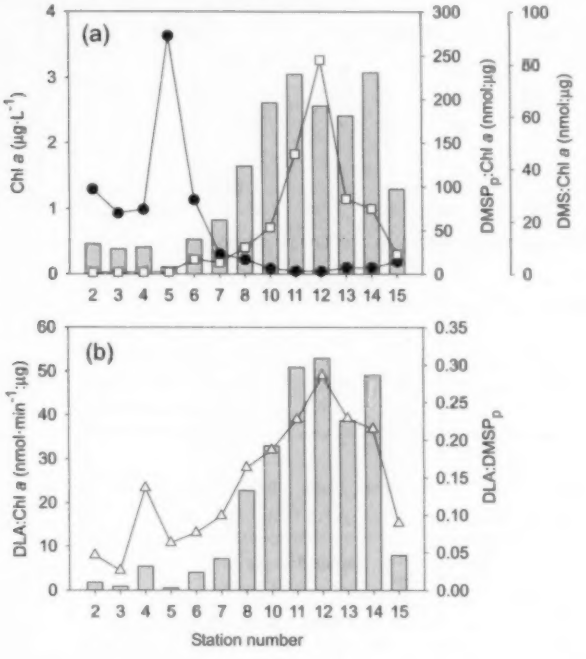

Fig. 5. Ratios of taxonomic pigment markers to Chl *a* at the surface (1–2 m depth) of each station. (*a*) Fucoxanthin (●) and alloxanthin (■) are the markers for diatoms and cryptophytes, respectively. (*b*) Divinyl Chl *a* (DVChl *a*) (▲), 19′-hexanoyloxy-fucoxanthin (Hex-Fuco) (●), and peridinin (□) are the markers for prochlorophytes, prymnesiophytes, and dinoflagellates, respectively.

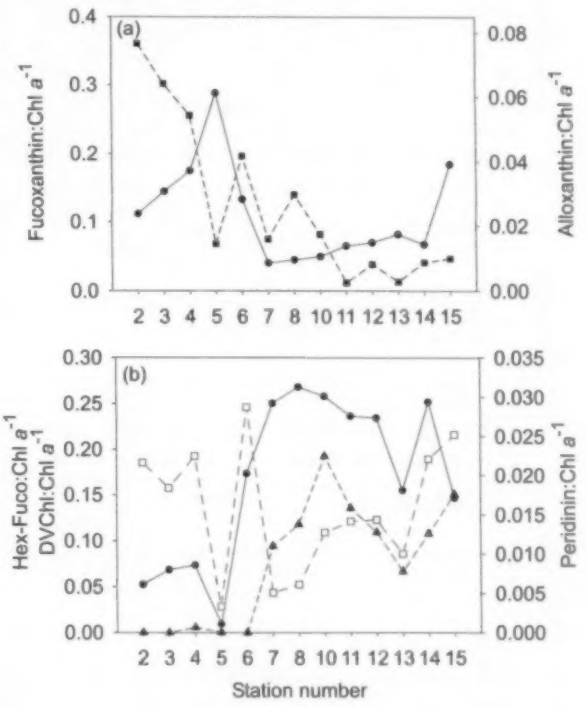

For the entire data set, the DLA per litre of seawater was weakly, but significantly, correlated with the dissolved DMS concentration ($r^2 = 0.22$, $P = 0.0002$, $n = 65$), but there were no clear differences among the sampling regions (Fig. 7*a*). The overall correlation between DLA and $DMSP_p$ was weak ($r^2 = 0.09$, $P = 0.015$, $n = 65$), but distinct relationships were observed for different water types (Fig. 7*b*). In the Sargasso Sea (Stations 10–14), DLA increased steeply as $DMSP_p$ increased, and the correlation was significant ($r^2 = 0.57$, $P = 0.002$, $n = 25$). A significant linear correlation between DLA and $DMSP_p$ ($r^2 = 0.77$, $P < 0.001$, $n = 15$) also was observed for the transitional stations (Stations 6–8), but the slope of the regression line (0.087) was less than that for the oligotrophic stations (0.17). By contrast, DLA was not significantly correlated with $DMSP_p$ in the Gulf of Maine (Stations 2–5: $r^2 = 0.018$, $P = 0.57$, $n = 20$) (Fig. 7*b*).

Based on in vitro rates of DLA measured under our assay conditions, DMS could be produced at rates from 4100 to 5200 nmol·L^{-1}·day^{-1} (Table 1), and at that rate the $DMSP_p$ pool could potentially turn over to DMS every 5–12 min (or 120–300 turnovers a day). The potential turnover rate was 2.5 times higher in the Sargasso Sea (Stations 10–14) than in the Gulf of Maine (Stations 2–4). These potential rates are compared with rates of DMS production measured in whole seawater samples incubated in the dark in the presence of DMDS to inhibit DMS consumption (Table 1). The potential DMS production rates as measured at substrate saturating DMSP in the in vitro DMSP lyase assays were three orders of magnitude higher than natural DMS production rates in situ (1.2–1.6 nmol·L^{-1}·day^{-1}).

Nutrient addition experiment

When an oligotrophic water sample from the Sargasso Sea was amended with 1 μmol ammonium·L^{-1} and 62.5 nmol phosphate·L^{-1}, Chl *a* increased exponentially from 0.097 to 1.25 μg·L^{-1} (a 13-fold increase in 2 days), while the unamended control showed only a 13% increase (from 0.097 to 0.11 μg·L^{-1}) (Fig. 8). Despite the large difference in Chl *a* response, DLA and DMS showed little or no difference between control and nutrient addition treatments, and their concentrations changed little from the initial values (Fig. 8). $DMSP_p$ did increase with nutrient addition, but the percentage increase was much less than that observed for Chl *a* (Fig. 8). Consequently, the $DMSP_p$:Chl *a* ratio decreased substantially in the nutrient addition treatment but showed a much smaller change in the control (Fig. 9). The initial $DMSP_p$:Chl *a* in the sample was 107 nmol·$μg^{-1}$, and after 2 days, this ratio decreased to 14.1 nmol·$μg^{-1}$ in the nutrient addition treatment, a decrease of 87%. In the control, by contrast, $DMSP_p$:Chl *a* after 2 days was much higher (86.3), only 19% less than the initial value.

© 2004 NRC Canada

Fig. 6. Depth profiles of DLA:Chl *a* (●) and diadinoxanthin:Chl *a* (○) for each station. Two data points were missing at Station 7, indicated by the broken line.

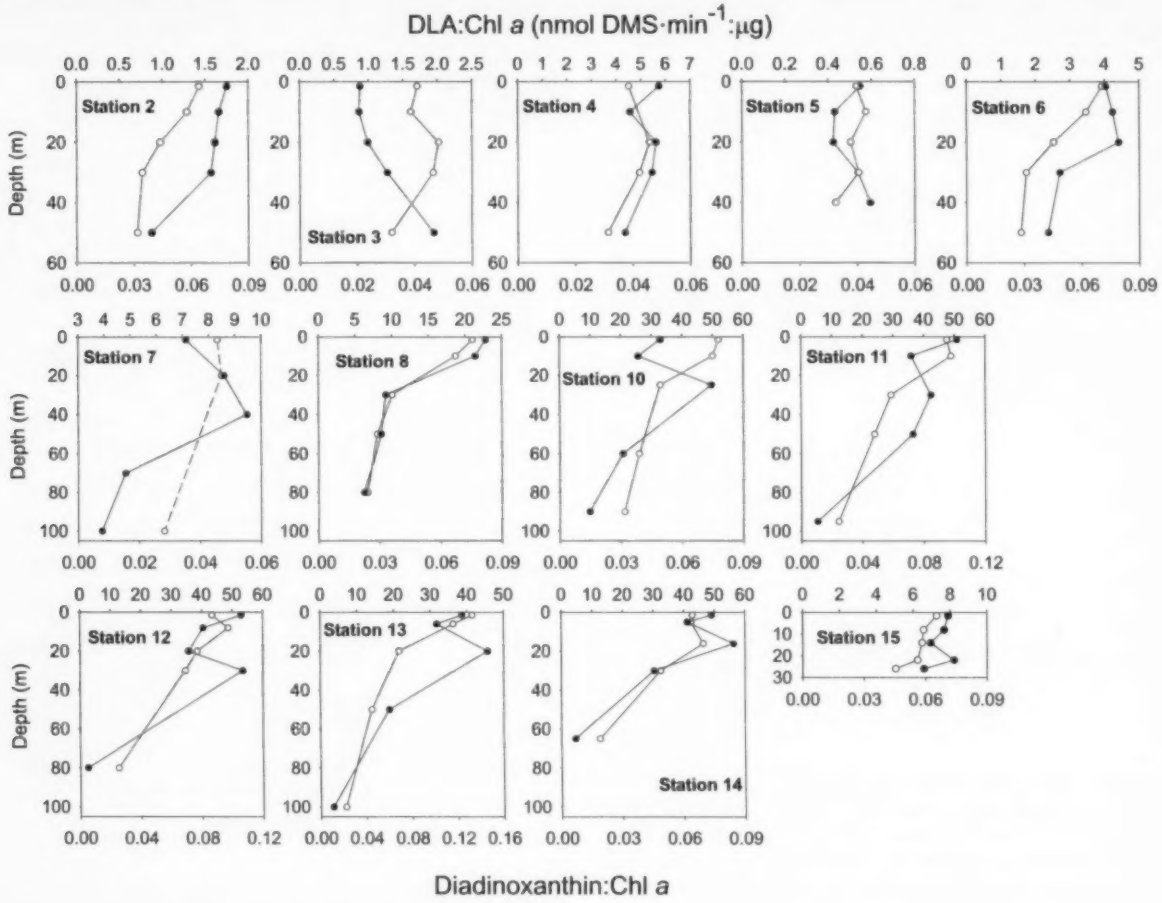

Similar large decreases were observed in DLA:Chl *a* and DMS:Chl *a* in the nutrient addition treatment (Fig. 9). DLA:Chl *a* decreased from 38.7 to 11.2 nmol·min^{-1}·µg^{-1} (a 71% reduction) during the first 24 h and decreased further to 2.7 nmol·min^{-1}·µg^{-1} (a 93% reduction) after 48 h. Compared with the controls, the nutrient-amended treatments had an 86% lower DLA:Chl *a* after 48 h (2.7 versus 20.2 nmol·min^{-1}·µg^{-1}). Likewise, DMS:Chl *a* showed no change after 2 days in the control but exhibited a 93% decrease (from 28.8 to 1.9 nmol·min^{-1}·µg^{-1}) with nutrient addition.

Discussion

This study presents some of the first DLA measurements from contrasting ocean waters, including oligotrophic regions. The range of rates of DLA that we measured in surface waters (0.82–5.36 nmol DMS·L^{-1}·min^{-1}) is somewhat higher than that measured by Steinke et al. (2002*a*) in a bloom of coccolithophores and dinoflagellates in the northern North Atlantic (0.17–2.37 nmol DMS·L^{-1}·min^{-1}). Our higher rates may reflect differences in the environmental characteristics of the waters sampled or the larger pore size filter (2.0 µm, polycarbonate) used by Steinke et al. (2002*a*) to capture plankton. We used Whatman GF/F glass-fiber filters to capture particles so that our DLA results would be directly comparable with Chl *a* data collected using the same filters. Because of their smaller effective pore size (0.7 µm), the GF/F filters may have retained some smaller DMSP lyase containing phytoplankton and also some bacteria (Scarratt et al. 2000). Size fractionation measurements carried out by Steinke et al. (2002*a*) within a dinoflagellate–coccolithophore bloom showed that >95% of the DLA was associated with particles >2 µm in diameter. In addition, they found a strong correlation between DLA and the dinoflagellate pigment peridinin. We did not carry out size fraction measurements during our 2002 cruise, but we have found that >90% of the DLA occurred in the >3 µm size fraction in coastal seawater from North Carolina sampled in July 2003 (H. Harada and R.P. Kiene, unpublished data). The size fractionation results, together with relationships between DLA and algal pigments (see discussion below), suggest that phytoplankton rather than bacterioplankton are the primary source of the DMSP lyase measured by us and by Steinke et al. (2002*a*). In addition, bacterioplankton typically convert

© 2004 NRC Canada

Fig. 7. Scatterplots of (*a*) DLA and DMS and (*b*) DLA and $DMSP_p$ for all samples. The Gulf of Maine area (●) was represented by Stations 2–5, the transitional area (○) by Stations 6–8, the Sargasso Sea (+) by Stations 10–14, and the North Carolina coast (▲) by Station 15. For all data, DLA and DMS showed a significant correlation ($r^2 = 0.21$, $P < 0.001$). Overall correlation between DLA and $DMSP_p$ was weak ($r^2 = 0.09$, $P = 0.014$), but there were higher and significant correlations between DLA and $DMSP_p$ in the Sargasso Sea ($r^2 = 0.57$, $P = 0.002$, regression slope = 0.17) and transitional zone ($r^2 = 0.77$, $P < 0.0001$, regression slope 0.087).

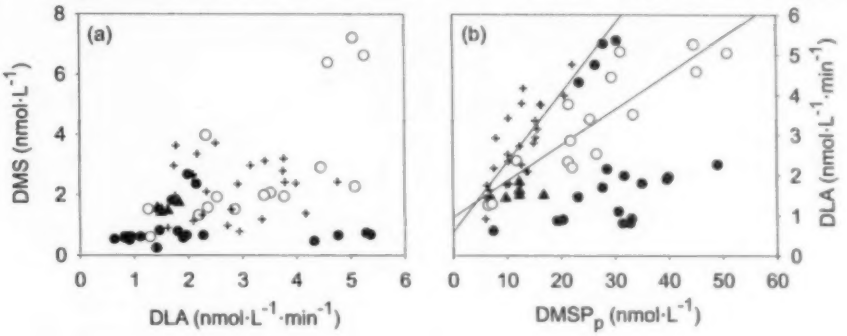

Table 1. Mean concentrations of $DMSP_p$ and DMS from surface depths (1–2 m) in different bodies of water together with estimated potential DMS production rates based on in vitro DLA and the actual DMS production rate in whole seawater samples.

Station(s)	Area	$DMSP_p$ (nmol·L^{-1})	DMS (nmol·L^{-1})	DLA rate (nmol DMS·L^{-1}·day^{-1})	Whole water DMS rate (nmol·L^{-1}·day^{-1})
2–4	Gulf of Maine	33.9±9.4	0.67±0.03	4056±3339	1.07±1.4
7 and 8	Transitional	23.3±6.0	1.81±0.66	5234±2943	1.60±0.7
10–14	Sargasso Sea	15.0±5.8	2.43±0.69	4556±1559	1.47±0.6
15	North Carolina shelf	18.5	1.43	2160	1.50

Note: Values are mean ± SD for the stations represented. Note that potential DMS production rates based on our enzyme assays are three orders of magnitude larger than the actual in situ production of DMS obtained from dark incubations of whole water containing 200 nmol dimethyldisulfide·L^{-1} to inhibit DMS consumption.

<10% of the DMSP that they take up to DMS (Kiene and Linn 2000), again arguing that they are a less likely source of lyase enzyme.

Spatial and depth-dependent patterns in DLA

Surface water DLA per unit Chl *a* was substantially higher in the warm, oligotrophic Sargasso Sea than in the cold, nutrient-rich Gulf of Maine. This trend is strikingly similar to that of the ratio of enzyme substrate ($DMSP_p$) and the product (DMS) to Chl *a* and the ratio of DLA to $DMSP_p$ (Fig. 4). Temperature did not appear to be a major factor governing the pattern for DLA, since there was no significant correlation between these two variables ($r^2 = 0.029$, $P = 0.17$, $n = 65$). Previous studies have shown that DMSP and DMS concentrations in a broad range of subtropical, temperate, and subarctic oceanic waters are relatively high under stratified conditions from spring through early fall and low during winter (Dacey et al. 1998; Simó and Pedrós-Alió 1999). The former period corresponds to increased solar radiation and thermal stratification of the water column in the northern Sargasso Sea (within the region that we sampled), which in turn results in nutrient limitation (Steinberg et al. 2001) and increased exposure of mixed-layer plankton to solar UV radiation (Simó and Pedrós-Alió 1999). Thus, the high DLA, DMSP, and DMS to Chl *a* ratios that we observed in surface waters of the Sargasso Sea may be related to high exposure to solar radiation (particularly solar UV) and (or) low nutrient availability that occur in shallow surface mixed layers under stratified conditions. Shallow mixed layers of 5–30 m, indeed, were observed at our Sargasso stations, indicating highly stratified conditions.

That solar radiation and nutrients influence the distribution of DLA, DMSP, and DMS is further suggested by the vertical patterns that we observed. The ratios of DMSP and DMS to Chl *a* decreased with depth (data not shown), similar to previously observed patterns for stratified open ocean waters (Belviso et al. 1993; Dacey et al. 1998). DLA:Chl *a* in the Sargasso Sea also was highest at the surface and decreased with depth following a similar trend to that of the photoprotective pigment diadinoxanthin. A similar relationship between DLA and diadinoxanthin was reported by Steinke et al. (2002*b*) for a North Sea algal bloom. We generally did not observe decreases in DLA:Chl *a* with depth in the productive waters of the Gulf of Maine or on Georges Bank (Stations 2–5), and DLA:Chl *a* was quite low at these stations, further suggesting that nutrient concentrations or penetration of solar radiation influences the distribution of DLA. The productive stations had low DLA:$DMSP_p$ compared with the Sargasso Sea stations (Fig. 4), so variations in Chl *a* are probably not the only factor influencing the pattern of DLA distribution.

The trend of higher DLA:Chl *a*, DLA:$DMSP_p$, and DMSP:Chl *a* in oligotrophic surface waters may also have been influenced by algal community composition. Based on marker pigment distributions, phytoplankton dominance in surface waters shifted from diatoms and cryptophytes at

© 2004 NRC Canada

Fig. 8. Effects of nutrient (nitrogen plus phosphorus) addition on (*a*) Chl *a*, (*b*) DLA, (*c*) $DMSP_p$, and (*d*) DMS concentrations in surface seawater samples collected at Station 13 (the oligotrophic Sargasso Sea). ●, unamended control; ▼, nitrogen plus phosphorus addition. Error bars represent the range for duplicate bottles in each treatment. The nutrient-treated samples were amended with 1 µmol ammonium·L^{-1} and 62.5 nmol phosphate·L^{-1} (N:P = 16:1). All samples were incubated in a deck incubator exposed to approximately 50% solar irradiance.

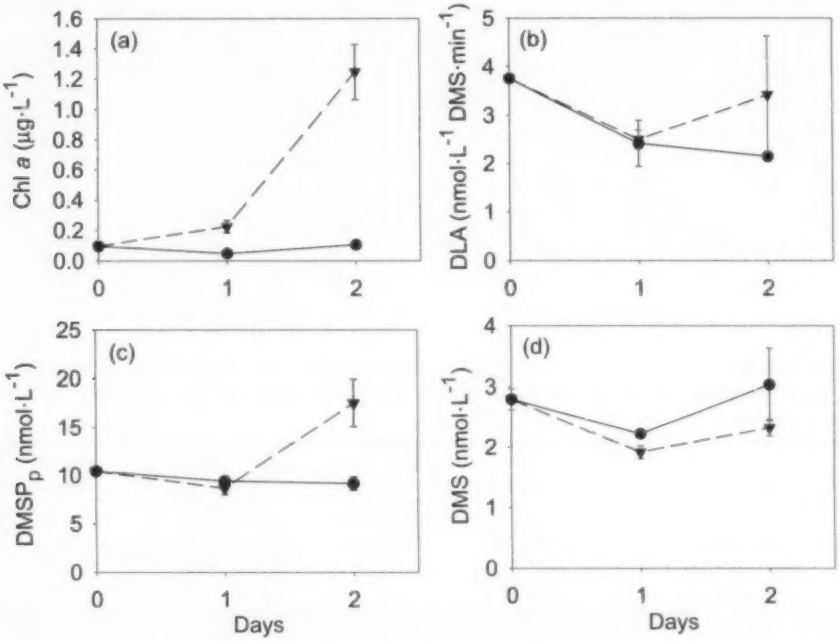

higher latitudes to prymnesiophytes and prochlorophytes in the oligotrophic Sargasso Sea. Diatoms and cryptophytes are not known to have high DMSP concentrations or DLA, whereas most prymnesiophytes have high DMSP and some have very active lyases (Steinke et al. 1996, 1998). We observed a significant correlation between DLA and 19′-hexanoyloxyfucoxanthin, the pigment marker for prymnesiophytes, but the relationship was weak (r^2 = 0.087, P = 0.02, n = 65), suggesting other factors control the distribution of DLA. A similar conclusion can be drawn for DMSP. This conclusion is further suggested by data from the transitional Station 6, where the marker pigments peridinin and 19′-hexanoyloxyfucoxanthin were relatively high, indicating that dinoflagellates and prymnesiophytes were abundant. As noted above, these phytoplankton groups are known to have high DMSP concentrations and DLA, yet we did not observe especially high DLA at this station, and DLA:Chl *a* and DMSP:Chl *a* were intermediate between those of the Gulf of Maine and the Sargasso Sea. This result suggests that DMSP concentrations and lyase activities may not depend only on community composition but also on some environmental factors. The fact that nutrient levels and the attenuation of solar radiation were intermediate at Station 6 supports our conclusion that these factors may exert strong control over the distribution of DMSP and DLA.

Can physiological roles of DMSP lyases help explain the distribution of DLA?

The high DLAs that we observed in filtered plankton could potentially turn over the large cellular pools of DMSP (i.e., $DMSP_p$) on a time scale of minutes if these enzymes were fully active in the cells. This finding suggests that lyase enzymes must have important functions in plankton. The physiological roles of DMSP and DMSP lyases in algae are still uncertain (Stefels 2000), but evidence points to some sort of role in stress response (Wolfe et al. 2002). Nutrient limitation is one form of stress that appears to promote high biomass-specific DMSP and DLA. In our shipboard experiment with surface water from a Sargasso Sea station, nutrient enrichment (nitrogen plus phosphorus addition) resulted in a rapid increase in Chl *a* and substantial decreases in the ratios of DLA, DMS, and $DMSP_p$ to Chl *a*. We do not know if these responses were due to a physiological change in the existing plankton population or to preferential growth of species low in DMSP and DLA. DMSP levels in cultured phytoplankton are known to increase under nitrogen-limited conditions (Grone and Kirst 1992; Keller and Korjeff-Bellows 1996; Keller et al. 1999*b*). This nitrogen effect may be due to replacement of nitrogen-containing osmolytes (e.g., glycine betaine or proline) by DMSP, although glycine betaine does not appear to replace DMSP even when nitrogen is abundant (Keller et al. 1999*a*, 1999*b*). Nonetheless, replacement of DMSP by nitrogen-containing osmolytes when nitrogen was supplied in our experiment could explain the decreases in $DMSP_p$:Chl *a* that we observed, but it would not explain the decrease in DLA:Chl *a* or DMS:Chl *a*. Nutrient limitation leads to increased oxidative stress and an increased need for photosynthetic overflow mechanisms, both of which have been suggested to increase DMSP production and lysis in

© 2004 NRC Canada

Fig. 9. Effects of nutrient addition on Chl *a* normalized (*a*) DMS, (*b*) DLA, (*c*) and $DMSP_p$ concentrations in surface seawater samples collected at Station 13 (the oligotrophic Sargasso Sea). Symbols: ●, unamended control; ▽, nitrogen plus phosphorus addition. Error bars represent the range of duplicate bottles for each treatment.. The nutrient-treated samples were amended with 1 μmol ammonium·L^{-1} and 62.5 nmol phosphate·L^{-1} (N:P = 16:1). All samples were incubated in a deck incubator exposed to approximately 50% solar irradiance.

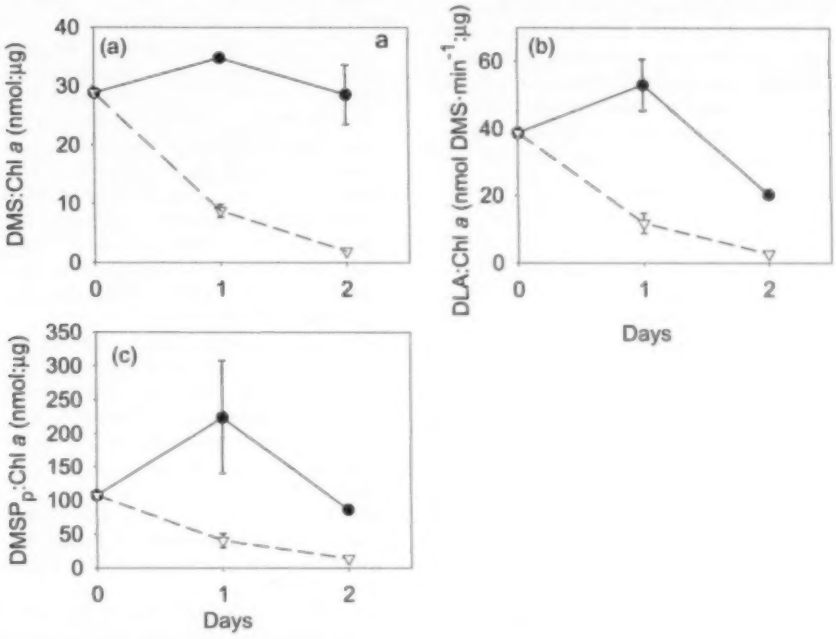

phytoplankton (Stefels 2000; Sunda et al. 2002). Relief from those stresses by increased nutrients could explain the diminishing DLA, DMSP, and DMS to Chl *a* ratios that we observed in our experiment and at least partly explain the decrease in the ratios that we observed between the oligotrophic Sargasso Sea and nutrient-rich waters of the Gulf of Maine.

High DLA, DMSP, and DMS to Chl *a* ratios in the surface waters of the Sargasso Sea could be related to oxidative stress experienced by surface-dwelling plankton (Sunda et al. 2002). UV radiation caused oxidative stress and inhibited photosynthesis in the dinoflagellate *Prorocentrum micans* (Lesser 1996), and this effect was heightened under nitrogen limitation (Litchman et al. 2002). Therefore, oxidative stress is likely to be important in stratified surface waters where exposure to solar radiation is high and nutrient availability is low. DMSP and its degradation products are effective oxygen radical scavengers (Steinke et al. 2002*b*; Sunda et al. 2002), and DMS and acrylate are, respectively, 60 and 20 times more reactive toward OH radicals than is DMSP. Thus, enzymatic cleavage of DMSP produces a large increase in OH radical scavenging ability, and DMSP lyase may regulate the antioxidant intensity of the system (Sunda et al. 2002). Another form of oxidative stress protection utilized by algae under nutrient limitation is overflow metabolism, whereby overreduction of the photosynthetic apparatus (and associated production of reactive oxygen species) is prevented by continued CO_2 fixation and biosynthesis of non-nutrient-containing compounds. Stefels (2000) suggested that DMSP may be used as a photosynthetic overflow metabolite under nutrient limitation or high-light conditions and that DMSP lyase may regulate the accumulation of intracellular DMSP.

DLA and DMS production in situ

DMSP lyases ultimately must be responsible for the DMS production in the ocean. The DLA that we measured represents the maximum, substrate-saturated rates in lysed or permeabilized cells, and it is not clear how these maximum potential rates relate to DMS production in situ. We observed that in vitro DLA rates were ~3000-fold higher than the in situ rates of DMS production occurring in natural water samples (Table 1). Since 5 mmol DMSP·L^{-1} was sufficient to saturate DLA in the assays, and the intracellular DMSP concentrations in most DMSP-producing phytoplankton is above this concentration (Keller et al. 1989), the DMSP lyases must not react freely with intracellular DMSP in the natural plankton populations. This conclusion agrees with results from phytoplankton culture studies, which suggest that the DMSP lysis reaction is highly regulated, possibly by physical separation of the substrate and the enzyme in vivo (Steinke et al. 1998). DMSP cleavage to DMS by algae is promoted by many different forms of cell damage (e.g., grazing or viral lysis) and physiological stress (oxidative stress, nutrient limitation, prolonged darkness) (Wolfe et al. 1997; Malin et al. 1998; Sunda et al. 2002). The exact mechanism of DMSP lyase regulation in vivo and in the sea remains to be elucidated.

For our entire data set, there was a positive correlation ($r^2 = 0.22$, $P < 0.001$, $n = 65$) between DLA and in situ water column DMS concentrations, but there were no distinct trends in the different regions that we sampled. DMS con-

© 2004 NRC Canada

centrations are controlled not only by rates of production from DMSP lysis but also by rates of loss from many processes including uptake by bacteria, photooxidation, and exchange with the atmosphere. These loss processes might have as much influence on DMS concentrations as its production by DLA. Strong correlation between DLA and $DMSP_p$ as well as high ratios of DLA, $DMSP_p$, and DMS to Chl *a* and DLA to $DMSP_p$ in the surface waters of oligotrophic Sargasso Sea imply that the demand for DMS or acrylate may be high in these waters, driving up the production of DMSP and the lyases that cleave it to DMS.

While in vitro DLA was much greater than in situ DMS production rates, the high DLA:Chl *a* values in oligotrophic surface waters were consistent with relatively high DMS concentrations in these waters and the very high DMS:Chl *a* values (Dacey et al. 1998). Assuming that most of the DLA that we measured was due to phytoplankton, this argues that direct output of DMS from phytoplankton could be a significant source of water column DMS. The Chl *a* specific DLA that we measured in plankton samples from the surface of the Sargasso Sea (33–53 nmol DMS·min^{-1}·μg Chl a^{-1} at Stations 10–14) were comparable with the in vitro lyase activity (52 nmol DMS·min^{-1}·μg Chl a^{-1}) reported for the axenic strain of the prymnesiophyte *Emiliania huxleyi* CCMP 373 isolated from the Sargasso Sea (Steinke et al. 1998). Based on the chemotaxonomic pigment analyses, the relative abundance of the prymnesiophytes was high at the Sargasso stations during our study. Thus, the presence of high-lyase prymnesiophytes, or other algae, combined with acclimation to nutrient poor and high-light conditions, may have contributed to the high DLA:Chl *a* and the high DMS:Chl *a* found in these oligotrophic waters.

In summary, biomass-specific DLA in marine plankton appears to be high when exposure to solar radiation is high and when nutrient availability is low, but other factors may be involved as well. Because the DLA in plankton is very high, it should contribute significantly to DMS production in the water column; however, further work will be needed to understand what factors control the production of DMSP lyases and how their activities are regulated in situ. Our DLA results are consistent with recently proposed functions for DMSP lyases in important physiological processes, such as antioxidant defenses and photosynthetic overflow metabolism. Our understanding of DLA is still limited and more research is needed to understand the physiological and geochemical roles of DMSP lyases.

Acknowledgements

This research was funded by NSF grants OCE-9907471 and OCE-0221122 and by the National Center for Coastal Ocean Science, National Ocean Service, National Oceanic and Atmospheric Administration. We thank the captain and crew of the R/V *Oceanus*, as well as other cruise participants, Rafel Simó, Maria Vila, Diedre Toole, Doris Slezak, Jody Bruton, Rex Malmstrom, and Alison Buchan. We are especially grateful to Dierdre Toole for providing us with algal pigment data and to Rafel Simó and Maria Vila for sharing DMS production rates.

References

Bates, T.S., Charlson, R.J., and Gammon, R.H. 1987. Evidence for the climatic role of marine biogenic sulphur. Nature (Lond.), **329**: 319–321.

Bates, T.S., Lamb, B.K., Guenther, A., Dignon, J., and Stoiber, R.E. 1992. Sulfur emissions to the atmosphere from natural sources. J. Atmos. Chem. **14**: 315–337.

Belviso, S., Buat-Menard, P., Putaud, J.-P., Nguyen, B., Claustre, H., and Neveux, J. 1993. Size distribution of dimethylsulfoniopropionate (DMSP) in areas of the tropical northeastern Atlantic Ocean and the Mediterranean Sea. Mar. Chem. **44**: 55–71.

Bidigare, R.R., and Trees, C.C. 2000. HPLC phytoplankton pigments: sampling, laboratory methods, and quality assurance procedures. *In* Ocean optics protocols for satellite ocean color sensor validation. Revision 2. Chap. 14. *Edited by* G.S. Fargion and J.L. Mueller. NASA TM 2000-209966, Goddard Space Flight Center, Greenbelt, Md. pp. 154–161.

Charlson, R.J., Lovelock, J.E., Andreae, M.O., and Warren, S.G. 1987. Oceanic phytoplankton, atmospheric sulfur, cloud albedo and climate. Nature (Lond.), **326**: 655–661.

Dacey, J.W.H., Howse, F.A., Michaels, A.F., and Wakeham, S.G. 1998. Temporal variability of dimethylsulfide and dimethylsulfoniopropionate in the Sargasso Sea. Deep-Sea Res. **45**: 2085–2104.

Grone, T., and Kirst, G.O. 1992. The effect of nitrogen deficiency, methionine and inhibitors of methionine metabolism on the DMSP contents of *Tetraselmis subcordiformis* (Stein). Mar. Biol. **112**: 497–503.

Keller, M.D., and Korjeff-Bellows, W. 1996. Physiological aspects of the production of dimethylsulfoniopropionate (DMSP) by marine phytoplankton. *In* Biological and environmental chemistry of DMSP and related sulfonium compounds. *Edited by* R.P. Kiene, P.T. Visscher, M.D. Keller, and G.O. Kirst. Plenum, New York. pp. 131–142.

Keller, M.D., Bellows, W.K., and Guillard, R.R.L. 1989. Dimethyl sulfide production in marine phytoplankton. *In* Biogenic sulfur in the environment. *Edited by* E. Saltzman and W.J. Cooper. American Chemical Society, New York. pp. 167–182.

Keller, M.D., Matrai, P.A., and Kiene, R.P. 1999*a*. Production of glycine betaine and dimethylsulfoniopropionate in marine phytoplankton: I. Batch cultures. Mar. Biol. **135**: 237–248.

Keller, M.D., Kiene, R.P., Matrai, P.A., and Bellows, W.K. 1999*b*. Production of glycine betaine and dimethylsulfoniopropionate in marine phytoplankton: II. N-limited chemostat cultures. Mar. Biol. **135**: 249–257.

Kiene, R.P., and Linn, L.J. 2000. The fate of dissolved dimethylsulfoniopropionate (DMSP) in seawater: tracer studies using ^{35}S-DMSP. Geochim. Cosmochim. Acta, **64**: 2797–2810.

Kiene, R.P., and Service, S.K. 1991. Decomposition of dissolved DMSP and DMS in estuarine waters: dependence on temperature and substrate concentration. Mar. Ecol. Prog. Ser. **76**: 1–11.

Ledyard, K.M., and Dacey, J.W.H. 1994. Dimethylsulfide production from dimethylsulfoniopropionate by a marine bacterium. Mar. Ecol. Prog. Ser. **110**: 95–103.

Lesser, M.P. 1996. Acclimation of phytoplankton to UV-B radiation: oxidative stress and photoinhibition of photosynthesis are not prevented by UV-absorbing compounds in the dinoflagellate *Prorocentrum micans*. Mar. Ecol. Prog. Ser. **132**: 287–297.

Litchman, E., Neale, P.J., and Banaszak, A.T. 2002. Increased sensitivity to ultraviolet radiation in nitrogen-limited dinoflagellates: photoprotection and photorepair. Limnol. Oceanogr. **47**: 86–94.

Mackey, M.D., Mackey, D.J., Higgins, H.W., and Wright, S.W. 1996. CHEMTAX — a program for estimating class abundances

© 2004 NRC Canada

from chemical markers: application to HPLC measurements of phytoplankton. Mar. Ecol. Prog. Ser. **144**: 265–283.

Malin, G., Wilson, W.H., Bratbak, G., Liss, P.S., and Mann, N.H. 1998. Elevated production of dimethylsulfide resulting from viral infection of cultures of *Phaeocystis pouchetii*. Limnol. Oceanogr. **43**: 1389–1393.

Niki, T., Kunugi, M., and Otsuki, A. 2000. DMSP-lyase activity in five phytoplankton species: its potential importance in DMS production. Mar. Biol. **136**: 759–764.

Scarratt, M., Cantin, G., Levasseur, M., and Michaud, S. 2000. Particle size-fractionated kinetics of DMS production: where does DMSP cleavage occur at the microscale? J. Sea Res. **43**: 245–252.

Simó, R., and Pedrós-Alió, C. 1999. Role of vertical mixing in controlling the oceanic production of dimethyl sulphide. Nature (Lond.), **402**: 396–399.

Stefels, J. 2000. Physiological aspects of the production and conversion of DMSP in marine algae and higher plants. J. Sea Res. **43**: 183–197.

Stefels, J., and VanBoekel, W.H.M. 1993. Production of DMS from dissolved DMSP in axenic cultures of the marine phytoplankton species *Phaeocystis* sp. Mar. Ecol. Prog. Ser. **97**: 11–18.

Steinberg, D.K., Carlson, C.A., Bates, N.R., Johnson, R.J., Michaels, A.F., and Knap, A.H. 2001. Overview of the US JGOFS Bermuda Atlantic Time-series Study (BATS): a decade-scale look at ocean biology and biogeochemistry. Deep-Sea Res. II. Top. Stud. Oceanogr. **48**: 1405–1447.

Steinke, M., Daniel, C., and Kirst, G.O. 1996. DMSP lyase in marine micro- and macroalgae: intraspecific differences in cleavage activity. *In* Biological and environmental chemistry of DMSP and related sulfonium compounds. *Edited by* R.P. Kiene, P.T. Visscher, M.D. Keller, and G.O. Kirst. Plenum, New York. pp. 317–324.

Steinke, M., Wolfe, G.V., and Kirst, G.O. 1998. Partial characterization of dimethylsulfoniopropionate (DMSP) lyase isozymes in 6 strains of *Emiliania huxleyi*. Mar. Ecol. Prog. Ser. **175**: 215–225.

Steinke, M., Malin, G., Turner, S.M., and Liss, P.S. 2000. Determinations of dimethylsulfoniopropionate (DMSP) lyases activity using headspace analysis of dimethylsulphide (DMS). J. Sea Res. **43**: 233–244.

Steinke, M., Malin, G., Archer, S.D., Burkill, P.H., and Liss, P.S. 2002*a*. DMS production in a coccolithophorid bloom: evidence for the importance of dinoflagellate DMSP lyases. Aquat. Microb. Ecol. **26**: 259–270.

Steinke, M., Malin, G., Gibb, S.W., and Burkill, P.H. 2002*b*. Vertical and temporal variability of DMSP lyase activity in a coccolithophorid bloom in the northern North Sea. Deep-Sea Res. **49**: 3001–3016.

Strickland, J.D.H., and Parsons, T.R. 1968. A practical handbook of seawater analysis. Fish. Res. Board Can. Bull. No. 167.

Sunda, W., Kieber, D.J., Kiene, R.P., and Huntsman, S. 2002. An antioxidant function for DMSP and DMS in marine algae. Nature (Lond.), **418**: 317–320.

Wolfe, G.V., Steinke, M., and Kirst, G.O. 1997. Grazing-activated chemical defense in a unicellular marine alga. Nature (Lond.), **387**: 894–897.

Wolfe, G.V., Strom, S.L., Holmes, J.L., Radzio, T., and Olson, M.B. 2002. Dimethylsulfoniopropionate cleavage by marine phytoplankton in response to mechanical, chemical, or dark stress. J. Phycol. **38**: 1–14.

Wright, S.W., Jeffrey, S.W., Mantoura, R.F.C., Llewellyn, C.A., Bjornland, T., Repeta, D., and Welschmeyer, N. 1991. Improved HPLC method for the analysis of chlorophylls and carotenoids from marine phytoplankton. Mar. Ecol. Prog. Ser. **77**: 183–196.

© 2004 NRC Canada

Influence of dinoflagellate diurnal vertical migrations on dimethylsulfoniopropionate and dimethylsulfide distribution and dynamics (St. Lawrence Estuary, Canada)[1]

Anissa Merzouk, Maurice Levasseur, Michael Scarratt, Sonia Michaud, and Michel Gosselin

Abstract: The influence of the diurnal vertical migration of the dinoflagellates *Alexandrium tamarense* and *Scrippsiella trochoidea* on dimethylsulfoniopropionate (DMSP) and dimethylsulfide (DMS) dynamics was studied during a 34-h Lagrangian experiment in the St. Lawrence Estuary in July 2000. Particulate DMSP ($DMSP_p$), dissolved DMSP ($DMSP_d$), and DMS exhibited diel patterns with minimum concentrations during the night and maximum concentrations around noon. $DMSP_p$ concentrations were correlated with the abundance of the two vertically migrating DMSP-rich dinoflagellates. The $DMSP_p$:Chl *a* ratio exhibited similar diel variations, suggesting a light-induced de novo DMSP synthesis during the day. Diel variations of the DMS:Chl *a* ratio suggest that the accumulation of DMS around noon resulted from physiological responses of the algae and (or) bacteria to light. Biological gross DMS production and bacterial DMS consumption were decoupled, leading to rapid fluctuations in DMS. These results show that in systems dominated by DMSP-rich dinoflagellates containing DMSP lyases, DMS concentrations may vary by as much as a factor of 10 over a 24-h period. Such diel variations must be considered when estimating the contribution of such systems to the DMS sea to air flux.

Résumé : Nous avons étudié l'influence de la migration verticale journalière des dinoflagellés *Alexandrium tomarense* et *Scrippsiella trochoidea* sur la dynamique du déméthylsulfoniopropionate (DMSP) et du sulfure de diméthyle (DMS) dans une expérience de type lagrangien de 34 h dans l'estuaire du Saint-Laurent en juillet 2000. Le DMSP particulaire ($DMSP_p$), le DMSP dissous ($DMSP_d$) et le DMS suivent tous des patterns journaliers avec des concentrations minimales durant la nuit et des concentrations maximales vers midi. Les concentrations de $DMSP_p$ sont en corrélation avec l'abondance des deux dinoflagellés à migration verticale qui sont riches en DMSP. Le rapport $DMSP_p$:Chl *a* suit des variations journalières semblables, ce qui indique une néosynthèse de DMSP induite par la lumière durant le jour. Les variations journalières du rapport DMS:Chl *a* indiquent que l'accumulation de DMS vers midi résulte de réactions physiologiques des algues et (ou) des bactéries à la lumière. La production biologique brute de DMS et la consommation bactérienne de DMS sont déphasées, ce qui entraîne des fluctuations rapides de DMS. Ces résultats démontrent que dans les systèmes dominés par des dinoflagellés riches en DMSP et contenant des DMSP lyases, les concentrations de DMS peuvent varier par un facteur allant jusqu'à 10 au cours d'une période 24 h. On doit tenir compte de ces variations journalières lorsqu'on estime la contribution de tels systèmes au flux de DMS de la mer à l'atmosphère.

[Traduit par la Rédaction]

Introduction

The production of the climatically active gas dimethylsulfide (DMS) in the ocean is controlled by several biological processes acting on different time scales. At mid- and high latitudes, maximum DMS concentrations are generally measured during the summer when the plankton community is dominated by strong producers of dimethylsulfoniopropionate (DMSP) (the algal precursor of DMS) and by a rapid turnover rate of the algal biomass (Kwint and Kramer 1996;

Received 14 March 2003. Accepted 13 March 2004. Published on the NRC Research Press Web site at http://cjfas.nrc.ca on 22 June 2004.
J17404

A. Merzouk[2] and M. Levasseur. Université Laval, Département de biologie (Québec-Océan), Pavillon Alexandre-Vachon, Québec, QC G1K 7P4, Canada.
M. Scarratt and S. Michaud. Fisheries and Oceans Canada, Maurice Lamontagne Institute, 850 Route de la mer, Mont-Joli, QC G5H 3Z4, Canada.
M. Gosselin. Institut des sciences de la mer à Rimouski (ISMER), Université du Québec à Rimouski, 310 Allée des Ursulines, Rimouski, QC G5L 3A1, Canada.

[1]This paper is part of the proceedings of the Third International Symposium on Biological and Environmental Chemistry of DMS(P) and Related Compounds, held in Rimouski (Québec), 26–28 September 2002.
[2]Corresponding author (e-mail: anissa.merzouk@giroq.ulaval.ca).

 doi: 10.1139/F04-066 © 2004 NRC Canada

Dacey et al. 1998; Kettle et al. 1999). The summer period is also marked by important variations in DMS concentrations on time scales of several days, with DMS peaks coinciding with the collapse of algal blooms and the release of DMSP in the environment (Matrai and Keller 1993; Dacey et al. 1998; Van Duyl et al. 1998). Recent studies have also reported large fluctuations in DMSP and DMS concentrations on hourly time scales. Causes for these rapid variations are not well understood but there are indications that they can result from vertical migration of dinoflagellates, physiological responses to the light regime, and impact of light on bacterial utilization of DMSP and DMS.

The diurnal vertical migration of dinoflagellates may generate short-term (hourly) variations in particulate DMSP ($DMSP_p$) concentrations. Some phytoplankton species, and dinoflagellates in particular, can perform diurnal vertical migrations, allowing them to efficiently use nutrients at depth during the night and solar radiation close to the surface during the day (Margalef 1978; Cullen and McIntyre 1998). Dinoflagellates are known for their high DMSP content (Keller et al. 1989), and short-term variations in the concentrations of $DMSP_p$ in surface waters of the Mediterranean Sea have been previously associated with vertical migration of dinoflagellates (Belviso et al. 2000). Several dinoflagellate species also possess DMSP lyase, the enzyme responsible for the cleavage of DMSP into DMS and acrylate. Consequently, dinoflagellates are often associated with high DMSP lyase activity (Steinke et al. 2002) and high DMS concentrations (Scarratt et al. 2002) in the ocean. Diel variations in the location of the dinoflagellates in the water column may thus result in important changes in both DMSP and DMS pool size.

DMSP and DMS variations on hourly time scales may also reflect physiological responses of the algae to the environment. During a 24-h on-deck microcosm experiment, Simó et al. (2002) showed that DMSP synthesis by phytoplankton varied in parallel with primary production and reached a maximum at noon, suggesting that DMSP biosynthesis is a diurnal process coupled to photosynthesis. A close coupling between DMSP production and primary production has also been observed in the field (Archer et al. 2001; Simó et al. 2002). This coupling may result from the physiological properties of DMSP. It has been proposed that DMSP synthesis could act as an overflow mechanism allowing the dissipation of energy and reduced sulfur in high light but nutrient-limiting conditions (Stefels 2000). More recently, the increase in DMSP generally measured in microalgae submitted to harmful levels of UV radiation or nutrient limitation was attributed to the potential antioxidant properties of DMSP (Sunda et al. 2002). Since DMS shares the same antioxidant property as DMSP, DMSP lyase containing algae may produce more DMS under stressing conditions (Sunda et al. 2002). Diel variations in the intensity of solar radiation (and particularly UV) may thus have indirect effects on seawater DMSP and DMS concentrations by controlling algal DMSP and DMS synthesis.

Short-term variations in DMS concentrations may also result from variations in bacterial DMS production and consumption. Bacteria are thought to be responsible for most of the DMSP cleavage into DMS in the oceans. Bacteria use DMSP as a carbon or a sulfur source and their uptake of DMSP may vary rapidly depending on substrate availability and their physiological state (Kiene et al. 2000). Because some bacteria also consume DMS (Kiene 1992; Kiene and Bates 1990), the net bacterial production of DMS reflects the balance between the two processes, which are generally positively correlated (Simó et al. 1995; Wolfe et al. 1999). Simó and Pedros-Alió (1999) demonstrated for the first time that bacterial DMSP and DMS consumption may vary during the day. During a 24-h on-deck microcosm experiment using water from the North Atlantic, they measured decreases in bacterial DMSP consumption at dawn and DMS consumption in the afternoon and at night. Causes for these variations were not identified and the demonstration of their occurrence in situ is still lacking.

Each year, blooms of the dinoflagellates *Alexandrium tamarense* and *Scrippsiella trochoidea* co-occur in the St. Lawrence Estuary during the summer months. Previous studies have shown elevated DMSP quotas (Keller et al. 1989; Levasseur et al. 1995) and presence of DMSP lyases (Niki et al. 2000; Wolfe et al. 2002) in strains of these two species. In July 2000, a cruise was conducted in the lower St. Lawrence Estuary with the main objective of determining the capacity of *A. tamarense* to perform vertical migration (J. Fauchot, Institut des Sciences de la Mer de Rimouski, Université du Québec à Rimouski, 310 Allée des Ursulines, Rimouski, QC G5L 3A1, Canada, unpublished data). We took this opportunity to acquire information on the influence of the diurnal migration of these DMSP-rich dinoflagellates on the distribution and cycling of DMSP and DMS.

Material and methods

The study was conducted aboard the CCGS *Martha L. Black* in the lower St. Lawrence Estuary (Fig. 1) on 8 and 9 July 2000. A water mass with high concentrations of *A. tamarense* and *S. trochoidea* was localized through a series of short rosette casts. The water mass was then marked with a drifting buoy and followed for 34 h during calm conditions (see wind speeds, Fig. 2*d*). Samples were collected every 2 h near the drifting buoy from an inflatable boat (Zodiac) launched from the main ship (stations T0–T16, Fig. 1). The inflatable boat was used to minimize mixing of the water mass during sampling. Vertical profiles of temperature, salinity, and in vivo Chl *a* fluorescence were obtained for all stations with a conductivity–temperature–depth (CTD) meter and fluorometer. Water was collected with a 5-L Niskin bottle at the first subsurface in vivo fluorescence maximum (between 2 and 6 m). This sampling depth corresponded to the maximum abundance of dinoflagellates in the mixed layer. The water collected for DMS(P) concentrations and rates determinations was taken directly from the Niskin bottle and prescreened on 202-μm Nitex mesh to remove large grazers. For DMS(P) concentration determination, water samples were gently transferred into 66-mL brown polyethylene bottles, leaving no headspace. For the incubations, larger volumes (10 L) of water were collected every 4 h and transferred gently into 10-L insulated containers, leaving no headspace. Water samples were also collected for nutrients analyses and phytoplankton species identification.

© 2004 NRC Canada

Fig. 1. Map of the lower St. Lawrence Estuary with the trajectory of the drifting buoy and the locations of the sampling stations.

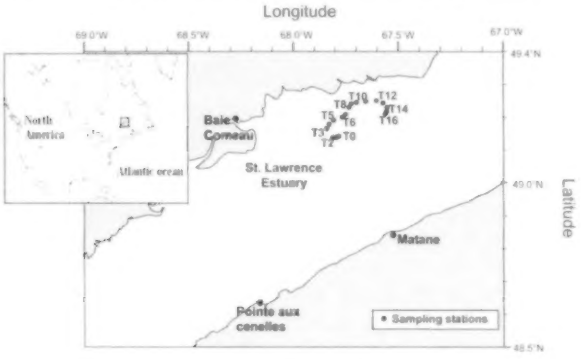

Phytoplankton abundances

Phytoplankton identification and enumeration were performed on samples preserved with acid Lugol using a settling column and inverted microscope. Total phytoplankton species were identified and enumerated for the water samples used for rate determinations, i.e., every 4 h at the subsurface fluorescence maximum.

DMS(P) concentrations

$DMSP_p$, dissolved DMSP ($DMSP_d$), and DMS concentrations were determined for all stations by gravity filtering 66-mL water samples through 47-mm Whatman GF/F filters (0.7 µm). For DMS samples, 24-mL serum bottles were filled with filtrate leaving no headspace, sealed with butyl septa, and crimped with aluminium seals. DMS samples were analysed within minutes of sampling. For $DMSP_d$ samples, 24-mL serum bottles were filled with 23 mL of filtrate and 1 mL of 10 mol·L^{-1} KOH solution, and sealed. For $DMSP_p$ samples, the filters were put in 24-mL serum bottles containing 23 mL of deionized water and 1 mL of 10 mol·L^{-1} KOH solution and sealed. All DMSP samples were stored at 4 °C in the dark and analysed within 4 weeks of collection. Sulfur gas analyses were performed using a purge and trap system coupled to a Varian 3400 gas chromatograph (see Scarratt et al. (2000) for details). DMSP samples were calibrated with a 5 ng DMSP·mL^{-1} standard prepared in 14-mL serum bottles containing 0.6 mL of 10 mol·L^{-1} KOH solution. DMS samples were calibrated against 46- to 912-µL injections of helium containing approximately 12 ng DMS·mL^{-1}, prepared using a permeation tube (KinTek). The quantification limits of the method were 0.04 nmol·L^{-1} for DMS and $DMSP_d$ and 0.008 nmol·L^{-1} for $DMSP_p$.

DMS production and consumption rates

DMS production and bacterial DMS consumption rates were determined every 4 h during on-deck dark incubations using water from the subsurface fluorescence maximum. Ten incubation bottles (66-mL brown polyethylene bottles with screwcaps), prerinsed with HCl, were filled with seawater, leaving no headspace. Four bottles were amended with methyl butyl ether (MBE) (30 µmol·L^{-1} final concentration), a specific inhibitor of bacterial DMS consumption (Visscher and Taylor 1993). Two unamended incubation bottles were immediately used for time zero values for both the control and the MBE treatment. The remaining bottles (four unamended controls and four containing MBE) were incubated in the dark in a thermostatic bath within 2.4 °C of in situ temperature. After 2 and 4 hours, duplicate bottles of both control and MBE treatments were gently mixed, gravity filtered, and analysed for $DMSP_p$, $DMSP_d$, and DMS concentrations, as described above. DMS production rates were determined from linear regressions of DMS concentrations versus time. The rates of bacterial DMS consumption were obtained from the difference in DMS production rates in the bottles with inhibitor (gross DMS production) and without inhibitor (net DMS production).

Results

Oceanographic setting

The Lagrangian experiment was characterized by sunny weather (Fig. 2) and very low wind speeds on 8 July (<2 m·s^{-1}) with a gradual increase on 9 July (Fig. 2*b*). The physical and biochemical characteristics of the water column during the study were typical of summer conditions for the St. Lawrence Estuary (Levasseur et al. 1984; Therriault and Levasseur 1985). The surface mixed layer, best delimited by the depth of the thermocline (Fig. 2*d*), varied between 10 and 15 m and was characterized by less saline (27–29 psu) and warmer (10–12 °C) water (Figs. 2*c* and 2*d*). In the upper 15 m of the water column, macronutrients concentrations were low (NO_3 < 0.3 µmol·L^{-1}, PO_4 < 0.3 µmol·L^{-1}, and SiO_4 < 1.5 µmol·L^{-1}; data not shown) and Chl *a* concentrations calculated from fluorescence were lower than 15 mg·m^{-3} (Fig. 2*e*). A sharp, deep chlorophyll maximum was observed at the thermocline (Fig. 2*e*).

Dinoflagellates, DMS(P) concentrations, and DMS(P):Chl *a* ratios

Throughout the time series, the phytoplankton community was dominated by diatoms (36–64% of total phytoplankton cell abundances), with flagellate and dinoflagellate contributions ranging from 24% to 40% and from 4% to 12% of the total cell abundances, respectively (data not shown). Most of the diatoms were concentrated in the deep fluorescence maximum located at the thermocline at approximately 10–15 m. The dinoflagellate assemblage was dominated by the species *A. tamarense*, *S. trochoidea*, and *Heterocapsa triquetra*, which were found mostly in the mixed layer where they formed a distinct subsurface fluorescence peak during the day, always shallower than the deep fluorescence maximum. The three dinoflagellate species exhibited diurnal vertical migrations during the sampling period (J. Fauchot, Institut des Sciences de la Mer à Rimouski, Université du Québec à Rimouski, 310 Allée des Ursulines, Rimouski, QC G5L 3A1, Canada, unpublished data). Their concentrations were low during the night in the upper mixed layer, increased during the morning to reach 60 000 cells·L^{-1} at 1000, and decreased more or less gradually during the afternoon to reach very low concentrations again during the night (Fig. 3*a*).

$DMSP_p$ concentrations varied between 4 and 122 nmol·L^{-1} and exhibited a diel pattern with maximum values measured

© 2004 NRC Canada

Fig. 2. Solar irradiance, wind speed, and structure of the water column during the Lagrangian experiment: (*a*) solar irradiance; (*b*) wind speed; (*c*) salinity (psu); (*d*) temperature (°C); (*e*) Chl *a* concentration (mg·m^{-3}) and sampling depths (circles). Grey areas represent the night.

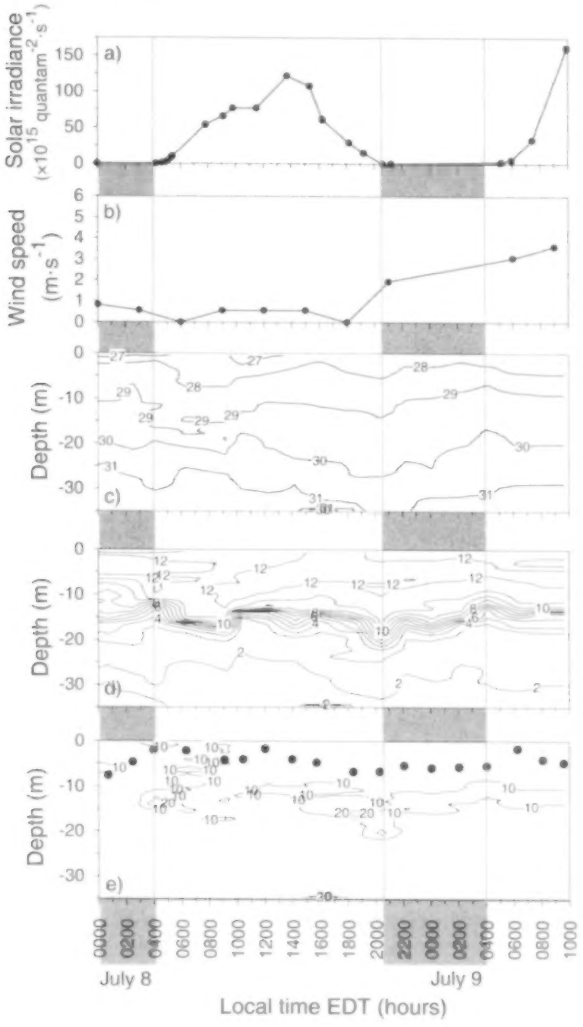

during the day (Fig. 3*b*). $DMSP_d$ concentrations varied between 2 and 11 nmol·L^{-1} and exhibited diel variations on 8 July with the highest concentrations during the day (Fig. 3*c*). DMS concentrations ranged from 0.6 to 6.2 nmol·L^{-1} and exhibited important short-term variations (Fig. 3*d*). DMS concentrations were below 2 nmol·L^{-1} during the night, increased during the morning and reached 4.5 nmol·L^{-1} around noon, decreased during the afternoon to reach 0.5 nmol·L^{-1} at 1800, and increased again to reach 4 nmol·L^{-1} during the evening. The evening peak in DMS concentrations was followed by a rapid decrease during the night.

Among all phytoplankton species present, $DMSP_p$ concentrations exhibited significant correlations only with the

Fig. 3. Temporal variations of dinoflagellates abundance and DMS(P) pools at the surface (<10 m): (*a*) abundances of the dinoflagellates *A. tamarense* (solid bars), *S. trochoidea* (open bars), and *H. triquetra* (hatched bars); total of three dinoflagellates (circles); (*b*) $DMSP_p$ concentrations; (*c*) $DMSP_d$ concentrations; (*d*) DMS concentrations. Error bars are the standard deviations of duplicate samples. Grey areas represent the night.

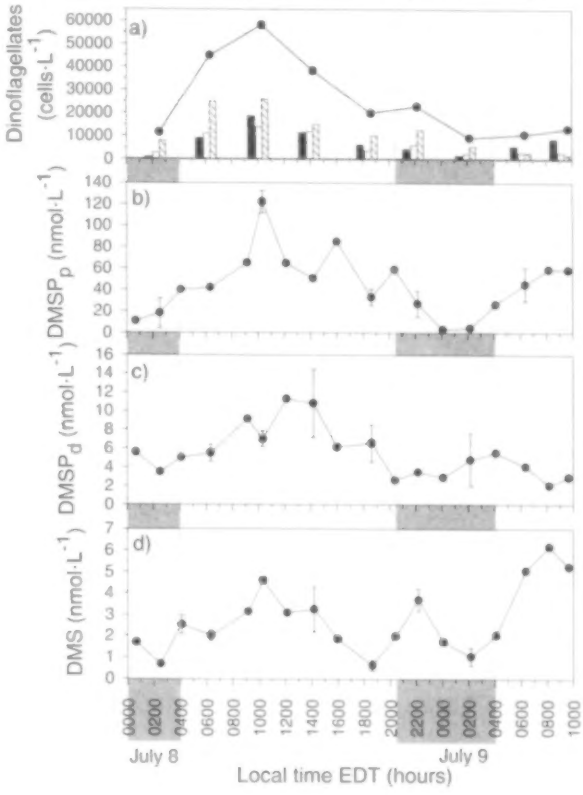

dinoflagellates *A. tamarense* and *S. trochoidea*, and $DMSP_d$ concentrations were significantly correlated only with *S. trochoidea*. DMS concentrations were significantly correlated with $DMSP_p$ concentrations (Table 1). No other phytoplankton taxa were correlated with either $DMSP_d$ or DMS.

The $DMSP_p$:Chl *a* and DMS:Chl *a* ratios varied between 1 and 16 mmol·g^{-1} and between 0.05 and 1.1 mmol·g^{-1}, respectively (Fig. 4*a*). The two ratios tended to vary in parallel, exhibiting minimum values at night and maximum values around noon. An increase in both ratios was also measured during the evening on 8 July. Chl *a* concentrations remained relatively constant during the sampling period, indicating that the variations in the ratios were mostly due to variations in $DMSP_p$ and DMS concentrations (Fig. 4*b*).

DMS production and consumption rates

The characteristics of the water incubated for biological rate determinations are presented in Table 2. Net DMS production ranged between –0.27 and 0.33 nmol·L^{-1}·h^{-1} with no net change measured during the first morning, a net DMS consumption measured at 1000 and 1400, and rates alternat-

© 2004 NRC Canada

Fig. 1. Map of the lower St. Lawrence Estuary with the trajectory of the drifting buoy and the locations of the sampling stations.

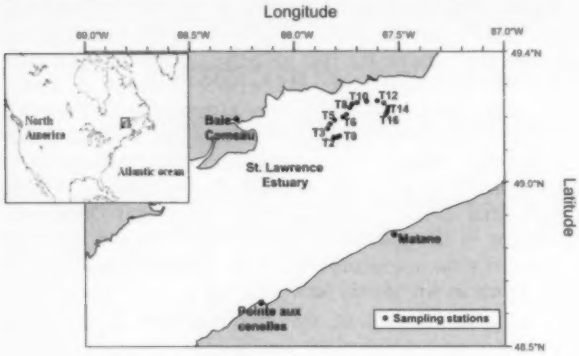

Phytoplankton abundances

Phytoplankton identification and enumeration were performed on samples preserved with acid Lugol using a settling column and inverted microscope. Total phytoplankton species were identified and enumerated for the water samples used for rate determinations, i.e., every 4 h at the subsurface fluorescence maximum.

DMS(P) concentrations

$DMSP_p$, dissolved DMSP ($DMSP_d$), and DMS concentrations were determined for all stations by gravity filtering 66-mL water samples through 47-mm Whatman GF/F filters (0.7 µm). For DMS samples, 24-mL serum bottles were filled with filtrate leaving no headspace, sealed with butyl septa, and crimped with aluminium seals. DMS samples were analysed within minutes of sampling. For $DMSP_d$ samples, 24-mL serum bottles were filled with 23 mL of filtrate and 1 mL of 10 mol·L^{-1} KOH solution, and sealed. For $DMSP_p$ samples, the filters were put in 24-mL serum bottles containing 23 mL of deionized water and 1 mL of 10 mol·L^{-1} KOH solution and sealed. All DMSP samples were stored at 4 °C in the dark and analysed within 4 weeks of collection. Sulfur gas analyses were performed using a purge and trap system coupled to a Varian 3400 gas chromatograph (see Scarratt et al. (2000) for details). DMSP samples were calibrated with a 5 ng DMSP·mL^{-1} standard prepared in 14-mL serum bottles containing 0.6 mL of 10 mol·L^{-1} KOH solution. DMS samples were calibrated against 46- to 912-µL injections of helium containing approximately 12 ng DMS·mL^{-1}, prepared using a permeation tube (KinTek). The quantification limits of the method were 0.04 nmol·L^{-1} for DMS and $DMSP_d$ and 0.008 nmol·L^{-1} for $DMSP_p$.

DMS production and consumption rates

DMS production and bacterial DMS consumption rates were determined every 4 h during on-deck dark incubations using water from the subsurface fluorescence maximum. Ten incubation bottles (66-mL brown polyethylene bottles with screwcaps), prerinsed with HCl, were filled with seawater, leaving no headspace. Four bottles were amended with methyl butyl ether (MBE) (30 µmol·L^{-1} final concentration), a specific inhibitor of bacterial DMS consumption (Visscher and Taylor 1993). Two unamended incubation bottles were immediately used for time zero values for both the control and the MBE treatment. The remaining bottles (four unamended controls and four containing MBE) were incubated in the dark in a thermostatic bath within 2.4 °C of in situ temperature. After 2 and 4 hours, duplicate bottles of both control and MBE treatments were gently mixed, gravity filtered, and analysed for $DMSP_p$, $DMSP_d$, and DMS concentrations, as described above. DMS production rates were determined from linear regressions of DMS concentrations versus time. The rates of bacterial DMS consumption were obtained from the difference in DMS production rates in the bottles with inhibitor (gross DMS production) and without inhibitor (net DMS production).

Results

Oceanographic setting

The Lagrangian experiment was characterized by sunny weather (Fig. 2*a*) and very low wind speeds on 8 July (<2 m·s^{-1}) with a gradual increase on 9 July (Fig. 2*b*). The physical and biochemical characteristics of the water column during the study were typical of summer conditions for the St. Lawrence Estuary (Levasseur et al. 1984; Therriault and Levasseur 1985). The surface mixed layer, best delimited by the depth of the thermocline (Fig. 2*d*), varied between 10 and 15 m and was characterized by less saline (27–29 psu) and warmer (10–12 °C) water (Figs. 2*c* and 2*d*). In the upper 15 m of the water column, macronutrients concentrations were low (NO_3 < 0.3 µmol·L^{-1}, PO_4 < 0.3 µmol·L^{-1}, and SiO_4 < 1.5 µmol·L^{-1}; data not shown) and Chl *a* concentrations calculated from fluorescence were lower than 15 mg·m^{-3} (Fig. 2*e*). A sharp, deep chlorophyll maximum was observed at the thermocline (Fig. 2*e*).

Dinoflagellates, DMS(P) concentrations, and DMS(P):Chl *a* ratios

Throughout the time series, the phytoplankton community was dominated by diatoms (36–64% of total phytoplankton cell abundances), with flagellate and dinoflagellate contributions ranging from 24% to 40% and from 4% to 12% of the total cell abundances, respectively (data not shown). Most of the diatoms were concentrated in the deep fluorescence maximum located at the thermocline at approximately 10–15 m. The dinoflagellate assemblage was dominated by the species *A. tamarense*, *S. trochoidea*, and *Heterocapsa triquetra*, which were found mostly in the mixed layer where they formed a distinct subsurface fluorescence peak during the day, always shallower than the deep fluorescence maximum. The three dinoflagellate species exhibited diurnal vertical migrations during the sampling period (J. Fauchot, Institut des Sciences de la Mer à Rimouski, Université du Québec à Rimouski, 310 Allée des Ursulines, Rimouski, QC G5L 3A1, Canada, unpublished data). Their concentrations were low during the night in the upper mixed layer, increased during the morning to reach 60 000 cells·L^{-1} at 1000, and decreased more or less gradually during the afternoon to reach very low concentrations again during the night (Fig. 3*a*).

$DMSP_p$ concentrations varied between 4 and 122 nmol·L^{-1} and exhibited a diel pattern with maximum values measured

© 2004 NRC Canada

Fig. 2. Solar irradiance, wind speed, and structure of the water column during the Lagrangian experiment: (*a*) solar irradiance; (*b*) wind speed; (*c*) salinity (psu); (*d*) temperature (°C); (*e*) Chl *a* concentration (mg·m^{-3}) and sampling depths (circles). Grey areas represent the night.

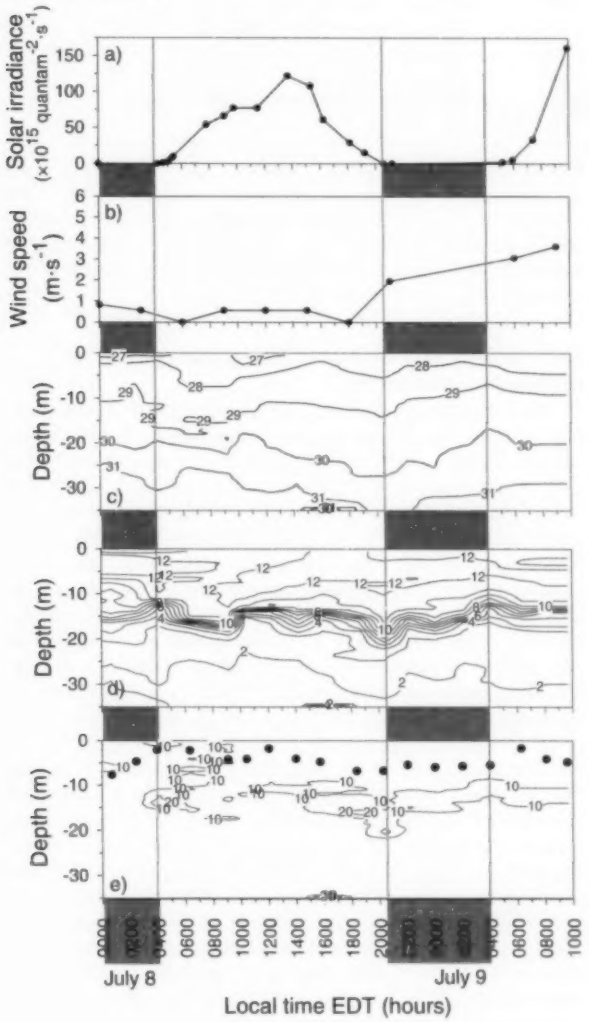

during the day (Fig. 3*b*). $DMSP_d$ concentrations varied between 2 and 11 nmol·L^{-1} and exhibited diel variations on 8 July with the highest concentrations during the day (Fig. 3*c*). DMS concentrations ranged from 0.6 to 6.2 nmol·L^{-1} and exhibited important short-term variations (Fig. 3*d*). DMS concentrations were below 2 nmol·L^{-1} during the night, increased during the morning and reached 4.5 nmol·L^{-1} around noon, decreased during the afternoon to reach 0.5 nmol·L^{-1} at 1800, and increased again to reach 4 nmol·L^{-1} during the evening. The evening peak in DMS concentrations was followed by a rapid decrease during the night.

Among all phytoplankton species present, $DMSP_p$ concentrations exhibited significant correlations only with the

Fig. 3. Temporal variations of dinoflagellates abundance and DMS(P) pools at the surface (<10 m): (*a*) abundances of the dinoflagellates *A. tamarense* (solid bars), *S. trochoidea* (open bars), and *H. triquetra* (hatched bars); total of three dinoflagellates (circles); (*b*) $DMSP_p$ concentrations; (*c*) $DMSP_d$ concentrations; (*d*) DMS concentrations. Error bars are the standard deviations of duplicate samples. Grey areas represent the night.

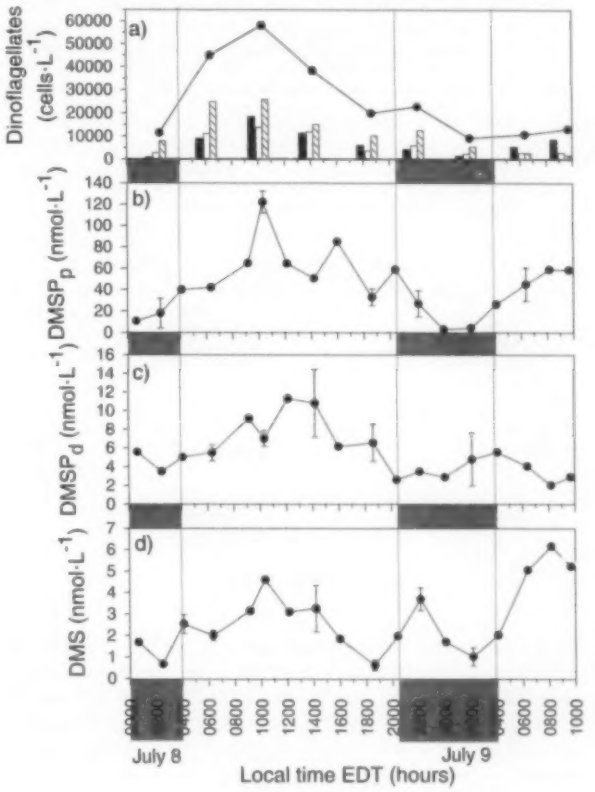

dinoflagellates *A. tamarense* and *S. trochoidea*, and $DMSP_d$ concentrations were significantly correlated only with *S. trochoidea*. DMS concentrations were significantly correlated with $DMSP_p$ concentrations (Table 1). No other phytoplankton taxa were correlated with either $DMSP_d$ or DMS.

The $DMSP_p$:Chl *a* and DMS:Chl *a* ratios varied between 1 and 16 mmol·g^{-1} and between 0.05 and 1.1 mmol·g^{-1}, respectively (Fig. 4*a*). The two ratios tended to vary in parallel, exhibiting minimum values at night and maximum values around noon. An increase in both ratios was also measured during the evening on 8 July. Chl *a* concentrations remained relatively constant during the sampling period, indicating that the variations in the ratios were mostly due to variations in $DMSP_p$ and DMS concentrations (Fig. 4*b*).

DMS production and consumption rates

The characteristics of the water incubated for biological rate determinations are presented in Table 2. Net DMS production ranged between –0.27 and 0.33 nmol·L^{-1}·h^{-1} with no net change measured during the first morning, a net DMS consumption measured at 1000 and 1400, and rates alternat-

© 2004 NRC Canada

Table 1. Pearson's correlation coefficients of regressions between in situ DMS(P) concentrations and abundances of various phytoplankton species during the Lagrangian experiment.

	$DMSP_p$ (nmol·L^{-1})	$DMSP_d$ (nmol·L^{-1})	DMS (nmol·L^{-1})
$DMSP_d$ (nmol·L^{-1}) (n = 18)	0.33 ns		
DMS (nmol·L^{-1}) (n = 18)	0.51 *	0.09 ns	
Alexandrium tamarense (cells·L^{-1}) (n = 9)	0.95 **	0.55 ns	0.54 ns
Scrippsiella trochoidea (cells·L^{-1}) (n = 9)	0.68 *	0.69 *	0.23 ns
Heterocapsa triquetra (cells·L^{-1}) (n = 9)	0.55 ns	0.50 ns	0.04 ns

Note: Two-tailed tests: *, $0.01 < p \leq 0.05$; **, $p \leq 0.01$; ns, not significant.

Fig. 4. Temporal variations of DMS(P):Chl *a* ratios and Chl *a*: (*a*) $DMSP_p$:Chl *a* ratio (open circles) and DMS:Chl *a* ratio (solid circles); (*b*) Chl *a* concentration. Grey areas represent the night.

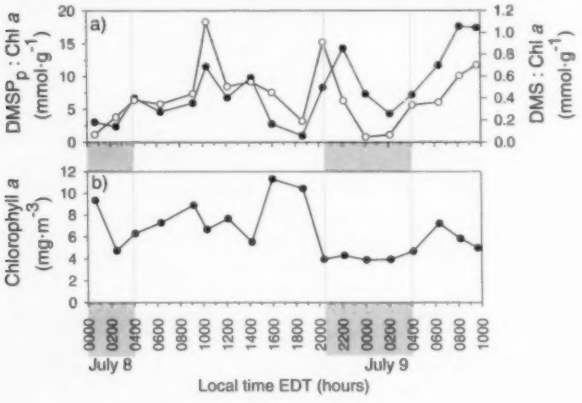

ing between net production and net consumption during the evening and night (Fig. 5*a*). DMS gross production rates varied between 0 and 0.55 nmol·L^{-1}·h^{-1} with a maximum measured in the evening (Fig. 5*b*). Bacterial DMS consumption was low (0.05 nmol·L^{-1}·h^{-1}) during the night on 8 July, increased progressively to reach a maximum of 0.33 nmol·L^{-1}·h^{-1} at 1400, remained at this level until 2200, and became undetectable at 0200 in the morning on 9 July (Fig. 5*b*).

The net biological DMS production rates measured during the dark incubations are compared with net DMS production rates calculated from changes in in situ DMS concentrations (Fig. 6*a*). The calculated (from in situ concentrations) and measured rates (from incubations) of DMS production exhibited similar patterns and were linearly related (as shown in Fig. 7; $r^2 = 0.85$; $p = 0.001$). However, the rates measured during the 4-h dark incubations systematically underestimated in situ DMS variations. When rates from the incubation experiments are multiplied by the regression coefficient of 2.9, they reproduce well the pattern of changes in DMS concentrations but still fail to reproduce the exact values, except for the evening peak (Fig. 6*b*).

Discussion

This study represents to our knowledge the first attempt to measure diel variations of DMS(P) pools and cycling processes in the field. Exceptionally calm and sunny conditions allowed us to follow for 34 h the vertical migration of two DMSP-rich dinoflagellate species, *A. tamarense* and *S. trochoidea*, and to determine their impact on DMS(P) concentrations and production. All sulfur pools and processes showed substantial short-term variations (on a time scale of hours), highlighting the complex and dynamic nature of the DMS(P) cycle.

Diel vertical migration of dinoflagellates and $DMSP_p$ distribution and synthesis

The vertical migration of the two dominant dinoflagellates had a significant impact on the distribution of $DMSP_p$ at the surface. $DMSP_p$ concentrations exhibited important diel variations characterized by minimum values at night and maximum values during the day, in phase with diurnal variations in the abundance of the vertically migrating dinoflagellates. The impact of the migration of *A. tamarense* and *S. trochoidea* on the $DMSP_p$ pool was expected, since these species are known to be strong DMSP producers, with cellular DMSP quotas measured for cultured strains of 265 and 384 pg·cell^{-1}, respectively (Keller et al. 1989). A similar DMSP quota of 274 pg·cell^{-1} was measured in an *A. tamarense* strain isolated from the study area (Levasseur et al. 1995). To estimate the potential contribution of these two dinoflagellates to the total $DMSP_p$ pool, we multiplied the published quotas for each species by their respective abundance. This rough calculation shows that despite being a minor component of the phytoplankton community (<3% of total phytoplankton abundance), the presence of the two dinoflagellates could explain between 33% and 100% of the total $DMSP_p$ measured. Their important contribution to the $DMSP_p$ pool coupled with the significant correlations existing between $DMSP_p$ concentrations and the abundance of these dinoflagellates indicates that their diurnal vertical migration was partly responsible for the observed diel changes in $DMSP_p$ in the surface mixed layer. These findings suggest that diurnal variations in $DMSP_p$ concentrations in surface waters owing to vertically migrating dinoflagellates are probably a frequent phenomenon that may have direct effects on the distribution and the dynamics of related sulfur compounds.

The diurnal vertical migration of the dinoflagellates may also have been accompanied by variations in DMSP synthesis rates. Evidences for de novo DMSP synthesis during the day can be best seen on the morning of 9 July when an important increase in $DMSP_p$ occurred without any coincident increase in dinoflagellate abundance. This hypothesis is further supported by the diel variations in $DMSP_p$:Chl *a* ratios which reached maximum values around noon on 8 July and increased during the morning on 9 July. This also agrees

© 2004 NRC Canada

Table 2. Physical and chemical characteristics of the water incubated for biological rate determinations.

Incubation	Sampling station	Date in 2000	Time	Depth (m)	Salinity (psu)	In situ temp. (°C)	Incubation temp. (°C)	Chl *a* ($mg \cdot m^{-3}$)	DMS ($nmol \cdot L^{-1}$)	$DMSP_d$ ($nmol \cdot L^{-1}$)	$DMSP_p$ ($nmol \cdot L^{-1}$)
1	T1	8 July	0230	4	28.4	12.4	10.0	4.7	0.7	3.5	18.0
2	T3	8 July	0622	2	27.4	11.4	10.0	7.3	2.0	5.5	41.9
3	T5	8 July	1020	4	27.4	11.5	10.0	6.7	4.6	7.0	122.2
4	T7	8 July	1412	4	28.3	12.7	12.0	4.5	3.2	10.8	50.6
5	T9	8 July	1838	6	28.4	12.1	12.0	10.4	0.6	6.6	33.0
6	T11	8 July	2210	5	28.3	12.5	12.0	4.3	3.7	3.5	27.0
7	T13	9 July	0210	5	28.5	12.2	12.0	3.9	1.0	4.8	4.3

Note: temp., temperature.

Fig. 5. Temporal variations of DMSP and DMS cycling rates obtained from 4-h dark incubations: (*a*) DMS net change; (*b*) DMS gross production (solid circles) and bacterial DMS consumption (open circles). Error bars are the standard error of regression slopes. Grey areas represent the night.

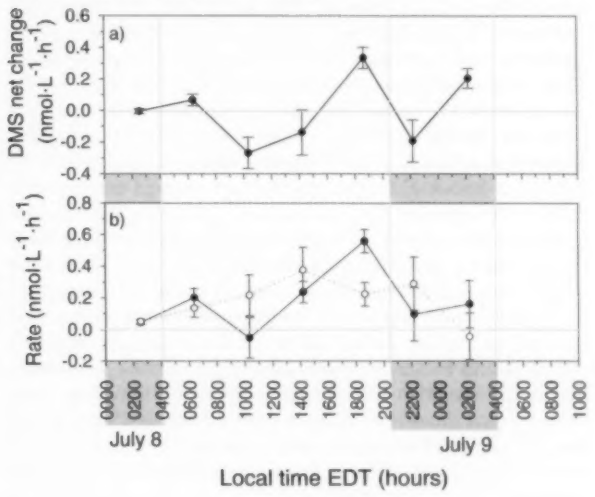

Fig. 6. Comparison of DMS net changes and DMS concentrations calculated by two different methods: (*a*) DMS net change measured during 4-h dark incubations (dotted line) and calculated from in situ DMS variations (solid line); (*b*) measured DMS concentrations (solid circles) and DMS concentrations ($nmol \cdot L^{-1}$) predicted from incubation rates (open circles). Grey areas represent the night.

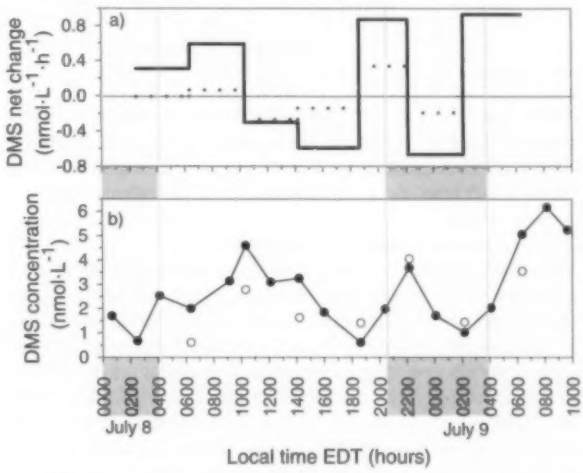

with studies showing that DMSP biosynthesis is a diurnal process coupled to photosynthesis and reaches maximum rates around noon (Archer et al. 2001; Simó et al. 2002). Diel covariations between dinoflagellates abundance and $DMSP_p$:Chl *a* ratios have also been observed in Barcelona Harbour (Belviso et al. 2000). In that case, the authors attributed the changes in the ratio entirely to variations in the composition of the phytoplankton assemblage owing to vertical migration of dinoflagellates. The diel variations in $DMSP_p$:Chl *a* ratios during this study could thus result from both de novo DMSP synthesis and vertical migration of the DMSP-rich dinoflagellates.

Diel variations in $DMSP_d$ concentrations

$DMSP_d$ concentrations were less variable than $DMSP_p$ but nevertheless exhibited diel variations on 8 July with values 2.5 times higher during the day than during the night. The covariation of the $DMSP_d$ pool with $DMSP_p$ and the significant correlation with *S. trochoidea* abundance suggest that the vertically migrating dinoflagellates were partly responsible for these variations. DMSP (and DMS, see below) may serve as an overflow mechanism for excess carbon (Stefels 2000) or reducing power in autotrophs (Sunda et al. 2002), with the excess DMSP being removed by exudation and cleavage to DMS. The peak in $DMSP_d$ measured on 8 July may thus result from a light-induced increase in algal synthesis and exudation of DMSP. Bacteria, which are sensitive to light, may also have contributed to the observed variations in $DMSP_d$. It has been recently shown that solar UV radiation may inhibit bacterial activity and growth during daytime, causing an accumulation of dissolved organic carbon (Gasol et al. 1998; Kuipers et al. 2000). DMSP-consuming bacteria seem to be sensitive to light as well, and Slezak et al. (2001) demonstrated reduced biological DMSP removal rate in samples exposed to natural surface solar radiation. Accumulation of $DMSP_d$ in surface water as observed on 8 July during our study may thus also result from the negative impact of solar radiation on DMSP-consuming bacteria. However, $DMSP_d$ did not accumulate during the morning of 9 July, while no increase in dinoflagellates was observed and very high solar intensities were measured, suggesting that the presence of the DMSP-rich dinoflagellates was essential. Whatever the mechanism(s) involved, these

© 2004 NRC Canada

Fig. 7. Linear relationship between DMS net change measured during 4-h dark incubations and calculated from in situ DMS variations. Open and solid circles represent daytime and nighttime values, respectively. The broken line represents the 1:1 line. $y = 2.93x + 0.18$; $r^2 = 0.85$, $p = 0.001$, $n = 7$.

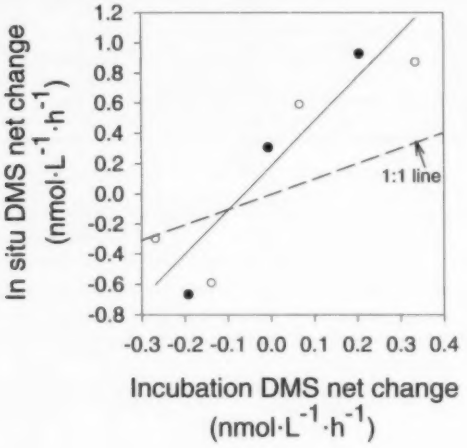

recent findings suggest that a light-induced disequilibrium between DMSP released from algal cells and bacterial $DMSP_d$ consumption may occur close to the surface during the day and lead to an accumulation of this compound.

Diel variations in DMS concentrations

DMS concentrations exhibited large and rapid short-term variations with maximum values more than seven times higher than minimum values. Like DMSP, DMS levels increased during the morning and decreased in the afternoon, suggesting either a direct link with solar radiation or an indirect effect through the migration of the dinoflagellates. DMS levels also peaked early in the night, a feature not seen in the DMSP pools, suggesting that another mechanism was at play.

The gradual increase in DMS concentrations during the morning and decrease during the afternoon suggest a light-induced response. The accumulation of DMS around noon is unexpected, since DMS loss by photooxidation should have been maximal at that time. DMS concentrations were correlated with $DMSP_p$, suggesting that the vertical migration of the DMSP producers was partly responsible for the rapid fluctuations in DMS concentrations. This covariation suggests a direct pathway of conversion from $DMSP_p$ to DMS and provides indirect evidence that *A. tamarense* and *S. trochoidea* strains from the St. Lawrence might also possess DMSP lyases like those tested by Wolfe et al. (2002) and Niki et al. (2000). Recent laboratory and field studies highlighted the important role played by dinoflagellate DMSP lyases in DMS production (Niki et al. 2000; Steinke et al. 2002). Sunda et al. (2002) recently proposed that DMSP and its breakdown products DMS and acrylate might have antioxidant properties. These compounds could efficiently scavenge harmful hydroxyl radicals (·OH) produced during photosynthesis in algal cells stressed by solar radiation or nutrient limitation. Taxa possessing DMSP lyases could furthermore enzymatically cleave DMSP into DMS and acrylate, since these compounds are even more effective antioxidants. The DMS produced could diffuse through cell membranes (Sunda et al. 2002), so that high DMS concentrations could be maintained in surface waters during the day when DMSP-rich algae possessing DMSP lyases are abundant. The antioxidant hypothesis may thus explain the peak in DMS measured around noon on 8 July and the increase in DMS measured during the morning on 9 July. Diel changes in DMS:Chl *a* ratios bring additional support to the hypothesis that the increase in DMS during the day resulted from a physiological response to irradiance by the dominant dinoflagellates. This is particularly true for the morning of 9 July when the DMS:Chl *a* ratio increased sharply, while no increases in the abundance of phytoplankton (reflected by Chl *a*) or of dinoflagellates were observed. This suggests that the increase in DMS is a physiological response of the algae to the increase in irradiance or, as discussed below, that the bacteria were responsible for the signal.

In addition to the light-induced increase in algal DMS production described above, the peak in DMS concentrations measured during the day may also result from photoinhibition of bacterial DMS consumption. Slezak et al. (2001) showed that solar radiation reduced the bacterial removal of DMS. Assuming that the negative effect of light persisted during the dark incubations, reduced biological DMS production and consumption during the day would be expected. Bacterial DMS consumption showed the opposite trend with high and low rates measured during the day and night, respectively. This suggests either that bacteria were not negatively impacted by light during the study or that the length of the dark incubations allowed a partial recovery of the light-induced damage to the bacteria. Although our current measurements do not allow for discrimination between the algal and bacterial responses to light, the large increase in DMS concentrations measured on both sampling days suggests that the effects of light on bacterial DMS consumption and algal production may have acted in synergy to create the large (factor 7) diel variations in DMS concentrations measured during our study.

The early-night peak in DMS

The strong peak in DMS and DMS:Chl *a* ratio measured at 2200 on 8 July could result from an increase of zooplankton grazing. Zooplankton were not sampled during this study but high concentrations of Euphausidiaceae were observed close to the surface at night from the inflatable boat. This confirms early measurements showing that the euphausids perform diurnal migration in the St. Lawrence accumulating close to the surface just after sunset (Simard et al. 1986). The sharp increase in DMSP:Chl *a* measured at 2000 just before the DMS peak could result from the presence of DMSP-rich zooplankters or fecal pellets. Laboratory and field studies have shown that copepods grazing on dinoflagellates could enhance DMS production by increasing the release of DMSP that become available for bacterial consumption (Dacey and Wakeham 1986; Christaki et al. 1996). Zooplankton grazing on algae with DMSP lytic capacity may also release the enzyme along with DMSP, resulting in an increase in DMS production independent of bacterial cleavage (Wolfe et al. 1997). These authors hypothesized that DMS and acrylate produced that way could serve as a chemical defence. The nighttime DMS peak could thus re-

© 2004 NRC Canada

sult from an increase in the grazing pressure by the migrating mesozooplankton.

Short-term variations in DMS production and consumption rates

As expected considering the large variations in DMS concentrations, DMS production and consumption rates also exhibited important short-term variability during our Lagrangian study. These variations were apparently not related to the availability of substrates. No significant relationships were found between DMS gross production and $DMSP_d$ concentrations ($r^2 = 0.08$, $p = 0.55$) or between DMS bacterial consumption and DMS concentrations ($r^2 = 0.41$, $p = 0.12$). We also found no significant relationship between DMS gross production and consumption ($r^2 = 0.03$, $p = 0.70$), indicating a decoupling between the two biological processes. These results contrast with studies reporting a tight coupling between DMS microbial consumption and production (Simó et al. 1995; Wolfe et al. 1999). However, other studies have also shown that departure from the equilibrium between DMS production and consumption may result in significant accumulations of DMS (Kwint and Kramer 1996; Van Duyl et al. 1998; Schultes et al. 2000). As a result of this decoupling, DMS net change during our study varied from positive to negative, but with no obvious diel cycle.

Our 4-h dark incubations failed to reproduce the measured in situ variations in DMS concentrations. As can be seen in this study, periods of net production or net consumption were relatively well reproduced, but net DMS changes measured during the dark incubations consistently underestimated rates estimated from temporal changes of in situ DMS concentrations by a factor of 2.9. It should be remembered that this threefold difference is a minimum, since the rates calculated from the in situ concentrations do not take into account DMS losses by photooxidation and ventilation. When corrected by the 2.9 factor (slope of the regression), a better agreement was found with in situ values, especially in recreating the night peak. This underestimation indicates that our incubations eliminated some processes increasing DMS production. This is consistent with our previous conclusions that light and mesozooplankton grazing, two mechanisms not present in our incubation, may have stimulated the production of DMS during our study.

Simó and Pedros-Alió (1999) demonstrated during a microcosm experiment that DMS production and consumption could vary over a 24-h period. Our results show that similar short-term variations in DMS gross production and consumption occur in the field. However, no clear similarity in patterns could be derived between the two experiments. This is not unexpected given the different approaches used (microcosm versus Lagrangian study) and the numerous and diverse physiological and ecological processes involved. But both experiments show that temporal variations in DMS concentrations may result from the net balance between different processes occurring during the day. This is an important finding, since most daily rate measurements are presently derived from incubations conducted for period shorter than 6 h. This could lead to important over- or under-estimation of the actual daily rates.

Acknowledgements

The authors wish to thank all scientists, officers, and crew of the CCGS *Martha L. Black* for their work and assistance during the cruise, Martine Lizotte for assistance with gas chromatography, and Lyse Bérard-Therriault for phytoplankton identification and enumeration. We also thank two reviewers for helpful comments on the manuscript. A.M. received a postgraduate scholarship from the Fond de la recherche sur la Nature et les Technologies. This project was supported by grants to M.L. from the Natural Sciences and Engineering Research Council of Canada and by Fisheries and Oceans Canada.

References

Archer, S.D., Widdicombe, C.E., Tarran, G.A., Rees, A.P., and Burkill, P.H. 2001. Production and turnover of particulate dimethylsulfoniopropionate during a coccolithophore bloom in the northern North Sea. Aquat. Microb. Ecol. **24**: 225–241.

Belviso, S., Christaki, U., Vidussi, F., Marty, J.-C., Vila, M., and Delgado, M. 2000. Diel variations of the DMSP-to-chlorophyll *a* ratio in northwestern Mediterranean surface waters. J. Mar. Syst. **25**: 119–128.

Christaki, U., Belviso, S., Dolan, J.R., and Corn, M. 1996. Assessment of the role of copepods and ciliates in the release to solution of particulate DMSP. Mar. Ecol. Prog. Ser. **141**: 119–127.

Cullen, J.J., and McIntyre, J.G. 1998. Behavior, physiology, and the niche of depth-regulating phytoplankton. *In* Physiological ecology of harmful algal blooms. *Edited by* D.M. Anderson, A.D. Cembella, and G.M. Hallegraeff. NATO ASI Series. Vol. G41. Springer-Verlag, Berlin and Heidelgberg. pp. 559–579.

Dacey, J.W.H., and Wakeham, S.G. 1986. Oceanic dimethylsulfide: production during zooplankton grazing on phytoplankton. Science (Wash., D.C.), **233**: 1314–1316.

Dacey, J.W.H., Howse, F.A., Michaels, A.F., and Wakeham, S.G. 1998. Temporal variability of dimethylsulfide and dimethylsulfoniopropionate in the Sargasso Sea. Deep-Sea Res. **45**: 2085–2104.

Gasol, J.M., Doval, M.D., Pinhassi, J., Calderon-Paz, J.I., Guixa-Boixareu, N., Vaque, D., and Pedros-Alio, C. 1998. Diel variations in bacterial heterotrophic activity and growth in the northwestern Mediterranean Sea. Mar. Ecol. Prog. Ser. **164**: 107–124.

Keller, M.D., Bellows, W.K., and Guillard, R.R.L. 1989. Dimethyl sulfide production in marine phytoplankton. *In* Biogenic sulfur in the environment. *Edited by* E.S. Saltzmann and E.M. Cooper. American Chemical Society Symposium Series. American Chemical Society, Washington, D.C. pp. 167–182.

Kettle, A.J., Andreae, M.O., Amouroux, D., Andreae, T.W., Bates, T.S., Berresheim, H., et al. 1999. A global database of sea surface dimethylsulfide (DMS) measurements and a procedure to predict sea surface DMS as a function of latitude, longitude, and month. Global Biogeochem. Cycles, **13**: 399–444.

Kiene, R.P. 1992. Dynamics of dimethyl sulfide and dimethylsulfoniopropionate in oceanic water samples. Mar. Chem. **37**: 29–52.

Kiene, R.P., and Bates, T.S. 1990. Biological removal of dimethyl sulphide from sea water. Nature (Lond.), **345**: 702–705.

Kiene, R.P., Linn, L.J., and Bruton, J.A. 2000. New and important roles for DMSP in marine microbial communities. J. Sea Res. **43**: 209–224

© 2004 NRC Canada

Kuipers, B., van Noort, G.J., Vosjan, J., and Herndl, G. 2000. Diel periodicity of bacterioplankton in the euphotic zone of the subtropical Atlantic Ocean. Mar. Ecol. Prog. Ser. **201**: 13–25.

Kwint, R.L.J., and Kramer, K.J.M. 1996. Annual cycle of the production and fate of DMS and DMSP in a marine coastal system. Mar. Ecol. Prog. Ser. **134**: 217–224.

Levasseur, M., Therriault, J.-C., and Legendre, L. 1984. Hierarchical control of phytoplankton succession by physical factors. Mar. Ecol. Prog. Ser. **19**: 211–222.

Levasseur, M., Gamache, T., St.-Pierre, I., and Michaud, S. 1995. Does the cost of NO_3^- reduction affect the production of harmful compounds by *Alexandrium excavatum*? *In* Harmful marine algal blooms. *Edited by* P. Lassus, G. Arzul, E. Erard, P. Gentien, and C. Marcaillou. Lavoisier, Paris, France. pp. 463–468.

Margalef, R. 1978. Life-forms of phytoplankton as survival alternatives in an unstable environment. Oceanol. Acta, **1**: 493–509.

Matrai, P.A., and Keller, M.D. 1993. Dimethylsulfide in a large-scale coccolithophore bloom in the Gulf of Maine. Continental Shelf Res. **13**: 831–843.

Niki, T., Kunugi, M., and Otsuki, A. 2000. DMSP-lyase activity in five marine phytoplankton species: its potential importance in DMS production. Mar. Biol. **136**: 759–764.

Scarratt, M., Cantin, G., Levasseur, M., and Michaud, S. 2000. Particle size-fractionation of DMS production: where does DMSP cleavage occur at the microscale? J. Sea Res. **43**: 245–252.

Scarratt, M.G., Levasseur, M., Michaud, S., Cantin, G., Gosselin, M., and de Mora, S.J. 2002. Influence of phytoplankton taxonomic profile on the distribution of dimethylsulfide and dimethylsulfoniopropionate in the northwest Atlantic. Mar. Ecol. Prog. Ser. **244**: 49–60.

Schultes, S., Levasseur, M., Michaud, S., Cantin, G., Wolfe, G., Gosselin, M., and de Mora, S. 2000. Dynamics of dimethylsulfide production from dissolved dimethylsulfoniopropionate in the Labrador Sea. Mar. Ecol. Prog. Ser. **202**: 27–40.

Simard, Y., Lacroix, G., and Legendre, L. 1986. Diel vertical migrations and nocturnal feeding of a dense coastal krill scattering layer (*Thysanoessa raschi* and *Meganyctiphanes norvegica*) in stratified surface waters. Mar. Biol. **91**: 93–105.

Simó, R., and Pedrós-Alió, C. 1999. Short-term variability in the open ocean cycle of dimethylsulfide. Global Biogeochem. Cycles, **13**: 1173–1181.

Simó, R., Grimalt, J.O., Pedrós-Alió, C., and Albaigés, J. 1995. Occurrence and transformation of dissolved dimethyl sulfur species in stratified seawater (western Mediterranean Sea). Mar. Ecol. Prog. Ser. **127**: 291–299.

Simó, R., Archer, S.D., Pedrós-Alió, C., Gilpin, L., and Stelfox-Widdicombe, C.E. 2002. Coupled dynamics of dimethylsulfoniopropionate and dimethylsulfide cycling and the microbial food web in surface waters of the North Atlantic. Limnol. Oceanogr. **47**: 53–61.

Slezak, D., Brugger, A., and Herndl, G.J. 2001. Impact of solar radiation on the biological removal of dimethylsulfoniopropionate and dimethylsulfide in marine surface waters. Aquat. Microb. Ecol. **25**: 87–97.

Stefels, J. 2000. Physiological aspects of the production and conversion of DMSP in marine algae and higher plants. J. Sea Res. **43**: 183–197.

Steinke, M., Malin, G., Archer, S.D., Burkhill, P.H., and Liss, P.S. 2002. DMS production in a coccolithophore bloom: evidence for the importance of dinoflagellate DMSP lyases. Aquat. Microb. Ecol. **26**: 259–270.

Sunda, W., Kieber, D.J., Kiene, R.P., and Huntsman, S. 2002. An antioxidant function for DMSP and DMS in marine algae. Nature (Lond.), **418**: 317–319.

Therriault, J.-C., and Levasseur, M. 1985. Control of phytoplankton production in the lower St. Lawrence Estuary: light and freshwater runoff. Nat. Can. **112**: 77–96.

Van Duyl, F.C., Gieskes, W.W.C., Kop, A.J., and Lewis, W.E. 1998. Biological control of short-term variations in the concentration of DMSP and DMS during a *Phaeocystis* spring bloom. J. Sea Res. **40**: 221–231.

Visscher, P.T., and Taylor, B.F. 1993. A new mechanism for the aerobic catabolism of dimethyl sulfide. Appl. Environ. Microbiol. **59**: 3784–3789.

Wolfe, G.V., Steinke, M., and Kirst, G.O. 1997. Grazing-activated chemical defence in a unicellular algae. Nature (Lond.), **387**: 894–897.

Wolfe, G.V., Levasseur, M., Cantin, G., and Michaud, S. 1999. Microbial consumption and production of dimethyl sulfide (DMS) in the Labrador Sea. Aquat. Microb. Ecol. **18**: 197–205.

Wolfe, G.V., Strom, S.L., Holmes, J.L., Radzio, T., and Olson, M.B. 2002. Dimethylsulfoniopropionate cleavage by marine phytoplankton in response to mechanical, chemical, or dark stress. J. Phycol. **38**: 948–960.

© 2004 NRC Canada

Particulate dimethylsulfoniopropionate and dimethylsulfoxide in relation to iron availability and algal community structure in the Peru Upwelling System[1]

S.F. Riseman and G.R. DiTullio

Abstract: The influence of iron on phytoplankton biogenic sulfur production, physiological status, and community structure in the Peruvian Upwelling System was investigated in September 2000. Vertical profiles of particulate dimethylsulfoniopropionate ($DMSP_p$) and dimethylsulfoxide ($DMSO_p$) were measured at stations along two transects passing from the high-iron waters of the continental shelf, across the Peru trench, to low-iron open-ocean waters. Although chlorophyll *a* (Chl *a*) biomass decreased significantly across the shelf, DMSPp and $DMSO_p$ concentrations relative to Chl *a* were higher at the offshore stations ($DMSP_p$:Chl *a* 2.3–6.4 times greater and $DMSO_p$:Chl *a* 2.6–4 times greater). These changes were associated with lower iron concentrations, as well as a shift from diatom-dominated communities to ones dominated by cryptophytes and haptophytes (based on algal pigment concentrations). The results of a shipboard iron-addition incubation experiment were similar to patterns observed on the transects. $DMSP_p$:Chl *a* ratios decreased with increasing iron and diatoms preferentially outgrew other taxa. The possible role of $DMSP_p$ and $DMSO_p$ as free radical scavengers (stimulated by iron limitation) was supported by the increased concentrations of these compounds measured under low-iron conditions, as well as by the positive correlations (r^2 = 0.69 and 0.82, respectively) observed between these compounds and the known antioxidant β-carotene.

Résumé : En septembre 2000, nous avons étudié l'influence du fer sur la production biogénique de soufre, ainsi que l'état physiologique et la composition de la communauté dans le système de la résurgence du Pérou. Nous avons mesuré les profils verticaux du diméthylsulfoniopropionate ($DMSP_p$) et du sulfoxyde de diméthyle ($DMSO_p$) particulaires à des stations le long de deux transects partant des eaux riches en fer du plateau continental, traversant la fosse du Pérou et rejoignant les eaux pauvres en fer de la haute-mer. Bien que la biomasse de chlorophylle décroisse significativement à travers le plateau continental, les concentrations de $DMSP_p$ et de $DMSO_p$ en fonction de la chlorophylle *a* sont plus élevées aux stations du large ($DMSP_p$:Chl *a* 2.3–6,4 fois plus élevé et $DMSO_p$:Chl *a* 2,6–4 fois plus élevé). Ces changements sont associés à des concentrations réduites de fer, ainsi qu'à un remplacement des communautés dominées par les diatomées par d'autres dominées par les cryptophytes et les haptophytes (d'après les concentrations des pigments des algues). Une expérience d'incubation avec addition de fer faite à bord a donné des résultats similaires aux patterns observés dans les transects. Un accroissement du fer s'accompagne d'un déclin des rapports $DMSP_p$:Chl *a* et une croissance préférentielles des diatomées par rapport aux autres taxons. Le rôle possible du $DMSP_p$ et du $DMSO_p$ comme « éboueurs » de radicaux libres (stimulés par la limitation du fer) est appuyé par l'augmentation des concentrations de ces composés dans les conditions de faibles concentrations de fer, ainsi que par les corrélations positives (r^2 = 0,69 et 0,82, respectivement) observées entre ces composés et l'antioxydant reconnu, la β-carotène.

[Traduit par la Rédaction]

Introduction

Biogeochemical cycling of sulfur compounds in the marine environment is thought to be intimately involved with atmospheric–oceanic processes and may significantly impact global climate change (Charlson et al. 1987; Andreae and Crutzen 1997). For instance, oceanic dimethylsulfide (DMS) concentrations have been shown to be positively correlated with the formation of cloud condensation nuclei (Falkowski et al. 1992). The coupling between the iron, sulfur, and carbon biogeochemical cycles has been suggested to explain the decrease in atmospheric pCO_2 levels during the last glacial

Received 12 February 2003. Accepted 8 January 2004. Published on the NRC Research Press Web site at http://cjfas.nrc.ca on 22 June 2004.
J17368

S.F. Riseman[2] and G.R. DiTullio. Hollings Marine Laboratory, College of Charleston, 331 Ft. Johnson Road, Charleston, SC 29412, U.S.A.

[1]This paper is part of the proceedings of the Third International Symposium on Biological and Environmental Chemistry of DMS(P) and Related Compounds, held in Rimouski (Québec), 26–28 September 2002.

[2]Corresponding author (e-mail: risemans@cofc.edu).

 doi: 10.1139/F04-052 © 2004 NRC Canada

maximum relative to interglacial periods (Martin 1990, 1992), but the exact physiological intracellular mechanisms in algae that are responsible for linking these cycles remain elusive.

Biological production of DMS occurs through the breakdown of dimethylsulfoniopropionate (DMSP) by the phytoplankton DMSP lyase enzyme and through bacterial conversion (Cantoni and Anderson 1956; Dacey and Wakeham 1986). DMSP production by marine phytoplankton has been intensely investigated over the past decade, yet we still know remarkably little about the factors influencing the production of this important compound or its exact physiological role in the cell. The putative functions of DMSP inside the cell include osmoregulation (Vairavamurthy et al. 1985), cryoprotection (Kirst et al. 1991), as a grazing deterrent (Wolfe et al. 1997), and as an overflow mechanism for excess carbon production under physiological stress conditions (Stefels 2000). The closely related compound dimethylsulfoxide (DMSO) is even more poorly understood. In fact, only recently has laboratory work provided evidence that there is a biogenic source for DMSO (Simó et al. 1998). As a consequence, relatively few data sets exist on the particulate pool of this compound and most oceanic measurements have been focused on the dissolved pool of DMSO.

Attention has recently been directed toward a possible antioxidant function for DMSP and DMSO. The potential function of DMSO as a free radical scavenger has been suggested (Simó et al. 1998; Lee and de Mora 1999) and recent laboratory evidence has shown that DMSP increases under oxidative stress conditions induced by either CO_2 or iron limitation (Sunda et al. 2002). The increase in cellular DMSP under iron stress conditions is consistent with the role of iron as a cofactor in the synthesis of various intracellular antioxidants such as catalase and dismutase enzyme systems. We hypothesized that if DMSP and DMSO levels are correlated with oxidative stress, then one might expect to see a change in cellular levels across natural gradients in iron concentrations.

The upwelling off the coast of Peru brings nutrient- and iron-rich water to the mixed layer supporting one of the most productive regions in the world. As this water is advected offshore, the biomass declines dramatically, while macronutrient concentrations remain relatively high, resulting in classic HNLC (high-nutrient low-chlorophyll) conditions. In September of 2000, an oceanographic cruise in this upwelling regime was undertaken to investigate the influence of iron on biogeochemical nutrient cycling. The results of this work have shown that phytoplankton in the Peruvian offshore HNLC waters are iron limited (Bruland et al. 2004; Hutchins et al. 2002; Eldridge et al. 2004). We report here on the concentrations of $DMSP_p$ and $DMSO_p$ on two cross-shelf transects off Peru spanning high to low dissolved iron waters. In addition, a shipboard iron addition experiment was conducted with water collected from the low-iron HNLC region to examine the influence of iron concentration on DMSP and DMSO production.

Material and methods

Transects

Two transects were conducted off the Peru coast in September 2000 (Fig. 1). Continuous underway surface measurements of algal pigments, photosynthetic efficiency of photosystem II (F_v/F_m), macronutrients, dissolved iron concentration, temperature, and salinity were conducted along the length of these transects and will be published elsewhere. We sampled three stations along the northern transect: a nearshore continental shelf station (station 18, 14 September; 8.325°S, 79.07°W), a midtransect station in the region of the trench (station 19, 15 September; 9.059°S, 80.279°W), and an offshore station (station 21, 16 September; 9.771°S, 81.606°W). We sampled a nearshore station (station 24, 18 September; 12.881°S, 76.571°W), a midshelf station (station 26, 19 September; 13.153°S, 76.686°W), and a trench station (station 28, 19 September; 13.648°S, 77.455°W) on the southern transect. Vertical profiles were sampled at each station just before sunrise using 10-L Niskin bottles mounted to a SeaBird CTD (conductivity–temperature–depth) rosette that provided vertical profiles of temperature, salinity, and percent oxygen saturation. Shipboard measurements of dissolved nutrients (nitrite plus nitrate, silicic acid, and phosphate) were made with a Lachat Quick Chem autoanalyzer. Quantum efficiency (F_v/F_m) and the functional cross section (σ_{PSII}) of photosystem II were measured using a fast repetition rate fluorometer (FRRF) (Fast^{tracka}, Chelsea Instruments Inc.). Samples were dark adapted for 15–30 min before FRRF analysis (FRRF protocol: eight sequences per acquisition, saturation flash width of 18 and interflash delay of 1, gain in autoranging mode with upper and lower thresholds of 70 and 15, respectively). Diel periodicity effects on F_v/F_m (Boyd and Abraham 2001)

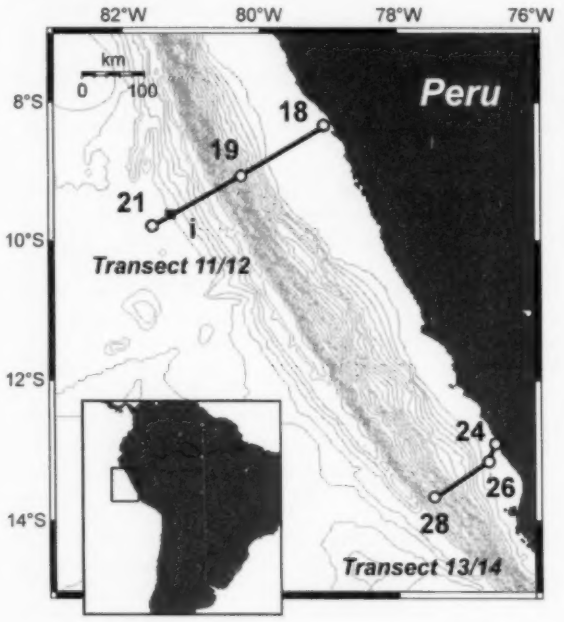

Fig. 1. Map of two transects sampled off of the Peruvian coast. Three stations were sampled on the northern transect (transect 11/12) and on the southern transect (transect 13/14). Stations are shown as open circles and are labeled with the station number. An iron fertilization experiment was conducted with water from the HNLC region of transect 11/12 (marked with a solid square and labeled *i*).

© 2004 NRC Canada

Table 1. Transect 11/12: depth-integrated and integral average concentrations of $DMSP_p$, $DMSO_p$, and pigments.

	Integral sums			Integral averages		
	Station 18	Station 19	Station 21	Station 18	Station 19	Station 21
$DMSP_p$[a]	128	521	319	4.41	7.66	4.75
$DMSO_p$[a]	77	256	122	2.66	3.76	1.82
Pigments[b]						
Chl *a*	46 314	46 584	26 721	1597	685	399
DVChl *a*	0	63 363	18 098	0	932	270
Chl *c*3	1 150	7 981	8 438	39.65	117	126
19′-Butanoyloxyfucoxanthin	167	1 635	4 832	5.75	24.04	72.12
Fucoxanthin	14 633	8 724	3 040	505	128	45.37
19′-Hexanoyloxyfucoxanthin	73	11 614	12 350	2.52	171	184
Alloxanthin	983	3 599	1 313	33.89	52.92	19.59
Peridinin	2 576	3 083	2 663	88.84	45.34	39.74
β-Carotene	8 116	16 603	6 243	280	244	93.18

Note: Concentrations were integrated from the surface to the base of the pycnocline (station 18, 0–29 m; station 19, 0–68 m; station 21, 0–67 m). Integral averages are the integral sums normalized to the total depth integrated.
[a]$DMSP_p$ and $DMSO_p$ are expressed in $\mu mol \cdot m^{-2}$ for integral sums and in $nmol \cdot L^{-1}$ for integral averages.
[b]Pigments are expressed in $\mu g \cdot m^{-2}$ for integral sums and in $ng \cdot L^{-1}$ for integral averages.

were avoided by sampling the stations (with the exception of station 26) at the same time in the early morning. Aliquots (0.5–2 L) of seawater were filtered onto Whatman GF/F filters and immediately frozen in liquid nitrogen for laboratory measurement of algal pigments using high-performance liquid chromatography (HPLC) (DiTullio and Geesey 2002).

Samples were collected for laboratory measurement of particulate DMSP ($DMSP_p$) and DMSO ($DMSO_p$). Seawater samples from each depth were filtered under low vacuum (≤5 psi (1 psi = 6.895 kPa)) onto Whatman GF/F filters. The filters were placed in gas-tight headspace vials with 5 mL of MeOH (Dacey et al. 1998) and stored in the dark at 4 °C until analysis. $DMSP_p$ and $DMSO_p$ were measured independently using cryogenic purge and trap gas chromatography. DMSP was converted to DMS via base hydrolyses in 1 $mol \cdot L^{-1}$ NaOH. The solution was sparged with high-purity helium gas (125 $mL \cdot min^{-1}$) for 25 min and DMS was cryogenically trapped in a teflon loop packed loosely with silanized glass wool. DMS was measured on an HP5890 Series II gas chromatograph fitted with a Chromosil 330 column and an FPD detector. The gas chromatograph was calibrated using a certified DMS standard permeation device (Vici Metronics).

A separate aliquot of the sample was used to measure $DMSO_p$. DMSP was first removed from the sample by base hydrolysis and sparging as described above. This process removed all DMSP from the sample as determined by a time series experiment (data not shown). $DMSO_p$ was then reduced to DMS using a modification of the sodium borohydride reduction method (Simó et al. 1996) that uses cobalt-doped sodium borohydride (Sigma) and relieves the necessity to neutralize the pH of the samples (in 1 $mol \cdot L^{-1}$ NaOH). The DMS was then collected and measured on the gas chromatograph as described above.

Shipboard iron-addition incubation

An iron addition experiment was conducted with water collected from the iron-depleted region of transect 11/12 between stations 19 and 21 (9.610°S, 81.312°W) (Fig. 1). Trace metal clean collection methods (as described in Bruland et al. 2001) were used to collect water from a depth of 8–10 m into an acid-cleaned 50-L carboy. Water from this carboy was dispensed into 2.3-L acid-cleaned polycarbonate bottles leaving no headspace. Triplicate bottles of three treatments, an unamended control, a low iron addition (0.2 $nmol \cdot L^{-1}$), and a high iron addition (2 $nmol \cdot L^{-1}$), were incubated in a spectrally adjusted deckboard incubator (Laws et al. 1990) for 3 days at 40% of the ambient light level. Iron additions were made with $FeCl_3$ in 0.01 $mol \cdot L^{-1}$ HCl. All seawater manipulations were performed under a class 100 laminar flow hood. Temperature in the incubator was maintained using flowing surface seawater. Initial and final measurements of algal pigments, dissolved nutrients, $DMSP_p$, and $DMSO_p$ were made using the methods described above.

Results

Transect 11/12: nearshore

Station 18 was located on the continental shelf with a bottom depth of 60 m. High dissolved iron concentrations of 6–8 $nmol \cdot L^{-1}$ in the surface waters and cooler temperatures (15.5 °C in the mixed layer) indicated that this water was recently upwelled (Bruland et al. 2004). Macronutrient concentrations were high and nonlimiting to photosynthetic production. Chlorophyll *a* (Chl *a*) concentrations were high at this station (Table 1), reaching a maximum of 2.45 $\mu g \cdot L^{-1}$ at 12 m in the upper pycnocline (Fig. 2*f*). High concentrations of fucoxanthin and the absence or low concentrations of accessory pigments diagnostic of other algal classes (Fig. 3*c*) indicated that the phytoplankton community consisted predominantly of diatoms. F_v/F_m has been shown to be a sensitive indicator of physiological stress due to iron limitation when macronutrients are nonlimiting (Kolber et al. 1994; Davey and Geider 2001; Sosik and Olson 2002). Values of F_v/F_m (0.41–0.50 in the upper 17 m) and σ_{PSII} (327–503 throughout the water column; Fig. 3*f*) reveal that the phytoplankton were not physiologically stressed at this station.

© 2004 NRC Canada

Fig. 2. Transect 11/12: profiles of (*a–c*) $DMSP_p$ and $DMSO_p$, (*d–f*) Chl *a* and DVChl *a*, and (*g–i*) $DMSP_p$:Chl *a* and $DMSO_p$:Chl *a*. Depth of the mixed layer is shown by a dotted line. Scales on the *x* axes are consistent between stations to facilitate comparison.

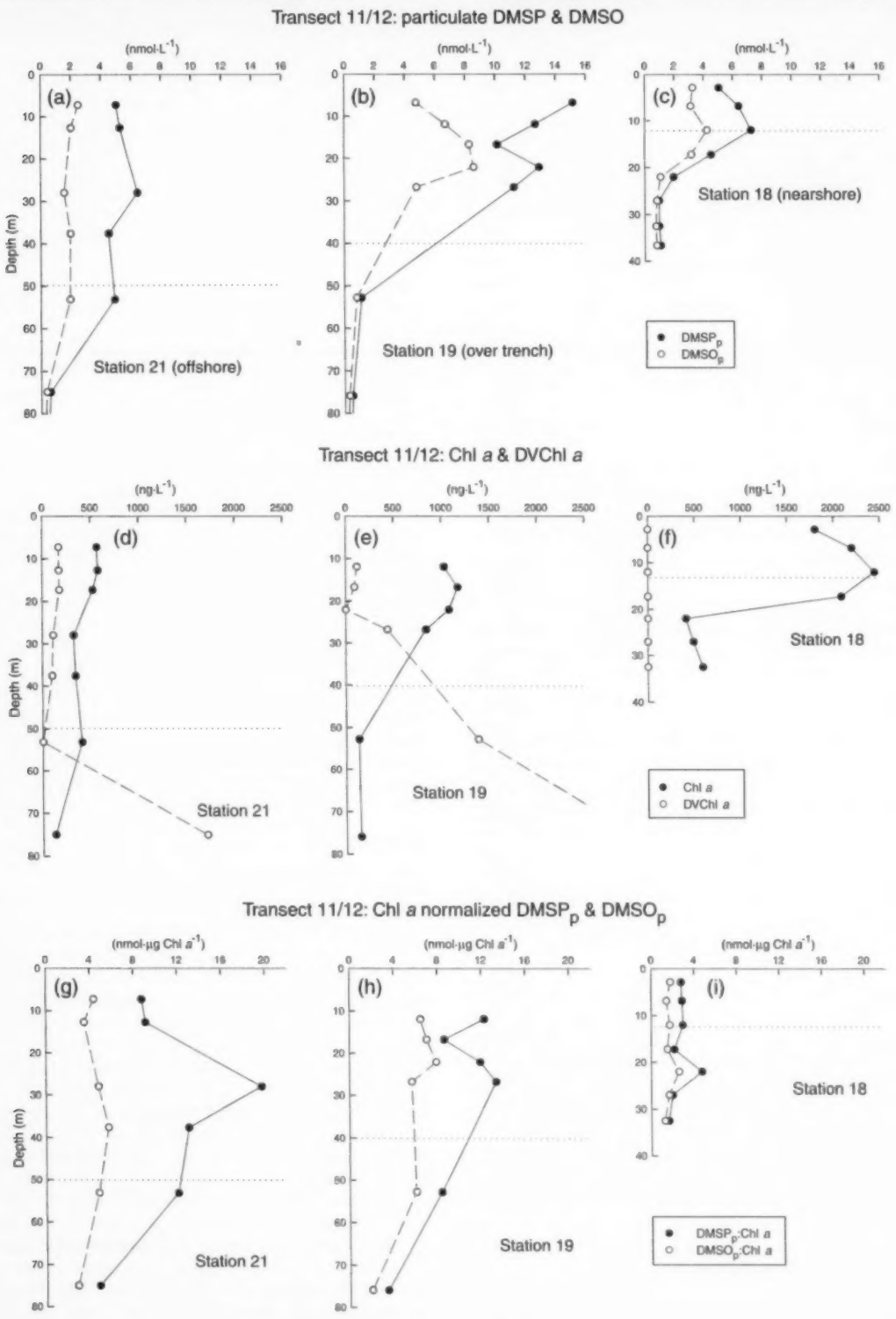

© 2004 NRC Canada

Fig. 3. Transect 11/12: profiles of (*a–c*) taxon-specific pigments and (*d–f*) photosynthetic efficiency (F_v/F_m) and the functional cross section of photosystem II (σ_{PSII}). Depth of the mixed layer is shown by a dotted line. Scales on the *x* axes are consistent between stations to facilitate comparison.

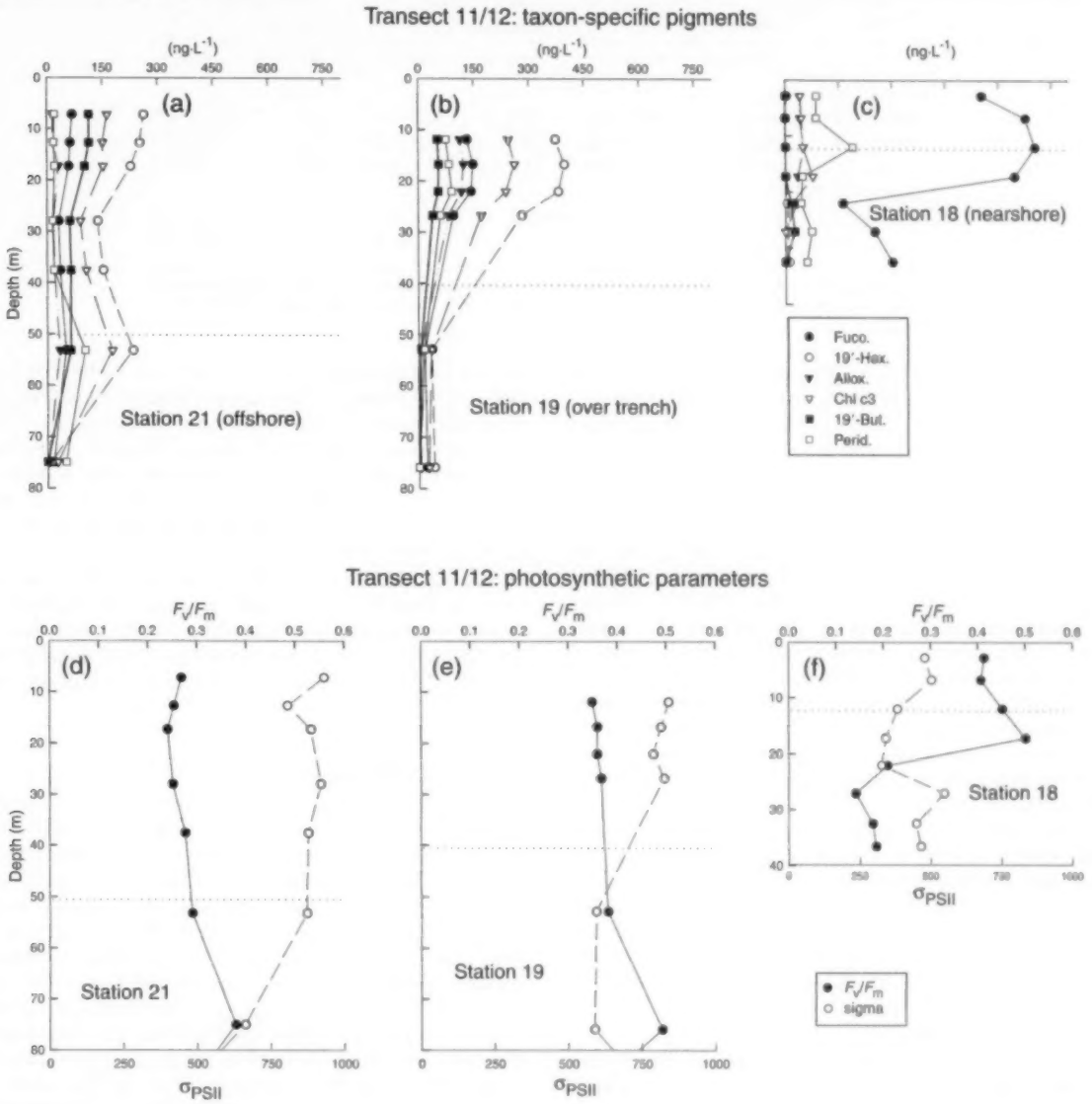

$DMSP_p$ (1–7 nmol·L^{-1}) and $DMSO_p$ (0.8–4 nmol·L^{-1}) concentrations exhibited depth profiles similar to that of Chl *a*, with the greatest concentrations occurring just below the base of the mixed layer and declining significantly below about 20 m (Fig. 2*c*). Chl *a* normalized concentrations were low and fairly constant throughout the sampled water column (Fig. 2*i*).

Transect 11/12: trench station

Station 19 was located in the middle of the transect over the Peru trench. Higher salinity and warmer temperature in the mixed layer (18.3 °C, 35.14 psu) suggest that this water had been advected offshore and had "aged" relative to station 18. Surface dissolved iron concentrations had dropped to approximately 0.56 nmol·L^{-1} (iron in this region was variable with lower concentrations nearby; Bruland et al. 2004). Macronutrient concentrations had declined from station 18 levels but were still present in nonlimiting concentrations (NO_x > 17 μmol·L^{-1}, PO_4^{3-} > 1.15 μmol·L^{-1}, $Si(OH)_4$ > 6 μmol·L^{-1}).

The depth-integrated (to the base of the pycnocline) Chl *a* was the same as at station 18 but the integral-average concentration was 57% lower with respect to station 18 because of the greater depth of the pycnocline (Fig. 2*e*; Table 1). Integrated divinyl Chl *a* (DVChl *a*) contributed 58% of the total Chl *a* (monovinyl plus divinyl) in the water column with most of the DVChl *a* found below the mixed layer (Fig. 2*e*;

© 2004 NRC Canada

Table 2. Ratios of particulate dimethylsulfoniopropionate ($DMSP_p$) and particulate dimethylsulfoxide ($DMSO_p$) to each other and to Chl *a*.

	$DMSO_p$:$DMSP_p$		$DMSP_p$:Chl *a* ($nmol \cdot \mu g^{-1}$)		$DMSO_p$:Chl *a* ($nmol \cdot \mu g^{-1}$)	
	Average	Range	Average	Range	Average	Range
Transect 11/12						
Station 18	0.63	0.49–0.84	2.9	2.0–4.8	1.8	1.4–2.6
Station 19	0.58	0.31–0.82	10.8	8.4–13.4	6.1	3.4–7.9
Station 21	0.39	0.24–0.50	12.6	8.8–19.7	4.6	3.5–5.7
Transect 13/14						
Station 24	0.83	0.40–1.42	1.1	0.8–1.3	0.9	0.6–1.5
Station 26	0.69	0.61–0.81	2.5	0.5–4.8	1.7	0.3–3.2
Station 28	0.51	0.38–0.66	7.0	4.1–11.0	3.6	1.7–5.2

Note: Average values were calculated from all samples at each station (excluding points below the pycnocline).

Table 1). The average fucoxanthin concentration dropped to about a quarter of station 18 levels, whereas the pigments 19′-butanoyloxyfucoxanthin (19′-but), alloxanthin, and especially Chl *c*3 and 19′-hexanoyloxyfucoxanthin (19′-hex) increased in concentration and relative to Chl *a* (Fig. 3*b*; Table 1). These changes in accessory pigment concentrations and pigment ratios indicated that diatoms accounted for much less of the total biomass, whereas cryptophytes and haptophytes were most abundant. These findings were similar to the surface community composition estimated by Chemtax analysis of pigment concentrations (G.R. DiTullio et al., unpublished[3]). F_v/F_m dropped to around 0.35 and σ_{PSII} increased to values above 790 in the mixed layer (Fig. 3*e*). F_v/F_m values were not as low as might be expected under iron limitation; however, cryptophytes, which have been shown to have relatively high F_v/F_m values in low-iron waters, were one of the dominant taxa at this station (Olson et al. 2000; Sosik and Olson 2002).

$DMSP_p$ and $DMSO_p$ concentrations were highest at this station, with a $DMSP_p$ maximum of 15 $nmol \cdot L^{-1}$ near the surface and $DMSO_p$ reaching a subsurface maximum of 8.6 $nmol \cdot L^{-1}$ at 20 m (Fig. 2*b*). Average Chl *a* normalized $DMSP_p$ and $DMSO_p$ concentrations increased 3.7- and 3.4-fold, respectively, relative to the iron-replete conditions observed at station 18 (Fig. 2*h*; Table 2).

Transect 11/12: offshore

Station 21 was located in the HNLC waters at the offshore end of the transect where the surface dissolved iron concentration had dropped to 0.08 $nmol \cdot L^{-1}$ (Bruland et al. 2004) and macronutrients were still present in nonlimiting concentrations (NO_x > 15 $\mu mol \cdot L^{-1}$, PO_4^{3-} > 1.25 $\mu mol \cdot L^{-1}$, $Si(OH)_4$ > 7 $\mu mol \cdot L^{-1}$). The water in the mixed layer was slightly deeper, warmer, and more saline than at the previous station.

This station had the lowest Chl *a* biomass (about 0.5 $\mu g \cdot L^{-1}$) on the transect (Fig. 2*d*). The integral average Chl *a* concentration was almost half of that at station 19 and about a quarter of that at station 18 (Table 1). Integrated DVChl *a* concentrations represented 40% of the total Chl *a*, indicating the importance of prochlorophytes below the mixed layer. Taxon-indicative pigment concentrations were similar to station 19 concentrations (Fig. 3*a*; Table 1). Unlike station 19, however, cryptophytes (based on alloxanthin concentrations) did not represent a major fraction of the biomass at this station. Low fucoxanthin levels show a negligible contribution of diatoms to the biomass throughout the water column. The F_v/F_m levels had dropped to about 0.25 at this station (Fig. 3*d*), indicating significant physiological stress, most likely because of iron limitation.

Average $DMSP_p$ and $DMSO_p$ concentrations in the mixed layer declined relative to those at station 19; however, this change was proportional to the drop in Chl *a* such that average Chl *a* normalized concentrations (12.6 and 4.6 $nmol \cdot \mu g$ Chl a^{-1}, respectively) were close to station 19 values (Table 2).

Transect 13/14: nearshore

Biomass was high at station 24 with Chl *a* concentrations reaching about 12 $\mu g \cdot L^{-1}$ near the surface (Fig. 4*f*) with an integral sum more than four times greater (~198 $mg \cdot m^{-2}$) than was observed at station 18 (Table 3). High biomass, warmer temperatures, and a stratified water column indicate that upwelled water had aged and the bloom was in a later stage than observed on transect 11/12. Similar to station 18, diatoms clearly dominated this community (with fucoxanthin levels exceeding 9 $\mu g \cdot L^{-1}$); however, Chl *c*3 levels were also high in the upper water column (Fig. 5*c*), reaching concentrations 20 times those at station 18. Near-surface increases in alloxanthin, peridinin, and 19′-hex show that cryptophytes, pelagophytes, dinoflagellates, and haptophytes were also present in the upper water column. Chemtax analysis suggests that the dominant taxa in the surface waters were diatoms followed by haptophytes and then cryptophytes (G.R. DiTullio et al., unpublished[3]). The presence of these other taxa may indicate the beginning of community succession triggered by decreasing iron and silicic acid. Surface dissolved iron concentrations were lower than at the northern shelf station (approximately 1.8 $nmol \cdot L^{-1}$; Bruland et al. 2004); however, F_v/F_m measurements (>0.5) in the upper water column (Fig. 5*f*) confirmed that the phytoplankton were not yet iron stressed.

[3] G.R. DiTullio, M.E. Geesey, J.M. Maucher, M.B. Alm, and S.F. Riseman. Physiological status and algal community composition in the Eastern Equatorial Peru Upwelling System.

© 2004 NRC Canada

Fig. 4. Transect 13/14: profiles of (*a–c*) $DMSP_p$ and $DMSO_p$, (*d–f*) Chl *a* and DVChl *a*, and (*g–i*) $DMSP_p$:Chl *a* and $DMSO_p$:Chl *a*. The depth of the mixed layer is shown by a dotted line. A break in the *x*-axis scale on the Chl profiles is marked by a shaded bar.

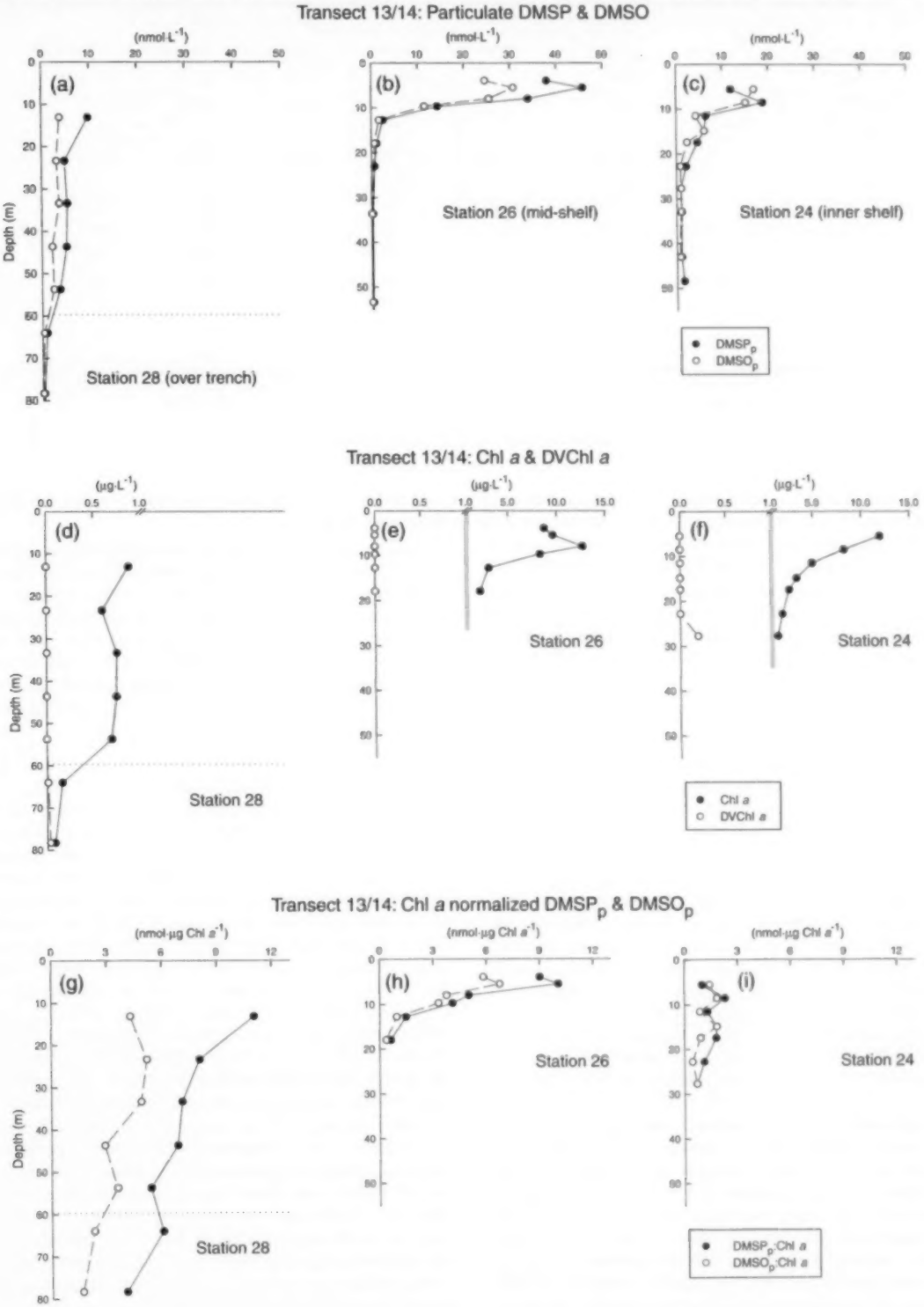

© 2004 NRC Canada

Table 3. Transect 13/14: depth-integrated sums and integral average concentrations of $DMSP_p$, $DMSO_p$, and pigments.

	Integral sums			Integral averages		
	Station 24	Station 26	Station 28	Station 24	Station 26	Station 28
$DMSP_p$[a]	212	322	355	7.07	12.88	4.55
$DMSO_p$[a]	215	222	182	7.16	8.88	2.33
Pigments[b]						
Chl *a*	197 510	113 761	41 187	6584	4550	526
DVChl *a*	933	0	353	31	0	5
Chl *c*3	16 898	15 002	8 187	563	600	105
19′-Butanoyloxyfucoxanthin	1 108	489	2 248	37	20	29
Fucoxanthin	129 851	112 807	10 947	4328	4512	140
19′-Hexanoyloxyfucoxanthin	1 427	591	7 942	48	24	101
Alloxanthin	1 467	1 082	3 433	49	43	44
Peridinin	1 896	0	2 841	63	0	36
β-Carotene	15 561	14 744	2 477	519	590	32

Note: Station 24 concentrations were integrated from the surface to 30 m and station 26 concentrations were integrated to 25 m, below which the waters were anoxic. Station 28 was integrated to the base of the pycnocline (78 m).

[a]$DMSP_p$ and $DMSO_p$ are expressed in $\mu mol \cdot m^{-2}$ for integral sums and in $nmol \cdot L^{-1}$ for integral averages.

[b]Pigments are expressed in $\mu g \cdot m^{-2}$ for integral sums and in $ng \cdot L^{-1}$ for integral averages.

$DMSP_p$ and $DMSO_p$ concentrations were higher than at the northern shelf station, reaching 18.9 and 16.9 $nmol \cdot L^{-1}$, respectively (Fig. 4*c*), both with integral average concentrations of about 7 $nmol \cdot L^{-1}$ (Table 3). Maximum $DMSP_p$ and $DMSO_p$ concentrations occurred in the upper 10 m (Fig. 4*c*), coinciding with the increase in biomass. Chl *a* normalized concentrations were low (Table 2) and fairly constant throughout the water column (Fig. 4*i*), similar to station 18.

Transect 13/14: middle shelf

Station 26 was located on the middle shelf. As with station 24, waters were highly stratified with anoxic conditions below about 25 m. In the upper 10 m, nitrate and phosphate levels were drawn down compared with station 24 (NO_x = 3.2 $\mu mol \cdot L^{-1}$, PO_4^{3-} = 0.5 μM, $Si(OH)_4$ = 8.9 $\mu mol \cdot L^{-1}$ at 4 m), and surface dissolved iron concentrations were low (0.1 – 0.8 $nmol \cdot L^{-1}$; Bruland et al. 2004). The maximum Chl *a* concentration (12.7 $\mu g \cdot L^{-1}$) was the same as at the previous station, but the distribution differed in that concentrations declined in the upper 10 m (Fig. 4*e*). Chemtax analysis and accessory pigment concentrations suggest that the community composition had not changed from station 24 (G.R. DiTullio et al., unpublished[3]). One notable difference was that fucoxanthin concentrations dropped off in the surface waters. Despite the low iron concentrations, F_v/F_m values in most of the water column remained high but dropped from 0.51 to 0.43 near the surface (Fig. 5*e*). The combination of pigment, nutrient, dissolved iron, and F_v/F_m data suggests that a community very similar to that of the nearshore station had recently drawn down nutrients and depleted iron in the near-surface waters causing a decline of biomass at these depths, driving maximum production slightly deeper. It appears that this biomass decline was primarily a result of diminishing diatom populations, as pigments other than fucoxanthin did not decrease as significantly in the upper water column. The variable effects of iron limitation on different taxa may explain the only moderate drop in F_v/F_m.

Station 24 had the highest concentrations of $DMSP_p$ and $DMSO_p$ observed on either transect (45.7 and 35.7 $nmol \cdot L^{-1}$, respectively) (Fig. 4*b*). Maximum integral average concentrations were also the highest (12.88 and 8.88 $nmol \cdot L^{-1}$, respectively) (Table 3). The peak in $DMSP_p$ and $DMSO_p$ concentrations occurred at around 5–6 m, slightly above the Chl *a* maximum. Chl *a* normalized $DMSP_p$ and $DMSO_p$ concentrations roughly doubled from those at station 24 (Table 2) and increased above 10 m (Fig. 4*h*).

Transect 13/14: off-shelf break

Station 28 was located well over the trench. As on the northern transect, this offshore station had a deeper mixed layer with warmer and more saline waters and biomass was only a fraction of levels seen at the two shelf stations. The integral average Chl *a* concentration was a fraction of station 26 and station 24 concentrations (8% and 12%, respectively) (Table 3) and was more similar to the offshore concentrations on transect 11/12. HPLC pigment analysis indicated that a mixed algal community was present at this station (Fig. 5*a*; Table 3). Chemtax analysis revealed that type 4 haptophytes (e.g., *Phaeocystis*), cryptophytes, and prasinophytes represented the largest fraction of the surface algal community, with diatoms, dinoflagellates, pelagophytes, and type 3 haptophytes (e.g., coccolithophorids) contributing a smaller proportion of the total Chl *a* (G.R. DiTullio et al., unpublished[3]). Dissolved iron was variable in this region (0.2–0.6 $nmol \cdot L^{-1}$); however, F_v/F_m values (0.27–0.35 in the mixed layer) had dropped markedly from shelf values (Fig. 5*d*), indicating increased physiological stress. Additionally, a flavodoxin index of 1.0 was reported, signifying physiological iron stress in this region (Maucher 2001).

Integral average concentrations of $DMSP_p$ and $DMSO_p$ at this station were similar to those observed at the offshore

© 2004 NRC Canada

Fig. 5. Transect 13/14: profiles of (*a–c*) taxon-specific pigments and (*d–f*) photosynthetic efficiency (F_v/F_m) and the functional cross section of photosystem II (σ_{PSII}). The depth of the mixed layer is shown by a dotted line. A break in the *x*-axis scale of the pigment profiles is marked by a shaded bar.

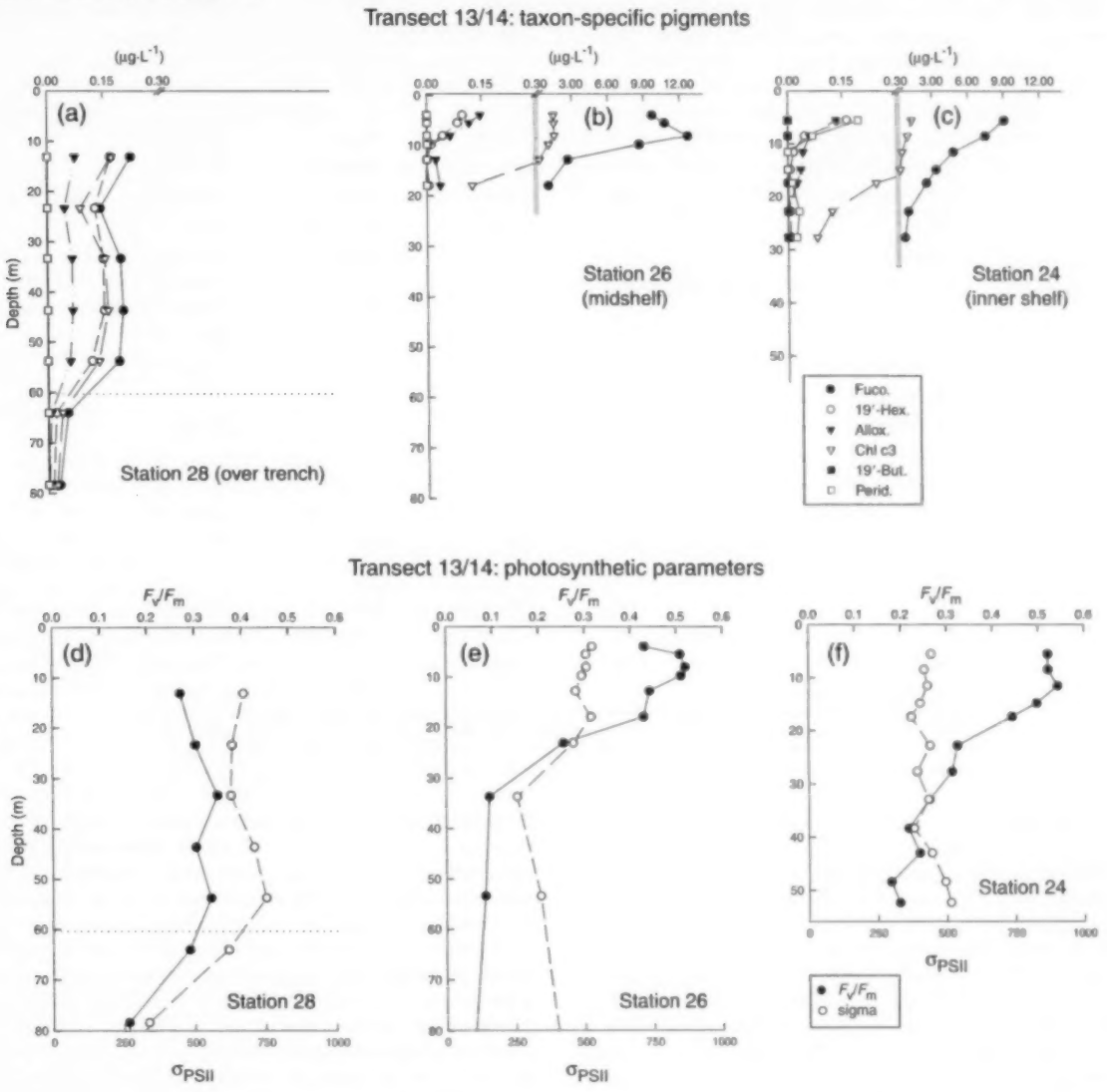

station of transect 11/12 (Table 3). Chl *a* normalized concentrations of $DMSP_p$ and $DMSO_p$ increased 6.4- and 4-fold, respectively, relative to station 24 but were not as high as the offshore concentrations on transect 11/12 (Table 2).

Iron addition incubation experiment

A summary of the initial and final pigment, nutrient, and $DMSP_p$ concentrations is provided in Table 4. Algal biomass in the initial water sample was similar to station 19 levels (Chl *a* = 1.3 μg·L^{-1}). Chemtax analysis revealed that at the time and location of initial water collection, the surface community was predominantly type 3 and type 4 haptophytes (G.R. DiTullio et al., unpublished[3]). Initial levels of $DMSP_p$ were higher than at both stations 19 and 21 (16.6 nmol·L^{-1} and 13.2 nmol·μg Chl *a*–1). Initial macronutrient concentrations were nonlimiting (NO_x = 16.2 μmol· L^{-1}, PO_4^{3-} = 1.1 μmol·L^{-1}, $Si(OH)_4$ = 8.1 μmol·L^{-1}).

After 3 days, Chl *a* increased as a function of iron concentration: no increase was observed in the control, whereas it more than doubled in the low-iron treatment and increased greater than fourfold in the high-iron treatment (Fig. 6*a*). There was a corresponding drawdown of nutrients, with the greatest drawdown observed in the high-iron treatment (Fig. 6*b*). Silicate to nitrate uptake ratios were low (<0.35) in all treatments but increased 59% with high iron (0.34) relative to the control (0.21). This trend in silicate to nitrate

© 2004 NRC Canada

Table 4. Initial and final concentrations of $DMSP_p$, algal pigments, and macronutrients for an iron addition incubation experiment conducted with HNLC water collected off of the Peruvian coast.

	Day 0	Control (day 3)	Low iron (day 3)	High iron (day 3)
Pigments ($ng \cdot L^{-1}$)				
Chl *a*	1258	1214±155	2710±1149	5241±1223
DVChl *a*	0	0	0	0
Chlorophyllide	4	19±12	55±17	101±36
Σ Phaeophorbide	19	245±112	432±223	513±180
Σ Phaeophytin	288	248±26	529±221	1022±335
Chl *c*3	312	223±55	454±146	745±177
Peridinin	32	0	200±198	253±121
19′-Butanoyloxyfucoxanthin	88	107±16	157±29	118±29
Fucoxanthin	178	381±39	993±441	2178±333
Prasinoxanthin	29	21±2	43±17	62±6
19′-Hexanoyloxyfucoxanthin	776	411±57	749±305	675±37
Alloxanthin	90	97±42	154±51	230±41
β-Carotene	55	51±13	176±80	352±87
$DMSP_p$				
$DMSP_p$ ($nmol \cdot L^{-1}$)	16.57	12.65±1.50	24.79±14.83	25.64±7.98
$DMSP_p$:Chl *a* ($nmol \cdot \mu g^{-1}$)	13.17	10.59±2.59	8.76±1.58	4.86±1.01
$DMSP_p$:β-carotene ($nmol \cdot \mu g^{-1}$)	301	189	141	73
Nutrients ($\mu mol \cdot L^{-1}$)				
NO_x	16.17	8.82±1.76	4.7±0.70	0.87±0.66
PO_4^{3-}	1.09	0.713±0.080	0.397±0.015	0.173±0.050
$Si(OH)_4$	8.08	6.51±0.560	5.12±0.367	2.89±0.626
$Si(OH)_4$:NO_x used (mol:mol)	—	0.213	0.258	0.339

Note: The control was unamended, the low-iron treatment was inoculated with iron to a final concentration of 0.217 $nmol \cdot L^{-1}$, and the high-iron treatment was brought to a final concentration of 2.17 $nmol \cdot L^{-1}$. Day 3 concentrations represent the mean ± 1 SD of three replicates for each treatment (two replicates for the control).

drawdown ratio was consistent with those reported by Hutchins et al. (2002) in nearby surface waters.

$DMSP_p$ concentrations decreased 24% in the control and increased about 50% and 55% in the low- and high-iron treatments, respectively, relative to the initial concentration; however, there were large differences in biomass between treatments. Chl *a* normalized concentrations decreased with increasing iron. $DMSP_p$:Chl *a* decreased approximately 20% in the control, 36% in the low-iron treatment, and 63% in the high-iron treatment (Fig. 6*c*). The $DMSP_p$:Chl *a* concentrations in the high-iron treatment were significantly lower than those in the control (one-way analysis of variance and Tukey pairwise comparison, $p = 0.029$), whereas the difference between the low-iron treatment and the control was not statistically significant ($p = 0.076$).

All pigment concentrations, with the exception of 19′-but, changed in response to iron addition (Table 4). The most marked change was the dramatic increase in fucoxanthin with the addition of iron (2.1, 5.6, and 12.2 times the initial concentration in the control, low-iron, and high-iron treatments, respectively). Chl *c*3 concentrations decreased slightly from initial values in the control but increased 1.5-fold in the low-iron and 2.4-fold in the high-iron treatments. Similarly, 19′-hex concentrations dropped 39% in the control but only slightly in the two iron treatments (3% in the low iron and 13% in the high iron). Concentrations of 19′-but did not show any pattern of response to iron addition. Changes in pigment concentrations indicate that although most taxa responded to iron addition, diatoms preferentially outgrew other groups and dominated the final community. Grazing increased substantially in all treatments and as a function of iron concentration, as indicated by increases in total phaeophorbide concentrations (12.9, 22.7, and 27 times initial levels in the control, low-iron, and high-iron treatments, respectively) and phaeophytin concentrations (0.86, 1.8, and 3.5 times initial levels in the control, low-iron, and high-iron treatments, respectively). This high level of grazing explains the lower than expected increase in Chl *a* based on the drawdown of nitrate.

Hutchins et al. (2002) presented the results of an iron addition experiment conducted with water collected at nearly the same time as the water used for the experiment described here. The measured values of initial nutrient and pigment concentrations were almost identical for the two experiments, as would be expected. Their lowest and highest iron addition treatments (0.2 and 2.5 $nmol \cdot L^{-1}$ final concentration) were close to our low-iron and high-iron treatments. Both experiments were incubated at the same light level, theirs for 5 days, whereas ours was ended on day 3. The results of the two experiments were almost identical, in terms of both the pattern of response and the actual concentrations of nutrients and algal pigments. Any notable differences (i.e., greater nutrient drawdown and higher concentrations of grazing-indicative pigments) can be explained by the longer

© 2004 NRC Canada

duration of their incubation. They reported that after the 5-day incubation, the majority of Chl *a* was contained within the <5 μm fraction and the diatoms that grew in response to iron addition were all pennates and mostly small unicellular *Nitzschia* spp. Given the similarity in initial and final pigment concentrations between our two incubations, it is likely that these same small pennate diatoms were the source of fucoxanthin increases in our treatments.

Discussion

$DMSP_p$ and $DMSO_p$ in the eastern equatorial Pacific and the Peru Upwelling

Although there are substantial records of DMS concentrations in the equatorial Pacific (Andreae 1985; Kieber et al. 1996; Bates and Quinn 1997; Kettle et al. 1999), records of its biogenic precursor DMSP are more limited and to our knowledge have not been measured in the Peru Upwelling before now. $DMSP_p$ concentrations in the mixed layer (0.98–45.7 nmol·L^{-1}) were generally lower than those reported from waters both east and west of the Galapagos Islands (0.8–174 nmol sulfur·dm^{-3}; Hatton et al. 1998) and were closer to those measured on transects of the equatorial Pacific (approximately 5–10 nmol·L^{-1}; Kettle et al. 1999) and during the IronEx II in situ iron fertilization experiment 1300 km west of the Galapagos Islands (approximately 5–16 nmol·L^{-1} before fertilization and 12.9–31.2 nmol·L^{-1} outside the fertilized patch; Turner et al. 1996). At the Peru transect stations, $DMSP_p$ integral sums ranged from 128 to 521 μmol·m^{-2} with integral average concentrations of 4.4–7.7 nmol·L^{-1}. Maximum $DMSP_p$ values were observed at the shelf stations of the two transects where biomass was the highest. Chl *a* normalized $DMSP_p$ concentrations were lowest at both of the nearshore shelf stations and increased offshore on both transects.

$DMSO_p$ remains poorly understood in the world's oceans. To date, there are few published $DMSO_p$ measurements. Table 5 summarizes our findings along with the published records of in situ $DMSO_p$ concentrations. The $DMSO_p$ data presented here are, to our knowledge, the first measurements reported from low latitudes. The $DMSO_p$ concentrations measured off Peru (0.1–30.8 nmol·L^{-1}) are remarkably similar to the majority of values reported from open waters in higher latitudes, whereas there is greater variation in $DMSO_p$:Chl *a* ratios. $DMSO_p$ integral sums (77–256 μmol· m^{-2}) and integral average concentrations (1.82–7.16 nmol·L^{-1}) were generally lower than those of $DMSP_p$. Similar to $DMSP_p$, $DMSO_p$ concentrations on the shelf or the shelf break were higher than at the associated offshore station, whereas $DMSO_p$:Chl *a* ratios increased offshore.

Unlike previous findings that have reported no or weak correlations between $DMSP_p$ and $DMSO_p$, we found that $DMSP_p$ and $DMSO_p$ were highly correlated (Fig. 7). A model II regression of data pooled from both transects revealed a highly significant correlation between $DMSP_p$ and $DMSO_p$ ($r^2 = 0.93$, $p \leq 0.01$, $n = 55$). One possible explanation for this strong correlation is that these compounds may have similar or related physiological functions in the cell (e.g., as components of an antioxidant system). Until we know more about the true physiological functions of these

Fig. 6. An iron addition experiment conducted with water collected using trace metal clean methods from the offshore HNLC region of transect 11/12. Water was collected into a single carboy and divided into three replicates each of three treatments: a control (unamended), a low iron addition (to a final concentration of 0.217 nmol·L^{-1}), and a high iron addition (to a final concentration of 2.17 nmol·L^{-1}). Bottles were incubated for 3 days. Initial (day 0) and final (day 3) concentrations of Chl *a* increased as a function of (*a*) iron with a corresponding drawdown of (*b*) macronutrients. (*c*) DMSP:Chl *a* ratios decreased as a function of iron concentration. The concentration in the high-iron treatment was significantly lower than the control concentration (analysis of variance and Tukey all pairwise comparison, $p < 0.05$), whereas differences between the two iron treatments and the low-iron treatment and the control were not significant. Triangles, NO_x; circles, $Si(OH)_4$; squares, PO_4^{3-}.

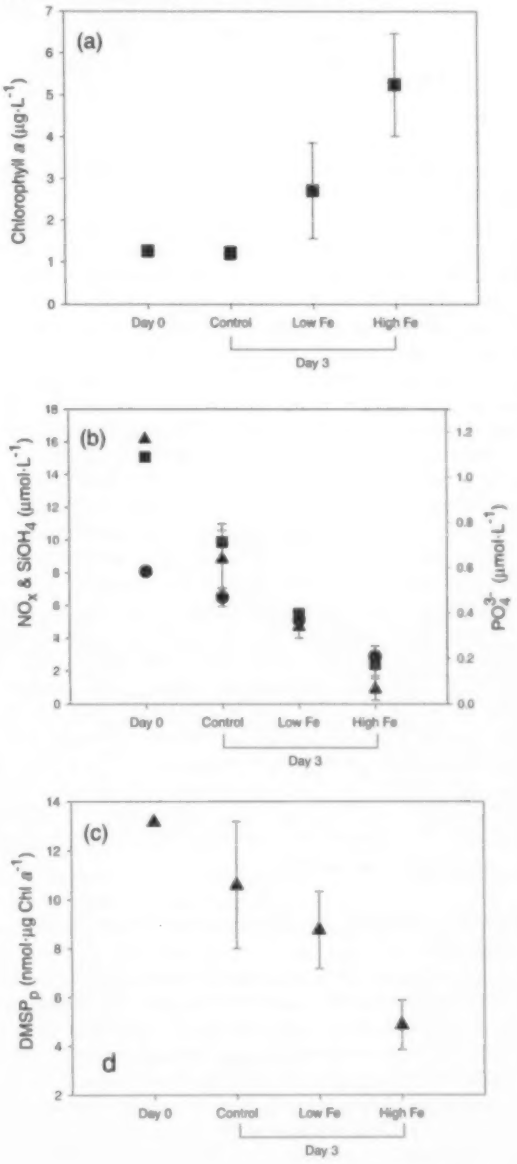

© 2004 NRC Canada

Table 5. Summary of $DMSO_p$, $DMSO_p$:Chl *a*, and $DMSO_p$:$DMSP_p$ from this investigation and all published in situ $DMSO_p$ records.

	$DMSO_p$ (nmol·L^{-1})		$DMSO_p$:Chl *a* (nmol·μg^{-1})		$DMSO_p$:$DMSP_p$	
	Range	Average	Range	Average	Range	Average
Water column						
Off Peru	0.1–30.8	6	0.3–7.9	3	0.24–1.42	0.62
North Sea[a]	2.7–16	7.5	0.99–2.93	1.71	0.04–0.75	0.39
Saguenay Fjord[b]	0–110	8.0	—	—	—	—
North Atlantic[c]	2.8–33	15.45	2.6–17.7	10.5	0.1–0.22	0.17
Mediterranean[c]	16	—	133	—	1.6	—
Arctic NOW[d]	0–16.9	0.37–3.68	0–6.86	0.83–1.69	0–41.8	3.07–11.6
Sea ice						
Arctic NOW[e]	1.35–102	13.7	0.01–4.5	0.22	0.01–1.1	0.07

Note: In cases where multiple average concentrations were reported, we provide the range. Both Bouillon et al. (2002) and Lee et al. (2001) reported on the same data set from the North Water Polynya (NOW); for this table, water column values were taken from the former, whereas sea ice values were taken from the latter.

[a]Simó et al. (1998).
[b]Lee et al. (1999).
[c]Simó et al. (2000).
[d]Bouillon et al. (2002).
[e]Lee et al. (2001).

two compounds, however, interpretation of these ratios is tentative.

The strong correlation of $DMSP_p$ and $DMSO_p$ resulted in relatively consistent $DMSO_p$:$DMSP_p$ ratios compared with other studies. We observed ratios that varied by a factor of less than 5 (0.31:1–1.42), whereas other studies have found this ratio to vary by a factor of 15 (Simó et al. 1998), 23 (Lee et al. 1999), and 21–107 (Bouillon et al. 2002). Despite the low variability that we observed in this ratio, on both transects the highest ratios occurred at the shelf stations where diatoms, generally poor DMSP producers (Keller et al. 1989), were more dominant. Lower $DMSO_p$:$DMSP_p$ ratios were observed offshore where DMSP-producing taxa (based on algal pigments) represented a larger fraction of the total Chl *a*. It was, therefore, largely cross-shelf changes in DMSP concentrations that had the greatest influence on the $DMSO_p$:$DMSP_p$ ratio. This pattern is consistent with the proposed hypotheses that significant variability in DMSP synthesis among different taxa is the primary factor influencing this ratio (Bouillon et al. 2002) and that DMSO synthesis may be more widespread among taxa relative to DMSP (Simó et al. 1998; Lee et al. 1999; Bouillon et al. 2002). Broad $DMSO_p$ production among different taxa is also supported by the stronger correlation of $DMSO_p$ with Chl *a* ($r^2 = 0.697$, $p < 0.01$) compared with that of $DMSP_p$ with Chl *a* ($r^2 = 0.48$, $p < 0.01$), suggesting that $DMSO_p$ production throughout the different transect communities was somewhat more uniform.

$DMSP_p$ and $DMSO_p$ in relation to iron and species composition

Our investigation of biogenic sulfur in the Peru Upwelling revealed that the $DMSP_p$ and $DMSO_p$ concentrations varied in conjunction with changes in dissolved iron concentrations, community composition, and algal biomass. Biomass-normalized $DMSP_p$ and $DMSO_p$ had the same pattern of distribution on both transects. The lowest concentrations of $DMSP_p$ and $DMSO_p$ relative to Chl *a* were observed in the freshly upwelled water on the shelf. This upwelling brings high levels of iron and macronutrients to the surface, stimulating primary production dominated by diatoms. Although biomass decreased significantly off the shelf, $DMSP_p$ and $DMSO_p$ production relative to Chl *a* was higher at these offshore stations. These increases were associated with declines in dissolved iron concentrations, lowered F_v/F_m, and community shifts to ones dominated by haptophytes and cryptophytes (in the case of the trench stations). The results of an iron addition experiment parallel the transect observations. In the bottle incubations, $DMSP_p$:Chl *a* ratios decreased as a function of the iron concentration. The initial algal community in the low-iron waters was predominantly composed of haptophytes; however, after iron addition, diatoms dominated.

Similar to our findings, most other investigations of iron and $DMSP_p$ have shown a decrease in $DMSP_p$ (when nor-

Fig. 7. A strong positive correlation between $DMSP_p$ and $DMSO_p$ was observed (Pearson product moment correlation: $r^2 = 0.916$, $p < 0.01$). A model II regression (reduced major axis method) yields the given relationship. Data are included from all depths (excluding depths below the pycnocline) at all stations sampled on two transects off northern Peru.

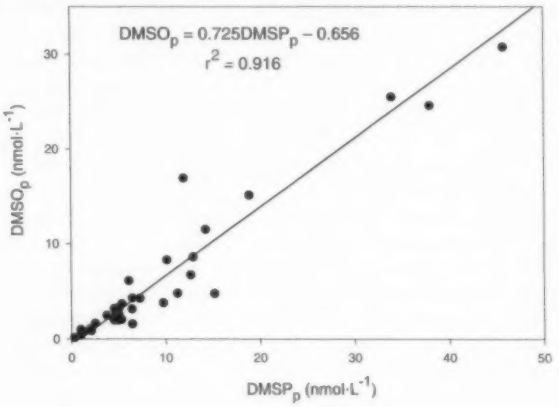

© 2004 NRC Canada

malized to Chl *a*) with iron addition, although the results are not typically presented in these terms. The large-scale in situ iron fertilization experiments conducted in the equatorial Pacific (IronEx II) and the Southern Ocean (SOIREE) reported a net increase in $DMSP_p$ concentrations with iron fertilization (Turner et al. 1996; Boyd et al. 2000). However, these findings are of limited utility in understanding the cellular response to iron addition because the data were not normalized to biomass. In both cases, iron fertilization resulted in a net decrease of DMSP:Chl *a* ratios. Shipboard incubation experiments in the Ross Sea resulted in an increase of $DMSP_p$ in response to iron, but the $DMSP_p$:Chl *a* ratio decreased by greater than 50% in the iron addition treatment compared with an increase in the control (DiTullio and Smith 1997). Similarly, iron addition incubations conducted in the Subantarctic Zone resulted in a decrease in $DMSP_p$:Chl *a* ratios in the +iron treatments of an iron–silicate experiment (DiTullio et al. 2001).

As has been noted for many of these studies and is the case for ours, interpretation of changes in $DMSP_p$ in natural communities is complicated by floristic shifts in response to changing iron availability. Invariably, iron addition experiments conducted in a variety of regions have resulted in a preferential increase in the diatom component of the community (Martin et al. 1989; Coale et al. 1996; Boyd et al. 2000). In general, oceanic diatoms are not thought to be major producers of DMSP based on the comparative studies of Keller et al. (1989). Owing to dramatic changes in the species contributing to the total Chl, normalizing particulate DMSP and DMSO values to this parameter could potentially lead to misinterpretation of the data or obscure taxon-specific responses to iron limitation. Decreases in both cell size and Chl content (chlorosis) under iron limitation (Sunda and Huntsman 1997) can also complicate interpretation of DMSP concentrations normalized to either cell number or total Chl.

Although few investigations of iron and DMSP have reported DMSP in terms of biovolume or intracellular concentration, two laboratory studies report an increase in intracellular concentrations of DMSP under iron limitation. Stefels and van Leeuwe (1998) found that cellular DMSP concentrations were 80% higher in iron-deplete compared with iron-replete *Phaeocystis* sp. cultures under high-light conditions, although this difference was not apparent under low-light conditions. Sunda et al. (2002) reported an increase in cellular DMSP under iron limitation in the centric diatom *Thalassiosira pseudonana*.

An antioxidant, free-radical scavenging function has recently been proposed for DMSO (Simó et al. 1998; Lee and de Mora 1999) and demonstrated for DMSP (Sunda et al. 2002). Such a function suggests the potential for greater synthesis of these compounds in HNLC regions where algae are experiencing iron-induced physiological stress. Shipboard incubations (Hutchins et al. 2002) and measurements of F_v/F_m and flavodoxin in the HNLC waters off the coast of Peru have shown that algae in this region are iron limited (G.R. DiTullio et al., unpublished[3]). Our investigations in this same system found the highest $DMSP_p$:Chl *a* and $DMSO_p$:Chl *a* ratios associated with low iron concentrations, a pattern supporting an antioxidant function for these compounds. Lee et al. (2001) suggested that DMSO may form part of a consortium of antioxidants, and comparisons of DMSO with other known antioxidants such as β-carotene might be revealing. Data from the two transects were pooled and a model II regression was performed. $DMSO_p$ was more strongly correlated with β-carotene ($r^2 = 0.82$, $p \leq 0.01$) (Fig. 8*a*) than with Chl *a*, lending further support to the antioxidant hypothesis. $DMSP_p$ was also more strongly correlated with β-carotene ($r^2 = 0.69$, $p \leq 0.01$) (Fig. 8*b*) than with Chl *a*, although less of the variation was explained by the regression.

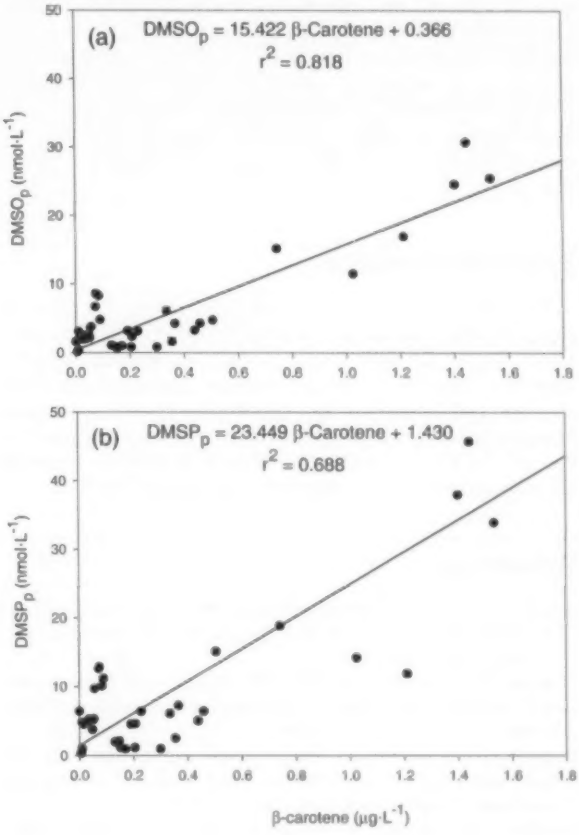

Fig. 8. Correlations between (*a*) $DMSO_p$ and (*b*) $DMSP_p$ and the known antioxidant β-carotene. The relationships given are based on model II regressions (reduced major axis method) of data from all depths (excluding depths below the pycnocline) at all stations sampled on two transects off northern Peru.

Our observations of dissolved iron, F_v/F_m, $DMSP_p$:Chl *a*, and $DMSO_p$:Chl *a* in the Peru Upwelling support an antioxidant function for DMSP and DMSO. However, there are limitations to the interpretation of our data because of changes in community composition. In most cases, the changes that we observed in dissolved iron concentration were associated with changes in the dominant taxa present, making it impossible to separate the effects of these different variables. Interestingly, the two shelf stations on transect 13/14 had very similar community compositions yet differed in dissolved iron concentrations and levels of physiological stress. $DMSP_p$ and $DMSO_p$ production per unit Chl were

© 2004 NRC Canada

higher in the lower iron waters, suggesting that the differences that we observed may not have been entirely due to species effects.

It is clear that concentrations of dissolved iron can influence net concentrations of $DMSP_p$ and $DMSO_p$ in the world's oceans. Whether this influence is due solely to the demonstrated effect that iron has on species composition and biomass or whether there is a direct biosynthetic change at the cellular level cannot be determined easily from studies of natural communities. Further laboratory work addressing the physiological responses of different taxa to iron stress is needed before accurate interpretation of field data is possible.

Acknowledgements

We would like to thank the following people for their assistance: Mel Alm for performing the FRRF measurements, Mark Geesey for HPLC analysis of the pigment samples, Jennifer Conn for shipboard nutrient measurements, Ken Bruland and Eden Rue for dissolved iron measurements, Geoffrey Smith for the trace metal clean collection of seawater, and the Captain and crew of the R/V *Melville*. Support for this research was provided by NSF OCE 9907931.

References

Andreae, M.O. 1985. Dimethylsulfide in the water column and the sediment pore waters of the Peru upwelling area. Limnol. Oceanogr. **30**: 1208–1218.

Andreae, M.O., and Crutzen, P.J. 1997. Atmospheric aerosols; biogeochemical sources and role in atmospheric chemistry. Science (Wash., D.C.), **276**: 1052–1058.

Bates, T.S., and Quinn, J.G. 1997. Dimethylsulfide (DMS) in the equatorial Pacific Ocean (1982 to 1996): evidence of a climate feedback? Geophys. Res. Lett. **24**: 861–864.

Bouillon, R.-C., Lee, P.A., de Mora, S.J., Levasseur, M., and Lovejoy, C. 2002. Vernal distribution of dimethylsulfide, dimethylsulphoniopropionate, and dimethylsulfoxide in the North Water in 1998. Deep-Sea Res. II. Top. Stud. Oceanogr. **49**: 5171–5189.

Boyd, P.W., and Abraham, E.R. 2001. Iron mediated changes in phytoplankton photosynthetic competence during SOIREE. Deep-Sea Res. II. Top. Stud. Oceanogr. **48**: 2529–2550.

Boyd, P., Watson, A.J., Law, C.S., Abraham, E.R., Trull, T., Murdoch, R., Bakker, D.C.E., Bowle, A.R., Buesseler, K.O., Chang, H., Charette, M., Croot, P., Downing, K., Frew, R., Gall, M., Hadfield, M., Hall, J., Harvey, M., Jameson, G., La Roche, J., Liddicoat, M., Ling, R., Maldonado, M.T., McKay, R.M.L., Nodder, S., Pickmere, S., Pridmore, R., Rintoul, S., Safi, K., Sutton, P., Strzepek, R., Tannenberger, K., Turner, S., Waite, A., and Zeldis, J. 2000. A mesoscale phytoplankton bloom in the polar Southern Ocean stimulated by iron fertilization. Nature (Lond.), **407**: 695–702.

Bruland, K.W., Rue, E.L., and Smith, G.J. 2001. Iron and macronutrients in California coastal upwelling regimes: implications for diatom blooms. Limnol. Oceanogr. **46**: 1661–1674.

Bruland, K.W., Rue, E.L., Smith, G.J., and DiTullio, G.R. 2004. Iron, macronutrients and diatom blooms in the Peru upwelling regime: brown and blue waters of Peru. Mar. Chem. In press.

Cantoni, G.L., and Anderson, D.G. 1956. Enzymatic cleavage of dimethylpropiothetin by *Polysiphona lanosa*. J. Biol. Chem. **22**: 171–177.

Charlson, R.J., Lovelock, J.E., Andrea, M.O., and Warren, S.G. 1987. Oceanic phytoplankton, atmospheric sulphur, cloud albedo, and climate. Nature (Lond.), **326**: 655–661.

Coale, K.H., Johnson, K.S., Fitzwater, S.E., Gordon, R.M., Tanner, S., Chavez, F.P., Ferioli, L., Sakamoto, C., Rogers, P., Millero, F., Steinberg, P., Nightingale, P., Cooper, D., Cochlan, W.P., Landry, M.R., Constantinou, J., Rollwagen, G., Trasvina, A., and Kudela, R. 1996. A massive phytoplankton bloom induced by an ecosystem-scale iron fertilization experiment in the Equatorial Pacific. Nature (Lond.), **383**: 495–501.

Dacey, J.W.H., and Wakeham, S.G. 1986. Oceanic dimethylsulfide: production during zooplankton grazing on phytoplankton. Science (Wash., D.C.), **233**: 1314–1316.

Dacey, J.W.H., Howse, F.A., Michaels, A.F., and Wakeham, S.G. 1998. Temporal variability of dimethylsulfide and dimethylsulfoniopropionate in the Sargasso Sea. Deep-Sea Res. I. Oceanogr. Res. Pap. **45**: 2085–2104.

Davey, M., and Geider, R.J. 2001. Impact of iron limitation on the photosynthetic apparatus of the diatom *Chaetoceros muelleri* (Bacillariophycea). J. Phycol. **37**: 987–1000.

DiTullio, G.R., and Geesey, M.E. 2002. Photosynthetic pigments in marine algae and bacteria. *In* The encyclopedia of environmental microbiology. *Edited by* G. Bitton. John Wiley & Sons, Inc., New York. pp. 2453–2470.

DiTullio, G.R., and Smith, W.O., Jr. 1997. Studies on dimethyl sulphide in Antarctic coastal waters. *In* Antarctic communities: species, structure and survival. *Edited by* B. Battaglia, J. Valencia, and D.W.H. Walton. Cambridge University Press, Cambridge, U.K. pp. 93–100.

DiTullio, G.R., Sedwick, P.N., Jones, D.R., Boyd, P.W., Crossley, A.C., and Hutchins, D.A. 2001. Effects of iron, silicate and light on dimethylsulfoniopropionate production in the Australian Subantarctic Zone. J. Geophys. Res.**106**: 31 585 – 31 595.

Eldridge, M.E., Trick, C.W., Alm, M.B., DiTullio, G.R., Rue, E.L., Bruland, K.W., Hutchins, D.A., and Wilhelm, S.W. 2004. Phytoplankton community response to a manipulation of bioavailable iron in HNLC waters of the subtropical Pacific Ocean. Aquat. Microb. Ecol. **35**: 79–91.

Falkowski, P.G., Kim, Y., Kolber, Z., Wilson, C., Wirick, C., and Cess, R. 1992. Natural versus anthropogenic factors affecting low-level cloud albedo over the North Atlantic. Science (Wash., D.C.), **256**: 1311–1313.

Hatton, A.D., Turner, S.M., Malin, G., and Liss, P.S. 1998. Dimethylsulphoxide and other biogenic sulphur compounds in the Galapagos Plume. Deep-Sea Res. II. Top. Stud. Oceanogr. **45**: 1043–1053.

Hutchins, D.A., Hare, C.E., Weaver, R.S., Zhang, Y., Firme, G.F., DiTullio, G.R., Alm, M.B., Riseman, S.F., Maucher, J.M., Geesey, M.E., Trick, C.G., Smith, G.J., Rue, E.L., Conn, J., and Bruland, K.W. 2002. Phytoplankton iron limitation in the Humbolt Current and Peru Upwelling. Limnol. Oceanogr. **47**: 997–1011.

Keller, M.D., Bellows, W.K., and Guillard, R.R.L. 1989. Dimethyl sulfide production in marine phytoplankton. *In* Biogenic sulfur in the environment. *Edited by* E.S. Saltzman and W.J. Cooper. American Chemical Society, Washington, D.C. pp. 167–182.

Kettle, A.J., Andreae, M.O., Amouroux, D., Andreae, T.W., Bates, T.S., Berresheim, H., et al. 1999. A global database of sea surface dimethylsulfide (DMS) measurements and a procedure to predict sea surface DMS as a function of latitude, longitude, and month. Global Biogeochem. Cycles, **13**: 339–444.

Kieber, D.J., Jiao, J., Kiene, R.P., and Bates, T.S. 1996. Impact of dimethylsulfide photochemistry on methyl sulfur cycling in the equatorial Pacific Ocean. J. Geophys. Res. **101**(C2): 3715–3722.

© 2004 NRC Canada

Kirst, G.O., Thiel, C., Wolff, H., Nothnagel, J., Wanzek, M., and Ulmke, R. 1991. Dimethylsulfoniopropionate (DMSP) in ice-algae and its possible biological role. Mar. Chem. **35**: 381–388.

Kolber, Z.S., Barber, R.T., Coale, K.H., Fitzwater, S.E., Greene, R.M., Johnson, K.S., Lindley, S.T., and Falkowski, P.G. 1994. Iron limitation of phytoplankton photosynthesis in the Equatorial Pacific Ocean. Nature (Lond.), **371**: 145–149.

Laws, E.A., DiTullio, G.R., Carder, K.L., Betzer, P.R., and Hawes, S. 1990. Primary production in the deep blue sea. Deep-Sea Res. **37**: 715–730.

Lee, P.A., and de Mora, S.J. 1999. Intracellular dimethylsulfoxide (DMSO) in unicellular marine algae: speculations on its origin and possible biological role. J. Phycol. **35**: 8–18.

Lee, P.A., de Mora, S.J., Chanut, J.-P., and Gosselin, M. 1999. Dimethylsulfoxide (DMSO) and related sulfur compounds in the Saguenay Fjord, Quebec. Can. J. Fish. Aquat. Sci. **56**: 1631–1638.

Lee, P.A., de Mora, S.J., Gosselin, M., Levasseur, M., Bouillon, R.-C., Nozais, C., and Michel, C. 2001. Particulate dimethylsulfoxide in Arctic sea-ice algal communities: the cryoprotectant hypothesis revisited. J. Phycol. **37**: 488–499.

Martin, J.H. 1990. Glacial–interglacial CO_2 change: the iron hypothesis. Palaeogeography, **5:** 1–13.

Martin, J.H. 1992. Iron as a limiting factor in oceanic productivity. *In* Primary production and biogeochemical cycles in the sea. *Edited by* P.G. Falkowski and A.D. Woodhead. Plenum Press, New York. pp. 123–136.

Martin, J.H., Gordon, R.M., Fitzwater, S.E., and Broenkow, W.W. 1989. VERTEX: phytoplankton/iron studies in the Gulf of Alaska. Deep-Sea Res. I. Oceanogr. Res. Pap. **36**: 649–680.

Maucher, J.M. 2001. Flavodoxin as a diagnostic indicator of iron stress in oceanic phytoplankton. M.S. thesis, University of Charleston, Charleston, S.C.

Olson, R.J., Sosik, H.M., Chekalyuk, A.M., and Shalapyonok, A. 2000. Effects of iron enrichment on phytoplankton in the Southern Ocean during late summer: active fluorescence and flow cytometric analyses. Deep-Sea Res. II. Top. Stud. Oceanogr. **47**: 3181–3200.

Simó, R., Grimalt, J.O., and Albaiges, J. 1996. Sequential method for the field determination of nanomolar concentrations of dimethyl sulfoxide in natural waters. Anal. Chem. **68**: 1493–1498.

Simó, R., Hatton, A., Malin, G., and Liss, P.S. 1998. Particulate dimethyl sulphoxide in seawater: production by microplankton. Mar. Ecol. Prog. Ser. **167**: 291–296.

Simó, R., PedrosAlio, C., Malin, G., and Grimalt, J.O. 2000. Biological turnover of DMS, DMSP and DMSO in contrasting open-sea waters. Mar. Ecol. Prog. Ser. **203**: 1–11.

Sosik, H.M., and Olson, R.J. 2002. Phytoplankton and iron limitation of photosynthetic efficiency in the Southern Ocean during late summer. Deep-Sea Res. I. Oceanogr. Res. Pap. **49**: 1195–1216.

Stefels, J. 2000. Physiological aspects of the production and conversion of DMSP in marine algae and higher plants. J. Sea Res. **43**: 183–197.

Stefels, J., and van Leeuwe, M.A. 1998. Effects of iron and light stress on the biochemical composition of Antarctic *Phaeocystis* sp. (Prymnesiophyceae). I. Intracellular DMSP concentrations. J. Phycol. **34**: 486–495.

Sunda, W.G., and Huntsman, S.A. 1997. Interrelated influence of iron, light and cell size on marine phytoplankton growth. Nature (Lond.), **390**: 389–392.

Sunda, W., Kieber, D.J., Kiene, R.P., and Huntsman, S. 2002. An antioxidant function for DMSP and DMS in marine algae. Nature (Lond.), **418**: 317–320.

Turner, S.M., Nightingale, P.D., Spokes, L.J., Liddicoat, M.I., and Liss, P.S. 1996. Increased dimethyl sulphide concentrations in sea water from *in situ* iron enrichment. Nature (Lond.), **383**: 513–516.

Vairavamurthy, A., Andreae, M.O., and Iverson, R.L. 1985. Biosynthesis of dimethylsulfide and dimethylpropiothetin by *Hymenomas carterae* in relation to sulfur source. Limnol. Oceanogr. **30**: 59–70.

Wolfe, G.V., Steinke, M., and Kirst, G.O. 1997. Grazing-activated chemical defense in a unicellular marine alga. Nature (Lond.), **387**: 394–897.

© 2004 NRC Canada

Possible impacts of zooplankton grazing on dimethylsulfide production in the Antarctic Ocean[1]

Nobue Kasamatsu, So Kawaguchi, Shuichi Watanabe, Tsuneo Odate, and Mitsuo Fukuchi

Abstract: The role of zooplankton grazing on dimethylsulfide (DMS) and dissolved dimethylsulfoniopropionate ($DMSP_d$) production was investigated in the Antarctic Ocean in January and February 2002. Dominant herbivorous macrozooplankton of this region, the Antarctic krill *Euphausia superba* and the tunicate *Salpa thompsoni*, were used in shipboard incubation experiments. The concentration of $DMSP_d$ + DMS increased in the water during incubation with krill. The production rate was 2.96 ± 2.78 nmol $DMSP_d$ + DMS·krill^{-1}·h^{-1} (mean ± SD). In addition, the $DMSP_d$ + DMS production rate was linearly related to the ingestion rate of krill ($r^2 = 0.664$, $p \leq 0.01$). Addition of salps to natural surface water, however, did not change the $DMSP_d$ + DMS concentrations. During the experiments, both animals fed on phytoplankton cells. The fecal pellets of krill contained broken phytoplankton cells, whereas those of salps contained unbroken cells. These results suggest that sloppy feeding by krill is a more likely mechanism for producing DMS and $DMSP_d$ than the direct ingestion of phytoplankton cells by salps. The decrease of DMS concentrations in the upper 200 m of the water column from January to February may be explained, in part, by changes in the composition of the macrozooplankton community.

Résumé : En janvier et février 2002, nous avons étudié le rôle du broutage du zooplancton sur la production de sulfure de diméthyle et de diméthylsulfoniopropionate dissous ($DMSP_d$) dans l'océan Antarctique. Nous avons aussi utilisé le krill antarctique *Euphausia superba* et le tunicier *Salpa thompsoni,* les espèces dominantes du macrozooplancton de la région, dans des expériences d'incubation à bord. Les concentrations de $DMSP_d$ + DMS augmentent dans l'eau durant l'incubation avec le krill. Le taux de production est de 2,96 ± 2,78 nmol $DMSP_d$ + DMS·krill^{-1}·h^{-1} (moyenne ± écart type). De plus, le taux de production de $DMSP_d$ + DMS est en corrélation linéaire avec le taux d'ingestion du krill ($r^2 = 0{,}664$, $p \leq 0{,}01$). En revanche, l'addition de salpes à de l'eau naturelle de surface ne change pas la concentration de $DMSP_d$ + DMS. Durant l'expérience, les deux espèces d'animaux se nourrissent de cellules du phytoplancton. Les boulettes fécales du krill contiennent des cellules de phytoplancton brisées, alors que celles des salpes contiennent des cellules intactes. Ces résultats indiquent que l'alimentation brouillonne du krill est un mécanisme plus probable de production de DMS et de $DMSP_d$ que l'ingestion directe des cellules du phytoplancton par les salpes. Le déclin des concentrations de DMS dans les 200 m supérieurs de la colonne d'eau en janvier et en février peut s'expliquer, en partie, par les changements dans la communauté du macrozooplancton.

[Traduit par la Rédaction]

Introduction

Dimethylsulfide (DMS) is the most abundant form of volatile sulfur in the ocean. According to the CLAW hypothesis (Charlson et al. 1987), marine DMS production may act as a climate regulatory mechanism via a feedback loop involving surface ocean temperature, phytoplankton, DMS, sulfate aerosol formation, and cloud albedo, although the existence of this feedback has not been proven. Recently, attention has been focused on assessing sinks and sources of DMS in the oceans and on the processes controlling the cycling of DMS in the marine environment. The different processes involved in marine DMS emission were reviewed by Liss et al. (1997). DMS is produced by the enzymatic cleavage of dimethylsulfoniopropionate (DMSP), an organic compound synthesized by many phytoplankton species that may serve as an osmolyte and cryoprotectant (Karsten et al. 1996; Kirst 1996). Since DMS is produced in seawater by the break-

Received 24 March 2003. Accepted 2 March 2004. Published on the NRC Research Press Web site at http://cjfas.nrc.ca on 23 June 2004.
J17407

N. Kasamatsu.[2] The Graduate University for Advanced Studies, 173-8515, 9-10 Kaga 1-chome, Itabashi-ku, Tokyo, Japan.
S. Kawaguchi.[3] National Research Institute of Far Seas Fisheries, 424-8633, 5-7-1 Orido, Shimizu, Japan.
S. Watanabe. Japan Marine Science and Technology Center, 237-0061, 2-15 Natsushimacho, Yokosuka, Japan.
T. Odate and M. Fukuchi. The Graduate University for Advanced Studies, 173-8515, 9-10 Kaga 1-chome, Itabashi-ku, Tokyo, Japan, and National Institute of Polar Research, 173-8515, 9-10 Kaga 1-chome, Itabashi-ku, Tokyo, Japan.

[1]This paper is part of the proceedings of the Third International Symposium on Biological and Environmental Chemistry of DMS(P) and Related Compounds, held in Rimouski (Québec), 26–28 September 2002.
[2]Corresponding author (e-mail: kasa@nipr.ac.jp).
[3]Present address: Australian Antarctic Division, Channel Highway, Kingston Tasmania 7050, Australia.

 doi: 10.1139/F04-072 © 2004 NRC Canada

down of its precursor, DMSP, one of the key steps towards better knowledge of DMS cycling in the ocean is to understand the rates of and controls on production and fate of DMSP. The conversion of DMSP into DMS may be influenced by bacterial activities (Kiene and Linn 2000), phytoplanktonic enzymes (Niki et al. 2000), and zooplankton grazing (Dacey and Wakeham 1986; Cantin et al. 1996; Wolfe et al. 2000). However, there is still a need for a proper evaluation of the role of zooplankton on DMS production in natural systems.

Dacey and Wakeham (1986) found that one third of the phytoplankton DMSP ingested by copepods was released in the seawater as DMS. Daly and DiTullio (1996) showed that DMS concentrations increased when krill were added to bottles filled with seawater during shipboard experiments. The interpretation of these results is, however, limited, as zooplankton ingestion rates were not measured during these experiments.

Zooplankton grazing experiments conducted during DMS studies were mainly done with copepods and krill, which are both known as sloppy feeders (Dacey and Wakeham 1986; Daly and DiTullio 1996; Tang et al. 2000*a*). Macrozooplankton have various grazing mechanisms in nature. To understand the impact of zooplankton on DMS production, we need to assess the effect of the different grazing mechanisms on DMS production. The Antarctic krill *Euphausia superba* and the tunicate *Salpa thompsoni* are both known as dominant macrozooplankton groups in the Antarctic Ocean. Although both krill and salps are filter feeders (e.g., Harbison et al. 1986), they have different grazing mechanisms. Krill are known as sloppy feeders, because they break algal cells with their mouthparts (Strom et al. 1997), whereas salps filter particles on their mucous nets and swallow them directly into their guts (Alldredge and Madin 1982). Breakage of the algal cells through sloppy feeding may result in greater dissolved DMSP ($DMSP_d$) production than does grazing by direct ingestion of cells without breakage (Kawaguchi 2001). Because of their different grazing mechanisms and their importance as consumers of primary producers in the Antarctic Ocean, we believe that it is important to compare the contribution of krill and salps to DMS production in this ocean system. The objective of this study was to determine the influence of macrozooplankton grazing on DMS dynamics in the Antarctic Ocean during the summertime.

Materials and methods

Water sampling

Sampling was carried out in the Australian sector of the Antarctic Ocean (approximately 65°S, 140°E) during cruise KH01-3 of the R/V *Hakuho-Maru* (University of Tokyo) in January 2002 and during the 43rd Japanese Antarctic Research Expedition Marine Science Cruise of the R/V *Tangaroa* in February 2002 (Table 1). Water samples were collected at 10 or 11 depths from 2 to 200 m with a rosette sampler equipped with 12-L Niskin bottles and a conductivity–temperature–depth (CTD) probe (SeaBird SBE911 plus). In addition, surface seawater was taken with a plastic bucket. On some occasions, seawater pumped by the ship from a depth of approximately 5 m was used for culture experiments (Table 2). These samples were used for the determination of DMS, $DMSP_d$, particulate DMSP ($DMSP_p$), and chlorophyll *a* (Chl *a*). For DMS(P) analyses, water samples were transferred with 100-mL glass syringes.

Incubation experiments

To determine the influence of macrozooplankton grazing on DMSP and DMS production, shipboard incubation experiments were conducted during the February cruise using the two dominant macrozooplankton species, the Antarctic krill *E. superba* and the tunicate *S. thompsoni* (Table 2). Krill and salp individuals were sampled by vertical tows with a NORPAC net at a hauling speed of 0.5 $m \cdot s^{-1}$. Salps were handled as gently as possible to avoid any damage to the animals. The animals were acclimated for several days under laboratory conditions, and only those in good condition were used for the experiments. This time span also ensured the regeneration of their mucous nets even if they were accidentally damaged during the sampling. Except for experiment 3, krill were collected before the February cruise and kept alive in the laboratory until performing the experiments. Approximate body length of krill and salps was 35 and 40 mm, respectively. All animals were kept in Whatman GF/F (nominal pore size of 0.7 μm) filtered seawater for 24 h before the beginning of the experiments to ensure that the gut contents of the animals were cleared out.

For the incubation experiments, water was collected at the sea surface or at the depth of the Chl *a* maximum, as described above, or pumped by the ship from a depth of approximately 5 m (Table 2). The water was transferred into a 75-L plastic bucket through 330-μm mesh, which removed macro- and meso-zooplankton. Initial concentrations of DMS, $DMSP_d$, $DMSP_p$, Chl *a*, and bacteria of the seawater in this 75-L bucket were determined in triplicate. The seawater was then immediately subdivided into six narrow-mouthed 10-L polycarbonate bottles as gently as possible. One animal each was placed in three of these bottles. The remaining three bottles without animals were incubated as controls. All of the labware was previously cleaned with diluted HCl.

All bottles were incubated, with a little headspace, for 6–24 h in a darkened roller incubator installed in a low-temperature room (approximately 0.5 °C). At the end of the incubation, subsamples were collected in each bottle for the determination of DMS(P), Chl *a*, and bacterial abundance. The appearance of fecal pellets in the incubation bottles was checked every 3–6 h. Fecal pellets were removed from the treatment bottles when they were present. They were observed and photographed under a microscope. Clearance rate of Chl *a* by macrozooplankton was calculated using the equation suggested by Frost (1972).

Sulfur determinations

DMS and DMSP concentrations were measured with a modified purge and trap apparatus as described by Watanabe et al. (1987) and Uzuka et al. (1996). For DMS measurement, an aliquot of 4–14 mL of seawater was filtered on a Whatman GF/F filter (47 mm) and the filtrate was introduced into a glass purge chamber. DMS concentration was determined on a gas chromatograph equipped with a flame photometric detector (Shimadzu GC-14B). For total DMSP

© 2004 NRC Canada

Table 1. Dominant zooplankton and integrated values for DMS, $DMSP_d$, $DMSP_p$, and Chl *a* in the water column (depth = 0–200 m).

Date	Sample location: Latitude (S)	Sample location: Longitude (E)	DMS ($mmol \cdot m^{-2}$)	$DMSP_d$ ($mmol \cdot m^{-2}$)	$DMSP_p$ ($mmol \cdot m^{-2}$)	Chl *a* ($mg \cdot m^{-2}$)	Dominant zooplankton
10 Jan. 2002	65°41′	140°08′	1.45	2.18	1.93	411.78	Krill
18 Feb. 2002	65°26′	139°51′	0.54	0.75	3.36	86.99	Salp

Table 2. Details of shipboard incubation experiments.

Experiment	Details of seawater used: Latitude (S)	Details of seawater used: Depth	Experimental animal	Initial Chl *a* ($\mu g \cdot L^{-1}$)	Initial $DMSP_d$+DMS ($nmol \cdot L^{-1}$)
1	66°26′	Chl *a* maximum (5 m)	Krill	4.20	4.83
2	64°00′	Chl *a* maximum (16 m)	Krill	0.83	6.20
3	65°26′	Surface	Krill	2.25	6.85
4	65°26′	Surface	Krill	1.38	3.81
5	64°00′	Pumped (5 m)	Salp	0.14	4.91
6	64°45′	Pumped (5 m)	Salp	0.34	10.54

($DMSP_t$) ($DMSP_t$ = $DMSP_d$ + $DMSP_p$) + DMS measurement, an aliquot of 4–14 mL of seawater sample was poured into a 30-mL serum bottle containing 4 mL of 6 mol $NaOH \cdot L^{-1}$. The alkali treatment permits the cleavage of $DMSP_t$ into gaseous DMS. For $DMSP_d$ + DMS measurement, an aliquot of 4–14 mL of seawater was filtered through a Whatman GF/F filter and the filtrate was poured into a serum bottle containing NaOH. Serum bottles were stored at 4 °C for at least 24 h to complete the cleavage before analyses. For DMSP analyses, the serum bottles were purged with pure nitrogen gas. $DMSP_d$ concentration was computed as the difference between $DMSP_d$ + DMS and DMS. $DMSP_p$ concentration was calculated as the difference between $DMSP_t$ + DMS and $DMSP_d$ + DMS. The analytical error for each measurement was 11%.

Pigment analysis

Samples for pigment analysis (Chl *a* and pheopigments) were filtered on Whatman GF/F filters. Pigments were extracted in dimethylformamid (Suzuki and Ishimaru 1990) for 24 h at approximately −80 °C. Concentrations of pigments were determined onboard the ship (Parsons et al. 1984) using a model 10AU Turner Designs fluorometer.

Bacterial abundance

Samples for the determination of bacterial abundance were fixed with 0.5% glutaraldehyde and kept refrigerated for later processing. At a shore laboratory, cells were stained with 4′,6-diamidino-2-phenylindole and counted by epifluorescence microscopy (Kirchman et al. 1982).

Statistical methods

Statistical analyses were conducted to evaluate the possible impacts of zooplankton on DMS(P) production, Chl *a* concentration, and bacterial abundance in the experimental seawater during the incubation. Because the values in the control bottles changed during the incubation periods as well as in the treatment bottles, differences of the final values between treatment bottles and control bottles (mean of three replicates for each experiment) were compiled for both krill and salps and applied to the tests. Because we were uncertain about the normality of the distribution of the values, we used both parametric (one-tailed *t* test) and nonparametric tests (the sign test) to assess the significance of their differences. Nonparametric tests are less powerful than parametric test but require fewer assumptions. Therefore, the results of the nonparametric tests will be more conservative (Zar 1996). To evaluate the relationship between the zooplankton grazing activity and DMS(P) production, a linear regression was fitted. Statistical analyses were conducted using Statview (version 5.0) software (SAS Institute Inc., Cary, N.C.).

Results

Overview of the survey site

In January 2002, the northern edge of the sea ice cover was observed near 65.5°S. In February, sea ice cover had retreated more than 93 km further south, near the coast of the Antarctic continent. The sampling station was thus free of ice in February. The surface mixed layer depth (defined as the depth where potential density is 0.1 greater than surface values) at the sampling station increased from 5 m in January to 50 m in February. An extensive phytoplankton bloom composed mainly of diatoms (M. Miki, University of Tokyo, Tokyo 113-8657, Japan, personal communication, e-mail: aa37057@mail.ecc.u-tokyo.ac.jp) was observed at the ice edge in January. Chl *a* concentrations integrated from 0 to 200 m were 412 $mg \cdot m^{-2}$ in January and 87 $mg \cdot m^{-2}$ in February (Table 1). The dominant macrozooplankton community changed from krill in January (J. Nishikawa, Ocean Research Institute, University of Tokyo, Tokyo 164-8639, Japan, personal communication, e-mail: jn@ori.u-tokyo.ac.jp) to salps in February (S. Kawaguchi, personal observation).

Concentrations of DMS and related compounds

In January, DMS and $DMSP_d$ concentrations integrated from 0 to 200 m were very high, reaching 1.45 and 2.18 $mmol \cdot m^{-2}$, respectively (Table 1). In February, these concentrations de-

© 2004 NRC Canada

Fig. 1. Differences in (*a*) Chl *a* concentrations and (*b*) $DMSP_d$ + DMS concentrations between treatment bottles and final control bottles (treatment minus final control) with the incubation time. The broken line indicates where the value of treatment bottles equals that of final control bottles. Positive values indicate that values of treatment bottles are higher than those of final control bottles.

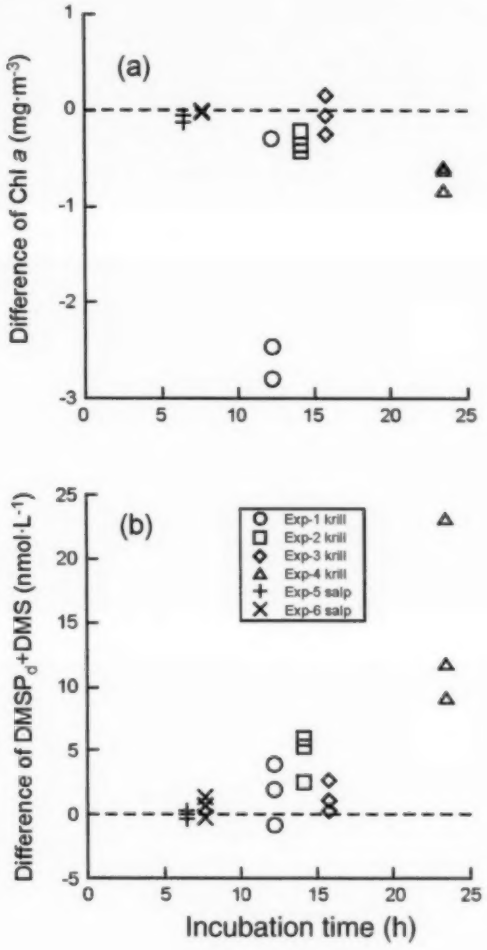

creased to 0.54 and 0.75 mmol·m^{-2}, respectively. In contrast with DMS and $DMSP_d$, $DMSP_p$ concentration increased from 1.93 mmol·m^{-2} in January to 3.36 mmol·m^{-2} in February (Table 1).

Krill experiments

During most experiments, krill ingested phytoplankton pigments. Chl *a* concentrations in treatment bottles were significantly lower than those of final control bottles (one-tailed *t* test, $t = -2.713$, $p \leq 0.05$, $n = 12$; sign test, $p \leq 0.01$, $n = 12$) (Fig. 1*a*). For all experiments, the clearance rate was 262 ± 239 mL·individual^{-1}·h^{-1} (mean ± SD) and the ingestion rate ranged from 0.00 to 0.48 µg Chl *a*·individual^{-1}·h^{-1} (Table 3). $DMSP_d$ + DMS concentrations in treatment bottles were significantly higher than in the final control bottles (one-tailed *t* test, $t = 2.937$, $p \leq 0.05$, $n = 12$; sign test, $p \leq 0.01$, $n = 12$) (Fig. 1*b*). Production rates of DMS and $DMSP_d$ + DMS were 2.91 ± 2.75 and 2.96 ± 2.78 nmol·individual^{-1}·h^{-1}, respectively (Table 4). Mean bacterial abundance under the different experimental conditions ranged from 1.1 to 1.4 × 10^5 cells·mL^{-1} (Table 5). There was a statistical significant difference in bacterial abundances between treatment bottles and final control (one-tailed *t* test, $t = 3.559$, $p \leq 0.01$, $n = 12$; sign test, $p \leq 0.05$, $n = 12$).

Table 3. Clearance and ingestion rates of zooplankton in shipboard incubation experiments.

Animal	Mean	Max.	Min.	SD	*n*
Clearance rate (mL·individual^{-1}·h^{-1})					
Krill	262.26	717.58	0.00	238.64	12
Salp	336.51	1047.96	5.34	400.42	6
Ingestion rate (µg Chl *a*·individual^{-1}·h^{-1})					
Krill	0.25	0.48	0.00	0.17	12
Salp	0.06	0.17	0.00	0.06	6

Note: Max., maximum; Min., minimum; *n*, the number of individuals.

Table 4. DMS and $DMSP_d$ + DMS production rates in shipboard incubation experiments.

Animal	Mean	Max.	Min.	SD	*n*
DMS production rates (nmol·individual^{-1}·h^{-1})					
Krill	2.91	7.26	–0.70	2.75	12
Salp	na	na	na	na	6
$DMSP_d$ + DMS production rates (nmol·individual^{-1}·h^{-1})					
Krill	2.96	9.86	–0.60	2.78	12
Salp	na	na	na	na	6

Note: Max., maximum; Min., minimum; *n*, the number of individuals; na, not applicable.

Table 5. Bacterial abundance in incubation experiments.

	Bacteria count (× 10^5 cells·mL^{-1}) (mean ±SD)		
Animal	Initial control	Final control	Treatment
Krill	1.1±0.7	1.2±0.7	1.4±0.7
Salp	1.0±0.5	0.9±0.2	0.8±0.2

Salp experiments

Initial Chl *a* concentrations in salp grazing experiments were lower than those in the krill experiments (Table 2). Significant statistical differences between Chl *a* concentrations in treatment bottles and final control bottles were observed (one-tailed *t* test, $t = -2.936$, $p \leq 0.05$, $n = 6$; sign test, $p \leq 0.05$, $n = 6$). During the experiments with salps, clearance rates ranged from 5.3 to 1048 mL·individual^{-1}·h^{-1}, while ingestion rates were 0.06 ± 0.06 µg Chl *a*·individual^{-1}·h^{-1} (mean ± SD) (Table 3). However, changes in $DMSP_d$ + DMS concentrations during the incubations were not statistically significant (one-tailed *t* test, $t = 1.071$, $p = 0.333$, $n = 6$; sign test, $p = 0.688$, $n = 6$) (Fig. 1*b*). Mean bacterial abundance under the different experimental conditions ranged from 0.8 to 1.0 × 10^5 cells·mL^{-1} (Table 5). There was no significant difference in bacterial abundance between the treatment bottles and final control bottles (one-tailed *t* test, $t = -1.777$, $p = 0.136$, $n = 6$; sign test, $p = 0.219$, $n = 6$).

© 2004 NRC Canada

Fig. 2. Relationship between $DMSP_d$ + DMS production rate and ingestion rate in the experimental cultures with krill. A linear regression line is also shown with the equation and statistics.

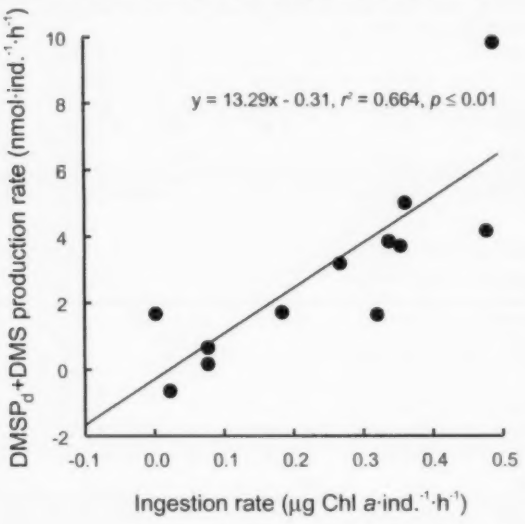

Relationship between ingestion rates and production rates

Ingestion rate of krill was linearly related to $DMSP_d$ + DMS production rate (linear regression, $r^2 = 0.664$, $p \leq 0.01$, $n = 12$) (Fig. 2). In one case, the $DMSP_d$ + DMS production rate of krill was calculated as a negative value. This may have been caused by the poor physiological condition of the krill.

Discussion

During this study, there were substantial changes in the position of the ice edge, in the concentrations of biogenic sulfur compounds and Chl *a*, and in the species composition of the macrozooplankton population. In January, the southernmost sampling station was located near the ice edge and the macrozooplankton community was dominated by krill. The integrated DMS value measured that month in the upper 200 m of the water column was relatively high (1.45 mmol·m^{-2}) near the ice edge where krill were the dominant macrozooplankton. DMS concentration at the sea surface was 31 nmol·L^{-1}, a value 15 times higher than those measured in most oceans areas (Aumont et al. 2002). In February, when the sea ice had retreated further south, the integrated DMS value (0–200 m) decreased to one third of that in January. DMS concentrations within the mixed layer were stable at approximately 3 nmol·L^{-1}, a value closer to the mean oceanic DMS concentration. The integrated $DMSP_d$ value in February also decreased to one third of the January value. In contrast with DMS and $DMSP_d$, the integrated $DMSP_p$ value in February showed about a twofold increase from that in January. The krill was replaced by salps during this interval. Phytoplankton biomass, estimated by Chl *a* concentrations, dramatically decreased from 412 mg·m^{-2} in January to 87 mg·m^{-2} in February, although the $DMSP_p$ integrated value

Fig. 3. Fecal pellets of (*a*) krill and (*b* and *c*) salps.

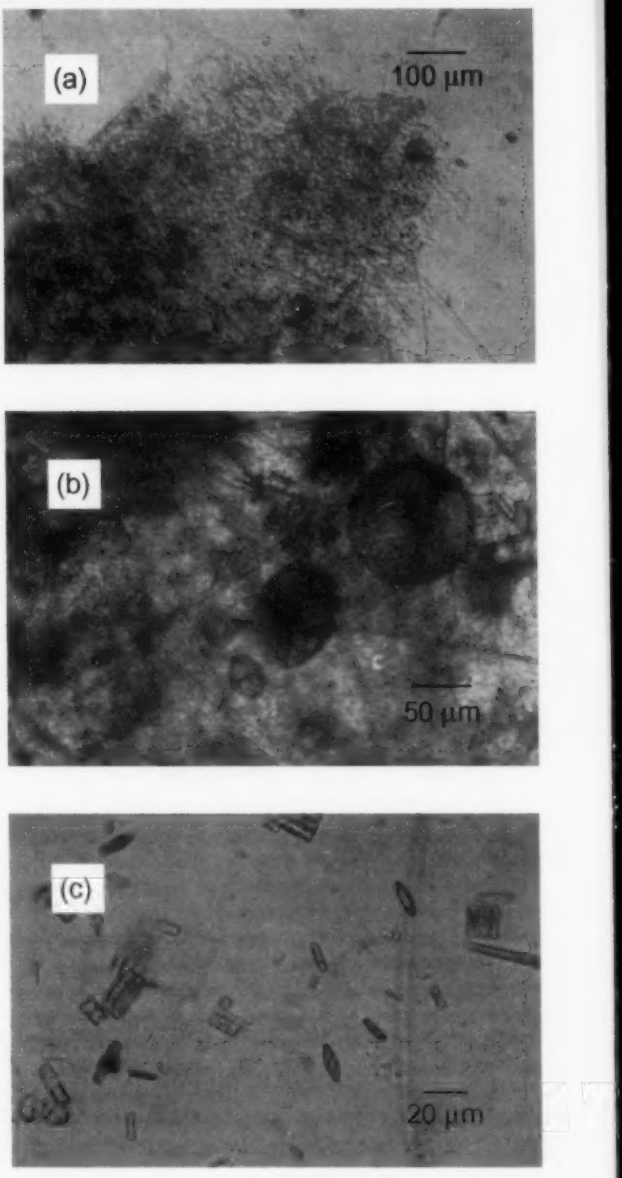

increased over the 2 months. This may be due to a change in the composition of the algal assemblage and (or) growth phase of the dominant phytoplankton species between January and February.

A complete change in the composition of the macrozooplankton community from krill to salps occurred during the study. This transition was accompanied by a large reduction in ambient DMS concentrations. Fecal pellets of krill, which are known to be sloppy feeders, contained destroyed phytoplankton cells (Fig. 3*a*), whereas those produced by salps contained unbroken phytoplankton cells (Figs. 3*b* and 3*c*). The difference in grazing mechanisms (sloppy feeding or di-

© 2004 NRC Canada

rect ingestion) may lead to differences in the magnitude of DMS and $DMSP_d$ release from the ingested phytoplankton cells. Therefore, among the many possible factors influencing DMS concentrations, we focused on the contribution of the various grazing impacts.

The ingestion rate of krill was linearly related to the $DMSP_d$ + DMS production rate ($r^2 = 0.664$, $p \leq 0.01$, $n = 12$). This indicates that krill grazing on phytoplankton is directly linked to the increasing $DMSP_d$ + DMS concentration. The difference in bacterial abundance between treatment bottles and final control bottles was significant. If the bacterial abundance has increased in the treatment bottles, it may also have affected the $DMSP_d$ + DMS production in krill experiments. However, the linear relationship found between ingestion rates of krill and $DMSP_d$ + DMS production rate supports the assumption that $DMSP_d$ + DMS production has been stimulated by krill grazing during the experiments.

The rate of $DMSP_d$ + DMS production by krill grazing in our study was 2.96 nmol·krill^{-1}·h^{-1} and the DMS production rate was 2.91 nmol·krill^{-1}·h^{-1}. DMS production rate through krill grazing reported by Daly and DiTullio (1996) accounted for only 5% of the value obtained in our work. Daly and DiTullio (1996) noted that their values may have been underestimated because of confinement effects. Furthermore, in their work, the initial Chl *a* concentration was low (0.31 mg·m^{-3}) compared with that of our krill incubation experiments. The containers that we used were relatively large (10 L) and were rotated during the experiment so that the phytoplankton were always suspended in the incubation bottles. Moreover, most of the animals used during our incubations were well adapted to the tanks and consequently less stressed than wild animals recently captured. All of our experimental conditions should have produced values with less experimental stress, which may be closer to the in situ value.

In the case of salps, clearance rates varied among individuals. Huntley et al. (1989) conducted shipboard incubation experiments and obtained maximum clearance rates of 376 mL·individual^{-1}·h^{-1} for *S. thompsoni* in the Antarctic Peninsula region. Pakhomov et al. (2002) reported that the clearance rate of *S. thompsoni* is a function of body length. According to their regression, the clearance rate of salps of 40 mm length should be 1491 mL·individual^{-1}·h^{-1}. In our study, clearance rates of salps ranged from 5.3 to 1048 mL·individual^{-1}·h^{-1} (337 mL·individual^{-1}·h^{-1} on average). Our clearance rates are slightly smaller than those of Pakhomov et al. (2002), but our maximum rates are only marginally higher than those of Huntley et al. (1989). Pakhomov et al. (2002) also reported that the changes in ingestion rates as a function of salp length are best represented by a power function. This equation gives an ingestion rate of 0.6 µg pigment·individual^{-1}·h^{-1} for a 40-mm animal. In our experiment, the ingestion rates of salps ranged between 0.0 and 0.2 µg Chl *a*·individual^{-1}·h^{-1}. These low values result mainly from the low Chl *a* concentrations present in our incubation vessels and not from the clearance performance. Hence, we believe that our incubation experiments on salps are appropriate for grazing experiments.

Our results indicate that krill grazing on phytoplankton was an important mechanism for producing $DMSP_d$ and DMS. On the other hand, salps had no detectable effect on the production of this biogenic gas. The difference in grazing mechanisms (sloppy feeding by krill or direct ingestion by salps) may have led to differences in the magnitude of DMS release from the ingested phytoplankton. What was the importance of zooplankton grazing on DMS and $DMSP_d$ concentrations in the field? In January, near the study site (65°S), krill abundance obtained by RMT net (0–800 m) was 64 individuals·1000 m^{-3} (S. Toczko, Ocean Research Institute, University of Tokyo, Tokyo 164-8639, Japan, personal communication, e-mail: stoczko@ori.u-tokyo.ac.jp). $DMSP_d$ + DMS production rates by the krill in January were calculated to be 0.2 nmol·m^{-3}·h^{-1} (based on a per individual rate of 2.96 nmol·individual^{-1}·h^{-1}). Turnover time expressed as ambient $DMSP_d$ + DMS integrated value (0–200 m) divided by the production rate by the krill assemblage in January was estimated to be 4 days. These values are comparable with the microbial turnover time of <1–3 days calculated in the Labrador Sea (Wolfe et al. 2000). Furthermore, if we assume an interannual variation range of 4.8–511 individuals·1000 m^{-3} (Loeb et al. 1997) at our study site, this means that $DMSP_d$ + DMS production rate by krill may vary interannually between 0.01 and 1.51 nmol·m^{-3}·h^{-1}. There are obviously many possible explanations for the rapid change in DMS concentrations measured between January and February, including the advection of a different water mass and changes in phytoplankton assemblage and (or) microbial activity (Liss et al. 1997; Simó 2001). Our results nevertheless suggest that the changes in macrozooplankton dominance and their corresponding impact on DMS production were at least partly responsible for the variations in DMS concentrations.

Bacteria attached to fecal pellets and damaged phytoplankton cells are known to play an important role in the transformation of DMSP and DMS (Scarratt et al. 2000). The effect of attached bacteria should have been negligible during our incubations, since fecal pellets were removed. However, attached bacteria may have been more abundant and (or) active on the fecal pellets from the krill than on those from the salps, which contained mostly intact cells. It is also important to consider the metabolism of DMSP by the zooplankters themselves. Some copepod species can accumulate a considerable amount of DMSP in their body, a pool that may represent more than 70% of $DMSP_p$ in ambient seawater (Tang et al. 1999, 2000*b*). It is assumed that zooplankton grazing affects zooplankton body DMSP content, thereby changing the partitioning of DMSP between the particulate and dissolved phases with a potential effect on DMS production (Tang 2000; Tang et al. 2000*a*, 2000*b*).

There is considerable discussion regarding the existence of competition between salps and krill in the Antarctic Ocean (e.g., Loeb et al. 1997; Kawaguchi et al. 1998). Nicol et al. (2000) showed clear separation of habitat by water masses between krill and salps. According to Pakhomov et al. (2002), krill and salps are adapted to different environmental conditions. Whether or not they are in competition, the abundance of the two species exhibits considerable intra- and interannual variation in space and time (Loeb et al. 1997; Kawaguchi et al. 1998). We believe that this important phenomenon has a strong influence in DMS distribution. Our results clearly indicate the potential importance of zoo-

© 2004 NRC Canada

plankton community structure and feeding mechanisms on DMS distributions in the Antarctic Ocean.

Moreover, if seawater temperature continues to increase, such as has already been observed in the Antarctic Peninsula region (e.g., Rott et al. 1996), there is a possibility that salps may spread into the high Antarctic regions with strong implications for the Antarctic biogeochemistry. The negative effect that this shift in zooplankton dominance may have on DMS net production may, however, be compensated (or exacerbated) by parallel changes in the abundance of DMSP-rich phytoplankton species and (or) bacterial DMS yields. A full appreciation of our results would thus require a better knowledge of the overall effect of these climate variations on the whole plankton community and associated net DMS production.

Acknowledgments

We wish to acknowledge support from Shizuo Tsunogai and Shinichiro Noriki, Hokkaido University. We would like to thank Captain Andrew Leachman and the crew of the R/V *Tangaroa* for their marvelous hospitality and efforts in helping us to carry out our sampling program. Thanks are extended to Makoto Terazaki and Hiroshi Ogawa for providing space aboard the R/V *Hakuho-Maru*. The captain and crew of the R/V *Hakuho-Maru* facilitated work in the Antarctic Ocean. We are grateful to Stephen Nicol of Australian Antarctic Division (AAD) for providing us with krill. We thank Jun Nishikawa, Sean Toczko, and Meguru Miki of the University of Tokyo for providing us with useful comments on zooplankton and phytoplankton abundance. We wish to thank Steve Candy of the AAD for his helpful advice on our statistical treatments. We would also like to thank Graham Hosie of the AAD, Michael Scarratt of Maurice Lamontagne Institute, Michel Gosselin and his colleague of Université du Québec à Rimouski for useful comments on the contents and suggestions on the English. The manuscript was considerably improved by critical and constructive comments made by the two anonymous referees and the Editors, Gary Sprules and Maurice Levasseur. This study was a part of the activities of JARE-43 financially supported by the Ministry of Education, Culture, Sports, Science and Technology, Grant-in-Aid for Special Purpose 11800009.

References

Alldredge, A.L., and Madin, L.P. 1982. Pelagic tunicates: unique herbivores in the marine plankton. BioScience, **32**: 655–663.

Aumont, O., Belviso, S., and Monfray, P. 2002. Dimethylsulfoniopropionate (DMSP) and dimethylsulfide (DMS) sea surface distributions simulated from a global three-dimensional ocean carbon cycle model. J. Geophys. Res. **107**(C4).

Cantin, G., Levasseur, M., Gosselin, M., and Michaud, S. 1996. Role of zooplankton in the mesoscale distribution of surface dimethylsulfide concentrations in the Gulf of St. Lawrence, Canada. Mar. Ecol. Prog. Ser. **141**: 103–117.

Charlson, R.J., Lovelock, J.E., Andreae, M.O., and Warren, S.G. 1987. Oceanic phytoplankton, atmospheric sulphur, cloud albedo and climate. Nature (Lond.), **326**: 655–661.

Dacey, J.W.H., and Wakeham, S.G. 1986. Oceanic dimethylsulfide: production during zooplankton grazing on phytoplankton. Science (Wash., D.C.), **233**: 1314–1316.

Daly, K.L., and DiTullio, G.R. 1996. Particulate dimethylsulfoniopropionate removal and dimethylsulfide production by zooplankton in the Southern Ocean. *In* Biological and environmental chemistry of DMSP and related sulfonium compounds. *Edited by* R.P. Kiene, P.T. Visscher, M.D. Keller, and G.O. Kirst. Plenum Press, New York. pp. 223–238.

Frost, B.W. 1972. Effects of size and concentration of food particles on the feeding behavior of the marine planktonic copepod *Calanus pacificus*. Limnol. Oceanogr. **17**: 805–815.

Harbison, G.R., McAlister, V.L., and Gilmer, R.W. 1986. The response of the salp, *Pegea confoederata*, to high levels of particulate material: starvation in the midst of plenty. Limnol. Oceanogr. **31**: 371–382.

Huntley, M.E., Sykes, P.F., and Marin, V. 1989. Biometry and trophodynamics of *Salpa thompsoni* foxton (Tunicata: Thaliacea) near the Antarctic Peninsula in austral summer, 1983–1984. Polar Biol. **10**: 59–70.

Karsten, U., Kuck, K., Vogt, C., and Kirst, G.O. 1996. Dimethylsufoniopropionate production in phototrophic organisms and its physiological function as a cryoprotectant. *In* Biological environmental chemistry of DMSP and related sulfonium compounds. *Edited by* R.P. Kiene, P.T. Visscher, M.D. Keller, and G.O. Kirst. Plenum Press, New York. pp. 143–153.

Kawaguchi, S. 2001. Recent topics on Antarctic krill research. Kaiyo Monthly Spec. Issue, **27**: 147–155. [In Japanese.]

Kawaguchi, S., Ichii, T., Naganobu, M., and de la Mare, W.K. 1998. Do krill and salps compete? Contrary evidence from the krill fisheries. CCAMLR Sci. **5**: 205–216.

Kiene, R.P., and Linn, L.J. 2000. The fate of dissolved dimethylsulfoniopropionate (DMSP) in seawater: tracer studies using ^{35}S-DMSP. Geochim. Cosmochim. Acta, **64**: 2797–2810.

Kirchman, D.J., Sigda, J., Kapuscinski, R., and Mitchell, R. 1982. Statistical analysis of the direct count method for enumerating bacteria. Appl. Environ. Microbiol. **44**: 376–382.

Kirst, G.O. 1996. Osmotic adjustment in phytoplankton and macroalgae. *In* Biological environmental chemistry of DMSP and related sulfonium compounds. *Edited by* R.P. Kiene, P.T. Visscher, M.D. Keller, and G.O. Kirst. Plenum Press, New York. pp. 121–129.

Liss, P.S., Hatton, A.D., Malin, G., Nighingale, P.D., and Turner, S.M. 1997. Marine sulphur emissions. Philos. Trans. R. Soc. Lond. B Biol. Sci. **352**: 159–169.

Loeb, V., Siegel, V., Holm-Hansen, O., Hewitt, R., Fraser, W., Trivelpiece, W., and Trivelpiece, S. 1997. Effects of sea-ice extent and krill or salp dominance on the Antarctic food web. Nature (Lond.), **387**: 897–900.

Nicol, S., Pauly, T., Bindoff, N.L., Wright, S., Thiele, D., Hosie, G.W., Strutton, P.G., and Woehler, E. 2000. Ocean circulation off east Antarctica affects ecosystem structure and sea-ice extent. Nature (Lond.), **406**: 504–507.

Niki, T., Kunugi, M., and Otsuki, A. 2000. DMSP-lyase activity in five marine phytoplankton species: its potential importance in DMS production. Mar. Biol. **136**: 759–764.

Pakhomov, E.A., Froneman, P.W., and Perissinotto, R. 2002. Salp/krill interactions in the Southern Ocean: spatial segregation and implications for the carbon flux. Deep Sea Res. II, **49**: 1881–1907.

Parsons, T.R., Maita, Y., and Lalli, C.M. 1984. A manual of chemical and biological methods for seawater analysis. Pergamon Press, Toronto, Ont.

Rott, H., Skvarca, P., and Nagler, T. 1996. Rapid collapse of northern Larsen Ice Shelf, Antarctica. Science (Wash., D.C.), **271**: 788–792.

Scarratt, M., Cantin, G., Levasseur, M., and Michaud, S. 2000. Particulate size-fractionated kinetics of DMS production: where does DMSP cleavage occur at the microscale? J. Sea Res. **43**: 245–252.

© 2004 NRC Canada

Simó, R. 2001. Production of atmospheric sulfur by oceanic plankton: biological, ecological and evolutionary links. Trends Ecol. Evol. **16**: 287–294.

Strom, S.L., Benner, R., Ziegler, S., and Dagg, M.J. 1997. Planktonic grazers are a potentially important source of marine dissolved organic carbon. Limnol. Oceanogr. **42**: 1364–1374.

Suzuki, R., and Ishimaru, T. 1990. An improved method for the determination of phytoplankton chlorophyll using *N,N*-dimethylformamide. J. Oceanogr. Soc. Jpn. **46**: 190–194.

Tang, K.W. 2000. Dynamics of dimethylsulfoniopropionate (DMSP) in a migratory grazer: a laboratory simulation study. J. Exp. Mar. Biol. Ecol. **243**: 283–293.

Tang, K.W., Dam, H.G., Visscher, P.T., and Fenn, T.D. 1999. Dimethylsulfoniopropionate (DMSP) in marine copepods and its relation with diets and salinity. Mar. Ecol. Prog. Ser. **179**: 71–79.

Tang, K.W., Fenn, T.D., Visscher, P.T., and Dam, H.G. 2000*a*. Regulation of body dimethylsulfoniopropionate (DMSP) content by the copepod *Temora longicornis*: a test of four mechanisms. Mar. Biol. **136**: 749–757.

Tang, K.W., Rogers, D.R., Dam, H.G., and Visscher, P.T. 2000*b*. Seasonal distribution of DMSP among seston, dissolved matter and zooplankton along a transect in the Long Island Sound estuary. Mar. Ecol. Prog. Ser. **206**: 1–11.

Uzuka, N., Watanabe, S., and Tsunogai, S. 1996. Dimethylsulfide in coastal zone of the east China Sea. J. Oceanogr. **52**: 313–321.

Watanabe, S., Demura, K., and Tsunogai, S. 1987. Determination of volatile organic sulfur compound concentrations in seawater. Bull. Fac. Fish. Hokkaido Univ. **38**: 286–292.

Wolfe, G.B., Levasseur, M., Cantin, G., and Michaud, S. 2000. DMSP and DMS dynamics and microzooplankton grazing in the Labrador Sea: application of the dilution technique. Deep Sea Res. I, **47**: 2243–2264.

Zar, J.H. 1996. Biostatistical analysis. 3rd ed. Prentice-Hall, Englewod Cliffs, N.J.

© 2004 NRC Canada

Vertically resolved cycling of dimethylsulfoniopropionate (DMSP) and dimethylsulfide (DMS) in the Northwest Atlantic in spring[1]

M. Levasseur, M. Scarratt, S. Roy, D. Laroche, S. Michaud, G. Cantin, M. Gosselin, and A. Vézina

Abstract: In May 1998, profiles of ambient concentration and net changes of particulate dimethylsulfoniopropionate ($DMSP_p$), dissolved dimethylsulfoniopropionate ($DMSP_d$), and dimethylsulfide (DMS) were measured in three biogeographic provinces of the Northwest Atlantic: Northwest Atlantic Continental Shelf (Grand Banks), North Atlantic Drift, and North Atlantic Subtropical Gyre (Sargasso Sea). All stations/depths exhibited large losses of $DMSP_p$ (up to 18.0 $nmol \cdot L^{-1} \cdot day^{-1}$). DMSP and DMS cycling varied in relation to the type and development stage of the plankton assemblages. The postdiatom bloom conditions on the Grand Banks were associated with an efficient utilization of DMSP by microzooplankton and bacteria. Bacterial DMS production balanced the DMS bacterial consumption, resulting in little net DMS production (0.3 $nmol \cdot L^{-1} \cdot day^{-1}$). This contrasted with the North Atlantic Drift and Sargasso Sea stations where flagellates were thriving and most of the $DMSP_p$ loss was recovered in the dissolved pool, indicating a less active microbial DMSP metabolism. $DMSP_d$ cleavage was high in these latter cases and exceeded DMS bacterial consumption, allowing a net production of DMS (up to 1.8 $nmol \cdot L^{-1} \cdot day^{-1}$). These results indicate that maximum DMS net production occurs in growing algal systems where the production of $DMSP_d$ resulting from microzooplankton grazing exceeds the bacterial requirement in carbon and sulfur.

Résumé : En mai 1998, nous avons mesuré les profils des concentrations ambiantes et des changements nets de diméthylsulfoniopropionate particulaire ($DMSP_p$), de diméthylsulfoniopropionate dissous ($DMSP_d$) et de sulfure de diméthyle (DMS) dans trois provinces biogéographiques du nord-ouest de l'Atlantique, soit le plateau continental (Grands Bancs), la dérive nord-atlantique et la gyre subtropicale de l'Atlantique nord (mer des Sargasses). Toutes les stations/profondeurs affichent d'importantes pertes de $DMSP_p$ (jusqu'à 18,0 $nmol \cdot L^{-1} \cdot jour^{-1}$). Le recyclage du DMSP et du DMS varie en fonction de la composition des communautés planctoniques et de leur stade de développement. Les conditions qui suivent l'efflorescence des diatomées sur les Grands Bancs sont associées à une utilisation efficace du DMSP par le microzooplancton et les bactéries. La production bactérienne de DMS contrebalance la consommation bactérienne de DMS, ce qui explique la faible production nette de DMS (0,3 $nmol \cdot L^{-1} \cdot jour^{-1}$). La situation est très différente dans les stations de la dérive nord-atlantique et de la mer des Sargasses où les flagellés foisonnent et où la plus grande partie de la perte de $DMSP_p$ est récupérée dans le pool de DMSP dissous, ce qui indique que le métabolisme bactérien du DMSP y est moins actif. Dans ces situations, la scission du $DMSP_d$ est importante et elle dépasse la consommation bactérienne de DMS, ce qui permet une production nette de DMS (jusqu'à 1,8 $nmol \cdot L^{-1} \cdot jour^{-1}$). Ces résultats indiquent que la production nette maximale de DMS se produit dans les systèmes d'algues en croissance, dans lesquels la production de $DMSP_d$ due au broutage du microzooplancton surpasse les besoins en carbone et en soufre des bactéries.

[Traduit par la Rédaction]

Received 7 March 2003. Accepted 19 October 2003. Published on the NRC Research Press Web site at http://cjfas.nrc.ca on 23 June 2004.
J17385

M. Levasseur,[2,3] **M. Scarratt, S. Roy, D. Laroche, S. Michaud, and G. Cantin.** Fisheries and Oceans Canada, Maurice Lamontagne Institute, 850, Route de la Mer, Mont-Joli, QC G5H 3Z4, Canada.
M. Gosselin. Institut des sciences de la mer, Université du Québec à Rimouski, 310, Allée des Ursulines, Rimouski, QC G5L 3A1, Canada.
A. Vézina. Fisheries and Oceans Canada, Bedford Institute of Oceanography, Dartmouth, NS B2Y 4A2, Canada.

[1]This paper is part of the proceedings of the Third International Symposium on Biological and Environmental Chemistry of DMS(P) and Related Compounds, held in Rimouski (Québec), 26–28 September 2002.
[2]Corresponding author (e-mail:maurice.levasseur@bio.ulaval.ca).
[3]Present address: Université Laval, Département de biologie, Québec-Océan, Sainte-Foy, QC G1K 7P4, Canada.

 doi: 10.1139/F04-026 © 2004 NRC Canada

Introduction

Dimethylsulfide (DMS) is the principal sulfur gas released from the oceans to the atmosphere. In the atmosphere, DMS is oxidized to form sulfate aerosols that, by increasing the scattering of solar radiation and the albedo of low clouds, may exert a cooling effect on climate (Charlson et al. 1992). DMS thus has the potential to generate a feedback loop between the marine biota and the climate (Charlson et al. 1987). This feedback hypothesis (referred to as the CLAW hypothesis from the names of the coauthors) has prompted considerable research in the last 15 years and as a consequence, our knowledge of the global distribution of DMS has increased substantially (see the compilation of Kettle et al. (1999)), as well as of the biological factors responsible for its production (see reviews by Simó 2001).

DMS production is intimately linked to the microbial food web in the ocean. The main precursor of DMS is dimethylsulfoniopropionate (DMSP), a compound produced by phytoplankton in which it may serve as an osmolyte (Vairavamurthy et al. 1985), cryoprotectant (Kirst et al. 1991), and antioxidant (Sunda et al. 2002). Cellular DMSP quotas are highly variable within phytoplankton, with the diatoms being weak producers and the prymnesiophytes and dinoflagellates being strong producers (Keller et al. 1989). The liberation of particulate (i.e., intracellular) DMSP ($DMSP_p$) to seawater as dissolved DMSP ($DMSP_d$) may result from exudation (Laroche et al. 1999) and cell lysis (Kwint and Kramer 1995). Zooplankton grazing may also release DMSP into the medium (Dacey and Wakeham 1986; Wolfe et al. 1997), although a significant part of the DMSP ingested can be metabolized directly by the organisms (Wolfe et al. 1994). Two major pathways of $DMSP_d$ degradation are known. The first and probably most prevalent (Kiene and Linn 2000) is demethylation, which is carried out essentially by bacteria and does not lead to the production of DMS (Kiene 1996). The second major pathway for $DMSP_d$ catabolism is enzymatic cleavage, which leads to DMS and acrylate and is carried out by bacterial (Yoch et al. 1997) or algal DMSP lyase (Stefels and Dijkhuizen 1996; Steinke et al. 1998). Finally, bacteria can also consume DMS (Wolfe et al. 1999; Simó et al. 2000). The cycling of DMSP/DMS in the oceans is thus directly linked to the dynamics of the entire microbial food web. However, the variability of the different sulfur pools is poorly known. In the Barents Sea, Matrai and Vernet (1997) demonstrated that the cycling of DMSP and DMS varied considerably depending on the type and physiological stage of the plankton systems, older algal systems being more productive in terms of DMS than those in the blooming phase. A later study provided an explanation for the previous observations that maximum DMS concentrations generally coincided with senescent blooms (Matrai and Keller 1993).

The Northwest Atlantic is one of the most productive regions of the world ocean in terms of DMS (Kettle et al. 1999). In spring, the area is characterized by a strong south–north gradient in DMSP and DMS concentrations with maximum values in the more productive northern waters (Scarratt et al. 2002). However, when normalized to chlorophyll *a* (Chl *a*) biomass, these pools show a different pattern, with high DMS:Chl *a* ratios in the Sargasso Sea (Scarratt et al. 2002). DMS bacterial production displays a more complex pattern in which the rates increase with both the phytoplankton biomass (as indicated by the concentration of Chl *a*) and water temperature (Scarratt et al. 2000; Schultes et al. 2000). This implies that DMS production is relatively high in the Sargasso Sea, notwithstanding the low biomass.

The objective of this study was to determine how the different biogenic sulfur pools ($DMSP_p$, $DMSP_d$, and DMS) covary at three stations representing the major biogeochemical provinces of the Northwest Atlantic Ocean (Longhurst 1995): the Northwest Atlantic Continental Shelf, the North Atlantic Drift, and the North Atlantic Subtropical Gyre. The distribution and daily changes in $DMSP_p$ were determined in four size fractions to highlight the relative contributions of different sizes of particulate material on the cycling of the biogenic sulfur compounds.

Materials and methods

Study area and sampling

Incubation experiments were conducted in the Northwest Atlantic from 1 to 16 May 1998. Other aspects of this cruise are reported elsewhere (Scarratt et al. 2000, 2002). Samples were collected in three different biogeographic provinces as described by Longhurst (1995): the Northwest Atlantic Continental Shelf (Grand Banks station), the North Atlantic Drift, and the North Atlantic Subtropical Gyre (Sargasso Sea station) (Fig. 1; Table 1). The study area ranges from 32 to 45°N and from 45 to 65°W. At each station, a vertical profile of temperature, salinity, and scalar photosynthetically active radiation was recorded using a conductivity–temperature–depth (CTD) meter (SeaBird 9/11-Plus equipped with an in vivo fluorometer and a LiCor underwater irradiance sensor) mounted on a rosette sampler. Using Niskin bottle samples, profiles were determined for nitrate, phosphate, Chl *a*, DMSP, and DMS over the upper 200 m of the water column (75 m for the Grand Banks station). Incubation experiments were conducted using samples from the surface mixed layer, fluorescence maximum, and 1% irradiance depths (Table 1). This water was first screened through 202-μm Nytex mesh to remove large grazers. Then, to determine initial conditions for the incubation experiments, subsamples were taken for $DMSP_p$, $DMSP_d$, DMS, nutrients, Chl *a*, and plankton enumeration and identification. The remaining water was subdivided into clear and dark bottles and incubated in situ at its original depth (see below). After 24 h, the incubated bottles were sampled for Chl *a*, $DMSP_p$, $DMSP_d$, DMS, and the different size fractions of $DMSP_p$.

Protocol for incubations

In situ incubations of 24-h duration were performed at the three stations using incubators suspended from a drifting buoy. The buoy consisted of a ballasted inflatable ball and mast with a radar reflector and light to aid tracking and recovery. A rectangular drogue was suspended from a Spectra line below the buoy at approximately the middepth of the mixed layer. Clear acrylic plastic racks were attached to the line and supported the incubation bottles (see below) at three depths determined from the CTD profile: the surface mixed layer (SML), the deep Chl maximum (DCM), and the depth of 1% surface irradiance. Incubation procedures were started as soon as possible after water sample collection. For each

© 2004 NRC Canada

Fig. 1. False-color SeaWiFS (Sea-viewing Wide Field Sensor) image of the study region in May 1998 showing Chl *a* concentration ($mg \cdot m^{-3}$). Approximate locations of incubation experiments are shown by red circles.

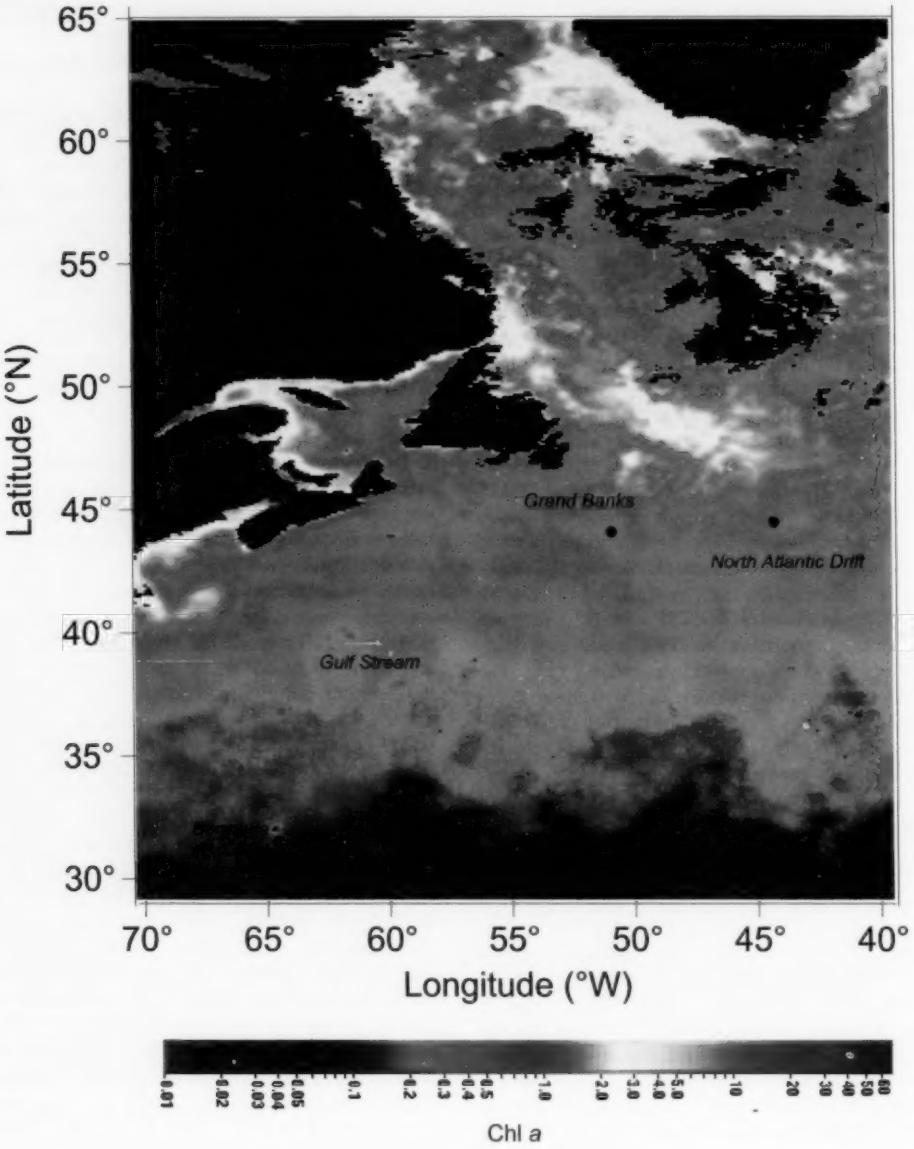

incubation, 600-mL polystyrene bottles were filled with water from each depth. All pouring and mixing was performed gently to avoid bubble formation, which could alter the concentration of DMS. Eight bottles (two clear, two dark, two clear plus methyl butyl ether (MBE), and two dark plus MBE) were incubated in the SML (4–5 m) and at the DCM and four bottles (two clear and two dark) were incubated at the depth of 1% irradiance. MBE, a known bacterial DMS consumption inhibitor (Visscher and Taylor 1993), was added to some bottles (30 $\mu mol \cdot L^{-1}$ final concentration) and bacterial DMS consumption rates were calculated by subtracting the net change in DMS in the bottles without MBE from the net change in the bottles containing MBE (see calculation section below). The bottles were placed in the acrylic racks and suspended from the buoy at the original depths of the water samples. Both the rack and the bottles were opaque to UV light. The buoy was deployed for 24 h beginning at 2030 for the North Atlantic Drift station and at 0830 for stations on the Grand Banks and in the Sargasso Sea. After 24 h, the bottles were recovered and stored briefly in the dark at their in situ temperature before sampling for $DMSP_p$, $DMSP_d$, DMS, and Chl *a*.

DMSP and DMS analyses

DMSP and DMS determinations (profile samples and initial and final incubation samples) were performed using the

© 2004 NRC Canada

Table 1. Physical, chemical, and biological properties and sampled depths of three stations visited in May 1998 in the Northwest Atlantic.

Characteristic	Grand Banks	North Atlantic Drift	Sargasso Sea
Location			
Latitude	44°28.9′N	44°70.9′N	32°16.6′N
Longitude	51°73.9′W	45°2.4′W	64°50.6′W
Oceanographic province	Northwest Atlantic Continental Shelf	North Atlantic Drift	North Atlantic Subtropical Gyre
Water depth (m)	82	4000	3400
Sampled depths (m)			
Surface mixed layer	4	4	5
Deep Chl *a* maximum	42	15	55
1% irradiance	60	63	93
Initial surface mixed layer conditions			
Sea surface temperature (°C)	6.1	15.2	20.2
Salinity (psu)	31.8	35.8	36.5
Chl *a* concentration ($\mu g \cdot L^{-1}$)	0.26	0.62	0.10
Nitrate ($\mu mol \cdot L^{-1}$)	0.09	2.64	0.18
Mean wind speed during 24 h ($m \cdot s^{-1}$)	4.0	13.6	11.9
Maximum wind speed during 24 h ($m \cdot s^{-1}$)	5.7	22.5	13.8
Cloud cover: mean during 24 h (%)	20	80	100

procedure described in Scarratt et al. (2002). Briefly, bottles were gently mixed and 250 mL was size-fractionated by gravity filtration using a sequential filtration apparatus (Sartorius) with four stages (pore size of 20, 11, 2, and 0.7 μm (Whatman GF/F)). Filtrate from the final stage (0.7 μm) was used to prepare $DMSP_d$ and DMS samples. Profiles were determined using a single sample at each depth. Incubation bottles were analyzed in duplicate.

DMS concentrations in the prepared samples were determined following purge, cryotrapping, and sulfur-specific gas chromatography procedures using a method derived from that of Leck and Bågander (1988). The system comprises a Varian STAR 3400 CX gas chromatograph (GC) equipped with a pulsed flame photometric detector and an SPB-1 sulfur capillary column (length 30 m, thickness 4.0 μm, 0.32 mm inside diameter; Supelco, Inc.). Samples were sparged with helium at 40 $mL \cdot min^{-1}$ in a heated purge vessel (70 °C) for 3 min. A water-cooled condenser (5 °C) followed by a drying tube containing small pellets (20 mesh) of $CaCl_2$ removed water vapor from the gas stream. The DMS was cryofocussed in a Teflon loop submerged in liquid nitrogen. The Teflon loop was subsequently placed in a hot water bath (approximately 70 °C), releasing the DMS onto the GC column. For the analysis of DMS samples, the GC was calibrated against microlitre injections of helium containing approximately 17 ng $DMS \cdot mL^{-1}$. This was prepared using a certified permeation tube (Kin-Tek) filled with DMS and kept at a constant 30 °C. For the analysis of DMSP, the GC was calibrated against gravimetric standards of DMSP (5.0 $ng \cdot mL^{-1}$ or 50 $ng \cdot mL^{-1}$ in distilled water) prepared in 10-mL serum vials containing 0.4 mL of KOH (10 $mol \cdot L^{-1}$). The analytical method has a precision of approximately 10% and a minimum quantification limit for both DMS and $DMSP_d$ of approximately 0.08 $nmol \cdot L^{-1}$. Total $DMSP_p$ was determined by summing the four particulate fractions. $DMSP_d$ concentrations were determined by subtracting the DMS concentration from DMS + $DMSP_d$ as determined in the hydrolyzed, filtered samples.

Calculation of DMSP and DMS transformation rates

DMSP and DMS transformation rates were determined from the net changes in DMS, $DMSP_d$, and $DMSP_p$ in the different incubation treatments over the 24-h incubation period. Because, in most cases, no significant difference was observed between light and dark treatments, the observed rates from the light and dark bottles at each depth were pooled to improve statistical significance. The following rates were determined using the net change in the treatments indicated: (*i*) net $DMSP_p$ production = mean change in $DMSP_p$ (total and size-fractionated), (*ii*) net $DMSP_d$ production = mean change in $DMSP_d$, (*iii*) net DMS production = mean change in DMS, (*iv*) DMS bacterial consumption = mean DMS change with MBE – mean DMS change without MBE, (*v*) gross DMS production ($DMSP_d$ cleavage) = net DMS production + DMS bacterial consumption, and (*vi*) gross $DMSP_p$ production = net $DMSP_p$ production + net $DMSP_d$ production + gross DMS production.

The mean rates from each group of four bottles (two light plus two dark) were tested for statistical significance (Student's two-tailed *t* test, null hypothesis $\mu \neq 0$, $p = 0.05$, $n = 4$). To test the DMS consumption rates, the differences between rates determined with and without MBE were tested for statistical significance (Student's one-tailed *t* test, null hypothesis $(\mu_1 - \mu_2) > 0$, $p = 0.05$, $n = 4$).

Chl *a* and nutrient determinations

Chl *a* and phaeopigments were determined using the fluorometric method described by Parsons et al. (1984). For each bottle, 250-mL subsamples were filtered onto Whatman GF/F filters and extracted with 90% acetone for 24 h at 4 °C. The fluorescence was measured with a Turner 111 fluorometer. Nitrate concentrations were determined at the

© 2004 NRC Canada

Fig. 2. Vertical profiles of (*a*) temperature (open triangles) and salinity (solid triangles), (*b*) nitrate (squares) and Chl *a* (circles), and (*c*) total $DMSP_p$ (squares), $DMSP_d$ (circles), and DMS (triangles) in the water column at the beginning of the Grand Banks incubation experiment. Dotted horizontal lines indicate the depths at which samples were taken for the incubation experiments.

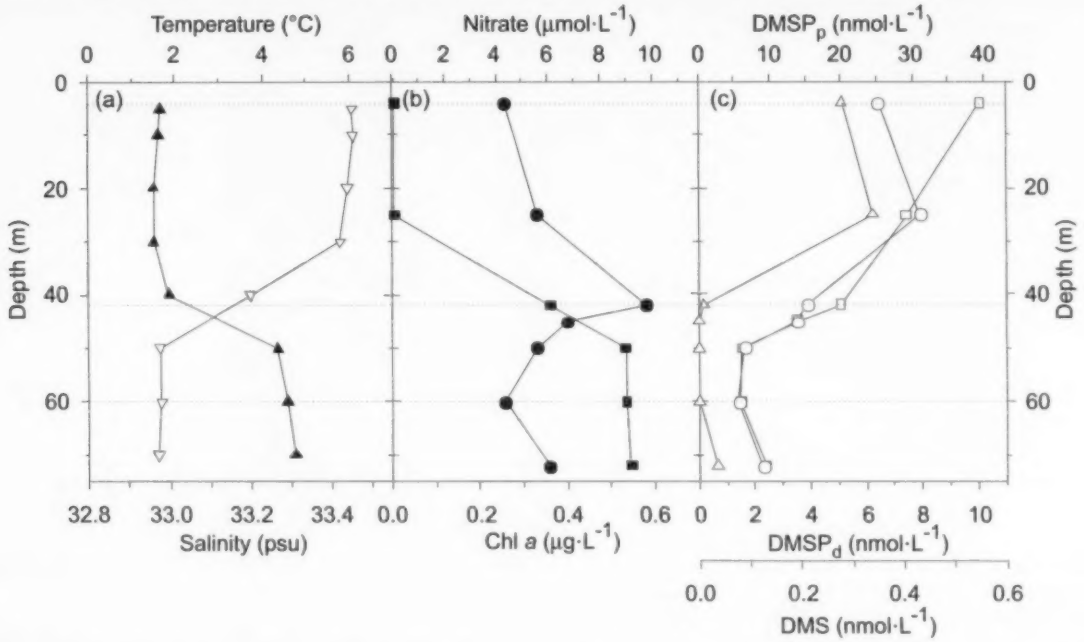

beginning of each incubation. At each station, a 50-mL sample was filtered through a Whatman GF/F glass fiber filter and the filtrate was frozen at –20 °C for later analysis using a Technicon autoanalyzer (Strickland and Parsons 1972).

Microplankton identification and enumeration

At the beginning of each incubation experiment, one 200-mL sample was fixed with 0.8 mL of acidic Lugol's fixative for later identification and counting of phytoplankton and microzooplankton cells using an inverted microscope at a magnification of 200 or 500× (Utermöhl technique: Utermöhl 1931; Lund et al. 1958).

Results

Grand Banks station

The Grand Banks station, the shallowest of the three (82 m), was characterized by a 30-m SML with salinity and temperature of approximately 32.9 psu and 6 °C, respectively (Fig. 2*a*). Nitrate concentrations were very low in the SML (<0.05 $\mu mol \cdot L^{-1}$) and increased to approximately 9 $\mu mol \cdot L^{-1}$ across the thermohalocline (Fig. 2*b*). Chl *a* concentrations varied between 0.3 and 0.4 $\mu g \cdot L^{-1}$ in the SML, reached 0.6 $\mu g \cdot L^{-1}$ at 40 m, and decreased to approximately 0.25 $\mu g \cdot L^{-1}$ below the nitracline. The plankton assemblage was composed mostly of small, unidentified flagellates, prymnesiophytes (mostly *Chrysochromulina* spp.), and dinoflagellates (Fig. 3*a*). Diatoms were present in low numbers, but we found many empty frustules, suggesting that our sampling took place during the declining phase of the spring diatom bloom. In contrast with Chl *a*, $DMSP_p$ concentrations were maximal in the SML (approximately 40 $nmol \cdot L^{-1}$) and decreased fairly steadily with depth to a minimum of approximately 5 $nmol \cdot L^{-1}$ at around 50–60 m (Fig. 2*c*). The phytoplankton species responsible for most of the Chl *a* signal were obviously different from those responsible for the $DMSP_p$ signal. $DMSP_p$ was evenly distributed in all size fractions except 11–20 μm, which contained little DMSP (Table 2). The three DMSP-rich fractions showed relatively small variations with depth. $DMSP_d$ concentrations ranged between 6 and 8 $nmol \cdot L^{-1}$ in the SML and decreased with depth below 30 m (Fig. 2*c*). DMS concentrations were very low (maximum of 0.3 $nmol \cdot L^{-1}$) in the SML and became undetectable between 40 and 60 m. A slight increase of the three sulfur pools was measured near the bottom of the water column. This could possibly be ascribed to resuspension of DMSP- and DMS-enriched sediments.

Incubations at the Grand Banks station were conducted at 4 (SML), 42 (DCM), and 60 m (1% surface irradiance) (dotted lines in Fig. 2). Small changes in Chl *a* concentrations were observed at all depths in both clear and dark bottles (Fig. 4*a*), but none of these were statistically significant ($p \geq 0.05$). The general characteristics of the DMSP and DMS dynamics at the Grand Banks station were similar at 4 and 42 m (Fig. 5*a*). At 4 m, the net loss of Chl *a* was accompanied by a significant ($p \leq 0.05$) net decrease in $DMSP_p$. Forty-five percent of the $DMSP_p$ pool was lost during that particular day at 4 m. Significant ($p \leq 0.05$) decreases in $DMSP_p$ were measured in all size fractions, except in the $DMSP_p$-poor 11–20 μm fraction where no change was measured (Fig. 6*a*). Essentially none of the $DMSP_p$ lost at 4 m (–17.7 $nmol \cdot L^{-1}$) was converted to the dissolved pool (Fig. 5*a*). A small but significant ($p \leq 0.05$) net DMS production of 0.3 $nmol \cdot L^{-1} \cdot day^{-1}$ was measured at that depth,

© 2004 NRC Canada

Fig. 3. Abundances of microplankton taxonomic groups in water from the three incubation depths at (*a*) the Grand Banks, (*b*) North Atlantic Drift, and (*c*) Sargasso Sea. The terms on the *y* axis refer to the incubation depth: surface mixed layer (SML), deep Chl maximum (DCM), and 1% irradiance.

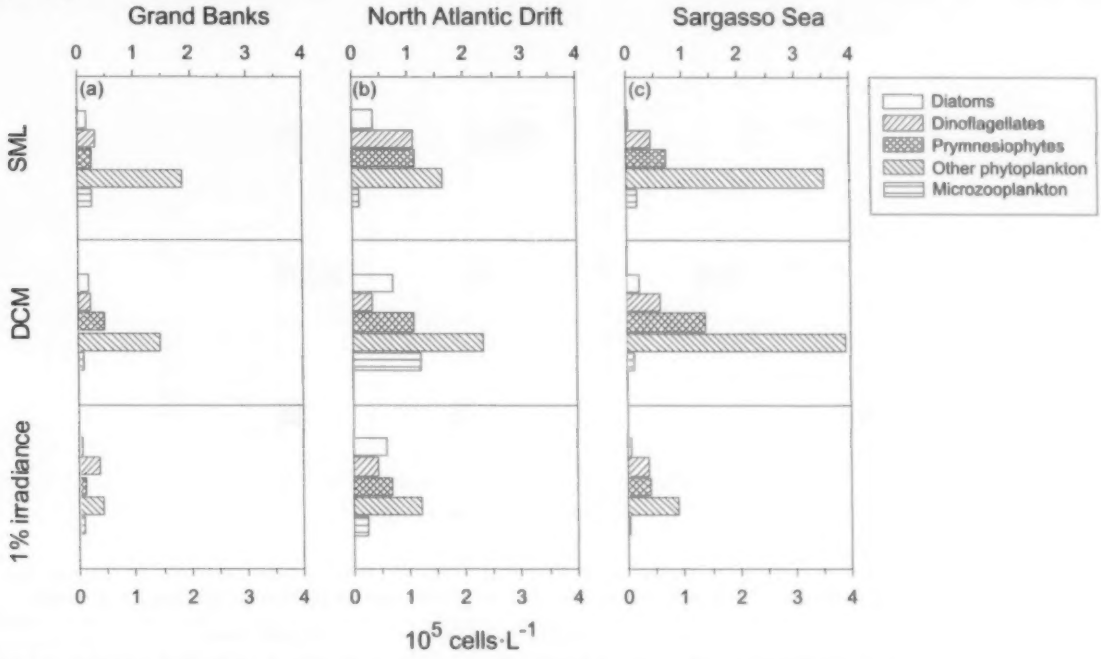

Table 2. Initial DMSP and DMS concentrations at the three incubation stations in the Northwest Atlantic.

Station	$DMSP_p$ (nmol·L^{-1})	$DMSP_d$ (nmol·L^{-1})	DMS (nmol·L^{-1})	Percentage of total $DMSP_p$			
				>20 µm	11–20 µm	2–11 µm	0.7–2 µm
Grand Banks							
Surface mixed layer	39.3	6.4	0.3	30	3	35	32
Deep Chl *a* maximum	19.9	3.9	0.01	51	1	33	15
1% irradiance	5.8	1.4	0.0	14	3	59	24
North Atlantic Drift							
Surface mixed layer	30.2	12.4	2.3	34	4	52	10
Deep Chl *a* maximum	23.2	6.2	1.7	22	4	65	9
1% irradiance	11.4	3.2	0.8	18	5	60	17
Sargasso Sea							
Surface mixed layer	21.7	5.4	2.2	7	5	76	12
Deep Chl *a* maximum	20.7	2.5	0.4	2	6	76	16
1% irradiance	2.8	1.4	0.0	5	10	67	18

Note: Four $DMSP_p$ size fractions are also presented as a percentage of total $DMSP_p$ concentrations.

but the results of the DMS bacterial consumption measurement were not significant. At 42 m, a significant ($p \leq 0.05$) $DMSP_p$ loss rate of 8.1 nmol·L^{-1}·day^{-1} was measured representing 41% of the $DMSP_p$ pool (Fig. 5*a*). This loss of $DMSP_p$ occurred mostly in the >20 µm size fraction (Fig. 6*a*) where most of the $DMSP_p$ was found. None of the DMSP lost from the particulate phase was recovered in the dissolved pool. DMS net production was negligible, but the MBE treatment indicates that DMS bacterial consumption was high (0.6 nmol·L^{-1}·day^{-1}) (Fig. 7*a*). At 60 m, no detectable variations in $DMSP_p$, $DMSP_d$, or DMS were measured.

North Atlantic Drift station

This station was the richest of the three stations studied in terms of both nitrate and Chl *a* (Fig. 8). The station was characterized by a more complex physical structure with the interleaving of three different water masses: a surface water mass of salinity 35.8 psu and temperature 15.2 °C (Fig. 8*a*) overlying an approximately 30-m-thick vertically homogeneous layer of 36.5 psu and 15.5 °C, which in turn mixed with a deep water mass of 35.7 psu and 13.7 °C at 200 m. Nitrate concentrations averaged 2.5 µmol·L^{-1} in the upper 50 m and increased gradually with depth to reach 7 µmol·L^{-1} at 200 m

© 2004 NRC Canada

Fig. 4. Net changes in Chl *a* during incubations at (*a*) the Grand Banks, (*b*) North Atlantic Drift, and (*c*) Sargasso Sea. The open and solid bars represent changes in clear and dark bottles, respectively. The error bars indicate the range of duplicates.

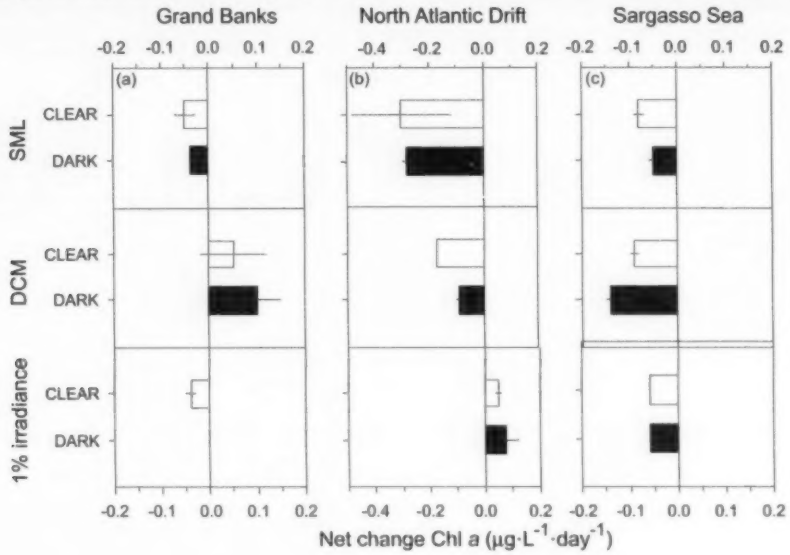

Fig. 5. Net changes in DMS and DMSP during incubations at (*a*) the Grand Banks, (*b*) North Atlantic Drift, and (*c*) Sargasso Sea. The open and solid bars represent changes in clear and dark bottles, respectively. The error bars indicate the range of duplicates.

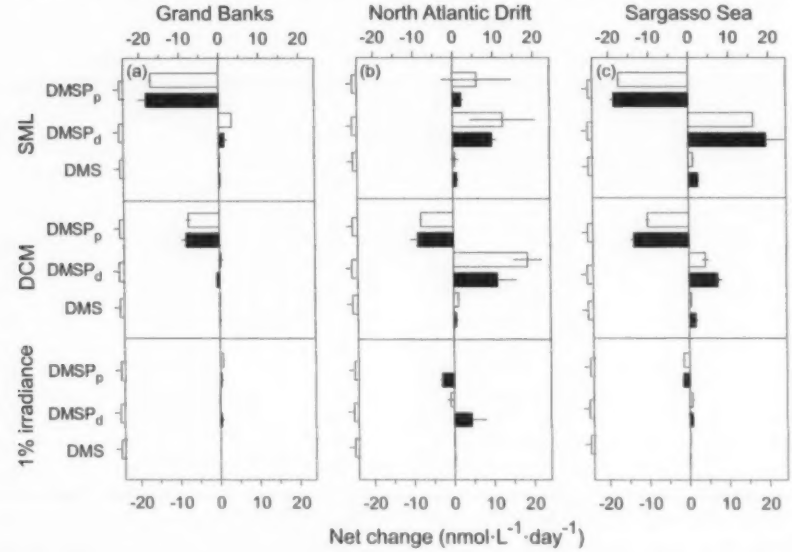

(Fig. 8*b*). Chl *a* concentrations varied between 0.5 and 0.6 µg·L^{-1} in the first 50 m and decreased sharply to less than 0.15 µg·L^{-1} below 50 m. This station was characterized by a large population of prymnesiophytes (mostly *Chrysochromulina* spp.) and dinoflagellates (mostly *Gyrodinium flagellare*) but also by more diatoms than at the Grand Banks and Sargasso Sea stations (Fig. 3*b*).

Vertical profiles of $DMSP_p$, $DMSP_d$, and DMS showed a strong similarity to the Chl *a* profile (Figs. 8*b* and 8*c*), with high values in the first 50 m and a sharp decline at the nitracline. Although Chl *a* concentrations were two times higher at this station, $DMSP_p$ concentrations were comparable with those measured at the Grand Banks station. Between 52% and 65% of the $DMSP_p$ was present in the 2–11 µm fraction (including *Chrysochromulina* spp.) and 18–34% in the >20 µm fraction (including most of the diatoms) (Table 2). Only small variations were observed with depth in the partitioning of the $DMSP_p$ between fractions. Below 50 m, DMS was undetectable but $DMSP_p$ and $DMSP_d$ were still present at low concentrations.

Incubations at the North Atlantic Drift station were conducted at 4, 15, and 63 m (dotted lines in Fig. 8). All three incubation depths were located in the 60-m-thick biomass-rich surface layer characterizing this station. Our results show

© 2004 NRC Canada

Fig. 6. Net changes in $DMSP_p$ by size fraction during incubations at (*a*) the Grand Banks, (*b*) North Atlantic Drift, and (*c*) Sargasso Sea. The open and solid bars represent changes in clear and dark bottles, respectively. The error bars indicate the range of duplicates.

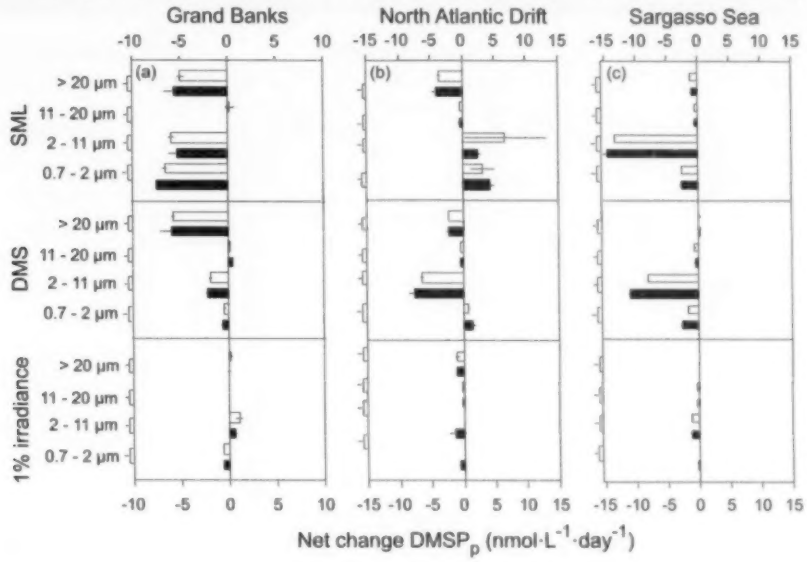

Fig. 7. Effects of the addition of MBE on the net change in DMS in incubations of the SML and DCM at (*a*) the Grand Banks, (*b*) North Atlantic Drift, and (*c*) Sargasso Sea. The difference between the two bars in each pair represents the DMS bacterial consumption rate.

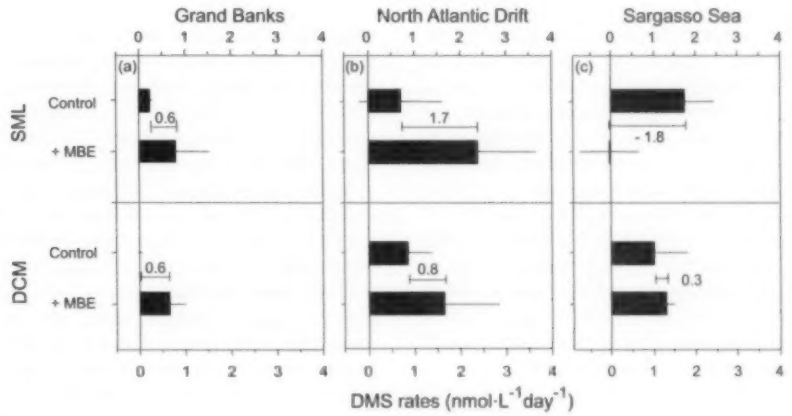

significant ($p \leq 0.05$) net decreases in Chl *a* at 4 and 15 m and an insignificant ($p \geq 0.05$) increase at 63 m (Fig. 4*b*). Variations in $DMSP_p$ concentrations (Fig. 5*b*) exhibited a different pattern with no significant change ($p \geq 0.05$) at 4 m and a large net decrease at 15 m (–8.5 nmol·L^{-1}·day^{-1}). At 63 m, there were no $DMSP_p$ rate data available from the clear bottles, since samples of one size fraction were lost (Figs. 5*b* and 6*b*). In terms of size-fractionated $DMSP_p$, only the changes in the >20 µm fraction were significant ($p \leq 0.05$) at all depths. However, the results generally indicate that the dynamics of $DMSP_p$ varied depending on the size of the particles (Fig. 6*b*). At 4 m, results from the clear bottles indicate an increase in $DMSP_p$ in the 2–11 µm fraction containing *Chrysochromulina* spp. but a decrease in the $DMSP_p$ present in the >20 µm fraction containing the diatoms. These results suggest that the diatoms were not growing and suffered significant losses at 4 m, whereas smaller cells were growing. This difference in the behavior of the larger and smaller cells may explain the difference observed in the daily variations of the Chl *a* (influenced mostly by the pigment-rich diatoms) and the $DMSP_p$ pools (influenced mostly by flagellates). At 15 m, $DMSP_p$ concentrations varied more like Chl *a* (Fig. 5*b*). At this depth, significant ($p \leq 0.05$) $DMSP_p$ decreases were observed in all but the smallest size fraction (Fig. 6*b*).

In contrast with the Grand Banks station, substantial net production of $DMSP_d$ was measured at the North Atlantic Drift station in both the SML (11.1 nmol·L^{-1}·day^{-1}) and the DCM (14.7 nmol·L^{-1}·day^{-1}) (Fig. 5*b*). However, the large error bars mean that these measurements are subject to con-

© 2004 NRC Canada

Fig. 8. Vertical profiles of (*a*) temperature (open triangles) and salinity (solid triangles), (*b*) nitrate (squares) and Chl *a* (circles), and (*c*) total $DMSP_p$ (squares), $DMSP_d$ (circles), and DMS (triangles) in the water column at the beginning of the North Atlantic Drift incubation experiment. Dotted horizontal lines indicate the depths at which samples were taken for the incubation experiments.

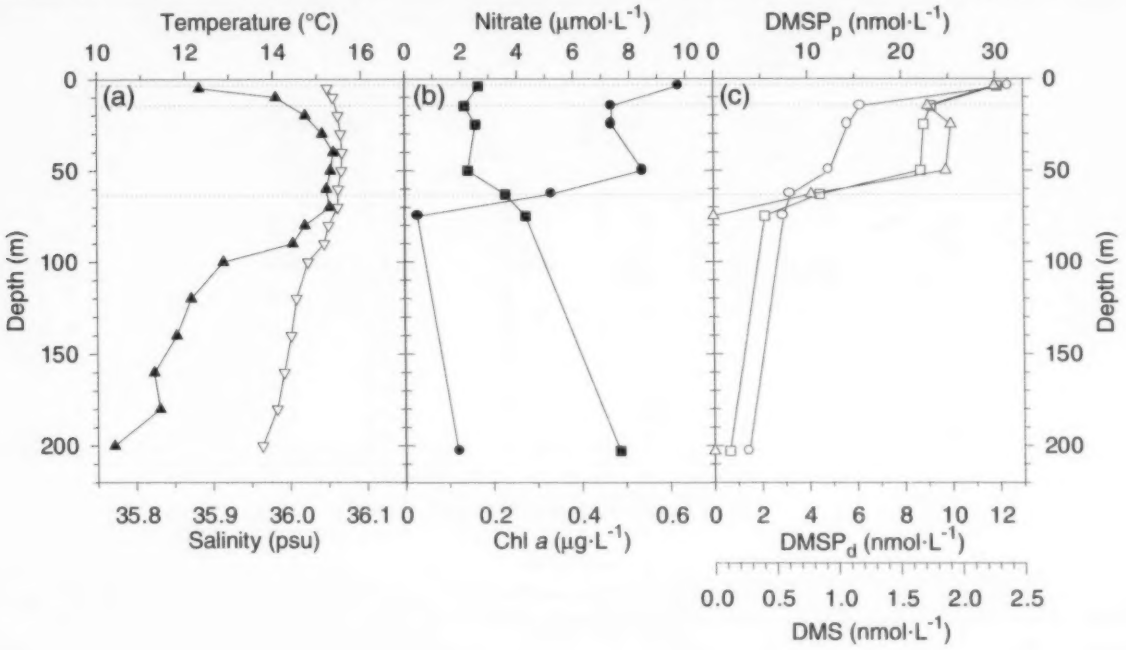

siderable uncertainty. In the DCM, the net production of $DMSP_d$ was higher than the loss rate of $DMSP_p$ (8.5 nmol·L^{-1}·day^{-1}), indicating possible $DMSP_p$ production at this depth. At 63 m, rates were much smaller and the net production of $DMSP_d$ corresponded to the decrease in $DMSP_p$ concentrations. Variations in DMS concentrations were relatively small at all depths and generally not significant ($p \geq 0.05$) during the incubations (Fig. 5*b*). Addition of MBE resulted in an increase in the measured DMS production rates at 4 and 15 m (Fig. 7*b*). These rates are statistically significant ($p \leq 0.05$) only at 4 m where bacterial DMS consumption can be estimated at 1.7 nmol·L^{-1}·day^{-1}. DMS production in the DCM was 0.9 nmol·L^{-1}·day^{-1}. DMS production was undetectable at the surface and at 63 m.

Sargasso Sea station

At sampling time (early May), the surface water was still fairly cool (20.2 °C) in the Sargasso Sea and the temperature profile revealed a thermocline located at around 30–40 m (Fig. 9*a*). Nitrate concentrations were under 0.2 μmol·L^{-1} in the top 60 m and increased sharply to 1.4 μmol·L^{-1} at 70–80 m (Fig. 9*b*). Chl *a* concentrations were approximately 0.1 μg·L^{-1} in the SML, reached 0.35 μg·L^{-1} in the nitracline between 60 and 80 m, and decreased to less than 0.01 μg·L^{-1} at 200 m. This station was also numerically dominated by unidentified flagellates (other phytoplankton in Fig. 3*c*), but dinoflagellates were also abundant and the prymnesiophyte group was composed almost exclusively of *Chrysochromulina* spp. Diatoms were almost absent in the SML but more abundant in the DCM. The DMSP and DMS pools showed little similarity to the Chl *a* profile (Fig. 9*c*). $DMSP_p$ concentrations remained stable at approximately 21 nmol·L^{-1} between the surface and the nitracline (60 m) where they sharply declined to less than 5 nmol·L^{-1}. The distribution of $DMSP_p$ in the different size fractions was approximately constant with depth with 67–76% found in the 2–11 μm fraction (Table 2). Less than 10% of the $DMSP_p$ was associated with the larger fraction containing most of the diatoms. The abundance of the pigment-rich but DMSP-poor diatoms in the DCM could thus explain the difference between the Chl *a* and $DMSP_p$ vertical profiles at this station. $DMSP_d$ concentrations were maximal close to the surface (5.4 nmol·L^{-1}) and decreased gradually in the top 60 m of the water column. The vertical distribution of DMS exhibited a similar pattern with maximum levels (2.2. nmol·L^{-1}) near the surface and decreasing concentrations with depth.

Incubations at the Sargasso Sea station were conducted at 5 (SML), 55 (DCM), and 93 m (1% surface irradiance) (dotted lines in Fig. 9). Significant ($p \leq 0.05$) net decreases in Chl *a* concentrations were measured at all depths, with the changes being slightly greater in the DCM (Fig. 4*c*). At 5 and 93 m, clear and dark bottles gave similar results, indicating no phytoplankton growth. At 55 m, the decrease in biomass was smaller in the clear bottles than in the dark bottles, indicating a Chl *a* gross production of 0.05 μg·L^{-1}·day^{-1}. A significant ($p \leq 0.05$) net loss of $DMSP_p$ was measured at all depths at this station (Fig. 5*c*), a loss occurring mostly in the dominant 2–11 μm size fraction (Fig. 6*c*). At 5 m, 98% of the loss of $DMSP_p$ was recovered in the dissolved pool, whereas 48% was recovered in the dissolved pool at 55 m (Fig. 5*c*). DMS net production rates at this station were among the highest that we measured during this study: 1.8

© 2004 NRC Canada

Fig. 9. Vertical profiles of (*a*) temperature (open triangles) and salinity (solid triangles), (*b*) nitrate (squares) and Chl *a* (circles), and (*c*) total $DMSP_p$ (squares), $DMSP_d$ (circles), and DMS (triangles) in the water column at the beginning of the Sargasso Sea incubation experiment. Dotted horizontal lines indicate the depths at which samples were taken for the incubation experiments.

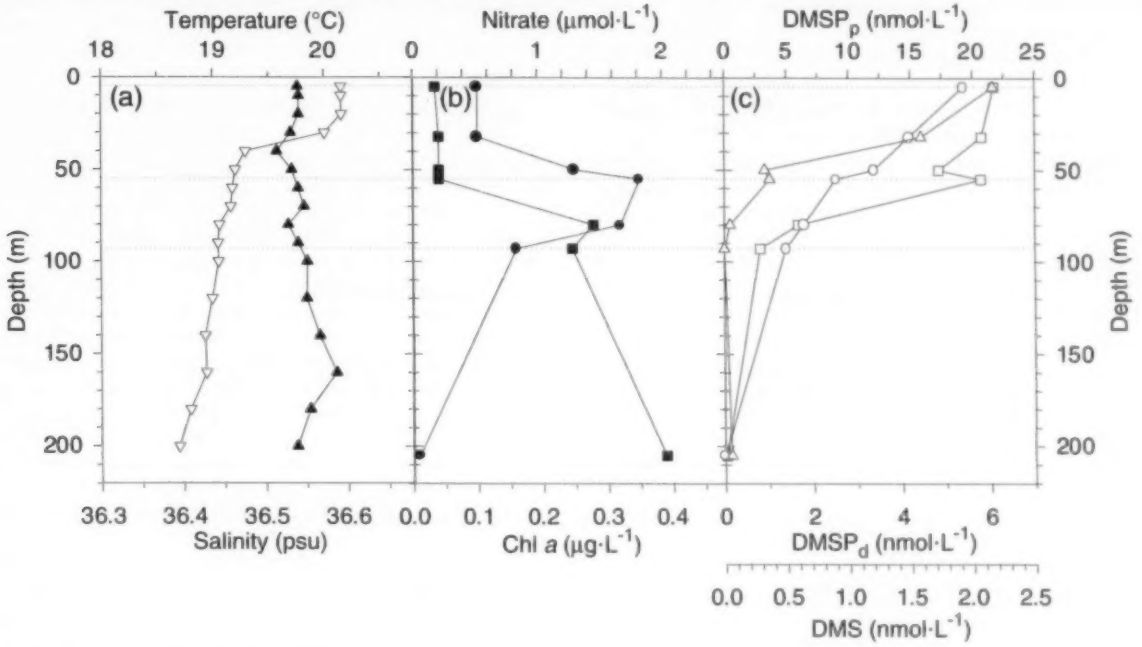

and 1.0 $nmol \cdot L^{-1} \cdot day^{-1}$ at 5 and 55 m, respectively. Addition of MBE at 5 m decreased the production of DMS, suggesting that MBE may have had an inhibitory effect on $DMSP_d$ cleavage (Fig. 7*c*). Consequently, DMS bacterial consumption could not be estimated at this depth. At 55 m, the addition of MBE did not change DMS production (Fig. 7*c*), indicating no significant bacterial DMS consumption. In contrast with the two other stations, DMS net production was lower in the clear bottles than in the dark bottles at 5 and 55 m in the Sargasso Sea (Fig. 5*c*). Photooxidation of DMS cannot totally explain these results, since DMS photooxidation is believed to be mainly controlled by UV light (René Bouillon, Dalhousie University, Halifax, N.S., personal communication), and our bottles were opaque to these wavelengths.

Discussion

The three stations were chosen to be representative of their respective provinces according to the seasonal physical water properties described by Longhurst (1995) and as such should reflect the prevailing conditions over a large area. SeaWiFS satellite derived Chl *a* images for the sampling period support this assumption, although examination of images from the period before the experiments shows that at the Grand Banks and North Atlantic Drift stations, the Chl *a* concentrations were higher 2 weeks before sampling. At the Grand Banks station, the low nitrate concentrations, the abundance of empty diatom frustules, and the absence of net production of Chl *a* in the SML indicate that the spring diatom bloom had reached the senescent phase. In contrast, the nitrate enrichment, seemingly related to the combined effect of a shallower nitracline and wind-induced mixing, was favoring the maintenance of an active phytoplankton assemblage dominated by flagellates and diatoms at the North Atlantic Drift station. Experiments in the Sargasso Sea were conducted at the same station where Dacey et al. (1998) collected a 2-year time series of biweekly vertical profiles of DMSP and DMS concentrations and other variables. Our Chl *a*, $DMSP_p$, $DMSP_d$, and DMS concentration measurements compare well with those of Dacey et al. (1998) for the same season. In general, they observed that the maximal $DMSP_p$ concentrations were always located above the DCM and that the maximal DMS concentrations were shallower than 40 m. Our results are in agreement with these previous findings. Overall, these observations suggest that the conditions observed in this study on the Grand Banks were transient, whereas those measured in the Sargasso Sea were representative of the summer period. The North Atlantic Drift station was located in a very hydrodynamically active area where the Gulf Stream and the Labrador Current converge, generating complex frontal systems (Clarke et al. 1980). The chemical and biological characteristics that we measured during our cruise may thus persist for extended periods of time along these fronts.

A schematic summary of the mean DMS and DMSP transformation rates for the two shallowest incubation depths at all stations is shown in Fig. 10. Only the SML and DCM values are given. Rates that were not significantly different from zero are noted as "0" (see Materials and methods). Our results reveal different cycling of the DMSP and DMS pools in each of the three provinces, differences seemingly related

© 2004 NRC Canada

Fig. 10. Schematic representation of the DMSP and DMS pools and transformation rates for the three stations in the Northwest Atlantic. Numbers in the boxes represent the pool size (nmol·L^{-1}), numbers in italics on the top of the boxes represent the measured net daily variations of each pool (nmol·L^{-1}·day^{-1}), and numbers on the arrows indicate the calculated daily flux between pools (nmol·L^{-1}·day^{-1}).

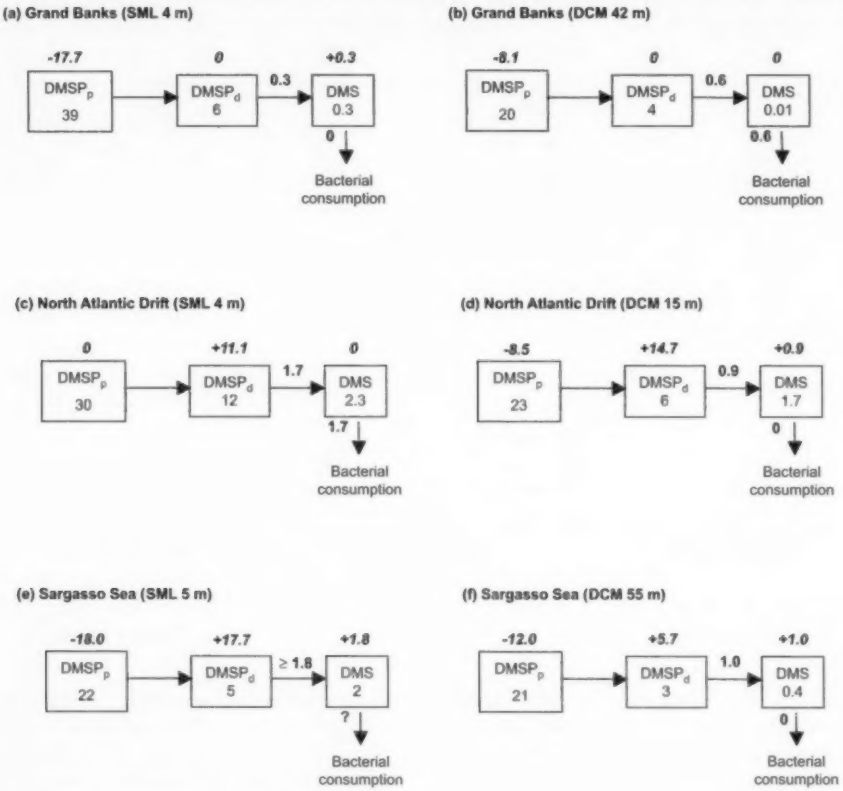

to the type and development stage of the prevailing plankton assemblage. Most stations exhibited high losses of $DMSP_p$ but different microbial DMSP cycling efficiency.

Grand Banks: fast DMSP cycling during postdiatom bloom conditions

At the Grand Banks station, 44% of the $DMSP_p$ was lost during our 24-h incubation in the SML and the DCM, as might be expected during a senescent bloom phase. Our size-fractionated $DMSP_p$ data indicate that both diatoms and smaller flagellates contributed to the loss of $DMSP_p$, with a higher contribution from diatoms in the DCM. The abundance of empty frustules suggests that diatom cell autolysis may have been the most important $DMSP_p$ loss mechanism at this station, whereas small flagellates may have experienced a high microzooplankton grazing pressure.

DMSP microbial cycling was very fast on the Grand Banks. The $DMSP_p$ lost from the particulate fraction was not recovered in the $DMSP_d$ pool. The unaccounted for DMSP cannot be attributed to storage by microzooplankton, since a net $DMSP_p$ loss was measured in the >20 μm size fraction where ciliates and zooflagellates, the dominant micrograzers, were found. Therefore, if the $DMSP_p$ was consumed by the microzooplankton, it must have been metabolized rapidly to other products, because it does not appear in either the particulate or dissolved pools. Archer et al. (2001) recently showed that ingested $DMSP_p$ by microzooplankton may provide up to 44% of their sulfur demand, indicating that $DMSP_p$ metabolism by microzooplankton may be important. Similarly, Wolfe et al. (1994) demonstrated in vitro that the heterotrophic dinoflagellate *Oxyrrhis marina* can take up and metabolize between 30% and 70% of algal DMSP without production of DMS. Thus, rapid metabolism by micrograzers represents a potentially important sink for DMSP. The other most likely sink for DMSP is bacterial uptake and demethylation. Uptake and storage of DMSP in bacterial cells is probably not important, however, as the size fraction containing the bulk of the bacteria (0.7–2.0 μm) did not show any increase in $DMSP_p$. This leaves only demethylation as a potential DMSP sink. This is consistent with previous measurements showing that demethylation is normally the dominant bacterial metabolism pathway for DMSP, especially in environments rich in dissolved organic carbon where the sulfur requirement of the bacteria is high (Kiene and Linn 2000; Kiene et al. 2000). These conditions were probably prevailing on the Grand Banks where high bacterial abundance was measured (Scarratt et al. 2000).

The Grand Banks station was similar to Station I (ice-covered waters) in Matrai and Vernet (1997), representing a physiologically older algal system with abundant diatoms that had stopped growing. Under these conditions, they also observed a depletion of $DMSP_d$ and DMS resulting from bi-

© 2004 NRC Canada

ological consumption. During our study, the rapid metabolism of DMSP by grazers or bacteria also prevented the accumulation of $DMSP_d$ in spite of the rapid loss of $DMSP_p$, whereas the high bacterial DMS consumption limited the net production of DMS. As a consequence, this microbial system was our least productive one in terms of DMS.

North Atlantic Drift: slow DMSP processing during flagellate bloom conditions

In contrast with the Grand Banks station, no significant $DMSP_p$ net change occurred in the surface water at the North Atlantic Drift station and a net loss occurred at 15 m. However, the large net $DMSP_d$ accumulation occurring at both 4 and 15 m suggests that gross DMSP production exceeded the net loss of $DMSP_p$. To balance the $DMSP_d$ net accumulation and DMS gross production measured during our incubations, gross $DMSP_p$ production of at least 11.1 and 6.2 $nmol \cdot L^{-1} \cdot day^{-1}$ must have taken place at 4 and 15 m, respectively. These $DMSP_p$ production rates fall below the range of those reported by Archer et al. (2001) during an *Emiliania huxleyi* bloom in the North Sea (15–46 $nmol \cdot L^{-1} \cdot day^{-1}$) and represented a doubling time of the $DMSP_p$ pool of between 2.7 and 3.7 days. Active $DMSP_p$ synthesis was thus occurring at this station. A sign of this productivity can be seen in our size-fractionated measurements at 4 m showing a net $DMSP_p$ production in the 2–11 μm fraction where *Chrysochromulina* spp., a known strong DMSP producer, was found (Keller et al. 1989). This species was probably also growing at 15 m, but its production may have been exceeded by grazing. Microzooplankton, which were particularly abundant at 15 m, may have been responsible for the loss of $DMSP_p$. Another potential grazer is *G. flagellare* (Scarratt et al. 2002), a dinoflagellate belonging to a genus known to have heterotrophic or mixotrophic members (Hansen 1992). The co-occurrence of *Chrysochromulina* spp., and *G. flagellare* may thus reflect a predator–prey relationship. $DMSP_p$ loss was also measured in the >20 μm fraction, suggesting that diatoms were the source of up to 50% of the $DMSP_d$ production at this station.

At the North Atlantic Drift station, a large accumulation of $DMSP_d$ was measured in the SML, suggesting a low rate of total microbial $DMSP_d$ utilization (cleavage and demethylation). This station was nevertheless characterized by high $DMSP_d$ cleavage rates (1.7 and 0.9 $nmol \cdot L^{-1} \cdot day^{-1}$), two times higher than on the Grand Banks, and relatively high DMS concentrations (2.3 and 1.7 $nmol \cdot L^{-1}$). The coincidence between high levels of DMS and high concentrations of *Chrysochromulina* spp. and *Gyrodinium* spp. has been reported in the past from field observations (Levasseur et al. 1994; Cantin et al. 1996), but the presence or absence of DMSP lyase (the enzyme that cleaves DMSP to DMS) in these taxa is not known. DMS bacterial consumption was not significant. This is an example where bacterial DMS gross production exceeds bacterial consumption, allowing a buildup of the DMS pool. This contrasts with the Grand Banks station where DMS gross production and consumption were in close balance.

From a DMSP/DMS cycling perspective, this station is similar to Station II (Polar front waters) in Matrai and Vernet (1997) where a high $DMSP_p$ production was measured but where most of the DMSP produced was converted to the dissolved pool. As for their polar front stations, our station in the North Atlantic Drift represented a physiologically active algal system. Under these conditions, the production of the substrates DMSP and DMS may exceed the carbon and sulfur requirement of the bacterial assemblage, resulting in an accumulation of both biogenic sulfur pools.

Sargasso Sea: a vertically stratified system

The $DMSP_p$ dynamics at the Sargasso Sea station were somewhat simpler than at the two previous stations with most of the $DMSP_p$ and daily changes occurring in one size fraction, 2–11 μm, composed largely of unidentified flagellates. A large portion of the $DMSP_p$ pool (as much as 82%) was also lost in 24 h at this station, indicating a strong disequilibrium between DMSP production and loss. During their annual cycle conducted at the same station, Dacey et al. (1998) also observed considerable short-term variability in $DMSP_p$ concentrations. They used estimates of phytoplankton growth and grazing in the Sargasso Sea to calculate the quantities of $DMSP_p$ processed by grazing each day. They estimated that grazing consumed between 10 and 15 nmol $DMSP_p \cdot L^{-1} \cdot day^{-1}$, or up to 80% of the daily $DMSP_p$ production, corresponding well to our findings at this station. This could be an example of grazing limitation in which phytoplankton standing stock, whose growth rate is normally balanced by zooplankton grazing in the Sargasso Sea, is rapidly consumed when the growth rate diminishes. Such "grazing control" has been described by many authors (e.g., Cullen 1995). Since the sky was completely overcast during our incubations, light deficiency could have limited phytoplankton growth, resulting in a decline in phytoplankton biomass as measured by $DMSP_p$ and Chl *a*. Our size-fractionated results also support the explanation of net losses of phytoplankton resulting from grazing. The relative magnitude of the $DMSP_p$ loss in each size fraction corresponds to the proportion of the total $DMSP_p$ found in each fraction. This suggests that the loss mechanism applies equally across the size spectrum, as might be expected from a light-induced reduction in growth rate and an evenly distributed grazing pressure.

The considerable decrease in $DMSP_p$ concentration observed in the Sargasso Sea in 1 day suggests that the equilibrium between $DMSP_p$ production and loss (grazing) may be highly sensitive to day-to-day variations in solar irradiance and may result in major $DMSP_p$ changes over short-term periods. From a modeling approach, and using Dacey et al.'s (1998) data, Lefèvre et al. (2003) also showed that microzooplankton grazing was the second (after the S:N ratio) most important variable affecting $DMSP_p$ productivity in the Sargasso Sea. Daily decreases of 80% of the $DMSP_p$ burden in the surface water represent a striking result and suggest that consecutive days of overcast conditions may have great impact on the DMSP pools and dynamics.

At the Sargasso Sea station, different microbial DMS and DMSP cycling patterns were found in the SML compared with the DCM. Essentially all of the $DMSP_p$ lost (98%) was recovered in the dissolved pool in the SML but only 30% was recovered in the DCM. Again, the loss of $DMSP_p$ measured in all size fractions, including the largest one, indicates that microzooplankton were not accumulating DMSP. In the SML, DMS net production was high (1.8 $nmol \cdot L^{-1} \cdot h^{-1}$), but

© 2004 NRC Canada

$DMSP_d$ cleavage still represented a minor sink for DMSP. The value of 1.8 nmol·L^{-1}·h^{-1} represents a minimum estimate for $DMSP_d$ cleavage in the SML, since the MBE-inhibited samples showed no DMS production and we thus have no measurements of bacterial DMS consumption. On the other hand, using an approach based on the addition of elevated concentrations of DMS in the water samples and following the decay of DMS over time, Scarratt et al. (2000) reported no DMS bacterial consumption in surface waters at this station. DMS bacterial consumption was thus probably low during our incubation. Our data also suggest a low utilization of DMSP by microzooplankton (metabolism) and (or) bacteria (demethylation) in the SML. At 5 m, the accumulation of DMSP in the dissolved pool can almost totally account for the loss of $DMSP_p$ and only a low demethylation rate (0.3 nmol·L^{-1}·day^{-1}) would be necessary to balance the loss. This is a surprising result, since, as previously mentioned, DMSP bacterial utilization is generally an order of magnitude greater than the cleavage rate (Kiene and Linn 2000). This would suggest a low sulfur demand by the bacterial assemblage in the SML. In the DCM, the accumulation of DMSP in the dissolved pool and $DMSP_d$ cleavage could only explain 48% of the loss in $DMSP_p$, leaving 52% to other loss processes (microzooplankton metabolism and (or) bacterial demethylation).

The SML of the Sargasso Sea may thus be viewed as a system characterized by high $DMSP_p$ production and loss where the production of $DMSP_d$ exceeds the bacterial requirement for carbon and sulfur. This is similar to the system previously described for the North Atlantic Drift station characterized by a growing algal community. On the other hand, the partitioning of the DMSP microbial utilization pathway observed in the DCM was more comparable with the one encountered on the Grand Banks and, as observed by Matrai and Vernet 1997, seems to be typical of mature algal systems.

In conclusion, comparison of the three stations suggests that water column DMS concentrations are controlled by the balance between DMSP and DMS sources and sinks. Loss of $DMSP_p$ may not necessarily be balanced by an increase in $DMSP_d$, depending on the relative importance of bacterial demethylation and assimilation of DMSP by grazers. It is also clear that the net DMS production and the DMS concentration in the water column are influenced by the rate of DMS consumption, with strong consumption preventing significant accumulation of DMS. The microplankton species assemblage appears to be an important factor influencing the distribution and dynamics of organic sulfur. The presence of known DMSP-producing species (*Chrysochromulina* sp. and *G. flagellare*) at the Sargasso Sea and North Atlantic Drift stations was clearly reflected in the abundance and distribution of DMS and DMSP. This underscores the importance of species-specific processes in DMS production. Grazing also appears to have an effect, with large losses of $DMSP_p$ coinciding with the presence of abundant microzooplankton. Finally, our results fit well with the explanation for the "summer DMS paradox" offered by Simó and Pedrós-Alió (1999). These authors pointed out that highest annual DMS concentrations in a broad range of subtropical, temperate, and subpolar oceans are found in summer, when surface Chl *a* levels are low. Our data suggest a scenario in which high DMS production (high $DMSP_d$ cleavage) and low DMS consumption combine to allow DMS to accumulate in actively growing algal systems even though the phytoplankton biomass is maintained at a low level by microzooplankton grazing. These conditions were found in the warmer waters of the North Atlantic Drift and Sargasso Sea. This lends further support to the CLAW hypothesis if such conditions are favored in a global warming scenario.

Acknowledgements

We are grateful to Alain Gagné, François Roy, Delphine Thibault, Marie-Lyne Dubé, and Lyse Bérard-Therriault for sample collection and analysis. We would like to thank the captain and crew members of the CCGS *Hudson* for their collaboration and Trevor Platt for providing SeaWiFS images. This research was funded as part of the Fisheries and Oceans Canada NODEM (Northern Oceans DMS Emission Models) program and grants from the Natural Sciences and Engineering Research Council of Canada to M.L. and M.G.

References

Archer, S.D., Widdicombe, C.E., Tarran, G.A., Rees, A.P., and Burkill, P.H. 2001. Production and turnover of particulate dimethylsulphoniopropionate during a coccolithophore bloom in the northern North Sea. Aquat. Microb. Ecol. **24**: 225–241.

Cantin, G., Levasseur, M., Gosselin, M., and Michaud, S. 1996. Role of zooplankton in the mesoscale distribution of surface dimethylsulfide concentrations in the Gulf of St. Lawrence, Canada. Mar. Ecol. Prog. Ser. **141**: 103–117.

Charlson, R.J., Lovelock, J.E., Andreae, M.O., and Warren, S.G. 1987. Oceanic phytoplankton, atmospheric sulphur, cloud albedo and climate. Nature (Lond.), **326**: 655–661.

Charlson, R.J., Schwartz, S.E., Hales, J.M., Cess, R.D., Coakley, J.A.J., Hansen, J.E., and Hofmann, D.J. 1992. Climate forcing by anthropogenic aerosols. Science (Wash., D.C.), **255**: 423–430.

Clarke, R.A., Hill, H.W., Reiniger, R.F., and Warren, B.A. 1980. Current system south and east of the Grand Banks of Newfoundland. J. Phys. Oceanogr. **10**: 25–65.

Cullen, J.J. 1995. Status of the iron hypothesis after the Open-Ocean Enrichment Experiment. Limnol. Oceanogr. **40**: 1336–1343.

Dacey, J.W.H., and Wakeham, S.G. 1986. Oceanic dimethylsulfide: production during zooplankton grazing on phytoplankton. Science (Wash., D.C.), **233**: 1314–1316.

Dacey, J.W.H., Howse, F.A., Michaels, A.F., and Wakeham, S.G. 1998. Temporal variability of dimethylsulfide and dimethylsulfoniopropionate in the Sargasso Sea. Deep-Sea Res. **45**: 2085–2104.

Hansen, P.J. 1992. Prey size selection, feeding rates and growth dynamics of heterotrophic dinoflagellates with special emphasis on *Gyrodinium spirale*. Mar. Biol. **114**: 327–334.

Keller, M.D., Bellows, W.K., and Guillard, R.R.L. 1989. Dimethylsulfide production in marine phytoplankton. *In* Biogenic sulfur in the environment. *Edited by* E.S. Saltzmann and E.M. Cooper. American Chemical Society Symposium Series. American Chemical Society, Washington, D.C. pp. 167–182.

Kettle, A.J., Andreae, M.O., Amouroux, D., Andreae, T.W., Bates, T.S., Berresheim, H., Bingemer, H., Boniforti, R., Curran, M.A.J., DiTullio, G.R., et al. 1999. A global database of sea surface dimethylsulfide (DMS) measurements and a procedure to predict sea surface DMS as a function of latitude, longitude, and month. Global Biogeochem. Cycles, **13**: 399–444.

© 2004 NRC Canada

Kiene, R.P. 1996. Production of methanethiol from dimethylsulfoniopropionate in marine surface waters. Mar. Chem. **54**: 69–83.

Kiene, R.P., and Linn, L.J. 2000. Distribution and turnover of dissolved DMSP and its relationship with bacterial production and dimethylsulfide in the Gulf of Mexico. Limnol. Oceanogr. **45**: 849–861.

Kiene, R.P., Linn, L.J., and Bruton, J.A. 2000. New and important roles for DMSP in marine microbial communities. J. Sea Res. **43**: 209–224.

Kirst, G.O., Thiel, C., Wolff, H., Nothnagel, J., Wanzek, M., and Ulmke, R. 1991. Dimethylsulfoniopropionate (DMSP) in ice-algae and its possible biological role. Mar. Chem. **35**: 381–388.

Kwint, R.L.J., and Kramer, K.J.M. 1995. Dimethylsulphide production by plankton communities. Mar. Ecol. Prog. Ser. **121**: 227–237.

Laroche, D., Vézina, A., Levasseur, M., Gosselin, M., Stefels, J., Keller, M.D., Matrai, P.A., and Kwint, R.L.J. 1999. DMSP synthesis and exudation in phytoplankton: a modeling approach. Mar. Ecol. Prog. Ser. **180**: 37–49.

Leck, C., and Bågander, L.E. 1988. Determination of reduced sulfur compounds in aquaous solutions using gas chromatography flame photometric detection. Anal. Chem. **60**: 1680–1683.

Lefèvre, M., Vézina, A., Levasseur, M., and Dacey, J.W.D. 2003. A model of dimethylsulfide dynamics for the subtropical Atlantic. Deep-Sea Res. I. Oceanogr. Res. Pap. **49**: 2221–2239.

Levasseur, M., Keller, M.D., Bonneau, E., D'Amours, D., and Bellows, W.K. 1994. Oceanographic basis of a DMS-related Atlantic cod (*Gadus morhua*) fishery problem: blackberry feed. Can. J. Fish. Aquat. Sci. **51**: 881–889.

Longhurst, A. 1995. Seasonal cycles of pelagic production and consumption. Prog. Oceanogr. **35**: 77–167.

Lund, J.W.G., Kipling, C., and Le Cren, E.D. 1958. The inverted microscope method of estimating algal numbers and the statistical basis of estimation by counting. Hydrobiologia, **11**: 143–178.

Matrai, P.A., and Keller, M.D. 1993. Dimethylsulfide in a large-scale coccolithophore bloom in the Gulf of Maine. Continental Shelf Res. **13**: 831–843.

Matrai, P.A., and Vernet, M. 1997. Dynamics of the vernal bloom in the marginal ice zone of the Barents Sea: dimethyl sulfide and dimethylsulfoniopropionate budgets. J. Geophys. Res. **102**: 22 965 – 22 979.

Parsons, T.R., Maita, Y., and Lalli, C.M. 1984. A manual of chemical and biological methods of seawater analysis. Pergamon, Oxford, U.K.

Scarratt, M.G., Levasseur, M., Schultes, S., Michaud, S., Cantin, G., Vézina, A., Gosselin, M., and de Mora, S.J. 2000. Production and consumption of dimethylsulfide (DMS) in North Atlantic waters. Mar. Ecol. Prog. Ser. **204**: 13–26.

Scarratt, M., Levasseur, M., Michaud, S., Cantin, G., Gosselin, M., and de Mora, S.J. 2002. Influence of phytoplankton taxonomic profile on the distribution of dimethylsulfide and dimethylsulfoniopropionate in the northwest Atlantic. Mar. Ecol. Prog. Ser. **244**: 49–61.

Schultes, S., Levasseur, M., Michaud, S., Cantin, G., Wolfe, G., Gosselin, M., and de Mora, S. 2000. Dynamics of dimethylsulfide production from dissolved dimethylsulfoniopropionate in the Labrador Sea. Mar. Ecol. Prog. Ser. **202**: 27–40.

Simó, R. 2001. Production of atmospheric sulfur by oceanic plankton: biogeochemical, ecological and evolutionary links. Trends Ecol. Evol. **16**: 287–294.

Simó, R., and Pedrós-Alió, C. 1999. Role of vertical mixing in controlling the oceanic production of dimethyl sulphide. Nature (Lond.), **402**: 396–397.

Simó, R., Pedros-Alio, C., Malin, G., and Grimalt, J.O. 2000. Biological turnover of DMS, DMSP and DMSO in contrasting open-sea waters. Mar. Ecol. Prog. Ser. **203**: 1–11.

Stefels, J., and Dijkhuizen, L. 1996. Characteristics of DMSP-lyase in *Phaeocystis* sp. (Prymnesiophyceae). Mar. Ecol. Prog. Ser. **131**: 307–313.

Steinke, M., Wolfe, G.V., and Kirst, G.O. 1998. Partial characterisation of dimethylsulfoniopropionate (DMSP) lyase isozymes in 6 strains of *Emiliania huxleyi*. Mar. Ecol. Prog. Ser. **175**: 215–225.

Strickland, J.D.H., and Parsons, T.R. 1972. A practical handbook of seawater analysis. Bull. Fish. Res. Board Can. No. 167.

Sunda, W.K.D.J., Kiene, R.P., and Huntsman, S. 2002. An antioxidant function for DMSP and DMS in marine algae. Nature (Lond.), **418**: 317–320.

Utermöhl, N. 1931. Neue wege in der quantitativen erfassung des planktons. Verh. Int. Ver. Theor. Angew. Limnol. **5**: 567–596.

Vairavamurthy, A., Andreae, M.O., and Iverson, R.L. 1985. Biosynthesis of dimethylsulfide and dimethylpropiothetin by *Hymenomonas carterae* in relation to sulfur source and salinity variations. Limnol. Oceanogr. **30**: 59–70.

Visscher, P.T., and Taylor, B.F. 1993. Aerobic and anaerobic degradation of a range of alkyl sulfides by a denitrifying marine bacterium. Appl. Environ. Microbiol. **59**: 4083–4089.

Wolfe, G.V., Sherr, E.B., and Sherr, B.F. 1994. Release and consumption of DMSP from *Emiliania huxleyi* during grazing by *Oxyrrhis marina*. Mar. Ecol. Prog. Ser. **111**: 111–119.

Wolfe, G.V., Steinke, M., and Kirst, G.O. 1997. Grazing-activated chemical defence in a unicellular marine alga. Nature (Lond.), **387**: 894–897.

Wolfe, G.V., Levasseur, M., Cantin, G., and Michaud, S. 1999. Microbial consumption and production of dimethyl sulfide (DMS) in the Labrador Sea. Aquat. Microb. Ecol. **18**: 197–205.

Yoch, D.C., Ansede, J.H., and Rabinowitz, K.S. 1997. Evidence for intracellular and extracellular dimethylsulfoniopropionate (DMSP) lyases and DMSP uptake sites in two species of marine bacteria. Appl. Environ. Microbiol. **63**: 3182–3188.

© 2004 NRC Canada

Dimethylsulfoniopropionate in six species of giant clams and the evolution of dimethylsulfide after death[1]

Richard W. Hill, John W.H. Dacey, Susan D. Hill, Ahser Edward, and Wayne A. Hicks

Abstract: Substantial accumulation of dimethylsulfoniopropionate (DMSP) is documented in tissues of all six of the common species of giant clams (Tridacnidae). Results include measures of DMSP concentrations in siphonal mantle, byssal mantle, adductor muscle, and gill tissues obtained by gas chromatography of alkalized extracts plus evidence of DMSP from mass spectrometry. Formation of dimethylsulfide (DMS) by tissues after death is documented. The tridacnid clams maintain symbiotic associations with populations of dinoflagellates, which live within the enlarged siphonal mantle. We postulated that because of their association with dinoflagellates, the clams would chronically accumulate DMSP to high concentrations. Our results show that DMSP occurs at over 30 mmol·kg^{-1} in many tissues of tridacnid clams (sometimes 50–60 mmol·kg^{-1}), meaning that these clams accumulate DMSP to the highest documented tissue concentrations in the animal kingdom. DMSP at such concentrations could affect multiple properties and functions. Our particular interest for this research was to assess whether postmortem breakdown of DMSP is responsible for the rapid development of potent off-odors and off-tastes that have blocked the commercial success of giant clam aquaculture. High concentrations of DMS produced in the day after death probably account for the peculiar perishability of giant clam tissues.

Résumé : Nous présentons des données qui montrent une accumulation importante de diméthylsulfoniopropionate (DMSP) dans les tissus des six espèces communes de moules géantes (Tridacnidae). Ces données comprennent des dosages des concentrations de DMSP par chromatographie en phase gazeuse d'extraits alcalinisés du manteau du siphon, du manteau du byssus, du muscle adducteur et des tissus branchiaux; d'autres données sur le DMSP ont été obtenues par spectrométrie de masse. Il y a aussi formation de sulfure de diméthyle (DMS) dans les tissus après la mort. Les moules tridacnidées maintiennent des relations symbiotiques avec des populations de dinoflagellés qui vivent dans le manteau élargi du siphon. Nous avons émis l'hypothèse que cette association avec les dinoflagellés amène les moules à accumuler de façon chronique de fortes concentrations de DMSP. Nos données confirment l'existence de concentrations de plus de 30 mmol·kg^{-1} (même 50–60 mmol·kg^{-1}) dans plusieurs tissus des moules tridacnidées, ce qui représente les plus fortes accumulations tissulaires connues de DMSP dans le règne animal. À de telles concentrations, le DMSP doit affecter de nombreuses propriétés et fonctions. Nous nous sommes intéressés, en particulier, dans ce travail à savoir si la dégradation après la mort du DMSP est responsable de l'apparition rapide des fortes odeurs et des saveurs désagréables qui nuisent au succès commercial de l'élevage des moules géantes. Les fortes concentrations de DMS qui se produisent durant la première journée qui suit la mort des moules géantes expliquent probablement la détérioration inusitée de leurs tissus.

[Traduit par la Rédaction]

Introduction

Although dimethylsulfoniopropionate (DMSP) is ordinarily thought of as an algal compound, it could in principle accumulate to high concentrations in animals that live in symbiotic association with algae. Such accumulation could have practical and physiological implications for the animals because DMSP can have important taste consequences in seafoods, can affect enzyme function, and may play roles in ameliorating tissue oxygen stress. We hypothesized that the

Received 1 February 2003. Accepted 7 November 2003. Published on the NRC Research Press Web site at http://cjfas.nrc.ca on 23 June 2004.
J17362

R.W. Hill[2] **and S.D. Hill.** Department of Zoology, Michigan State University, East Lansing, MI 48824, U.S.A.
J.W.H. Dacey. Department of Biology, Woods Hole Oceanographic Institution, Woods Hole, MA 02543, U.S.A.
A. Edward. College of Micronesia – FSM, P.O. Box 159, Kolonia, Pohnpei, Federated States of Micronesia 96941.
W.A. Hicks. Department of Biochemistry and Molecular Biology, Michigan State University, East Lansing, MI 48824, U.S.A.

[1]This paper is part of the proceedings of the Third International Symposium on Biological and Environmental Chemistry of DMS(P) and Related Compounds, held in Rimouski (Québec), 26–28 September 2002.
[2]Corresponding author (e-mail: hillr@msu.edu).

 doi: 10.1139/F04-029 © 2004 NRC Canada

giant clams of the family Tridacnidae accumulate DMSP because they maintain symbiotic associations with dinoflagellates, termed zooxanthellae. The zooxanthellae, which belong to two of the major subdivisions of *Symbiodinium* (Rowan 1998), occur primarily in the siphonal mantle tissue, where they live and multiply extracellularly in a system of specialized tubules (Norton et al. 1992). The clams, which occupy exposed locations in the clear, shallow waters of Indo-Pacific coral reefs, present their extensive siphonal mantle tissue to the sun, enabling high photosynthetic rates by their zooxanthellae; the clams sometimes acquire over 90% of all of their organic carbon input from their zooxanthellae (Klumpp and Griffiths 1994), and evidence indicates that the zooxanthellae may meet at least 45% of the nitrogen requirements of the clams by manufacturing organic nitrogen compounds from ammonium nitrogen (Hawkins and Klumpp 1995). We recently reported for the first time that certain giant clams not only accumulate DMSP but also reach tissue concentrations higher than those documented for any other animals (Hill et al. 2000). Indeed, the concentrations of DMSP that we measured in giant clams were an order of magnitude higher than the highest tissue concentrations ever observed in fish, crustaceans, or other bivalve or gastropod mollusks, all of which, if they accumulate DMSP at all, acquire DMSP from ingested foods rather than endogenous symbionts (Hill et al. 2000).

A principal purpose of the present research was to enhance the definitiveness of our original report. For one thing, our earlier identification of DMSP was based entirely on gas chromatographic results (e.g., the column retention time of presumptive dimethylsulfide (DMS) liberated by alkalization of clam tissues matched the retention time of DMS reagent). In the research we now report, we returned tissues at liquid nitrogen temperature to the United States from western Pacific islands and analyzed these well-preserved materials by mass spectrometry as well as gas chromatography, providing definitive evidence for DMSP in the clam tissues. Another shortcoming of our earlier report was that only two of the eight or nine species of tridacnid clams were studied. In this report, we address all six of the common species in the family Tridacnidae.

Our second principal purpose in this research was to test our hypothesis (Hill et al. 2000) that DMS is evolved by giant clam tissues soon after death because of the postmortem breakdown of tissue DMSP. This hypothesis is of significant practical interest because giant clams are noted for developing offensive tastes and odors soon after death (Peavey and Riley 1993, 1994), and the off-tastes and off-odors have constituted significant obstacles for the commercial success of tridacnid aquaculture. We hypothesized that DMS, a well known agent of off-tastes in seafoods, is responsible for the problems observed with giant clams, the tissues of which are poised to generate substantial quantities of DMS because of their peculiarly high DMSP concentrations.

Materials and methods

Tissues for study of chemical composition

Hippopus hippopus (13–28 cm shell length), *Tridacna maxima* (12–19 cm), and *Tridacna squamosa* (12–20 cm) were collected in the wild and *Tridacna derasa* (19–21 cm) was obtained alive from government aquaculture facilities in the Federated States of Micronesia (Pohnpei and Kosrae); wild collection and export of tissues were by Permits Nos. 000304 and 00-001 from the Office of Marine and Coastal Resource Management, Pohnpei State Government. *Hippopus hippopus* (13–14 cm), *Tridacna crocea* (7–9 cm), *T. derasa* (16–19 cm), and *Tridacna gigas* (12–17 cm) were also obtained alive, mostly as aquacultured specimens, in the Republic of Palau from Belau Aquaculture; export of tissues was by certificate EXP.2000-102 from the Ministry of Resources and Development, Republic of Palau.

Tissues were taken from clams immediately after death in the Federated States of Micronesia and Palau in March 2000. A siphonal mantle sample was cut from the middle of the siphonal mantle of each clam; the cuts were made through the entire tissue and perpendicular to the tissue surface so as to include the pigmented surface layer and the relatively unpigmented inner layer of this mantle tissue in their natural proportions. A byssal mantle sample was cut in a similar manner from the mantle tissue near the byssal aperture, tissue that does not receive sunlight. The sample of adductor muscle was cut from the interior of the muscle. Cuts for the gill sample were made perpendicular to the long axis of a gill so as to include the full lengths of the gill lamellae. All samples were blotted on paper towels and weighed promptly after being cut. Samples were then placed in Corning cryogenic vials (polypropylene) and frozen immediately using dry ice. They were later transferred to an MVE dry dewar at liquid nitrogen temperature for transport to the United States where they were refrigerated at –80 °C until assay by mass spectrometry, gas chromatography, and fluorometry (for pheophytin).

Chemical assays

For mass spectrometry, an approximately 0.7-g piece of tissue was powdered by grinding in a mortar at liquid nitrogen temperature and extracted twice into a methanol–chloroform–water solution (12:5:1). Separation of the solution into aqueous and chloroform phases was then induced. The aqueous phase was removed, acidified (HCl), enriched with 10 µmol of trigonelline (Sigma; 1-methylpyridinium-3-carboxylate) as a semiquantitative internal standard, and passed sequentially through three resin columns: (*i*) Bio-Rad Laboratories AG 1-X8 (200–400 mesh, Cl^- form) prepared by washing to equilibrium with 1 mol·L^{-1} NaOH, (*ii*) Bio-Rad Bio-Rex 70 (100–200 mesh, Na^+ form) previously protonated by washing with 1 mol·L^{-1} HCl, and (*iii*) Bio-Rad AG 50W-X8 (200–400 mesh, Na^+ form) previously protonated by washing with 1 mol·L^{-1} HCl. Distilled, deionized water was passed through the columns following the sample. Afterward, the AG 50 column was eluted with 2.5 mol·L^{-1} HCl. The elution solution was lyophilized and stored at –20 °C until a fast atom bombardment mass spectrum was obtained using a Jeol JMF HX 110 mass spectrometer. An index of DMSP concentration was calculated as the ratio of the mass-135 signal over the mass-138 signal (trigonelline) normalized to the weight of tissue assayed.

For analysis by gas chromatography and fluorometry, an approximately 1-g piece of tissue was minced while still semifrozen and placed in 25 mL of reagent-grade methanol in a glass vial sealed with a Teflon-faced butyl-rubber sep-

© 2004 NRC Canada

Table 1. Concentration of DMSP ($\mu mol \cdot g^{-1}$) in four tissues of six species of giant clams.

	Siphonal mantle		Byssal mantle		Adductor muscle		Gill	
Species	Mean ± SE	Range	Mean ± SE	Range	Mean ± SE	Range	Mean ± SE	Range
H. hippopus (n = 8)	6.76±1.54	1.5–15.7	9.67±1.50	3.4–16.4	3.95±1.07	1.2–9.5	17.6±7.51	7.0–47.4
T. crocea (n = 6)	29.7±2.98	16.5–34.6	43.2±3.85	29.2–57.5	2.59±0.34	1.5–3.4	25.6	
T. derasa (n = 9)	16.5±2.33	6.0–27.1	11.9±1.09	7.2–16.6	5.75±1.64	1.4–13.9	7.83±0.47	6.3–8.8
T. gigas (n = 7)	25.9±1.47	21.5–32.4	17.3±1.73	11.7–23.4	10.7±1.92	4.8–16.9	22.5±1.39	18.5–26.1
T. maxima (n = 7)	29.6±3.20	15.4–41.5	29.9±4.05	14.7–42.7	3.29±0.20	2.4–3.8	34.7±2.24	27.0–41.4
T. squamosa (n = 5)	37.7±4.05	24.5–47.6	36.8±5.75	23.5–57.7	5.04±1.05	2.8–8.5	42.3±2.43	38.4–51.5

Note: Adductor muscle for one *T. derasa* was not analyzed. For gill, n is 5 for *H. hippopus*, 1 for *T. crocea*, 5 for *T. derasa*, and 5 for *T. gigas*, and as tabulated for the other species.

tum (Regis Technology). After 24 h of extraction in the dark with periodic shaking, 1.0 mL of methanol was withdrawn by glass syringe from each tissue extraction vial and placed in 25 mL of 2 $mol \cdot L^{-1}$ KOH in a sealed analysis glass vial. Incubation in cold base quantitatively converts DMSP to DMS (Dacey and Blough 1987). After base incubation, DMS was measured in headspace samples by gas chromatography using a Chromosil 330 (Supelco) column for separation, Sievers 350B sulfur chemiluminescence detector, and Hewlett Packard 3395 integrator. Standards were prepared in 25 mL of 2 $mol \cdot L^{-1}$ KOH plus 1 mL of methanol using reagent-grade DMS (Fluka) in vials identical to those used for alkalization of tissue extracts.

Chlorophyll was measured to serve as an index of the density of zooxanthellae. In fact, because some chlorophyll could have degraded to pheophytin during shipment and sample preparation, and because our interest was not in chlorophyll itself but in an index of relative levels of zooxanthellae, we degraded all chlorophyll by acidification (3 mmol $HCl \cdot L^{-1}$) and measured total pheopigment levels as our index (Hill et al. 1995). For pheopigment assay, 0.5 mL of methanol was withdrawn by glass syringe from each tissue extraction vial (as earlier described) and placed in 6.5 mL of reagent-grade methanol. Additional serial dilutions were carried out in methanol if necessary to place a sample onto the linear portion of the calibration curve. Pheopigment *a* was measured using a Turner 10-AU fluorometer calibrated using standards of chlorophyll *a* from spinach (Sigma) in methanol (acidified exactly as unknowns) following procedures recommended by Holm-Hansen and Riemann (1978).

Postmortem DMS production

DMS production by tissues of *T. maxima* and *T. squamosa* after death was studied in August and September 2000 in Pohnpei and Palau using an HNU Systems PI-52 photoionization detector, Chromosil 330 column, and Hewlett Packard 3395 integrator transported to Pohnpei and Palau and operated with air from scuba tanks. Clams collected without injury (e.g., by chiseling out of coral rock with byssus intact) and maintained in running seawater after collection were killed at a defined moment within 10–20 h of collection. Pieces of adductor muscle and siphonal mantle tissue were placed in glass vials closed with Teflon-faced septa and sealed with crimped aluminum rings. Gas was periodically removed for analysis. For calibration, we injected headspace samples from standards of reagent-grade DMS (Fluka) in 2 $mol \cdot L^{-1}$ KOH. To determine absolute DMS concentrations in the headspaces of the standards, exact replicates of the standards were prepared in Woods Hole and calibrated, at temperatures matching those in Pohnpei and Palau, against a VICI Metronics DMS permeation tube that was factory calibrated to U.S. National Institute of Standards and Technology standards.

Total DMSP in the tissues used for the postmortem DMS study in Palau was measured by extracting samples of the tissues in 75% ethanol. Ethanol was used in these assays because ethanol was locally available, whereas methanol was not. Samples of the extracts were alkalized in 2 $mol \cdot L^{-1}$ KOH and assayed much as described earlier for total tissue DMSP using standards prepared in a background of 2$mol \cdot L^{-1}$ KOH and ethanol.

Results

Chemical assays

Tridacna maxima and *T. squamosa* exhibited the pattern of tissue DMSP concentrations reported for the species in earlier research (Hill et al. 2000) in that the siphonal mantle, byssal mantle, and gill tissue were similar to each other in DMSP concentration and over five times more concentrated in DMSP than the adductor muscle (Table 1). This pattern appears to be consistent for these species, as we have also observed it in other data collections not yet reported. The present research reveals that the pattern also exists in *T. crocea*. However, in *T. derasa*, *T. gigas*, and *H. hippopus*, although the adductor muscle is least concentrated in DMSP, the difference between it and other tissues is not as dramatic, and in *H. hippopus*, there is only one tissue that is dramatically high in DMSP, the gill.

Judging from our data on pheophytin *a*, the byssal mantle tissue, which occurs along the shell margins farthest from the light-exposed part of the mantle, is always far less concentrated in chlorophyll than the siphonal mantle tissue, which houses the principal population of zooxanthellae and is presented to the sun (Table 2). The adductor muscle and gill are almost devoid of chlorophyll in all six species of giant clams.

A point of particular interest is whether DMSP occurs at high concentrations in the animal tissues of the clams as opposed to being simply associated with algal cells positioned within the animal tissues. Abundant evidence indicates, in fact, that DMSP occurs in the animal tissues. For example, in *T. crocea*, *T. maxima*, and *T. squamosa*, the byssal mantle is at least as concentrated in DMSP as the siphonal mantle

© 2004 NRC Canada

Table 2. Concentration of pheophytin *a* ($\mu g \cdot g^{-1}$, mean ± SE) in four tissues of six species of giant clams.

Species	Siphonal mantle	Byssal mantle	Adductor muscle	Gill
H. hippopus (n = 8)	245±49.6	89.7±27.3	5.82±2.5	0.74±0.5
T. crocea (n = 6)	530±64.8	15.8±10.4	2.51±0.8	1.96
T. derasa (n = 9)	174±33.0	15.0±6.8	0.34±0.2	0.21±0.1
T. gigas (n = 7)	205±20.3	39.0±8.6	8.61±1.5	3.78±1.2
T. maxima (n = 7)	283±37.8	23.3±6.7	1.38±0.3	2.18±0.9
T. squamosa (n = 5)	431±70.5	48.8±26.5	2.15±0.5	7.83±5.7

Note: Adductor muscle for one *T. derasa* was not analyzed. For gill, n is 5 for *H. hippopus*, 1 for *T. crocea*, 5 for *T. derasa*, 5 for *T. gigas*, and as tabulated for the other species.

Fig. 1. DMSP concentration as a function of pheophytin *a* concentration for all 154 tissue samples analyzed by both methods. Symbols identify tissue type: ●, siphonal mantle; ○, byssal mantle; ▲, adductor; △, gill.

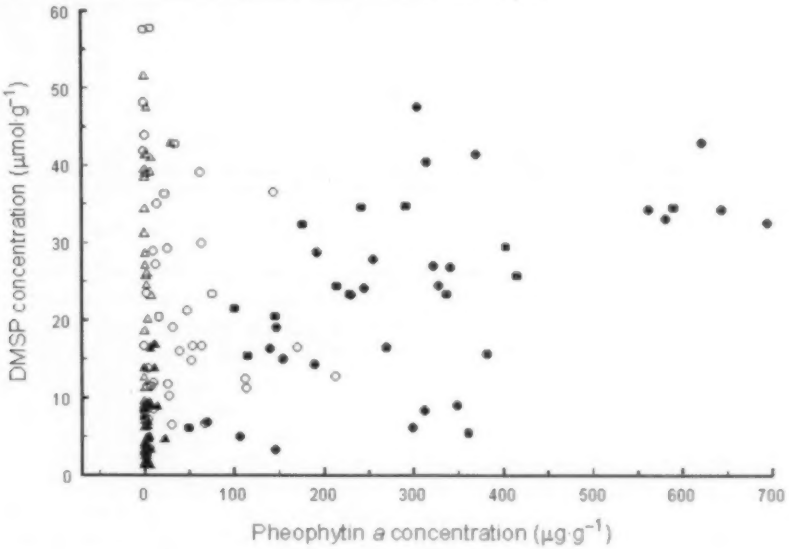

(Table 1), even though, on average, its concentration of chlorophyll is only 3–11% as high as that of the siphonal mantle. The data on the byssal mantle indicate that a tissue may contain a high concentration of DMSP without having a high density of zooxanthellae. Similarly, the gills often have high concentrations of DMSP while being virtually devoid of zooxanthellae. Overall, the DMSP concentration of tissues bears little predictable relationship to the density of zooxanthellae in the tissues (as gauged by chlorophyll concentration) (Fig. 1). The correlation between the two variables is statistically significant (r = 0.58, $p < 0.01$, n = 42) for siphonal mantle, and that relationship seems to be principally responsible for the fact that the correlation for all tissues taken together is statistically significant (r = 0.30, $p < 0.01$, n = 154). However, low chlorophyll concentrations do not at all preclude high DMSP concentrations. (For tissues other than siphonal mantle, r = 0.08, indicating a non-significant correlation, but the analysis using r is of qualitative use only because the data are so heteroscedastic.)

Mass spectra were obtained for 57 tissue samples representing all six species in approximately equal numbers and representing the siphonal mantle, byssal mantle, and adductor tissues in approximately equal numbers. A signature was observed at mass 135 in essentially every sample analyzed, documenting the presence of DMSP. The only sample that did not exhibit a mass-135 signature was one that gas chromatography indicated was virtually devoid of DMSP. Overall, a rough correlation exists between the magnitude of the signature at mass 135 and the DMSP concentration measured by gas chromatography (Fig. 2) (the correlation coefficient is not calculated because of the extreme heteroscedasticity of the data). An important result from the mass spectrometry of the samples eluted from the Bio-Rex 70 resin was the absence from all samples of a signature at mass 164, indicating that the tissues of giant clams contain little or no *S*-methylmethionine.

Postmortem DMS production

Following death, significant DMS production often occurs from the siphonal mantle tissue of *T. maxima* and *T. squamosa* within the first 10 h, and within 24 h, a marked efflux of DMS from siphonal mantle is universal (Figs. 3 and 4). On the other hand, some samples of adductor muscle evolve almost no DMS even after 24–48 h, and the samples of adductor muscle that produce significant DMS inevitably produce far less than siphonal mantle tissue from the same

© 2004 NRC Canada

Fig. 2. Index of DMSP concentration from mass spectrometry as a function of the DMSP concentration from gas chromatography in 57 samples analyzed by both methods. The index of DMSP concentration from mass spectra was calculated as the magnitude of the mass-135 signal divided by the magnitude of the trigonelline signal normalized for the weight of the tissue sample analyzed.

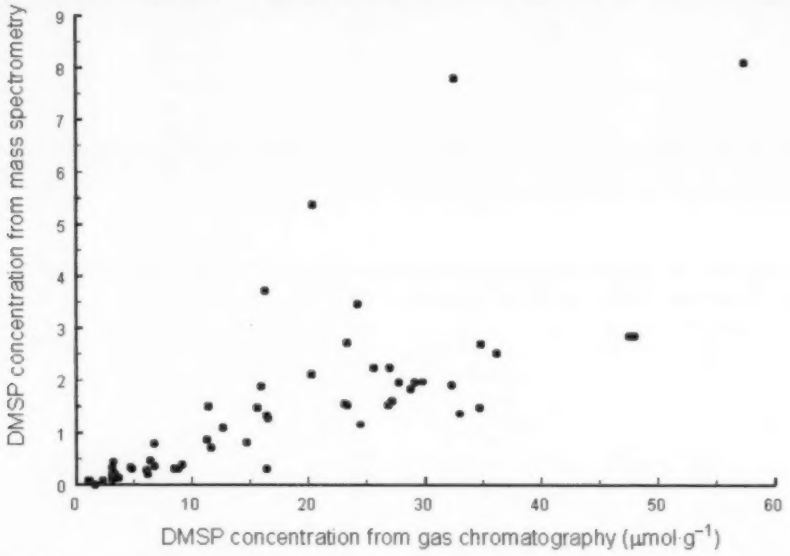

Fig. 3. Accumulation of DMS in sealed vials containing pieces of siphonal mantle tissue (solid symbols) and adductor muscle tissue (open symbols) of four *T. maxima* (11–21 cm shell length) and two *T. squamosa* (11–15 cm) collected in Pohnpei as a function of time after death. Each piece of tissue weighed about 3 g and was sealed in a 38-mL vial. The temperature was 25–30 °C. Solid and open symbols are matched for individual clams. The lowermost squares and triangles represent *T. squamosa*.

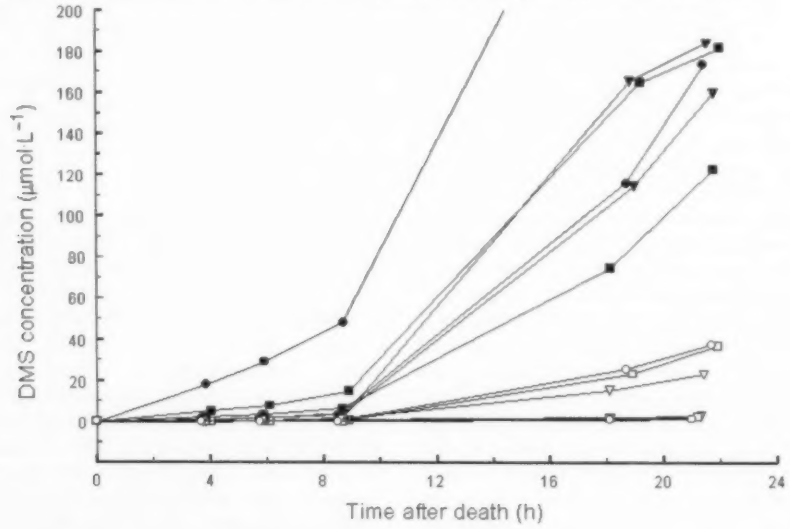

animal (Figs. 3 and 4). At 20–25 h, the quantity of DMS accumulated in the gas phase in the vials containing siphonal mantle samples (Fig. 4) was 310–2700 nmol·g^{-1}, whereas our assays of the same siphonal tissues by alcohol extraction and gas chromatography detected 29–48 μmol DMSP·g^{-1}; the DMS accumulated in the gas phase of adductor samples was 8–240 nmol·g^{-1}, whereas the adductor samples contained 1–20 μmol DMSP·g^{-1}. Thus, the fraction of DMSP accumulated in net fashion as DMS gas was not great. At 21–22 h, the quantity of DMS accumulated in the gas phase in the siphonal mantle vials was 1600–2400 nmol·g^{-1}, whereas that accumulated in adductor muscle vials was 18–450 nmol·g^{-1} (Fig. 3).

Discussion

The preponderance of evidence indicates that for the tridacnid clams, a chronic accumulation of DMSP in many of their tissues is a special consequence of their symbiotic association with dinoflagellates. DMSP occurs in tissues that

© 2004 NRC Canada

Fig. 4. Accumulation of DMS in sealed vials containing pieces of siphonal mantle tissue (solid symbols) and adductor muscle tissue (open symbols) of three *T. maxima* (13–21 cm shell length) and five *T. squamosa* (19–26 cm) collected in Palau as a function of time after death. Each piece of tissue weighed about 1 g and was sealed in an 11-mL vial. The temperature was around 5 °C for the first 6 h but thereafter was about 30 °C. Solid and open symbols are matched for individual clams. *Tridacna maxima* are represented by the uppermost circles, squares, and diamonds for siphonal mantle tissue and by the uppermost circles and squares and lowermost diamonds for adductor muscle tissue.

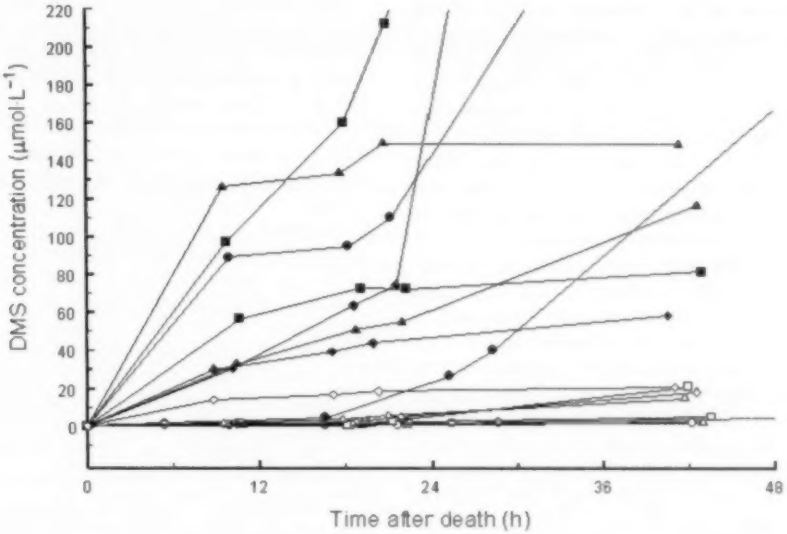

harbor few, if any, zooxanthellae, indicating that DMSP is transported throughout the clams from the siphonal mantle, where photosynthesis occurs, along with nutritional and other algal products. The evidence for DMSP in the tissues of the clams is twofold, namely that a mass-135 signature is a virtually universal feature of the mass spectra of giant clam tissues and that alkalization at room temperature very rapidly gives rise to DMS; furthermore, the mass spectra indicate that giant clam tissues are free of *S*-methylmethionine, an unlikely but theoretically possible alternative source of DMS. An intriguing attribute of the distribution of DMSP within individual clams is that the various tissues of single individuals often differ dramatically in DMSP concentrations. This research expands knowledge of the heterogeneous nature of DMSP accumulation by bringing to light that species differ in systematic ways in their patterns of DMSP distribution within individuals (Table 1). If DMSP has metabolic or other consequences for the tissues in which it occurs, the pattern of DMSP distribution within a clam's body could be subject to adaptive evolution. The adductor muscle, to take the example of a particular tissue, is consistently low in DMSP concentration. Is this a passive consequence of the tissue structure and composition of adductor muscle, or has adductor muscle evolved properties that specifically act to exclude DMSP? There seems to be no basis for deciding at present.

The tissue concentrations of DMSP observed in giant clams are extraordinary for animals. Hill et al. (2000) reviewed the literature on DMSP in animals and found that values reported for fish, crustaceans, and other mollusks, all of which acquire DMSP through food ingestion, are essentially always below 3–4 $\mu mol \cdot g^{-1}$. About the only exception is a single reported instance of 30–40 $\mu mol \cdot g^{-1}$ in pteropods (Levasseur et al. 1994), but this case is not directly comparable with the sort of data reported here because, of necessity, the pteropod assay included gut contents and thus did not directly reveal tissue concentrations. In giant clams, even disregarding the siphonal mantle where abundant algal DMSP is presumably confounded with animal tissue DMSP, concentrations of DMSP of 30 $\mu mol \cdot g^{-1}$ or higher are commonplace, and values as high as 40–60 $\mu mol \cdot g^{-1}$ are regularly encountered. Animals that have evolved symbioses with microbes can potentially accumulate unusual concentrations of microbial products. The giant clams seem to represent the most extreme case of accumulation of DMSP.

There are three ways in which a plausible case can presently be made that DMSP in giant clam tissues could have significant consequences. First, as stressed already by Hill et al. (2000), evidence exists that DMSP at the concentrations observed could perturb the function of certain enzymes (Nishiguchi and Somero 1992; Karsten et al. 1996). Because of the potential for such effects, giant clams might have evolved specialized enzyme forms differing from the enzyme homologs in other mollusks, notably enzyme forms adapted to function within a high-DMSP environment. A second potential consequence of the presence of high DMSP concentrations is that, according to some evidence, DMSP and DMS are capable of acting to ameliorate tissue oxygen stress (Sunda et al. 2002). The tridacnid clams face the challenge that they expose their siphonal mantle tissue to high insolation at high water temperatures so as to provide their algal symbionts with sunlight, and furthermore, the clams have vigorous photosynthetic activity proceeding within the substance of their siphonal mantle tissue. Just as the algae might themselves benefit from compounds that ameliorate oxygen stress, the animal tissues of the clams might also

© 2004 NRC Canada

benefit. If DMSP and DMS can help relieve oxygen stress, they could play adaptive roles in clam tissues.

With the publication of this research, the third potential consequence of high DMSP concentrations in tridacnid tissues is the best established. A major reason that the aquaculture of giant clams in western Pacific nations has failed is that their meat is exceptionally perishable because of the rapid postmortem development of a "particularly offensive and pervasive odor", even if the clams are refrigerated with the viscera removed (Peavey and Riley 1993, 1994). Comparing siphonal mantle and adductor meat, a disagreeable "seaweed-like" odor has been particularly associated with the mantle (Cowan 1988), and the mantle is far less commercially valuable than the adductor (Hill et al. 2000). On the island of Pohnpei, the government aquaculture project persuaded several up-scale restaurants catering to tourists to carry cultured tridacnids on their menus, but the venture ended when restaurant owners factored in that the clams needed to be kept alive until served because of their peculiar tendency to develop off-tastes and off-odors soon after death. Based on the data we here present and our experiences with the odors of dead tridacnids, we believe that the postmortem evolution of DMS from tissue DMSP is the cause of this problem. To put the problem in perspective, tissue concentrations of DMSP in cod and other finfish in the range of 0.2–1.0 $\mu mol \cdot g^{-1}$ are considered high and commercially problematic because of the offensive odors that can be caused by postmortem DMS formation (Hill et al. 2000); even the adductor muscles of giant clams contain higher concentrations. Knowing the cause of the postmortem off-tastes and off-odors in giant clams sets the stage for a rational approach to a solution to the problem (e.g., development of chemically specific methods to prevent DMS formation). The offensive tastes and smells are a consequence of the symbiotic association of these remarkable animals with algae, a relationship that during life provides the clams with beneficial access to photosynthetic products.

Acknowledgements

Douglas Gage, Mark Dennett, and David Kulis assisted with chemical analyses. Larry Sharron helped procure clams in Palau. This study was funded by the Comer Science and Education Foundation, Michigan Sea Grant, and Woods Hole Oceanographic Institution Sea Grant. This is Woods Hole Oceanographic Institution contribution No. 10821.

References

Cowan, L. 1988. Use of giant clams in Japanese cuisine. *In* Giant clams in Asia and the Pacific. *Edited by* J.W. Copland and J.S. Lucas. Australian Centre for International Agricultural Research, Canberra, Australia. pp. 256–257.

Dacey, J.W.H., and Blough, N.V. 1987. Hydroxide decomposition of dimethylsulfoniopropionate to form dimethylsulfide. Geophys. Res. Lett. **14**: 1246–1249.

Hawkins, A.J.S., and Klumpp, D.W. 1995. Nutrition of the giant clam *Tridacna gigas* (L.). 2. Relative contributions of filter-feeding and the ammonium-nitrogen acquired and recycled by symbiotic algae towards total nitrogen requirements for tissue growth and metabolism. J. Exp. Mar. Biol. Ecol. **190**: 263–290.

Hill, R.W., Dacey, J.W.H., and Krupp, D.A. 1995. Dimethylsulfoniopropionate in reef corals. Bull. Mar. Sci. **57**: 489–494.

Hill, R.W., Dacey, J.W.H., and Edward, A. 2000. Dimethylsulfoniopropionate in giant clams (Tridacnidae). Biol. Bull. (Woods Hole), **199**: 108–115.

Holm-Hansen, O., and Riemann, B. 1978. Chlorophyll *a* determination: improvements in methodology. Oikos, **30**: 438–447.

Karsten, U., Kück, K., Vogt, C., and Kirst, G.O. 1996. Dimethylsulfoniopropionate production in phototrophic organisms and its physiological function as a cryoprotectant. *In* Biological and environmental chemistry of DMSP and related sulfonium compounds. *Edited by* R.P. Kiene, P.T. Visscher, M.D. Keller, and G.O. Kirst. Plenum, New York. pp. 143–153.

Klumpp, D.W., and Griffiths, C.L. 1994. Contributions of phototrophic and heterotrophic nutrition to the metabolic and growth requirements of four species of giant clam (Tridacnidae). Mar. Ecol. Prog. Ser. **115**: 103–115.

Levasseur, M., Keller, M.D., Bonneau, E., D'Amours, D., and Bellows, W.K. 1994. Oceanographic basis of a DMS-related Atlantic cod (*Gadus morhua*) fishery problem: blackberry feed. Can. J. Fish. Aquat. Sci. **51**: 881–889.

Nishiguchi, M.K., and Somero, G.N. 1992. Temperature- and concentration-dependence of compatibility of the organic osmolyte β-dimethylsulfoniopropionate. Cryobiology, **29**: 118–124.

Norton, J.H., Shepherd, M.A., Long, H.M., and Fitt, W.K. 1992. The zooxanthellal tubular system in the giant clam. Biol. Bull. (Woods Hole), **183**: 503–506.

Peavey, S., and Riley, J. 1993. Sensory evaluation of fresh and frozen giant clams. Res. Rep. 93-02. National Aquaculture Center, Federated States of Micronesia. (Available from the senior author of this paper.)

Peavey, S., and Riley, J. 1994. Marketing giant clams in the local foodservice industry: a case study. Res. Rep. 94-01. National Aquaculture Center, Federated States of Micronesia. (Available from the senior author of this paper.)

Rowan, R. 1998. Diversity and ecology of zooxanthellae on coral reefs. J. Phycol. **34**: 407–417.

Sunda, W., Kieber, D.J., Kiene, R.P., and Huntsman, S. 2002. An antioxidant function for DMSP and DMS in marine algae. Nature (Lond.), **418**: 317–320.

© 2004 NRC Canada

Modelling of the seasonal patterns of dimethylsulphide production and fate during 1989 at a site in the North Sea[1]

Stephen D. Archer, Francis J. Gilbert, J. Icarus Allen, Jerry Blackford, and Philip D. Nightingale

Abstract: This modelling study aimed to extend our understanding of the biogeochemistry of the climatically active gas dimethylsulphide (DMS) in marine surface waters to an annual cycle. Processes involved in the production and fate of DMS and its precursor β-dimethylsulphoniopropionate (DMSP), a product of phytoplankton synthesis, were incorporated into a complex, coupled one-dimensional physical ecosystem model (European Regional Seas Ecosystem Model (ERSEM) and the General Ocean Turbulence Model (GOTM)) to create a model of DMS biogeochemistry at a seasonally stratified site in the North Sea for 1989. The model was validated against nutrient concentrations, biological standing stocks, biological production, DMS and DMSP concentrations, and DMS sea to air flux determined throughout 1989 during the North Sea Project. The validation results demonstrated that complex ecosystem models, combined with a comprehensive network of processes that control the production and fate of DMSP and DMS, could accurately mimic DMS biogeochemistry. The model provides insights into the impact of seasonally changing physical forcing on the relative contribution of individual processes to DMS production and sea to air flux.

Résumé : Notre étude de modélisation vise à placer dans un cycle annuel nos connaissances de la biogéochimie du sulfure de diméthyle (DMS), un gaz qui affecte le climat, dans les eaux marines superficielles. Nous avons incorporé les processus impliqués dans la production et le sort du DMS et de son précurseur le β-diméthylsulfoniopropionate (DMSP), un produit de synthèse du phytoplancton, dans le modèle ERSEM (« European Regional Seas Ecosystem Model »), un modèle physique, complexe, unidimensionel et couplé de l'écosystème et dans le modèle GOTM (« General Ocean Turbulence Model »). Nous avons ainsi mis au point un modèle de la biogéochimie du DMS appliqué à des données de 1989 provenant d'un site à stratification saisonnière de la mer du Nord. Nous l'avons validé avec des données de concentrations de nutriments, de biomasses biologiques, de production biologique, de concentrations de DMS et de DMSP et de flux de DMS de la mer à l'atmosphère obtenues en 1989 dans le cadre du Projet de la mer du Nord (« North Sea Project »). Les résultats de cette validation démontrent que des modèles complexes de l'écosystème, combinés à un réseau complet des processus qui contrôlent la production et le sort du DMSP et du DMS, peuvent représenter de façon exacte la biogéochimie du DMS. Le modèle fournit des perspectives intéressantes sur l'impact du forçage physique, qui varie d'une saison à l'autre, sur les contributions relatives des divers processus particuliers à la production du DMS et à son passage de la mer à l'atmosphère.

[Traduit par la Rédaction]

Introduction

The volatile sulphur compound dimethylsulphide (DMS) is generally supersaturated in the surface waters of the ocean, and its sea to air flux and subsequent oxidation represent an important source of sulphur compounds and sulphate aerosols in the marine boundary layer (Bonsang et al. 1980; Clarke et al. 1998). These aerosols influence albedo, particularly in the remote marine atmosphere, by directly backscattering incoming solar radiation and indirectly by forming cloud condensation nuclei and increasing cloud-top reflectivity (Charlson et al. 1987; Shaw 1987). Recent estimates of the global oceanic flux of DMS lie somewhere between 15 and 33 Tg S·year^{-1} depending on the method used to calculate the rate of sea to air flux (Kettle and Andreae 2000). However, such estimates are based on a relatively limited understanding of how this flux varies seasonally or of the factors that dictate the seasonal variation.

Sea to air flux is generally a relatively minor portion (1–10%) of total DMS removal from surface waters at the end

Received 1 February 2003. Accepted 19 November 2003. Published on the NRC Research Press Web site at http://cjfas.nrc.ca on 23 June 2004.
J17359

S.D. Archer,[2] F.J. Gilbert, J.I. Allen, J. Blackford, and P.D. Nightingale. Plymouth Marine Laboratory, Prospect Place, Plymouth PL1 3DH, U.K.

[1]This paper is part of the proceedings of the Third International Symposium on Biological and Environmental Chemistry of DMS(P) and Related Compounds, held in Rimouski (Québec), 26–28 September 2002.

[2]Corresponding author (e-mail: stda@pml.ac.uk).

 doi: 10.1139/F04-028 © 2004 NRC Canada

of a complex network of biological and physiochemical production processes (Bates et al. 1994; Kieber et al. 1996; Archer et al. 2002*a*). The two most critical factors that affect DMS flux rates across the air–sea interface are wind speed and surface DMS concentration. DMS is a breakdown product of β-dimethylsulphoniopropionate (DMSP) synthesized by phytoplankton (Gage et al. 1997) and thought to have a number of physiological roles but principally to act as an osmolyte or compatible solute (reviewed in Stefels 2000). DMS surface concentrations are intricately linked to biological processes that transform DMSP to DMS, including grazing, bacterial production, and viral lysis (Dacey and Wakeham 1986; Malin et al. 1998; Kiene and Linn 2000). Once produced, the two major loss processes of DMS are generally considered to be consumption by bacteria (Kiene and Bates 1990; Zubkov et al. 2001) and photolysis (Kieber et al. 1996; Brugger et al. 1998). Physical processes, particularly those that control the depth of the surface mixed layer, impact on the production rates of particulate DMSP ($DMSP_p$), may influence the yield of DMS production from DMSP on both short and long time scales (Simó and Pedrós-Alió 1999*a*), and are likely to have an influence on the contribution of each DMS removal process (Kieber et al. 1996).

Few field studies are able to combine the suite of measured parameters and high-resolution, seasonal time series required to understand biogeochemical cycles in the oceans on an annual basis. In the case of DMS, several studies have examined the seasonality of DMS and DMSP concentrations in coastal (Turner et al. 1988; Leck et al. 1990; Kwint and Kramer 1996) and oceanic waters (Dacey et al. 1998) in relation to biological and physical parameters. These studies have demonstrated that surface concentrations of DMS are poorly related to chlorophyll, phytoplankton biomass, or primary production, possibly because of the complex series of processes that transform phytoplankton DMSP to DMS. Similarly on a global scale, DMS concentrations show poor correlations with chlorophyll or nutrient concentrations (Kettle et al. 1999). On the other hand, a number of intensive short-term studies have successfully quantified and partitioned the contribution of key processes involved in producing and removing DMS in surface waters (Bates et al. 1994; Simó and Pedrós-Alió 1999*b*; Archer et al. 2002*a*).

Here, we use a modelling approach to link the understanding developed through such detailed process studies to seasonal patterns of DMS production and fate. Within this seasonal context, our aims were to (*i*) evaluate our understanding of the processes that control the production and fate of DMS, (*ii*) estimate the annual budgets of $DMSP_p$ production and its transformation to DMS and sea to air flux, (*iii*) demonstrate the impact of seasonally varying meteorological forcing on DMS production and fate, and (*iv*) determine the importance of certain biological processes in the transformation of $DMSP_p$ to DMS.

To achieve this, we incorporated pathways involved in the production and fate of DMSP and DMS into a coupled one-dimensional physical ecosystem model of a seasonally stratified site in the North Sea. Several other modelling studies describe the production and fate of DMS over seasonal time scales (Gabric et al. 1995; Jodwalis et al. 2000; Lefèvre et al. 2002), including in the southern North Sea (van den Berg et al. 1996). However, the present study differs in the high level of complexity of the ecosystem model and its coupling to a high-resolution physical model. The biological components of the model are intimately controlled by the high-resolution physical forcing. In addition, the model benefits from the continued development of our understanding of the processes that govern DMS(P) biogeochemistry in surface waters. Consequently, the DMS(P) production and transformation processes that are incorporated into the model are of greater detail than has previously been undertaken.

Fig. 1. Location of station CS in the North Sea.

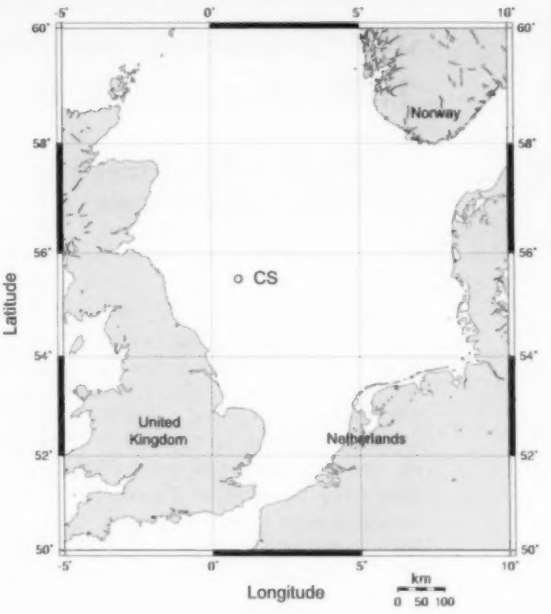

The site chosen to evaluate this model was sampled during the North Sea Project (Simpson 1993) from August 1988 to October 1989 for physical and biological parameters (Joint and Pomroy 1993; Prandle et al. 1997) including DMSP and DMS concentrations (Turner et al. 1996). The site, labelled CS in the North Sea Project, is situated at 55°30′N, 0°55′E (Fig. 1) in approximately 85 m of water. By comparison with many of the other North Sea sites, CS is relatively unaffected by direct terrigenous inputs of nutrients, with the regeneration through biological processes dominating the nutrient inputs (Howarth et al. 1993).

Methods

DMSP and DMS production and transformation processes have been incorporated into a version of the European Regional Seas Ecosystem Model (ERSEM) (Baretta-Bekker et al. 1998), coupled with the physics of the General Ocean Turbulence Model (GOTM) (Burchard et al. 1999).

The physical model

GOTM is a one-dimensional physical model that is designed as a generic system for marine modelling. The system is constructed so that the user may decide between a number of options to suit the region or scales being modelled. In this case, the GOTM k–ε turbulence closure option

© 2004 NRC Canada

is applied and forced with six-hourly resolution sea surface meteorology and tidal constituents. The meteorological forcing data (air temperature at 2 m (T_A), 10-m winds, cloud cover, dew point temperature (T_D), and mean sea level pressure (P_A)) were supplied by the European Centre for Medium-range Weather Forecasts. The T_D and P_A data were used to calculate relative humidity based on the formulation in Wallace and Hobbs (1977) using the calculation of the saturation vapour pressure (E_S) of Tetens (1930). Evaporation and precipitation are not considered. The tidal constituents for M2 and S2 tides used to force the model were taken from the simulations described in Sinha and Pingree (1997). This physical forcing is used to calculated the time evolution of temperature, salinity, turbulence, and hence the coefficients of vertical eddy diffusivity throughout the water column. This method has been demonstrated to give good simulations of observed turbulent dissipation data in the stratified waters of the northern North Sea (Burchard et al. 2002). At the sea surface, fluxes of heat and momentum are calculated using the bulk formulas outlined in Castellari et al. (1998).

The ecosystem model

ERSEM is a generic ecosystem model originally used in the North Sea (Baretta et al. 1995) but recently applied successfully to more oligotrophic waters (Zavatarelli et al. 2000; Allen et al. 2002). Detailed descriptions of ERSEM and its pelagic submodels are given in Baretta et al. (1995), Baretta-Bekker et al. (1995, 1998), and Ebenhöh et al. (1997). In ERSEM, the ecosystem is represented as a network of interacting physical, chemical, and biological processes. A "functional group" approach is used to describe the biological components consisting of primary producers, consumers, and decomposers, which in turn are subdivided on the basis of trophic links and (or) size (a schematic of the ERSEM trophic links is given in Fig. 2*a*). The dynamics of each functional group are dictated by physiological (ingestion, respiration, excretion, and egestion) and population (growth, mortality, and migration) processes that are described by fluxes of nutrients between groups. Each functional group consists of components of carbon, nitrogen, and phosphorus, and silicon in the case of diatoms.

Gross primary production is a function of temperature, availability of and adaptation to light, silicate concentration in the case of diatoms, and phytoplankton biomass. The phytoplankton community consists of four functional types: picophytoplankton (0.2–2.0 μm), phytoflagellates (2–20 μm), phototrophic dinoflagellates (20–200 μm), and diatoms (20–200 μm). Photosynthetically active light at the sea surface is modelled from astronomical values that are corrected for cloud cover. Extinction of light through the water column is a function of particulate concentrations and phytoplankton biomass and is given a background extinction parameter. Mesozooplankton, microzooplankton, and heterotrophic flagellates make up the consumers. Grazing uptake is a function of maximal ingestion rate, temperature, food availability, and zooplankton biomass. Zooplankton mortality occurs in the model at a constant rate and may be triggered by low oxygen concentration. Each zooplankton functional group is predated upon (Fig. 2*a*).

There are three bacterioplankton functional groups in the model that differ in the dissolved food source that they can utilize. One group utilizes only dissolved organic matter (DOM), one group is able to take up dissolved DMSP ($DMSP_d$) and DOM, and the third group is able to consume DMS and DOM. In natural waters, whether the same bacteria are able to utilize $DMSP_d$ and DMS (e.g., González et al. 1999) or the different processes are carried out by different taxonomic/functional groups (e.g., Visscher et al. 1992) is uncertain. Bacterial uptake is a function of potential assimilation rate, temperature, oxygen availability, nutrient quotient, and the concentration of the food source.

The DMS model

The processes and parameters included in the DMS model and incorporated into ERSEM (shown in Fig. 2*b*) are mathematically described in eqs. 1–21. This is a modification of the model described in Archer et al. (2002*a*). The rate processes that transform $DMSP_p$ to DMS and standing stocks of $DMSP_p$, $DMSP_d$, and DMS quantified during a 6-day Lagrangian experiment in the northern North Sea were well represented by the parameters applied in the original model (Archer et al. 2002*a*), albeit over only a 6-day period during the summer.

The four phytoplankton functional groups invest a constant proportion of gross carbon production in DMSP synthesis such that

$$(1) \qquad \frac{\partial \mathrm{DMSP_p}}{\partial t} = q_n \frac{\partial P_n}{\partial t}$$

where P_n represents the biomass of the different taxa (Table 1; Fig. 2*a*) and q_n is the cell quota for each taxon (Table 1). The group-specific $DMSP_p$ cell quotas used in the model (Table 1) are based on measurements by Keller et al. (1989) and Corn et al. (1996). Similar values were used to explain the partition of $DMSP_p$ standing stocks among phytoplankton groups in the northern North Sea (Archer et al. 2002*b*).

The processes controlling $DMSP_d$ cycling are described by the following equation:

$$(2) \qquad \frac{\partial \mathrm{DMSP_d}}{\partial t} = q_n \cdot r_{\mathrm{DMSP_d}} [\text{production of DOC}] - \text{uptake}_{\mathrm{DMSP_d}} - \text{transformation}_{\mathrm{DMSP_d}} \pm \text{transport}_{\mathrm{DMSP_d}}$$

Production of $DMSP_d$ occurs as a fixed proportion (r_{DMSP_d}) of dissolved organic carbon (DOC) production (eq. 3). In the model, $DMSP_p$ loss from phytoplankton occurs through grazing by all three groups of grazers (e.g., Christaki et al. 1996), through mortality resulting from cell lysis (Nguyen et al. 1988; Malin et al. 1998), and through exudation (Vairavamurthy et al. 1985). In each case, DMSP lyase enzymes contained in the phytoplankton cells may react with DMSP to form DMS and acrylate (Stefels and Dijkhuizen 1996; Wolfe and Steinke 1996). The factors that control this reaction and hence the proportion of DMS produced are poorly understood. In the model, $DMSP_d$ and DMS production from phytoplankton occurs in a 9:1 molar ratio irrespective of which process causes the release. In terms of carbon, this equates to 9:0.4 $DMSP_d$:DMS with the remaining carbon assumed to be acrylate, which contributes to the DOC pool.

© 2004 NRC Canada

Fig. 2. Diagrammatic representation of (*a*) the pelagic food web of the ERSEM model and (*b*) DMS- and DMSP-related processes incorporated into the model.

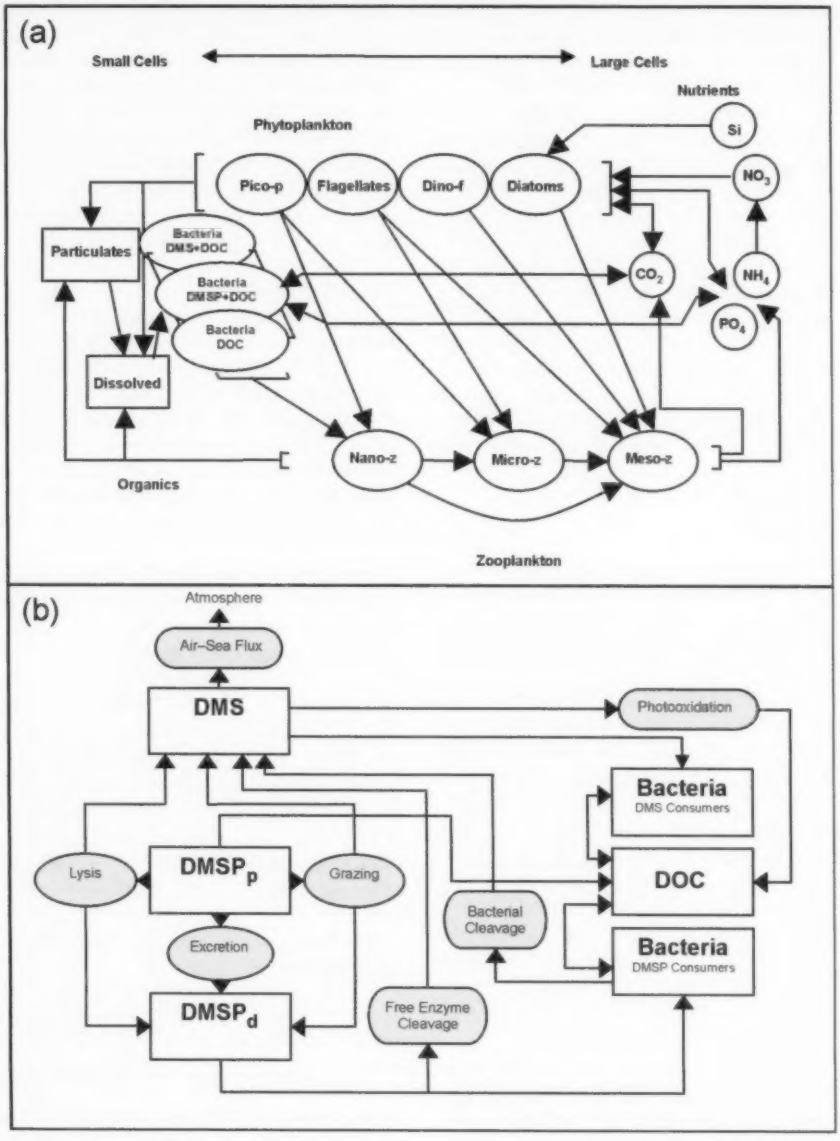

The production of DOC is described as follows:

(3) Production of DOC = lysis + exudation + grazing

In the model, cell lysis is a product of nutrient stress and causes total release of $DMSP_p$ to the dissolved phase. Nutrient-stressed lysis is calculated from a rate (r_{lysis}) modified by a dynamic nutrient limitation factor (nl):

$$(4) \qquad \text{Lysis} = \frac{1.0}{\text{nl} + 0.1} r_{\text{lysis}} \cdot P_n^C$$

The nutrient currency being described in each equation is indicated as C for carbon, N for nitrogen, or P for phosphate. The nutrient limitation factor (nl) employs "Droop kinetics" (Droop 1974). This is a function of the internal cell ratios of C:N ($q^N = P^N/P^C$) and C:P ($q^P = P^P/P^C$) and the maximum C:N and C:P ratios ($q^{(N,P)}P_{max}$), having subtracted the structural content of the cell ($q^{(N,P)}P_{min}$) from each. A separate limitation factor is calculated for each phytoplankton group (P_n) constrained between a range of 0–1.

Exudation of $DMSP_p$ from cells is a combination of activity exudation and exudation caused by nutrient stress. Exudation consists of two elements:

$$(5) \qquad \text{Exudation} = e_a + e_n$$

where e_a is the activity exudation of a fixed proportion (p_{ex}) of photosynthesis:

$$(6) \qquad e_a = \text{photosynthesis} \cdot p_{ex}$$

© 2004 NRC Canada

Table 1. Biological components and their size distribution in the ERSEM–GOTM–DMS model and parameters used in the model to describe the processes that produce $DMSP_p$, $DMSP_d$, and DMS.

Notation	Description	
Biological component		
P_1	Diatoms	20–200 μm
P_2	Phytoflagellates	2–20 μm
P_3	Picophytoplankton	0.2–2 μm
P_4	Phototrophic dinoflagellates	20–200 μm
Z_4	Mesozooplankton	200 μm
Z_5	Microzooplankton	100 μm
Z_6	Heterotrophic nanoflagellates	<10 μm
B_1	Bacteria DOC consumers	
B_2	Bacteria $DMSP_d$ consumers	
B_3	Bacteria DMS consumers	
Parameter		
q_1	Proportion of cell carbon composed of $DMSP_p$ in diatoms	0.01
q_2	Proportion of cell carbon composed of $DMSP_p$ in phytoflagellates	0.05
q_3	Proportion of cell carbon composed of $DMSP_p$ in picophytoplankton	0.025
q_4	Proportion of cell carbon composed of $DMSP_p$ in dinoflagellates	0.08
r_{DMSP_d}	Carbon ratio of $DMSP_d$ released from $DMSP_p$	0.9
r_{DMS}	Carbon ratio of DMS released from $DMSP_p$	0.04
f_1	Fixed fraction of $DMSP_d$ uptake by bacteria cleaved to DMS	0.1
f_2	Fixed fraction of $DMSP_d$ cleaved to DMS by "free enzymes"	0.01
f_3	Maximum rate of photolysis of DMS to DOC	0.25
f_4	Carbon ratio DMS:$DMSP_d$	0.4
$h_{(DMSP_d, DMS)}$	Michaelis–Menten substrate limitation value	0.35
h_l	Michaelis–Menten light limition value	5

and e_n is the nutrient stressed exudation of the potential assimilate $(1.0 - p_{ex})$ (it is assumed that stressed cells cannot assimilate nutrients):

$$(7) \qquad e_n = \text{photosynthesis} \cdot (1.0 - \text{nl}) \cdot (1.0 - p_{ex})$$

In a modelling study, Laroche et al. (1999) calculated an upper limit of 11%·day^{-1} for the leakage of DMSP from phytoplankton in culture and illustrated that the amount released may vary in relation to growth rate and between taxa.

Grazing rates are a function of maximal ingestion rate (r_{ing}, defined at 10 °C), a temperature factor (t), total food concentration (F^C_{tot}), the half-saturation constant (h_g, the food concentration where uptake is 0.5 the maximum rate), and the grazer biomass (Z_n):

$$(8) \qquad \text{Grazing} = r_{ing} \frac{F^C_{tot}}{(F^C_{tot} + h_g)} t \cdot Z^C_n$$

All three groups of grazers are assumed to assimilate 30% of ingested $DMSP_p$ with 70% released at a constant ratio (Table 1) as either $DMSP_d$ or DMS and acrylate. Little is known of the assimilation efficiencies of grazers for DMSP, DMS, or acrylate. Between 30% and 100% of phytoplankton DMSP ingested by protozoans was estimated to have been released as $DMSP_d$ or DMS in laboratory studies (Wolfe et al. 1994; Christaki et al. 1996). Copepod taxa vary in the extent to which they incorporate DMSP (Tang et al. 1999) and presumably in the proportion of ingested $DMSP_p$ released as $DMSP_d$ and DMS. No account is taken of the potential $DMSP_d$ and DMS production resulting from zooplankton mortality.

The temperature response factor (t) is common to all functional groups, taking the form of a $Q10$ function of the ambient temperature (T):

$$(9) \qquad t = Q^{(T-10.0)/10.0}$$

where Q in the model has a value of 2 for each functional group.

Bacterial uptake is a function of potential assimilation rate (r_{ass}), the temperature factor (t), a limitation if low oxygen conditions apply (eO_2), limitation because of the nutrient quotient of the food source and the availability of inorganic nutrients if required (n_{DMSP_d}, eq. 12), bacterial biomass (B) constrained by the total amount of available substrate, and DOM (R_{DOM}). It is described by the following equation:

$$(10) \qquad \text{Uptake}_{DMSP_d} = \min(r_{ass} \cdot t \cdot eO_2 \cdot n_{DMSP_d} \cdot B)$$

Oxygen limitation is described as

$$(11) \qquad eO_2 = \frac{O_{rel}}{(O_{rel} + h_{ox})}$$

where h_{ox} is the concentration of oxygen.

Nutrient limitation is described as

© 2004 NRC Canada

$$(12)\quad n_{\mathrm{DMSP_d}} = \min\left[\frac{(\mathrm{NH_4} + R^{\mathrm{N}}_{\mathrm{DOM}})}{(\mathrm{NH_4} + R^{\mathrm{N}}_{\mathrm{DOM}} + h_{\mathrm{N}})}, \frac{(\mathrm{PO_4} + R^{\mathrm{P}}_{\mathrm{DOM}})}{(\mathrm{PO_4} + R^{\mathrm{P}}_{\mathrm{DOM}} + h_{\mathrm{P}})}, \frac{\mathrm{DMSP_d}}{(\mathrm{DMSP_d} + h_{\mathrm{DMSP_d}})}\right]$$

where h_N and h_P are the concentrations of available nitrogen and phosphate at which the limitation factor equals 0.5.

Once in the dissolved phase, $DMSP_d$ may be cleaved by "free" DMSP lyase enzymes (Scarratt et al. 2000) or utilized by bacteria (Kiene and Linn 2000; Zubkov et al. 2001). One of the three functional groups of bacteria in the model is able to utilize $DMSP_d$ in combination with the DOC pool. The $DMSP_d$ that they process is either demethylated/demethiolated or cleaved to DMS and acrylate at a constant rate (f_1) (Table 1):

$$(13)\quad \text{Bacterial cleavage} = f_1 \cdot \text{uptake}_{\mathrm{DMSP_d}}$$

The factors that may vary this proportion are discussed in Kiene et al. (2000) but are not included in the model.

"Free" $DMSP_d$ lyase may transform $DMSP_d$ to DMS (e.g., Scarratt et al. 2000). This process is included in the model at a fixed proportion (f_2) (Table 1) of the $DMSP_d$ concentration:

$$(14)\quad \text{Enzymatic cleavage} = f_2 \cdot \mathrm{DMSP_d^C}$$

Thus, the transformation of $DMSP_d$ is described as follows:

$$(15)\quad \text{Transformation}_{\mathrm{DMSP_d}} = \text{bacterial cleavage} + \text{enzymatic cleavage}$$

$DMSP_d$ is transported through the water column as a consequence of turbulence driven by physical processes: wind, tide, friction between thermally stratified layers, and an eddy diffusion coefficient (k_z). The direction of transport is dictated by the vertical gradient as described in the following equation:

$$(16)\quad \text{Transport}_{\mathrm{DMSP_d}} = \frac{\partial(k_z \cdot \partial \mathrm{DMSP_d}/\partial z)}{\partial z}$$

In the model, DMS is removed by bacteria, by photolysis, and by sea to air flux (Fig. 2*b*):

$$(17)\quad \frac{\partial \mathrm{DMS}}{\partial t} = q_n \cdot r_{\mathrm{DMS}}[\text{production of DOC}] - \text{uptake}_{\mathrm{DMS}} - f_4 \cdot \text{transformation}_{\mathrm{DMSP_d}} - \text{air–sea flux} \pm \text{transport}_{\mathrm{DMS}}$$

A separate functional group of bacteria consumes DMS in combination with DOC (uptake_{DMS}), described in analogous terms to the uptake of $DMSP_d$ by the $DMSP_d$-consuming bacteria (eq. 10). As a result of transformation (eq. 15), the five carbon atoms of $DMSP_d$ produce two atoms of DMS carbon defined by the carbon ratio f_4 (Table 1).

Photooxidation of DMS is described as follows:

$$(18)\quad \text{Photooxidation} = f_3 \cdot \frac{\text{irradiance}}{\text{irradiance} + h_1} \cdot \mathrm{DMS}$$

There is increasing evidence that DMS photolysis is chiefly driven by UV wavelengths (Kieber et al. 1996; Brugger et al. 1998) but this is unresolved in the model. The sea to air flux equation (Nightingale et al. 2000) uses an empirical derivation of the transfer or piston velocity (k_{DMS}) and the concentration difference (ΔDMS) across the sea surface. The transfer velocity requires sea surface temperature (degrees Celsius) and wind speed at a height of 10 m (metres per second):

$$(19)\quad \text{Air–sea flux} = k_{\mathrm{DMS}} \cdot \Delta\mathrm{DMS}$$

$$(20)\quad k_{\mathrm{DMS}} = (1.46 \times 10^{-4} \cdot T_{\mathrm{sst}}^2 + 1.36 \times 10^{-2} \cdot T_{\mathrm{sst}} + 0.474) \times (0.222 \cdot \mathrm{wind}^2 + 0.333 \cdot \mathrm{wind})$$

$$(21)\quad \Delta\mathrm{DMS} = \mathrm{DMS}_{\text{sea surface}} - \mathrm{DMS}_{\mathrm{air}}$$

where DMS_{air} is assumed to be zero. DMS is subject to the same physical transport as $DMSP_d$ (eq. 16).

Model setup

The physical model was initialized with a generic, fully mixed winter temperature and salinity profile. To correctly reproduce the observed water column structure, a simple assimilation method using the relaxation method described in Burchard et al. (1999) was applied to take account of horizontal advective processes. Temperature and salinity profiles were recorded at CS during the North Sea Project at approximately monthly intervals and are assimilated into the model on the appropriate dates with a fixed relaxation time of 2 weeks. Without this, the mixed layer is found to be too shallow. Sharples and Tett (1994) have previously noted the underestimation of the depth of the mixed layer at this site when using one-dimensional turbulence models.

The ERSEM formulation of the biogeochemical processes defining biological dynamics is retained in the present model as are the parameter values described in Baretta-Bekker et al. (1997). The ecological model was initialized with in situ winter nutrient concentrations measured during the North Sea Project (Lowry et al. 1992) and the winter biomass estimates used to initialize the simulations described in Baretta et al. (1995). The model was run using a 3-year repeating cycle of forcing data for 1987 as a "spin-up" period to allow the model to reach a quasi-equilibrium state and provide initial conditions for the 1988 model run. The simulations presented here are for 1989.

Results and discussion

The physical environment and seasonal changes

The physical environment and biological response are used to define four separate seasons or regimes. The assimilation of temperature and salinity profiles using a relaxation technique (see above) precludes a meaningful validation of the physical model but produces a realistic environment in which to explore the ecosystem response to seasonally changing physical forcing and its impact on DMS(P) biogeochemistry. The Richardson number (Ri), defined as the ratio of buoyancy frequency to shear frequency, has been calculated to illustrate the stability of the water column. The critical value for stability is taken to be 0.25. Essentially, the water column consists of a three-layer system: a surface mixed layer

© 2004 NRC Canada

Fig. 3. Contour plot of values of the Richardson number (Ri) for the water column at CS during 1989 (open areas, Ri < 0.25; lightly shaded areas, 0.25 < Ri < 100; darker shaded areas, Ri > 100). Four seasons are defined in terms of water column structure: (*a*) winter mixed, days 1–33 and 354–365, (*b*) spring transitional, days 34–114, (*c*) summer, stratified, days 115–263, and (*d*) autumn stratified, days 264–353.

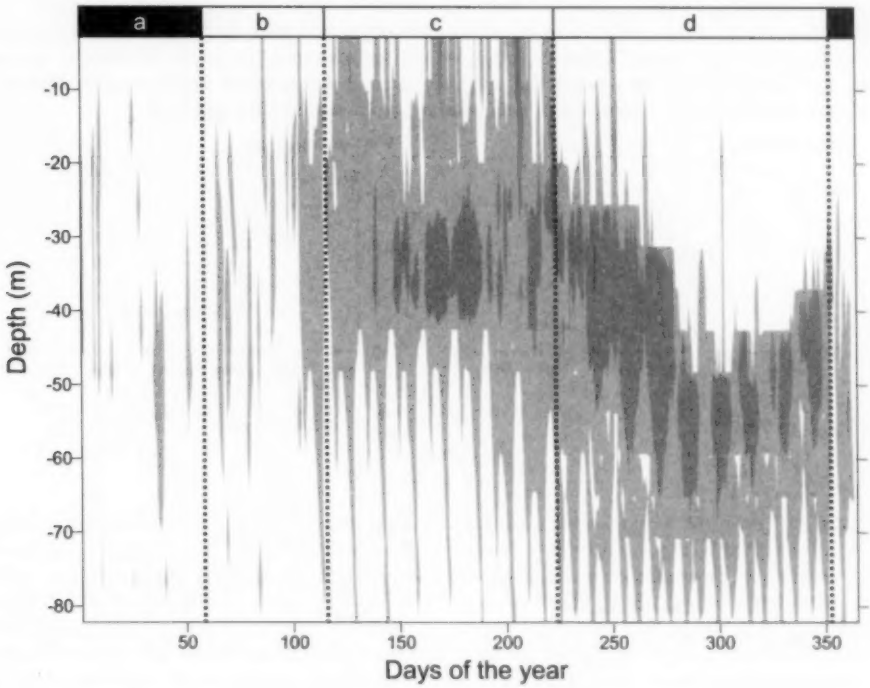

(Ri < 0.25) that varies from the full column depth during winter months to <20 m on some days during the summer months, a stable midwater layer (Ri > 0.25) that forms in early May and persists through the summer months, extending from roughly 20 m to >30 m before it deepens and is eventually eroded, and a mixed bottom layer (Ri < 0.25) (Fig. 3).

The physical environment and biological response are used to define four separate seasons or regimes (Fig. 3) to illustrate the seasonal variations in DMS(P) biogeochemistry. These are (*i*) "winter mixed", when the water column is essentially fully mixed and phytoplankton productivity is at a minimum, (*ii*) "spring transitional", when increasing day length during March and April enhances phytoplankton production in a water column that is starting to show signs of stabilizing, (*iii*) "summer stratified", during which the three-layer water column is stable and the intermediate layer lies within the euphotic layer, and (*iv*) "autumn stratified', the regime when the depth of the surface mixed layer exceeds 30 m; although the water column remains stratified with a stable middle layer, this layer deepens to lie below the euphotic layer for most of this period.

Comparison of the seasonal trends in modelled nutrients, biological standing stocks, and rate processes at CS with empirical data

In general, the model output of nutrient concentrations and standing stocks of the components of the plankton tallies with measurements made during the North Sea Project in the vicinity of CS (Lowry et al. 1992) (Fig. 4). The modelled seasonal trend in phytoplankton taxonomy and abundance is characteristic of temperate shelf seas. In the model, the picophytoplankton are first to respond to increasing irradiance and high nutrient concentrations in late winter – early spring, during the transitional period (Fig. 5). No empirical data are available to directly validate this occurrence, but significant production by picophytoplankton has been recorded in early spring in the Celtic Sea (Rees et al. 1999) and in a similar water column in the Celtic Sea (G. Tarran, Plymouth Marine Laboratory, Plymouth, PL1 3DH, U.K., unpublished data). The picophytoplankton bloom triggers the expansion of the heterotrophic flagellate population in mid-March. A peak in diatom biomass succeeds the picophytoplankton bloom as the water column begins to exhibit thermal stratification. The diatom bloom is largely responsible for the maximum chlorophyll *a* concentrations throughout the year of 3.3 $mg \cdot m^{-3}$ in early April. Following the decline of the diatom bloom at the end of the transitional season, largely resulting from depletion of available nutrients, the picophytoplankton population recovers briefly but is outcompeted for nutrients and light by a rapidly growing phytoflagellate population that benefits from stratification of the water column. The phytoflagellates reached a maximum biomass in late April – early May. The microzooplankton population tracks that of the phytoflagellates, accounting in part for the decline in phytoflagellate abundance in late May. A combination of light variability and wind/tidally induced turbulence results in a constantly fluctuating

© 2004 NRC Canada

Fig. 4. Simulated seasonal trends in nutrient concentrations and phytoplankton and zooplankton biomass for CS during 1989 and a comparison with field data collected during the North Sea Project. To enable comparison with field data, the values of nutrient concentration are integrated for the top 10 m, and those for the biological components, for the top 30 m. Field data (circles) for (*a–c*) nutrients were measured at CS in 1989. Because of the relative scarcity of data for (*d*) chlorophyll *a*, (*e–g*) phytoplankton, and (*h* and *i*) micrograzers, the same validation approach as applied by Baretta-Bekker et al. (1997) is used. Values are mean ± 1 SD of measurements determined in 1989 at CS or at one of three stations with similar physical characteristics within International Council for the Exploration of the Sea box 7′, sampled during the same period. Microscope analysis of phytoplankton samples did not distinguish between dinoflagellates and other flagellates. As a result, Fig. 4*f* compares combined flagellate populations for field and modelled data. The field data for (*j*) mesozooplankton is a composite of data collected at CS during 1988 and 1989.

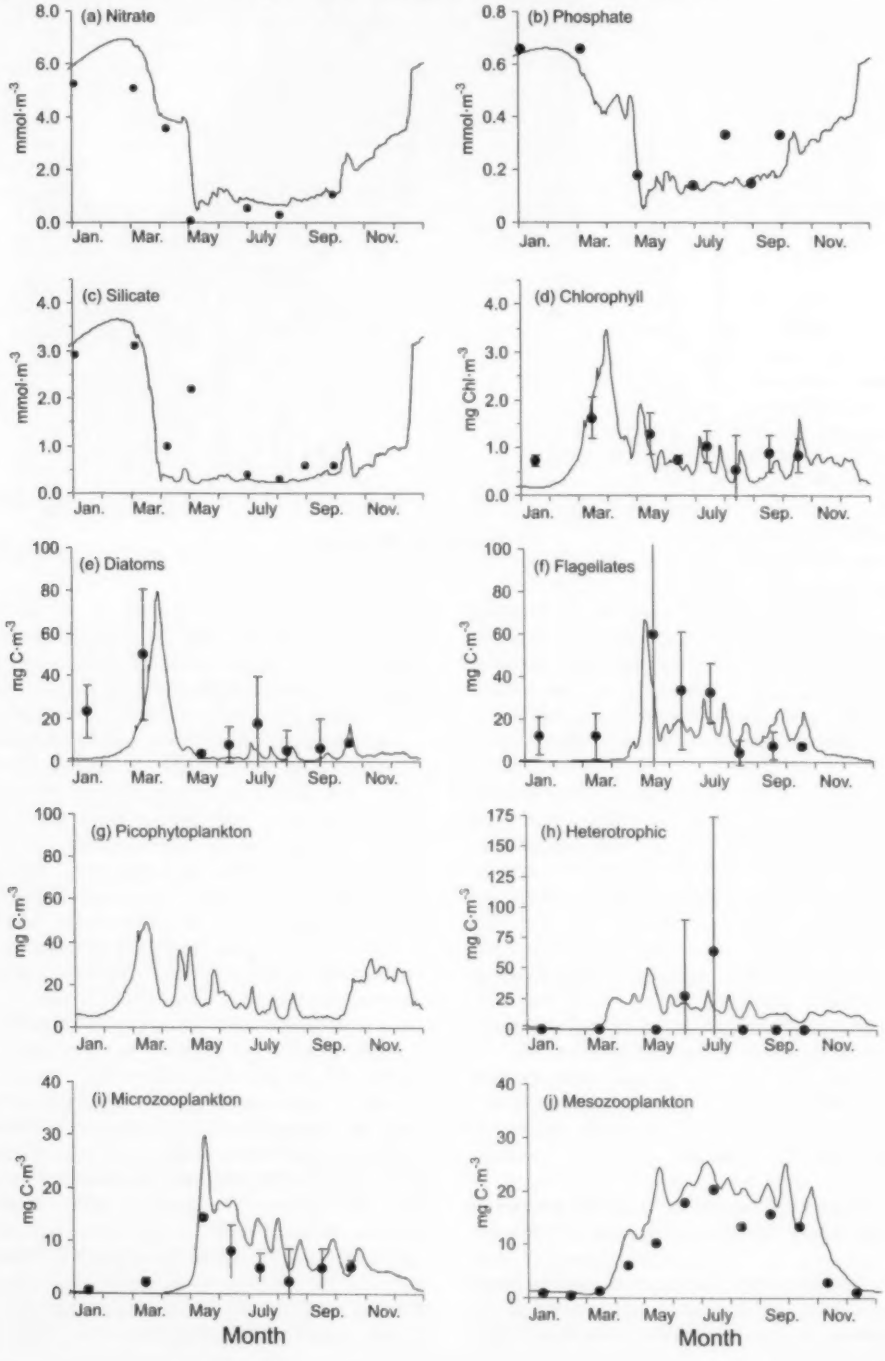

© 2004 NRC Canada

Fig. 5. Simulated net primary production for CS in 1989 in the surface mixed layer compared with primary production measured as ^{14}C accumulation at CS during 1989 (triangles) (Joint and Pomroy 1993).

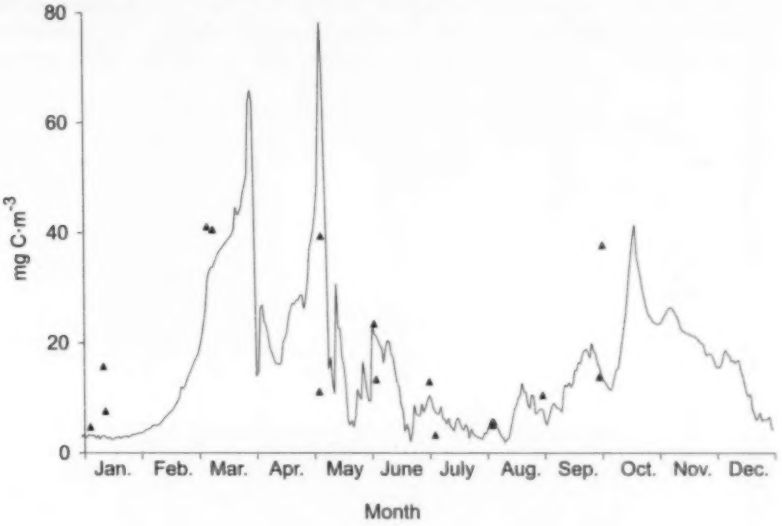

phytoplankton population throughout the stratified period. An increasing abundance of phototrophic dinoflagellates occurs as the middle layer deepens and this maintains the phytoplankton biomass through September and October. The magnitude and temporal trends in primary production determined as ^{14}C uptake rates over 24-h incubations compare favourably with modelled estimates of net primary production at CS (Joint and Pomroy 1993) (Fig. 5).

Model-generated bacterial biomass and composition are more difficult to validate, as no comparable measurements were made during the North Sea Project. In the northern North Sea in summer, total bacterial biomass was estimated to range between 30 and 40 mg $C \cdot m^{-3}$ in the surface and middle layers of the water column (Zubkov et al. 2001). Slightly higher but comparable bacterial biomass (40–50 mg $C \cdot m^{-3}$) is generated in the top 30 m by the model during June and July (data not shown). More importantly, net bacterial production generated by the model compares favourably with estimates of bacterial production carried out in similar waters of the Celtic Sea (Joint et al. 2001) (Fig. 6). The composition of the bacteria generated by the model is a product of $DMSP_d$ and DMS availability. Zubkov et al. (2001) found that a subpopulation of bacteria related to the genus *Roseobacter* constituted 45–48% of bacterial biomass in the waters of the northern North Sea in summer. These bacteria appeared to be the dominant consumers of $DMSP_d$ in these waters. This supports the almost 50% contribution to bacterial biomass contributed by the $DMSP_d$-consuming functional group in summer that is generated by the model (Fig. 6), but the seasonal trends generated by the model remain to be validated for the remainder of the year.

Production of $DMSP_p$, $DMSP_d$, and DMS

The close coupling between physical forcing and biological activity is illustrated by the modelled temporal and vertical trends in the concentrations of $DMSP_p$, $DMSP_d$, and DMS (Fig. 7), which clearly relate to the physical regimes defined above (Fig. 3). Very little production of $DMSP_p$ occurred in the winter mixed period (Fig. 7; Table 2). During the spring transitional period, high total water column standing stocks of $DMSP_p$ of >50 mg $S \cdot m^{-2}$ (Fig. 7) were produced by picophytoplankton and to a lesser extent diatoms (Fig. 8). Relatively high concentrations of $DMSP_p$ occurred in both the surface mixed and intermediate layers during the summer stratified period (Fig. 7). Particularly high concentrations of >3.5 mg $S \cdot m^{-3}$ were associated with phytoflagellate production in the surface layer during May (Fig. 8) and high concentrations were produced by phytoflagellates and dinoflagellates in the intermediate layer later in the summer stratified season (Fig 7). High concentrations of $DMSP_p$ were observed in an intermediate water layer during summer in the northern North Sea associated with relatively high abundance of the dinoflagellate *Prorocentrum minimum* (Archer et al. 2002*b*). The total annual production of $DMSP_p$ amounts to 5242 mg $S \cdot m^{-2} \cdot year^{-1}$ (Table 2), equivalent to 9812 mg $C \cdot m^{-2} \cdot year^{-1}$. Seventy percent of the annual $DMSP_p$ production occurred in the surface mixed layer, while as much as 29% was produced by the phytoplankton in the stable, intermediate water layer during the summer stratified period. The highest daily average production rates of 12.87 and 11.36 mg $S \cdot m^{-2}$ occurred in the surface mixed layer during the summer and autumn stratified periods (Table 2).

The proportion of gross carbon production invested in the synthesis of DMSP by phytoplankton ranges from slightly more than 1% to almost 5% in the surface mixed layer (Fig. 7). Highest proportions occur during the stratified periods in summer and autumn when the phytoplankton are dominated by flagellate and dinoflagellate taxa with DMSP quotas of 0.05 and 0.08 of cell carbon, respectively (Table 1). The minimum ratios coincide with the peak in diatom production in spring. $DMSP_p$ production rates determined in dilution experiments were equivalent to approximately 10% of primary production determined as ^{14}C uptake rates in surface waters during summer in the northern North Sea (Ar-

© 2004 NRC Canada

Fig. 6. (*a*) Simulated mean monthly bacterial production for CS in 1989 in the surface mixed layer (×) compared with bacterial production determined from [^{3}H]thymidine uptake rates in similar waters of the Celtic Sea (bars) (Joint et al. 2001). The range of values depicted by the bars is a product of using commonly applied bacterial cell carbon contents to calculate bacterial production from thymidine uptake rates. (*b*) Proportion that the three functional groups of bacteria contribute to total bacterial biomass for the surface mixed layer as simulated by the model for 1989 at CS (broken line, DOC consumers; thick line, DMSP consumers; thin line, DMS consumers).

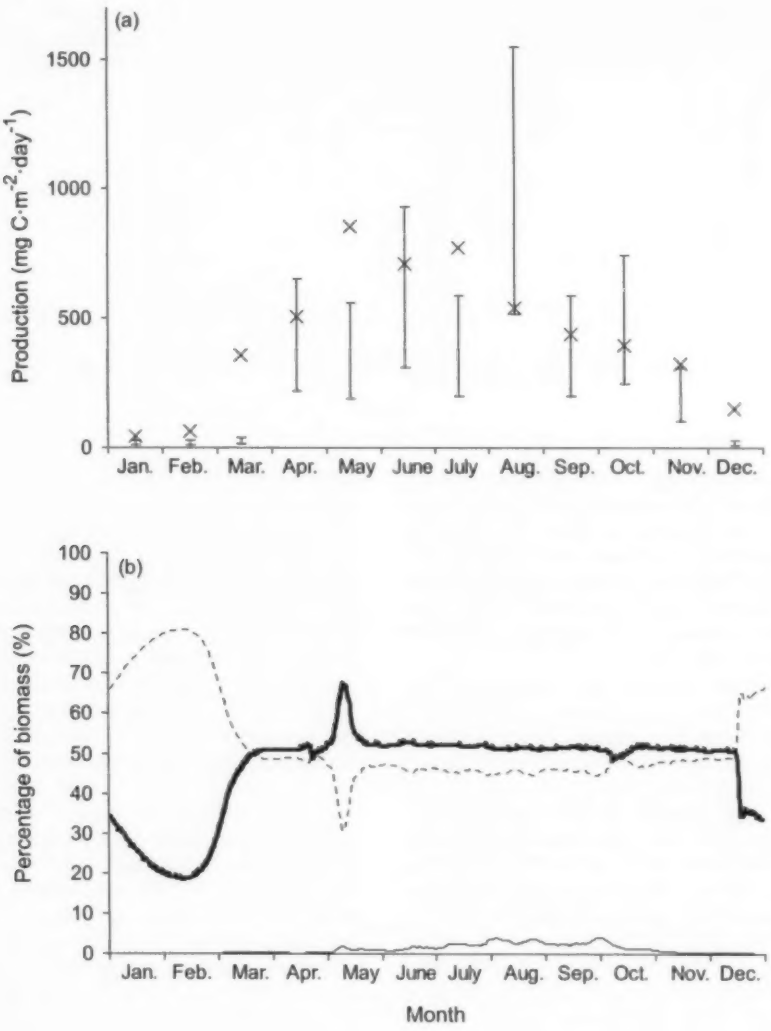

cher et al. 2001). Using an alternative approach to estimate $DMSP_p$ production, a slightly lower average of 7% of ^{14}C primary production was estimated in the North Atlantic (Simó et al. 2002).

As would be expected, the seasonal and vertical trends in $DMSP_d$ and DMS concentrations generated by the model are closely related to those of $DMSP_p$ (Fig. 7). Maximum concentrations of both compounds occur near the surface in May as a result of the peak in phytoflagellate biomass and maximum $DMSP_p$ concentrations. Both $DMSP_d$ and DMS occur at concentrations above 0.01 mg S·m^{-3} in surface waters during most of the year, dropping below this level only during the winter mixed period (Fig. 7). $DMSP_d$ production rates vary from seasonal average yields of 0.36–0.64 of the gross production of $DMSP_p$ during the winter mixed and summer stratified periods, respectively (Table 3). The yield of DMS production averaged 0.10 and 0.13 of $DMSP_p$ production in the spring transitional and summer stratified periods, respectively (Table 3). These values are comparable with measurements made in the northern North Sea in summer over a 6-day period when approximately 0.14 of the $DMSP_p$ produced by phytoplankton was transformed to DMS (Archer et al. 2002*a*). Somewhat higher estimates of 0.11–0.56 were recorded at the same time of year in the North Atlantic during a similar Lagrangian experiment (Simó and Pedrós-Alió 1999*b*). In the northwestern Pacific, DMS

© 2004 NRC Canada

Fig. 7. Contour plots of the temporal and vertical concentrations (mg S·m^{-3}) of (*a*) $DMSP_p$, (*b*) $DMSP_d$, and (*c*) DMS as simulated by the model for 1989 at CS.

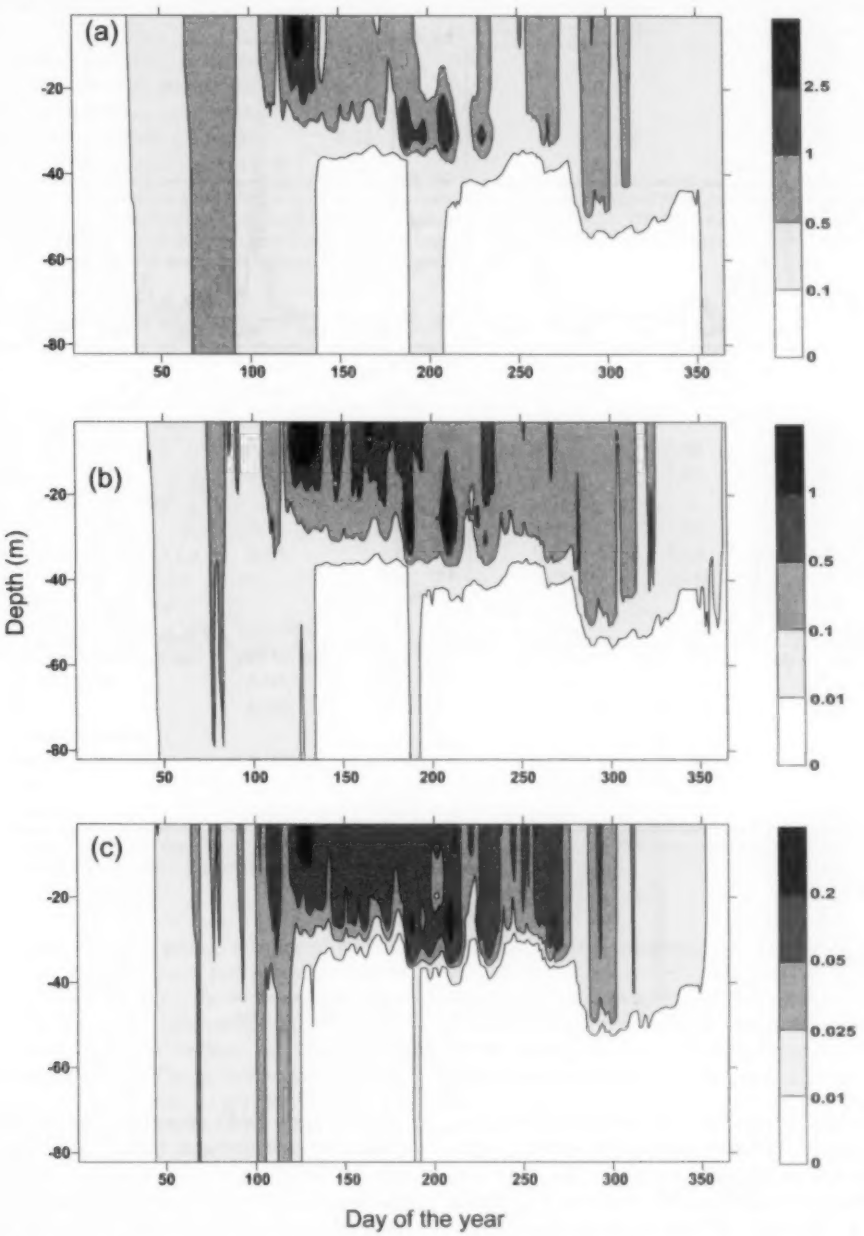

Table 2. Annual production of $DMSP_p$ (mg S·m^{-2}) (mean daily rates of production (mg S·m^{-2}·day^{-1}) in parentheses) in each layer of the water column and in the total water column and for each season as defined in Fig. 3.

Water column	Winter mixed	Spring transitional	Summer stratified	Autumn stratified	Annual
Surface	57 (1.27)	664 (8.20)	1918 (12.87)	1022 (11.36)	3661 (11.36)
Intermediate	1 (0.02)	38 (0.46)	1462 (9.82)	13 (0.15)	1514 (4.15)
Bottom	1 (0.01)	9 (0.11)	56 (0.38)	1 (0.02)	67 (0.18)
Total	59 (1.30)	710 (8.77)	3436 (23.06)	1037 (11.52)	5242 (14.36)

© 2004 NRC Canada

Fig. 8. Simulated standing stocks (solid line) and concentrations (broken line) of $DMSP_p$ in the surface mixed layer contributed by (*a*) picophytoplankton, (*b*) phytoflagellates, (*c*) diatoms, and (*d*) autotrophic dinoflagellates; (*e*) percent total phytoplankton carbon biomass comprising $DMSP_p$.

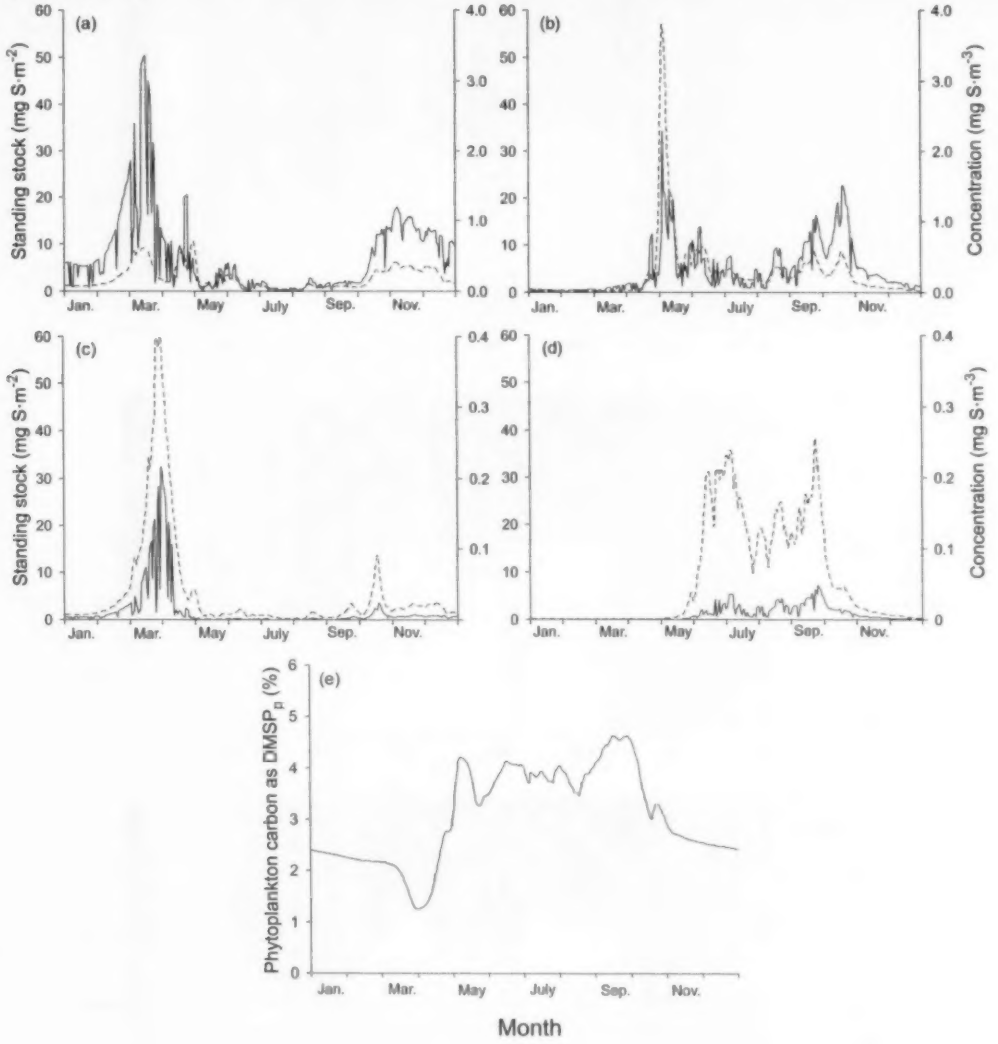

production equalled 0.27 times the total sulphate ($^{35}SO_4$) assimilation (Bates et al. 1994), also higher than values generated by the model. One explanation for this is that the yield calculated from the model relates DMS production to gross $DMSP_p$ production. The three short-term studies all differ in approach but are all likely to have underestimated gross DMSP production. Alternatively, the model suggests that production and removal processes may vary substantially over short time scales, and if this is real, the timing of short-term studies may be critical. More than 60% of the gross $DMSP_p$ production is transformed to either $DMSP_d$ or DMS in the model. The remainder is lost as particulate organic matter or is metabolized by the cells. In the model, no account is taken of the potential production of $DMSP_d$ and DMS from particulate organic matter.

$DMSP_d$ and DMS concentrations are the product of high production and removal rates (Table 4). Although for the sake of clarity, these rates may be averaged for each of the four seasons, they vary substantially over much shorter time scales (Fig. 9). In the model, the dynamic nature of these production and removal processes is a response to variability in physical forcing.

Leakage and lysis of phytoplankton cells contribute a substantial proportion of the DMS produced, either directly or as a product of $DMSP_d$ production, in the model. Leakage and lysis account for 78% of the annual $DMSP_d$ production in the surface mixed layer (Table 4). An average of 87% of $DMSP_d$ production occurs because of leakage and lysis during the spring transitional period because nutrient depletion and hence cell leakage and lysis play a major part in the de-

© 2004 NRC Canada

Table 3. Yields in the transformation of $DMSP_p$ to atmospheric DMS.

Yield	Winter mixed	Spring transitional	Summer stratified	Autumn stratified	Annual
$DMSP_d$ production/$DMSP_p$ production	0.36	0.45	0.64	0.5	0.56
DMS production/$DMSP_p$ production	0.12	0.09	0.13	0.1	0.12
DMS production/$DMSP_d$ consumption	0.35	0.23	0.22	0.21	0.22
DMS sea to air flux/DMS production	0.131	0.087	0.076	0.059	0.075
DMS sea to air flux/$DMSP_p$ production	0.015	0.007	0.01	0.006	0.008

Note: Values are in proportions of sulphur over the surface mixed layer and are calculated from the totals for each season. $DMSP_d$ production includes leakage by phytoplankton cells, lysis, and grazing processes. $DMSP_d$ consumption includes cleavage by free enzymes, bacterial cleavage, and consumption by bacteria. DMS production includes cleavage of $DMSP_d$ by free enzymes and by bacteria and during cell leakage, lysis, and grazing.

Table 4. Production and removal processes for $DMSP_d$ and DMS in the surface mixed layer.

	Winter mixed	Spring transitional	Summer stratified	Autumn stratified	Annual
$DMSP_d$ production processes					
Leakage and lysis	0.42	3.21	6.6	3.68	4.37 (78%)
Grazing	0.04	0.46	1.58	1.95	1.23 (22%)
$DMSP_d$ removal processes					
Bacterial consumption	0.39	2.8	6.96	4.94	4.73 (90%)
Bacterial cleavage	0.04	0.28	0.7	0.49	0.47 (9%)
Cleavage by free enzymes	0	0.03	0.08	0.05	0.05 (1%)
DMS production processes					
Bacterial cleavage	0.03998	0.28	0.696	0.494	0.480 (42%)
Cleavage by free enzymes	0.004	0.031	0.077	0.055	0.053 (5%)
Leakage and lysis	0.047	0.357	0.733	0.409	0.485 (42%)
Grazing	0.004	0.051	0.176	0.216	0.137 (14%)
DMS removal processes					
Bacterial consumption	0.051	0.476	1.237	0.969	0.856 (77%)
Photolysis	0.021	0.104	0.278	0.121	0.169 (15%)
Sea to air flux	0.02	0.063	0.129	0.07	0.086 (8%)

Note: Values are average daily rates (mg $S \cdot m^{-2} \cdot day^{-1}$) for each season and annually. The proportion that each process contributed to production or removal over the year is given in parentheses.

cline of the diatom population. An annual average of 42% of DMS production results directly from leakage and lysis of phytoplankton cells (Table 4; Fig. 9). Few studies have quantified DMS or $DMSP_d$ production resulting from leakage or lysis, particularly in natural waters, and hence, how realistic the model results are is difficult to verify. Certainly, relatively high rates of lysis are a general feature of ERSEM. However, increased production of $DMSP_d$/DMS has often been observed during the stationary phase of batch cultures, presumably because of increased leakage or cell lysis resulting from nutrient limitation (e.g., Stefels and van Boekel 1993; Laroche et al. 1999). There is also increasing evidence that in natural phytoplankton populations, cell death and subsequent lysis play an important role in phytoplankton succession (e.g., Brussard et al. 1995; Agustí et al. 1998). A relatively high proportion of phytoplankton may be in a compromised or lytic state and this may change seasonally in relation to environmental conditions, including nutrient availability (e.g., Agustí and Sánchez 2002). The model results highlight the need for further studies to address the relationship between phytoplankton viability and release rates of DMS and (or) $DMSP_d$.

Grazing plays a substantial but less significant role than leakage and lysis in the production of DMS, either directly (Fig. 9) or via $DMSP_d$, in the model. The proportion of $DMSP_d$ excreted by grazers ranges from a seasonal average of 9% during the winter mixed period to 35% during the autumn stratified period and averages 22% during the year (Table 4). An annual average of 14% of DMS production is directly released by grazers (Table 4). Few studies have been able to quantify the relative roles of DMS/$DMSP_d$ production processes in natural waters. Budgets of the fate of $DMSP_p$ developed from ship-based Lagrangian experiments suggest that grazing may account for the majority of the transformation of $DMSP_p$ to the dissolved phase (Archer et al. 2002*a*; Simó et al. 2002). However, both of these budgets covered relatively short periods of time when the bulk of the phytoplankton communities were actively growing and hence when nutrient-related excretion or lysis may not have been significant.

The model results confirm the importance of bacterial consumption and the relatively minor role of sea to air flux as loss processes of DMS in surface waters (Fig. 9). Bacterial consumption of DMS accounts for a seasonal average of

© 2004 NRC Canada

Fig. 9. Simulated seasonal patterns of DMS (*a* and *b*) production rates and (*c* and *d*) removal rates in the surface mixed layer at CS in 1989.

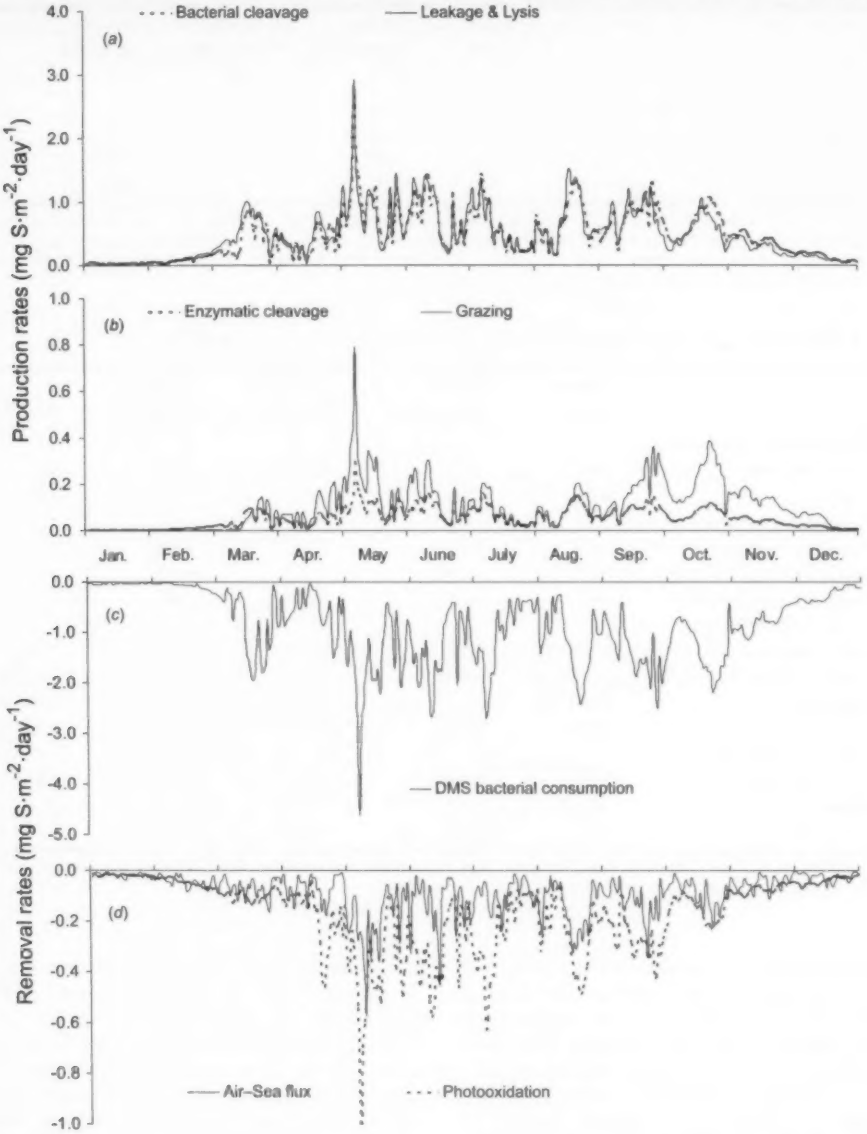

between 56% and 84% of the total removal of DMS in the surface mixed layer in winter and autumn, respectively (Table 4). Photolysis of DMS averages 15% of the annual removal and varies more than 20-fold between winter and summer average values (Table 4). The seasonally averaged proportion of DMS lost from the surface layer resulting from sea to air flux varies from 11% in winter to 4% in summer (Table 4), reflecting the higher winter wind speeds and lower rates of bacterial metabolism and photolysis in the winter mixed period.

Comparison of DMS, $DMSP_d$, and $DMSP_p$ concentrations with field data

DMS, $DMSP_d$, and $DMSP_p$ concentrations generated by the model are generally comparable with values measured in the vicinity of CS and mimic the seasonal trends observed during the North Sea Project (Fig. 10). The direct comparisons indicate that concentrations of DMS and $DMSP_p$ simulated by the model are of similar magnitude to measured values but that simulated $DMSP_d$ concentrations are overestimated by the model (Fig. 10). The bias in $DMSP_d$ concentration may, in part, be a product of the scarcity of field data available for comparison and the inherent difficulties of accurately determining $DMSP_d$ concentrations. Additionally, the model may overestimate production rates and (or) underestimate loss rates of $DMSP_d$. Interestingly, the plots of temporal trends in simulated seasonal cycle and field data suggest a closer correspondence for $DMSP_d$ than for either DMS or $DMSP_p$ despite the bias indicated by comparison between individual data points. High seasonal variability in

© 2004 NRC Canada

Fig. 10. Comparison of simulated concentrations and field data collected during the North Sea Project (NSP) for (*a* and *b*) DMS, (*c* and *d*) $DMSP_d$, and (*e* and *f*) $DMSP_p$ in 1989. Figures 10*a*, 10*c*, and 10*e* illustrate the temporal trend in simulated daily concentration in the surface mixed layer and measurements (diamonds) made in surface waters at CS or one of three stations with similar physical characteristics within International Council for the Exploration of the Sea box 7′ and 20 km of CS. Figures 10*b*, 10*d*, and 10*f* directly compare the same field data with simulated concentrations. Because of the relative scarcity of the field data, the simulated concentrations used for the direct comparison (Figs. 10*b*, 10*c*, and 10*f*) are weekly (3 days on either side of the sampling date) mean values.

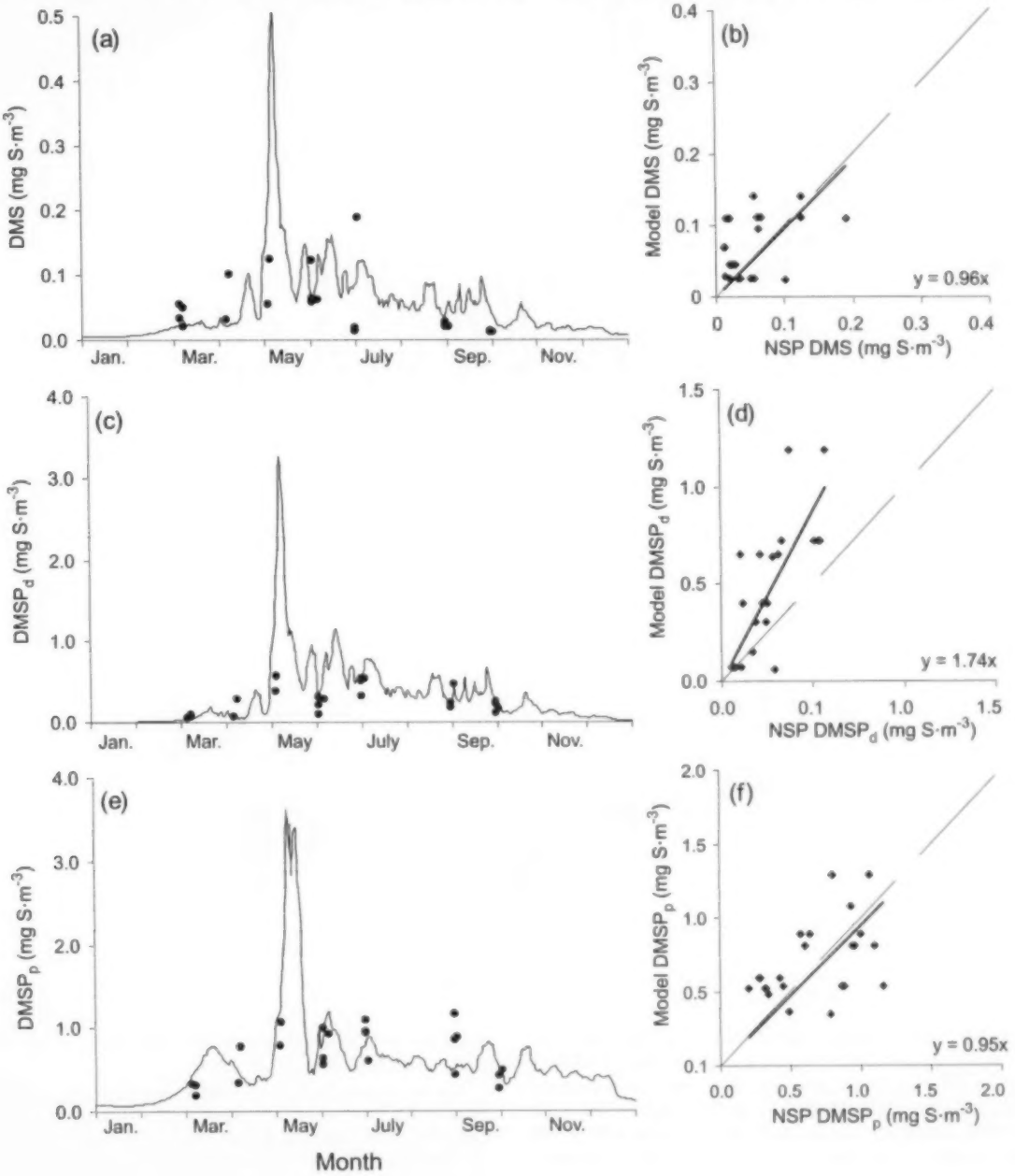

DMS surface concentrations, as simulated by the model, has been observed in studies with greater sampling frequency at a coastal site in the Baltic Sea (Leck et al. 1990) and at a shallow, tidal inlet on the Netherlands coast (Kwint and Kramer 1996).

DMS flux at CS and comparison with empirical data and other estimates

Variable wind speed is largely responsible for the substantial changes in modelled DMS sea to air flux from day to day (Fig. 11). The daily variability confirms the importance

© 2004 NRC Canada

Fig. 11. (*a*) Simulated daily sea to air flux of DMS at CS in 1989 compared with estimates generated from DMS concentrations measured at CS during the North Sea Project using modelled wind speed and temperature but based on a variety of methods of applying the data as explained in Turner et al. (1996). The diamonds mark the central point in the range of values produced by the various calculation methods. (*b*) Sea surface temperature (SST) (curve) and wind speed (spikes) used in the model to derive DMS sea to air flux.

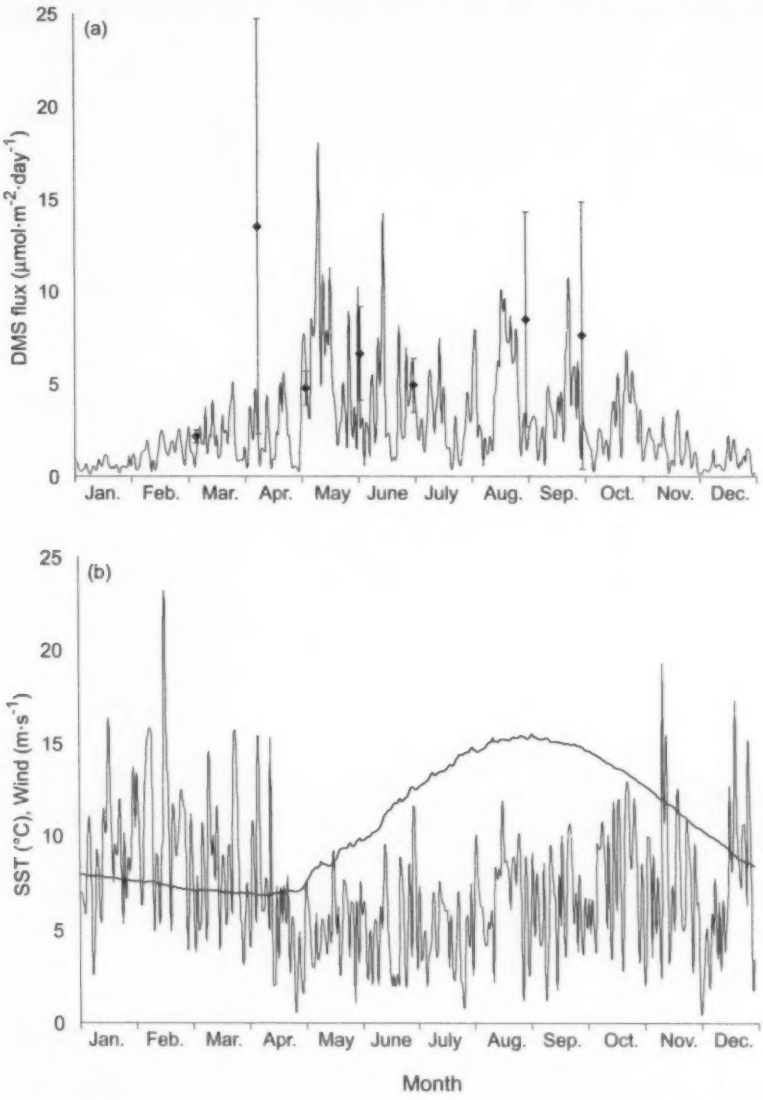

of applying high-resolution wind speed, in this case six-hourly data points, to estimates of sea to air flux (Archer et al. 2002*a*). Highest fluxes coincide with maximum concentrations of DMS in the surface mixed layer during the peak of the phytoflagellate bloom that is a product of the increased stability of the water column at the start of the summer stratified period. However, only slightly lower flux rates are maintained through to September and October, in part because of relatively high DMS concentrations throughout the summer and generally higher winds in the autumn. A similar seasonal trend in sea to air flux of DMS was generated for the open sea region of the southern North Sea by coupling several DMS production processes to the FYFY model (van den Berg et al. 1996).

The modelled cumulative annual sea to air flux of DMS in 1989 in the vicinity of CS amounted to 31.4 mg $S \cdot m^{-2} \cdot year^{-1}$. Turner et al. (1996) calculated a spatially averaged emission of DMS from the southern North Sea, including the region within which station CS lies, from February to October 1989 of 39.7 mg $S \cdot m^{-2} \cdot year^{-1}$. The close correspondence between these two estimates is somewhat fortuitous given the large DMS concentration gradients recorded over the southern North Sea (Turner et al. 1996) and the different methods of calculating transfer velocities. Turner et al. (1996) used a

© 2004 NRC Canada

Fig. 12. Illustrations of the impact of proportional changes in model parameters on the predicted annual DMS sea to air flux at CS in 1989 for (*a*) the proportion of phytoflagellate carbon comprising DMSP (standard: $q_2 = 0.05$), (*b*) the fraction of $DMSP_d$ uptake by bacteria cleaved to DMS (standard: $f_1 = 0.10$), (*c*) the efficiency of assimilation of $DMSP_p$ by grazers (standard = 30%), (*d*) the carbon ratio of DMS released from $DMSP_p$ during leakage, lysis, and grazing (standard: $r_{DMS} = 0.04$), (*e*) the carbon ratio of DMS released from $DMSP_p$ during only leakage and lysis (standard: $r_{DMS} = 0.04$), and (*f*) the carbon ratio of DMS released from $DMSP_p$ during only grazing (standard: $r_{DMS} = 0.04$).

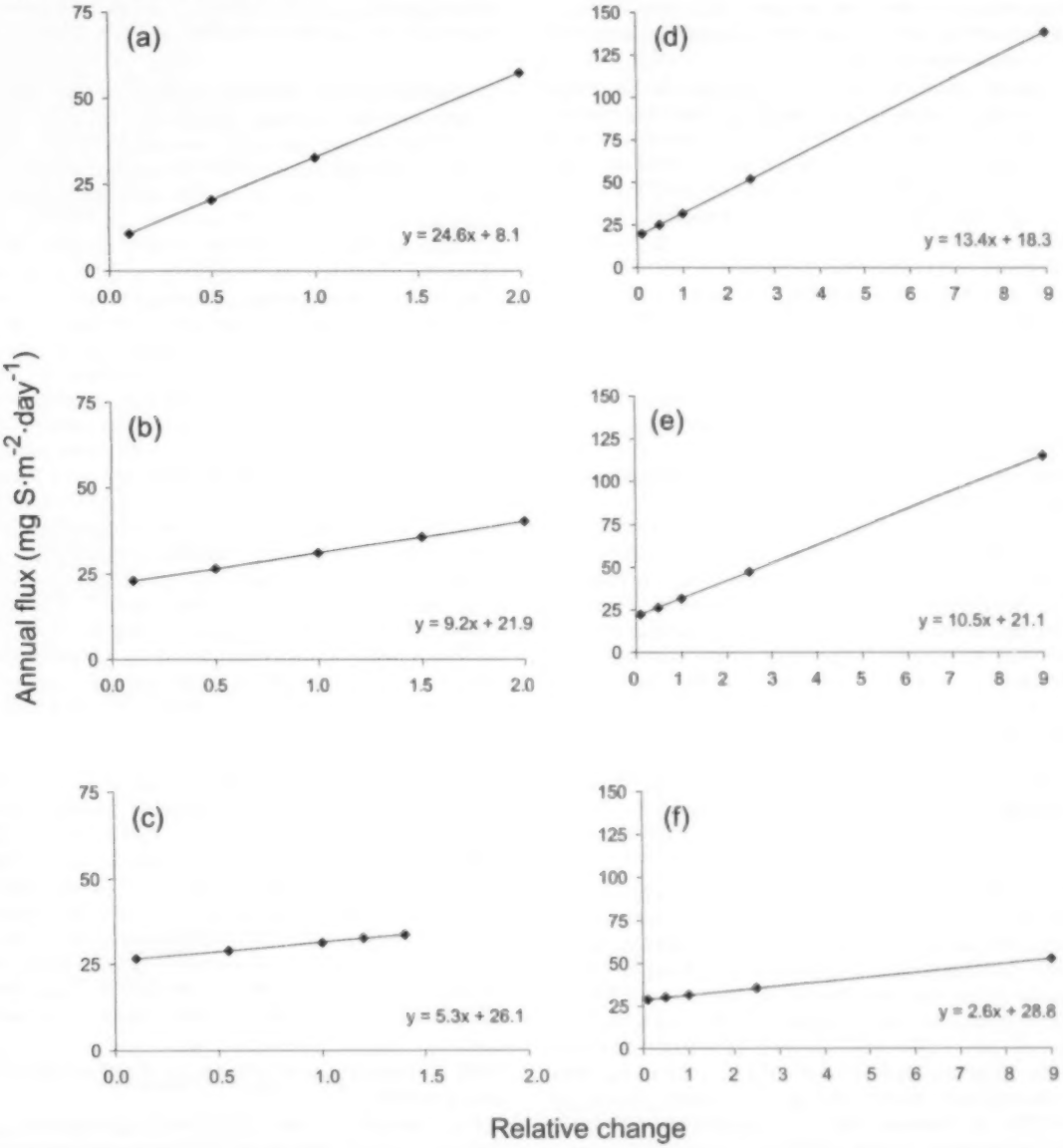

modification of the Liss and Merlivat (1986) relationships and mean monthly wind speeds. The present model calculations are based on the relationship of Nightingale et al. (2000) and use wind speeds interpolated for each time step between six-hourly rates. A more comprehensive validation of the magnitude and seasonality of DMS flux generated in the model is provided in Fig. 11. The model output for 1989 shows generally good agreement with estimates of DMS sea to air flux calculated from DMS concentrations measured in surface waters and using modelled wind speeds for a variety of methods of calculating the transfer velocity (Turner et al. 1996).

Sensitivity of the model to key biological parameters

A series of simple sensitivity tests were carried out to determine the importance of biological processes thought to be key determinants of DMS production. The tests related the cumulative annual DMS sea to air flux to proportional

© 2004 NRC Canada

changes in the parameterization of the standard run (Fig. 12). The changes in parameterization do not significantly alter the carbon and nutrient dynamics of the model. The parameters that are changed merely alter the portioning of a subset of the total carbon flux, and as a result, a linear relationship is produced by plotting proportional changes in parameter values against the annual DMS flux. Hence, a comparison of the slopes of the best fit line indicates the importance of each parameter.

The model was most sensitive to changes in the proportion of phytoplankton carbon comprising DMSP, confirming the need to fully resolve the role(s) of and controls on DMSP production by phytoplankton. A change in the DMSP content of only the phytoflagellate population had a greater impact on sea to air flux than proportional changes in any of the parameters that affect the processes that transform $DMSP_p$ to DMS (Fig. 12). A doubling of the cell DMSP content (q_2) (Table 1) to 0.10 for the phytoflagellate population, a value within the range of measured phytoplankton DMSP contents (e.g., Matrai and Keller 1994), increased the DMS flux from 31.4 to 57.3 mg $S \cdot m^{-2} \cdot year^{-1}$ (Fig. 12*a*).

The activity of DMSP lyase enzymes is likely to determine the proportion of $DMSP_p$ that is transformed to either $DMSP_d$ or DMS during leakage, lysis, or grazing of phytoplankton cells. A doubling of the parameter that controls the proportion of DMS produced from $DMSP_p$ (r_{DMS}) (Table 1) during these processes results in an increase in DMS sea to air flux from 31.4 to 45.1 mg $S \cdot m^{-2} \cdot year^{-1}$ (Figs. 12*d*–12*f*). The choice of $r_{DMS} = 0.04$ for the standard run was based on close coupling between $DMSP_p$ removal rates by microzooplankton and $DMSP_d$ consumption rates by bacteria observed over a 6-day Lagrangian experiment in the northern North Sea in summer, suggesting little direct production of DMS by grazers (Archer et al. 2002*a*). Furthermore, turnover rates of DMS appear to be approximately an order of magnitude lower than those of $DMSP_d$ (Ledyard and Dacey 1996; Kiene and Linn 2000; Zubkov et al. 2001). As bacterial uptake of $DMSP_d$ and DMS generally dominates removal processes, this indicates that a similar partition in the molar ratio of production is likely to occur.

The model is less sensitive to the level of assimilation of $DMSP_d$ by heterotrophs. DMSP may be an important source of carbon and particularly sulphur for both bacteria (Kiene and Linn 2000) and grazers (Simó et al. 2002). Metabolic demand for sulphur may determine the proportion of $DMSP_d$ taken up by bacteria that is cleaved to DMS (f_1) (Table 1) and may act as a key control on DMS production (Kiene et al. 2000). In the model, f_1 is fixed at 0.10 based on measurements in both coastal shelf and oceanic waters (Kiene and Linn 2000). A decrease in the demand for sulphur by $DMSP_d$-consuming bacteria resulting in a doubling in the quantity cleaved to DMS would raise the DMS sea to air flux from 31.4 to 40.3 mg $S \cdot m^{-2} \cdot year^{-1}$ (Fig. 12*b*). Although several laboratory studies have been able to budget the fate of phytoplankton DMSP that is ingested by grazers (Wolfe et al. 1994; Christaki et al. 1996), little is known about the factors controlling the level of assimilation (Tang et al. 1999). Alteration of the level of $DMSP_d$ and DMS released by grazers from 70% of that ingested to 100%, a 1.4-fold increase, would raise the DMS flux to 33.7 mg $S \cdot m^{-2} \cdot year^{-1}$ (Fig. 12*c*). In waters of the northern North Sea, the similar rates of $DMSP_p$ consumption by microzooplankton and uptake rates of $DMSP_d$ by bacteria suggest that little $DMSP_p$ was assimilated by the grazers and that altering the level of assimilation would have a major impact on DMS production rates (Archer et al. 2002*a*). However, the present model suggests that on an annual time scale, grazing processes are less important as a source of $DMSP_d$ and (or) DMS production.

Limitations of the DMS(P) processes in the model

Although the processes included in ERSEM to describe the DMS(P) biogeochemistry are more complex than many of the models produced to date for similar purposes, they are by no means comprehensive. The sensitivity analysis demonstrated the importance of accurately simulating the phytoplankton production of DMSP if DMS production is to be predicted effectively by modelling analyses. It is undoubtedly an oversimplification to have invariant cell quotas for each phytoplankton functional group, as used in the present study. An expanding number of functions have been accredited to cellular DMSP and it may be beneficial to include the more important controls on DMSP cell quota in ecosystem models of this complexity. The roles and activity of DMSP lyase enzymes, particularly those of the phytoplankton, remain poorly understood. How these enzymes react during the variety of processes that cause DMSP release from phytoplankton is one of the keys to correctly modelling DMS production. Bacterial metabolism of $DMSP_d$ acts as a substantial sink of potential DMS production, and the sensitivity analysis confirmed that the degree to which bacteria cleave $DMSP_d$ to DMS is one of the key biological controls of DMS production. Demarcation of the bacterial population into three functional groups replicated both seasonal trends in bacterial production and the limited evidence available for the functional composition of bacterioplankton communities. How this functional composition varies seasonally is uncertain but is likely to affect $DMSP_d$ and DMS dynamics considerably and may be advantageously incorporated among the modelled processes in future. Viral infection of phytoplankton may prove to be an important cause of $DMSP_p$ release in natural communities, and viral components of the mortality of phytoplankton and bacteria are planned for inclusion in the model. Parameterization of DMS photolysis in the present study is too simple and will benefit from the incorporation of the correct wavelength dependency and influence of DOM as more is learnt about the process.

DMS concentrations in relation to plankton biomass and rate processes

One approach to estimating DMS concentration globally and its seasonal variation has been to develop proxies of DMS concentration that can then be derived either from remotely sensed data (Simó and Dachs 2002) or, for instance, from a simple biogeochemical model coupled to an ocean general circulation model (Aumont et al. 2002). The complexity of the coupled ERSEM–GOTM model and its DMS(P) production and transformation processes allows an examination of how several modelled state variables or rates that may be of value as proxies of DMS correlate with modelled DMS concentration over an annual cycle at a single station.

© 2004 NRC Canada

Fig. 13. Plots of the daily output from the model for 1989 in the surface mixed layer of DMS concentration verses (*a*) phytoplankton biomass, (*b*) net primary production, and (*c*) net bacterial production.

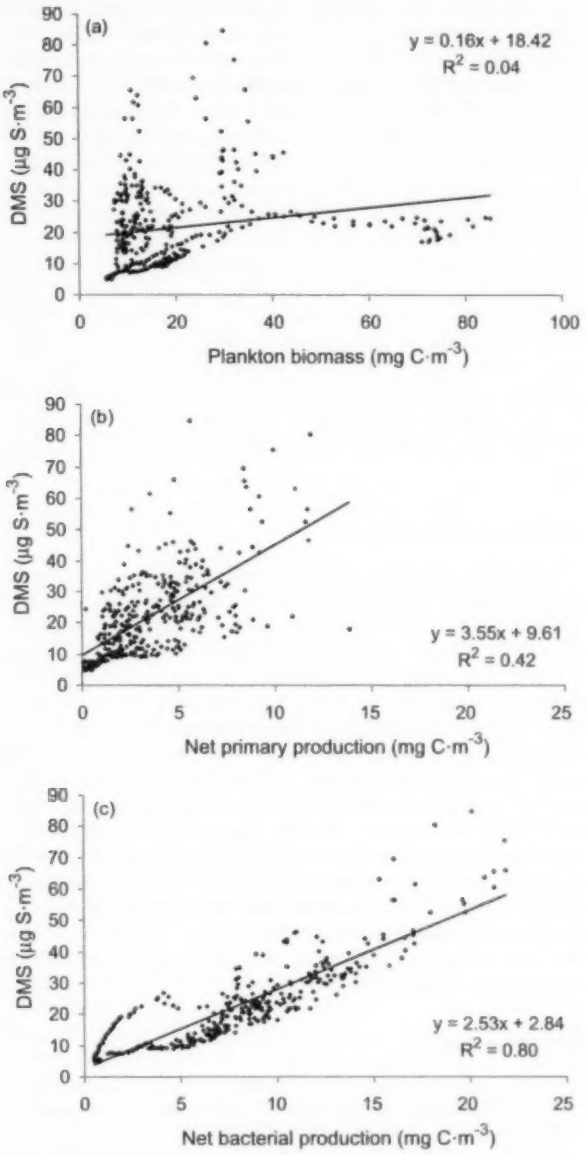

We show the relationship between daily concentrations of DMS generated by the model in the surface mixed layer and modelled phytoplankton biomass, primary production, and bacterial production (Fig. 13). The exercise confirms the poor correlation often found between parameters of phytoplankton "biomass", for instance chlorophyll *a*, and DMS concentration (e.g., Turner et al. 1988; Leck et al. 1990; Kettle et al. 1999) and illustrates that this poor correlation is likely to hold at a single site over the course of an annual cycle (Fig. 13*a*).

It may be more fruitful to use estimates of rate processes, possibly in combination with "biomass", to derive DMS concentration. Recent advances in algorithm development have enabled rates of net primary production to be estimated from remotely sensed data (Campbell et al. 2002). Net primary production generated by the model explains 42% of the variation in DMS concentration, considerably higher than phytoplankton biomass alone (Fig. 13*b*). Lawrence (1993) demonstrated the benefit of relating seawater DMS concentrations to phytoplankton growth rate rather than phytoplankton population density in a modelling examination of potential climate feedback cycles. Anderson et al. (2001) predicted DMS concentrations on a global scale as a product of chlorophyll, light, and a nutrient limitation term, all factors that determine phytoplankton production. Recently, Aumont et al. (2002) have shown a nonlinear relationship between the ratio of DMS to $DMSP_p$ and an index based on the ratio of fucoxanthin and peridinin to the total pigment concentration, the "Fp ratio", that may indicate the "trophic status" of the phytoplankton.

In the present model, DMS concentration is highly correlated with heterotrophic rate processes. For instance, net bacterial production explains 80% of the variation in DMS concentration in the surface mixed layer (Fig. 13*c*). This is not surprising, as bacterial production has a multifaceted influence on DMS concentrations, ranging from the impact on $DMSP_p$ production through competition for nutrients between phytoplankton and bacteria to consumption and transformation of $DMSP_d$ and the direct consumption of DMS. This emphasizes the fact that $DMSP_d$ and DMS are components of the labile DOC (and sulphur) fraction. Deriving the rates of heterotrophic processes, such as bacterial production, from remotely sensed data will not be straightforward and may involve a combination of modelling and algorithm development, but it may be a productive route by which we can link the complex DMS(P) processes of the ecological models of the type presented here to remotely sensed data, enabling more accurate spatial and temporal extrapolation of DMS concentrations and flux.

Model complexity and potential for extrapolation in time and space

The ERSEM–GOTM–DMS model presented here is the most complex model used to date to simulate a seasonal cycle of DMS biogeochemistry. By incorporating greater complexity in the ecosystem coupled to a high-resolution physical model, together with a more comprehensive series of processes involved in controlling DMS concentration and flux, the present model is intended to provide a more realistic response to meteorologically driven physical forcing. One issue that the present study raises is how complex do models of the processes that govern DMS sea to air flux need to be? One of the limiting factors governing model development and extrapolation to greater spatial and temporal scales and one explanation for the use of DMS proxies as an alternative strategy has been computing time and cost. The relatively simple model of van den Berg et al. (1996) was successfully used to simulate DMS sea to air flux for the whole of the southern North Sea at 22.5 km × 22.5 km resolution. The more complex DMS production model of Gabric et al.

© 2004 NRC Canada

(1993) has subsequently been used to simulate and calibrate a seasonal cycle of DMS flux in the subantarctic region of the Southern Ocean (Gabric et al. 1995) and to investigate the potential impact of climate change on DMS flux (Gabric et al. 1998). However, the influence of oceanic physical forcing on the ecosystem or DMS(P) processes is not taken into account in either case. Recently, Lefèvre et al. (2002) have presented a model used to simulate DMSP and DMS concentrations at Hydrostation S in the Sargasso Sea that uses a diagnostic approach to model the physical environment. Although the Lefèvre et al. (2002) and present model have been developed with similar aims in mind, they differ markedly in community structure, in the dynamics of the ecosystem, in the parameterization of the DMS(P) production and removal processes, and in the physical model. Both models benefit from an ever-expanding number of studies that address the processes controlling DMSP production, its transformation to DMS, and the fate of DMS, including flux across the air–sea interface. It is informative, therefore, to compare the structure and parameterization of some of the key processes in the two models. To match the in situ data sets available, the Lefèvre et al. (2002) model uses several parameters that are adjusted both seasonally and with depth. The cell quota of DMSP is varied in relation to photosynthetically active radiation, while the carbon to chlorophyll ratio and particle sinking velocities are varied in relation to the zenithal angle. Depth dependence of these parameters is adjusted in relation to light extinction. The seasonally varying parameters are used to enable the model to simulate the impact of a changing succession of phytoplankton functional groups. Here, in contrast, the DMS process descriptions are coupled to a complex generic ecosystem model (ERSEM) that is designed to reproduce the range of spatial and temporal dynamics observed in the North Sea (Baretta-Bekker et al. 1997) and other marine environments (Allen et al. 2002; Blackford and Burkill 2002). Hence, the observed seasonal and depth varying dynamics of the DMS system are inherent in the ecosystem model process descriptions. As a result, DMSP to carbon and hence DMSP to chlorophyll ratios vary in relation to the phytoplankton community composition that is a product of each group's differing response to physical forcing, ability to compete for nutrients with other phytoplankton and bacteria, and their susceptibility to predation from a dynamically varying grazer community.

A novel aspect of the present model is the incorporation of three bacterial functional groups, two of which directly impact on the DMS(P) dynamics, while the third does so indirectly by competing for nutrients and available DOC. The population of each bacterial functional group and their activity vary seasonally in a dynamic manner (Fig. 6). This is in contrast with the Lefèvre et al. (2002) model in which there is no bacterial compartment. Instead, a constant 40% of $DMSP_d$ is transformed to DMS each day and this is the only route for DMS production. In the present model, a fixed proportion of the $DMSP_d$ that is consumed by bacteria is cleaved to DMS (f_1) (Table 1). However, the quantity of $DMSP_d$ cleaved by bacteria varies in relation to the $DMSP_d$-consuming bacterial uptake (eq. 10), and DMS is also produced directly from phytoplankton cell lysis, grazing, and the activity of free enzymes (Fig. 2). Similarly, in the Lefèvre et al. (2002) model, DMS consumption is an invariant 0.4 day^{-1}, while in the present model, it is a function of five parameters (eq. 10) and DMS-consuming bacteria are explicitly represented.

Admittedly, parameterization of these DMS producing and removal processes is based on relatively few experimental studies (see above in the Results and discussion) and our knowledge of how and why they vary is still developing. However, inclusion in the model allows their relative contributions to DMS production and loss to be compared on a seasonal basis and the causes of the seasonal variations to be explored in greater detail. It may also facilitate the evaluation of alternative, possibly simpler approaches to estimate DMS concentration on greater regional scales. Alternatively, computational constraints on the extrapolation of such models to three dimensions and greater temporal scales are continually being resolved as computing power advances and becomes more affordable. Given the acknowledged complexity of the processes that govern sea surface DMS concentration and sea to air flux, the impact of changing physical forcing, both seasonally and in the longer term, is likely to be multifaceted and require a comprehensive model to understand and predict the direction of any feedback mechanism.

Acknowledgements

This work was supported by funding from the U.K. Joint Grant Scheme (JGS reference Nos. 595 and 813) with the Environmental Sciences Department, QuinetiQ, through the Plymouth Marine Laboratory research programme Microbially Driven Biogeochemical Cycles funded by the U.K. Natural Environment Research Council and through the BASICS programme funded by the European Commission. We acknowledge the efforts of the personnel who undertook the North Sea Project sampling programme with which this model is validated, particularly the measurements of DMS and DMSP concentration by Sue Turner and Gill Malin. Ian Joint kindly provided the bacterial production data for validation purposes. We are grateful for both intellectual and financial support from Arnold Taylor, Peter Burkill, and Geoff Smith in the development of the model. Finally, we thank the two anonymous reviewers who helped to considerably improve the manuscript.

References

Agustí, S., and Sánchez, M.C. 2002. Cell viability in natural phytoplankton communities quantified by a membrane permeability probe. Limnol. Oceanogr. **47**: 818–828.

Agustí, S., Satta, M.P., Mura, M.P., and Benavent, E. 1998. Dissolved esterase activity as tracer of phytoplankton lysis: evidence of high phytoplankton lysis rates in the NW Mediterranean. Limnol. Oceanogr. **43**: 1836–1849.

Allen, J.I., Somerfield, P.J., and Siddorn, J.R. 2002. Primary and bacterial production in the Mediterranean Sea: a modelling study. J. Mar. Syst. **33–34**: 473–495.

Anderson, T.R., Spall, S.A., Yool, A., Cipollini, P., Challenor, P.G., and Fasham, M.J.R. 2001. Global fields of sea surface dimethylsulfide predicted from chlorophyll, nutrients and light. J. Mar. Syst. **30**: 1–20.

Archer, S.D., Widdicombe, C.E., Tarran, G.A., Rees, A.P., and Burkill, P.H. 2001. Production and turnover of particulate

© 2004 NRC Canada

dimethylsulphoniopropionate during a coccolithophore bloom in the northern North Sea. Aquat. Microb.Ecol. **24**: 225–241.

Archer, S.D., Gilbert, F.J., Nightingale, P.D., Zubkov, M.V., Taylor, A.H., Smith, G.C., and Burkill, P.H. 2002*a*. Transformation of dimethylsulphoniopropionate to dimethyl sulphide during summer in the North Sea with an examination of key processes via a modelling approach. Deep-Sea Res. II, **49**: 3067–3101.

Archer, S.D., Smith, G.C., Nightingale, P.D., Widdicombe, C.E., Tarran, G.A., Rees, A.P., and Burkill, P.H. 2002*b*. Dynamics of particulate dimethylsulphoniopropionate during a Lagrangian experiment in the northern North Sea. Deep-Sea Res. II, **49**: 2979–2999.

Aumont, O., Belviso, S., and Monfray, P. 2002. Dimethylsulfoniopropionate (DMSP) and dimethylsulfide (DMS) sea surface distributions simulated from a global three-dimensional ocean carbon model. J. Geophys. Res. **107**(C4): 1–21.

Baretta, J.W., Ebenhöh, W., and Ruardij, P. 1995. The European Regional Seas Ecosystem Model, a complex marine ecosystem model. Neth. J. Sea Res. **33**: 233–246.

Baretta-Bekker, J.G., Baretta, J.W., and Rasmussen, E.K. 1995. The microbial food web in the European Regional Seas Ecosystem Model. Neth. J. Sea Res. **33**: 363–379.

Baretta-Bekker, J.G., Baretta, J.W., and Ebenhöh, W. 1997. Microbial dynamics in the marine ecosystem model ERSEM II with decoupled carbon assimilation and nutrient uptake. J. Sea Res. **38**: 195–212.

Baretta-Bekker, J.G., Baretta, J.W., Hansen, A.S., and Riemann, B. 1998. An improved model of carbon and nutrient dynamics in the microbial food web in marine enclosures. Aquat. Microb. Ecol. **14**: 91–108.

Bates, T.S., Kiene, R.P., Wolfe, G.V., Matrai, P.A., Chavez, F.P., Buck, K.R., Blomquist, B.W., and Cuhel, R.L. 1994. The cycling of sulfur in surface seawater of the Northeast Pacific. J. Geophys. Res. **99**: 7835–7843.

Blackford, J.C., and Burkill, P.H. 2002. Planktonic community structure and carbon cycling in the Arabian Sea as a result of monsoonal forcing: the application of a generic model. J. Mar. Syst. **36**: 239–267.

Bonsang, B., Nguyen, B.C., Gaudry, A., and Lambert, G. 1980. Sulfate enrichment in marine aerosols owing to biogenic gaseous sulfur compounds. J. Geophys. Res. **85**: 7410–7416.

Brugger, A., Slezak, D., Obernosterer, I., and Herndl, G.J. 1998. Photolysis of dimethylsulfide in the northern Adriatic Sea: dependence on substrate concentration, irradiance and DOC concentration. Mar. Chem. **59**: 321–331.

Brussard, C.P.D., Reigman, R., Noordeloos, A.A.M., Cadée, G.C., Witte, H., Kop, A.J., Nieuwland, G., van Duyl, F.C., and Bak, R.P.M. 1995. Effects of grazing, sedimentation and phytoplankton cell lysis on the structure of a coastal pelagic food web. Mar. Ecol. Prog. Ser. **123**: 259–271.

Burchard, H., Bolding, K., and Villarreal, M.R. 1999. GOTM — a general ocean turbulence model. Theory, applications and test cases. Tech. Rep. EUR 18745 EN. European Commission.

Burchard, H., Bolding, K., Rippeth, T.P., Stips, A., Simpson, J.H., and Sundermann, J. 2002. Microstructure of turbulence in the northern North Sea: a comparative study of observations and model simulations. J. Sea Res. **47**: 223–238.

Campbell, J., Antoine, D., Armstrong, R., Arrigo, K., Balch, W., Barber, R., Behrenfeld, M., Bidigare, R., Bishop, J., Carr, M.E., Esaias, W., Falkowski, P., Hoepffner, N., Iverson, R., Kiefer, D., Lohrenz, S., Marra, J., Morel, A., Ryan, J., Vedernikov, V., Waters, K., Yentsch, C., and Yoder, J. 2002. Comparison of algorithms for estimating ocean primary production from surface chlorophyll, temperature and irradiance. Global Biogeochem. Cycles, **16**. Article No. 1035.

Castellari, S., Pinardi, N., and Learman, K. 1998. A model of air sea interactions in the Mediterranean Sea. J. Mar. Syst. **18**: 89–114.

Charlson, R.J., Lovelock, J.E., Andreae, M.O., and Warren, S.G. 1987. Oceanic phytoplankton, atmospheric sulfur, cloud albedo and climate. Nature (Lond.), **326**: 655–661.

Christaki, U., Belviso, S., Dolan, J.R., and Corn, M. 1996. Assessment of the role of copepods and ciliates in the release to solution of particulate DMSP. Mar. Ecol. Prog. Ser. **141**: 119–127.

Clarke, A.D., Davis, D., Kapustin, V.N., Eisele, F., Chen, G., Paluch, I., Lenschow, D., Bandy, A.R., Thornton, D., Moore, K., Mauldin, L., Tanner, D., Litchy, M., Carroll, M.A., Collins, J., and Albercook, C. 1998. Particle nucleation in the tropical boundary layer and its coupling to marine sulfur sources. Science (Wash., D.C.), **282**: 89–92.

Corn, M., Belviso, S., Partensky, F., Simon, N., and Christaki, U. 1996. Origin and importance of picoplanktonic DMSP. *In* Biological and environmental chemistry of DMSP and related sulfonium compounds. *Edited by* R.P. Kiene, P.T. Visscher, M.D. Keller, and G.O. Kirst. Plenum Press, New York. pp. 191–201.

Dacey, J.W.H., and Wakeham, S.G. 1986. Oceanic dimethylsulfide — production during zooplankton grazing on phytoplankton. Science (Wash., D.C.), **233**: 1314–1316.

Dacey, J.W.H., Howse, F.A., Michaels, A.F., and Wakeham, S.G. 1998. Temporal variability of dimethylsulfoniopropionate in the Sargasso Sea. Deep-Sea Res. I, **45**: 2085–2104.

Droop, M.R. 1974. The nutrient status of algal cells in continuous culture. J. Mar. Biol. Assoc. U.K. **54**: 825–855.

Ebenhöh, W., Baretta, J.W., and Baretta-Bekker, J.G. 1997. The primary production module in a marine ecosystem model ERSEM II. J. Sea Res. **38**: 173–194.

Gabric, A., Murray, N., Stone, L., and Kohl, M. 1993. Modelling the production of dimethylsulfide during a phytoplankton bloom. J. Geophys. Res. **94**: 9731–9742.

Gabric, A.J., Ayers, G.P., and Sander, G.C. 1995. Independent marine and atmospheric model estimates of the sea–air flux of dimethylsulfide in the Southern Ocean. Geophys. Res. Lett. **22**: 3521–3524.

Gabric, A.J., Whetton, P.H., Boers, R., and Ayers, G.P. 1998. The impact of simulated climate change on the air–sea flux of dimethylsulphide in the subantarctic Southern Ocean. Tellus Ser. B Chem. Phys. Meteorol. **50**: 388–399.

Gage, D.A., Rhodes, D., Nolte, K.D., Hicks, W.A., Leustek, T., Cooper, A.J.L., and Hanson, A.D. 1997. A new route for synthesis of dimethylsulphoniopropionate in marine algae. Nature (Lond.), **387**: 891–894.

González, J.M., Kiene, R.P., and Moran, M.A. 1999. Transformation of sulfur compounds by an abundant lineage of marine bacteria in the alpha-subclass of the class Proteobacteria. Appl. Environ. Microbiol. **65**: 3810–3819.

Howarth, M.J., Dyer, K.R., Joint, I.R., Hydes, D.J., Purdie, D.A., Edmunds, H., Jones, J.E., Lowry, R.K., Moffat, T.J., Pomroy, A.J., and Proctor, R. 1993. Seasonal cycles and their spatial variability. Philos. Trans. R. Soc. Lond. Ser. A Math. Phys. **343**: 383–403.

Jodwalis, C.W., Benner, R.L., and Eslinger, D.L. 2000. Modeling of dimethyl sulfide ocean mixing, biological production, and sea-to-air flux for high latitudes. J. Geophys. Res. **105**: 14 387 – 14 399.

Joint, I., and Pomroy, A. 1993. Phytoplankton biomass and production in the southern North Sea. Mar. Ecol. Prog. Ser. **99**: 169–182.

Joint, I., Wollast, R., Chou, L., Batten, S., Edwards, E., Hirst, A., Burkill, P., Groom, S., Gibb, S., Miller, A., Hydes, D., Dehairs, F., Antia, A., Barlow, R., Rees, A., Pomroy, A., Brockmann, U.,

© 2004 NRC Canada

Cummings, D., Lampitt, R., Loijens, M., Mantoura, F., Miller, P., Raabe, T., Alvarez-Salgado, X., Stelfox, C., and Woolfenden, J. 2001. Pelagic production at the Celtic Sea shelf break. Deep-Sea Res. II, **48**: 3049–3081.

Keller, M.D., Bellows, W.K., and Guillard, R.R.L. 1989. Dimethyl sulfide production in marine-phytoplankton. Am. Chem. Soc. Symp. Ser. **393**: 167–182.

Kettle, A.J., and Andreae, M.O. 2000. Flux of dimethylsulfide from the oceans: a comparison of updated data sets and flux models. J. Geophys. Res. **105**: 26 793 – 26 808.

Kettle, A.J., Andreae, M.O., Amouroux, D., Andreae, T.W., Bates, T.S., Berresheim, H., Bingemer, H., et al. 1999. A global database of sea surface dimethylsulfide (DMS) measurements and a procedure to predict sea surface DMS as a function of latitude, longitude, and month. Global Biogeochem. Cycles, **13**: 399–444.

Kieber, D.J., Jiao, J.F., Kiene, R.P., and Bates, T.S. 1996. Impact of dimethylsulfide photochemistry on methyl sulfur cycling in the Equatorial Pacific Ocean. J. Geophys. Res. **101**: 3715–3722.

Kiene, R.P., and Bates, T.S. 1990. Biological removal of dimethyl sulfide from sea-water. Nature (Lond.), **345**: 702–705.

Kiene, R.P., and Linn, L.J. 2000. Distribution and turnover of dissolved DMSP and its relationship with bacterial production and dimethylsulfide in the Gulf of Mexico. Limnol. Oceanogr. **45**: 849–861.

Kiene, R.P., Linn, L.J., and Bruton, J.A. 2000. New and important roles for DMSP in marine microbial communities. J. Sea Res. **43**: 209–224.

Kwint, R.L.J., and Kramer, K.J.M. 1996. Dimethylsulphide production by plankton communities. Mar. Ecol. Prog. Ser. **121**: 227–237.

Laroche, D., Vézina, A.F., Levasseur, M., Gosselin, M., Stefels, J., Keller, M.D., Matrai, P.A., and Kwint, R.L.J. 1999. DMSP synthesis and exudation in phytoplankton: a modelling approach. Mar. Ecol. Prog. Ser. **180**: 37–49.

Lawrence, M.G. 1993. An empirical analysis of the strength of the phytoplankton–dimethylsulfide–cloud–climate feedback cycle. J. Geophys. Res. **98**: 20 663 – 20 673.

Leck, C., Larsson, U., Bagander, L.E., Johansson, S., and Hajdu, S. 1990. Dimethyl sulfide in the Baltic Sea — annual variability in relation to biological activity. J. Geophys. Res. **95**: 3353–3363.

Ledyard, K.M., and Dacey, J.W.H. 1996. Microbial cycling of DMSP and DMS in coastal and oligotrophic seawater. Limnol. Oceanogr. **41**: 33–40.

Lefèvre, M., Vézina, A., Levasseur, M., and Dacey, J.W.H. 2002. A model of dimethylsulphide dynamics for the subtropical North Atlantic. Deep-Sea Res. I, **49**: 2221–2239.

Liss, P.S., and Merlivat, L. 1986. Air–sea gas exchange rates: introduction and synthesis. *In* The role of air–sea gas exchange in geochemical cycling. *Edited by* P. Buat-Ménard. Reidel, Dordrecht, the Netherlands. pp. 113–127.

Lowry, R., Cranmer, K., and Rickards, L. 1992. North Sea Project CD ROM and users guide. British Oceanographic Data Centre, Natural Environment Research Council, Swindon, U.K.

Malin, G., Wilson, W.H., Bratbak, G., Liss, P.S., and Mann, N.H. 1998. Elevated production of dimethylsulfide resulting from viral infection of cultures of *Phaeocystis pouchetii*. Limnol. Oceanogr. **43**: 1389–1393.

Matrai, P.A., and Keller, M.D. 1994. Total organic sulfur and dimethylsulfoniopropionate in marine phytoplankton — intracellular variations. Mar. Biol. **119**: 61–68.

Nguyen, B.C., Belviso, S., Mihalopoulos, N., Gostan, J., and Nival, P. 1988. Dimethyl sulfide production during natural phytoplanktonic blooms. Mar. Chem. **24**: 133–141.

Nightingale, P.D., Malin, G., Law, C.S., Watson, A.J., Liss, P.S., Liddicoat, M.I., Boutin, J., and Upstill-Goddard, R.C. 2000. *In situ* evaluation of air–sea gas exchange parameterizations using novel conservative and volatile tracers. Global Biogeochem. Cycles, **14**: 373–387.

Prandle, D., Hydes, D.J., Jarvis, J., and McManus, J. 1997. The seasonal cycles of temperature, salinity, nutrients and suspended sediment in the southern North Sea in 1988 and 1989. Estuarine Coastal Shelf Sci. **45**: 669–680.

Rees, A.P., Joint, I.R., and Donald, K.M. 1999. Early spring bloom phytoplankton–nutrient dynamics at the Celtic Sea shelf edge. Deep-Sea Res. I, **46**: 483–510.

Scarratt, M., Cantin, G., Levasseur, M., and Michaud, S. 2000. Particle size-fractionated kinetics of DMS production: where does DMSP cleavage occur at the microscale? J. Sea Res. **43**: 245–252.

Sharples, J., and Tett, P. 1994. Modelling of the effect of physical variability on the midwater chlorophyll maximum. J. Mar. Res. **52**: 219–238.

Shaw, G.E. 1987. Aerosols as climate regulators: a climate biosphere linkage? Atmos. Environ. **21**: 985–986.

Simó, R., and Dachs, J. 2002. Global ocean emission of dimethylsulfide predicted from biogeophysical data. Global Biogeochem. Cycles, **16**. Article No. 1078.

Simó, R., and Pedrós-Alió, C. 1999*a*. Short-term variability in the open ocean cycle of dimethylsulfide. Global Biogeochem. Cycles, **13**: 1173–1181.

Simó, R., and Pedrós-Alió, C. 1999*b*. Role of vertical mixing in controlling the oceanic production of dimethyl sulphide. Nature (Lond.), **402**: 396–399.

Simó, R., Archer, S.D., Pedrós-Alió, C., Gilpin, L., and Widdicombe, C.E. 2002. Coupled dynamics of dimethylsulfide cycling and the microbial food-web in surface waters of the North Atlantic. Limnol. Oceanogr. **47**: 53–61.

Simpson, J.H. 1993. The North Sea Project — an overview and the way forward. Philos. Trans. R. Soc. Lond. Ser. A Math. Phys. **343**: 585–596.

Sinha, B., and Pingree, R.D. 1997. The principal lunar semidiurnal tide and its harmonics: baseline solutions for M-2 and M-4 constituents on the Northwest European continental shelf. Continental Shelf Res. **17**: 1321–1365.

Stefels, J. 2000. Physiological aspects of the production and conversion of DMSP in marine algae and higher plants. J. Sea Res. **43**: 183–197.

Stefels, J., and Dijkhuizen, L. 1996. Characteristics of DMSP-lyase in *Phaeocystis* sp. (*Prymnesiophyceae*). Mar. Ecol. Prog. Ser. **131**: 307–313.

Stefels, J., and van Boekel, W.H.M. 1993. Production of DMS from dissolved DMSP in axenic cultures of the marine phytoplankton species *Phaeocystis* sp. Mar. Ecol. Prog. Ser. **97**: 11–18.

Tang, K.W., Dam, H.G., Visscher, P.T., and Fenn, T.D. 1999. Dimethyl-sulfoniopropionate (DMSP) in marine copepods and its relation with diets and salinity. Mar. Ecol. Prog. Ser. **179**: 71–79.

Tetens, O. 1930. Uber einige meteorologische Begriffe. Z. Geophys. **6**: 297–309.

Turner, S.M., Malin, G., Liss, P.S., Harbour, D.S., and Holligan, P.M. 1988. The seasonal-variation of dimethyl sulfide and dimethylsulfoniopropionate concentrations in nearshore waters. Limnol. Oceanogr. **33**: 364–375.

Turner, S.M., Malin, G., Nightingale, P.D., and Liss, P.S. 1996. Seasonal variation of dimethyl sulphide in the North Sea and an assessment of fluxes to the atmosphere. Mar. Chem. **54**: 245–262.

Vairavamurthy, A., Andreae, M.O., and Iverson, R.L. 1985. Biosynthesis of dimethylsulfide and dimethylpropiothetin by *Hyme-*

© 2004 NRC Canada

nomonas carterae in relation to sulfur source and salinity variations. Limnol. Oceanogr. **30**: 59–70.

van den Berg, A.J., Turner, S.M., van Duyl, F.C., and Ruardij, P. 1996. Model structure and analysis of dimethylsulphide (DMS) production in the southern North Sea, considering phytoplankton dimethylsulphoniopropionate(DMSP)-lyase and eutrophication effects. Mar. Ecol. Prog. Ser. **145**: 233–244.

Visscher, P.T., Diaz, M.R., and Taylor, B.F. 1992. Enumeration of bacteria which cleave or demethylate dimethylsulfoniopropionate in the Caribbean Sea. Mar. Ecol. Prog. Ser. **89**: 293–296.

Wallace, J.M.A., and Hobbs, P.V. 1977. Atmospheric science: an introductory survey. Academic Press, San Diego, Calif.

Wolfe, G.V., and Steinke, M. 1996. Grazing-activated production of dimethyl sulfide (DMS) by two clones of *Emiliania huxleyi*. Limnol. Oceanogr. **41**: 1151–1160.

Wolfe, G.V., Sherr, E.B., and Sherr, B.F. 1994. Release and consumption of DMSP from *Emiliania huxleyi* during grazing by *Oxyrrhis marina*. Mar. Ecol. Prog. Ser. **111**: 111–120.

Zavatarelli, M., Baretta, J.W., Baretta-Bekker, J.G., and Pinardi, N. 2000. The dynamics of the Adriatic Sea ecosystem. An idealised model study. Deep-Sea Res. I, **47**: 937–970.

Zubkov, M.V., Fuchs, B.M., Archer, S.D., Kiene, R.P., Amann, R., and Burkill, P.H. 2001. Linking the composition of bacterioplankton to rapid turnover of dissolved dimethylsulphoniopropionate in an algal bloom in the North Sea. Environ. Microbiol. **3**: 304–311.

© 2004 NRC Canada

Behaviour of the ocean DMS(P) pools in the Sargasso Sea viewed in a coupled physical–biogeochemical ocean model[1]

Yvonnick Le Clainche, Maurice Levasseur, Alain Vézina, John W.H. Dacey, and François J. Saucier

Abstract: The dimethylsulfide (DMS) production model NODEM (Northern Oceans DMS Emission Model) was coupled with the water column ocean model GOTM (General Ocean Turbulence Model) that includes a two-equation k–ε turbulence scheme. This coupled physical–biogeochemical ocean model represents a significant improvement over the previous uncoupled version of NODEM that was driven by a diagnostic vertical mixing scheme. Using the same set of biogeochemical parameters, the coupled model is used to simulate the annual cycles of 1992 and 1993 at Hydrostation S in the Sargasso Sea. The better reproduction of the turbulent mixing environment corrects some deficiencies in nitrogen cycling, especially in the seasonal evolution of the nutrient concentrations. Hence, the coupled model captures the late-winter chlorophyll- and DMS(P)-rich blooms. It is also more adept at reproducing the vertical distribution of chlorophyll and DMS(P) in summer. Moreover, the DMS pool becomes less dependent on parameters controlling the nitrogen cycle and relatively more sensitive to parameters related to the sulfur cycle. Finally, the coupled model reproduces some of the observed differences in DMS(P) pools between 1992 and 1993, the latter being an independent data set not used in calibrating the initial version of NODEM.

Résumé : Le modèle NODEM (« Northern Oceans DMS Emission Model ») de production de dimethylsulfide (DMS) a été couplé avec le modèle 1-D d'océan GOTM (« General Ocean Turbulence Model »), qui inclue un schéma de la turbulence océanique du second ordre de type k–ε. Ce modèle couplé physique et biogéochimique constitue une amélioration significative de la précédente version non couplée de NODEM, qui s'appuyait sur un schéma diagnostique pour le mélange vertical. Reprenant les mêmes paramètres biogéochimiques, le modèle couplé a été utilizé pour simuler le cycle saisonnier des années 1992 et 1993 à la station S en mer des Sargasses. La meilleure prise en compte de l'aspect turbulent du mélange océanique corrige certains défauts dans la représentation du cycle de l'azote, en particulier l'évolution saisonnière des concentrations en nutriments. Le modèle couplé capture maintenant les floraisons phytoplanctoniques de fin d'hiver et les pics en chlorophylle et en DMS(P) qui les caractérisent. Il améliore également la représentation des distributions verticales de chlorophylle et de DMS(P) en été. De plus, le réservoir de DMS est moins dépendant des paramètres contrôlant le cycle de l'azote, et relativement plus sensible aux paramètres reliés au cycle du souffre. Finalement, le modèle couplé reproduit certaines des différences observées entre 1992 et 1993 dans les réservoirs de DMS(P), la dernière année constituant un jeu de données indépendant qui n'a pas été utilizé pour la calibration de la version initiale de NODEM.

Introduction

Dimethylsulfide (DMS) is the most abundant form of volatile organic sulfur in the ocean. It results from the enzymatic cleavage of dimethylsulfoniopropionate (DMSP) (Malin and Kirst 1997), which is an organic sulfur compound produced by many phytoplankton species (Keller 1989). The ventilation of DMS is the largest known natural source of atmospheric sulfur (Bates et al. 1992; Andreae and Crutzen 1997). The most recent estimates (Kettle and Andreae 2000)

Received 24 March 2003. Accepted 20 November 2003. Published on the NRC Research Press Web site at http://cjfas.nrc.ca on 23 June 2004.
J17406

Y. Le Clainche[2] and M. Levasseur. Québec-Océan, Département de Biologie, Université Laval, Pavillon Alexandre-Vachon, Québec, QC G1K 7P4, Canada.
A. Vézina. Fisheries and Ocean Canada, Bedford Institute of Oceanography, Dartmouth, NS B2Y 4A2, Canada.
J.W.H. Dacey. Department of Biology, Woods Hole Oceanographic Institution, Redfield 3 MS32, Woods Hole, MA 02543, U.S.A.
F.J. Saucier. Fisheries and Ocean Canada, Maurice Lamontagne Institute, 850 route de la Mer, Mont-Joli, QC G5H 3Z4, Canada.

[1]This paper is part of the proceedings of the Third International Symposium on Biological and Environmental Chemistry of DMS(P) and Related Compounds, held in Rimouski (Québec), 26–28 September 2002.
[2]Corresponding author (e-mail: yvonnick.leclainche@giroq.ulaval.ca).

 doi: 10.1139/F04-027 © 2004 NRC Canada

of DMS emission from the world's ocean range from 15 × 10^{12} to 33 × 10^{12} g S·year^{-1}, about one-third of global anthropogenic sulfur emissions (Rodhe 1999). Because the residence time of DMS sulfur in the atmosphere is longer than that of anthropogenic sulfur, marine DMS emissions contribute approximately 40% of the global atmospheric sulfur burden (Chin and Jacob 1996). However, sea surface DMS concentrations and emissions show wide variations over time and space (Kettle and Andreae 2000), which result from complex biological cycling in a highly dynamical physical environment.

In the marine atmosphere, DMS is oxidized to form non-sea-salt sulfate and methanesulfonate aerosols (Andreae and Crutzen 1997), which affect the radiative balance of the earth. These aerosols can have direct effects by absorbing and reflecting incoming solar radiation (Mitchell et al. 1995). They can also have indirect effects by acting as cloud condensation nuclei, thereby changing the microphysical properties of clouds, in particular increasing their albedo (Falkowski et al. 1992; Clarke et al. 1998). Consequently, DMS emissions may have a cooling effect on climate that partly counteracts the warming effect of greenhouse gases. Moreover, Charlson et al. (1987) have postulated that an increase in solar irradiance makes phytoplankton produce more DMS. They have proposed a negative feedback between oceanic DMS and climate involving DMS emission – cloud condensation nuclei – cloud albedo – solar radiation – temperature. Both empirical analysis (Foley et al. 1991; Lawrence 1993) and regional (Gabric et al. 1998, 2001) and global (Bopp et al. 2003) modeling studies to assess this DMS–climate feedback have shown a small but nonnegligible negative feedback on warming. Nevertheless, the hypothesis formulated by Charlson et al. (1987), known as the CLAW hypothesis, is still under investigation, since the response of DMS production in surface waters to modifications of climatic factors is not understood (Simó 2001).

The first-order impact of climate change will be on air–sea heat fluxes, temperature, wind stress, and consequently the stratification of the upper ocean (Houghton et al. 2001). Mixing in the upper ocean depends strongly on wind and temperature and controls marine ecosystem dynamics (Mann and Lazier 1991), including the biogenic production and vertical distribution of particulate DMSP ($DMSP_p$) and DMS (e.g., Simó and Pedrós-Alió 1999; Jodwalis et al. 2000; Simó et al. 2002). Clearly, short-duration events in the ecosystem at low levels are very important and depend critically on the accurate representation of turbulent quantities such as the depth of the mixed layer and temperature to understand the ocean DMS production and its response to climate change.

We have developed a one-dimensional DMS production model based on an ecosystem model. This model, called NODEM for Northern Oceans DMS Emission Model (Lefèvre et al. 2002), has been calibrated in the Sargasso Sea using measured time series of DMS(P) collected in 1992 at Hydrostation S (32°10′N, 64°30′W) by Dacey et al. (1998). The vertical diffusivity profiles needed to run this model were computed by a direct parameterization (Denman and Gargett 1983). This diagnostic approach used semimonthly density profiles observed at BATS station (31°50′N, 64°10′W) and linearly interpolated for each day of 1992 and winds recorded at the Bermuda airport weather station. This type of parameterization cannot reproduce adequately the dynamics of the mixed layer, especially its response to rapid changes in atmospheric forcing.

To investigate the impact of ocean physics on DMS production, we constructed a one-dimensional coupled physical–biogeochemical ocean model by coupling NODEM with GOTM (General Ocean Turbulence Model) (Burchard et al. 1999; http://www.gotm.net), a water column ocean model that includes a two-equation turbulence parameterization scheme. The different components of the coupled GOTM–NODEM model are described in the next section. The main goal of this study was to validate this new coupled model. Thus, we performed a new simulation at the Hydrostation S site for 1992, comparable with the previous one performed with the uncoupled version of NODEM (Lefèvre et al. 2002). We used the same set of parameters that were adjusted in the 1992 uncoupled simulation. But the vertical turbulent exchange processes are now simulated by GOTM accordingly to its second-order turbulent closure scheme. This allows the examination of the impact of this more realistic representation of vertical mixing on the NODEM predictions of DMS(P) concentrations for 1992. We also conducted the same parametric sensitivity analysis as in the uncoupled version of NODEM to estimate the impact of wind-induced turbulence on the DMS(P) pools simulated. Finally, we validated NODEM on a second complete annual cycle (1993), independent of the annual cycle used to calibrate the initial NODEM model.

Description of the coupled model

Physical ocean model

GOTM is a one-dimensional numerical model of the ocean water column that implements a number of standard turbulence closure schemes for accurate simulation of vertical turbulent exchange processes in the marine environment (Burchard et al. 1999; http://www.gotm.net). For this study, we chose the widely used k–ε turbulence closure scheme (Burchard and Baumert 1995; Burchard and Petersen 1999). The turbulent kinetic energy k and the dissipation rate ε are calculated via prognostic equations, which consider turbulence generation by wind, buoyancy, and shear productions, as well as dissipation and turbulent diffusion. These equations can be found in the reference GOTM technical report (Burchard et al. 1999).

It is assumed that all tracers (temperature, nutrients, phytoplankton, etc.) have the same eddy diffusivity ν_t, which is based on the assumption of fully developed turbulence. The eddy diffusivity ν_t is function of the turbulent kinetic energy k, the normalized dissipation rate ε, and a nondimensional stability function c_μ that is calculated following the method of Kantha and Clayson (1994). We use also the parameterization derived from Large et al. (1994) to promote increased mixing induced by shear instability and internal wave activity under stably stratified situations (Kantha and Clayson 1994), such as summer conditions in the Sargasso Sea. When k becomes smaller than 10^{-6} m^2·s^{-2} (diagnostic for stable stratification), the eddy diffusivity ν_t is calculated as the sum of a shear-induced diffusivity ν_t^{SI} (modeled as a

© 2004 NRC Canada

Fig. 1. Schematic view of the NODEM model structure. The black boxes represent the six nitrogen compartments of the model and the solid black arrows indicate the nitrogen fluxes among these compartments. The shaded ellipses represent the three sulfur pools (the $DMSP_p$ pool is included in phytoplankton). The two additional trapezoids illustrate free sulfate (S) and dimethyl sulfoxide (DMSO), which represent sinks for DMS and $DMSP_d$. The shaded arrows indicate the sulfur fluxes among the five sulfur pools. The shaded broken arrows illustrate the influence of physical factors.

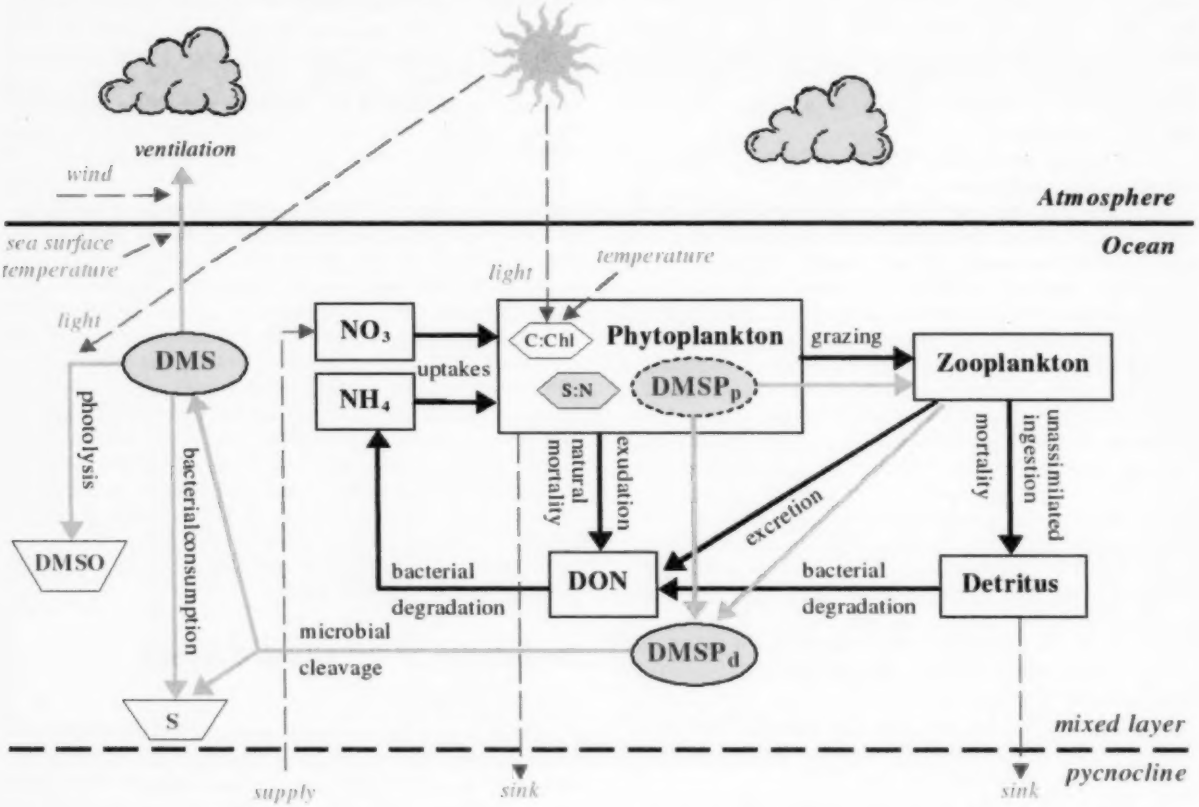

strongly decreasing function of the Richardson number gradient) and a constant internal wave-induced diffusivity ν_t^{IW} (10^{-4} $m^2 \cdot s^{-1}$ for tracers).

Ecosystem and DMS(P) cycle model

NODEM is an ecosystem model based on nitrogen fluxes that also simulates the DMS(P) cycle. Its initial uncoupled version is discussed in detail in Lefèvre et al. (2002). For the coupling with the physical ocean model, two distinct modules for the ecosystem and the DMS(P) cycle have been integrated into the modular structure of GOTM. The ecosystem module computes primary production and the nitrogen fluxes among six compartments: phytoplankton, microzooplankton, detritus, dissolved organic nitrogen (DON), ammonium (NH_4^+), and nitrate (NO_3^-). The DMS(P) cycle module simulates three sulfur components: $DMSP_p$, dissolved DMSP ($DMSP_d$), and DMS. The scheme presented sums up the main characteristics of the NODEM model (Fig. 1).

The biogeochemical tracers are introduced in GOTM using the general equation

$$(1) \qquad \frac{\partial X}{\partial t} - \frac{\partial}{\partial z}\left(Xw + \nu_t \frac{\partial X}{\partial z}\right) = P(X) - S(X)$$

For a tracer X, the turbulent flux $\nu_t \frac{\partial X}{\partial z}$ is calculated as the product of the eddy diffusivity ν_t with the vertical gradient of this tracer. The vertical movement of the tracer (e.g., sedimentation) is related to the vertical velocity w. The terms $P(X)$ and $S(X)$ on the right-hand side of the equation represent the sum of the production sources and the sum of the sinks, respectively. The complete equations for all of the state variables implemented in NODEM are presented in Appendix A. Thereafter, we recall the main characteristics of NODEM, which is fully described in Lefèvre et al. (2002).

The primary production computed by the ecosystem module is controlled by (*i*) photosynthetically available radiation, (*ii*) NO_3^- availability determined by vertical mixing from below (new production), (*iii*) NH_4^+ remineralized in the euphotic zone (regenerated production), and (*iv*) ambient water temperature. The underwater light field in the euphotic zone that is used to compute the photosynthetic activity is calculated from 400–700 nm by a spectral module (Sathyendranath and Platt 1988). The model assumes that, in oligotrophic waters like in Bermuda, most of the mortality is due to microzooplankton grazing, whereas natural mortality resulting from cell lysis represents a minor contribution (Bissett et al.

© 2004 NRC Canada

1994). Dead phytoplankton is instantaneously routed to the dissolved pool assuming that cell lysis occurs rapidly. The grazing function assumes a high affinity of microzooplankton for phytoplankton (Bissett et al. 1994), that is, maximal grazing rates are obtained at low phytoplankton concentrations (low half-saturation constant). The unassimilated part (30%) of the ingested nitrogen (Doney et al. 1996) is channeled to the detritus pool. Microzooplankton nitrogen is lost through mortality (sum of predation and export) to the detritus pool and excretion to the DON pool. Sloppy feeding (dissolved organic matter release by cell rupture during grazing) is considered to be included in the excretion rate (Fasham et al. 1990). Detrital nitrogen and DON are remineralized to DON and NH_4^+, respectively.

$DMSP_p$ is produced by phytoplankton proportionally to primary production through the S_{DMSP}:N cell quota that varies with time and depth (see below). Three processes lead to the release of $DMSP_d$ in the water: phytoplankton cell lysis, phytoplankton exudation, and microzooplankton excretion. Potential release of $DMSP_d$ by cells rupturing during feeding is included in our excretion term. In the absence of information about the exudation of DMSP relative to that of DON, the exudation rate for DMSP is set as the same as for DON. It is assumed that all of the $DMSP_p$ grazed by microzooplankton is excreted directly to the dissolved pool (Lefèvre et al. 2002). Thus, there is no accumulation of $DMSP_p$ into microzooplankton or into detritus produced by microzooplankton. $DMSP_d$ undergoes microbial degradation either to DMS or to other sulfur compounds ("S" sink on Fig. 1). The microbial DMS yield (percentage of $DMSP_d$ cleaved to DMS) is set at 40% and includes both bacterial and algal conversion. Finally, DMS is lost through bacterial consumption, photolysis, and ventilation to the atmosphere.

We used the same set of parameters for both nitrogen and sulfur cycling, which were adjusted in the 1992 uncoupled simulation. They are fully discussed in Lefèvre et al. (2002) and are summed up in Appendix A (Table A1).

Seasonal variations of parameters

The initial work with the uncoupled NODEM (Lefèvre at al. 2002) found it necessary to impose seasonal and depth variations on some key parameters to reproduce the main characteristics of the chlorophyll *a* (Chl *a*) (Michaels and Knap 1996) and DMS(P) data (Dacey et al. 1998) in the Sargasso Sea. This approach was retained in the coupled model. The varying parameters are the phytoplankton cell and detritus sinking rates, the C:Chl cell ratio, and the S_{DMSP}:N cell ratio. Their variations aim to simulate the influence of seasonal change in phytoplankton composition. In winter and early spring, when vertical mixing enhances the supply of nutrients, the phytoplankton community is dominated by larger algae (higher sinking rates), which are characterized by low C:Chl ratio and low S_{DMSP}:N quota. In the summer stratified and stable waters, the phytoplankton community is dominated by smaller algae (lower sinking rates), which are characterized by higher C:Chl ratio and S_{DMSP}:N quota.

In agreement with the modeling study at BATS of Hurtt and Amstrong (1996), the phytoplankton cells and detritus sinking rates used in NODEM were kept very low throughout the year. However, they vary from 0.01 to 0.1 m·day^{-1} and from 0.02 to 0.2 m·day^{-1}, respectively, and are keyed to the zenithal angle of the sun. In accord with the observations of Malone et al. (1993), the C:Chl cell ratio is forced to vary in surface waters from 50 to 100 mg C·mg Chl^{-1}. This variation follows a sinusoidal function throughout the year, also based on the zenithal angle of the sun. The DMSP quota is known to vary not only among species (Keller 1989) but also with environmental forcing like nutrient availability (Keller et al. 1999). In the model, the surface S_{DMSP}:N quota varies from 0.1 to 0.5 mg S·mg N^{-1} based on a linear function of the surface irradiance at noon, which is highly variable from day to day. For the depth dependence, both the C:Chl ratio and the S_{DMSP}:N quota follow the underwater extinction of the irradiance. As mentioned in Lefèvre et al. (2002), the calibration is based on in situ measurements of S_{DMSP}:Chl ratio at Hydrostation S from the 1992 data set of Dacey et al. (1998) and from the NODEM II cruise (Scarratt et al. 2002). The C:Chl cell ratio converges to 20 mg C·mg Chl^{-1} at the bottom of the euphotic zone (~ 140 m) and the S_{DMSP}:N quota converges to 0.1 mg S·mg N^{-1}. These ranges of variation are unchanged for the simulation of the independent year 1993. We show seasonal mean profiles of the two ratios calculated for January–February–March, April–May–June, July–August–September, and October–November–December of year 1992 in Fig. 2.

The complete formulations for the seasonal variation at the surface and for the variations with depth can be found in Lefèvre at al. (2002). The extreme annual values for the zenithal angle of the sun depend only on geographical location. In contrast, the extreme annual values for the surface irradiance at noon change slightly (<10%) from year to year. They were determined for each year by a standalone run of the radiation spectral model.

Technical characteristics of the simulation

Numerics

Because the focus is on the dynamics within the mixed layer, only the first 250 m of the water column are considered. The vertical discretization is regular with 250 layers of 1 m thickness from the surface to 250 m depth. A further simulation extending over 500 m with 500 vertical levels of 1 m thickness was also performed. Its results, both for the physics and for the ecosystem and the DMS cycle, are identical to the results presented in this study. The vertical resolution is the same for the physical mean flow (u, v, temperature, and salinity) and the biogeochemical (phytoplankton, microzooplankton, detritus, DON, NH_4^+, NO_3^-, $DMSP_p$, $DMSP_d$, and DMS) variables. At each vertical level, they represent the mean value for the 1-m vertical interval and are thus determined at the centres of the interval. The turbulent quantities (k, ε, ν_t, and c_μ) are discretized on the same grid but are positioned at the interface of the intervals.

The simple diffusion equation (general eq. 1) for a mean flow quantity such as tracers is fully implicitly discretized over two time levels. This leads for each transport equation to a system of linear equations with a tridiagonal matrix, which is solved by means of the simplified Gaussian elimination (see GOTM report (Burchard et al. 1999; http://www.gotm.net) for a complete description). This calculation is done in the general transport module of GOTM. The main

© 2004 NRC Canada

Fig. 2. Seasonal mean profiles for January–February–March (JFM), April–May–June (AMJ), July–August–September (JAS), and October–November–December (OND) 1992 for (*a*) C:Chl ratio and (*b*) S_{DMSP}:N quota as simulated by the coupled model.

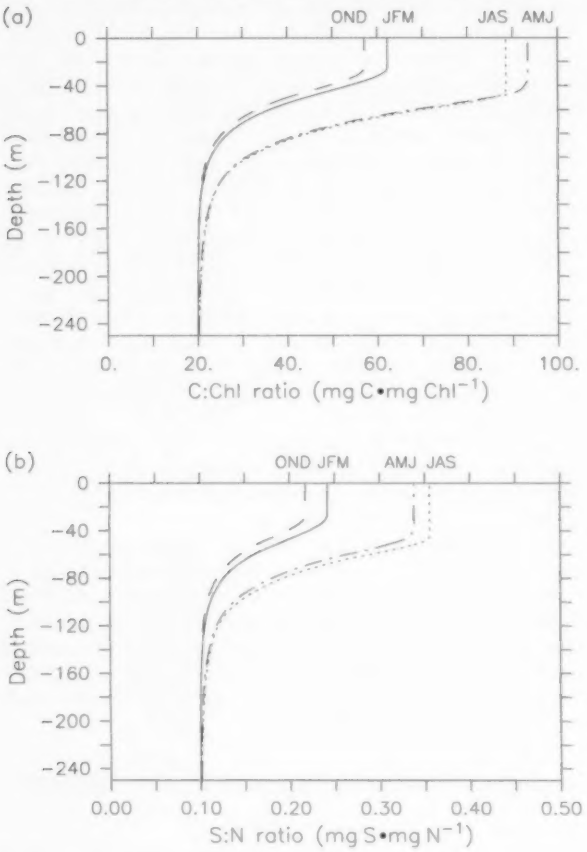

time step for the physics (hydrodynamic equations, temperature and salinity equations, turbulence equations) is 15 min. The time step for the biological processes (primary production and nitrogen fluxes) and the processes involved in the DMS(P) cycle is 1 h. Thus, the source and sink terms (see Appendix A) for each of the biogeochemical variables are computed every four physical time steps. Each calculated budget is directly added to the appropriate variable, independently of the transport equation. However, all of these variables undergo vertical turbulent mixing and sinking (for phytoplankton and detritus) every physical time step (i.e., 15 min). Their transport equations are thus resolved by the general transport module according to zero on the right-hand side of the equation.

The simulation starts on 1 January 1991 and ends on 31 December 1993. Whereas the spinup of the ocean occurs rapidly (on turbulent time scales), the ecosystem model takes a few months to reach near steady state. Thus, the first year is discarded and we concentrate on the solutions for the years 1992 and 1993. This approach differs from the previous uncoupled simulation of NODEM (Lefèvre et al. 2002), where the solution for 1992 was obtained after 2 years of setup with the same 1992 forcing.

Surface forcing and bottom boundary conditions

The wind stresses are calculated through a bulk formula using the daily mean wind velocity components (at 10 m height) given by the NCEP–CDAS reanalysis (Kalnay et al. 1996). The wind is prescribed as a surface boundary condition for the momentum equations.

The net heat flux is split into two components: the shortwave incident solar radiation (reduced by the sea surface albedo) and the nonsolar heat flux including the contributions of the latent, sensible, and infrared radiation. The nonsolar heat flux is considered as a boundary condition at the surface and is calculated through a bulk formula as a function of the sea surface temperature (prognostic), the relative humidity, the air temperature (at 2 m height), the surface air pressure, and the cloud fraction. The daily mean values of the meteorological fields come from the NCEP–CDAS reanalysis (Kalnay et al. 1996). The solar flux is a source term in the temperature equation. A radiation spectral model (Sathyendranath and Platt 1988), already used in the previous uncoupled NODEM simulation, is called by GOTM to compute the surface irradiance and underwater spectral light field from 400 to 700 nm. The spectral model also requires the mean wind speed, the relative humidity, the air temperature, and the cloud fraction. To calculate the impact of aerosols in the Sargasso Sea, the air mass type is set to the maritime tropical one and the horizontal visibility length scale is fixed to 20 km.

The freshwater flux through the surface is not considered in the salinity equation (see below). At the bottom boundary, only the NO_3^- concentration is fixed to its initial value of 40 mg N·m^{-3} (2.8 mmol·m^{-3}) from BATS data (Michaels and Knap 1996). As confirmed by the further simulation extending over 500 m, the bottom boundary conditions have no influence on the euphotic zone (approximately top 150 m), which represents our main domain of interest.

Control of the physical model

The sea surface salinity and the sea surface temperature are restored every day towards daily data interpolated from the Hydrostation S data set (obtained via http://www.bbsr.edu) reported in Knap et al. (1993, 1994, 1995, 1997). The sea surface salinity relaxation replaces the effect of the surface freshwater flux, which is more accurate than attempting to specify freshwater flux. The sea surface temperature relaxation corresponds to a first-order Taylor expansion of the total surface net heat flux around sea surface temperature and acts as a flux correction.

The depth profiles of salinity and temperature from the Hydrostation S data set, interpolated both in time (to obtain daily profiles) and over depth (to obtain vertical profiles at 1-m resolution), are also used to control the physical model. The restoring towards temperature and salinity observations on the whole water column (250 m) is done with a relaxation time constant of 10 days. This diagnostic method accounts for the effects of lateral fluxes of heat and salt (via horizontal advection/diffusion) that cannot be represented explicitly by one-dimensional models.

Initialization

The physical model is initialized with temperature and salinity profiles for 1 January 1991, interpolated from the data

© 2004 NRC Canada

set at Hydrostation S. The initial NO_3^- concentration profile is taken from BATS data (Michaels and Knap 1996). The phytoplankton concentration is set to 1 mg N·m^{-3} from surface to 150 m depth and 0.1 mg N·m^{-3} below. The microzooplankton is set to 0.1 mg N·m^{-3} from surface to 150 m depth and 0.01 mg N·m^{-3} below. The $DMSP_p$ concentration is set to 0.1 mg S·m^{-3} from surface to 150 m depth and 0.01 mg S·m^{-3} below following the phytoplankton profile according to a constant S:N ratio of 0.1 mg S·mg N^{-1}. The $DMSP_d$ and DMS concentrations, as well as all of the others variables, are set to zero. Tests with different initial conditions have showed no sensitivity.

Results and discussion

The annual cycles of upper ocean temperature (from the surface to 250 m depth) simulated by GOTM for 1992 and 1993 are shown in Fig. 3*b*. The temperature data from Hydrostation S (Knap et al. 1993, 1994, 1995, 1997), interpolated to the model grid and for each day, are shown for comparison in Fig. 3*c*. Not surprisingly, given the use of relaxation, the simulated temperature structures of the upper ocean for both 1992 and 1993 are close to the observed structures. In contrast with the classic diagnostic of the mixed layer depth based on the 0.5 °C temperature deviation from the surface temperature (used in Lefèvre et al. 2002), the turbulent mixed layer depth is defined as the depth where turbulent kinetic energy decreases to less than 10^{-6} m^2·s^{-2} (the solid line in Fig. 3*b* indicates that depth). This approach provides a dynamically based view of the mixed layer variability and better visualizes the short-term mixing events related to the high variability of the wind forcing (shown in parallel in Fig. 3*a*).

Impact of prognostic turbulent mixed layer modeling on the NODEM simulation (1992)

The coupled model simulates two deep vertical mixing events during winter 1992 in mid-February and at the end of March (Fig. 3*b*). Strong winds induce significant mixing below the nitracline, producing an input of nutrients in the upper ocean from depth (Fig. 4*a*). Primary production is enhanced and two short phytoplankton blooms develop (Fig. 5*b*). This pattern is in good agreement with the observations of Chl *a* (Fig. 5*a*) at the Bermuda BATS station near Hydrostation S (Michaels and Knap 1996). Because we use winds from the NCEP reanalysis that are daily means for a relatively large area (grid cell of 1.85° in longitude and 1.90° in latitude centred on the position 31.42°N, 63.75°W), the timing of local events cannot be captured very precisely. This may introduce a time lag between the simulated and observed blooms (Fig. 5*d*). Moreover, simulated Chl *a* concentrations are overestimated near the bottom of the mixed layer. In contrast, simulated Chl *a* concentrations are underestimated in the top 50 m. Because phytoplankton concentration as nitrogen is maximum in the top 50 m of the water column, this feature may result from the C:Chl ratio profile calculated for the winter season. The surface C:Chl ratio may be too high, whereas the threshold of 20 mg C·mg Chl^{-1} may be too low at depth. High vertical mixing during this period tends to homogenize phytoplankton community structure in the vertical. The use of the irradiance profile to simulate the depth variation in C:Chl may overestimate the vertical structure, as irradiance is not influenced by the mixing.

Nevertheless, the simulation of two winter blooms as observed represents a major improvement compared with the previous uncoupled simulation of NODEM based on a diagnostic mixing model, which was unable to capture the episodic winter nutrient inputs and the associated phytoplankton blooms (Figs. 4*b*, 5*c*, and 5*d*). On the contrary, the uncoupled NODEM model simulated a constant vertical gradient in the nutrient fields. Without changing any of the ecosystem parameters, the coupling with the ocean turbulence model allows one to reproduce the dynamics of nutrients in winter (Lipschultz 2001). This has repercussions on the $DMSP_p$ and DMS concentrations simulated during winter. In accordance with the data of Dacey et al. (1998) (Figs. 6*a* and 7*a*), the coupled model simulates a peak of $DMSP_p$ during February 1992 (Fig. 6*b*) followed by an increase in DMS (Fig. 7*b*). Actually, the observations show two short peaks, but this difference may also result from the inaccuracy of the wind forcing used. As mentioned by Dacey et al. (1998), the peak of $DMSP_p$ is linked to increases in primary production and phytoplankton biomass, and the rapid response of the DMS pool results from the development of microzooplankton biomass and associated grazing. The coupled model reproduces this dynamic initiated by the deep winter vertical mixing event. This was not captured by the uncoupled NODEM simulation (Figs. 6*c* and 7*c*).

The summer period is characterized by strong stratification and typically a 5- to 20-m deep mixed layer (Fig. 3*b*). Nutrients show very low surface concentrations (Fig. 4*a*) and negligible NO_3^- concentrations in the euphotic zone. The nitrogen cycle is supported by efficient recycling of the dissolved nitrogen pool to NH_4^+ via the microbial loop (Michaels et al. 1994). Thanks to the depth variation of the C:Chl ratio, the development of a subsurface Chl maximum near 100 m was already reproduced in the uncoupled NODEM simulation (Fig. 5*c*). But with better resolved mixing into the euphotic zone, the coupled model simulates higher biomass and Chl levels (Fig. 5*b*), which are closer to the observations. In agreement with the data of Dacey et al. (1998), it also reproduces the $DMSP_p$ and DMS subsurface maxima around 40 m that are well above the Chl *a* maximum, in particular during July 1992. In the uncoupled NODEM simulation, the diagnostic model generated not enough vertical mixing under stable conditions. Moreover, this simulation was characterized by unrealistically high concentrations of NH_4^+, which dominate the nutrient field (Fig. 4*b*) and stimulate large regenerated production. The rapid turnover prevented an increase of the phytoplankton biomass, but on the other hand, the microzooplankton biomass was enhanced within the mixed layer. Higher concentrations of DMS were thus simulated by the uncoupled version of NODEM in the top 20 m of the ocean and appeared strongly dependent on the variations of the S:N surface ratio. Coupling NODEM with a prognostic turbulent mixing model allows us to correct this weakness of the uncoupled simulation.

Finally, the better parameterization of the turbulent mixing regime and mixed layer depth dynamics affects the dynamics of the nitrogen cycle both in winter and in summer and consequently the variations in the DMS(P) pools. In comparison with the previous uncoupled NODEM version,

© 2004 NRC Canada

Fig. 3. Annual cycle for 1992 and 1993 of (*a*) wind forcing at sea surface from NCEP reanalysis (Kalnay et al. 1996), (*b*) ocean temperature in the upper 250 m and turbulent mixed layer depth (solid line added) as simulated by the coupled model, and (*c*) ocean temperature in the upper 250 m as interpolated from the Hydrostation S data set (Knap et al. 1993, 1994, 1995, 1997).

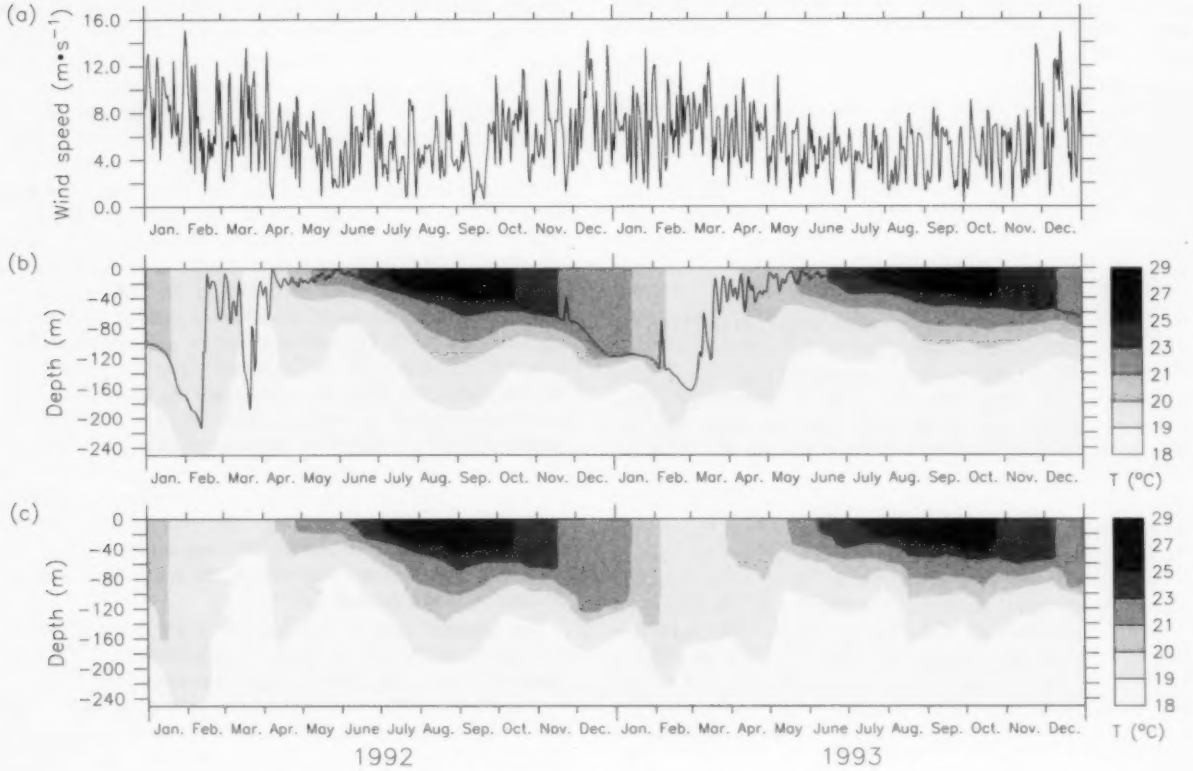

Fig. 4. Annual cycle for 1992 and 1993 of nutrient (NO_3^- and NH_4^+) concentration in the upper 250 m ocean simulated by (*a*) the coupled GOTM–NODEM model and (*b*) the uncoupled NODEM, only for 1992.

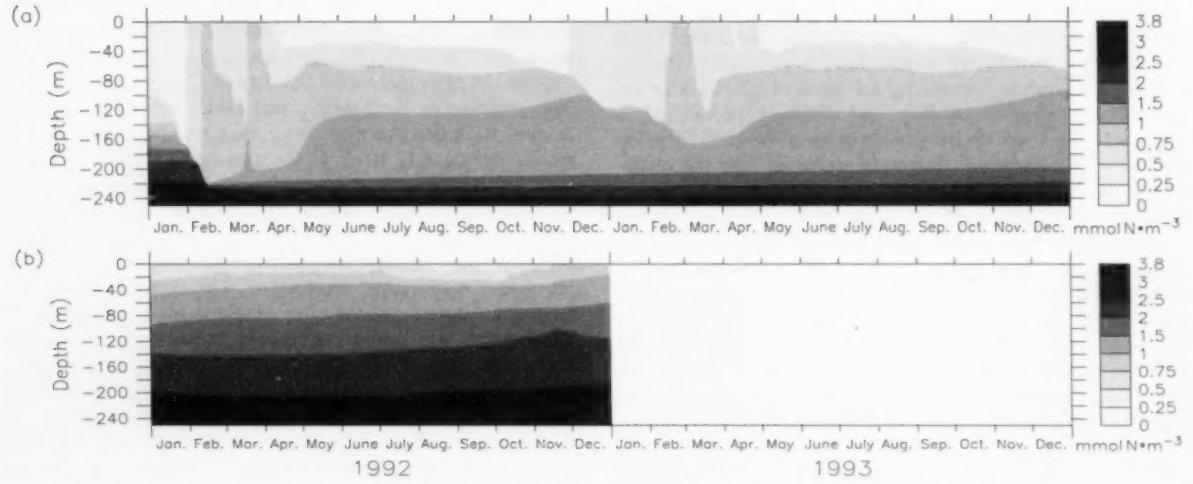

the coupled GOTM–NODEM model simulates a more active system during late winter blooms and a less active system that is nutrient limited in summer. This results from a better reproduction of the seasonal evolution of the nutrient field within the euphotic zone.

Impact on parametric sensitivity of NODEM

The parametric sensitivity analysis with the uncoupled NODEM model (Lefèvre et al. 2002) showed that $DMSP_p$ was dependent mostly on parameters controlling phytoplankton biomass, whereas DMS was dependent mostly on parame-

© 2004 NRC Canada

Fig. 5. Annual cycle for 1992 and 1993 of Chl *a* concentration in the upper 250 m of ocean (*a*) interpolated from the BATS data set (Michaels and Knap 1996), (*b*) simulated by the coupled model, and (*c*) simulated by the uncoupled NODEM and of Chl *a* in (*d*) 0- to 140-m integrated stocks interpolated from BATS data (red line), simulated by the coupled model (blue line), and simulated by the uncoupled NODEM, only for 1992 (green line).

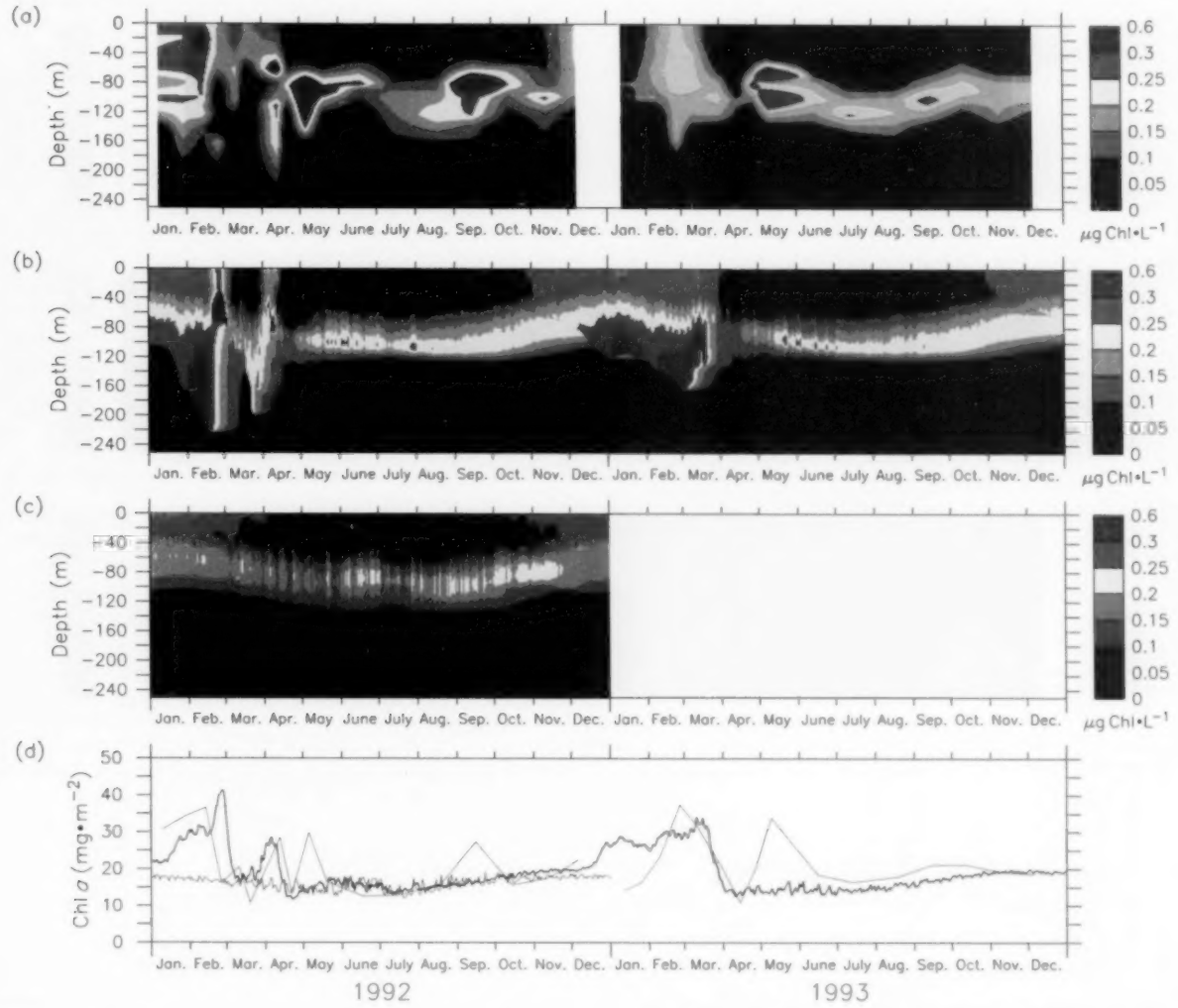

ters controlling phytoplankton productivity. To estimate the impact of the turbulent mixing model on the major biological processes controlling the $DMSP_p$ and DMS pools, we conduct the same parametric sensitivity analysis as in the previous uncoupled study. For each parameter k used by NODEM (see Appendix A, Table A1), we performed two sensitivity simulations with a variation of this single parameter by plus or minus 50%. All of the sensitivity simulations used the same initialization technique as the reference simulation and started on 1 January 1991. As in Lefèvre et al. (2002), we calculated the index of sensitivity S_k of the parameter k on the year 1992 as follows:

$$(2) \qquad S_k = \frac{\left(\overline{\mathrm{DMS(P)}_{k_{max}}} - \overline{\mathrm{DMS(P)}_{k_{min}}}\right)}{\overline{\mathrm{DMS(P)}_k}}$$

where $\overline{\mathrm{DMS(P)}_k}$, $\overline{\mathrm{DMS(P)}_{k_{min}}}$, and $\overline{\mathrm{DMS(P)}_{k_{max}}}$ are the annual DMS or $DMSP_p$ averaged over the upper 60 m and simulated for the reference value of the parameter k, the upper value k_{max} ($1.5 \times k$), and the lower value k_{min} ($0.5 \times k$), respectively.

The sensitivity indices of the 1992 annual $DMSP_p$ and DMS budgets greater than 0.1 are plotted in decreasing order in Figs. 8*a* and 8*b*, respectively. The results are broadly similar to those obtained with the uncoupled version of NODEM (see fig. 9 in Lefèvre et al. 2002). In particular, the most sensitive parameter remains the variable S_{DMSP}:N cell quota. When its minimum and maximum values of variation at the sea surface are changed by 50%, both $DMSP_p$ and DMS budgets are altered by about 100%. However, some notable differences appear between the coupled and the uncoupled mode. In the coupled GOTM–NODEM model, the DMS budget is less dependent on parameters linked to phyto-

© 2004 NRC Canada

Fig. 6. Annual cycle for 1992 and 1993 of $DMSP_p$ concentration in the upper 140 m of ocean (*a*) interpolated from the observation data set of Dacey et al. (1998), (*b*) simulated by the coupled model, and (*c*) simulated by the uncoupled NODEM and of $DMSP_p$ in (*d*) 0- to 140-m integrated stocks interpolated from observations (red line), simulated by the coupled model (blue line), and simulated by the uncoupled NODEM, only for 1992 (green line).

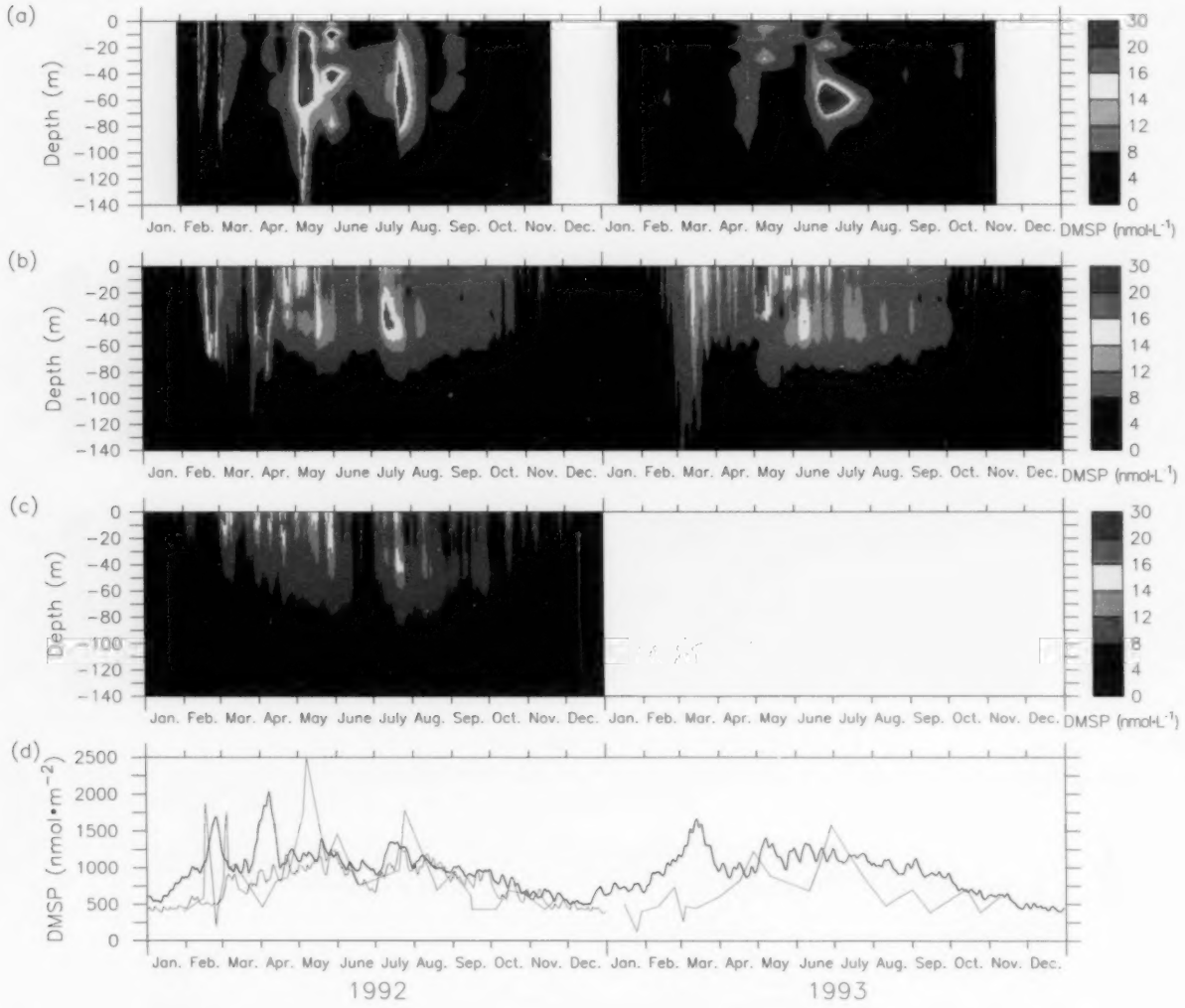

plankton productivity (C:Chl ratio, photosynthetic efficiency, phytoplankton maximum assimilation rate). In contrast with the uncoupled NODEM simulation, the more realistic lower concentration of NH_4^+ simulated by the coupled model (Fig. 4*a*) limits the possible enhancement of regenerated primary production due to those parameters variations. The increase over 0.1 of the DMS sensitivity to parameters linked to the NH_4^+ pool (remineralization of DON, NH_4^+ uptake) confirms this change. In this more nutrient-limited system simulated by the coupled model, the turnover of phytoplankton biomass is weaker during most of the year, especially in the upper 60 m. The production of DMS via the grazing pathway is reduced compared with the uncoupled NODEM simulation. The sensitivity of DMS to parameters related to microzooplankton (grazing half-saturation coefficient, maximum grazing rate, excretion rate, natural mortality) is reduced, whereas the sensitivity of $DMSP_p$ is enhanced. With regard to the reductions of the sensitivity of DMS to the parameters controlling the nitrogen cycle, the parameters involved in DMS removal (DMS bacterial degradation, photolysis) appear to be more important to the variations in the DMS budget. Overall, the coupling with the prognostic turbulent mixing model makes the DMS pool less sensitive to the nitrogen dynamics of the system.

Limitations of the coupled model

Driven by the increase in biomass at the beginning of April, which is coherent with the observations (Fig. 5), the coupled model simulates a large peak of $DMSP_p$ production in the upper ocean that is not present in the observations. However, the local maximum of DMS that develops just af-

© 2004 NRC Canada

Fig. 7. Annual cycle for 1992 and 1993 of DMS concentration in the upper 140 m of ocean (*a*) interpolated from the observation data set of Dacey et al. (1998), (*b*) simulated by the coupled model, and (*c*) simulated by the uncoupled NODEM and of DMS in (*d*) 0- to 140-m integrated stocks interpolated from observations (red line), simulated by the coupled model (blue line), and simulated by the uncoupled NODEM, only for 1992 (green line).

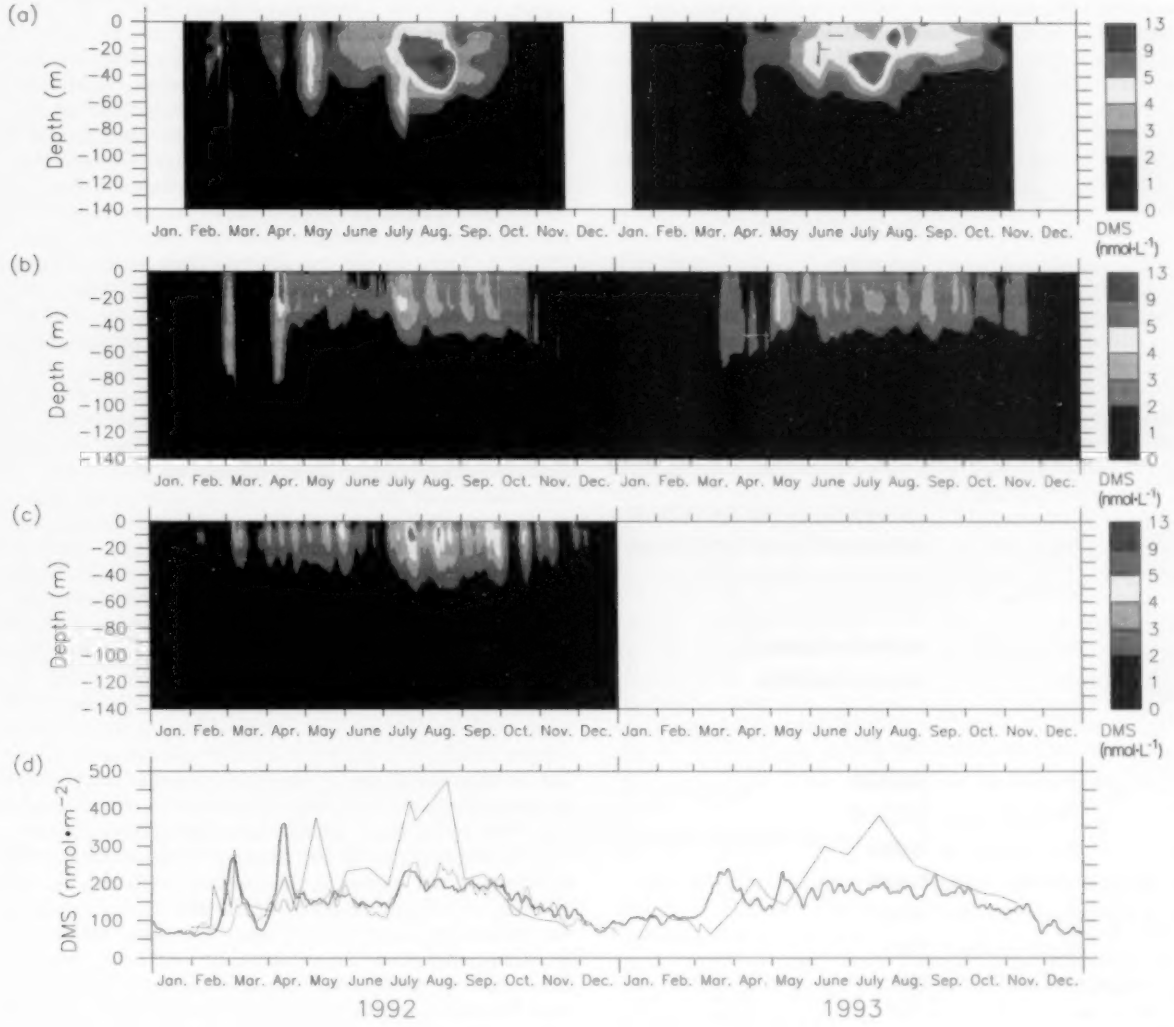

ter is found in the data, but with smaller amplitude. The DMS(P) cycle simulated by the coupled model appears to be too productive during April 1992, especially the production of $DMSP_p$. The very sensitive parameter S:N ratio at the sea surface, which varies according to the surface irradiance at noon, reaches high values during April. Such values do not agree with a phytoplankton community dominated by low DMSP producers, which should dominate during this period (Michaels et al. 1994). This result shows the limitations of our parameterization in reproducing the seasonal effects on community structure.

The coupled model captures the winter blooms but not the subsurface blooms that occur during May and September 1992 and also during May 1993. For these three periods, the temperature contours (Fig. 3*c*) point to important upward displacements of the 19 °C isotherm that characterize the passage of mesoscale eddies (McGillicuddy et al. 1998). The upwelling mechanism associated with such eddies involves NO_3^- injection that stimulates phytoplankton growth (McGillicuddy et al. 1998). The observed subsurface Chl increases may result from this mechanism and thus cannot be reproduced with a one-dimensional model, irrespective of the vertical turbulence representation that is used. A three-dimensional eddy-resolving ocean model is needed to capture this mesoscale variability. The peaks of $DMSP_p$ and DMS observed during May 1992 seem to be also linked to the passage of the eddy. However, the mechanism involved is less clear, since the other subsurface blooms in September 1992 and May 1993 are not accompanied by increases of $DMSP_p$ and especially of DMS.

© 2004 NRC Canada

Fig. 8. Sensitivity index of 1992 annual (*a*) $DMSP_p$ and (*b*) DMS budgets averaged over the upper 60 m when parameters used in the coupled model are varied by ±50%. Black bars indicate positive sensitivity indices (increase of budget when the parameter is increased by 50%) and shaded ones indicate negative indices. Zoo., zooplankton; Phyto., phytoplankton; half-sat., half-saturation coefficient.

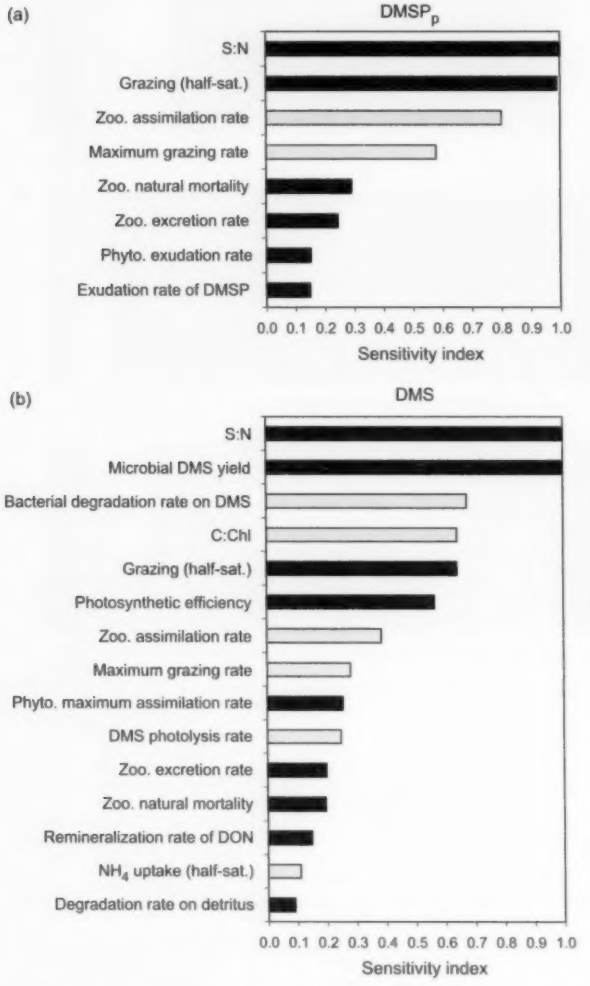

Limitations of parameterizations of DMS dynamics

Despite a more realistic simulation of the summer ecosystem dynamics, the coupled model tends to overestimate $DMSP_p$ concentrations in the top 40 m (Fig. 6*b*) and to underestimate the DMS summer peak (Fig. 7*b*). Considering the large $DMSP_p$ pool simulated in summer, the underestimation of DMS concentration does not result from a lack of $DMSP_p$ synthesis. The simulated $DMSP_d$ pool (not shown), which presents a structure similar to that of DMS, is also not underestimated compared with the data. The weakness of the summer DMS peak may result from incorrect modeling of the DMS budget.

Our sensitivity analysis has confirmed the high sensitivity of DMS concentration to DMS yield (which determined the gross production of DMS from the $DMSP_d$ pool) and to parameters controlling DMS removal (DMS bacterial degradation, photolysis). The DMS yield was fixed at 40% in our model, leading to a high correlation between DMS and $DMSP_d$ variations (not shown) that is not observed in situ (Dacey et al. 1998). Different field studies (Ledyard and Dacey 1996; Simó and Pedrós-Alió 1999; Scarratt et al. 2000) have shown both spatial and temporal variations of the DMS yield. Based on different data in the Northern Hemisphere, Simó and Pedrós-Alió (1999) proposed that DMS yield varies with mixed layer depth. Their asymmetric relationship presents a minimum yield at a mixed layer depth of 15–20 m. These are the depths found from April to September at BATS. The introduction of a variable DMS yield in the model may well be desirable. However, the only published study does not offer a solution to the model underestimate of summer DMS concentrations.

Photolysis is an important sink for DMS in the upper ocean. In the model, its parameterization is based on visible radiation following Kieber et al. (1996). However, recent field studies (Toole et al. 2003) indicate the predominance of UV radiation on the photochemistry of DMS. This suggests an overestimation of the photolysis in summer by our model (R-C. Bouillon, Department of Oceanography, Dalhousie University, Halifax, NS B3H 4J1, Canada, personal communication). The UV radiation is not yet computed in our spectral module. A specific modeling study is needed to test the influence of a photolysis parameterization based on UV radiation.

The bacterial degradation rate on DMS is also one of the most sensitive parameter for DMS (Fig. 8*b*). It is fixed to 0.4·day^{-1} in NODEM. This value is in the range of the values estimated by Kiene (1992) and Kiene and Linn (2000) in the Sargasso Sea, but it may display a seasonal variability (Ledyard and Dacey 1996). In contrast with the zero-dimensional DMS model developed by Gabric et al. (1993), bacteria are not explicitly modeled in NODEM. Because they play an important role in the production and consumption of volatile sulfur and are under the influence of physical forcing (temperature, UV radiation, mixing), they may contribute to the variability of the system (Simò 2001). However, the understanding and quantification of their exact role need to be studied thoroughly in both field and numerical modeling studies.

Validation with independent data (1993)

The coupled model predictions for the independent 1993 data using the same ecosystem parameters as for the calibration year 1992 are similar to the 1992 results and reproduce the main structure of the 1993 annual cycle. However, we should note that the variations of the S:N ratio and the depth dependence of the C:Chl ratio are changed because they are linked to the surface irradiance, which differs between years. The coupled model succeeds in capturing part of the interannual variability between 1992 and 1993. Both simulations and observations (Michaels and Knap 1996) point to only one deep winter mixing event occurring in 1993 leading to a single winter phytoplankton bloom (Fig. 4*d*). This contrasts with the multiple blooms observed and simulated for 1992.

© 2004 NRC Canada

Moreover, the lower depth of winter mixing in 1993 is also well captured. On the other hand, the model does not reproduce the higher intensity of the subsurface Chl maximum in summer 1993 than in summer 1992.

The same limitations are found in this second year of simulation as in the first one. The simulated winter bloom shows a time lag compared with the observations, and the vertical profile of Chl *a* shows an important gradient with subsurface values higher than near the surface. The subsurface increase of Chl *a* in May 1993 that is possibly linked to the passage of an eddy (see Fig. 3) is not reproduced. The $DMSP_p$ and DMS concentrations reach a peak in May 1993, when the S:N surface ratio calculated reaches its highest values. An increase of $DMSP_p$ is observed in May 1993 but is not as marked as in the model simulation.

The simulated 0- to 140-m integrated stocks of $DMSP_p$ and DMS are comparable between 1992 and 1993, whereas the observations show significant differences. The observed $DMSP_p$ pool is smaller in 1993; consequently, the model overestimation is stronger for 1993 than for 1992. However, in accord with the observations of Dacey et al. (1998), the intensity of the $DMSP_p$ and DMS peaks simulated in winter and spring 1993 is reduced in comparison with 1992. In summer, the observed DMS peak is broader (stretched over a longer period) and lower in 1993 than in 1992. The model differs little in its simulation of summer dynamics between these two years. However, because the model simulates a broader and lower DMS peak than observed, it is closer to the 1993 summer DMS data than to the 1992 summer data.

These comparisons indicate that using prognostic mixed layer physics is not sufficient to reproduce all of the interannual variability in the DMS pool dynamics. Improvements of the ecosystem model itself are required. The present parameterization used to mimic seasonal changes in phytoplankton composition is obviously a simplification that limits our model. The problems described above occurred equally in both years of the simulation (i.e., variations of the C:Chl ratio with depth, high variability of the S:N ratio, underestimation of summer DMS peak). Moreover, the model does not simulate the lower $DMSP_p$ concentrations measured in 1993 even though it reproduces the Chl levels correctly for both years. The S:N ratio is the most sensitive parameter of the model, but processes controlling the S_{DMSP}:N quota are not yet well known (Simò 2001). The parameterization of this ratio should be a priority for future field and modeling work to replace the semiempirical approach. Incidentally, the complex variations of the phytoplankton community structure need also to be addressed by a more sophisticated implicit parameterization (Denman 2003) or ultimately by a functional group approach. The representation of the role of bacteria needs also to be investigated in detail.

In summary, we have constructed a new one-dimensional coupled physical–biogeochemical ocean model by coupling the DMS production model NODEM with the water column ocean model GOTM that includes a two-equation k–ε turbulence closure scheme (Burchard et al. 1999). This model proved to be a significant improvement over a previous version of NODEM that was driven by a diagnostic vertical mixing scheme (Lefèvre et al. 2002). Using the same set of biogeochemical parameters as the uncoupled NODEM version, the coupled model GOTM–NODEM was able to improve the simulations of the 1992 time series of DMS(P) collected at Hydrostation S by Dacey et al. (1998). Simply by better reproduction of the mixing environment, the coupled model was able to capture winter phytoplankton blooms largely missed by the uncoupled model. Moreover, the coupled model proved to be more adept at reproducing summer stratification at Hydrostation S and consequently the prediction of the summer vertical structure in phytoplankton biomass and DMS concentration. This points to the importance of high-resolution prognostic physical modeling in reproducing not only the variability in biological–chemical systems that affect DMS(P) concentrations but also their dynamics during stable periods when nutrient recycling dominates. The use of prognostic mixing also changed our view of the model parameters that are most critical to predictions of DMS(P) levels. Compared with the previous version of NODEM, and compared also with most previously published models that use bulk mixing parameterizations (Vezina 2004), parameters related to the sulfur cycle become more important in relation to parameters controlling the nitrogen cycle. A better representation of mixing corrects deficiencies in nitrogen cycling and shifts the sensitivities towards the sulfur parameters. Finally, the coupled model was able to reproduce some of the observed differences in DMS dynamics between 1992 and 1993, the latter being an independent data set not used in developing NODEM. Based on this work, significant improvements in DMS modeling will arise first from developing better parameterizations of the time and space dependence of processes that affect DMS removal, as well as those affecting DMS production (e.g., phytoplankton growth and variability in cell sulfur quota). Secondly, extensions to eddy-resolving three-dimensional modeling should bring some improvements to ocean areas like BATS that are known to be influenced by a strong eddy field.

Acknowledgements

This work was supported in part by the Government of Canada's Climate Change Action Fund and by the Canadian–SOLAS Network (Surface Ocean – Lower Atmosphere Study) of the Natural Sciences and Engineering Research Council of Canada and the Canadian Foundation for Climate and Atmospheric Sciences. The authors wish to thank the entire GOTM project team for the code of GOTM and in particular H. Burchard, K. Bolding, and P.P. Mathieu for their help. We also thank the team of the Bermuda Research Station for the Hydrostation S data set (available from www.bbsr.edu) and the team of the NCEP/NCAR 40-year reanalysis project for atmospheric data. Most of the graphics in this paper were created with the Ferret program. Ferret is a product of NOAA's Pacific Marine Environmental Laboratory (www.ferret.noaa.gov). We are grateful to the two anonymous reviewers for their constructive comments on the first version of this manuscript.

References

Andreae, M.O., and Crutzen, P.J. 1997. Atmospheric aerosols: biogeochemical sources and role in the atmospheric chemistry. Science (Wash., D.C.), **276**: 1052–1058.

© 2004 NRC Canada

Bates, T.S., Lamb, B.K., Guenther, A., Dignon, J., and Stoiber, R.E. 1992. Sulfur emissions to the atmosphere from natural sources. J. Atmos. Chem. **14**: 315–337.

Bissett, W.P., Meyers, M.B., Walsh, J.G., and Muller-Karger, F.E. 1994. The effects of temporal variability of mixed layer depth on primary productivity around Bermuda. J. Geophys. Res. **99**(C4): 7539–7553.

Bopp, L., Aumont, O., Belviso, S., and Monfray, P. 2003. Potential impact of climate change on marine dimethylsulfide emissions. Tellus Ser. B Chem. Phys. Meteorol. **55**: 11–22.

Burchard, H., and Baumert, H. 1995. On the performance of a mixed-layer model based on the k–ε turbulence closure. J. Geophys. Res. **100**(C5): 8523–8540.

Burchard, H., and Petersen, O. 1999. Models of turbulence in the marine environment — a comparative study of two-equation turbulence models. J. Mar. Syst. **21**: 29–53.

Burchard, H., Bolding, K., and Villarreal, M.R. 1999. GOTM — a general ocean turbulence model. Theory, applications and test cases. Tech. Rep. EUR 18745, European Commission.

Charlson, R.J., Lovelock, J.E., Andreae, M.O., and Warren, S.G. 1987. Oceanic phytoplankon, atmospheric sulfur, cloud albedo and climate. Nature (Lond.), **326**: 655–661.

Chin, M., and Jacob, D.J. 1996. Anthropogenic and natural contributions to tropospheric sulfate: a global model analysis. J. Gephys. Res. **101**(D13): 18 691 – 18 699.

Clarke, A.D., Varmer, J.L., Eisele, F., Maudlin, R.L., Tanner, D., and Litchy, M. 1998. Particle nucleation in the tropical boundary layer and its coupling to marine sulfur sources. Science (Wash., D.C.), **282**: 89–92.

Dacey, J.W.H., Howse, F.A., Michaels, A.F., and Wakeham, S.G. 1998. Temporal variability of dimethylsulfide and dimethylsulfoniopropionate in the Sargasso Sea. Deep-Sea Res. I, **45**: 2085–2104.

Denman, K.L. 2003. Modelling planktonic ecosystems: parameterizing complexity. Prog. Oceanogr. **57**(3–4): 429–452.

Denman, K.L., and Gargett, A.E. 1983. Time and space scales of vertical mixing and advection of phytoplankton in the upper ocean. Limnol. Oceanogr. **28**: 801–815.

Doney, S.C., Glover, D.M., and Najjar, R.G. 1996. A new coupled, one-dimensionnal biological–physical model for the upper ocean: applications to the JGOFS Bermuda Atlantic time-series study (BATS) site. Deep-Sea Res. II, **43**(2–3): 591–624.

Falkowski, P.G., Kim, Y., Kolber, Z., Wilson, C., Wirik, C., and Cess, R. 1992. Natural versus anthropogenic factors affecting low-level cloud albedo over the North Atlantic. Science (Wash., D.C.), **256**: 1311–1313.

Fasham, M.J.R., Ducklow, H.W., and McKelvie, S.M. 1990. A nitrogen-based model of plankton dynamics in the oceanic mixed layer. J. Mar. Res. **48**: 591–639.

Foley, J.A., Taylor, K.E., and Ghan, S.J. 1991. Planktonic dimethylsulfide and cloud albedo: an estimate of the feedback response. Clim. Change, **18**: 1–15.

Gabric, A., Murray, N., Stone, L., and Kohl, M. 1993. Modeling the production of dimethylsulfide during a phytoplankton bloom. J. Geophys. Res. **98**(C12): 22 805 – 22 816.

Gabric, A.J., Whetton, P.H., Boers, R., and Ayers, G.P. 1998. The impact of simulated climate change on the air-sea flux of dimethylsulphide in the subantarctic Southern Ocean. Tellus Ser. B Chem. Phys. Meteorol. **50**: 388–399.

Gabric, A.J., Whetton, P.H., and Cropp, R. 2001. Dimethylsulphide production in the subantarctic southern ocean under enhanced greenhouse gas conditions. Tellus Ser. B Chem. Phys. Meteorol. **53**: 273–287.

Houghton, J.T., Ding, Y., Griggs, D.J., Noguer, M., Van der Linden, P.J., and Xiaosu, D. (*Editors*). 2001. Climate change 2001: the scientific basis. Contribution of Working Group I to the Third Assessment Report of the Intergovernmental Panel on Climate Change (IPCC). Cambridge University Press, Cambridge,U.K.

Hurtt, G.C., and Armstrong, R.A. 1996. A pelagic ecosystem model calibrated with BATS data. Deep-Sea Res. II, **43**(2–3): 653–683.

Jodwalis, C.M., Benner, R.L., and Eslinger, D.L. 2000. Modeling of dimethyl sulfide ocean mixing, biological production, and sea-to-air flux for high latitudes. J. Geophys. Res. **105**(D11): 14 387 – 14 399.

Kalnay, E., Kanamitsu, M., Kistler, R., Collins, W., Deaven, D., Gandin, L., Iredell, M., Saha, S., White, G., Woollen, J., et al. 1996. The NCEP/NCAR 40-year reanalysis project. B. Am. Meteorol. Soc. **77**: 437–472.

Kantha, L.H., and Clayson, C.A. 1994. An improved mixed layer model for geophysical applications. J. Geophys. Res. **99**(C12): 25 235 – 25 266.

Keller, M.D. 1989. Dimethyl sulfide production and marine phytoplankton: the importance of species composition and cell size. Biol. Oceanogr. **6**(5–6): 375–382.

Keller, M.D., Kiene, R.P., Matrai, P.A., and Bellows, W.K. 1999. Production of glycine betaine and dimethylsulfoniopropionate in marine phytoplankton. II. N-limited chemostat cultures. Mar. Biol. **135**: 249–257.

Kettle, A.J., and Andreae, M.O. 2000. Flux of dimethylsulfide from the oceans: a comparison of updated data sets and flux models. J. Geophys. Res. **105**(D22): 26 793 – 26 808.

Kieber, D.J., Jiao, J., Kiene, R.P., and Bates, T.S. 1996. Impact of dimethylsulfide photochemistry on methyl sulfur cycling in the Equatorial Pacific Ocean. J. Geophys. Res. **101**(C2): 3715–3722.

Kiene, R.P. 1992. Dynamics of dimethylsulfide and dimethylsulfoniopropionate in oceanic water samples. Mar. Chem. **37**(1–2): 29–52.

Kiene, R.P., and Linn, L.J. 2000. The fate of dissolved dimethylsulfoniopropionate (DMSP) in seawater: tracer studies using ^{35}S-DMSP. Geochim. Cosmochim. Acta, **64**: 2797–2810.

Knap, A.H., Michaels, A.F., Dow, R.L., Johnson, R.J., Gundersen, K., Sorensen, J.C., et al. 1993. Bermuda Atlantic time-series study. BATS Data Rep. B-3. Joint Global Ocean Flux Study. pp. 25–36.

Knap, A.H., Michaels, A.F., Dow, R.L., Johnson, R.J., Gundersen, K., Sorensen, J.C., et al. 1994. Bermuda Atlantic time-series study. BATS Data Rep. B-4. Joint Global Ocean Flux Study. pp. 37–48.

Knap, A.H., Michaels, A.F., Dow, R.L., Johnson, R.J., Gundersen, K., Sorensen, J.C., et al. 1995. Bermuda Atlantic time-series study. BATS Data Rep. B-5. Joint Global Ocean Flux Study. pp. 49–60.

Knap, A.H., Michaels, A.F., Hansell, D., Bahr, F., Bates, N., Becker, S., et al. 1997. Bermuda Atlantic time-series study. BATS Data Rep. B-6. Joint Global Ocean Flux Study. pp. 61–72.

Large, W.G., McWilliams, J.C., and Doney, S.C. 1994. Oceanic vertical mixing: a review and a model with nonlocal boundary layer parameterization. Rev. Geophys. **32**: 363–403.

Lawrence, M.G. 1993. An empirical analysis of the strength of the phytoplankton–dimethylsulfide–cloud–climate feedback cycle. J. Geophys. Res. **98**(D11): 20 633–20 673.

Ledyard, K.M., and Dacey, J.W.H. 1996. Microbial cycling of DMSP and DMS in coastal and oligotrophic seawater. Limnol. Oceanogr. **41**: 33–40.

Lefèvre, M., Vézina, A., Levasseur, M., and Dacey, J.W.H. 2002. A model of dimethylsulfide dynamics for the subtropical North Atlantic. Deep-Sea Res. I, **49**: 2221–2239.

Lipschultz, F. 2001. A time-series assessment of the nitrogen cycle at BATS. Deep-Sea Res. II, **48**(8–9): 1897–1924.

© 2004 NRC Canada

Malin, G., and Kirst, G.O. 1997. Algal production of dimethylsulfide and its atmospheric role. J. Phycol. **33**: 889–896.

Malone, T.C., Pike, S.E., and Conley, D.J. 1993. Transient variations in phytoplankton productivity at the JGOFS Bermuda time series station. Deep-Sea Res. I, **40**: 903–924.

Mann, K.H., and Lazier, R.N. 1991. Dynamics of marine ecosystems, biological–physical interactions in the oceans. Blackwell Scientific Publications, Boston, Mass.

McGillicuddy, J.D.J., Robinson, A.R., Siegel, D.A., Jannasch, H.W., Johnson, R., Dickey, T.D., McNeil, J., Michaels, A.F., and Knap, A.H. 1998. Influence of mesoscale eddies on the new production in the Sargasso Sea. Nature (Lond.), **394**: 263–266.

Michaels, A.F., and Knap, A.H. 1996. Overview of the U.S. JGOFS Bermuda Atlantic time-series study and the Hydrostation S program. Deep-Sea Res. II, **43**(2–3): 157–198.

Michaels, A.F., Knap, A.H., Dow, R.L., Gundersen, K., Johnson, R.J., Sorensen, J.C., Close, A., Knauer, G.A., Lohrentz, S.E., Asper, V.A., et al. 1994. Seasonal patterns of ocean biogeochemistry at the U.S. JGOFS Bermuda Atlantic time-series study site. Deep-Sea Res. I, **41**: 1013–1038.

Mitchell, J.F.B., Johns, T.C., Gregory, J.M., and Tett, S.F.B. 1995. Climate response to increasing levels of greenhouse gases and sulfate aerosols. Nature (Lond.), **376**: 501–504.

Rodhe, H. 1999. Human impact on the atmospheric sulfur balance. Tellus Ser. A–B, **51**: 110–122.

Sathyendranath, S., and Platt, T. 1988. The spectral irradiance field at the surface and in the interior of the ocean: a model for application in oceanography and remote sensing. J. Gephys. Res. **98**(C8): 9270–9280.

Sathyendranath, S., and Platt, T. 1989. Computation of aquatic primary production: extended formalism to include effect of angular and spectral distribution of light. Limnol. Oceanogr. **34**: 188–198.

Sathyendranath, S., Platt, T., Caverhill, C.M., Warnock, R.E., and Lewis, M.R. 1989. Remote sensing of oceanic primary production: computations using a spectral model. Deep-Sea Res. I, **36**: 431–453.

Scarratt, M., Cantin, G., Levasseur, M., and Michaud, S. 2000. Particle size-fractionated kinetics of DMS production: where does DMSP cleavage occur at the microscale? J. Sea Res. **43**(3–4): 245–252.

Scarratt, M., Levasseur, M., Michaud, S., Cantin, G., Gosselin, M., and de Mora, M.J. 2002. Influence of phytoplankton taxonomic profile on the distribution of dimethylsulfide and dimethylsulfoniopropionate in the northwest Atlantic. Mar. Ecol. Prog. Ser. **244**: 49–61.

Simó, R. 2001. Production of atmospheric sulfur by oceanic plankton: biogeochemical, ecological and evolutionary links. Trends Ecol. Evol. **16**: 287–294.

Simó, R., and Pedrós-Alió, C. 1999. Role of vertical mixing in controlling the oceanic production of dimethyl sulphide. Nature (Lond.), **402**: 396–397.

Simó, R., Archer, S.D., Pedrós-Alió, C., Gilpin, L., and Stelfox-Widdicombe, C.E. 2002. Coupled dynamics of dimethylsulfoniopropriate and dimethylsulfide cycling and the microbial food web in surface waters of the North Atlantic. Limnol. Oceanogr. **47**: 53–61.

Toole, D.A., Kieber, D.J., Kiene, R.P., Siegel, D.A., and Nelson, N.B. 2003. Photolysis and the dimethylsulfide (DMS) summer paradox in the Sargasso Sea. Limnol. Oceanogr. **48**: 1088–1100.

Vézina, A.F. 2004. Towards modelling marine DMS production and emissions over regional and global scales. Can. J. Fish. Aquat. Sci. **61**(5). This issue.

Wanninkhof, R. 1992. Relationship between wind speed and gas exchange over the ocean. J. Geophys. Res. **97**(C5): 7373–7382.

Appendix A

This appendix presents the complete equations for the nitrogen cycling and sulfur cycling state variables used in the model. The left-hand side of the equations follows the general form of the transport equation (eq. 1), where the term $\nu_t \frac{\partial X}{\partial z}$ represents the turbulent flux of the quantity X. The right-hand side points out the production and consumption terms that are calculated by the accurate module. The functions for phytoplankton growth, photosynthesis, and grazing are also depicted. A description of these parameters, including units and values used in the model, is presented in Table A1. We kept the same parameter values as in the uncoupled NODEM simulation, which are fully discussed in Lefèvre et al. (2002).

Equation for nitrogen cycling (ecosystem module)

Phytoplankton:

$$\text{(A1)}\quad \frac{\partial P}{\partial t} - \frac{\partial}{\partial z}\left(s_1 P + \nu_t \frac{\partial P}{\partial z}\right) = (P\mu_{(\mathrm{PAR},\mathrm{NH_4},\mathrm{NO_3},T)}) - (P(e_1 + m_1) + Zg_{(P,T)})$$

Phytoplankton growth (μ) is controlled by light (P^B is the light-dependent production), temperature (T), and nitrogen availability as follows:

$$\text{(A2)}\quad \mu = P^B q_1 \left(\frac{[\mathrm{NO_3}]^2}{\mathrm{Ks}^2_{\mathrm{NH_4}} + [\mathrm{NO_3}]^2} + \frac{[\mathrm{NH_4}]^2}{\mathrm{Ks}^2_{\mathrm{NH_4}} + [\mathrm{NH_4}]^2}\right) e^{-0.069(T_0 - T)}$$

Photosynthesis P^B is a function (Sathyendranath et al. 1989; Sathyendranath and Platt 1989) of photosynthetically active radiation at the sea surface irradiance (I_0), underwater attenuation light coefficient (k_z) due to water and algae particles, maximum rate of photosynthesis (P^B_m) at saturated irradiance normalized to algal biomass, and photosynthetic efficiency at low irradiance (α^B). The surface irradiance (I_0) and the underwater light field ($I_{0_{\lambda,\mathrm{doy}}}$) in the euphotic zone are calculated by a spectral model from 400 to 700 nm (Sathyendranath and Platt 1988). Thus, P^B depends on depth (z), wavelength (λ), the day of the year (doy), the day length (dl), and the time of the day (t):

$$\text{(A3)}\quad P^B = P^B_m \left(1 - e^{-(\alpha^B_\lambda I_{0_{\lambda,\mathrm{doy}}} \sin(\pi t/\mathrm{dl}) e^{-k_z z})/P^B_m}\right)$$

Microzooplankton:

$$\text{(A4)}\quad \frac{\partial Z}{\partial t} - \frac{\partial}{\partial z}\left(\nu_t \frac{\partial Z}{\partial z}\right) = (Z g_{(P,T)} a) - (Z(e_2 + m_2))$$

Grazing (g) is controlled by temperature (T) and phytoplankton (P) availability as follows:

$$\text{(A5)}\quad g = V_m \frac{[P]^2}{\mathrm{Ks}^2 + [P]^2} e^{-0.069(T_0 - T)}$$

© 2004 NRC Canada

Table A1. Parameters of the nitrogen and sulfur cycling used in NODEM.

Parameter	Symbol	Value	Units	Equation(s)
C:Chl cell ratio	q_1	Variable between 50 and 100	mg C·mg Chl^{-1}	A2
C:N biomass ratio	q_3	5.7	mg C·mg N^{-1}	
Photosynthetic maximum assimilation rate	P_m^B	4.5	mg C·mg $Chl^{-1}·h^{-1}$	A3
Photosynthetic efficiency	α^B	0.05	mg C.mg $Chl^{-1}.h^{-1}$/(Einsteins·$m^{-2}·s^{-1}$)	A3
Half-saturation coefficient, NO_3^- uptake	Ks_{NO_3}	0.2	mmol N·m^{-3}	A2, A9
Half-saturation coefficient, NH_4^+ uptake	Ks_{NH_4}	0.15	mmol N·m^{-3}	A2, A8
Reference temperature	T_0	20	°C	A2, A5
Phytoplankton exudation rate	e_1	0.03	day^{-1}	A1, A7, A11
Microzooplankton excretion rate	e_2	0.05	day^{-1}	A4, A7
Phytoplankton sinking rate	s_1	Variable between 0.01 and 0.1	m·day^{-1}	A1
Detritus sinking rate	s_2	Variable between 0.02 and 0.2	m·day^{-1}	A6
Phytoplankton natural mortality	m_1	0.01	day^{-1}	A1, A7, A11
Microzooplankton natural mortality	m_2	0.06	day^{-1}	A4, A6
Maximum grazing rate	V_m	1	day^{-1}	A5
Half-saturation coefficient, grazing	Ks	0.15	mmol N·m^{-3}	A5
Microzooplankton assimilation efficiency	a	70	%	A4, A6
Bacterial degradation rate on detritus	δ_1	0.4	day^{-1}	A6, A7
Remineralization rate of DON to NH_4^+	δ_2	0.1	day^{-1}	A7, A8
S_{DMSP_p} cell quota	q_2	Variable between 0.1 and 0.5	mg S·mg N^{-1}	A10, A11
Microbial degradation rate on $DMSP_d$	δ_3	3	day^{-1}	A11, A12
Bacterial degradation rate on DMS	δ_4	0.01	day^{-1}	A12
Microbial DMS yield (% of cleavage)	γ	40	%	A12
DMS photolysis rate	ϕ	0.003	$h^{-1}·(W·m^{-2})^{-1}$	A12

Detritus:

$$\text{(A6)}\quad \frac{\partial D}{\partial t} - \frac{\partial}{\partial z}\left(s_2 D + \nu_t \frac{\partial D}{\partial z}\right) = (Z(g_{(P,T)}(1-a)+m_2)) - D\delta_1$$

DON:

$$\text{(A7)}\quad \frac{\partial \mathrm{DON}}{\partial t} - \frac{\partial}{\partial z}\left(\nu_t \frac{\partial \mathrm{DON}}{\partial z}\right) = (P(m_1+e_1) + Ze_2 + D\delta_1) - \mathrm{DON}\,\delta_2$$

NH_4^+:

$$\text{(A8)}\quad \frac{\partial \mathrm{NH_4}}{\partial t} - \frac{\partial}{\partial z}\left(\nu_t \frac{\partial \mathrm{NH_4}}{\partial z}\right) = \mathrm{DON}\,\delta_2 - P\mu_{(\mathrm{PAR},\mathrm{NH_4},T)}$$

NO_3^-:

$$\text{(A9)}\quad \frac{\partial \mathrm{NO_3}}{\partial t} - \frac{\partial}{\partial z}\left(\nu_t \frac{\partial \mathrm{NO_3}}{\partial z}\right) = -P\mu_{(\mathrm{PAR},\mathrm{NO_3},T)}$$

Equations for sulfur cycling (DMS(P) cycle module)

$DMSP_p$:

$$\text{(A10)}\quad \frac{\partial \mathrm{DMSP_p}}{\partial t} - \frac{\partial}{\partial z}\left(\nu_t \frac{\partial \mathrm{DMSP_p}}{\partial z}\right) = \frac{\partial (Pq_2)}{\partial t}$$

$DMSP_d$:

$$\text{(A11)}\quad \frac{\partial \mathrm{DMSP_d}}{\partial t} - \frac{\partial}{\partial z}\left(\nu_t \frac{\partial \mathrm{DMSP_d}}{\partial z}\right) = (P(m_1+e_1) + Zg_{(P,T)})\,q_2 - \mathrm{DMSP_d}\,\delta_3$$

© 2004 NRC Canada

DMS:

$$\text{(A12)}\quad \frac{\partial \mathrm{DMS}}{\partial t} - \frac{\partial}{\partial z}\left(\nu_t \frac{\partial \mathrm{DMS}}{\partial z}\right) = \mathrm{DMSP}_d \delta_3 \gamma - \mathrm{DMS}(\phi_z + \delta_4)$$

Photolysis (ϕ_z) follows the irradiance extinction profile (Kieber et al. 1996).

At the surface level of the model, the sea to air flux of DMS added to the sink terms is controlled by the transfert velocity *kw* calculated following Wanninkhof (1992) as follows:

$$\text{(A13)}\quad F_{\mathrm{DMS}} = k_w \mathrm{DMS}.$$

© 2004 NRC Canada

Assessment of a global climatology of oceanic dimethylsulfide (DMS) concentrations based on SeaWiFS imagery (1998–2001)[1]

S. Belviso, C. Moulin, L. Bopp, and J. Stefels

Abstract: A method is developed to estimate sea-surface particulate dimethylsulfoniopropionate ($DMSP_p$) and dimethylsulfide (DMS) concentrations from sea-surface concentrations of chlorophyll *a* (Chl *a*). When compared with previous studies, the 1° × 1° global climatology of oceanic DMS concentrations computed from 4 years (1998–2001) of Chl *a* measurements derived from SeaWiFS (satellite-based, sea-viewing wide field of view sensor) exhibits lower seasonal variability in the southern hemisphere than in the northern hemisphere. A first evaluation of the method shows that it reasonably well represents $DMSP_p$ and DMS in the North Atlantic subtropical gyre, in large blooms of mixed populations of diatoms and *Phaeocystis* spp., and in massive blooms of *Phaeocystis* spp. but fails for large, almost pure blooms of diatoms. $DMSP_p$ and DMS concentrations derived from SeaWiFS were also compared with spatially and temporally coincident in situ measurements acquired independently in the Atlantic between 39°N and 45°N and in subtropical and subantarctic Indian Ocean surface waters. Moderate spring and summer phytoplankton blooms there exhibited similar trends in $DMSP_p$ and DMS levels vs. moderate blooms of mixed populations of prymnesiophytes and dinoflagellates investigated by others. Measured DMS largely exceeded simulated DMS concentrations, whereas measured and simulated $DMSP_p$ levels were in close agreement. DMS accumulation is tentatively attributed to dinoflagellate DMSP lyase activity.

Résumé : Nous avons mis au point une méthode pour estimer les concentrations du diméthylsulfoniopropionate particulaire ($DMSP_p$) et du sulfure de diméthyle (DMS) dans les eaux superficielles de la mer à partir des concentrations de chlorophylle *a* (Chl *a*) à la surface de l'océan. Par comparaison aux études antérieures, la climatologie globale à l'échelle 1° × 1° des concentrations de DMS océanique calculée à partir de données de Chl *a* sur quatre années (1998–2001) obtenues par le senseur SeaWiFS affiche moins de variabilité saisonnière dans l'hémisphère sud que dans le nord. Une première évaluation de la méthode montre qu'elle produit une représentation assez exacte du $DMSP_p$ et du DMS dans la gyre subtropicale de l'Atlantique nord, dans les grandes efflorescences de peuplements mixtes de diatomées et de *Phaeocystis* spp. et dans les efflorescences massives de *Phaeocystis* spp., mais qu'elle ne fonctionne pas pour les grandes efflorescences presque pures de diatomées. Les concentrations de $DSMP_p$ et de DMS obtenues à partir des données SeaWiFS ont aussi pu être comparées à des mesures indépendantes faites sur place et à la même période dans l'Atlantique entre les latitudes 39°N et 45°N et dans les eaux de surface des régions subtropicale et subantarctique de l'océan Indien. Dans les efflorescences modérées de phytoplancton au printemps et en été dans ces régions, les concentrations de $DMSP_p$ et de DMS affichent des tendances semblables à celles signalées par d'autres auteurs pour des efflorescences modérées de peuplements mixtes de prymnésiophytes et de dinoflagellés. Les concentrations de DMS mesurées dépassent de beaucoup les concentrations simulées, alors que celles de $DMSP_p$ s'accordent de près aux concentrations simulées. L'accumulation de DMS est attribuée de façon préliminaire à l'activité de la DMSP lyase chez les dinoflagellés.

[Traduit par la Rédaction]

Introduction

To assess the climate effects of anthropogenic sulfate aerosols in three-dimensional (3-D) atmospheric models, it is necessary to simulate the spatial and temporal distributions of natural sulfur gases and aerosols emitted at the Earth's surface. Dimethylsulfide (DMS) is an important sulfur compound produced naturally in the sea by the phytoplankton from its precursor dimethylsulfoniopropionate (DMSP). DMS is present in the seawater at sufficient con-

Received 12 February 2003. Accepted 5 November 2003. Published on the NRC Research Press Web site at http://cjfas.nrc.ca on 24 June 2004.
J17366

S. Belviso,[2] C. Moulin, and L. Bopp. Laboratoire des Sciences du Climat et de l'Environnement, UMR CEA-CNRS 1572, CEN/Saclay, Bât 709, L'Orme des Merisiers, 91191 Gif-sur-Yvette, France.
J. Stefels. University of Groningen, Department of Marine Biology, P.O. Box 14, 9750 AA Haren, the Netherlands.

[1]This paper is part of the proceedings of the Third International Symposium on Biological and Environmental Chemistry of DMS(P) and Related Compounds, held in Rimouski (Québec), 26–28 September 2002.

[2]Corresponding author (e-mail: belviso@lsce.saclay.cea.fr).

 doi: 10.1139/F04-001 © 2004 NRC Canada

centrations to sustain a large flux to the atmosphere, where it is photooxydized to form hygroscopic sulfur aerosols. Jones et al. (2001) demonstrated in a sensitivity test that a doubling of oceanic DMS emissions would reduce the effects of anthropogenic sulfate aerosol on cloud albedo and on precipitation efficiency (the "indirect" sulfate aerosol forcing effects) by over 25%. Thus, changes in natural DMS emissions appear to significantly affect estimates of the magnitude of anthropogenic sulfate forcing.

Most current atmospheric sulfur models rely on the global database of sea-surface DMS concentration measurements assembled by Kettle et al. (1999) to compute the atmospheric fluxes of DMS. This database, initially derived from 15 617 measurements, was processed to create a monthly climatology on a 1° latitude × 1° longitude grid. Because this data set does not provide a complete coverage of the oceans, Kettle et al. (1999), following Longhurst et al. (1995), divided the Earth's oceans into a series of 57 biogeochemical provinces and calculated the average DMS concentration in each province. Several oceanic provinces are satisfactorily sampled (North Atlantic, Equatorial Pacific, etc.), but some others, mostly in the southern hemisphere, have so few data available that the average DMS concentration from an adjacent province was used to fill the gap. This global database of sea-surface DMS concentrations was recently updated (Kettle and Andreae (2000), hereafter referred to as K&A2000), using observations collected in the South Subtropical Convergence, Subantarctic, and North Atlantic Drift provinces by Sciare et al. (1999) and Belviso et al. (2000). The major drawback of this unique database is that the sea-surface DMS concentrations in the poorly sampled oceanic provinces are subject to strong changes when new data are added to the database.

Attempts to correlate DMS with variables that can be mapped globally have been carried out (Kettle et al. 1999). With respect to DMS concentration, the highest linear correlation was found with particulate DMSP ($DMSP_p$) concentration, but the coefficient of correlation (r^2) was only 0.24. With respect to $DMSP_p$ and chlorophyll *a* (Chl *a*) concentrations, r^2 was only 0.14. These two relationships are thus not accurate enough to estimate the sea-surface distribution of DMS from the global distribution of Chl *a* measured from space by ocean-color sensors.

In a recent study by Anderson et al. (2001), the Chl *a* concentration of the K&A2000 database, when available, was merged with global fields of nutrients and light to generate a *CJQ* index, where *C* is the chlorophyll concentration, *J* is the mean daily short-wave radiation flux, and *Q* is a nutrient-limitation term. The product of *C*, *J*, and *Q* exhibits considerably higher variations than the primary production. Log(*CJQ*) was shown to be significantly linearly correlated with DMS in the range of 2.3–22 nmol·L^{-1}. The relationship suppresses the DMS variability in low-concentration areas (<2.3 nmol·L^{-1}). This is certainly the major weakness of this method as low DMS levels account for about half of the DMS measurements of the K&A2000 database and concern wide areas of the open ocean (high and mid-latitudes in the winter hemisphere, subtropical gyres).

In the work of Simó and Dachs (2002), the Kettle et al. (1999) database of DMS and Chl *a* was extended by adding the climatological mixed-layer depths (MLD). A double-equation algorithm with Chl *a* and MLD was found to explain a large fraction of the variance for surface DMS concentration. The global distribution of oceanic DMS is estimated from the 1997–2000 satellite-based, sea-viewing wide field of view sensor (SeaWiFS) measurements of the sea-surface Chl *a* concentration and from a global MLD climatology. In more than 80% of cases, the DMS concentration appears to be solely a nonlinear function of the MLD.

An alternative method is proposed in the modeling study of Aumont et al. (2002) that makes use of nonlinear parameterizations to relate DMS concentration to Chl *a* and to a community structure index (Fp ratio), both parameters being calculated independently within the global 3-D ocean carbon cycle model. Their results show that the use of the Fp ratio, in addition to Chl *a*, leads to much more realistic estimates of the sea-surface DMS concentration. The major difficulty in using this method is that, contrary to Chl *a*, the Fp ratio is not routinely measured at the global scale.

In this study, we modified the method of Aumont et al. (2002) by estimating the Fp ratio directly from Chl *a*, so that sea-surface DMS concentration can be computed solely from SeaWiFS ocean-color measurements. We also slightly revised diagnostic relationships used by Aumont et al. (2002) to relate $DMSP_p$ and DMS concentrations to Chl *a* and Fp ratio. The relevance of these relationships to predict $DMSP_p$ and DMS concentrations is assessed in different areas of the North Atlantic and Indian oceans, and a global monthly climatology of sea-surface DMS concentration based on 4 years (1998–2001) of SeaWiFS data is presented. The relevance of this climatology is assessed by comparison only with K&A2000 data sets because most current atmospheric sulfur models rely on the DMS climatology of K&A2000. It is not the scope of this article to conduct a full intercomparison exercise between the DMS climatologies of K&A2000, Anderson et al. (2001), Simó and Dachs (2002), and the present one.

Description of the method

The principle of our method is similar to that developed by Aumont et al. (2002). It relies basically on two relationships:

$$(1a) \quad DMSP_p = \text{micro-}DMSP_p\, f(\text{Fp ratio, Chl } a) + \text{nano-}DMSP_p\, f(\text{Fp ratio, Chl } a)$$

$$(1b) \quad DMS = f(DMSP_p, \text{Fp ratio})$$

where Chl *a* is the sea-surface chlorophyll concentration and Fp ratio is the community structure index. This index represents the proportion of microphytoplankton within the whole phytoplankton community and is defined as the ratio of the integrated concentrations of fucoxanthin and peridinin to the sum of the integrated concentrations of diagnostic pigments of all taxa in the phytoplanktonic community (Claustre 1994). Contrary to the approach of Aumont et al. (2002), the Fp ratio is determined directly from Chl *a* in this study.

The three relationships used in eqs. 1*a* and 1*b* are obtained statistically using the scarce sets of coincident measurements of the required parameters. The amount of available data is thus crucial in this approach to ensure the validity of the relationships at the global scale. We used pig-

© 2004 NRC Canada

Fig. 1. Empirical relationships based on cruise data used to predict dimethylsulfoniopropionate ($DMSP_p$) and dimethylsulfide (DMS) concentrations from weekly mean chlorophyll maps from SeaWiFS data: (*a*) community structure ratio vs. Chl *a* concentration (see eq. 2*a*); (*b*) microplanktonic $DMSP_p$ vs. microplanktonic Chl *a* (see eq. 3); (*c*) nanoplanktonic $DMSP_p$ vs. nanoplanktonic + picoplanktonic Chl *a* (see eqs. 4*a* and 4*b*); (*d*) DMS-to-$DMSP_p$ ratio vs. the community structure index (see eq. 5*a*).

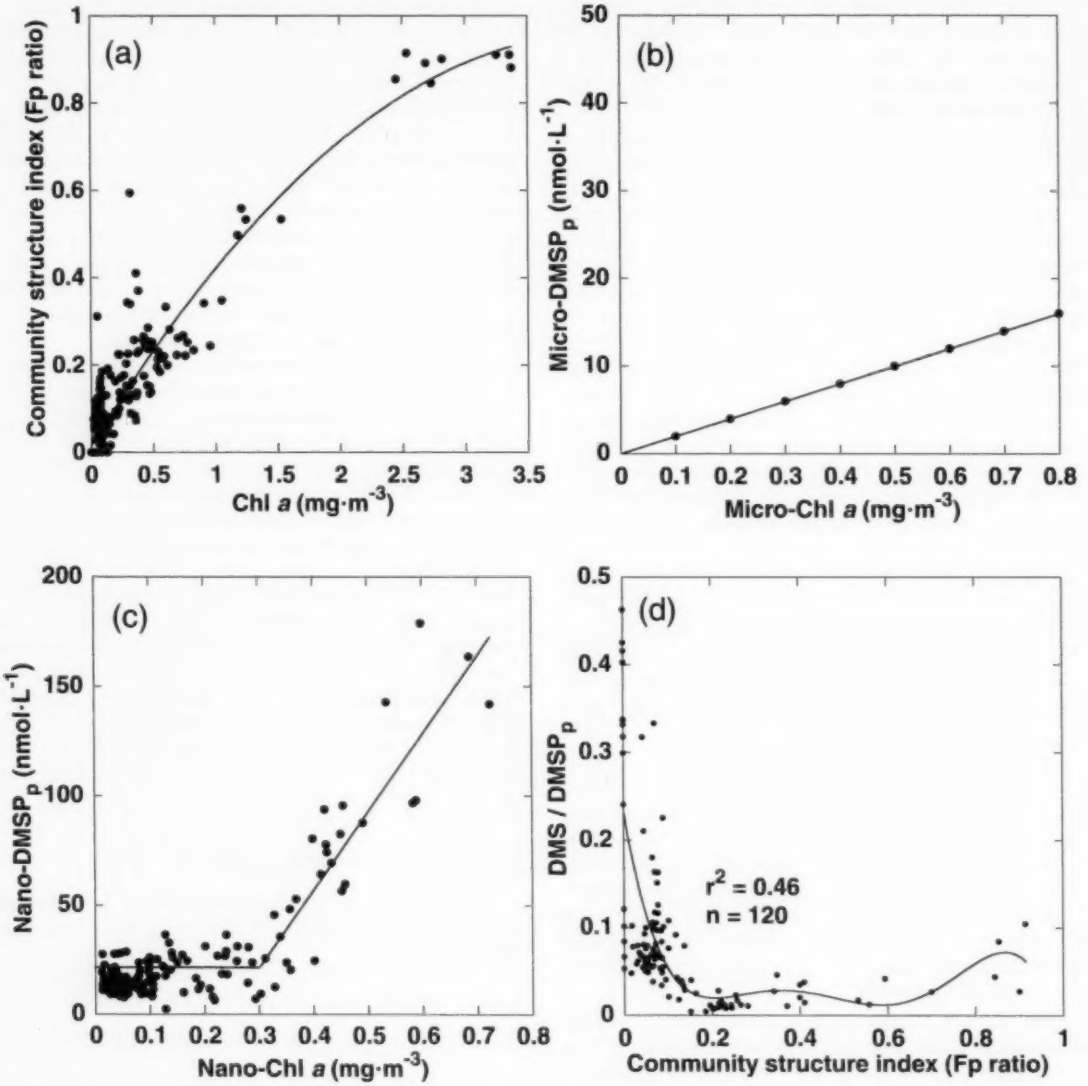

ment measurements performed during five cruises carried out in the Atlantic Ocean, the Mediterranean Sea, and the Indian sector of the Southern Ocean (Belviso et al. 2001) to relate the Fp ratio to the Chl *a* concentration. The proportion of microphytoplankton within the whole phytoplankton community increases nonlinearly with Chl *a* (Fig. 1*a*), the best fit relationship (r^2 = 0.89, n = 195) in the range 0–3.5 mg·m^{-3} being

(2*a*) $\text{Fp} = 0.01682 + (0.48047\text{Chl } a) - (0.062878(\text{Chl } a)^2)$ for Chl $a \leq 3.5$ mg·m^{-3}

Despite the good correlation coefficient, the high dispersion of Fp ratio data for Chl *a* lower than 0.5 mg·m^{-3} shows the limitation of this Chl *a* based approach to represent the complexity of phytoplankton communities in the open ocean (Fig. 1*a*). Because of the lack of high Chl *a* data, we used a conservative relationship to compute the Fp ratio:

(2*b*) Fp = 0.92 for Chl $a > 3.5$ mg·m^{-3}

The contribution of microphytoplankton (diatoms plus dinoflagellates) to the total concentration of Chl *a* is assumed to be Fp × Chl *a* (Vidussi et al. 2001). A ratio of 20 mmol·g^{-1} is taken to be typical of phytoplankton communities dominated by microphytoplankton, i.e., diatoms and, to a lesser extent, dinoflagellates (Aumont et al. 2002). Micro-$DMSP_p$ in eq. 1*a* was thus parameterized as follows (see also Fig. 1*b*):

© 2004 NRC Canada

(3) micro-$DMSP_p$ = 20 × Chl *a* × Fp

The diagnostic relationship of nano-$DMSP_p$ in eq. 1*a* used by Aumont et al. (2002) has been revised in an empirical way to improve the quality of the fit. In our work, the term "nano" encompasses nano- and pico-sized phytoplankton. We show a scatterplot of the contribution of the remaining phytoplankton community to Chl *a* and $DMSP_p$ (nano-Chl *a* and nano-$DMSP_p$) (Fig. 1*c*). A new equation was developed whereby nano-$DMSP_p$ is invariant with Chl *a* in the range of 0 to 0.3 mg·m^{-3} and is a linear function of Chl *a* above 0.3 mg·m^{-3}:

(4*a*) nano-$DMSP_p$ = 21 nmol·L^{-1} for nano-Chl *a* ≤ 0.3 mg·m^{-3}

(4*b*) nano-$DMSP_p$ = 356.4nano-Chl *a* – 85.5 for nano-Chl *a* > 0.3 mg·m^{-3}

The diagnostic relationship of DMS used by Aumont et al. (2002) has also been revised by removing data from the Norwegian fjords because they are believed not to be relevant for global-scale studies. These data will, however, be used in the next section (where Table 1 is presented and discussed) to independently evaluate the relevance of the diagnostics of $DMSP_p$ and DMS concentrations for coastal waters. The revised DMS-to-$DMSP_p$ ratios from the different cruises are plotted against Fp ratios (in the range of 0 to 0.92; Fig. 1*d*). These ratios are significantly correlated (r^2 = 0.46, n = 120), the best fit being obtained with a fifth-order polynome:

(5) $DMS/DMSP_p = 0.231 - 3.038Fp + 16.0Fp^2 - 38.05Fp^3 + 41.12Fp^4 - 16.32Fp^5$

The sea-surface DMS concentration can thus be deduced directly from the surface chlorophyll concentration measured at sea or from space by using eqs. 1*a*, 2, 3, 4, and 5.

Application to discrete Chl *a* measurements from Atlantic waters

Most of the data points gathered in Figs. 1*c* and 1*d* were obtained from surveys carried out in Atlantic surface waters with Chl *a* levels lower than 3.5 mg·m^{-3} (Aumont et al. 2002). Published and unpublished $DMSP_p$ and DMS data from the Atlantic Ocean are shown to independently evaluate the relevance of our diagnostics of $DMSP_p$ and DMS concentrations (Table 1). In this validation data set, Chl *a* ranges from 0.1 mg·m^{-3} in the Sargasso Sea (Scarratt et al. 2000) to 11.5 mg·m^{-3} in the Labrador Sea (Cantin et al. 1999). Our $DMSP_p$ estimates show virtually no difference with observations in the oligotrophic waters of the Sargasso Sea. Our relationships also very well simulate $DMSP_p$ levels for the intense *Phaeocystis*-dominated bloom off the Dutch coast. Moreover, in the Labrador Sea (Cantin et al. 1999) and the Ullsfjord in Northern Norway (Belviso et al., unpublished data) where Chl *a* was in the range of 2.2 to 11.5 mg·m^{-3} and where phytoplankton was dominated by diatoms and, to a lesser extent, *P. pouchetii*, the accuracy of our $DMSP_p$ estimates is better than 50%. Estimates for $DMSP_p$ associated with moderate blooms of *Chrysochromulina* (Scarratt et al. 2000) and *E. huxleyi* (Archer et al. 2001) are –29% and about –7% of the observations, respectively. Estimates for $DMSP_p$ associated with blooms of diatoms as observed in the central North Sea and the Balsfjord and Malangen fjords (Belviso et al., unpublished data) are in the range of 130% to 2000% of the observations. $DMSP_p$ is highly overestimated there mainly because the $DMSP_p$-to-Chl *a* ratio of microphytoplankton is 2- to 10-fold lower than that used in eq. 3 (Table 1) and because our calculation adds 8% of the Chl *a* as nano-Chl *a*, which represents about 200 nmol·L^{-1} $DMSP_p$ at a total Chl *a* concentration of 10 mg·m^{-3}. Thus, the diagnostic of $DMSP_p$ does not resolve $DMSP_p$ variability in almost pure diatom blooms but does a fairly good job in areas where prymnesiophytes proliferate, which constitute large tracts of the North Atlantic Ocean.

Contrary to the $DMSP_p$ estimates of diatom-dominated blooms, which are systematically highly overestimated (see above), DMS estimates are in the range of –64% to +655% of observations. Blooms of mixed populations of diatoms and *Phaeocystis* exhibit DMS estimates in the range of –2% to +160% of the observations. DMS estimates for moderate blooms of *Chrysochromulina* spp. and *E. huxleyi* are –72% and –62% of the observations, respectively. Our model also markedly overestimates $DMSP_p$ and DMS levels associated with a bloom of unknown flagellates from the Gulf Stream. In low-DMS areas, as observed in the Titanic and Grand Banks sampling sites (Scarratt et al. 2000), estimated DMS is –30% and +130% of observations, respectively. Finally, the DMS estimate for the Sargasso Sea is only 9% lower than in reality.

Thus, the present diagnostics resolve DMS variability both in low- and high-DMS areas of the Atlantic Ocean, even if $DMSP_p$ and DMS levels in diatom-dominated blooms of the North Sea and north Norwegian fjords are not well represented. With these limitations in mind, the method is suitable for use in combination with nearly global ocean-color data from the SeaWiFS. Assuming that Chl *a* is estimated from space with 35% error at the most, the relative error using the set of equations is 25%, 33%, and 50% for Chl *a* levels equal to 0.1, 1, and 10 mg·m^{-3}, respectively.

Application to SeaWiFS ocean-color data

Global fields of Chl *a* were obtained from 4 years (1998–2001) of monthly composites of SeaWiFS Chl *a*. The data were regridded onto a 1° grid. Equations 2*a* and 2*b* were used to estimate the Fp ratio from SeaWiFS Chl *a*, and both parameters were then used in eqs. 1*a*, 3, 4*a*, 4*b*, and 5 to retrieve monthly near-global gridded fields of DMS concentration. We show the monthly mean maps of sea-surface DMS concentration for January, April, July, and October (Fig. 2). Compared with the results of K&A2000, our estimates show a much higher spatial variability in frontal and upwelling regions in particular, which was expected as the distribution of the biology in oceans is far from being uniform. We thus expect this approach to strongly improve the capability of our global source to capture DMS concentration variability at the meso-scale. Note that no data are available at high latitude during winter in both hemispheres because SeaWiFS observations are limited to regions with sufficient solar irradiance. We also show the geographical limits of four se-

© 2004 NRC Canada

Table 1. Validation of dimethylsulfoniopropionate ($DMSP_p$) and dimethylsulfide (DMS) estimates from Chl *a* levels measured in contrasted areas of the Atlantic Ocean (1 SD in parentheses).

Sampling sites	Dominant phytoplankton	Chl *a* ($mg \cdot m^{-3}$)	$DMSP_p$[a] (nM)	$DMSP_p$[b] (nM)	$\Delta DMSP_p$[c] (%)	DMS[a] (nM)	DMS[b] (nM)	ΔDMS[c] (%)	References
Sargasso Sea	Dinoflagellates	0.10	21.5	21.7	–0.9	2.0	2.2	–9.1	Scarratt et al. 2000
Grand Banks	Cryptophyceae	0.26	22.1	39.4	–44	0.7	0.3	+130	
Titanic	*Chaetoceros* spp.	0.25	22.1	8.5	+160	0.7	1	–30	
	Chrysochromulina spp.	0.52	56.1	78.9	–29	1.2	4.3	–72	
North Atlantic Drift	Dinoflagellates	0.62	74.8	30.2	+150	2.0	2.3	–13	
Gulf Stream	Flagellates	0.85	109	11.7	+830	3.1	0.3	+940	
North Atlantic	*E. huxleyi* and *P. minimum*	0.7 (0.2)	80.2 (34)	74.7 (20.1)	6.8	2.1 (1.0)	5.5 (2.3)	–62	Archer et al. 2001
		$n = 8$	$n = 8$	$n = 8$		$n = 8$	$n = 8$		
North Sea	Diatoms	3.1 (1.6)	120 (32)	22.7 (10.8)	+350	5.7 (2.6)	0.8 (0.5)	+580	Cruise ESCAPE 2
Apr. 1998		$n = 47$	$n = 47$	$n = 47$		$n = 47$	$n = 47$		Belviso et al., unpublished
Balsfjord	Diatoms	6.3	178	22.4	+690	11.2	5.0	+124	Cruise ESCAPE 1
Apr. 1997		7.8	241	23.3	+930	15.2	6.5	+134	Belviso et al., unpublished
		11.1	379	33.2	+1040	23.9	6.3	+279	
		10.9	371	17.5	+2020	23.4	3.1	+655	
		2.7	99	24.7	+300	7.1	5.3	+34	
Malangen	Diatoms	5.4	141	15.1	+830	8.9	11.7	–24	Cruise ESCAPE 1
Apr. 1997		4.5	105	24.3	+330	6.7	12.7	–47	Belviso et al., unpublished
		2.7	99	12.1	+720	7.1	12.3	–42	
		5.2	132	46.9	+180	8.3	9.4	–12	
Ullsfjord	Diatoms	6.7	195	32	+510	12.3	34	–64	Cruise ESCAPE 1
Apr. 1997		5.4	140	52.6	+170	8.9	24.5	–64	Belviso et al., unpublished
		7.1	211	92.3	+130	13.3	14.6	–9	
	Diatoms and *P. pouchetii*	2.2	129	88.3	+46	6.4	5.4	+18	
	Diatoms and *P. pouchetii*	5.8	157	184	–15	9.9	9.7	–2	
Labrador Sea	Diatoms and *P. pouchetii*	11.5	400	270	+48	25	ND	ND	Cantin et al. 1999
North Sea, Texel	*P. globosa*	9.0 (3.2)	291 (133)	263 (94)	+10.6	18.4 (8.4)	16.5 (6.9)	+11.5	Cruise ESCAPE 2
Apr. 1998		$n = 21$	$n = 21$	$n = 21$		$n = 21$	$n = 21$		Belviso et al., unpublished

Note: ND, no data.
[a]Estimated.
[b]Measured.
[c](Estimated – measured)·measured $^{-1}$.

© 2004 NRC Canada

Fig. 2. Global climatologies of dimethylsulfide (DMS) concentration for January, April, July, and October created from SeaWiFS maps of Chl *a* (1998–2001) and the database of Kettle and Andreae (2000), left and right columns, respectively.

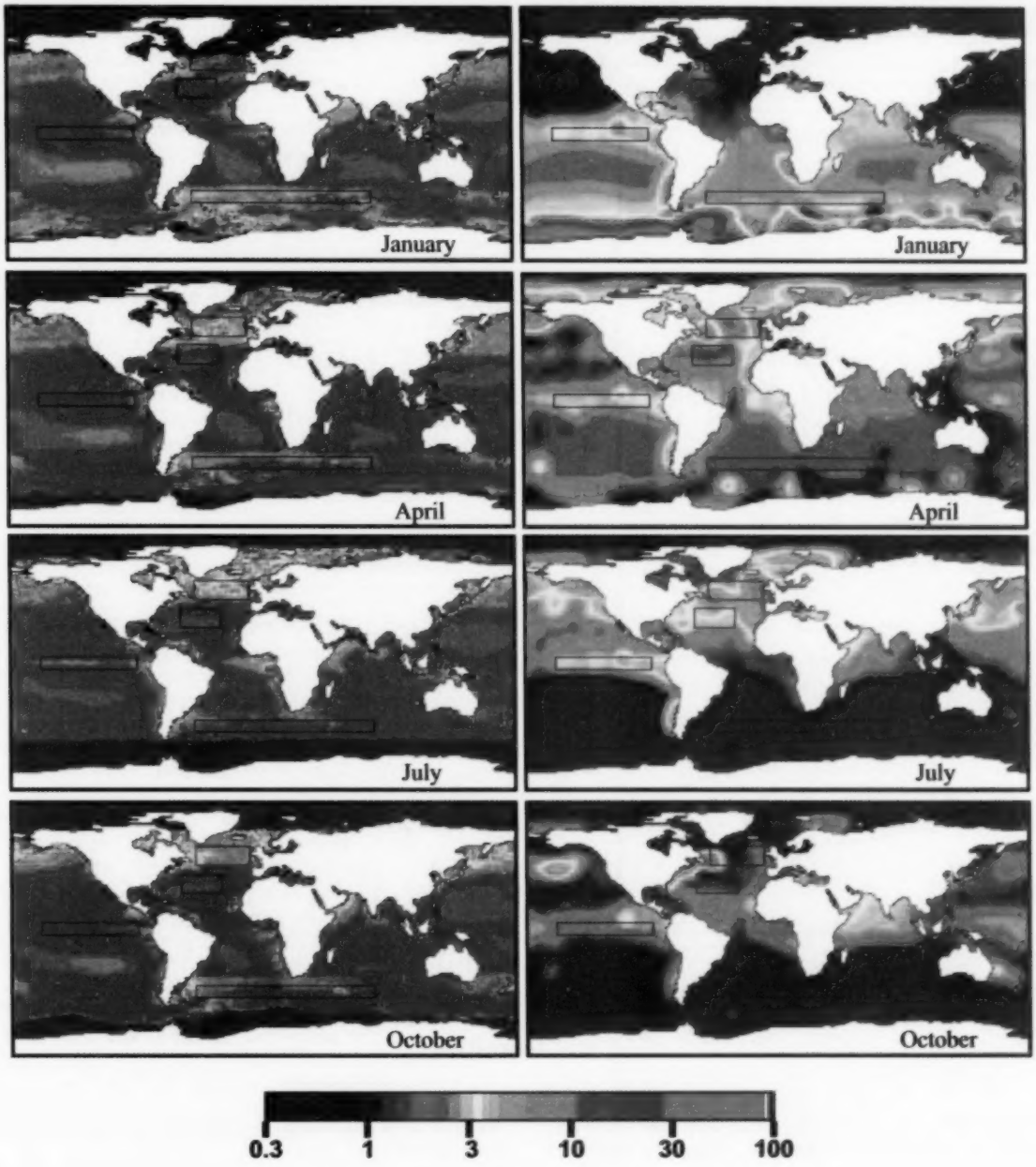

lected oceanic areas, the locations of which roughly correspond to the biogeochemical provinces NADR (northern high latitudes of the Atlantic Ocean), NAST (northern midlatitudes of the Atlantic Ocean), PEQD (Equatorial Pacific) and SSTC (southern midlatitudes of the Indian and Atlantic oceans) as defined by Longhurst et al. (1995) and used by Kettle et al. (1999) to construct monthly maps of the DMS distribution from a database of existing measurements (Fig. 2). These regions were selected because they efficiently summarize the similarities and differences between both climatologies, but also because they correspond to well-documented regions for which the K&A2000 database is likely to be the most reliable. We display the seasonal variations of DMS deduced from the K&A2000 monthly maps and as predicted by SeaWiFS imagery for these four regions (Fig. 3).

Substantial differences between the SeaWIFS and K&A2000 data sets are observed in NADR in late spring

© 2004 NRC Canada

Fig. 3. Comparison of the Kettle and Andreae (2000; ●) and SeaWiFS-derived (□) seasonal variabilities of monthly mean dimethylsulfide (DMS) concentration in four selected biogeochemical provinces: (*a*) northern high latitudes of the Atlantic Ocean (NADR); (*b*) northern midlatitudes of the Atlantic Ocean (NAST); (*c*) Equatorial Pacific (PEQD); (*d*) southern midlatitudes of the Indian and Atlantic oceans (SSTC).

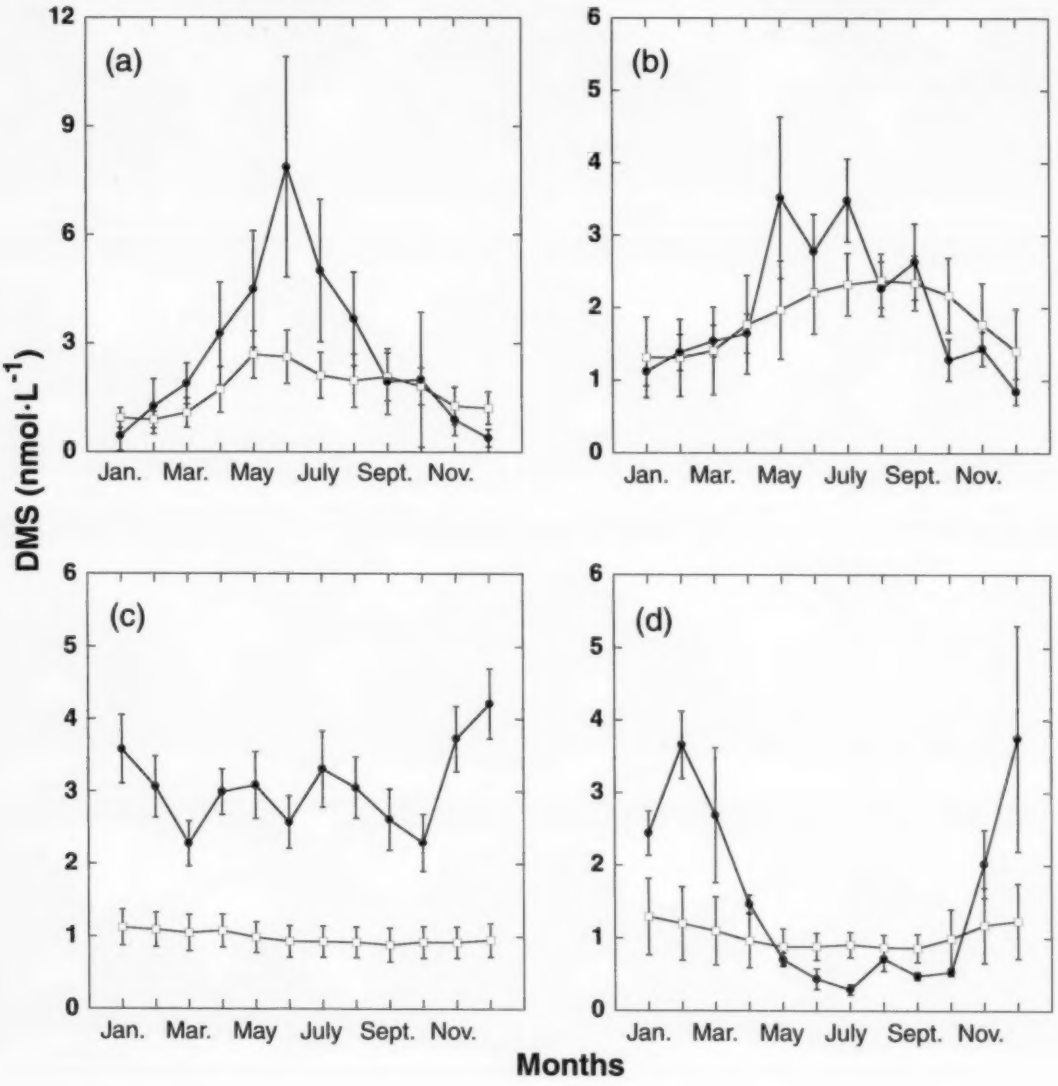

and summer (Fig. 3*a*) as the May–June–July maximum concentration of K&A2000 is roughly twice the SeaWiFS-derived concentration. The seasonal cycles of DMS in NAST compare rather well (Fig. 3*b*). Equatorial regions are characterized by small seasonal changes (Fig. 3*c*). However, the DMS simulated in this work is roughly one-third that of K&A2000. This problem may be related to an underestimate of the DMS-to-$DMSP_p$ ratio in these high-nutrient low-chlorophyll areas. Unfortunately, the Equatorial Pacific, which has been investigated extensively for DMS, has received much less attention for $DMSP_p$. It appears that our approach markedly underestimates the amplitude of the DMS seasonal variations in the area SSTC (Fig. 3*d*).

Validation of the SeaWiFS estimates of surface DMS concentration

Data sets gathered in the comprehensive database of DMS measurements assembled by Kettle et al. (1999) are dated 1997 and earlier; thus, they are not suitable for use in evaluating SeaWiFS-derived $DMSP_p$ and DMS concentrations with temporally and spatially coincident observations. POLDER and OCTS ocean-color data available between November 1996 and June 1997 are coincident in space and time with cruises numbered 132 (Ross Sea) and 133 (Labrador Sea) in Kettle et al. (1999). Unfortunately, DMS data from both cruises are not yet available on line at http://saga.pmel.noaa.gov/dmsserver/index.php. The Kettle

© 2004 NRC Canada

database has been updated recently (K&A2000) by the addition of measurements from Belviso et al. (2000), Sciare et al. (1999), and J. Sciare (Laboratoire des Sciences du Climat et de L'Environnement, UMR CEA-CNRS 1572, CEN/Saclay, Bât 709, L'Orme des Merisiers, 91191 Gif-sur-Yvette, France, unpublished data). Because the parameterizations of $DMSP_p$ and DMS make use of data from Belviso et al. (2000), only the measurements from J. Sciare in the Indian Ocean were suitable for the evaluation exercise. Here we used a second independent data set of $DMSP_p$ and DMS concentrations measured in a sector of the North Atlantic Ocean between Portugal and Acores (38°N–44°N, 17°W–22°W) as part of the recent French research project POMME (Programme Océan Multidisciplinaire Méso-Echelle). The coupling of mesoscale dynamical and biological processes was one of the major objectives of POMME. During the first leg of the three cruises carried out in 2001 (each roughly 20 days long), a hydrographic survey was carried out with a resolution of about 50 km (Fig. 4). To benefit from the rather high resolution in space and time of the validation data set, we used here SeaWiFS 8-day mean global fields of Chl *a* at 9-km resolution instead of monthly composites to compute DMS concentrations. Unfortunately, these cruises did not benefit from SeaWiFS scheduling in local area coverage (LAC) mode (1-km resolution) for real-time image support and real-time validation of DMS estimates.

Case 1: Northeast Atlantic surface waters

The winter mixed-layer depth discontinuity zone divides the Northeast Atlantic basin into two regions: a rather productive zone, with a strong spring bloom to the north associated with a deep winter mixed layer, and a more oligotrophic region to the south, with characteristics similar to those of the subtropical gyre. DMS and $DMSP_p$ measurements were carried out in the upper 80 m of the water column and analyses were performed at sea following the methodology described in Belviso et al. (2001). The depth of the surface layer that contributes 90% of the upwelling marine radiance, Z_{90} (Morel 1988), varies inversely with Chl *a*. For the Chl *a* values typical of the POMME region (see Figs. 5*a*, 5*d*, and 5*g*), Z_{90} varies from about 20 m for Chl $a = 0.1$ mg·m^{-3} to slightly less than 10 m for Chl $a = 1$ mg·m^{-3}. Consequently, in winter and spring (POMME 1 and 2), zonal averages of $DMSP_p$ and DMS concentrations were calculated from surface samples only (Figs. 5*b*, 5*c*, 5*e*, and 5*f*). In late summer, during cruise POMME 3, zonal averages of $DMSP_p$ and DMS concentrations were calculated from surface and 20-m-deep samples (Figs. 5*h* and 5*i*). In winter, zonally averaged SeaWiFS-derived $DMSP_p$ concentrations are 1.5- to 6-fold higher than observations north of 42°N (Fig. 5*b*). The agreement is better south of 42°N where simulated and measured $DMSP_p$ concentrations are within a factor of two. Corresponding simulated DMS concentrations are 1.5- to 4-fold higher than observations north of 42°N and 1.2- to 2.2-fold higher than observations south of 42°N (Fig. 5*c*). In spring, north of 42°N, simulated $DMSP_p$ is 1.5- to 3-fold higher than observations, whereas south of 42°N, simulated $DMSP_p$ is in very close agreement with the observations (Fig. 5*e*). North of 42°N, DMS concentrations are within a factor of two of the observations. The simulations fail to reproduce the high-DMS concentrations measured south of 40°N

Fig. 4. Network of hydrographic stations from which zonal-averaged dimethylsulfoniopropionate ($DMSP_p$) and dimethylsulfide (DMS) concentrations were calculated: (*a*) cruise POMME 1 (3–23 February 2001); (*b*) cruise POMME 2 (22 February to 13 March 2001); (*c*) cruise POMME 3 (23 August to 13 September 2001). Figures in the maps correspond to station numbers.

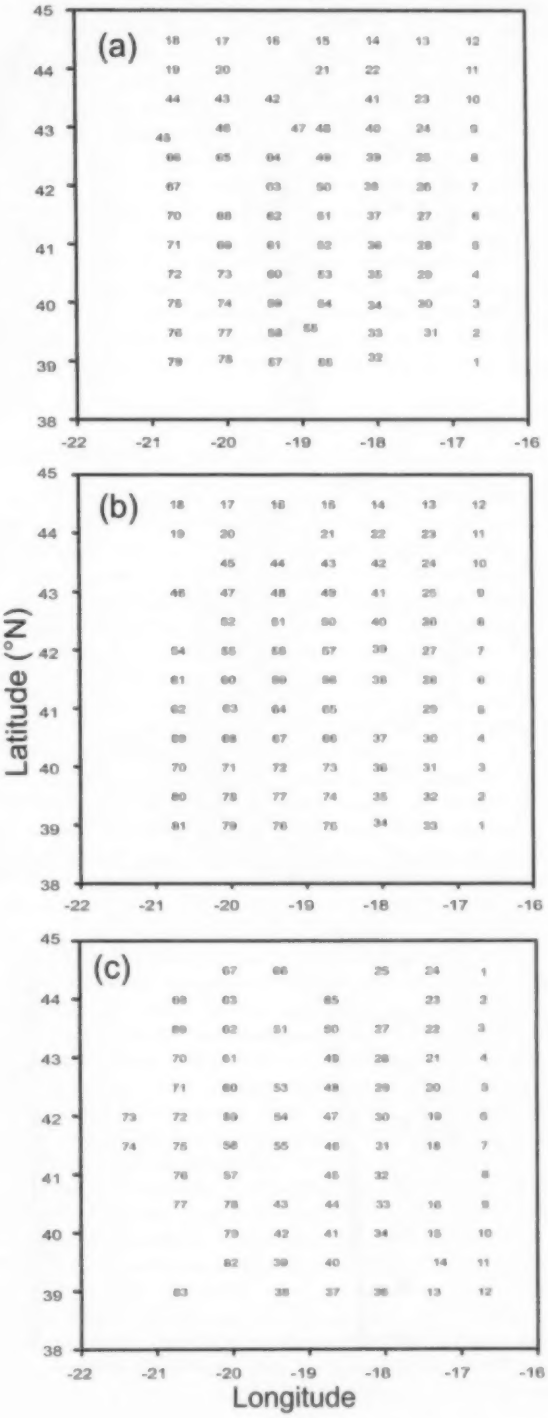

© 2004 NRC Canada

Fig. 5. Comparison of observed (□, thick line) zonal-averaged concentrations of Chl *a* (from SeaWiFS), dimethylsulfoniopropionate ($DMSP_p$), and dimethylsulfide (DMS) with SeaWiFS-derived predictions (●, thin line) of $DMSP_p$ and DMS concentrations in the POMME area.

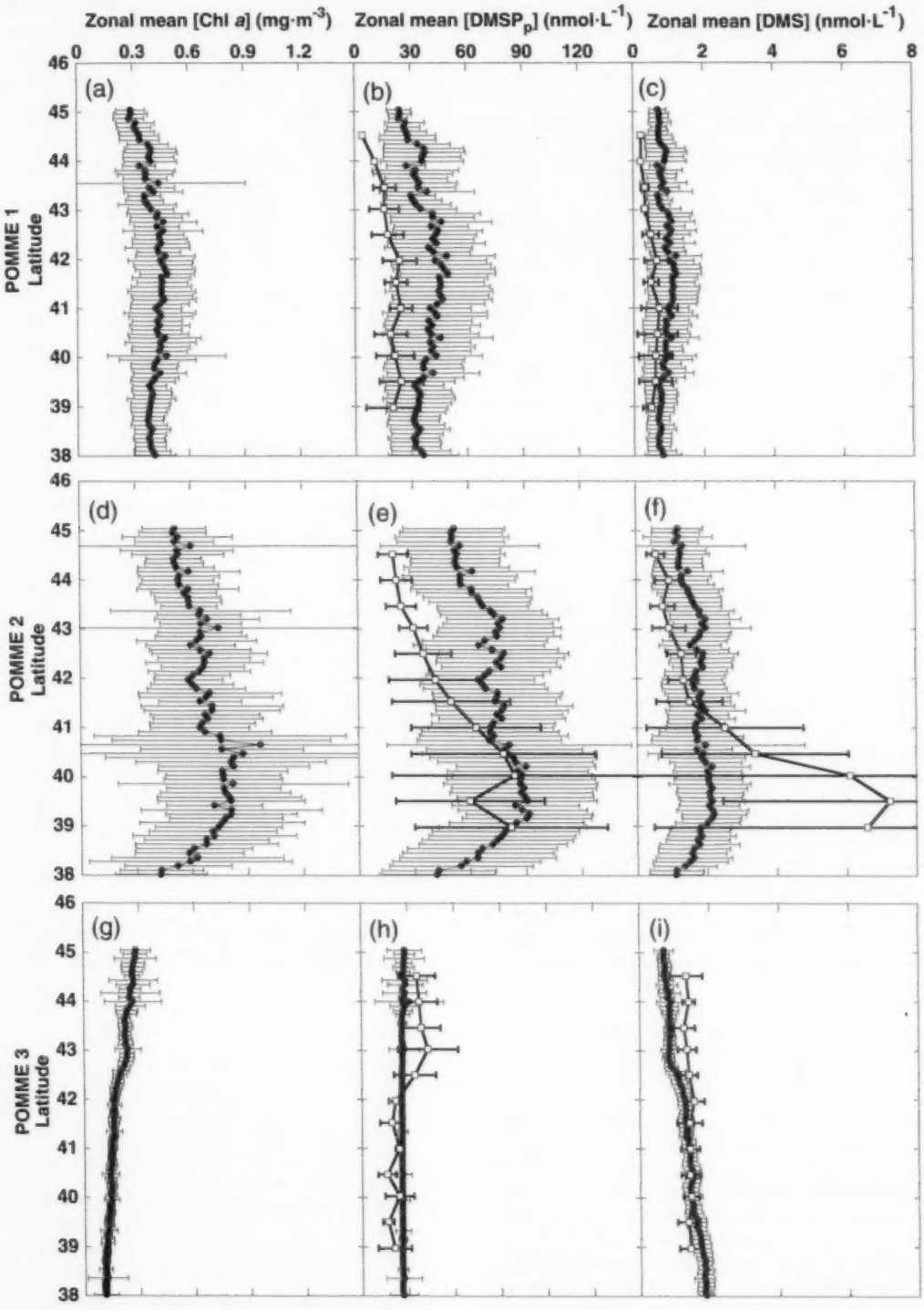

© 2004 NRC Canada

(Fig. 5*f*). In this area, however, the zonal variability of DMS was huge (see error bars) because the DMS highs were restricted to the southwest sector of the domain (data not shown). This situation in which simulated DMS is markedly underestimated but $DMSP_p$ is well simulated very much resembles the situations associated with moderate blooms of *Chrysochromulina* spp. and *E. huxleyi* in Atlantic waters (Table 1). In late summer, simulated $DMSP_p$ and DMS concentrations are within a factor of two of the observations. Thus, it appears that the diagnostics of the $DMSP_p$ and DMS concentrations mainly reduce the zonal variability of the compounds in Northeast Atlantic surface waters at midlatitudes. This mainly results from the overestimation of $DMSP_p$ concentration in the deep winter mixed layer and from the underestimation of the DMS spring bloom in more stratified waters. The $DMSP_p$ and DMS content of the more oligotrophic waters of the northern edge of the North Atlantic subtropical gyre in late summer are predicted with higher accuracy.

Case 2: Indian Ocean surface waters

DMSP and DMS concentrations were measured in December 1997 and August 1998 during cruises of R/V *Marion Dufresne* (Sciare et al. (1999) and Sciare et al., unpublished data, respectively). Each trip consisted of three legs: (1) from La Réunion Island (20°S, 56°E) to Crozet Island (46°S, 50°E); (2) from Crozet Island to Kerguelen Island (49°S, 69°E); and (3) from Kerguelen Island to Amsterdam Island (37°S, 77°E). We compare the SeaWiFS-derived $DMSP_p$ and DMS concentrations with observed sea-surface DMSP and DMS concentrations in December 1997 and August 1998 (Fig. 6). Weekly mean chlorophyll maps from SeaWiFS data were used for evaluating predicted versus observed DMSP and DMS levels. Note that Figs. 6*a* and 6*c* show observed total DMSP levels ($DMSP_t$), i.e., the cumulated levels of particulate DMSP ($DMSP_p$) and dissolved DMSP ($DMSP_d$), whereas eqs. 3*a* and 3*b* involve only $DMSP_p$. Indeed, in subtropical and subantarctic waters of the Indian Ocean during December 1997 and August 1998, $DMSP_d$ accounted for 20% to 80% of $DMSP_t$. $DMSP_d$ is a very labile compound, usually exhibiting turnover times on the order of hours rather than days (e.g., Zubkov et al. 2001). Because $DMSP_d$ is released from phytoplankton by direct excretion, grazing, or viral lysis, it is expected that measured $DMSP_d$ results from the turnover of $DMSP_p$ produced in the previous few days. Thus, it is more appropriate to compare predicted $DMSP_p$ and observed $DMSP_t$ than to compare directly predicted and observed $DMSP_p$ concentrations. In other words, observed $DMSP_t$ concentrations are more adapted to a comparison with predicted mean $DMSP_p$ because they provide a longer integration over time.

As seen here, SeaWiFS data in combination with eqs. 1–5 markedly overestimate $DMSP_p$ in August 1998 inside the chlorophyll patch (Fig. 6*a*). The SeaWiFS data predict a four- to five-fold enhancement of $DMSP_p$ in the patch, whereas observations show a twofold increase. Outside the chlorophyll patch and during the first three-quarters of the winter cruise, predicted and observed DMSP concentrations are almost the same. During the last quarter of the cruise, SeaWiFS data overestimate $DMSP_p$ about twofold. In August, observed and predicted DMS levels exhibit almost similar fluctuations in the range of 0.4 to 3 nmol·L^{-1} except near cruise end as for $DMSP_p$ (Fig. 6*b*). It appears that the use of SeaWiFS data in combination with eqs. 1–5 generally compares very well with the winter observations.

Three major $DMSP_p$ peaks are predicted via the SeaWiFS data at the location of the chlorophyll patches crossed during the December 1997 trip (Fig. 6*c*). The predicted magnitudes are in close agreement with the field observations except near cruise end (Kerguelen Plateau), where predicted $DMSP_p$ is twofold higher than observed. Outside these chlorophyll patches, predicted $DMSP_p$ concentrations are similar in subtropical waters or elsewhere up to threefold lower than observed. Three major DMS peaks are also predicted by the SeaWiFS data at the location of the chlorophyll patches (Fig. 6*d*). DMS field observations also were clearly enhanced at these locations. The SeaWiFS-derived magnitude of the first two DMS peaks, however, is considerably lower (5- to 10-fold) than observed, with better agreement on the third peak. Outside the chlorophyll patches, baseline DMS is up to 20-fold lower than observed except in subtropical waters where estimates and observations are in close agreement.

Discussion

It appears that one major problem with SeaWiFS-based predictions is an underestimation of DMS concentrations in subantarctic waters during the summer. Again, this situation in which simulated DMS is markedly underestimated but $DMSP_p$ is well simulated very much resembles the situations associated with the moderate blooms of *Chrysochromulina* spp. and *E. huxleyi* in Atlantic waters and the spring bloom in the POMME area. The approach described here using SeaWiFS data results in an oceanic DMS baseline concentration of about 0.5 nmol·L^{-1}, about fourfold lower than the baseline of 2.3 nmol·L^{-1} reported by Anderson et al. (2001). Both Fig. 6*b* and Table 1 show that SeaWiFS-derived DMS concentrations vary over a wider range of values (0.5–41 nmol·L^{-1}) than DMS concentrations derived from the *CJQ* index of Anderson et al. (2001). The use of weekly mean chlorophyll maps from SeaWiFS data in combination with the nonlinear eqs. 2–5 improves the representation of the low- and high-DMS areas. Evidence is given in this study of the proper representation of DMS concentrations in subtropical gyres. Evidence is also given of the proper representation of DMS levels associated with *Phaeocystis* spp. blooms. In the winter hemispheres at midlatitudes, the difference between observed and simulated DMS levels is generally lower than a factor of two except north of 42°N where larger discrepancies were noted. In the winter hemisphere at high latitudes in the absence of SeaWiFS data and to provide a global coverage of the oceanic domain, we recommend, according to Belviso et al. (2000) and the POMME 1 survey, to take 0.2 nmol·L^{-1} as the winter reference for marine DMS. As shown here, our approach fails to reproduce the observed high (4–30 nmol·L^{-1}) DMS levels associated with the fairly well estimated moderate (60–150 nmol·L^{-1}) DMSP levels. The largest discrepancy was observed in the Indian Ocean during summer. Unfortunately, no supporting parameters were measured during the December 1997 cruise, so the dominant phytoplanktonic popula-

© 2004 NRC Canada

Fig. 6. Comparison of observed (□, thick line) concentrations of total dimethylsulfoniopropionate ($DMSP_t$) and dimethylsulfide (DMS) concentrations with SeaWiFS-derived predictions (●, thin line) of $DMSP_p$ and DMS concentrations in the Indian Ocean along the track of R/V *Marion Dufresne* from La Réunion Island to Amsterdam Island.

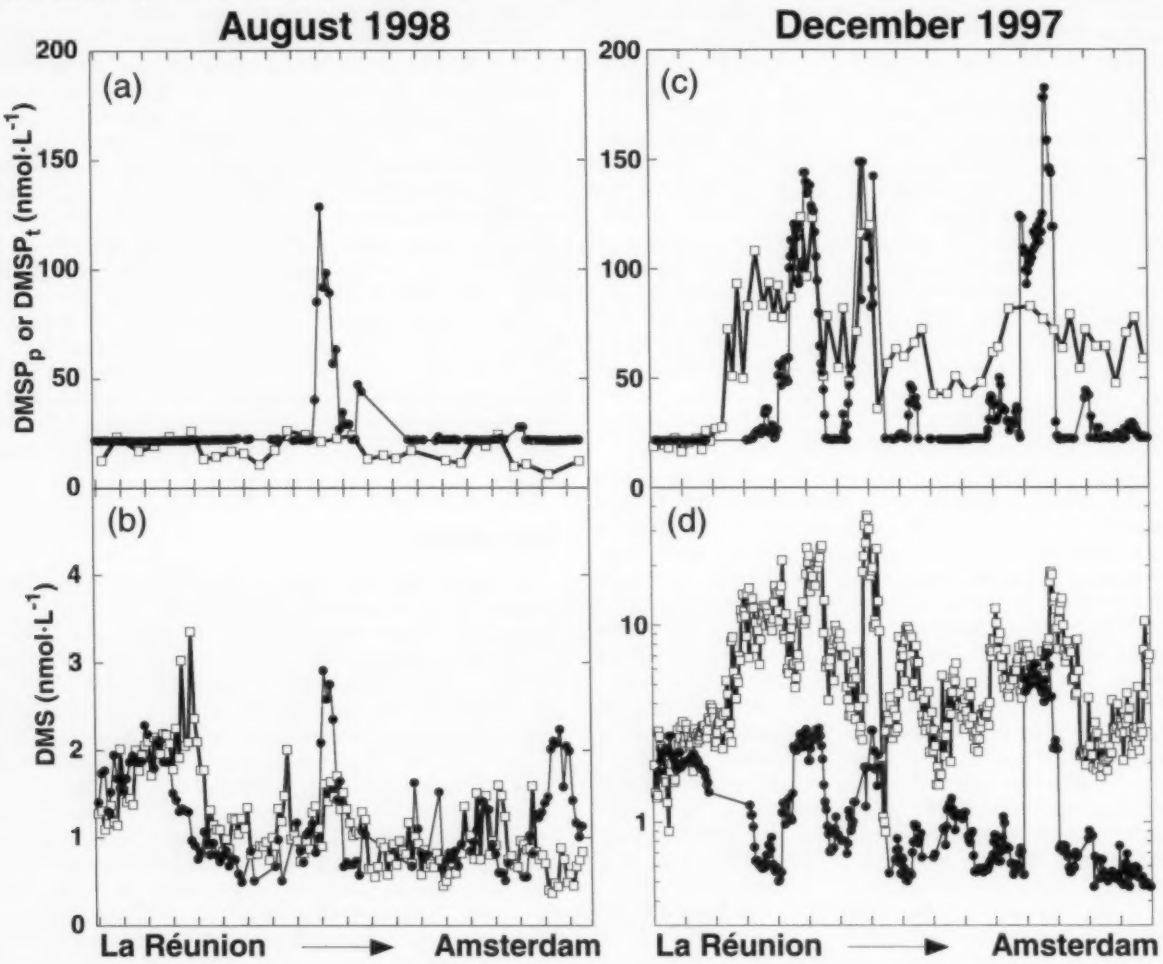

tions in these waters are unknown. Very high DMS levels in association with very high concentrations of $DMSP_d$ and low $DMSP_p$ (Sciare et al. 1999) could result from senescence of a phytoplanktonic bloom. Indeed, in the senescence phase, phytoplankton autolysis or zooplankton grazing releases to solution compounds present in the phytoplanktonic cell, where they can undergo microbial degradation. Enzymatic cleavage by DMSP lyase is thought to be the major process for DMS production in marine environments. Dissolved DMSP is available to bacteria in surface waters. To maintain DMS and $DMSP_d$ at the very high levels observed in December 1997, it may be suggested, according to Kiene et al. (2000) who highlighted the high metabolic value of $DMSP_d$ for bacteria, that bacterial sulfur demand and bacterial DMS consumption in the area was low and that a relatively high proportion of $DMSP_d$ was available for DMS production from bacterial enzymatic cleavage of DMSP. Pathways for nonbacterial production of DMS have been also acknowledged, e.g., Steinke et al. (2002), where the majority of DMSP lyase activity occurred in particles >10 µm and was related to the presence of dinoflagellates. Fiala et al. (1998) reported at the KERFIX station, 60 miles southwest of the Kerguelen Islands, that the >10-µm size fraction contributed 60% to total phytoplankton integrated biomass during summer blooms. Large autotrophic dinoflagellates, mainly *Prorocentrum* spp., were associated with the summer phytoplankton maxima and accounted for >80% of the total autotroph carbon biomass. In November and December, the presence of the large heterotrophic dinoflagellates *Protoperidinium* spp. and *Gyrodinium* spp. contributed a high proportion of total carbon biomass. Archer et al. (2001) and Steinke et al. (2002) agreed on the presence of dinoflagellates in *E. huxleyi* blooms from the northern North Sea and the North Atlantic. The *Chrysochromulina* spp. bloom investigated by Scarratt et al. (2000) was in fact located very close to the North Atlantic Drift sampling station where dinoflagellates were the dominant phytoplankton. Thus, it is not unlikely that dinoflagellates were also present

© 2004 NRC Canada

in the *Chrysochromulina* spp. bloom. A phytoplankton bloom took also place in the southwestern portion of the POMME area during spring 2001. The $DMSP_p$ size fractionation experiment carried out there showed that $DMSP_p$ was mainly present in the <10-µm fraction (S. Belviso, unpublished data). According to Belviso et al. (2001), it is likely that prymnesiophytes and pelagophytes accounted for nanoplanktonic $DMSP_p$ and that dinoflagellates accounted for the remaining microplanktonic form of $DMSP_p$ in North Atlantic waters. Thus, evidence is given of the presence of dinoflagellates in the four moderate phytoplankton blooms investigated where $DMSP_p$ was well diagnosed but DMS was markedly underestimated by SeaWiFS data in combination with eqs. 1–5. Assuming that all other DMS-controlling processes were equal, a weak assumption, it is suggested that the DMS enhancements resulted from the DMSP lyase activities of dinoflagellates.

In conclusion, our SeaWiFS-derived climatology of sea-surface DMS concentration is an alternative (1) to K&A2000 in which monthly fields of DMS concentration still lack stability and heavily rely on a scheme of substitutions, especially in regions of the southern hemisphere where observations remain poorly numerous, and (2) to the approach of Anderson et al. (2001), which does not resolve DMS variability in low-DMS areas. A means to characterize the global distribution of $DMSP_p$, the major intermediate in DMS production, and a key for the investigation of the interannual variations of the marine source of DMS are also provided. The diagnostic relationships adopted here, in combination with Chl levels obtained by either ship-based measurements or remotely sensed, resolve the DMS variability in subtropical gyres, in large blooms of mixed populations of diatoms and *Phaeocystis* spp., and in massive blooms of *Phaeocystis* spp. but fails for large almost pure blooms of diatoms. Moreover, they provide accurate estimates of $DMSP_p$ concentrations in spring and summer moderate blooms of mixed populations of prymnesiophytes and dinoflagellates in the North Atlantic and, possibly, subantarctic waters of the Indian Ocean. Related DMS levels, however, are markedly underestimated, a situation which results in a clear reduction of the seasonal amplitude of DMS variations. Our method does not resolve the variations of DMS in the Equatorial Pacific.

The Fp ratio is clearly the critical parameter of the method described in this paper. We estimated this parameter from the Chl *a* concentration with the help of a simple relationship, although it also strongly depends on the phytoplankton populations. The use of more complete estimates of the Fp ratio based on biological modeling (e.g., Laws et al. 2000) would likely improve the accuracy of the method. Improved remote-sensing techniques may also provide additional information on the phytoplankton population (Loisel et al. 2001), and it is likely that recent high-performance ocean-color sensors such as MODIS or MERIS would enable the global survey of some phytoplankton-related parameters.

Acknowledgements

We acknowledge the Goddard Active Archive Centre, under the auspices of the National Aeronautics and Space Administration, for provision of the SeaWiFS ocean-colour data. DMSP and DMS concentrations in Indian Ocean subtropical and subantarctic waters during winter are courtesy of J. Sciare. We thank I. Lefevre, C. Valant, and O. Aumont for contributing to DMSP/DMS analyses during the POMME cruises. This work was supported by the national program PROOF of INSU/CNRS and EU under contract MAS3-CT96-0050 (ESCAPE project). This is Laboratoire des Sciences du Climat et de l'Environnement (LSCE) contribution No. 1006.

References

Anderson, T.R., Spall, S.A.,Yool, A., Cipollini, P., Challenor, P.G., and Fasham, M.J.R. 2001. Global fields of sea surface dimethylsulfide predicted from chlorophyll, nutrients and light. J. Mar. Syst. **30**: 1–20.

Archer, S.D., Widdicombe, C.E., Tarran, G.A., Rees, A.P., and Burkill, P.H. 2001. Production and turnover of particulate dimethylsulphoniopropionate during a coccolithopohore bloom in the northern North Sea. Aquat. Microb. Ecol. **24**: 225–241.

Aumont, O., Belviso, S., and Monfray, P. 2002. Dimethylsulfoniopropionate (DMSP) and dimethylsulfide (DMS) sea surface distributions simulated from a global 3-D ocean carbon cycle model. J. Geophys. Res. **107**(C4) (doi: 10.1029/1999JC000111).

Belviso, S., Morrow, R., and Mihalopoulos, N. 2000. An Atlantic meridional transect of surface water DMS concentrations with 10–15 km horizontal resolution and close examination of ocean circulation. J. Geophys. Res. **105**(D11): 14 423 – 14 431.

Belviso, S., Claustre, H., and Marty, J.-C. 2001. Evaluation of the utility of chemo-taxonomic pigments as a surrogate for particulate DMSP. Limnol. Oceanogr. **46**(4): 989–995.

Cantin, G., Levasseur, M., Schultes, S., and Michaud, S. 1999. Dimethylsulfide (DMS) production by size-fractionated particles in the Labrador Sea. Aquat. Microb. Ecol. **19**: 307–312.

Claustre, H. 1994. The trophic status of various oceanic provinces as revealed by phytoplankton, pigment signatures. Limnol. Oceanogr. **39**(5): 1206–1210.

Fiala, M., Kopczynska, E.E., Jeandel, C., Oriol, L., and Vetion, G. 1998. Seasonal and interannual variability of size-fractionated phytoplankton biomass and community structure at station Kerfix, off the Kerguelen Islands, Antarctica. J. Plank. Res. **20**(7): 1341–1356.

Jones, A., Roberts, D.L., Woodage, M.J., and Johnson, C.E. 2001. Indirect sulphate aerosol forcing in a climate model with an interactive sulphur cycle. J. Geophys. Res. **106**(D17): 20 293 – 20 310.

Kettle, A.J., and Andreae, M.O. 2000. Flux of dimethylsulfide from the oceans: a comparison of updated data sets and flux models. J. Geophys. Res. **105**(D22): 26 793 – 26 808.

Kettle, A.J., Andreae, M.O., Amouroux, D., Andreae, T.W., Bates, T.S., Berresheim, H., Bingemer, H., Boniforti, R., Curran, M.A.J., DiTullio, G.R., Helas, G., Jones, G.B., Keller, M.D., Kiene, R.P., Leck, C., Levasseur, M., Malin, G., Maspero, M., Matrai, P., McTaggart, A.R., Mihalopoulos, N., Nguyen, B.C., Novo, A., Putaud, J.P., Rapsomanikis, S., Roberts, G., Schebeske, G., Sharma, S., Simó, R., Staubes, R., Turner, S., and Uher, G. 1999. A global database of sea surface dimethylsulfide (DMS) measurements and a procedure to predict sea surface DMS as a function of latitude, longitude, and month. Global Biogeochem. Cycles, **13**(2): 399–444.

Kiene, R.P., Linn, L.J., and Burton, J.A. 2000. New and important roles for DMSP in marine microbial communities, J. Sea Res. **43**(3–4): 209–224.

© 2004 NRC Canada

Laws, E.A., Falkowski, P.G., Smith, W.O., Jr., Ducklow, H., and McCarthy, J.J. 2000. Temperature effects on export production in the open ocean. Global Biogeochem. Cycles, **14**(4): 1231–1246.

Loisel, H., Bosc, E., Stramski, D., Oubelkheir, K., and Deschamps, P.Y. 2001. Seasonal variability of the backscattering coefficient in the Mediterranean Sea based on satellite SeaWiFS imagery. Geophys. Res. Lett. **28**(22): 4203–4206.

Longhurst, A., Sathyendranath, S., Platt, T., and Caverhill, C. 1995. An estimate of global primary production in the ocean from satellite radiometer data. J. Plank. Res. **17**(6): 1245–1271.

Morel, A. 1988. Optical modelling of the upper ocean in relation to its biogenous matter content (Case 1 waters). J. Geophys. Res. **93**: 10 747 – 10 768.

Scarratt, M.G., Levasseur, M., Schultes, S., Michaud, S., Cantin, G., Vézina, A., Gosselin, M., and de Mora, S.J. 2000. Production and consumption of dimethylsulfide (DMS) in North Atlantic waters. Mar. Ecol. Prog. Ser. **204**: 13–26.

Sciare, J., Mihalopoulos, N., and Nguyen, B.C. 1999. Summertime seawater concentrations of dimethylsulfide in the western Indian Ocean: reconciliation of fluxes and spatial variability with long-term atmospheric observations. J. Atmos. Chem. **32**: 357–373.

Simó, R., and Dachs, J. 2002. Global ocean emission of dimethylsulfide predicted from biogeophysical data. Global Biogeochem. Cycles, **16**(4) (doi: 10.1029/2001GB001829).

Steinke, M., Malin, G., Archer, S.D., Burkill, P.H., and Liss, P.S. 2002. DMS production in a coccolithophorid bloom: evidence for the importance of dinoflagellate DMSP lyases. Aquat. Microb. Ecol. **26**: 259–270.

Vidussi, F., Claustre, H., Manca, B.B., Luchetta, A., and Marty, J.C. 2001. Phytoplankton pigment distribution in relation to upper thermocline circulation in the eastern Mediterranean Sea during winter. J. Geophys. Res. **106**(C9): 19 939 – 19 956.

Zubkov, M.V., Fuchs, B.M., Archer, S.D., Kiene, R.P., Amann, R., and Burkill, P.H. 2001. Linking the composition of bacterioplankton to rapid turnover of dissolved dimethylsulfoniopropionate in an algal bloom in the North Sea. Environ. Microb. **3**: 304–311.

© 2004 NRC Canada

Sulphur isotopic composition of aerosols over the western North Atlantic Ocean[1]

Moire A. Wadleigh

Abstract: During spring (1998) and fall (1999) cruises of the Northern Oceans Dimethylsulphide (DMS) Emissions Model programme (NODEM II and III), size-segregated atmospheric aerosol samples were collected above the western North Atlantic Ocean. The soluble portion of the aerosols was analyzed for concentrations of sulphate, sodium, nitrate, and methane sulphonic acid (MSA). Sulphur isotopic compositions were measured on total soluble sulphur. The stable isotope data conform to a mixing model involving contributions from biogenic, anthropogenic, and sea salt sulphur sources. Biogenic sulphur fractions calculated using stable isotopic compositions range from 0.00 to 0.64 of the total sulphate, higher than most previously reported values. %MSA/NSS (non-sea-salt) SO_4^{2-} ranges from 0 to 94. The data suggest that sulphates of clearly biogenic origin (MSA) are formed in areas where surface-ocean DMS concentrations are high. These sulphates contribute to aerosol mass in particles up to 3 μm in diameter. This seems to occur by condensation onto existing aerosols. Stable isotope data indicate that these existing aerosols can be of either biogenic or anthropogenic origin depending on the size fraction and geographic location. Stable isotope data also reveal other areas where sulphate aerosols of biogenic origin are produced, not associated with MSA.

Résumé : Lors de missions en mer au printemps 1998 et à l'automne 1999 dans le cadre des programmes NODEM II et III (« Northern Oceans Dimethylsulphide (DMS) Emissions Model »), des échantillons d'aérosols fractionnés d'après la taille ont été récoltés au-dessus de la région occidentale de l'Atlantique nord. Les concentrations de sulfate, de sodium, de nitrate et d'acide méthanesulfonique (MSA) ont été déterminées dans la portion soluble des aérosols. Les compositions isotopiques du soufre mesurées dans le soufre dissous total s'accordent avec un modèle de brassage qui combine les contributions des sources de soufre biogéniques et anthropiques, ainsi que celle des sels de mer. Les fractions de soufre biogénique calculées d'après la composition des isotopes stables représentent 0,00 à 0,64 du sulfate total, des valeurs supérieures à la plupart de celles rapportées jusqu'à maintenant. Le rapport % MSA/SO_4^{2-} d'origine NSS (sels non marins) varie de 0 à 94. Les données indiquent que les sulfates qui sont nettement d'origine biogénique (MSA) se forment dans les régions où les concentrations de DMS à la surface de l'océan sont élevées. Ces sulfates contribuent à la masse des aérosols dans des particules pouvant atteindre 3 μm de diamètre. Cela semble se produire par condensation sur des aérosols déjà présents. Les données d'isotopes stables indiquent que ces aérosols préexistants peuvent être d'origine biogénique ou anthropique, selon la taille de la fraction et la position géographique. Les données d'isotopes stables révèlent aussi l'existence d'autres régions où il y a production d'aérosols à sulfates d'origine biogénique, mais non associés au MSA.

[Traduit par la Rédaction]

Introduction

The marine SO_4^{2-} aerosol consists of primary sea salt aerosol produced by bursting bubbles at the ocean surface and secondary non-sea-salt (NSS) aerosol formed by gas to particle conversion of compounds such as SO_2 and dimethylsulphide (DMS) (O'Dowd et al. 1997).

NSS SO_4^{2-} aerosol particles are predominantly <1 μm in diameter. Turner et al. (1996) have suggested that aerosols of this size can alter the earth's radiation balance directly by scattering incoming solar radiation and also indirectly by acting as nuclei for cloud condensation. Because NSS SO_4^{2-} aerosols may partially counteract the warming effects of greenhouse gases, it is important to understand the origins of the SO_2 and DMS from which they are thought to form.

DMS is readily oxidized, and low atmospheric concentrations can make it difficult to observe directly. The principal products of its oxidation include methane sulphonic acid (MSA) and SO_2, which is further oxidized to SO_4^{2-} in the atmosphere. Charlson et al. (1987) proposed that DMS released into near-surface layers of the oceans by phytoplankton is the largest source of SO_4^{2-} aerosols and cloud condensation nuclei in the marine troposphere. If true, phytoplankton productivity may influence global climate. Direct evidence that DMS oxidation contributes new particles to the fine NSS SO_4^{2-} aerosol fraction has remained elu-

Received 12 February 2003. Accepted 13 March 2004. Published on the NRC Research Press Web site at http://cjfas.nrc.ca on 30 June 2004.
J17370

M.A. Wadleigh. Department of Earth Sciences, Memorial University, St. John's, NL A1B 3X5, Canada (e-mail: moire@esd.mun.ca).

[1]This paper is part of the proceedings of the Third International Symposium on Biological and Environmental Chemistry of DMS(P) and Related Compounds, held in Rimouski (Québec), 26–28 September 2002.

 doi: 10.1139/F04-073 © 2004 NRC Canada

sive. However, assuming that it does occur, many studies have attempted to distinguish this aerosol from NSS SO_4^{2-} of anthropogenic or volcanic origin. Some have relied on modelling (e.g., Gondwe et al. 2003), while others have launched monitoring programmes to measure atmospheric DMS and its oxidation products in the marine atmosphere (e.g., Sciare et al. 2000). Measured quantities of NSS SO_4^{2-} cannot be uniquely associated with DMS unless one can distinguish its contribution from other sources of SO_2. And as long as the aerosol contribution from DMS remains unknown, or is included within the total NSS SO_4^{2-} fraction, judging the significance of the climate effects remains difficult.

Because DMS is the only known source of MSA, MSA/NSS SO_4^{2-} ratios have been suggested as a proxy for estimating the proportion of DMS-derived aerosols. Both MSA and NSS SO_4^{2-} are thought to have similar physical and chemical properties making them subject to the same transport processes and removal mechanisms. If the ratio of MSA to NSS SO_4^{2-} were constant in purely marine air masses, this ratio would be a useful tracer of the biogenic contribution to NSS SO_4^{2-}. However, previous studies have reported a trend towards higher ratios at higher latitudes (Berresheim 1987; Bates et al. 1992). This is presumably due to the temperature dependence of the branching ratio for DMS oxidation mechanisms by which DMS oxidizes more readily to MSA and less readily to SO_2 at lower temperatures (Bates et al. 1992; Wayne 2000). So while MSA is an important indicator of biological activity, it cannot be quantitatively related to the biogenic component.

Stable isotopes of sulphur offer a way of unequivocally distinguishing atmospheric aerosols of biogenic origin from those of anthropogenic or volcanic origin. The method is based on the premise that different sources of sulphur are isotopically distinct from one another and that these isotopic signatures are retained by the newly formed aerosols. This is not a new tool, but its application has been limited until recently by the demands of sample size. Recent advances in instrumentation (continuous-flow isotope ratio mass spectrometry) have enabled the accurate determination of isotopic compositions in samples containing as little as 8 μg of sulphur. This means that sufficient aerosol mass can be collected on each stage of a cascade impactor to yield an isotope measurement, providing unique insight into the sources of NSS SO_4^{2-} throughout a range of aerosol size fractions.

The atmospheric sulphur-containing aerosol over the western North Atlantic Ocean is derived from sea salt, DMS, and anthropogenic sources. Sea salt SO_4^{2-} has a well-defined isotopic value of $\delta^{34}S = +21‰$. Its fractional contribution is conventionally calculated assuming the mass ratio of SO_4^{2-} to sodium of 0.252 in bulk seawater. Phytoplankton obtain sulphur from seawater SO_4^{2-}. This value should be reflected in the DMS produced by the phytoplankton and in the SO_4^{2-} oxidation products of this DMS. SO_4^{2-} $\delta^{34}S$ values between 15‰ and 19‰ are expected from the oxidation of DMS over the oceans (Calhoun et al. 1991). Anthropogenic sulphur sources, which are dominated by fossil fuel combustion, have distinctly different sulphur isotopic compositions averaging between 0‰ and 6‰ (Wadleigh et al. 1996; Norman et al. 1999). Aerosol particles produced from biogenic marine and anthropogenic continental sources should, therefore, be isotopically distinguishable from each other.

This paper reports chemical and sulphur isotopic analyses of size-segregated aerosol samples collected during two cruises in the western North Atlantic Ocean aboard the CCGS *Hudson* in May 1998 and September 1999 (Fig. 1). The cruises were coordinated by Dr. Maurice Levasseur of the Institute Maurice Lamontagne, Fisheries and Oceans Canada (Mont-Joli, QC G5H 3Z4, Canada) as part of the Northern Oceans DMS Emissions Model programme (NODEM). Hereafter, the 1998 cruise will be referred to as NODEM II and the 1999 cruise as NODEM III.

Materials and methods

An Andersen–Sierra high-volume air sampler fitted with a Graseby five-stage cascade impactor was installed above the ship's bridge approximately 10 m above the sea surface. Aerosol particles were collected onto Whatman 41 filters for NODEM II and onto Whatman quartz fibre filters for NODEM III. Sampling duration varied from 8 to 51 h at a flow rate of 1.1 $m^3 \cdot min^{-1}$. This technique separated the particles in each sample into the following aerodynamic equivalent diameter ranges: stage 1, >7.2 μm; stage 2, 3.0–7.2 μm; stage 3, 1.5–3.0 μm; stage 4, 0.95–1.5 μm; stage 5, 0.49–0.95 μm; and stage 6, <0.49 μm. Blank filters were used to account for any contamination acquired during sample handling.

Nine samples (consisting of six size fractions each) were collected during each cruise. Soluble material on the filters was ultrasonically extracted into 50 mL of deionized water for 1 h. All size fractions from NODEM II were analyzed individually for SO_4^{2-}, Na^+, NO_3^-, and MSA by ion chromatography using a Dionex DX-100 ion chromatograph. $\delta^{34}S$ of total sulphur for the same size fractions was measured by continuous-flow isotope ratio mass spectrometry on a Carlo Erba elemental analyzer interfaced to a Finnigan MAT 252 isotope ratio mass spectrometer. The two largest size fractions (>3.0 μm) were dominated by sea salt; therefore, similar measurements were made on only the four smallest size fractions for NODEM III. Samples were slowly evaporated first in acid-washed polyethylene snap-cap containers and then in 10 mm × 10 mm tin cups. SO_4^{2-} precipitated into the tin cups as the solution evaporated. All analyses were performed in the environmental geochemistry laboratories at Memorial University (St. John's, NL A1B 3X5, Canada).

Sea salt SO_4^{2-} contributions were calculated by comparing the SO_4^{2-}/Na^+ ratio of the sample with that of bulk ocean water, assuming Na+ to be conservative. The isotopic composition of NSS SO_4^{2-} ($\delta^{34}S_{NSS}$) was calculated from the isotopic composition of the sample's total SO_4^{2-} ($\delta^{34}S_{measured}$) using the equation

$$\delta^{34}S_{NSS} = \left(\frac{1}{f_{NSS}}\right) \times [\delta^{34}S_{measured} - (f_{SS}\,\delta^{34}S_{SS})]$$

where $\delta^{34}S_{SS}$ is the measured or accepted $\delta^{34}S$ value for seawater SO_4^{2-} and f_{NSS} and f_{SS} are the fractions of NSS SO_4^{2-} and SS SO_4^{2-}, respectively, calculated as described above. $\delta^{34}S$ values are reported with respect to the Canyon Diablo

© 2004 NRC Canada

Fig. 1. Map of the western North Atlantic Ocean showing 4-day air mass back-trajectories for each of the sampled periods: shaded lines, NODEM II samples; broken lines, NODEM III samples. The inset shows the cruise tracks of the CCGS *Hudson* during NODEM II (polygons) and NODEM III (ellipses) with the samples identified by number. Samples collected during NODEM II and III are prefixed by II and III, respectively.

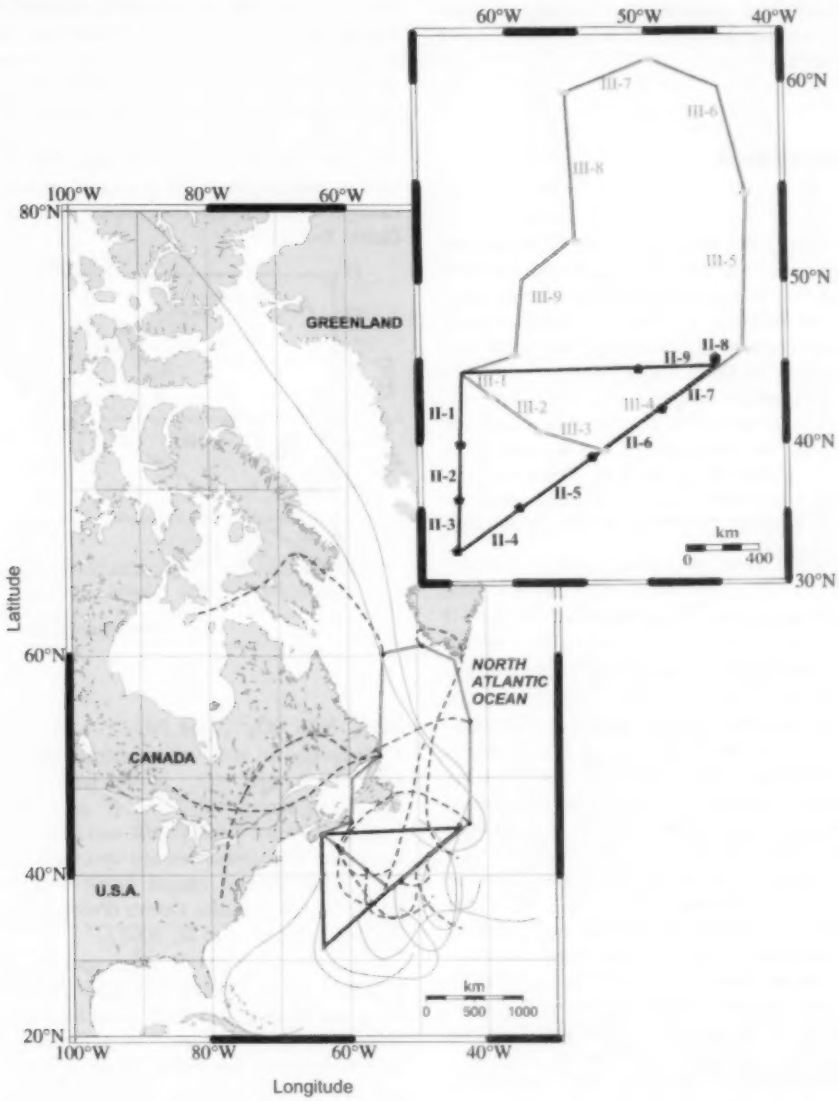

Troilite international standard. Isotopic compositions were calibrated using NBS-127 ($BaSO_4$, $\delta^{34}S$ = +20.3‰), NBS-123 (ZnS, $\delta^{34}S$ = +17.3‰), and MUN-py (FeS_2, internal reference, $\delta^{34}S$ = 1.26‰).

The Meteorological Service of Canada provided 4-day air mass back-trajectories for each sampling period using the method of Olson et al. (1978). These trajectories (Fig. 1) suggest that few of the sampling periods were directly under the influence of continental air masses.

Other scientists on these cruises measured DMS concentrations in surface seawater. The values were low but variable, ranging from <1 to 9 nmol·L^{-1} during NODEM II and from <1 to 3 nmol·L^{-1} during NODEM III. Elevated concentrations were associated with a bloom of *Chrysochromulina* in the North Atlantic Drift during NODEM II and with the west Greenland shelf during NODEM III (M. Scarratt, Institut Maurice Lamontagne, Fisheries and Oceans Canada, 850 route de la Mer, Mont-Joli, QC G5H 3Z4, Canada, personal communication). Calculated fluxes of DMS to the atmosphere ranged from <1 to 30 µmol·m^{-2}·day^{-1} during NODEM II, with high values again associated with the phytoplankton bloom, and from <1 to 20 µmol·m^{-2}·day^{-1} during NODEM III, the highest flux being associated with Hurricane Floyd (M. Scarratt, Institut Maurice Lamontagne,

© 2004 NRC Canada

Fisheries and Oceans Canada, 850 route de la Mer, Mont-Joli, QC G5H 3Z4, Canada, personal communication). Atmospheric DMS concentrations were not measured and can only be inferred from flux calculations and using MSA and NSS SO_4^{2-} as proxies. The relationship between seawater DMS concentrations and the aerosol data will be the subject of a separate contribution.

Results and discussion

Sulphur isotopes

Aerosol sulphur isotopic composition is plotted versus sea salt fraction (f_{ss}, percent) for all size-segregated samples collected during NODEM II and III (excluding the two largest size fractions from NODEM III; Fig. 2). Superimposed on this figure is a triangular plot illustrating the apportionment of aerosols between the three major sulphur sources in the North Atlantic atmosphere: biogenic (A), sea spray (B), and anthropogenic (C). Using values of +18 ± 2‰ for end-member A (bio), +21‰ for end-member B (ss), and +3 ± 2‰ for end-member C (anth) (McArdle et al. 1998; Norman et al. 1999; Wadleigh et al. 2001), we can calculate the approximate fraction of biogenic SO_4^{2-} in the North Atlantic aerosols using the equation

$$\delta^{34}S_{meas} = \delta^{34}S_{bio} f_{bio} + \delta^{34}S_{anth} f_{anth} + \delta^{34}S_{ss} f_{ss}$$

where $f_{bio} + f_{anth} + f_{ss} = 1$. These biogenic SO_4^{2-} fractions are presented for the size fractions <3.0 μm (Table 1). Larger size fractions are not included in this table because there were only a few cases in which biological contributions were a significant component of the total SO_4^{2-} for size fractions >3.0 μm. Large uncertainties (10–40%) are inherent in these calculations because of the large range in sea salt concentrations and the range in $\delta^{34}S$ of the biogenic and anthropogenic end-members. However, biogenic contributions to total SO_4^{2-} of >40% (corresponding to $f_{bio} = 0.4$) are evident in one third of the NODEM II samples and >30% in one quarter of the NODEM III samples. Biogenic contributions to NSS SO_4^{2-} ranged from 4% to 65% (mean = 35%) for the submicron size fraction. These values are substantially greater than those of Patris et al. (2000) and Turekian et al. (2001) who reported biogenic contributions generally <35%, and ~11%, respectively, of the NSS SO_4^{2-} fraction in fine particles (<0.8 μm) from the North Atlantic.

Sulphur isotopes are plotted by sample as a function of aerosol size for NODEM II (Fig. 3*a*) and NODEM III (Fig. 3*b*). Isotope data for particles >3.0 μm from NODEM II are also included (Fig. 3*a*). Between 70% and 100% of the sulphur in this size range was of sea salt origin, so it is not surprising that their $\delta^{34}S$ values are constrained to a narrow range between +16‰ and +21‰. As particle size decreases, the range of isotopic compositions changes (+5‰ to +19‰), reflecting the change from sea salt to anthropogenic and (or) biogenic sources of particles (this is effectively illustrated in Fig. 4). In general, isotopic compositions decrease with decreasing particle size. The average sea salt contribution to particles <0.95 μm is 15%.

Fig. 2. Sulphur isotopic composition of size-segregated aerosols for both NODEM II (squares) and NODEM III (diamonds) plotted versus percent sea spray (PSS). PSS values were calculated assuming sodium to be conservative. The solid lines represent a triangular plot defining the mixing regions for the known sources of sulphur. Point A represents the marine biogenic end-member ($\delta^{34}S \approx 18$‰, PSS ≈ 0). Point B represents the sea spray end-member ($\delta^{34}S = 21$‰, PSS = 100). Point C represents the continental/anthropogenic end-member ($\delta^{34}S \approx 3$‰, PSS ≈ 0). Samples with PSS > 50 tend to plot along the mixing line between C and B, between anthropogenic and sea spray sources, whereas samples with PSS < 50 plot between A, B, and C, indicating a significant biogenic sulphur component. CDT, Canyon Diablo Troilite.

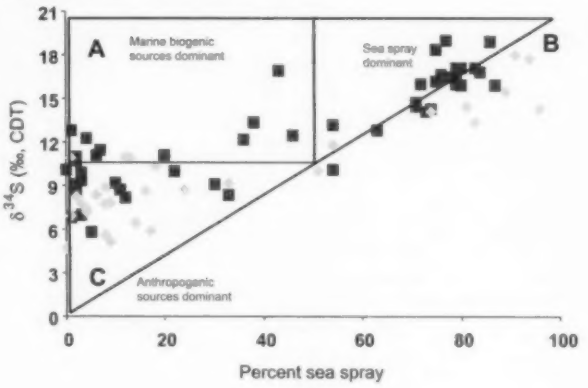

MSA, NSS SO_4^{2-}, and NO_3^-

Variations in total atmospheric concentrations for MSA, NSS SO_4^{2-}, and NO_3^- in the four smallest size fractions measured during NODEM II and III are illustrated in Figs. 5*a* and 5*b*, respectively, and their minimum, maximum, and mean concentrations are specified (Table 2). In general, these concentration ranges agree with those reported elsewhere for the Atlantic Ocean (Prospero et al. 1995; Patris et al. 2000; Turekian et al. 2001).

Concentrations of all three species were higher during NODEM II than during NODEM III. No marine sources of NO_3^- are known, and high concentrations of NO_3^- are considered to be an indicator of anthropogenic influence. The only trajectories for NODEM II to show direct continental influence have source regions in the Canadian Arctic (Fig. 1), whereas three of the air mass back-trajectories for NODEM III sample periods suggest continental source regions. But the higher NO_3^- concentrations in NODEM II samples indicate anthropogenic influence. This apparent discrepancy is consistent with Berresheim et al.'s (1991) conclusion that the boundary layer atmosphere over the western North Atlantic Ocean is impacted by continental air during all seasons. NODEM II sampling took place exclusively in this impacted region, with the result that even air masses originating over the ocean carry an anthropogenic signal. NSS SO_4^{2-} in NODEM II may also be of primarily anthropogenic origin, owing to the same long-range transport. The lower concentrations of species measured during the 1999 NODEM III cruise are more typical of remote marine con-

© 2004 NRC Canada

Table 1. Biogenic SO_4^{2-} fraction (f_{bio}) of aerosols with a diameter of <3.0 μm.

Sample	Stage 3 (1.5–3.0 μm)	Stage 4 (0.95–1.5 μm)	Stage 5 (0.49–0.95 μm)	Stage 6 (<0.49 μm)
NODEM II				
1	—	0.04	0.03	—
2	—	—	0.12	0.23
3	—	0.05	0.37	0.24
4	0.13	0.23	0.47	0.51
5	0.00	0.08	0.49	0.64
6	—	0.21	0.38	0.49
7	0.42	0.57	0.30	nd
8	—	—	0.20	0.35
9	—	—	0.25	0.43
NODEM III				
1	—	0.33	0.29	0.30
2	0.52	0.27	0.11	0.08
3	0.25	0.25	0.06	0.37
4	nd	nd	—	—
5	—	—	0.28	0.38
6	—	0.01	0.22	0.21
7	—	—	—	0.09
8	—	—	0.04	0.07
9	—	0.18	—	0.23

Fig. 3. Isotopic compositions of aerosols plotted as a function of aerosol size for (*a*) NODEM II and (*b*) NODEM III samples. CDT, Canyon Diablo Troilite.

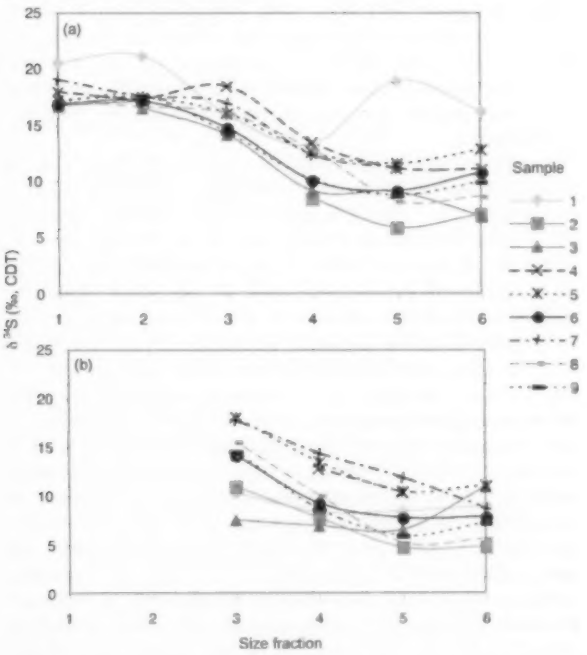

Fig. 4. $\delta^{34}S$ versus percent sea spray (PSS) for the four smallest size fractions. (*a*) NODEM II; (*b*) NODEM III. Points A, B, and C represent the biogenic, sea spray, and anthropogenic end-members, respectively. PSS values increase with increasing particle size. Diamonds, stage 6; squares, stage 5; triangles, stage 4; crosses, stage 3.

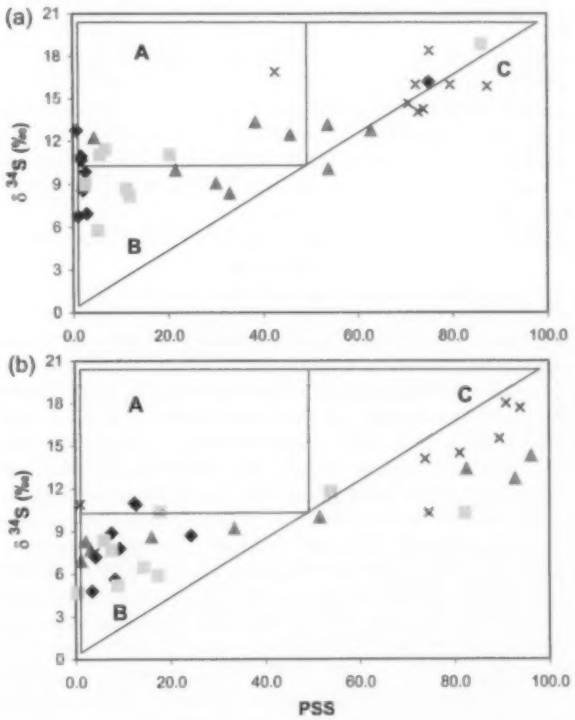

centrations consistent with the northerly latitudes sampled (Quinn et al. 1990).

Although Figs. 5*a* and 5*b* and Table 2 are based on combined values from all four of the smallest size fractions, patterns of species concentrations also appear in the individual size fractions. These are illustrated for NODEM II (Fig. 6)

© 2004 NRC Canada

Table 2. Minimum (Min.), maximum (Max.), and mean concentrations of MSA, NSS SO_4^{2-}, and NO_3^- in <3.0-μm size fractions for the NODEM II and III surveys.

	NODEM II			NODEM III		
Concentration (nmol·m^{-3})	Min.	Max.	Mean	Min.	Max.	Mean
MSA	0.17	0.64	0.36	0.16	0.40	0.21
NSS SO_4^{2-}	4.5	25	13	1.5	12	8.3
NO_3^-	3.3	32	14	0.030	5.3	1.5

Fig. 5. Combined total [MSA] (dot-dashed lines), [NSS SO_4^{2-}] (solid lines), and [NO_3^-] (dashed lines) in nmol·m^{-3} for the four smallest size fractions (<3.0 μm) collected during (*a*) NODEM II and (*b*) NODEM III.

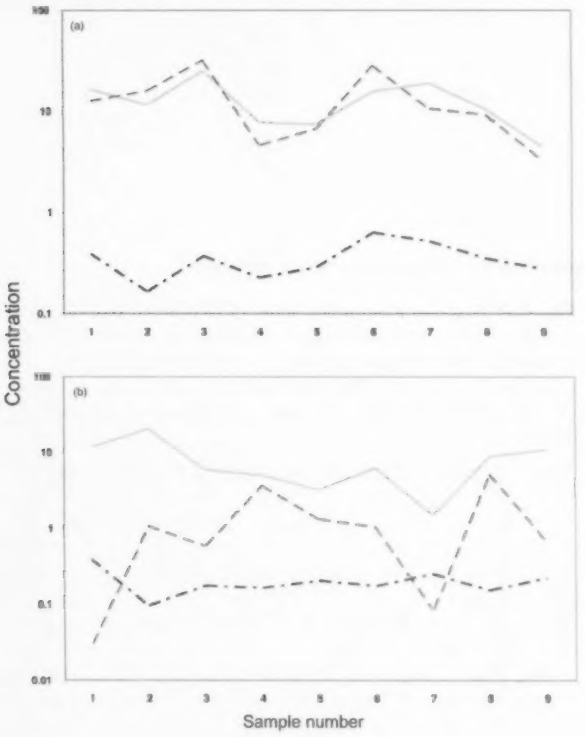

and NODEM III (Fig. 7). NO_3^- concentrations tend to increase with increasing particle size. This is particularly evident in the NODEM II data. Concentrations during NODEM III are almost an order of magnitude lower and fewer data are reported. NSS SO_4^{2-} concentrations tend to decrease with increasing particle size. Where sufficient data exist for comparison, [NO_3^-] and [NSS SO_4^{2-}] patterns always correspond. Samples in the two smallest size fractions (<0.95 μm) contained between 62% and 100% of the total MSA. This agrees well with other reported data for the Atlantic (Sciare et al. 2000). [MSA] decreases with increasing size fraction. In some size fractions, [MSA] and [NSS SO_4^{2-}] patterns correspond (<0.49 μm, NODEM II and III; 0.49–0.95 μm, NODEM III; 0.95–1.5 μm, NODEM II), whereas in others, they are opposed (0.49–0.95 μm, NODEM II; 0.95–1.5 μm, NODEM III; 1.5–3.0 μm, NODEM II and III).

%MSA/NSS SO_4^{2-}

MSA/NSS mass ratios are presented for the four size fractions <3.0 μm measured in this study (Table 3) and are also illustrated graphically (Figs. 6 and 7). Values were fairly low and constant for the NODEM II data, ranging from 0% to 6.8% and showing no obvious size dependence. The only unusual feature in the ratio for NODEM II was its sudden decrease in the 1.5–3.0 μm size fraction for sample 7. The decrease was due to a concomitant rise in [NSS SO_4^{2-}] and fall in [MSA]. For NODEM III, however, the values were higher and their range more variable, extending from 0% to 94%, with the highest and most dramatic change in values found preferentially in the 0.95–3.0 μm particle size range and associated with sample 7. The increase in ratio was due primarily to a sudden decrease in [NSS SO_4^{2-}] in the three smallest size fractions but an increase in [MSA] in the 1.5–3.0 μm fraction. The higher ratios observed in NODEM III are consistent with the more northerly latitudes sampled. Turekian et al. (2001) observed a decrease in the ratio %MSA/biogenic NSS SO_4^{2-} with decreasing particle size in aerosols collected at Bermuda. They interpreted this observation to represent significant production of biogenic NSS SO_4^{2-} via aqueous-phase oxidation pathways. No consistent trend with particle size was observed in either the NODEM II or III data.

Regions of high DMS concentration in the water column were encountered in the area of sample 7 of the NODEM II cruise and in the area of sample 7 of the NODEM III cruise. The former is associated with a bloom of *Chrysochromulina* in the North Atlantic Drift; the latter is associated with the high biological productivity area of the west Greenland shelf. The highest %MSA/NSS SO_4^{2-} ratios in this study correspond to these samples. In addition, both MSA and NSS for these two samples are spread over the four smallest size fractions. Biogenic SO_4^{2-} fractions calculated using stable isotope data for sample 7 of NODEM II (Table 1) are also among the highest values, ranging from 30% to 57% of the total SO_4^{2-}. Unfortunately, high sea salt concentrations made it impossible to calculate the biogenic fraction for sample 7 of NODEM III. Taken together, these results support the suggestion that phytoplankton produce DMS and that oxidation of this DMS produces or enhances submicrometre-sized aerosol particles thought to influence the earth's albedo. In the two areas of high DMS production, the calculated biogenic fractions of sulphur and (or) concentrations of MSA were higher than in other areas. Since MSA is not expected to form new aerosol particles, its correlation with NSS SO_4^{2-} suggests preferential condensation onto existing NSS SO_4^{2-} particles, primarily <0.95 μm in diameter.

Nevertheless, high MSA concentrations and ratios are not an exclusive indicator of biogenic aerosols in this study. Sev-

© 2004 NRC Canada

Fig. 6. Variation in [NO_3^-] (crosses), [NSS SO_4^{2-}] (squares), [MSA] (diamonds), and %[MSA]/[NSS SO_4^{2-}] (bold line) according to individual size fraction for NODEM II. (*a*) <0.49 μm; (*b*) 0.49–0.95 μm; (*c*) 0.95–1.5 μm; (*d*) 1.5–3.0 μm. All concentrations are in nmol·m^{-3}.

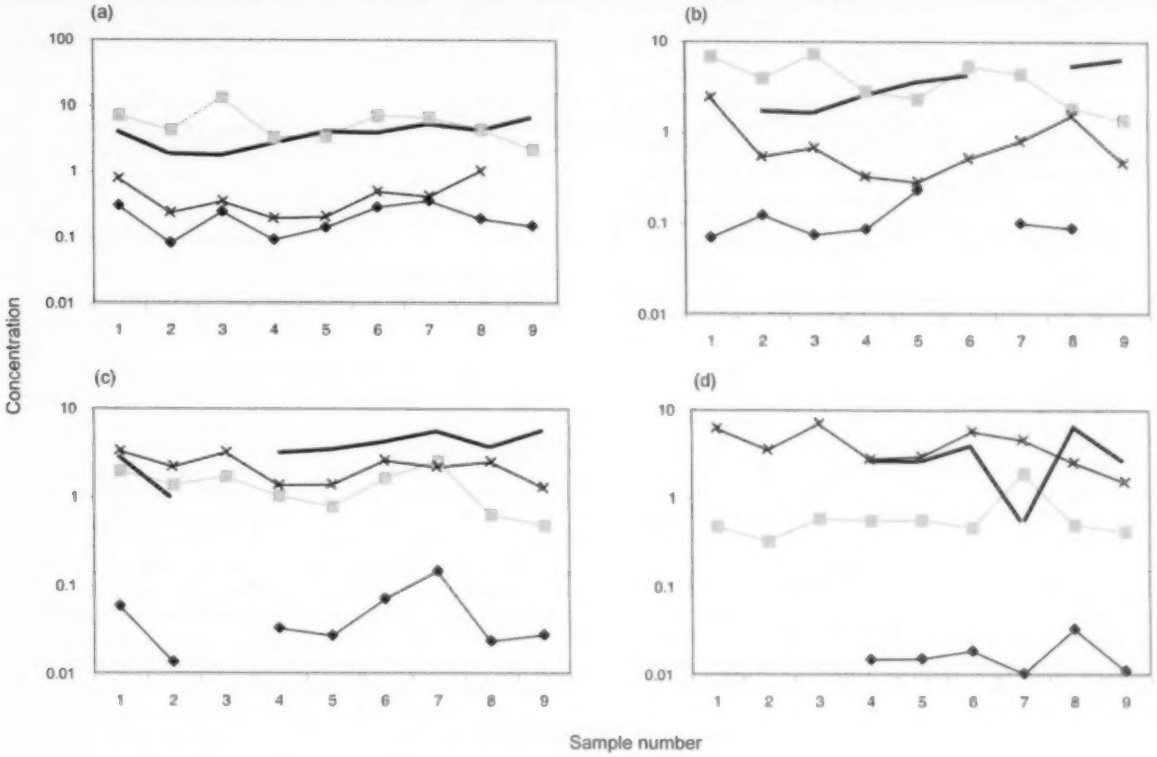

eral other samples contained significant biogenic contributions as determined by stable isotopic compositions (see Table 1: NODEM II, samples 4, 5, and 6; NODEM III, samples 1, 2, and 5). Of particular interest in this regard is NODEM III sample 5. This sample corresponds to the encounter with Hurricane Floyd and the highest calculated DMS fluxes on the cruise. There is nothing remarkable about [MSA] or [NSS SO_4^{2-}], but this sample has the highest biogenic SO_4^{2-} contribution in the submicrometre size fraction of all NODEM III samples based on stable isotope measurements.

Oxidation of DMS forms two condensable species, MSA and sulphuric acid, which contribute to the submicrometre aerosol mass (Kreidenweiss et al. 1989). MSA is not expected to form new particles by condensation but may contribute to the growth of existing particles by depositing onto them (Brasseur et al. 1999). Sulphuric acid has a sufficiently low vapour pressure that it is capable of forming new particles and can also enhance growth of existing particles. MSA and NSS SO_4^{2-} are positively correlated for both NODEM II and III (r = 0.789) for the four smallest size fractions, but there is a considerable degree of scatter. The slope of the line corresponds to a %[MSA]/[NSS SO_4^{2-}] ratio of 2.4, similar to background values for the western North Atlantic Ocean. The greatest mass of both MSA (79% for NODEM II, 84% for NODEM III) and NSS (75% for NODEM II, 84% for NODEM III) is in the submicrometre size fraction. Correlation of MSA with NSS SO_4^{2-} means that biogenic NSS SO_4^{2-} has formed its own particles and MSA has condensed onto them or that MSA has deposited onto existing anthropogenic SO_4^{2-} particles or both. These observations are consistent with the differential incorporation of biogenic sulphur as a function of particle size. Isotope data suggest that the submicrometre fraction includes biogenic and anthropogenic SO_4^{2-}, favouring one of the latter two explanations.

In conclusion, this work has used stable sulphur isotopes for distinguishing sea salt, biogenic, and anthropogenic sources of aerosol NSS SO_4^{2-} in the marine environment. Calculated biogenic SO_4^{2-} fractions from these parts of the western North Atlantic Ocean are much higher than previously reported. %MSA/NSS SO_4^{2-} ratios are broadly similar to previously reported values for this area, but there are specific examples of particularly high ratios related to known areas of high productivity, with the highest ratios in high-latitude regions.

The observed dependence of isotopic composition on aerosol size yielded additional clues to the formation and composition of the submicrometre aerosol, considered to influence the earth's albedo. The data from this study suggest that sulphates of clearly biogenic origin (MSA) are formed in areas where surface-ocean DMS concentrations are high. Calculations based on stable isotope data support the biogenic origin of these aerosols. These sulphates contribute to the

© 2004 NRC Canada

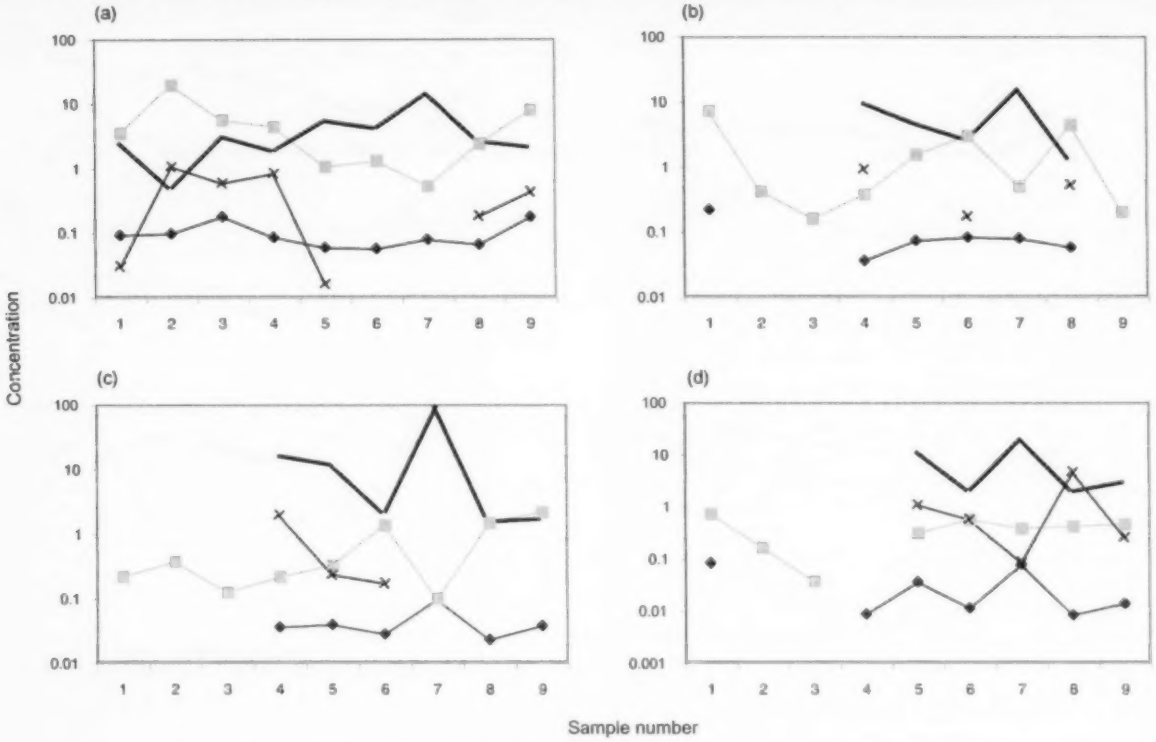

Fig. 7. Variation in [NO_3^-] (crosses), [NSS SO_4^{2-}] (squares), [MSA] (diamonds), and %[MSA]/[NSS SO_4^{2-}] (bold line) according to individual size fraction for NODEM III. (*a*) <0.49 μm; (*b*) 0.49–0.95 μm; (*c*) 0.95–1.5 μm; (*d*) 1.5–3.0 μm. All concentrations are in nmol·m^{-3}.

Table 3. %MSA/NSS SO_4^{2-} for aerosols with diameter of <3.0 μm

Sample	Stage 3 (1.5–3.0 μm)	Stage 4 (0.95–1.5 μm)	Stage 5 (0.49–0.95 μm)	Stage 6 (<0.49 μm)
NODEM II				
1	0	3.0	0	4.2
2	0	1.0	1.7	1.9
3	0	0	1.7	1.8
4	2.7	3.2	2.6	2.7
5	2.7	3.5	3.6	4.1
6	4.0	4.3	4.3	4.0
7	0.5	5.6	0	5.4
8	6.7	3.8	5.4	4.3
9	2.6	5.8	6.4	6.8
NODEM III				
1	11	0	3.0	2.6
2	—	—	—	0.5
3	0	0	0	3.2
4	—	16	9.6	1.9
5	12	12	4.7	5.5
6	2.0	2.0	2.7	4.2
7	20	94	16	15
8	2.0	1.6	1.3	2.7
9	2.9	1.7	0	2.2

submicrometre aerosol mass likely by condensing onto existing aerosols (size range of <0.45 to 3.0 μm). Stable isotope data indicate that these existing aerosols can be of both biogenic and anthropogenic origin. Stable isotope data also identified other NSS SO_4^{2-} aerosols with a significant biogenic component not associated with MSA.

© 2004 NRC Canada

Acknowledgements

Funding for this research was provided by a grant from the Natural Sciences and Engineering Research Council of Canada to the author and from the Climate Change Action Fund to M. Levasseur. The author would also like to thank G. Quinlan for his assistance in preparation of the manuscript and Alison Pye for field and laboratory assistance. The manuscript was improved by the comments from two anonymous reviewers.

References

Bates, T., Calhoun, J., and Quinn, P. 1992. Variations in the methanesulphonate to sulphate molar ratio in submicrometre marine aerosol particles over the south Pacific Ocean. J. Geophys. Res. **97**: 9859–9865.

Berresheim, H. 1987. Biogenic sulphur emissions from the Subantarctic and Antarctic oceans. J. Geophys. Res. **92**: 13 245 – 13 262.

Berresheim, H., Andreae, M.O., Iverson, R.L., and Li, S.M. 1991. Seasonal variations of dimethylsulphide emissions and atmospheric sulphur and nitrogen species over the western north Atlantic Ocean. Tellus Ser. B Chem. Phys. Meteorol. **43**: 353–372.

Brasseur, G.P., Orlando, J.J., and Tyndall, G.S. 1999. Atmospheric chemistry and global change. Oxford University Press, New York.

Calhoun, J.A., Bates, T.S., and Charlson, R.J. 1991. Sulphur isotope measurements of sub-micrometre sulphate aerosol particles over the Pacific Ocean. Geophys. Res. Lett. **18**: 1877–1880.

Charlson, R., Lovelock, J., Andreae, M., and Warren, S. 1987. Oceanic phytoplankton, atmospheric sulphur, cloud albedo and climate: a geophysiological feedback. Nature (Lond.), **326**: 655–661.

Gondwe, M., Krol, M., Gieskes, W., Klaassen, W., and de Baar, H. 2003. The contribution of ocean-leaving DMS to the global atmospheric burdens of DMS, MSA, SO_2, and NSS SO_4^{2-}. Global Biogeochem. Cycles, **17**: 1–18.

Kreidenweiss, S.M., Flagan, R.C., Seinfeld, J.H., and Okuyama, K. 1989. Binary nucleation of methanesulphonic acid and water. J. Aerosol Sci. **20**: 587–607.

McArdle, N.C., Liss, P.S., and Dennis, P. 1998. An isotopic study of atmospheric sulphur at three sites in Wales and at Mace Head, Eire. J. Geophys. Res. **103**: 31 079 – 31 094.

Norman, A.L., Barrie, L.A., Toom-Sauntry, D., Sirois, A., Krouse, H.R., Li, S.M., and Sharma, S. 1999. Sources of aerosol sulphate at Alert: apportionment using stable isotopes. J. Geophys. Res. **104**: 11 619 – 11 631.

O'Dowd, C., Smith, M., Constredine, I., and Lowe, J. 1997. Marine aerosol, sea salt, and the marine sulphur cycle: a short review. Atmos. Environ. **31**: 73–80.

Olson, M.P., Oikawa, K.K., and MacAfee, A.W. 1978. A trajectory model applied to the long-range transport of air pollutants: a technical description and some model intercomparisons, *LRTAP 78-4*, Atmospheric Environment Service, Downsview, Ont.

Patris, N., Mihlopoulos, N., and Baboukas, D. 2000. Isotopic composition of sulphur in size-resolved marine aerosols above the Atlantic Ocean. J. Geoph$_2$ Res. **105**: 14 449 – 14 457.

Prospero, J.M., Savoie, D.L., Arimoto, R., Olafsson, H., and Hjartarson, H. 1995. Sources of aerosol nitrate and non-sea salt sulphate in the Iceland region. Sci. Total Environ. **160**: 181–191.

Quinn, P.K., Bates, T.S., Johnson, J.E., Covert, D.S., and Charlson, R.J. 1990. Interactions between the sulphur and reduced nitrogen cycles over the central Pacific Ocean. J. Geophys. Res. **95**: 16 405 – 16 416.

Sciare, J., Baboukas, E., Kanakidou, M., Krischke, U., Belviso, H., Bardouki, H., and Mihalopoulos, N. 2000. Spatial and temporal variability of atmospheric sulphur-containing gases and particles during the Albatross campaign. J. Geophys. Res. **105**: 14 433 – 14 448.

Turekian, V.C., Macko, S.A., and Keene, W.C. 2001. Application of stable sulphur isotopes to differentiate sources of size-resolved particulate sulphate in polluted marine air at Bermuda during spring. Geophys. Res. Lett. **28**: 1491–1494.

Turner, S., Nightingale, P., Spokes, L., Liddicoat, M., and Liss, P. 1996. Increased dimethyl sulphide concentrations in sea water from in situ iron enrichment. Nature (Lond.), **383**: 513–516.

Wadleigh, M.A., Schwarcz, H.P., and Kramer, J.R. 1996. Isotopic evidence for the origin of sulphate in coastal rain. Tellus Ser. B Chem. Phys. Meteorol. **48**: 44–59.

Wadleigh, M.A., Schwarcz, H.P., and Kramer, J.R. 2001. Areal distribution of sulphur and oxygen isotopes in sulphate of rain over eastern North America. J. Geophys. Res. **106**: 20 883 – 20 895.

Wayne, R.P. 2000. Chemistry of atmospheres. 3rd ed. Oxford University Press, New York.

© 2004 NRC Canada

Will marine dimethylsulfide emissions amplify or alleviate global warming? A model study[1]

Laurent Bopp, Olivier Boucher, Olivier Aumont, Sauveur Belviso, Jean-Louis Dufresne, Mai Pham, and Patrick Monfray

Abstract: Dimethylsulfide (DMS) is the most abundant volatile sulfur compound at the sea surface and has a strong marine phytoplanktonic origin. Once outgased into the atmosphere, it contributes to the formation of sulfate aerosol particles that affect the radiative budget as precursors of cloud condensation nuclei (CCN). It has been postulated that climate may be partly modulated by variations in DMS production. We test this hypothesis in the context of anthropogenic climate change and present here, modelled for the first time, an estimate of the radiative impact resulting from changes in DMS air–sea fluxes caused by global warming. At 2× CO_2, our model estimates a small increase (3%) in the global DMS flux to the atmosphere but with large spatial heterogeneities (from –15% to 30%). The radiative perturbation resulting from the DMS-induced change in cloud albedo is estimated to be –0.05 $W \cdot m^{-2}$, which represents only a small negative climate feedback on global warming. However, there are large regional changes, such as a perturbation of up to –1.5 $W \cdot m^{-2}$ in summer between 40°S and 50°S, that can impact the regional climate. In the Southern Ocean, the radiative impact resulting from changes in the DMS cycle may partly alleviate the radiative forcing resulting from anthropogenic CO_2.

Résumé : Le sulfure de diméthyle (DMS) est le composé sulfuré volatil le plus abondant à la surface de la mer et il provient en grande partie du phytoplancton marin. Une fois libéré dans l'atmosphère, il contribue à former des particules de sulfate en aérosol qui affectent le bilan des radiations en tant que précurseurs de noyaux de condensation des nuages (CCN). On a aussi émis l'hypothèse selon laquelle le climat est en partie contrôlé par les variations de la production de DMS. Nous vérifions cette hypothèse dans le contexte des changements anthropiques du climat et nous présentons une estimation, obtenue par modélisation, de l'impact sur les radiations causé par les changements des flux air–mer de DMS dus au réchauffement global. À des concentrations doublées de CO_2 (2× CO_2), le modèle prédit un faible accroissement (3 %) du flux global de DMS vers l'atmosphère, mais une importante hétérogénéité spatiale (de –15 % à 30 %). La perturbation relative estimée des radiations due aux changements d'albédo des nuages est de –0,05 $W \cdot m^{-2}$, ce qui représente seulement une faible rétroaction négative au réchauffement global. Il y a, cependant, de grands changements régionaux, tels qu'une perturbation pouvant atteindre –1,5 $W \cdot m^{-2}$ en été entre les latitudes 40°S et 50°S, qui peuvent affecter le climat régional. Dans l'océan austral, l'impact sur les radiations dû aux changements dans le cycle du DMS peut, en partie, diminuer le forçage relatif relié au CO_2 anthropique.

[Traduit par la Rédaction]

Introduction

The sea-to-air flux of dimethylsulfide (DMS) is controlled by the DMS concentration at the sea surface and by the magnitude of the DMS transfer velocity across the air–sea interface, which both depend on climate variables. Sea-to-air transfer velocity mainly varies with sea-surface temperature and wind velocity (Liss and Merlivat 1986; Wanninkhof 1992; Nightingale et al. 2000). Sea-surface DMS concentration is also regulated by climate variables such as solar irradiance, sea-surface temperature, and ocean physics through their control on the marine biology.

Received 5 August 2003. Accepted 27 November 2003. Published on the NRC Research Press Web site at http://cjfas.nrc.ca on 24 June 2004.
J17686

L. Bopp[2] and S. Belviso. Laboratoire des Sciences du Climat et de l'Environnement/IPSL, CEA/CNRS, F-91191 Gif sur Yvette, France.
O. Boucher. Laboratoire d'Optique Atmosphérique, CNRS/USTL, F-59655 Villeneuve d'Ascq CEDEX, France.
O. Aumont. Laboratoire d'Océanographie et de Dynamique du Climat/IPSL, Université Paris VI, F-75252 Paris CEDEX 5, France.
J.-L. Dufresne. Laboratoire de Météorologie Dynamique/IPSL, Université Paris VI, F-75252 Paris CEDEX 5, France.
M. Pham. Service d'Aéronomie/IPSL, Université Paris VI, F-75252 Paris CEDEX 5, France.
P. Monfray. Laboratoire d'Etudes en Géodésie et Océanographie Spatiales, F-31400 Toulouse, France.

[1]This paper is part of the proceedings of the Third International Symposium on Biological and Environmental Chemistry of DMS(P) and Related Compounds, held in Rimouski (Québec), 26–28 September 2002.
[2]Corresponding author (e-mail: bopp@lsce.saclay.cea.fr).

 doi: 10.1139/F04-045 © 2004 NRC Canada

It has been postulated that the Earth's climate is partly regulated by variations in DMS emissions through a DMS – cloud concentration nuclei (CCN) – cloud albedo feedback (Charlson et al. 1987). However, there are large uncertainties both on the sign and on the magnitude of this feedback (Liss et al. 1994), and it is still not clear whether this mechanism can play a role in future climate change.

A first step has been accomplished by Gabric et al. (1998, 2001) with the coupling of a general circulation model together with a DMS production model to investigate the response of DMS emissions to climate change. Based on a 10° × 20° area in the sub-antarctic Southern Ocean, south of Australia, Gabric et al. (2001) estimate an increase in DMS emissions of 5% by 2080 (corresponding to an equivalent CO_2 tripling relative to pre-industrial levels). With this modest increased percentage, they find a small negative radiative impact, which, they conclude, confirms the minor role for DMS-derived aerosols in climate regulation. But this study is essentially a regional one and it is difficult to extend such results to the world ocean. Penner et al. (2001) estimated a small increase in global DMS flux between the years 2000 and 2100, with global DMS fluxes of 26.0 and 27.7 Tg S·year^{-1}, respectively. This estimate is for constant marine DMS concentrations and thus includes only the effects of changing wind speed and sea-surface temperature, which were estimated from the climate system model of the National Center for Atmospheric Research (NCAR). Moreover, Penner et al. (2001) did not estimate the impact of such changes on the radiation budget.

In a previous paper (Bopp et al. 2003), a model of the global distribution of sea-surface DMS concentrations (Aumont et al. 2002) was coupled to an atmosphere–ocean general circulation model (Barthelet et al. 1998) to predict the evolution of DMS sea-surface concentrations and air–sea fluxes in the context of global warming. Here, we propose to extend the previous study and to propagate the changes in air–sea DMS fluxes to the atmosphere sulfur cycle and climate. To predict the impact of changes in marine DMS emissions on the atmospheric sulfur cycle and the radiative budget of the Earth, we use a global model of the atmospheric sulfur cycle. The aim of this study is to give a first quantitative assessment of the role of DMS emissions in future climate change.

To test the robustness of our results, we perform additional simulations. In particular, we use two different parameterizations for the air–sea gas exchange transfer function (Liss and Merlivat 1986; Nightingale et al. 2000) and two different parameterizations for the relationship between the atmospheric sulfate mass and the cloud droplet number (CDN) concentration (Boucher and Lohmann 1995).

Methods

Marine DMS emissions

Sea-surface DMS concentrations for 1× CO_2 and 2× CO_2 conditions are obtained from the work of Bopp et al. (2003). (Note that 1× CO_2 corresponds here to 1990 (350 ppmv (parts per million by volume)) rather than to pre-industrial conditions.) In this previous work, the transient climate response to increased atmospheric CO_2 was obtained from simulations with the Institut Pierre-Simon Laplace Coupled Model 1 (IPSL-CM1) ocean–atmosphere general circulation model (OAGCM) (Barthelet et al. 1998). The transient climate run consists of a global-warming scenario in which atmospheric pCO_2 was increased from 350 ppmv (1× CO_2) at a rate of 1% per year, reaching 700 ppmv (2× CO_2) after about 70 years.

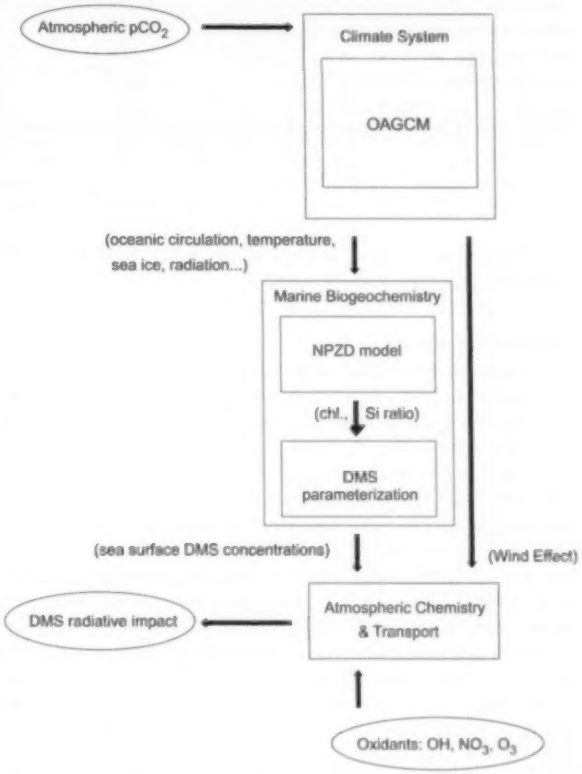

Fig. 1. The suite of models used for this study includes an atmosphere–ocean general circulation model (OAGCM), an oceanic biogeochemical scheme incorporating parameterizations of air–sea dimethylsulfide (DMS) emissions, and a model of the global atmospheric sulfur cycle. NPZD, nutrient, phytoplankton, zooplankton, and detritus model; chl, surface chlorophyll.

This transient climate was then used to force a marine biogeochemical scheme (Fig. 1) and to predict the evolution of marine biology (Bopp et al. 2001). The biogeochemical scheme used for this study is a nutrient, phytoplankton, zooplankton and detritus (NPZD) type model. Phytoplankton growth depends on the local conditions of light, temperature, and turbulence and considers PO_4^{3-} as the only limiting nutrient. Parameterizations of DMS, as nonlinear functions of surface chlorophyll concentrations (a proxy of the phytoplankton biomass) and Si ratios (computed as the ratio of the local simulated production of biogenic silica to the maximum production of biogenic silica and used as a proxy of the phytoplankton composition) were applied to predict DMS sea-surface concentrations (Bopp et al. 2003). Those relationships (DMS as a function of surface chlorophyll and Si ratio) have been established from datasets obtained during several cruises carried out in contrasted areas of the world oceans. The marine biogeochemical scheme and the DMS

© 2004 NRC Canada

Table 1. Characteristics of the experiments performed in this study

Experiment	CONTROL	GWdms	GW	CTLgex	GWgex	CTLcdn	GWcdn
Oceanic DMS concentration	1× CO_2	2× CO_2	2× CO_2	1× CO_2	2× CO_2	1× CO_2	2× CO_2
Wind speed correction factor	—	—	2× CO_2	—	2× CO_2	—	2× CO_2
Sea–air transfer function	Nightingale	Nightingale	Nightingale	Liss	Liss	Nightingale	Nightingale
Sulfate to CDNC relationship	D	D	D	D	D	A	A
Oceanic DMS emission flux	29.47	29.77 (+1%)	30.23 (+3%)	19.97	20.48 (+3%)	29.47	30.23 (+3%)
DMS burden	0.077	0.078	0.079	0.053	0.054	0.077	0.079
Radiative impact (90°N–90°S)	—	–0.03	–0.05	—	–0.05	—	–0.045
Radiative impact (40°S–60°N)	—	–0.25	–0.37	—	–0.35	—	–0.29

Note: Oceanic dimethylsulfide (DMS) concentrations for 1× CO_2 and 2× CO_2 and the wind speed correction factor are obtained form the work of Bopp et al. (2003). The sea–air transfer function for DMS emissions are from Nightingale et al. (2000) or Liss and Merlivat (1986). The relationship between cloud droplet number concentration (CDNC) and the sulfate mass concentration are taken from Boucher and Lohmann (1995) and correspond to relationships A and D of this paper. Oceanic DMS fluxes are given in Tg S·year^{-1}, DMS burdens in Tg S, and radiative impacts in W·m^{-2}.

parameterizations that were used are fully described and evaluated in Aumont et al. (2002).

Sulfur cycle model

A model of the global atmospheric sulfur cycle is used to propagate the DMS fluxes into the atmosphere and to compute the associated radiative impact through changes in the cloud properties (Fig. 1). The model used in this study was developed in the framework of the atmospheric general circulation model (AGCM) of the Laboratoire de Météorologie Dynamique and is fully described in Boucher et al. (2002). Only aspects relevant to the DMS cycle are recalled here. Sea-surface DMS concentrations are prescribed from Bopp et al. (2003) on a monthly basis but DMS fluxes are computed interactively in the atmospheric sulfur cycle model on an hourly basis to take into account the short temporal variability of winds. This differs from our previous work (Bopp et al. 2003) in which DMS fluxes were estimated using monthly means of winds. Once emitted into the atmosphere, DMS is oxidized in the gas phase by OH and NO_3 radicals. Oxidation of DMS by NO_3 produces SO_2 and oxidation of DMS by OH produces either SO_2 or dimethylsulfoxide (DMSO). We also included the oxidation of DMS by O_3 in the gas phase (producing SO_2 only) and aqueous phase (producing DMSO only) as introduced in Boucher et al. (2003). DMSO is oxidized in the gas phase by OH to produce SO_2 and methanesulfonic acid (MSA). No heterogeneous sink is included for DMS and DMSO. All reaction rates are given in Boucher et al. (2002, 2003). The monthly concentrations of oxidants are prescribed from the IMAGES model (Müller and Brasseur 1995), except H_2O_2, which is calculated interactively in the model.

Experimental design

We provide a list and characteristics of the seven experiments performed with our global model of the atmospheric sulfur cycle (Table 1). All of the experiments use the same meteorology, i.e., the dynamics of the global atmospheric model is forced by present-day climatologies and the radiative impact of changing DMS emissions does not feedback on the simulated meteorology. The different experiments also use the same sources of sulfur compounds other than marine DMS. In particular, the industrial sources of SO_2 are taken from the EDGAR 2.0 database (Olivier et al. 1996) and are representative of year 1990. We also include anthropogenic sources of H_2S (Watts 2000) and volcanic sources of SO_2 (Andres and Kasgnoc 1998).

The seven experiments differ (*i*) by their marine DMS concentrations, taken from Bopp et al. (2003), (*ii*) by the parameterization of air–sea DMS exchange (Nightingale et al. (2000) or Liss and Merlivat (1986)) used to compute interactively the DMS fluxes, and (*iii*) by the parameterization of the sulfate mass to cloud droplet number concentration (CDNC) relationship (Boucher and Lohmann 1995).

In the three different control experiments (CONTROL, CTLgex, and CTLcdn), marine DMS concentrations are set to their 1× CO_2 value. In the "global-warming" experiments (GW, GWgex, and GWcdn), marine DMS concentrations are set to their 2× CO_2 value and we correct the air–sea DMS flux by applying a scaling factor on the 10-m wind speed, which accounts for the changes in wind speed as simulated in the OAGCM 1× CO_2 and 2× CO_2 experiments. This scaling factor is applied as a two-dimensional (latitude–longitude) monthly average and is estimated from the changes in wind stress in the OAGCM experiments (Fig. 1). We also perform an additional sensitivity experiment (GWdms) similar to GW but without the correction factor on wind speed in order to separate effects of the changes in marine DMS concentrations and wind speed. We do not account in these experiments for changes in the DMS air–sea transfer velocity induced by the change in sea-surface temperature and sea ice.

For our baseline experiments (CONTROL and GW), we use the parameterization of Nightingale et al. (2000) to compute the air–sea DMS fluxes. The sensitivity of the results to the choice of the gas exchange parameterization is tested in the CTLgex and GWgex experiments using the parameterization of Liss and Merlivat (1986) instead of Nightingale et al. (2000).

For our baseline experiments (CONTROL and GW), we use the relationship D of Boucher and Lohmann (1995) to relate the cloud droplet number concentration to the atmospheric sulfate mass concentration. This calculation is only diagnostic and therefore only includes the first indirect effect (change in cloud optical properties for a fixed liquid water content). Although very uncertain, the second indirect effect (resulting from a reduction in precipitation efficiency) may be of magnitude similar to that of the first indirect effect. The radiative impact on clouds because of changes in DMS emissions is computed as the difference in top-of-atmosphere radiative fluxes between the global-warming and

© 2004 NRC Canada

Fig. 2. Zonally averaged change (global warming minus control) of (*a*) sea-surface temperature (SST, solid line,°C) and mixed layer depth (broken line, m, log-scale), (*b*) surface chlorophyll (solid line, mg·m^{-3}) and relative abundance of siliceous phytoplankton species (Si ratio, broken line, %), (*c*) dimethylsulfide (DMS) sea-surface concentration (solid line, nM) and wind effect (dotted line, %), (*d*) DMS flux to the atmosphere (solid line, µmol·day^{-1}·m^{-2}). In the last panel (*d*), the solid lines represent both effects of changes in marine DMS and winds (GW minus CONTROL), and the broken lines represent the effect of sea-surface DMS concentration changes alone (GWdms minus CONTROL). In the same panel, the dotted line represents both effects (marine DMS and winds) but using the Liss and Merlivat (1986) parameterization (GWgex minus CTLgex). Panels (*a*), (*b*), and (*c*) recall the main results of Bopp et al. (2003).

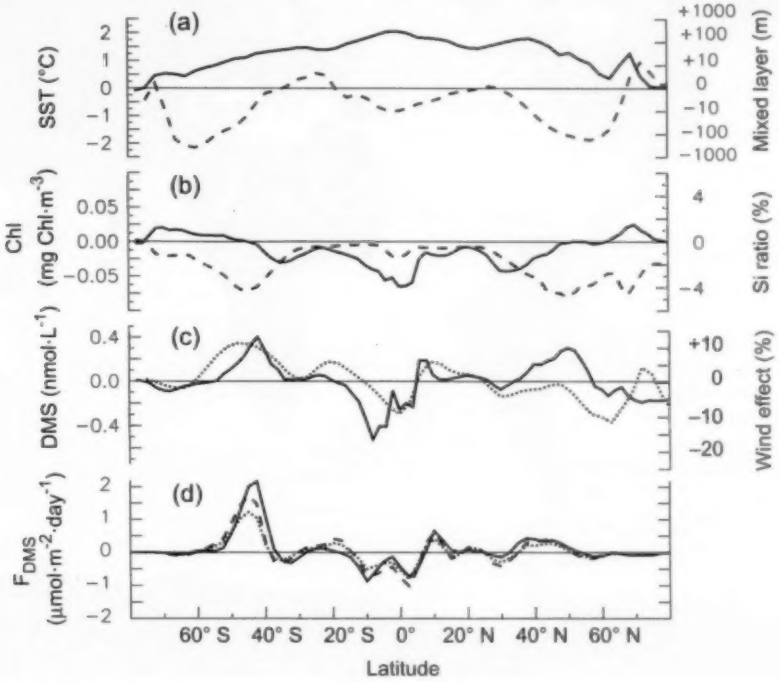

control experiments (i.e., with DMS emissions at 2× CO_2 and 1× CO_2, respectively). The minimum background cloud droplet number concentration is prescribed at 50 cm^{-3} (a larger value than in Boucher and Lohmann (1995), thus decreasing the cloud sensitivity to CDNC at low CDNC). The robustness of our results to this relationship is tested in CTLcdn and GWcdn, which are identical to CONTROL and GW except that we use the relationship A of Boucher and Lohmann (1995) to relate the cloud droplet number concentration to the atmospheric sulfate mass. With relationship D, there is only one log–log regression line between sulfate mass and CDNC, taken as identical over the continents and the oceans, whereas relationship A distinguishes between continental and marine air.

The model was run 18 months for each experiment and we present results for the last 12 months. The spin-up time of 6 months is long enough considering the short life of aerosols.

Results

We first recall the main results of Bopp et al. (2003) in which the authors focus on the modelled marine productivity and marine DMS concentrations responses to climate change (Figs. 2*a*–2*c*). The biogeochemical model used in this previous study predicts a 9% global decrease in the mean annual primary production and a small decrease of global sea-surface DMS concentrations (ca. –1%). It also predicts opposing changes between the high and low latitudes (Figs. 2*b*–2*c*). In the low latitudes, climate-induced changes (reduced nutrient supply caused by increased stratification of the upper ocean and decreased intensity of tropical upwellings) decrease marine production (–20%) and consequently lead to lower DMS concentrations. In the high latitudes, climate-induced changes (a longer growing season caused by increased stratification of the upper ocean) increase marine production (30%). In the 40°–60° band (north and south), the model also shows a poleward retreat of siliceous species (considered as low-DMS producers) and their replacement by nonsiliceous species (considered as high-DMS producers). This shift in the phytoplankton ecosystem (depicted as the Si ratio in Fig. 2*b*) is responsible for a DMS concentration increase in the midlatitudes at 2× CO_2.

Results, mechanisms, and uncertainties of the response of marine production and DMS concentrations to climate change are described in more details in Bopp et al. (2001, 2003). Here, we investigate how these changes propagate up to sea-to-air DMS emissions and to the atmospheric sulfur cycle.

DMS flux to the atmosphere

From our baseline experiments (CONTROL and GW) and on global average, the DMS flux to the atmosphere is in-

© 2004 NRC Canada

Fig. 3. Change in annual dimethylsulfide (DMS) flux between CONTROL and GW experiments. Units are μmol·day^{-1}·m^{-2} and contours are every 0.5 μmol·day^{-1}·m^{-2}. Shaded areas indicate increase in DMS flux by more than 0.5 μmol·day^{-1}·m^{-2}.

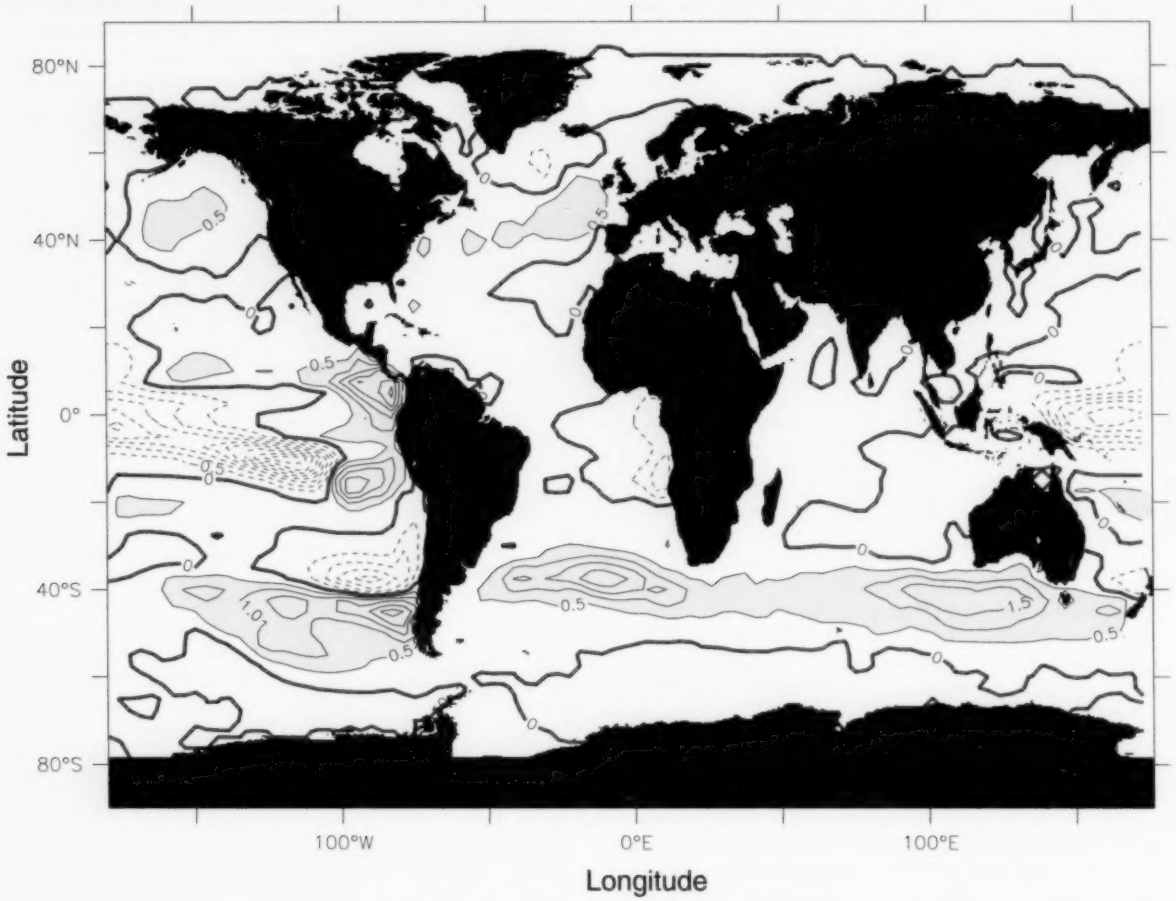

creased by about 3%, from 29.47 Tg S·year^{-1} at 1× CO_2 conditions to 30.23 Tg S·year^{-1} at 2× CO_2 conditions (Table 1). This increase is very similar to the one that we predicted using the same DMS concentrations changes but monthly means of winds in Bopp et al. (2003) instead of hourly winds used here. The lack of impact of using high-frequency winds to compute DMS fluxes may be partly explained by the fact that marine DMS concentrations are supplied at low frequency to the atmospheric model: this impact could be stronger if the ocean biogeochemical model and the atmospheric sulfur cycle model were fully coupled.

Differences between GW and CONTROL also show a large spatial heterogeneity in the change in DMS fluxes (Fig. 3). In the tropical Pacific Ocean, the DMS fluxes are reduced by up to 10 μmol·m^{-2}·day^{-1} (or –50%). Conversely, in the subtropical and subantarctic zones, DMS fluxes are strongly enhanced by up to 6 μmol·m^{-2}·day^{-1} (or 50%). These regional changes and the latitudinal opposition (Fig. 2*d*) are driven by variations in DMS concentrations. Stronger winds in the Southern Ocean and weaker winds in the equatorial region at 2× CO_2 amplify the large heterogeneity. In the 40°S–60°S band, for example, the model predicts almost a 20% increase in the annual DMS flux. In this region, the effect of wind changes (estimated from GW minus GWdms) alone accounts for one-quarter of the total increase (a 5% increase), whereas the major effect is due to changes in sea-surface DMS concentrations (a 15% increase). On global average, the effects of changes in marine DMS and wind speed (estimated from GW, GWdms, and CONTROL) account for 0.30 Tg S·year^{-1} and 0.46 Tg S·year^{-1} of the total increase, respectively (Table 1). The effect of wind speed is small on zonal average compared with the effect of marine DMS but is relatively larger on global average because of the cancellation of the marine DMS effect between tropical and midlatitude regions.

The additional experiments using the Liss and Merlivat (1986) parameterization for the air–sea gas exchange (CTLgex and GWgex) also show an increase of the global DMS flux to the atmosphere. But this increase (+0.51 Tg S·year^{-1}) is only two-thirds of that simulated with the Nightingale et al. (2000) parameterization (+0.76 Tg S·year^{-1}) (Table 1 and Fig. 2*d*). As shown by Jones et al. (2001) and Boucher et al. (2003), the use of Liss and Merlivat (1986) instead of Nightingale et al. (2000)

© 2004 NRC Canada

parameterization for the air–sea gas exchange also reduces the mean global DMS flux (from 29.47 TgS·year^{-1} to 19.97 Tg S·year^{-1}) in the control experiment. Thus, the relative increase of DMS flux is almost identical in the two global-warming experiments (+3%).

Atmospheric DMS and sulfate

At 2× CO_2 and for our baseline scenario (GW), the mean atmospheric DMS burden is very similar to its 1× CO_2 value (0.077 Tg S at 1× CO_2 vs. 0.079 Tg S at 2× CO_2). The DMS lifetime is also unchanged at about 0.9 day. The small increase in the DMS burden is accompanied by a very small decrease in the sulfate burden, probably because of a shift of sulfate production in regions where wet scavenging is more efficient.

However, the differences in the spatial distribution of DMS emissions result in large regional differences of atmospheric DMS concentrations. The changes in the distribution of DMS mixing ratios at the surface follow the changes in marine DMS emissions. In the Southern Ocean, DMS mixing ratio is increased by up to 50 pptv (parts per trillion by volume) (or 25%). It is decreased by up to 40 pptv (or –50%) in the western Equatorial Pacific Ocean.

Again, changes in atmospheric DMS concentrations computed using the Liss and Merlivat (1986) parameterization (GWgex minus CTLgex) are considerably lower than in our baseline scenario but are very similar in terms of relative changes.

Indirect radiative effect

The radiative impact in clear sky (or direct effect) induced by the changes in sulfate aerosol burden is negligible. As mentioned above, we focus here on the radiative impact in cloudy sky and consider only the first indirect radiative effect (changes in cloud optical properties for fixed liquid water content).

The change in radiative flux (computed as annually and globally averaged top-of-atmosphere radiative flux) between the GW and CONTROL experiments (with DMS emissions set to their 2× CO_2 and 1× CO_2 values, respectively) is very small at –0.052 W·m^{-2}. Again, this modest global figure conceals large spatial and temporal heterogeneities. In regions where DMS emissions are increased by global warming, sulfate mass and the cloud droplet number concentration increase. Through the associated changes in cloud optical properties, this increase in DMS emission leads to an albedo increase and a negative impact on the radiative budget. Accordingly, a decrease in DMS emissions leads to an albedo decrease and a positive impact on the radiative budget.

The radiative impact of changes in DMS emissions at 2× CO_2 reaches 1 W·m^{-2} in the western Equatorial Pacific Ocean and off the west coasts of Angola and Chile, whereas in the Southern Ocean between 40°S and 60°S and in the eastern Equatorial Pacific Ocean the radiative impact of changes in DMS emissions reaches –1 W·m^{-2} (Fig. 4*a*). A comparison of Figs. 3 and 4*a* shows very similar patterns for the changes in DMS emissions and the associated radiative impact: on a whole and because of the short life span of atmospheric DMS, the atmospheric sulfur cycle model seems to closely reflect the changes in DMS emissions.

The spatial heterogeneity described above and found in the changes in the raditiave budget is combined to a temporal heterogeneity. At mid- and high latitudes, changes in DMS emissions resulting from global warming and the associated radiative impact are highly seasonal. In the 40°S–60°S band, the DMS radiative impact reaches its maximum in summer, with values up to –1.5 W·m^{-2}, whereas winter values are only ca. –0.1 W·m^{-2} (Fig. 5). This seasonal feature refects the biogenic nature of DMS and its short life in the atmosphere. The impact of global warming on DMS emissions and on the associated radiative effect is maximum in summer during the productivity season and minimum in winter when deep convection and low light levels inhibit the biological activity.

Discussion

Large effect in the Southern Ocean

One of the major findings from the present study is that the simulated radiative impact of changes in DMS emisions is especially pronounced in the Southern Ocean (up to –1 W·m^{-2} for the annual mean and up to –1.5 W·m^{-2} in summer) compared with anywhere else on the globe. In particular, although marine DMS changes are more or less symmetrical between the northern hemisphere (NH) and southern (SH) hemisphere, the largest effect on the radiative budget is clearly located in the SH. There are several reasons why this symmetry in marine DMS change does not translate into a similar symmetry in the radiative impact (Fig. 6). Firstly, the surface covered by the ocean is less in the NH than in the SH. Secondly, the amplification of the change in DMS flux resulting from changes in wind speed occurs only in the SH. Finally, the radiative impact is expected to be negligible in polluted regions where the cloud droplet number concentration and the indirect aerosol forcing are already large. But the radiative impact induced by changes in DMS was estimated assuming constant anthropogenic emissions of SO_2 over the period of doubling CO_2 concentrations, and these emissions and those of other aerosol types are expected to change in the future. There are observed negative trends in sulfate aerosol emissions and concentrations over Europe and North America (Boucher and Pham 2002), although emissions are expected to continue to grow over Asia and some other regions of the world.

The enhanced DMS production and associated negative radiative impact that we predict in the Southern Ocean is qualitatively consistent with previous studies (Gabric et al. 1998, 2001) using regional models of marine DMS production. In the subantarctic Southern Ocean, Gabric et al. (1998, 2001) also predict an increase in DMS flux (ca. +5%) and a negative perturbation to radiative forcing (–0.29 W·m^{-2}) under doubled CO_2 conditions.

Sensitivity experiments

The additional sensitivity experiments that we performed enable us to test the robustness of our results to the choice of (*i*) the air–sea flux parameterization and (2) the sulfate mass – cloud droplet number relationship. Interestingly, our results show a similar radiative impact (Fig. 6) no matter how we parameterize the air–sea exchange of DMS (Nightingale et al. (2000) or Liss and Merlivat (1986)), whereas the absolute

© 2004 NRC Canada

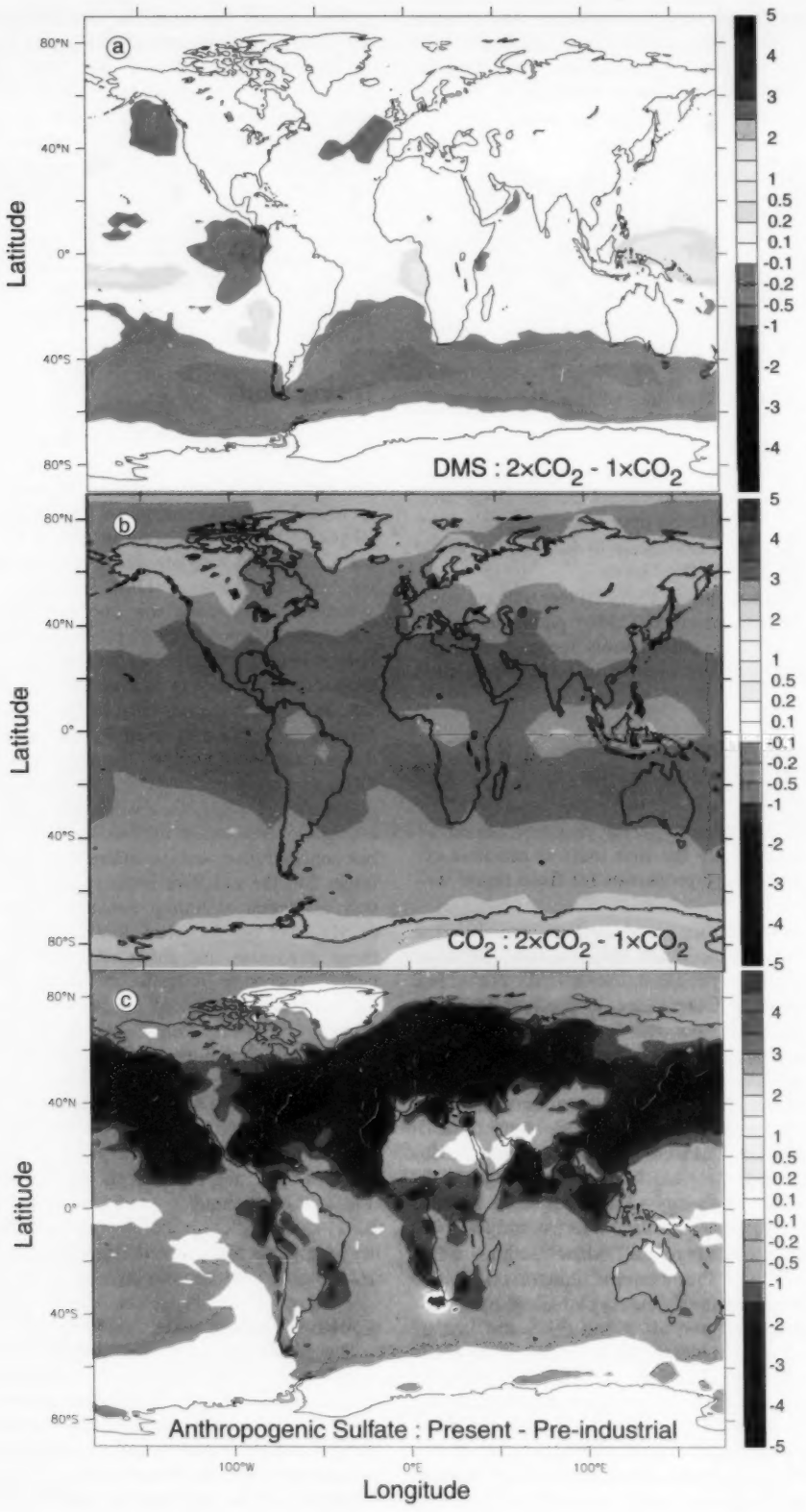

© 2004 NRC Canada

Fig. 4. (*a*) Annually averaged radiative impact on clouds (first indirect effect only) resulting from changes in dimethylsulfide (DMS) fluxes associated with a CO_2 doubling (GW minus CONTROL). (*b*) The corresponding annually averaged radiative forcing resulting from CO_2 (from 1× CO_2 or 350 ppmv to 2× CO_2 or 700 ppmv), computed with the Laboratoire Météorologie Dynamique (LMD) model (Laurent Z.X. Li, Laboratoire de Météorologie Dynamique, Université de Paris 6, Case Postale 99, 4 place Jussieu, F-75252 Paris, CEDEX 05, France, personal communication), is also shown for comparison. (*c*) Also shown for comparison is the annually averaged indirect radiative forcing resulting from anthropogenic sulfate from present-day relative to pre-industrial conditions, computed with the same global model of the atmospheric sulfur cycle from Boucher and Pham (2002). Numbers along the color scale are expressed in $W \cdot m^{-2}$ and the color scale is the same for all three panels.

Fig. 5. Latitude–time diagram of the radiative impact (first indirect effect) induced by changes in the dimethylsulfide (DMS) flux (GW minus CONTROL, zonal mean, unit is $W \cdot m^{-2}$ and contour lines are every 0.1 $W \cdot m^{-2}$).

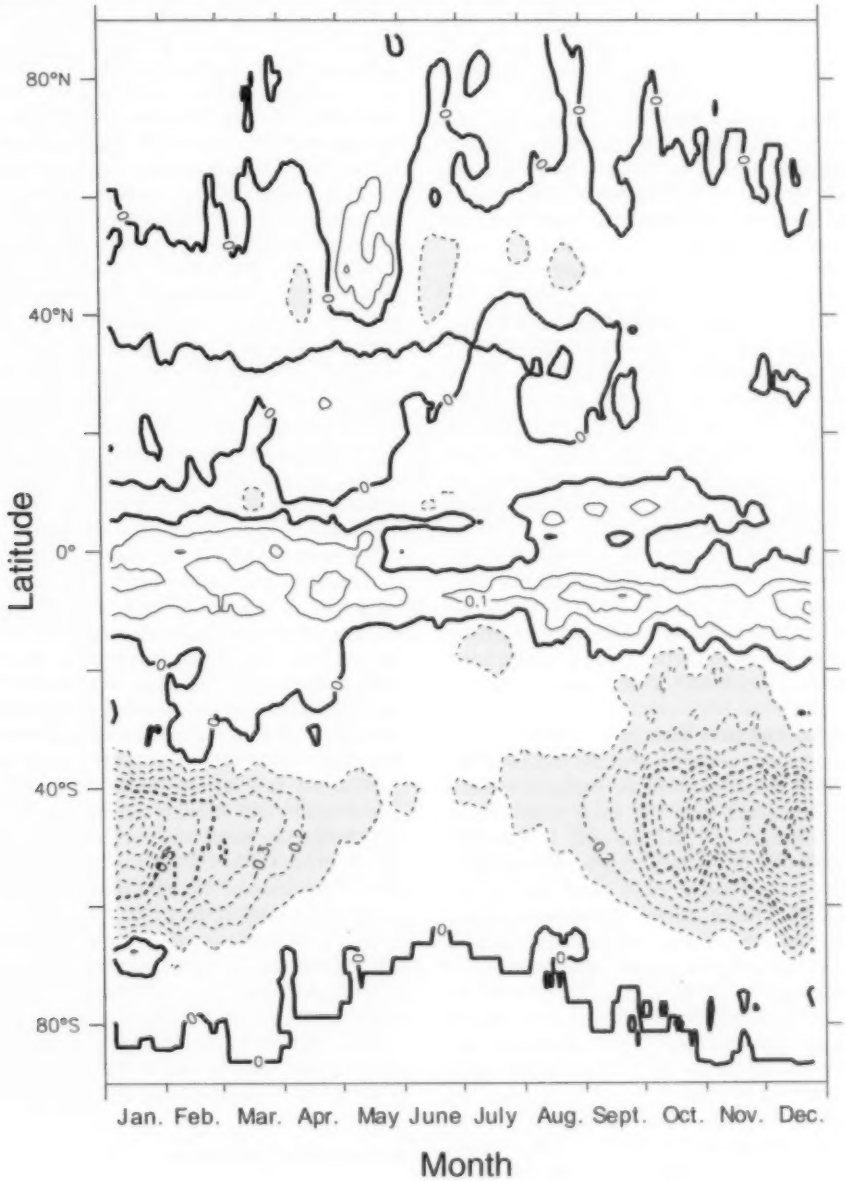

© 2004 NRC Canada

Fig. 6. Zonally averaged change (global warming minus control) of annual radiative impact resulting from changes in dimethylsulfide (DMS) emissions (in $W \cdot m^{-2}$). Different sensibility tests are shown: solid line is GW minus CONTROL, dotted line is GWgex minus CTLgex, and broken line is GWcdn minus CTLcdn.

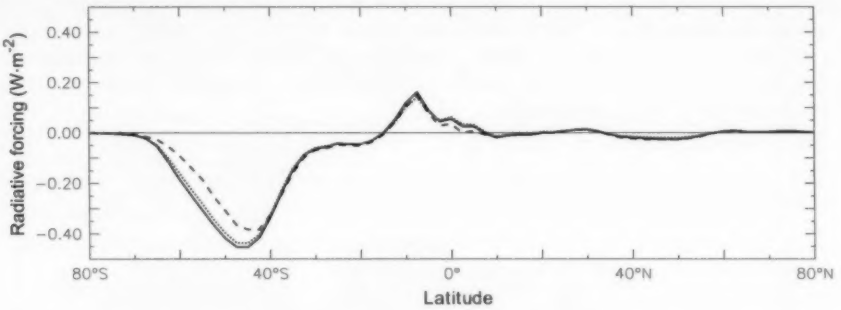

changes in DMS emissions and atmospheric concentrations are not the same in the two cases. In the unpolluted marine air of the Southern Ocean, a smaller increase in DMS emissions with Liss and Merlivat (1986) parameterization than with Nightingale et al. (2000) results in the same radiative impact at 2× CO_2 (ca. –0.35 $W \cdot m^{-2}$).

Second, our results show that using the relationship A of Boucher and Lohmann (1995), instead of relationship D, significantly reduces the absolute values of the radiative impact resulting from changes in DMS emissions (Fig. 6). This is particularly true in the Southern Ocean (–0.29 $W \cdot m^{-2}$ vs. –0.37 $W \cdot m^{-2}$). With relationship A, which distinguishes marine and continental air, the slope of the log–log regression lines between the sulfate mass concentration and the cloud droplet number concentration is reduced over oceans and increased over continents. Accordingly, a change in DMS emissions over the oceans will have less effect on the cloud droplet number concentration and the radiative budget. However, our main conclusions concerning the radiative impact of changes in DMS emissions caused by global warming remain unchanged: the radiative impact is very small globally (around –0.05 $W \cdot m^{-2}$) but is significant (ca. –0.3 to –0.4 $W \cdot m^{-2}$) in the unpolluted Southern Ocean.

Comparison with CO_2 radiative forcing

In this study, we compare our estimate of the radiative impact of changes in DMS emissions with the radiative forcing of CO_2 at 2× CO_2, computed with the same atmospheric GCM from the Laboratoire de Météorologie Dynamique (Laurent Li, Laboratoire de Météorologie Dynamique, Université de Paris 6, Case Postale 99, 4 place Jussieu, F-75252 Paris, CEDEX 05, France, personal communication). In the subantarctic Southern Ocean, the radiative impact caused by changes in DMS emissions may partly counteract the CO_2 radiative forcing (–0.5 $W \cdot m^{-2}$ vs. 2.5 $W \cdot m^{-2}$ in zonal annual means). Moreover, the DMS radiative impact differs from the CO_2 radiative forcing by its seasonality. Although CO_2 radiative forcing is more or less constant over the year, the DMS radiative impact reaches its maximum in summer, with values up to –1.5 $W \cdot m^{-2}$ in the 40°S–60°S band. Nevertheless, the strength of the DMS – CCN – cloud albedo feedback is found to be small at the global scale when compared with the CO_2 radiative forcing.

In conclusion, following previous work on modelling the marine DMS response to climate change (Bopp et al. 2003) and using an atmospheric model of the global sulfur cycle, we estimate the impact of future climate change on DMS fluxes to the atmosphere and the associated radiative impact through changes in cloud albedo. At 2× CO_2, the DMS flux is similar to its 1× CO_2 value (at about 29 Tg $S \cdot year^{-1}$); however, it displays large regional contrasts: a reduction (–15%) of the DMS flux in the tropical band and an increase (30%) in the midlatitudes of the southern hemisphere. In this paper, we focus on how those changes propagate up to the atmospheric sulfur cycle and to the Earth's radiative budget.

Changes in marine DMS emissions at 2× CO_2 significantly impact the regional radiative budget, up to –1.5 $W \cdot m^{-2}$ in summer between 40°S and 50°S. In the Southern Ocean, this radiative impact may partly cancel out the radiative forcing of anthropogenic CO_2 (2.5–3 $W \cdot m^{-2}$ at 2× CO_2). The strength of the DMS – CCN – cloud albedo feedback is nevertheless found to be small at the global scale.

We have tested the robustness of our results to some of the parameterizations we employ. In particular, we show that the use of the Liss and Merlivat (1986) parameterization for the air–sea gas exchange, instead of the more recent Nightingale et al. (2000) parametrization, does not affect our results in terms of radiative impact. Second, we show that the use of another parameterization for the relationship between the sulfate mass concentration and the cloud droplet number may slightly modify the magnitude of the estimated impact, but that our conclusions remain qualitatively the same.

Our results still strongly depend on the skill of our models to simulate marine productivity, on the relationships that we use to predict DMS from biological variables, and on the parameterization of the aerosol indirect effect used in the atmospheric model of the sulfur cycle. Improvements in all aspects will be necessary to develop greater confidence in such future predictions. In particular, the role of sea-salt particles as CCN and the potential change in sea salt induced by changes in wind speed should also be considered. Although such a study must be viewed as a sensitivity study more than a prediction, it represents a first step toward the assessment of the DMS – cloud albedo climate feedback loop.

Acknowledgments

This work was supported by the Environment and Climate Programme of the European Community (IRONAGE contract EVK2-1999-00227 and PHOENICS contract EVK2-

© 2004 NRC Canada

CT-2001-00098) and the French national programmes PROOF and PNCA of CNRS/INSU. Computing time was provided by CNRS/IDRIS under projects 020040 and 021167. The Laboratoire d'Optique Atmosphérique is an institute of the "Fédération de Recherche" FR1818 of the CNRS. This is Laboratoire des Sciences du Climat et de l'Environnement contribution No. 1033.

References

Andres R.J., and Kasgnoc, A.D. 1998. A time-averaged inventory of subaerial volcanic sulfur emissions, J. Geophys. Res. **103**: 25 251 – 25 261.

Aumont, O., Belviso, S., and Monfray, P. 2002. Dimethylsulfoniopropionate (DMSP) and dimethylsulfide (DMS) sea surface distributions simulated from a global 3-D ocean carbon cycle model. J. Geophys. Res. **107**(C4). [doi:10.1029/1999JC000111]

Barthelet, P., Bony, S., Braconnot, P., Braun, A., Cariolle, D., Cohen-Solal, E., Dufresne, J.-L., Delecluse, P., Déqué, M., Fairhead, L., Filiberti, M.-A., Forichon, M., Grandpeix, J.-Y., Guilyardi, E., Houssais, M.-N., Imbard, M., Le Treut, H., Lévy, C., Li, Z., Madec, G., Marquet, P., Marti, O., Planton, S., Terray, L., Thual, O., and Valcke, S. 1998. Simulations couplées globales des changements climatiques associés à une augmentation de la teneur atmosphérique en CO_2. C.R. Acad. Sci. Paris, **326**: 677–684.

Bopp, L., Monfray, P., Aumont, O., Dufresne, J.-L., Le Treut, H., Madec, G., Terray, L., and Orr, J. 2001. Potential impact of climate change on marine export production. Global Biogeochem. Cycles, **15**: 81–99.

Bopp, L., Aumont, O., Belviso, S., and Monfray, P. 2003. Potential impact of climate change on marine DMS (dimethylsulfide) emissions. Tellus, **55B**: 11–22.

Boucher, O., and Lohmann, U. 1995. The sulfate–CCN–cloud-albedo effect: a sensitivity study with two general circulation models. Tellus, **47B**: 281–300.

Boucher, O., and Pham, M. 2002. History of sulfate aerosol radiative forcings. Geophys. Res. Lett. **29**, 1308. [doi:10.1029/2001GL014048]

Boucher, O., Pham, M., and Venkataraman, C. 2002. Simulation of the atmospheric sulfur cycle in the Laboratoire de Météorologie Dynamique General Circulation Model. Model description, model evaluation, and global and European budgets. Notes scientifiques du pôle de modélisation, IPSL, Paris, France. [http://www.ipsl.jussieu.fr/poles/Modelisation/NotesSciences.htm]

Boucher, O., Moulin, C., Belviso, S., Aumont, O., Bopp, L., Cosme, E., von Kuhlmann, R., Lawrence, M.G., Pham, M., Reddy, M.S., Sciare, J., and Venkataraman, C. 2003. DMS atmospheric concentrations and sulphate aerosol indirect radiative forcing: a sensitivity study to the DMS source representation and oxidation. Atmos. Chem. Phys. **3**: 49–65.

Charlson, R.J., Lovelock, J.E., Andreae, M.O., and Warren, S.G. 1987. Oceanic phytoplankton, atmospheric sulphur, cloud albedo and climate. Nature (Lond.), **326**: 655–661.

Gabric, A.J., Whetton, P.H., Boers, R., and Ayers, G.P. 1998. The impact of simulated climate change on the air–sea flux of dimethylsulphide in the subantarctic Southern Ocean. Tellus, **50B**: 388–399.

Gabric, A.J., Whetton, P.H., and Cropp, R. 2001. Dimethylsulphide production in the subantarctic Southern Ocean under enhanced greenhouse conditions. Tellus, **53B**: 273–287.

Jones, A., Roberts, D., Woodage, M., and Johnson, C. 2001. Indirect sulphate aerosols forcing in a climate model with an interactive sulphur cycle. J. Geophys. Res. **106**: 20 293 – 20 310.

Liss, P., and Merlivat, L. 1986. Air–sea gas exchange: introduction and synthesis. *In* The role of air–sea exchange in geochemical cycling. *Edited by* P. Buat-Ménard. D. Reidel, Dordrecht.

Liss, P., Malin, G., Turner, S.M., and Holligan, P.M. 1994. Dimethylsulphide and Phaeocystis: a review. J. Mar. Sys. **5**: 41–53.

Müller, J.F., and Brasseur, G. 1995. IMAGES: a three-dimensional chemical transport model of the global troposphere. J. Geophys. Res. **100**: 16 455 – 16 490.

Nightingale, P.D., Malin, G., Law, C.S., Watson, A.J., Liss, P.S., Liddicoat, M.I., Boutin, J., and Upstill-Goddard, R.C. 2000. In-situ evaluation of air–sea exchange parameterizations using novel conservative and volatile tracers. Global Biogeochem. Cycles, **14**: 373–387.

Olivier, J.G.J., Bouwman, A.F., Van der Maas, C.W.M., Berdowski, J.J.M., Veldt, C., Bloos, J.P.J., Visschedijk, A.J.H., Zandveld, P.Y.J., and Haverlag, J.L. 1996. Description of EDGAR version 2.0: a set of global emission inventories of greenhouse gases and ozone-depleting substances for all anthropogenic and most natural sources on a per country basis and on 1° × 1° grid. National Institute of Public Health and the Environment (RIVM) Report No. 771060 002.

Penner, J., Andreae, M., Annegarn, H., Barrie, L., Feichter, J., Hegg, D., Jayaraman, A., Leaitch, R., Murphy, D., Nganga, J., and Pitari, G. 2001. Aerosols, their direct and indirect effects. *In* Climate change 2001. The Scientific Basis, Contribution of Working Group I to the Third Assessment Report of the Intergovernmental Panel on Climate Change. Cambridge University Press, New York. pp. 289–348.

Wanninkhof, R. 1992. Relationship between wind speed and gas exchange over the ocean. J. Geophys. Res. **97**: 7373–7382.

Watts S.F. 2000. The mass budgets of carbonyl sulfide, dimethylsulfide, carbon disulfide and hydrogen sulfide. Atmos. Environ. **34**: 761–779.

© 2004 NRC Canada

PERSPECTIVE / PERSPECTIVE

Direct measurements of biogenic dimethylsulphide fluxes from the oceans: a synthesis[1]

H.J. Zemmelink, J.W.H. Dacey, and E.J. Hintsa

Abstract: This paper provides a brief overview of the state-of-the-art of techniques that are currently used for field measurements of trace gas fluxes and the subsequent derivation of gas transfer rates over the oceans. Special attention is given to the relaxed eddy accumulation (REA) and gradient flux (GF) techniques, which rely on empirical functions thus far mainly validated over land. The universality of these functions and their application at sea have not yet been fully evaluated. New experiments have shown that the emission of dimethylsulphide (DMS) can be measured by the REA and GF techniques. Moreover, these measurements have provided parameterizations of gas exchange rates that are within the range of relationships between wind speed and gas transfer that have recently been derived from eddy correlation (EC) and deliberate tracer measurements. Using DMS as a model, gas is potentially a powerful approach to intercalibrate the REA, GF, and EC techniques, test their applicability in the marine environment, and investigate processes that determine trace gas exchange across the ocean surface.

Résumé : Nous présentons ici une courte synthèse des meilleures techniques courantes utilisées pour mesurer en nature les flux de gaz en traces et pour ensuite dériver les taux de transferts des gaz au-dessus des océans. Il est particulièrement question des techniques REA (« Relaxed Eddy Accumulation », méthode simplifiée d'accumulation des tourbillons) et GF (« Gradient Flux », méthode de gradient des flux) qui reposent sur des fonctions empiriques validées jusqu'à maintenant surtout sur le continent. L'universalité de ces fonctions et leur application à l'environnement marin n'ont pas encore été complètement évaluées. De nouvelles expériences indiquent que l'émission de sulfure de diméthyle (DMS) peut être mesurée par les techniques REA et GF. De plus, ces mesures ont fourni des paramètres pour les taux d'échanges gazeux qui se situent dans la gamme des relations entre la vitesse du vent et le transfert des gaz obtenues récemment par la méthode EC (« Eddy Correlation », méthode des corrélations turbulentes) et par des additions délibérées de traceurs (« deliberate tracer method »). L'utilisation du DMS comme gaz modèle pourrait permettre de calibrer les méthodes REA, GF et EC entre elles, de vérifier leur applicabilité au milieu marin et d'étudier les processus qui déterminent les échanges de gaz en traces de part et d'autre de la surface des océans.

[Traduit par la Rédaction]

Introduction

Ocean–atmosphere interactions and feedback mechanisms are key processes that need to be quantified to understand the role of the oceans in atmospheric chemistry and global climate. The biogenic gas dimethylsulphide (DMS) and its precursor dimethylsulphoniopropionate (DMSP) are at the center of attention of international research programs such as SOLAS (Surface Ocean – Lower Atmosphere Study) because of the potential of DMS to regulate climate. Since Lovelock et al. (1972) reported that DMS emissions from the oceans could possibly close the global sulphur budget, empirical evidence for a DMS-driven negative climate feedback has been found (Ayers and Gillet 2000; Sciare et al. 2000). This supports the suggestion of Charlson et al. (1987) and more recently Andreae and Crutzen (1997) that atmospheric oxidation products of DMS are part of one of the major feedback mechanisms linking the global biosphere and climate, with a possible cooling capacity of about 4 °C (Watson and Liss 1998).

Received 1 February 2003. Accepted 7 November 2003. Published on the NRC Research Press Web site at http://cjfas.nrc.ca on 24 June 2004.
J17361

H.J. Zemmelink,[2] J.W.H. Dacey, and E.J. Hintsa. Woods Hole Oceanographic Institution, Woods Hole, MA 02543, U.S.A.

[1]This paper is part of the proceedings of the Third International Symposium on Biological and Environmental Chemistry of DMS(P) and Related Compounds, held in Rimouski (Québec), 26–28 September 2002.

[2]Corresponding author (e-mail: hzemmelink@whoi.edu).

 doi: 10.1139/F04-047 © 2004 NRC Canada

Table 1. Parameterizations of gas transfer (k) as a function of wind speed (U) at an elevation of 10 m.

Parameterization	Equation
Liss and Merlivat 1986	$k = 0.17U$ ($U \leq 3.6$ m·s^{-1})
Liss and Merlivat 1986	$k = 2.85U - 9.65$ ($3.6 < U \leq 13$ m·s^{-1})
Liss and Merlivat 1986	$k = 5.9U - 49.3$ ($U > 13$ m·s^{-1})
Wanninkhof 1992	$k = 0.39U^2$ (long-term-averaged winds)
Wanninkhof 1992	$k = 0.31U^2$ (short-term-averaged winds)
McGillis et al. 2001*a*	$k = 3.3 + 0.026U^3$
Nightingale et al. 2000	$k_{600} = 0.33U + 0.222U^2$, $R^2 = 0.80$
Jacobs et al. 1999	$k = (0.54\pm0.08)U^2$, $R^2 = 0.17$
Hintsa et al. 2004 (FAIRS–GF)	$k = (0.18\pm0.03)U^2$, $R^2 = 0.18$
Zemmelink et al. 2004*a* (FAIRS–REA)	$k = (0.61\pm0.06)U^2$, $R^2 = 0.36$
Zemmelink et al. 2004*b* (GasEx-2001–GF)	$k = (0.60\pm0.04)U^2$, $R^2 = 0.28$
Zemmelink et al. 2004*b* (pooled GasEx–FAIRS)	$k = (0.48\pm0.09)U^2$, $R^2 = 0.31$

Note: Gas transfer rates or velocities are normalized to a Schmidt number of 660.

DMS and its oxidation products affect atmospheric chemistry in various ways (Andreae and Crutzen 1997). Once emitted from the oceans, DMS is oxidized by free radicals such as OH and NO_3 to form a variety of products including methane sulphonic acid and sulphur dioxide, part of which in turn are oxidized to form non-sea-salt sulphate (NSS sulphate). Even with an understanding of the dynamics of DMS in the atmosphere, current models are still unable to simulate the oceanic climate feedback system. The uncertainty of the atmospheric burden is at least equal to the uncertainty in the magnitude of the sea to air fluxes. The most recent estimates of the sea to air flux of DMS range from 15 to 33 Tg S·year^{-1} (Kettle and Andreae 2000), a significant contribution to the global atmospheric sulphur burden and the dominant one over large regions of the oceans. Gondwe et al. (2003) recently estimated the average contribution of DMS to the overall atmospheric sulphur burden at 18%, but this percentage varies greatly: 43% in the relative pristine Southern Hemisphere and 9% in the Northern Hemisphere because of the dominance of sulphur from fossil fuel burning.

Commonly used gas exchange models rely on the assumption that the flux (F) of a gas across the air–water interface is the product of the air–water concentration disequilibrium (ΔC) and a kinetic parameter, the transfer velocity (k_{gas}), which quantifies the rate at which the gas crosses the air–sea interface:

$$(1) \qquad F = k_{gas}\,\Delta C$$

The air–water disequilibrium for most volatile compounds is highly variable because it is a function of time, location, meteorological conditions, and chemical/biological processes. Even when spatial and seasonal surface water concentrations are fairly well known, it remains difficult to calculate fluxes because the rate of transfer across the water surface is uncertain (Wanninkhof 1992). Although parameterizations of k_{gas} as a function of wind speed are available (Liss and Merlivat 1986; Wanninkhof 1992; Erickson 1993), the fundamental physical nature of k_{gas} remains poorly understood and it is usually parameterized as the waterside transfer velocity (k_w) as a function of wind speed (U) and temperature in the form

$$(2) \qquad k_w \approx aU^x \mathrm{Sc}^n$$

where Sc is the dimensionless Schmidt number: the ratio of the kinematic viscosity of water (ν, metres per second squared) and the molecular diffusivity of the gas (D, metres per second squared), Sc = ν/D. Molecular diffusivities have been quantified for a range of gases (e.g., Jähne et al. 1987; Wanninkhof 1992; Saltzman et al. 1993) and the kinematic viscosity of seawater is well known. The Sc exponent, n, is a function of surface characteristics and has been determined to be –2/3 for smooth water surfaces (wind speed ≤3.6 m·s^{-1}) and –1/2 for rough surfaces (wind speed >3.6 m·s^{-1}). The wind speed exponent (x) expresses the wind speed dependency of k. Estimates of x range from linear (Liss and Merlivat 1986) to cubic (Wanninkhof and McGillis 1999). The regression coefficient a is derived from the best fit through observed values of k. Estimates of the regression coefficient vary from a factor of 2 between the most commonly applied parameterizations of Liss and Merlivat (1986) and Wanninkhof (1992) to a factor of 3 between parameterizations that are based on the direct measurement of k in the field (Table 1).

Usually, transfer velocities are normalized to the Sc of CO_2 in seawater at 20 °C with a salinity of 35‰ (Sc = 660) by means of the Sc dependence

$$(3) \qquad k_{660} = k_w(660/\mathrm{Sc})^n$$

Extrapolating measured fluxes of one gas to estimate fluxes of other gases requires conversion through the Sc using $k_{gas\,A} = k_{gas\,B}(\mathrm{Sc}_{gas\,A}/\mathrm{Sc}_{gas\,B})^n$. However, the power dependence of Sc changes under wave-breaking conditions where poorly soluble gases are transported relatively more efficiently by bubbles than more soluble gases (Woolf 1993). Hence, Sc conversions are valid only as long as k remains independent of the gas solubility (Asher and Wanninkhof 1998*a*). The effect of bubbles on air–sea gas exchange is a topic of ongoing research and still far from resolution (Donelan et al. 2002 and references therein). In addition, the solubility and aqueous reactivity of a gas determine whether gas transfer will be limited by the waterside or airside. For gases with low solubility, the gas transfer is predominantly controlled by the liquid phase. The exchange of gases with high solubilities is limited by transfer through the airside. Gases that have an intermediate solubility, such as DMS,

© 2004 NRC Canada

will experience part liquid and part airside control, and the predominance will depend on turbulence and the temperature dependence of the gas solubility (McGillis et al. 2000). A correction should be applied for the airside control of moderately soluble gases if gas exchange rates are expressed in terms of k_{660} (the waterside controlled transfer velocity of CO_2).

The two most commonly applied gas exchange parameterizations have been developed by Liss and Merlivat (1986) and Wanninkhof (1992). That of Liss and Merlivat (1986) was deduced from a deliberate tracer experiment with sulphur hexafluoride (SF_6) in a lake for wind speeds up to 8 $m \cdot s^{-1}$ and from wind tunnel data at higher wind speeds. That of Wanninkhof (1992) is a quadratic fit in agreement with the global mean transfer velocity determined from the oceanic uptake of bomb-derived radiocarbon. Purposefully released tracers have been used more recently in oceanic settings (Asher and Wanninkhof 1998*a*, 1998*b*; Nightingale et al. 2000). These bulk parameterizations have the drawback that they yield relationships averaged over longer time intervals and over larger spatial scales for oceanic conditions that may be hard to characterize because of their variability. In other words, these parameterizations do not provide adequate insight into the temporal and spatial variability of k.

Direct determination of k in the field would clearly be preferable but has proven to be difficult. A number of techniques have been developed in recent years (reviewed by Asher and Wanninkhof 1998*a*; Fairall et al. 2000). Examples of techniques in the aqueous phase are the dissolved gas balance technique (Wallace and Wirick 1992; Farmer et al. 1993) and the controlled flux method (Jähne et al. 1989; Hauβecker et al. 1995). Both of these are used to determine the change of a quantity (the concentration of a gas or heat, respectively) over time. Although these techniques provide insight into physical processes that control gas transfer and give a direct estimate of the budget of the measured tracer, conversion to gas transfer rates of other gases using eq. 3 might still be unreliable because of the effect of breaking waves (and solubility). A major disadvantage of the controlled flux method lies in its inability to measure the bubble-mediated component. In contrast, micrometeorological techniques in the airside allow the field measurement of fluxes and the derivation of transfer velocities without recourse to other gases, on time scales of less than an hour for most sea states. These techniques link atmospheric turbulence, generated by the friction between air and the sea surface and by density variations (buoyancy) in the atmosphere (determining atmospheric stability), to gas exchange. Several micrometeorological techniques have been applied for the measurement of turbulence and gas fluxes at sea, among which are the eddy correlation, relaxed eddy accumulation, and profiling techniques.

Micrometeorological techniques used for field estimates of gas transfer

Eddy correlation

Eddy correlation (EC) is the most straightforward and basic approach for flux measurement, where the flux (moles per square metre per second) is obtained from the product of concurrent instantaneous measurements of the fluctuations of vertical velocity w' (metres per second) and gas concentration or mixing ratio χ_c' (moles of gas per mole of air):

$$(4) \qquad F_c = \rho_a \overline{(w' \chi_c')}$$

where ρ_a (moles per cubic metre) is the density of dry air and the overbar denotes a time average. EC gives an unambiguous result for the absolute flux but requires instruments that are capable of high-resolution measurements of both air motion and air composition at frequencies of approximately 10 Hz. This is easily achieved for fast-response air motion sensors such as sonic anemometers, but the availability of suitable trace gas sensors, often infrared absorption devices, is limited to gases such as O_3, SO_2, NO, NO_2, CH_4, and CO_2.

Unfortunately, trace gas fluxes over the ocean are often at the limit of detection of fast-response sensors, thus hampering the applicability of EC in the marine environment. Another method to estimate the absolute flux was proposed by Desjardins (1977), who suggested a variant of EC that does not rely on fast-response gas sensors. This technique is known as eddy accumulation in which air is drawn from the immediate vicinity of an anemometer measuring vertical wind speed (w) and subsequently diverted into one of two accumulators on the basis of the sign of w at a pumping rate proportional to the magnitude of w. Sampling air at a rate proportional to the vertical wind velocity is, however, extremely difficult to achieve in real time. Other techniques of measuring fluxes generally require some empirically determined relationship to estimate the flux. Two such methods are the relaxed eddy accumulation (REA) and the profiling or gradient flux (GF) techniques, which allow the storage of gases and later analysis.

Relaxed eddy accumulation

Businger and Oncley (1990) examined sets of raw EC measurements of vertical wind speed, humidity, and temperature and noted that if measurements of temperature and humidity were segregated according to the sign of the vertical wind speed, then the flux was proportional to the product of the standard deviation of the vertical wind speed, σ_w (metres per second), and the difference between the two samples:

$$(5) \qquad F_c = \beta \sigma_w (\overline{C}_u - \overline{C}_d)$$

where β is the eddy accumulation coefficient (dimensionless) and $\overline{C}$ is the mean concentration (moles per cubic metre) in the upward- and downward-moving eddies. This observation allows for the application of the REA method, which is based on sampling air into updraft and downdraft reservoirs at a constant flow rate rather than proportionally to the vertical wind speed, w, as in the case of true eddy accumulation. For a Gaussian distribution, the β factor is a constant (0.627; Wyngaard and Moeng 1992). However, several field experiments yielded β values that were on average between 0.56 and 0.60 (Businger and Oncley 1990; Baker et al. 1992; Pattey et al. 1993), sometimes showing considerable scatter with ranges from 0.2 to 0.9 (e.g., Oncley et al. 1993; Beverland et al. 1996). It is still uncertain whether β is absolutely constant or varies systematically, depending on the relative contribution of buoyancy and friction to turbulence. Businger and Oncley (1990) and more recently Andreas et

© 2004 NRC Canada

al. (1998) proposed β as a general function of stability (z/L, where z is the measurement height (metres) and L is the Obukhov length (metres), which reflects the relative contribution of buoyancy and friction to the production of turbulence). However, only a weak systematic variation was detected and could not be reproduced by other authors (e.g., Beverland et al. 1996). Most studies use a constant literature value for β between 0.56 and 0.60 or derive β from EC measurements.

Often, a sampling threshold around zero (metres per second) vertical wind speed is used, where neither updraft nor downdraft air is sampled. This deadband approach has the advantage of increasing the concentration difference between the two collection reservoirs because sampling is biased toward larger eddies (those with sufficient vertical velocity to exceed the threshold), which tend to move farther along the concentration gradient. The quantitative effect of the deadband on the REA measurements is still a matter of investigation. However, it is generally accepted that the increase in concentration difference must be balanced by a decrease in β. The correction for the increased concentration difference was evaluated by Businger and Oncley (1990) and more recently by Pattey et al. (1993). Both studies found an exponential decrease in β with increasing deadband. Businger and Oncley (1990) proposed

$$\beta = \beta_0 \exp(-0.75 w_0/\sigma_w) \quad (6)$$

where w_0 (metres per second) is the deadband vertical wind velocity threshold for REA measurements. When w is within $\pm w_0$, air is discarded. Businger and Oncley (1990) found that β_0 was insensitive to atmospheric stability.

Gradient flux

With the GF technique (Businger et al. 1971) the flux is derived from the difference in concentration between two or more elevations using Monin-Obukhov similarity theory (the MOST theory states that turbulent statistics are universal functions of z/L when normalized by the appropriate scaling parameter (Monin and Obukhov 1954)

$$C(z) - C(z_0) = \frac{C_*}{k}(\ln(z/z_0) - \Psi(z/L) + \Psi(z_0/L)) \quad (7)$$

where $C(z)$ (moles per cubic metre) is the concentration at height z (metres), Ψ (dimensionless) is the integrated flux profile function that corrects for atmospheric stability (Paulson 1970), k is the von Karman constant (0.4), z_0 is a reference height, and L (metres) is the Obukhov length:

$$L = \frac{\overline{\theta} u_*^3}{k g F_\theta} \quad (8)$$

where θ is the virtual temperature (overbar denotes an average), u_* (metres per second) is the friction velocity, which can be derived from EC measurements of wind speed, g is the acceleration due to gravity, and F_θ is the buoyancy flux (derived from EC measurements). The C_* (eq. 7) is determined from the least-squares-fitted slope of $C(z)$ as a function of $(\ln(z) - \Psi(z/L))$, the stability-corrected height. The flux is then calculated from

$$F_c = C_* u_* \quad (9)$$

Although EC, REA, and GF techniques have been used extensively over terrestrial systems, their application to air–sea gas exchange is relatively new and there has been an intense effort in the last decade to improve these techniques and to evaluate their accuracy and applicability in the marine environment (Fairall et al. 2000). Specific problems in the marine environment are platform motion, flow distortion caused by the sampling platform, and environmental factors unique to the ocean such as atmosphere–wave interactions.

Generally, EC and wind speed measurements (e.g., of F_θ, u_*, and σ_w) are considered to be accurate, usually within 10%. The accuracy of the EC method is due to the fact that all corrections and flux calculations can be carried out in postprocessing procedures after the field measurements; needless to say, this advantage is also highly appropriate for measurements over sea.

The applicability and performance of the GF method are not only determined by the accuracy of EC but also by the choice of the appropriate measurement heights. The vertical distance should be large enough that it allows concentration differences that are resolvable by available sensors. But the concentrations should also yield a log-linear profile that is, unfortunately, easily disturbed by factors such as flow distortion or waves. The deformation of the log-linear profile is difficult to predict and depends on (wind and wave) conditions during the measurement. In addition, the applicability of Monin–Obukhov similarity theory, the basis of the GF technique, appears to be valid where the generation of turbulence is dominated by friction between the surface and the wind (Edson and Fairall 1998; Edson et al. 2002) but can be questioned over mature seas and swell when turbulence has a strong dependency on waves.

Although EC and wind speed measurements can be corrected for systematic error effects such as an offset in the vertical wind speed and a vertical tilt of the wind sensor, REA measurements cannot be corrected for such errors. This is due to the fact that REA depends on an instantaneous reaction of the sampling system to changes in wind speed. Offset and tilt typically introduce flux errors on the order of 10–20%. An additional systematic error is caused by the delay time between the wind measurement and the reaction of valves in the sampling system that control the distribution of samples over the appropriate down- or updraft collection reservoir. A mismatch between the wind measurement and the distribution of the samples can result in an underestimation of the flux. However, the use of valves that can respond with a frequency of 20–50 Hz will minimize the delay and allows measurements with a (delay introduced) error of about 10%. Recent tests of the universality of the empirical functions for REA showed that β in the marine environment is indeed not dependent on atmospheric stability and varies around 0.56 (Zemmelink et al. 2004*a*), in agreement with observations made over terrestrial systems that yield numbers in the vicinity of 0.56–0.58 (Andreas et al. 1998).

Field estimates of gas transfer rates

From recent experiments involving field measurement of gas fluxes by a variety of micrometeorological techniques, organized by the U.S. (GasEx-1998, FAIRS, GasEx-2001) and the European Union (ASGAMAGE), a number of rela-

© 2004 NRC Canada

Fig. 1. Summary of proposed short-term relationships between gas transfer velocities (k_{660}) and wind speed ($U_{10,n}$, measured at an elevation of 10 m during neutral conditions). Equations are given in Table 1. Abbreviations refer to the gases that were measured (CO_2, carbon dioxide; DMS, dimethylsulphide) and the micrometeorological technique used (EC, eddy correlation; GF, gradient flux; REA, relaxed eddy accumulation; DT, deliberate tracer.

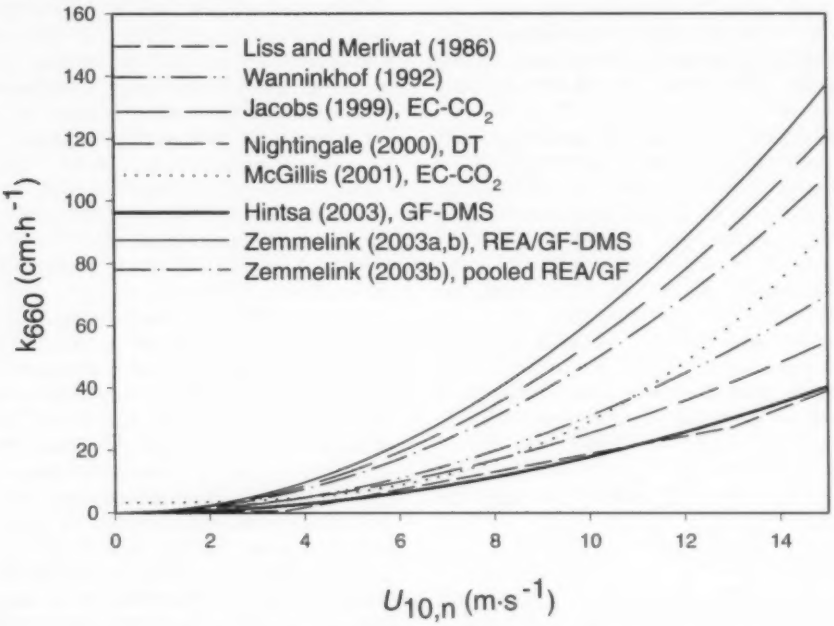

tionships between gas transfer and wind velocities have been proposed (Table 1). These parameterizations relate k_w to short-term measurements of wind speed. This is an important distinction because owing to the nonlinear dependence of gas exchange on wind speed, k estimated over long time periods with variable winds will necessarily be somewhat higher than corresponding estimates over short time scales with more steady winds (for the same average wind speed; Wanninkhof 1992).

Most parameterizations incorporate a nonlinear relationship between gas transfer and wind speed. For example, a cubic dependence between k and wind speed was derived from EC measurements of CO_2 flux conducted during GasEx-1998. The cubic dependency incorporates the retardation of gas transfer at low to intermediate winds by surfactants and bubble-enhanced transfer at higher winds (Wanninkhof and McGillis 1999; McGillis et al. 2001*a*). It is noteworthy that a quadratic fit through the same data corresponds very closely to the Wanninkhof (1992) relationship (Fig. 1). The GasEx-1998 results obtained by EC were within uncertainty in agreement with gas transfer velocities derived from concomitant gradient measurements of the CO_2 and DMS flux and with results derived from SF_6–^{3}He dual tracer release experiments (McGillis et al. 2001*b*). A quadratic relation was derived from EC measurements of CO_2 flux over a coastal shelf sea conducted during ASGAMAGE (Jacobs et al. 1999). These EC results were on average a factor of 2.5 higher than k derived from a simultaneous deliberate tracer experiment (Nightingale et al. 2000), which showed a wind speed dependence intermediate between the relationships proposed by Liss and Merlivat (1986) and Wanninkhof (1992). Part of the difference between the results from the two methods could be explained by near-surface gradients of the inert tracers that caused an underestimation of k up to 25% (Jacobs et al. 2002). In addition, a 10% overestimation of the EC estimates could have been caused by biological activity and river discharge affecting surface water CO_2 (Jacobs et al. 2002).

Air–sea exchange coefficients in the upper range of commonly used parameterizations were required to be able to close mass budgets of sulphur cycles over the Pacific Ocean (Yvon et al. 1996; Chin et al. 1998). While the studies of GasEx-1998, Yvon et al. (1996), and Putaud and Nguyen (1996) may have given some insight into the magnitude of k_{DMS}, they did not provide a relationship between k_{DMS} and U or other mechanisms that control gas exchange. More recent experiments, FAIRS (Fluxes, Air–Sea Interaction, and Remote Sensing conducted in 2000; Jessup et al. 2002) and GasEx-2001, allowed the derivation of a parameterization for k_{DMS}. REA and GF techniques were used during those cruises, thus providing the opportunity to measure fluxes in duplicate and compare the applicability of both techniques in the marine environment.

Transfer velocities for DMS from FAIRS and GasEx-2001 are characterized by a considerable amount of scatter that increases with increasing wind speed to over an order of magnitude (Fig. 2). This is in agreement with the scatter observed in EC and GF measurements of the CO_2 flux conducted during ASGAMAGE, GasEx-1998, and GasEx-2001 (Jacobs et al. 1999; McGillis et al. 2001*b*; Zemmelink et al. 2004*b*).

The FAIRS gas transfer rates of DMS derived from REA were on average about a factor of 2 higher than estimates derived from GF measurements simultaneously applied during

© 2004 NRC Canada

Fig. 2. Gas transfer velocities (k_{660}) as a function of wind speed (measured at an elevation of 10 m during neutral conditions). All transfer velocities are based on dimethylsulphide (DMS) fluxes. □, derived from relaxed eddy accumulation measurements conducted during FAIRS; ■, derived from gradient flux measurements conducted during FAIRS; ▲, derived from gradient flux measurements conducted during GasEx-2001.

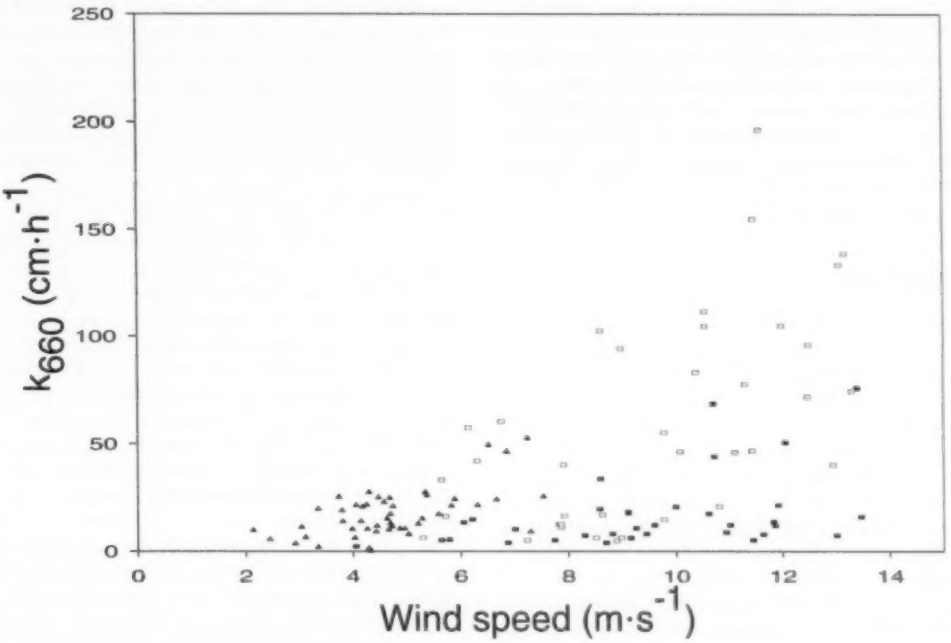

the cruise. No straightforward explanation could be given for the observed discrepancy; however, the effect of sea state and environmental conditions on the measurements is still under consideration. There was no firm rationale to prefer one technique over the other in the marine environment except perhaps that the GF method is less susceptible to ship motion. The GF technique was used for the measurement of DMS fluxes during the GasEx-2001 cruise. Concomitant profile measurements of water vapor fluxes showed that Monin–Obukhov similarity was valid during the meteorological and sea state conditions encountered during the GasEx-2001 cruise (Edson et al. 2002). The relationship between gas transfer and wind speed derived from the GF measurements conducted during GasEx-2001 was very similar to the parameterization derived from REA measurements conducted during FAIRS, and so the data sets were combined to derive a DMS-based gas transfer parameterization for wind speeds between 2 and 13 m·s^{-1}. The relationship derived from the pooled data set was in close agreement with the parameterization found by Jacobs et al. (1999) from EC CO_2 flux measurements. However, the equation derived from the merged FAIRS–GasEx data set was significantly higher than the relationship derived from GF measurements during FAIRS. It was emphasized that there is no reason to assume that either of the two methods used during FAIRS (GF and REA) was erroneous! Moreover, there is no argument to prefer one parameterization over the other. The agreement between the GasEx-GF and FAIRS–REA data sets might have been coincidental. It should be kept in mind that different water characteristics in the two areas, such as the occurrence of surfactants, waves, and swell (FAIRS was conducted at the edge of the California Current and GasEx-2001 in the midequatorial Pacific), are likely to have affected gas exchange and the results of the two techniques.

Right now, the influences of surfactants, waves, and swell are not taken into account during the application and interpretation of micrometeorological measurement techniques. In other words, lacking appropriate parameterizations for those influences on the applied techniques, it is not yet possible to ascribe the discrepancies and (or) agreement between techniques and campaigns to well-defined causes.

The parameterizations derived from the field measurements and the commonly applied parameterizations proposed by LM86 and W92 differ by up to a factor of 2–3 (Fig. 1). This is small compared with results obtained with EC techniques during the late 1970s and early 1980s, which showed much larger values of k (Wesely et al. 1982; Broecker et al. 1986; Smith and Jones 1986). These initial experiments have led to technologically improved EC instruments, especially with respect to gas sensors, and to new insights into data quality and the corrections to be applied. Currently, the EC technique may be regarded as a reasonably reliable method for determining CO_2 fluxes over the sea. However, all field measurements show a substantial amount of scatter, which results from a combination of effects such as surface and temporal nonhomogeneity, variations in wind speed, and a small signal to noise ratio (some of which are discussed in Jacobs et al. 2002). The conclusion can be drawn that field measurements have not resulted in a convincing parameterization of gas exchange (as a function of wind speed) yet. The scatter in the data suggests that parameterizations based on wind speed alone oversimplify gas exchange and

© 2004 NRC Canada

do not provide adequate insight into the processes that cause the scatter. Indeed, Bock et al. (1999) emphasized that gas exchange is only indirectly affected by wind speed. Other environmental parameters, such as waves, surface films, and subsurface turbulence, are intermittently linked and influence gas exchange in a more direct manner. Progress in understanding processes that affect gas exchange is most likely to come from a detailed study of the upwind source area of the flux including wind, waves, and surface turbulence. Footprint models allow the determination of this source area and the in situ quantification of parameters that define the magnitude of the flux and will be a valuable addition to future studies of gas exchange.

Recommendations

Recent experiments have shown that DMS fluxes can be measured by the REA and GF techniques. Moreover, parameterizations of gas exchange rates as a function of wind speed that were derived from these measurements are in reasonable agreement with parameterizations derived from EC and deliberate tracer measurements. Using DMS as a model gas is potentially a powerful tool for future projects that aim at (*i*) the testing and intercalibration of the REA, GF, and EC techniques in the marine environment, (*ii*) the investigation of processes that control fluxes, and (*iii*) the estimation of trace gas budgets on regional to global scales.

In contrast with the EC technique, REA and GF do not measure absolute fluxes, and although models that REA and GF rely on appear to be applicable in the marine environment, further testing under different conditions is needed before we can be fully confident in the application of these techniques. The lack of fast-response DMS sensors has allowed few EC measurements (Mitchell 2001), but new developments in gas analysis using mass spectrometry should make EC feasible for DMS (e.g., Bandy et al. 2002; Spicer et al. 1996). Bypassing the traditional approach for EC (based on continuous high-frequency sampling of air), fluxes can also be calculated from only a subset of the whole time series by taking quick samples at a low frequency (Rinne et al. 2000). Based on this approach, an EC system was developed that makes eddy covariance flux measurements possible using relatively slow sensors such as for methanol (Rinne et al. 2001). At this point, however, the use of micrometeorological techniques for field measurements of the flux of any gas in the marine environment is still in its infancy and intercalibration of techniques is required.

Although micrometeorological methods yield average net fluxes and exchange rates for areas with a length scale of about 10–1000 m (as a rule of thumb, 100 times the measurement height), they do not provide insight into processes that occur on the much smaller scales where fluxes are truly controlled or at the larger length scales that are needed to study biosphere–climate interactions. In the case of DMS, gas exchange might dominate removal in the upper metre of the water column, while biological consumption seems to be the most important removal pathway when the whole mixed layer is considered (Kieber et al. 1996). The combination of small-scale in situ studies, using, for example, enclosures, and the study of processes that occur in the source area of micrometeorological measurements will provide valuable information on the production and fate of DMS in relation to food web dynamics and environmental conditions. Such combined studies might eventually lead to general, global ecology laws that make it feasible to link near-surface dynamics to (DMS) fluxes.

Upscaling from micrometeorological measurements to regional and global scales is possible with airborne measurements that are able to integrate over surface areas with length scales up to hundreds of kilometres. Estimates of air–sea gas transfer can be made by satellite observations of sea surface roughness and thus coupled to the occurrence of waves (Glover et al. 2001). Still, to convert the surface roughness to gas transfer rates and eventually into fluxes, fundamental knowledge on the relationship between surface roughness and gas transfer is needed in combination with information on chemical and biological processes in the surface ocean that determine gas concentrations and fluxes. In addition, comparison of large-scale measurements with in situ measurements is needed to correctly interpret the obtained data. However, interactions between the different length scales can be complex and nonlinear (Jarvis and McNaughton 1986; Klaassen 1992) and results obtained by different flux measurement techniques operating on different scales might not be directly comparable. This remains to be evaluated in future work at sea.

In conclusion, micrometeorological methods cannot address all scales of interest for air–sea gas exchange processes. But they do provide insight into turbulence and biogeochemical processes that determine gas exchange, atmospheric transport, and subsequently atmospheric chemistry. In addition, eddy correlation, (relaxed) eddy accumulation, and profiling methods are most appropriate for the intensive as well as long-term investigation of net exchange over large regions and hence are valuable tools for nutrient cycle and budget studies.

The biogenic gas DMS can be used to investigate the applicability of EC, REA, and GF systems in the marine environment. Moreover, measurement of DMS fluxes provides an indication of the accuracy of EC, REA, and GF systems for the measurement of fluxes of other trace gases. There can be little doubt that the use of DMS as a model gas will strongly contribute to our current knowledge of the coupling between ocean biogeochemistry and global climate.

References

Andreae, M.O., and Crutzen, P.J. 1997. Atmospheric aerosols: biogeochemical sources and role in atmospheric chemistry. Science (Wash., D.C.), **276**: 1052–1058.

Andreas, E.L., Hill, R.J., Gosz, J.R., Moore, D.I., Otto, W.D., and Sarma, A.D. 1998. Stability dependence of the eddy-accumulation coefficients for momentum and scalars. Boundary Layer Meteorol. **86**: 409–420.

Asher, W., and Wanninkhof, R. 1998*a*. Transient tracers and air–sea gas transfer. J. Geophys. Res. **103**: 15 939 – 15 958.

Asher, W.E., and Wanninkhof, R. 1998*b*. The effect of bubble-mediated gas transfer on purposeful dual-gaseous tracer experiments. J. Geophys. Res. **103**: 10 555 – 10 560.

Ayers, G.P., and Gillett, R.W. 2000. DMS and its oxidation products in the remote marine atmosphere: implications for climate and atmospheric chemistry. J. Sea Res. **43**: 275–286.

© 2004 NRC Canada

Baker, J.M., Norman, J.M., and Bland, W.L. 1992. Field-scale application of flux measurement by conditional sampling. Agric. For. Meteor. **62**: 31–52.

Bandy, A.R., Thornton, D.C., Tu, F.H., Blomquist, B.W., Nadler, W., Mitchell, G.M., and Lenschow, D.H. 2002. Determination of the vertical flux of dimethyl sulfide by eddy correlation and atmospheric pressure ionization mass spectrometry (APIMS). J. Geophys. Res. **107**(D24): 4743 (doi: 10.1029/2002JD002472).

Beverland, I.J., Oneill, D.H., Scott, S.L., and Moncrieff, J.B. 1996. Design, construction and operation of flux measurement systems using the conditional sampling technique. Atmos. Environ. **30**: 3209–3220.

Bock, E.J., Hara, T., Frew, N.M., and McGillis, W.R. 1999. Relationship between air–sea gas transfer and short wind waves. J. Geophys. Res. **104**: 25 821 – 25 831.

Broecker, W.S., Ledwell, J.R., Takahashi, T., Weiss, R., Merlivat, L., Memery, L., Peng, T.H., Jähne, B., and Munnich K.O. 1986. Isotopic versus micrometeorological ocean CO_2 fluxes: a serious conflict. J. Geophys. Res. **91**: 10 517 – 10 527.

Businger, J.A., and Oncley, S.P. 1990. Flux measurement with conditional sampling. J. Atmos. Ocean. Technol. **7**: 349–352.

Businger, J.A., Wyngaard, J.C., Izumi, Y., and Bradley, E.F. 1971. Flux profile relationships in the atmospheric surface layer. J. Atmos. Sci. **28**: 181–189.

Charlson, R.J., Lovelock, J.E., Andreae, M.O., and Warren, S.G. 1987. Oceanic phytoplankton, atmospheric sulfur, cloud albedo and climate. Nature (Lond.), **326**: 655–661.

Chin, M., Rood, R.B., Allen, D.J., Andreae, M.O., Thompson, A.M., Lin, S.J., Atlas, R.M., and Ardizzone, J.V. 1998. Processes controlling dimethylsulfide over the ocean: case studies using a 3-D model driven by assimilated meteorological fields, J. Geophys. Res. **103**: 8341–8353.

Desjardins, R.L. 1977. Energy budget by an eddy correlation method. J. Appl. Meteorol. **16**: 248–250.

Donelan, M.A., Drennan, W., Saltzman, E., and Wanninkhof, R. (*Editors*). 2002. Gas transfer at water surfaces. Geophys. Monogr. Ser. **127**.

Edson, J.B., and Fairall, C.W. 1998. Similarity relationships in the marine atmospheric surface layer for terms in the TKE and scalar variance budgets. J. Atmos. Sci. **55**: 2311–2328.

Edson, J.B., Zappa, C., and McGillis, W. 2002. Scalar flux profile relationships for water vapor over the open ocean. *In* Fifteenth Conference on boundary layer and turbulence. Extended abstracts. American Meteorological Society, Boston, Mass.

Erickson, D.J., III. 1993. A stability dependent theory for air–sea gas exchange. J. Geophys. Res. **98**: 8471–8488.

Fairall, C.W., Hare, J.E., Edson, J.B., and McGillis, W. 2000. Parameterization and micrometeorological measurement of air–sea gas transfer. Boundary Layer Meteorol. **96**: 63–105.

Farmer, D.M., McNeil, C.L., and Johnson, B.D. 1993. Evidence for the importance of bubbles in increasing air–sea gas flux. Nature (Lond.), **361**: 620–623.

Glover, D.M., Frew, N.M., McCue, S.J., and Bock, E.J. 2001. A multi-year time series of global gas transfer velocity from the TOPEX dual frequency, normalized radar backscatter algorithm. *In* Gas transfer at water surfaces. *Edited by* M.A. Donelan, W. Drennan, E. Saltzman, and R. Wanninkhof. Geophys. Monogr. Ser. **127**: 325–332.

Gondwe, M., Krol, M., Gieskes, W.W.C., Klaassen, W., and de Baar, H.J.W. 2003. The contribution of ocean-derived DMS to the global atmospheric burdens of DMS, MSA, SO_2 and NSS-SO_4^{2-}. Global Biogeochem. Cycles, **17**: 1056 (doi: 10.1029/2002GB001937).

Haußecker, H., Reinelt, S., and Jähne, B. 1995. Heat as a proxy tracer for gas exchange measurements in the field: principle and technical realization. *In* Air–water gas transfer. *Edited by* B. Jähne and E.C. Monahan. Aeon, Hanau, Germany. pp. 405–413.

Hintsa, E.J., Dacey, J.W.H., McGillis, W.R., Edson, J.B., Zappa, C.J., and Zemmelink, H.J. 2004. Sea-to-air fluxes from measurements of the atmospheric gradient of dimethylsulfide and comparison with simultaneous relaxed eddy accumulation measurements. J. Geophys. Res. **109**: C01026 (doi: 10.1029/2002JC001617).

Jacobs, C.M.J., Kohsiek, W., and Oost, W.A. 1999. Air–sea fluxes and transfer velocity of CO_2 over the North Sea: results from ASGAMAGE. Tellus, **51**: 629–641.

Jacobs, C., Kjeld, J.F., Nightingale, P., Upstill-Goddard, R., Larsen, S., and Oost, W. 2002. Possible errors in CO_2 air–sea transfer velocity from deliberate tracer releases and eddy covariance measurements due to near-surface concentration gradients. J. Geophys. Res. **107** (doi: 10.1029/2001JC000983).

Jähne, B., Heinz, G., and Dietrich, W. 1987. Measurements of the diffusion coefficients of sparingly soluble gases in water. J. Geophys. Res. **92**: 10 767 – 10 776.

Jähne, B., Libner, P., Fischer, R., Billen, T., and Plate, E.J. 1989. Investigating the transfer processes across the free aqueous viscous boundary layer by the controlled flux method. Tellus, **41**: 177–195.

Jarvis, P.G., and McNaughton, K.G. 1986. Stomatal control of transpiration: scaling up from leaf to region. Adv. Ecol. Res. **15**: 1–49.

Jessup, A.T., Asher, W.E., Plant, W.J., McGillis, W.R., Zappa, C.J., Hintsa, E.H., Dacey, J.W.H., Farmer, D.M., Gemmrich, J., Vagle, S., Reising, S.C., and Zemmelink, H.J. 2002. The FAIRS experiment. IEEE Geosci. Remote Sens. Soc. Newsl. **123**: 12–17.

Kettle, A.J., and Andreae, M.O. 2000. Flux of dimethylsulfide from the oceans: a comparison of updated data sets and flux models. J. Geophys. Res. **105**: 26 793 – 26 808.

Kieber, D.J., Jianfu, J., Kiene, R.P., and Bates, T.S. 1996. Impact of dimethylsulfide photochemistry on methyl sulfur cycling in the equatorial Pacific Ocean. J. Geophys. Res. **101**: 3715–3722.

Klaassen, W. 1992. Average fluxes from heterogeneous vegetated regions. Boundary Layer Meteorol. **58**: 329–354.

Liss, P.S., and Merlivat, L. 1986. Air–sea gas exchange rates: introduction and synthesis. *In* The role of air–sea exchange in geochemical cycling. *Edited by* P. Buat-Ménard. D. Reidel, Boston, Mass. pp. 113–129.

Lovelock, J.E., Maggs, R.J., and Rasmussen, R.A. 1972. Atmospheric dimethyl sulfide and the natural sulfur cycle. Nature (Lond.), **237**: 452–453.

McGillis, W.R., Dacey, J.W.H., Frew, N.M., Bock, E.J., and Nelson, R.K. 2000. Water–air flux of dimethylsulfide. J. Geophys. Res. **105**: 1187–1193.

McGillis, W.R., Edson, J.B., Hare, J.E., and Fairall, C.W. 2001*a*. Direct covariance air–sea CO_2 fluxes. J. Geophys. Res. **106**: 16 729 – 16 745.

McGillis, W.R., Edson, J.B., Ware, J.D., Dacey, J.W.H., Hare, J.E., Fairall, C.W., and Wanninkhof, R. 2001*b*. Carbon dioxide flux techniques performed during GasEx-98. Mar. Chem. **75**: 267–280.

Mitchell, G.M. 2001. Determination of vertical fluxes of sulfur dioxide and dimethyl sulfide in the remote marine atmosphere by eddy correlation and an airborne isotopic dilution atmospheric pressure ionization mass spectrometer. Ph.D. thesis, Drexel University, Philadelphia, Pa.

Monin, A.S., and Obukhov, A.M.O. 1954. Fundamentale Gesetzmäßigkeiten der turbulenten vermischung in der bodennahen schicht der atmosphäre. *In* Sammelband zur statistischen theory der turbulenz. *Edited by* H. Goering. Deutsche Akademie der Wissenschaften zu Berlin, Berlin. pp. 199–226.

© 2004 NRC Canada

Nightingale, P.D., Malin, G., Law, C.S., Watson, A.J., Liss, P.S., Liddicoat, M.I., Boutin, J., and Upstill-Goddard, R.C. 2000. In situ evaluation of air–sea gas exchange parameterizations using novel conservative and volatile tracers. Global Biogeochem. Cycles, **14**: 373–387.

Oncley, S.P., Delany, A.C., Horst, T.W., and Tans, P.P. 1993. Verification of flux measurements using relaxed eddy accumulation. Atmos. Environ. Part A Gen. Top. **27**: 2417–2426.

Pattey, E., Desjardins, R.L., and Rochette, P. 1993. Accuracy of the relaxed eddy-accumulation technique, evaluated using CO_2 flux measurements. Boundary Layer Meteorol. **66**: 341–355.

Paulson, C.A. 1970. The mathematical representation of wind speed and profile temperatures in the unstable atmospheric surface layer. J. Appl. Meteorol. **9**: 857–861.

Putaud, J.P., and Nguyen, B.C. 1996. Assessment of dimethylsulfide sea–air exchange rate. J. Geophys. Res. **101**: 4403–4411.

Rinne, H.J.I., Delany, A.C., Greenberg, J.P., and Guenther, A.B. 2000. A true eddy accumulation system for trace gas fluxes using disjunct eddy sampling method. J. Geophys. Res. **105**: 24 791 – 24 798.

Rinne, H.J.I., Guenther, A.B., Warneke, C., de Gouw, J.A., and Luxembourg, S.L. 2001. Disjunct eddy covariance technique for trace gas flux measurements. Geophys. Res. Lett. **28**: 3139–3142.

Saltzman, E.S., King, D.B., Holmen, K., and Leck, C. 1993. Experimental determination of the diffusion coefficient of dimethylsulfide in water. J. Geophys. Res. **98**: 16 481 – 16 486.

Sciare, J., Mihalopoulos, N., and Dentener, F.J. 2000. Interannual variability of atmospheric dimethylsulfide in the southern Indian Ocean. J. Geophys. Res. **105**: 26 369 – 26 377.

Smith, S.D., and Jones, E.P. 1986. Isotopic and micrometeorological ocean CO_2 fluxes: different time and space scale. J. Geophys. Res. **91**: 10 529 – 10 532.

Spicer, C.W., Kenny, D.V., Chapman, E., Busness, K.M., and Berkowitz, C.M. 1996. Observations of dimethyl sulfide over the western North Atlantic Ocean using an airborne tandem mass spectrometer. J. Geophys. Res. **101**: 29 137 – 29 147.

Wallace, D.W.R., and Wirick, C.D. 1992. Large air–sea gas fluxes associated with breaking waves. Nature (Lond.), **356**: 694–696.

Wanninkhof, R. 1992. Relationship between wind speed and gas exchange over the ocean. J. Geophys. Res. **97**: 7373–7382.

Wanninkhof, R., and McGillis, W.R. 1999. A cubic relationship between air–sea CO_2 exchange and wind speed. Geophys. Res. Lett. **26**: 1889–1892.

Watson, A.J., and Liss, P.S. 1998. Marine biological controls on climate via the carbon and sulphur geochemical cycles. Philos. Trans. R. Soc. Lond. B Biol. Sci. **353**: 41–51.

Wesely, M.L., Cook, D.R., Hart, R.L., and Williams, R.M. 1982. Air–sea exchange of CO_2 and evidence for enhanced upward fluxes. J. Geophys. Res. **87**: 8827–8832.

Woolf, D.K. 1993. Bubbles and the air–sea transfer velocity of gases. Atmos. Ocean, **31**: 517–540.

Wyngaard, J.C., and Moeng, C.H. 1992. Parameterizing turbulent diffusion through the joint probability density. Boundary Layer Meteorol. **60**: 1–13.

Yvon, S.A., Saltzman, E.S., Bates, T.S., Cooper, D.J. 1996. Atmospheric sulfur cycling in the tropical Pacific marine boundary layer (12°S, 135°W): a comparison of field data and model results. 1. Dimethylsulfide. J. Geophys. Res. **101**: 6899–6910.

Zemmelink, H.J., Gieskes, W.W.C., Klaassen, W., Beukema, W.J., de Groot, H.W., de Baar, H.J.W., Hintsa, E.J., McGillis, W.R., and Dacey, J.W.H. 2004*a*. Relaxed eddy accumulation measurements of the sea-to-air transfer of dimethylsulfide over the northeastern Pacific. J. Geophys. Res. **109**: C01025 (doi: 10.1029/2002JC001616).

Zemmelink, H.J., Gieskes, W.W.C., Klaassen, W., de Groot, H.W., de Baar, H.J.W., Dacey, J.W.H., Hintsa, E.J., and McGillis, W.R. 2004*b*. Air–sea gas transfer rates derived from atmospheric dimethyl sulphide fluxes. J. Geophys. Res. In press.

© 2004 NRC Canada

PERSPECTIVE / PERSPECTIVE

Ecosystem modelling of the cycling of marine dimethylsulfide: a review of current approaches and of the potential for extrapolation to global scales[1]

Alain F. Vézina

Abstract: There is rising interest from oceanic and atmospheric scientists in the potential role of dimethylsulphide (DMS) in regulating global climate. The increased availability of field observations of DMS and related compounds (DMS(P)) and of their transformation rates in the ocean has stimulated the development of ecosystem models of marine sulfur cycling. The models cover a wide range of complexity levels and spatial/temporal scales, from zero-dimensional local simulations spanning a few days to regional/global simulations driven by ocean general circulation models. The degree of complexity required to model DMS(P) dynamics, particularly the differentiation into phytoplankton species or groups, remains an important open question. First attempts to drive these models with vertically resolved turbulence models suggest interesting interactions between DMS(P) dynamics and fine-scale ocean mixing that can modify fluxes of DMS to the atmosphere. Recent models also bring into focus the strong affinities between the cycling of DMS(P) and that of dissolved organic carbon in the surface ocean. Formal parameter estimation techniques, which are increasingly used in ecosystem modelling of carbon and nitrogen dynamics, should play a stronger role in the development of DMS sulfur modelling. Extrapolation of DMS cycling and fluxes to the global scale presently relies largely on empirical approach. A semiempirical approach, based on a simple ecosystem model, is shown to reproduce gross features of the global distribution of DMS in the surface ocean. This shows promise for the continuing development of ecosystem models for global modelling of marine sulfur fluxes to the atmosphere.

Résumé : Il y a un intérêt croissant parmi les chercheurs en sciences océaniques et atmosphériques dans le rôle potentiel du diméthylsulfide (DMS) dans la régulation du climat global. La plus grande disponibilité des observations du DMS et des composés associés (DMS(P)) et de leurs taux de transformation en milieu océanique a stimulé le développement de modèles écosystémiques du cyclage du soufre marin. Ces modèles couvrent une vaste gamme de niveaux de complexité et d'échelles spatio-temporelles, allant de simulations locales zéro-dimensionelles sur quelques jours à des simulations régionales et globales conduites par des modèles de la circulation générale des océans. Une question importante demeure le niveau de complexité requis pour modéliser la dynamique du DMS(P), particulièrement la différentiation entre les divers groupes ou espèces de phytoplancton. Les premières tentatives pour forcer ces modèles avec des modèles de turbulence à haute résolution verticale suggèrent des interactions intéressantes entre la dynamique du DMS(P) et le mélange océanique à petite échelle qui peuvent modifier les flux de DMS vers l'atmosphère. Des modèles récents mettent aussi en lumière la grande affinité entre le cyclage du DMS(P) et celui du carbone organique dissous à la surface de l'océan. Les techniques formelles d'estimation des paramètres, utilisées de plus en plus dans la modélisation de la dynamique du carbone et de l'azote, devrait jouer un rôle plus important dans le développement de la modélisation de la dynamique du DMS. Présentement, l'extrapolation du cyclage et des flux de DMS des échelles locales aux échelles globales s'appuie sur des approches empiriques. On montre ici qu'une approche semi-empirique, basée sur un modèle écosystémique simplifié, peut reproduire les principales caractéristiques de la répartition globale du DMS à la surface des océans. Ceci est prometteur pour la poursuite du développement des modèles écosystémiques pour la modélisation globale des flux de soufre marin vers l'atmosphère.

Received 12 February 2003. Accepted 15 December 2003. Published on the NRC Research Press Web site at http://cjfas.nrc.ca on 24 June 2004.
J17367

A.F. Vézina. Fisheries and Oceans Canada, Bedford Institute of Oceanography, 1 Challenger Drive, Dartmouth, NS B2Y 4A2, Canada (e-mail: vezinaa@dfo-mpo.gc.ca).

[1]This paper is part of the proceedings of the Third International Symposium on Biological and Environmental Chemistry of DMS(P) and Related Compounds, held in Rimouski (Québec), 26–28 September 2002.

 doi: 10.1139/F04-025 © 2004 NRC Canada

Introduction

Dimethylsulfide (DMS) is the most important volatile organic sulfur compound produced by the oceans and is a key link in the global sulfur cycle (Malin et al. 1992). DMS is the major source of non-sea-salt sulfate aerosols over the oceans (Andreae and Crutzen 1997) and is a significant contributor to coastal sulfate aerosols as well (Levasseur et al. 1997). The marine production of DMS and associated aerosols may respond to climate change in a way that could partly counteract greenhouse gas related warming (Charlson et al. 1987). For all of these reasons, there has been increased interest in quantifying DMS concentration in the surface ocean ($[DMS]_{SW}$) and DMS emissions into the atmosphere (F_{DMS}) and in understanding the factors that regulate $[DMS]_{SW}$ and F_{DMS}. At a minimum, such knowledge is required to correctly specify the sulfur fluxes that drive aerosols in global and regional climate models (Chin et al. 1998). Furthermore, improved knowledge of DMS fluxes and of their regulation is critical for investigations of the potential links between DMS and a changing climate (Lawrence 1993).

DMS is a product of biological activity in the surface ocean. $[DMS]_{SW}$ depends on photosynthetic and heterotrophic processes involving phytoplankton, zooplankton, and bacteria (Malin et al. 1992). Ecosystem modelling is thus a natural tool to investigate how $[DMS]_{SW}$ is regulated. Ecosystem modelling also provides the ability to simulate how $[DMS]_{SW}$ might respond to changes in climate forcing of ecosystem processes. Gabric et al. (1993) developed the first marine ecosystem model that incorporates sulfur dynamics. Since then the observations required to construct and evaluate such models have improved and there has been a notable increase in the number of ecosystem models developed to simulate marine sulfur dynamics (hereafter DMS ecosystem models). One of the goals of this review is to provide a brief overview of this burgeoning field from an arms-length perspective rooted in ecosystem modelling of carbon and nitrogen dynamics (hereafter C/N ecosystem models). These two areas of modelling have much in common and it is useful to bring some of these commonalities into focus.

Despite the power of ecosystem modelling, it can be reasonably pointed out that too little is known about many of the processes and parameters incorporated into these models to provide predictive power (Anderson et al. 2001). This has led to a search for simple empirical relationships that can be used to interpolate $[DMS]_{SW}$ from variables that can be measured more easily over regional and global scales (Anderson et al. 2001; Aumont et al. 2002). These empirical relationships can also be used to extrapolate $[DMS]_{SW}$ to conditions not encountered during observations, thus to provide indications of how $[DMS]_{SW}$ and F_{DMS} might respond to a changing climate. However, empirical models might not be suitable for extrapolation because the parameters derived from fitting observations do not necessarily apply to conditions that were not observed. Process-based ecosystem models, if they can be shown to be robust, may provide a better tool for extrapolation. In any case, ecosystem models do link outcomes (in this case $[DMS]_{SW}$) more transparently to processes and allow richer analyses of the sensitivity of these outcomes to different assumptions. With that in mind, a second goal of this review is to briefly explore the potential for global modelling of $[DMS]_{SW}$ with a semiempirical algorithm based on the simple DMS ecosystem model developed by Lawrence (1993).

Basic principles

All current DMS ecosystem models share basic principles (illustrated in Fig. 1). The focus of the models is the planktonic ecosystem that resides in the surface mixed layer of the ocean. The growth rate of phytoplankton is modelled as a function of irradiance, nutrient, and temperature levels in the mixed layer. These forcing factors are all dependent on the intensity of vertical mixing that is in large part reflected in the depth of the mixed layer. The resulting photosynthetic production (approximately growth rate × biomass) is balanced by zooplankton grazing, natural mortality processes (e.g., cell lysis), and net changes in phytoplankton biomass. The biomass of phytoplankton and flows to other compartments are simulated in units of the limiting nutrient, usually taken to be nitrogen, but can be expressed in other units (e.g., carbon) using conversion factors. These principles underpin both DMS and C/N ecosystem models.

In this simple model, the flows into the DMS pool are a function of the mortality and grazing flows. The simplest way is to start by assuming a fixed ratio of DMS per unit of biomass within phytoplankton cells. The DMS inside cells is generally in the form of its precursor dimethylsulfoniopropionate (DMSP) and this DMSP is typically referred to as particulate DMSP ($DMSP_p$). The DMS released to the water column is the product of the biomass flows through the grazing and mortality pathways with this fixed DMSP quota. This assumes that all of the DMSP released in the water, now dissolved DMSP ($DMSP_d$), is instantaneously transformed into DMS. Most models actually include $DMSP_d$ as a separate compartment as explained below. The released DMS is then subject to bacterial and photochemical loss processes and to ventilation to the atmosphere. These are processes specific to DMS ecosystem models. However, DMS and $DMSP_d$ are part of the dissolved organic matter (DOM) pool. Consequently, the dynamics of DMS + $DMSP_d$ have much in common with those of dissolved organic carbon (DOC), an increasingly important part of C/N ecosystem modelling (Christian and Anderson 2002).

Thus, current DMS ecosystem models can be broken down into three submodels: (*i*) an ecological structure, basically a C/N ecosystem model, that determines primary production and its fate through a trophic network, (*ii*) a physical arena that regulates the rate of primary production, and (*iii*) a DMS(P) dynamics model that determines the fate of DMS(P) once it is released in the water. There are no feedbacks between these submodels, and DMS(P) dynamics are driven by the physical and nutrient dynamics. I will here review the current DMS ecosystem models in terms of these submodels and examine how the development of these submodels in DMS ecosystem models compares with that in C/N ecosystem models.

Overview of sulfur dynamics ecosystem models

Ecological structure

The first DMS ecosystem model (Gabric et al. 1993) was

© 2004 NRC Canada

Fig. 1. Schematic of the fundamental processes common to DMS ecosystem models. P, phytoplankton; Z, zooplankton; S:P, ratio of sulfur (as $DMSP_p$) to phytoplankton biomass; $[DMS]_{sw}$, concentration of DMS in surface waters; mort, mortality.

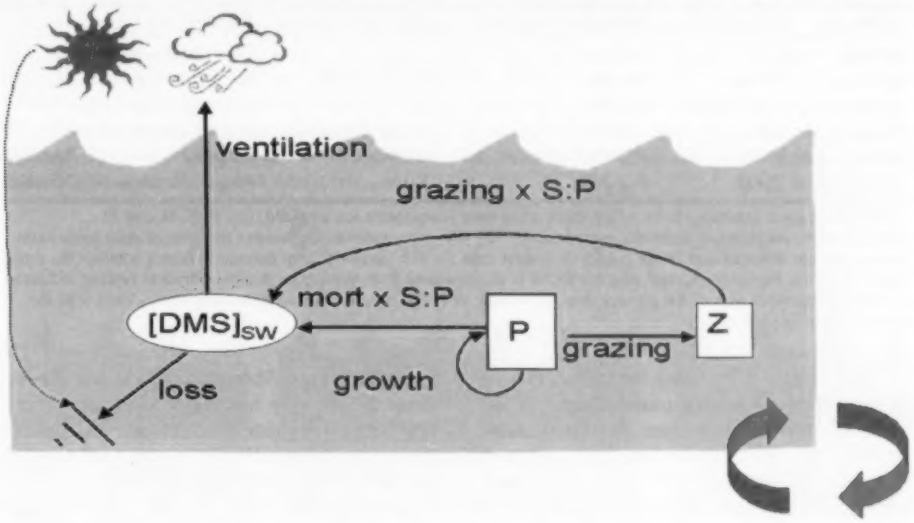

based on the Moloney et al. (1986) model, which simulates nitrogen flows through phytoplankton, bacteria, detritus (particulate and dissolved), and three size-based groups of zooplankton. Gabric et al. (1993) added DMS and $DMSP_d$ as state variables, linear relations to calculate sulfur flows to the DMS(P) pools as a function of the simulated nitrogen flows, and sinks for $DMSP_d$ and DMS (bacterial consumption, photooxidation, and ventilation). They used their model initially to simulate short-term phytoplankton bloom dynamics and to investigate the sensitivity of simulated DMS concentrations to variations in the controlling parameters of the model. This model has been extended to investigate a range of problems, including the interaction between the spring bloom and DMS dynamics in the Barents Sea (Gabric et al. 1999), DMS dynamics observed during a Lagrangian experiment in the North Sea (Watts and Bigg 2001), and the impact of climate change on air–sea fluxes of DMS in the subantarctic ocean south of Australia (Gabric et al. 1998, 2001). Recently, DMS ecosystem models with different structures and parameterizations have appeared in the literature (Table 1).

DMS ecosystem models published to date tend to be ecologically complex, with multiple phytoplankton and zooplankton compartments. Early C/N ecosystem models tended to have less ecological detail. The PZND (phytoplankton, zooplankton, nutrients, and detritus) model structure, which lumps all phytoplankton and zooplankton types into single compartments, is still a common ecological structure in C/N ecosystem modelling. Only one published DMS ecosystem model (Lefèvre et al. 2002) used the PZND structure. This makes it more difficult to compare DMS and C/N ecosystem modelling. The adoption of the PZND structure by Lefèvre et al. (2002) made it easier for them to compare the parameters they used to simulate nitrogen dynamics to the parameters used in a number of C/N modelling studies at the same study site. On the other hand, the tendency to minimize ecological detail in C/N ecosystem modelling may not be an optimal approach (Doney 1999). More complicated C/N models for biogeochemical applications (Moore et al. 2002) are beginning to appear. Nevertheless, simple PZND models continue to play a strong role in C/N ecosystem modelling (Franks 2002; Newberger et al. 2003).

The rationale for splitting the phytoplankton into different groups in DMS ecosystem models is that DMS(P) quotas vary enormously among phytoplankton groups. A rough generalization is that most diatoms are low DMS(P) producers whereas groups such as prymnesiophytes and coccolithophores include high-DMS(P)-producing species. It seems important then to distinguish a priori between low- and high-DMS(P) phytoplankton groups in the model. This in turn encourages the differentiation of zooplankton groups because these phytoplankton groups have different fates in the food web. Gabric et al. (1999) indicated from their modelling work that the different characteristics of the spring bloom and resulting DMS dynamics in contrasting stations across the Arctic Polar front can be reproduced satisfactorily with only one phytoplankton compartment. van den Berg et al. (1996) ran sensitivity experiments that point to the discrimination between species that produce DMSP lyase (e.g., *Phaeocystis*) and those that do not as the important distinction to maintain in the models. This issue is far from settled and more modelling work targeted specifically at this problem is important to guide the development of DMS ecosystem models.

Physical forcing

Most DMS ecosystem models have used box approximations of the mixed layer for physical forcing (Table 1). The mixed layer is treated as an instantaneously and homogeneously mixed box. A mixing rate is applied that renews part of the contents of the box each simulated day. Boundary conditions that specify physical, chemical, and biological conditions below the box determine how this mixing rate affects properties inside the box. The thickness of the box (mixed layer depth), mixing rate, and boundary conditions have been generally assumed or specified from observations,

© 2004 NRC Canada

Table 1. Variations in ecological structure, level of description of the microbial loop, and physical forcing found among published DMS ecosystem models.

Source	Ecological structure	Microbial loop	Physical forcing
Lawrence 1993	PZ	None	Box (zero-dimensional)
Gabric et al. 1993	PZ_3ND	B and DOM	Box (zero-dimensional)
van den Berg et al. 1996	P_2ZND	B	Box (two-dimensional)
Archer et al. 2002	P_3Z_3ND	B and DOM	Box (zero-dimensional)
Lefèvre et al. 2002	PZND	DOM	Diagnostic (one-dimensional)
Jodwalis et al. 2000	P_2Z_2ND	None	Prognostic (one-dimensional)

Note: Ecological structure shows which basic ecosystem components are included, i.e., P, Z, N, and D (phytoplankton, zooplankton, nutrients, and detritus). The subscripts indicate the number of types of each basic components that are differentiated in the model (if greater than 1). The microbial loop column indicates whether the model resolves bacteria explicitly (B) and whether DOM is distinguished from particulate detritus. Physical forcing indicates the level of representation of the physics (box, diagnostic or prognostic in order of increasing complexity) with the dimensionality in parentheses.

although van den Berg et al. (1996) used the output from a circulation model. This box approximation is simple to implement and works well for the short time periods (blooms and field experiments) that have been the focus of most DMS ecosystem models to date. However, it can be difficult to implement realistically for longer seasonal to annual time scales. In those cases, seasonal changes in mixed layer depth, mixing rate, and vertical gradient all need to be specified and errors in the specifications can have a large impact on the simulations (Eigenheer et al. 1996). Moreover, the instantaneously mixed representation of the mixed layer is only a rough approximation of the real physics of the mixed layer. Simulations of plankton dynamics are known to be sensitive to the physical model used to drive the ecosystem model (Chen and Annan 2000).

These considerations have led to the increasing use of sophisticated physical models to drive C/N ecosystem models (Archer 1995). These models attempt to represent the evolution of the mixed layer and mixing rates from first principles, relating the mixed layer to the vertical density structure and surface forcing (heat, freshwater, and momentum fluxes). They can be run in diagnostic mode where the temperature and salinity structure is prescribed by observations and maintained fixed throughout the simulation (Tian et al. 2001) or in prognostic mode where the temperature and salinity are allowed to evolve with the simulated changes in mixing characteristics (Doney et al. 1996). Prognostic mixed layer simulations allow detailed investigations of the interactions between ocean physics and plankton dynamics and are now a common tool in C/N ecosystem modelling. To date, only one published DMS ecosystem modelling study has used prognostic physical modelling (Jodwalis et al. 2000).

This study has revealed interesting features of the interaction between ocean physics (in a one-dimensional sense) and DMS production and air–sea fluxes. Jodwalis et al. (2000) have shown that DMS fluxes are influenced by dynamic interactions between vertical mixing throughout the water column and DMS(P) production. DMS(P) compounds that have accumulated at depth under the summer pycnocline are mixed back towards the surface during fall overturn, enhancing the DMS production and emission that arises from increased fall production. Moreover, Jodwalis et al. (2000) suggested that the strength of DMS emissions may depend on the frequency of meteorological events that affect the mixed layer. Short intervals (a few days or less) between wind events may not allow sufficient time to recharge the DMS(P) pools near the surface. The resulting DMS emissions may be smaller than expected from considering only climatological $[DMS]_{SW}$ and wind speed. Only prognostic physical models, forced by real meteorological data, can reveal such interactions and further work in that area may well yield new insights into factors regulating DMS emissions from the ocean surface.

DMS(P) dynamics

The structures and parameterizations used in DMS(P) dynamics models are summarized in Fig. 2. The production of DMS in the water column largely arises from the bacteria cleaving $DMSP_d$ into DMS (Malin et al. 1992). Therefore, most DMS ecosystem models introduce both DMS and $DMSP_d$ as explicit compartments. The $DMSP_d$ pool is supplied by processes that release DMSP from phytoplankton cells (e.g., exudation, lysis, and grazing). $DMSP_d$ is consumed by bacteria, with a proportion of that consumption routed to the DMS pool through a DMS yield parameter. This parameter determines the proportion of the $DMSP_d$ consumption that is cleaved to DMS, the remainder being demethylated to supply bacterial sulfur requirements. These models also allow for direct production of DMS from the phytoplankton cells through the activity of intra- and extracellular DMSP lyase. Archer et al. (2002) added another level of complexity by distinguishing between bacterial DMSP and DMS consumers. Some models have ignored the intermediate $DMSP_d$ link and produce DMS directly from cell lysis and grazing. The advantage of this approach is that it eliminates some parameters, such as the DMS yield, that are difficult to estimate with precision. The disadvantage is that it ignores microbial interactions with the DMS(P) pool that may act to decouple DMS production from primary production and grazing.

Most DMS ecosystem models have used simple linear dynamics to simulate the production of DMS from DMSP (Fig. 2). The flux of sulfur from one pool to another is either proportional to the concentration of the substrate or proportional to the product of the substrate concentration and the bacterial biomass. These parameterizations reflect the lack of knowledge about factors regulating DMS production, although this situation is improving, rather than any firm evi-

© 2004 NRC Canada

Fig. 2. Schematic of the (*a–c*) compartmental structures and (*d–f*) functional relationships used to represent the dynamics of DMS and related compounds (DMS(P)) in DMS ecosystem models. (*a*) Direct production and consumption of DMS (Lawrence 1993; Jodwalis et al. 2000). (*b*) Dependence of the production and consumption dynamics of DMS on the dynamics of its precursor $DMSP_d$ (Gabric et al. 1993; van den Berg et al. 1996; Lefèvre et al. 2002). (*c*) Same as Fig. 2*b* but with separation between $DMSP_d$- and DMS-consuming bacteria (Archer et al. 2002). (*d*) Linear dependence of DMS(P) transformation fluxes ($F^C_{DMS(P)}$) on DMS(P) concentration (Gabric et al. 1993; Lawrence 1993; Jodwalis et al. 2000; Lefèvre et al. 2002). (*e*) Linear dependence of $F^C_{DMS(P)}$ on bacterial and DMS(P) concentrations (van den Berg et al. 1996) (different curves are for different values of *B*, bacterial biomass). (*f*) Nonlinear kinetics of DMS(P) utilization rates competing with other forms of DOC (Archer et al. 2002). The two curves represent the uptake velocities of DMS(P) ($V_{DMS(P)}$) and DOC (V_{DOC}) as a function of DOC concentration when the half-saturation constant for DMS(P) ($H_{DMS(P)}$) is set lower than that for DOC as a whole (H_{DOC}).

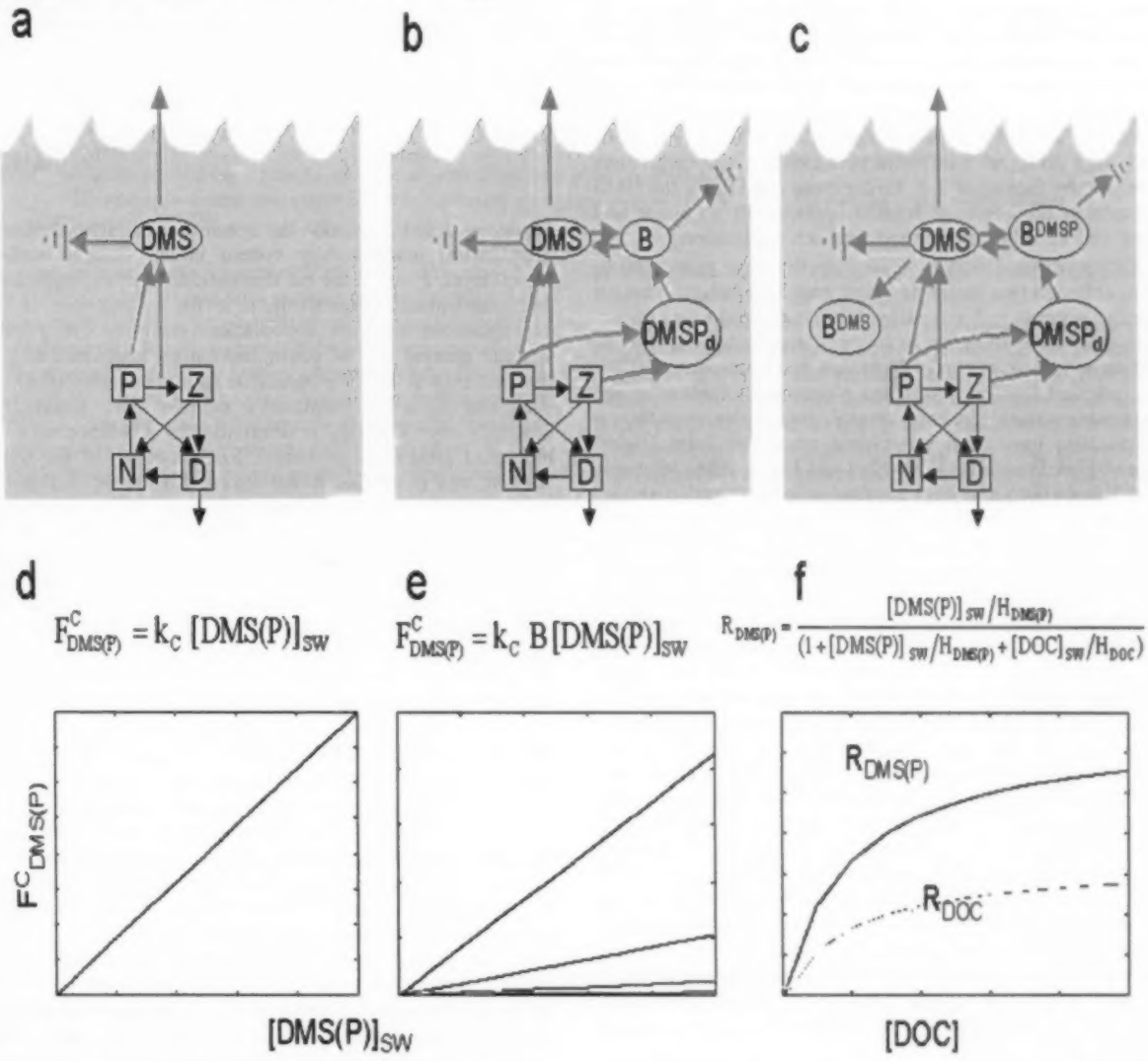

dence that transformation rates are actually linear. Archer et al. (2002) is the only model that uses nonlinear kinetics to represent the bacterial assimilation of $DMSP_d$ and DMS. This is analogous to the parameterizations used in C/N ecosystem models to represent bacterial incorporation of DOM (Christian and Anderson 2002). In fact, Archer et al. (2002) treat $DMSP_d$ and DMS as labile fractions of DOM that are potential sources of carbon for bacteria. This is the most realistic approach in light of recent estimations that DMS(P) compounds can satisfy a substantial proportion of the bacterial carbon demand (Kiene and Linn 2000). This also points to a common theoretical framework for the DOM and DMS(P) submodels of C/N and DMS ecosystem models, respectively.

However, increasing model complexity increases the number of parameters that need to be specified. This is a serious

© 2004 NRC Canada

issue because most of the parameters involved in DMS(P) transformation fluxes remain poorly known. There are large differences among parameter values used in the DMS(P) part of various DMS ecosystem models (Table 2). In most cases, the parameter values were determined from laboratory or field measurements, with some or all of the parameters adjusted by trial and error to improve the correspondance between model simulations and measurements of the state variables. Only Watts and Bigg (2001) used formal parameter estimation techniques to estimate parameter values that minimize model–data misfits. In part, these differences in parameter values reflect differences in model structure and functional relationships. However, large differences in parameters appear among different applications of the same model. Compare the parameters used for applications of the Gabric et al. (1993) model (Gabric et al. 1993, 1999; Watts and Bigg 2001) with different periods/sites. The parameters can vary by factors of 2–5. Under these conditions, the DMS ecosystem models have limited applicability in space and time and must be recalibrated for each application.

C/N ecosystem models suffer from the same general problem, although two recent developments have helped improve their robustness and generality. First, the introduction of formal parameter estimation techniques, also called data assimilation or inverse methods (Robinson and Lermusiaux 2002), has allowed more rigorous and objective estimation of the parameter values. Second, several time series at different ocean sites have been established under the Joint Global Ocean Flux Study (JGOFS) (Karl and Lucas 1996; Michaels and Knap 1996) and have resulted in multiannual data sets that can be used for model development (Lawson et al. 1996). The combination of parameter estimation and time series data has allowed experimentation with different model structures (Spitz et al. 2001). The different model structures are applied on the same data and the results of the numerical experiments can be compared much more transparently when the parameters are estimated objectively rather than when they are obtained by trial and error. As a result, C/N ecosystem models are now emerging that can reproduce dynamics at contrasting sites (e.g., subtropical versus subpolar (Hurtt and Armstrong 1999) or Pacific versus Atlantic (Spitz and Abbott 2000)) with a common parameter set. At present, only one oceanic multiannual time series of DMS(P) observations (Dacey et al. 1999) is available for model development and only one DMS modelling study (Watts and Bigg 2001) has used a formal parameter estimation technique. Based on the experience from C/N ecosystem modelling, enhancement of DMS(P) time series observations combined with increased use of formal parameter estimation constitutes a reasonable prescription for improvement in the robustness and generality of DMS ecosystem models.

Sensitivity analysis

Sensitivity analysis is an important part of mathematical modelling in general and ecosystem modelling in particular. It is required to establish how model parameters control the behaviour of the model. Most parameters of an ecosystem model are not precisely known and it is crucial to determine which parameters strongly influence model output and which ones can be given lower priority for improvement. Specifically, sensitivity analyses of DMS ecosystem models have been used to better understand the controls on surface $[DMS]_{SW}$ and their relative importance. But before examining those results, some insight into controlling processes can be gained by examining the simplest model depicted in Fig. 1. Lawrence (1993) derived a set of three equations that describe this system:

$$(1) \quad \frac{dP}{dt} = \mu P - m_P - gPZ$$

$$(2) \quad \frac{dZ}{dt} = \gamma gPZ - m_Z Z$$

$$(3) \quad \frac{d[DMS]_{SW}}{dt} = \beta(m_P P + gPZ) - K_C[DMS]_{SW} - \frac{K_L}{Z_M}[DMS]_{SW}$$

Equations 1 and 2 describe the dynamics of a phytoplankton–zooplankton predator–prey system in the oceanic surface mixed layer, P and Z are the concentrations of phytoplankton and zooplankton, respectively, μ is the growth rate of the phytoplankton, m_P is the phytoplankton mortality rate, g is the specific grazing rate of phytoplankton by zooplankton, γ is the efficiency at which zooplankton assimilates phytoplankton prey, and m_Z is the zooplankton mortality rate. Equation 3 describes how $[DMS]_{SW}$ is determined by a balance between biological production processes, loss processes in the water column, and ventilation to the atmosphere. In eq. 3, β is the ratio of $DMSP_p$ to phytoplankton biomass, K_C is the rate of DMS consumption in the water column, K_L is the piston velocity at the air–sea interface, and Z_M is the depth of the mixed layer. Lawrence (1993) also derived the steady-state solution for $[DMS]_{SW}$:

$$(4) \quad [DMS]_{SW} = \frac{\mu\beta P}{\frac{K_L}{Z_M} + K_C}$$

and the steady-state solution for P:

$$(5) \quad P = \frac{m_Z}{\gamma g}$$

Substituting eq. 5 into eq. 4 yields

$$(6) \quad [DMS]_{SW} = \frac{\mu\beta m_Z}{\left(\frac{K_L}{Z_M} + K_C\right)\gamma g}$$

which indicates that, according to this simple model, $[DMS]_{SW}$ at steady state is positively related to the phytoplankton growth rate, the DMS(P) quota, and zooplankton mortality and is inversely related to the sum of the DMS ventilation and loss rate constants, scaled by the flux of phytoplankton biomass assimilated by the zooplankton. Fundamentally, $[DMS]_{SW}$ appears as a balance between the production of DMS(P) compounds (phytoplankton growth rate × DMS(P) quota) that enhances $[DMS]_{SW}$ and the assimilation of phytoplankton by the zooplankton (not just the grazing mortality) that depresses $[DMS]_{SW}$.

© 2004 NRC Canada

Table 2. Variations in specified parameters controlling the dynamics of DMS and related compounds among published DMS ecosystem models.

Model	S:N (mg S·mg N^{-1})	K_{DMSP_d} (day^{-1})	K_{DMS} (day^{-1})	DMS yield (%)	K_{photo} (day^{-1})
Gabric et al. 1993	0.3	1.0	0.95	33	0.5
van den Berg et al. 1996	0.03–0.2[a]	na	na	18	na
Gabric et al. 1999	0.04–0.2	0.23–0.53	0.18–0.52	30–50	0–1.3[b]
Jodwalis et al. 2000	0.02–0.3[c]	na	na	na	1.08
Watts and Bigg 2001	0.3	0.49	0.4	68	0.24
Archer et al. 2002	na	4.2	4.2	17	0.25
Lefèvre et al. 2002	0.1–0.5	3.0	0.4	40	0.6–0.8

Note: S:N is the S($DMSP_p$) to N ratio in phytoplankton cells; K_{DMSP_d} and K_{DMS} are the rate constants for bacterial consumption of $DMSP_d$ and DMS, respectively; DMS yield is the ratio of DMS produced to $DMSP_d$ consumed via bacterial degradation; K_{photo} is the rate constant of photooxidation; "na" means that the parameter is not included in the corresponding model or that there was not sufficient information in the published source to convert it into units common with the other models.

[a]Calculated from original units (nmol DMSP·mg C^{-1}) assuming a molecular mass of 134 for DMSP and a carbon to nitrogen ratio of 5.7 (by weight).

[b]Maximum rate (1.3·day^{-1}) scaled by the ratio of mean mixed layer to surface irradiance.

[c]Calculated from original units (mmol DMSP·L^{-1}) assuming a molecular mass of 134 for DMSP and a carbon to cell volume ratio of 0.1 (Montagnes et al. 1994).

Equation 6 points to fundamental processes that may control $[DMS]_{SW}$ and to potential reasons why it has been difficult to relate $[DMS]_{SW}$ to phytoplankton biomass (as measured by chlorophyll). It also suggests that processes important in C/N ecosystem models, such as phytoplankton growth and zooplankton grazing, are also critical for predictions of $[DMS]_{SW}$. Simple scaling arguments also suggest that some of these parameters may be more critical than others. For example, average piston velocities over the surface ocean typically range between 2 and 3 m·day^{-1} and DMS loss rates are on the order of 1·day^{-1}. However, mixed layer depths range between 10 and 100 m; hence, the impact of variations in ventilation losses is likely to be small relative to that of variations in biological/photochemical loss rates. Similarly, zooplankton mortality rates are generally much smaller than zooplankton grazing and assimilation rates. Again, the impact of variations in zooplankton mortality on $[DMS]_{SW}$ is likely to be minor compared with that of variations in zooplankton grazing.

With this in mind, it is instructive to look at the results of several sensitivity analyses of DMS ecosystem models (Table 3). I consider only sensitivity analyses where all model parameters have been systematically perturbed from their base value and the impact on $[DMS]_{SW}$ has been quantified. Such sensitivity analyses have been published only for the Gabric et al. (1993) model and its variants as well as for the Lefèvre et al. (2002) model. This does not cover the full range of DMS ecosystem models that have been published and this summary may not be generally representative of the sensitivity responses of DMS ecosystem models. Nevertheless, it is interesting to note that the sensitivity analyses consistently point to parameters controlling phytoplankton growth rate and zooplankton grazing as among the most sensitive. The models do not agree on the importance of the DMS(P) quota, but two out of three rank it very high. The first-order DMS loss to bacterial consumption in the water column is a moderately to highly sensitive parameter whereas the ventilation loss has a minor impact. The zooplankton assimilation efficiency has a significant impact in all of the models whereas zooplankton mortality has a small to negligible impact. These results are broadly consistent with the analysis of the simple model.

The more complex models in Table 3 include $DMSP_d$ as an intermediate in the production of DMS and, in the case of Gabric et al. (1993) and variants, model bacterial dynamics explicitly. The sensitivity analyses indicate that these additional parameters have an impact on simulations of $[DMS]_{SW}$. However, they do not rank higher than the basic growth and grazing/assimilation processes included in the Lawrence (1993) model. The exception is the yield of DMS from microbial consumption of $DMSP_d$, which is a critical parameter in the Lefèvre et al. (2002) model. However, this model has a unique structure among DMS ecosystem models, separating $DMSP_d$ from DMS without an explicit bacterial compartment. This structure puts the microbial yield in a central role mediating all of the transformation from $DMSP_d$ to DMS.

Overall, the sensitivity analyses indicate that detailed understanding of microbial processes involved in sulfur transformations, although certainly important, must rest first on a solid foundation describing phytoplankton growth and grazing/assimilation. Another feature of these sensitivity analyses is that parameters that control nitrogen (or carbon) dynamics rank high in relation to sulfur-specific parameters in controlling $[DMS]_{SW}$. In other words, getting the carbon and nitrogen part of DMS ecosystem models right is at least as important as getting the sulfur dynamics part right. Watts and Bigg (2001) made a similar point based on the results of their parameter estimation study where they found that carbon and nitrogen parameters needed as much adjustment as sulfur parameters in minimizing the model–data misfits.

Potential for extrapolation to global scales

One important focus of recent research in marine sulfur cycling is to quantify global fluxes of marine DMS to the atmosphere and to investigate how these fluxes might respond to global warming. Current attempts at global extrapolation and simulation of DMS fluxes rely on empirical models (Anderson et al. 2001; Aumont et al. 2002). This

© 2004 NRC Canada

Table 3. Summary of the results of sensitivity analyses on the Gabric et al. (1993) model, a modified version of the Gabric et al. (1993) model (Gabric et al. 1999), and the Lefèvre et al. (2002) model.

Parameter group	Submodel	Gabric et al. 1993	Gabric et al. 1999	Lefèvre et al. 2002
Phytoplankton growth rate	N	1	4	3, 5, 9
DMS(P) quotum	S	2	9	1
Zooplankton assimilation efficiency	N	4, 5	7, 8	7
Zooplankton grazing rate	N	3, 7	1	4, 8
Zooplankton mortality rate	N	Low	Low	10
DMS loss rate	S	8	2,3	6
Ventilation	S	Low	Low	Low
Microbial DMS yield	S	Low	6, 10	2
Bacterial growth	N	6, 9, 10	5	na

Note: When appropriate, the parameters of these models are assigned to categories defined from the simple model (Fig. 1; eqs. 1, 2, and 3). Parameters that cannot be mapped on the structure of the simple model (i.e., microbial parameters) are added on the last rows of the table. Parameter groups are also assigned to the C/N (ecological structure) submodel (N) or the DMS(P) dynamics submodel (S). The numbers in the table give the rank order of the sensitivity of $[DMS]_{SW}$ to the parameters belonging to each group (with rank 1 being the most influential parameter). Only the 10 most sensitive parameters are ranked; those that fall below rank 10 are marked as "low" (for low influence). "na" means that there are no parameters in the model that fall into that category.

parallels the longer history in global modelling of biogenic carbon fluxes, which in its early phase relied almost entirely on empirical relationships for extrapolation to global scales (Eppley and Peterson 1979; Martin et al. 1987). These are still used to great advantage but there is an increasing emphasis in incorporating dynamic ecosystem models into global circulation models (Moore et al. 2002). It is probable that the same evolution will occur in the marine sulfur field as DMS ecosystem models become more common and better understood. In that spirit, I explore the potential of a simple DMS ecosystem model (eq. 4) to reproduce the latitudinal profile of annual $[DMS]_{SW}$ (Kettle et al. 1999). This is not presented here as a new global model — much more work would be required to test it rigorously and this is outside the scope of this review.

The two published empirical approaches to global extrapolation start from very different premises. Anderson et al. (2001) developed their model by matching globally gridded estimates of putative independent variables with $[DMS]_{SW}$ observations from the Kettle et al. (1999) database. They found a significant relationship between $[DMS]_{SW}$ and the product of surface chlorophyll (milligrams per cubic metre), surface shortwave radiation (watts per square metre), and a nutrient limitation term calculated from nitrate concentrations (millimoles per cubic metre). This relationship emerged only after extensive smoothing of the data. This model does not resolve $[DMS]_{SW}$ variability at small and mesoscales and at low $[DMS]_{SW}$ (below 2.29 nmoles·L^{-1}). Aumont et al. (2002) in contrast developed their model from the results of small to mesoscale studies and then extrapolated the model to global scales. The independent variables of their model are also quite different from Anderson et al. (2001). The Aumont et al. (2002) model is in fact a pair of regression models that predict first $DMSP_p$ and then the ratio of $[DMS]_{SW}$ to $DMSP_p$ as a function of chlorophyll and a trophic index. This trophic index is the ratio of diatoms to total phytoplankton biomass. This is based on observations from the field surveys that communities dominated by diatoms produce less $DMSP_p$ per unit biomass and also display lower ratios of $[DMS]_{SW}$ to $DMSP_p$. This is also consistent with the general finding that diatoms are low DMS producers. Therefore, the Anderson et al. (2001) model emphasizes phytoplankton growth as a controlling variable whereas the Aumont et al. (2002) model emphasizes the impact of community structure.

Another approach is to use the relationship derived by Lawrence (1993) from the steady-state solution of his simple ecosystem model (eq. 4). Lawrence (1993) did in fact use this equation to estimate $[DMS]_{SW}$ for his modelling of the strength of the DMS feedback on climate. However, he made a calculation only for the tropical ocean. With the availability of global ocean data products, it is possible to extrapolate his model to the global scale. Equation 4 is used instead of eq. 6 because phytoplankton biomass data are available on global scales, which makes it much easier to implement the model.

All three models were implemented using globally gridded data sets from the data repository at http://ingrid.ldeo.columbia.edu/. For each model, the $[DMS]_{SW}$ is calculated from the required independent variables averaged zonally over 46 4° latitude bins (from 90°S to 90°N). The averaging of independent variable data and the $[DMS]_{SW}$ calculations were first done for 16 combinations of four major ocean basins (Atlantic, North Pacific, South Pacific, and Indian) and four seasons (January–March, April–June, July–September, and October–December). The basin- and season-specific results were then averaged to give global predicted meridional $[DMS]_{SW}$ profiles that can be compared with the global meridional $[DMS]_{SW}$ profile from Kettle et al. (1999). The Anderson et al. (2001) and Aumont et al. (2002) models were implemented exactly as described in the original references. The trophic index required by the Aumont et al. (2002) model was estimated from the silicate fields as described by Aumont et al. (2002).

The Lawrence (1993) model requires the phytoplankton growth rate. This was estimated using a simple growth model as a function of surface irradiance, nitrate concentrations, temperature, and mixed-layer depth (adapted from Sharples (1999), described in Appendix A). The DMSP quota (90 nmol S·mg Chl^{-1}) was the mean quota used by Lefèvre et al. (2002). The phytoplankton biomass was obtained from gridded data as for the empirical models. A global mean piston velocity (2.5 m·day^{-1}, Bates et al. 1987) was used and the rate constant of DMS consumption was fixed at 0.9·day^{-1} following Lawrence (1993). However, this fixed consump-

© 2004 NRC Canada

Fig. 3. Global latitudinal profiles of annual surface ocean DMS ($[DMS]_{SW}$) extracted from fig. 6 in Kettle et al. (1999) (solid line) and predicted by the empirical models of Anderson et al. (2001) (broken line) and Aumont et al. (2002) (dotted line) and by the semiempirical algorithm derived from the model of Lawrence (1993) (dashed–dotted line).

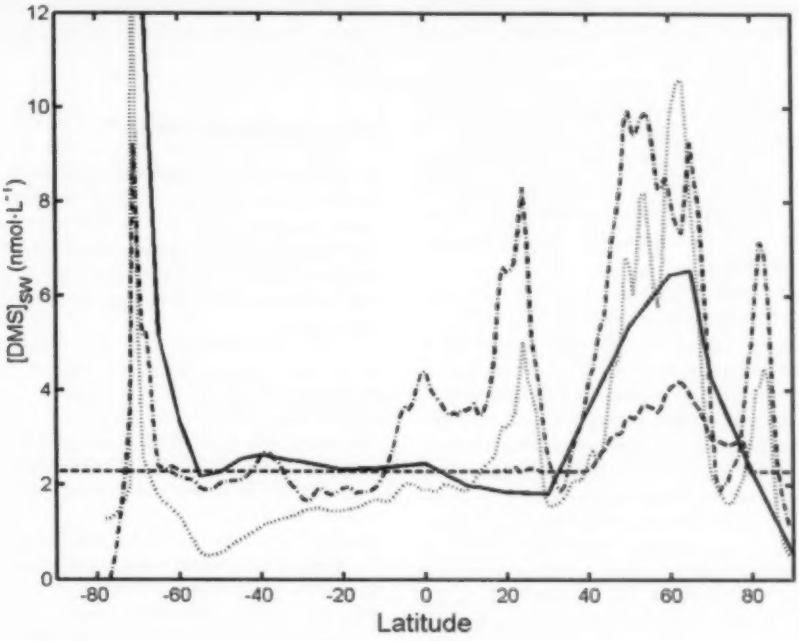

tion rate constant does not account for photochemical degradation, which is light dependent and therefore varies with latitude. To account for this, a term K'_C was added to K_C, where $K'_C = \phi I_0/4$, where $\phi = 0.072$ $m^2 \cdot W^{-1} \cdot day^{-1}$ and I_0 is the incident shortwave radiation (watts per square metre) and photolytically active radiation is assumed to represent 25% of the total radiation (Lefèvre et al. 2002).

The latitudinal profile of annual $[DMS]_{SW}$ from Kettle et al. (1999) is replotted along with the profiles predicted by the empirical models and the steady-state solution to Lawrence (1993)'s model (Fig. 3). The Kettle et al. (1999) profile is itself a model that interpolates sparse data. It cannot be viewed as a proper validation data set, especially as it smooths out much of the seasonal and geographic variability. This comparison is meant only to illustrate the behaviour of the different models.

All models and the Kettle et al. (1999) profile display a broad maximum in $[DMS]_{SW}$ between 30 and 70°N and low and relatively uniform $[DMS]_{SW}$ between 10 and 70°S. The profile from the Anderson et al. (2001) model is much smoother than those produced by the other models, but this is expected given the smoothing involved in developing the model in the first place. The Aumont et al. (2002) and Lawrence (1993) models display similar latitudinal features, even though they arise from completely different foundations. Both generate a spike in $[DMS]_{SW}$ between 70 and 80°S that is also seen in the Kettle et al. (1999) profile and both overestimate $[DMS]_{SW}$ in the tropical Northern Hemisphere (10–30°N). However, the overestimate by the Lawrence (1993) model is stronger and broader, encompassing the equatorial ocean, than that from the Aumont et al. (2002) model. It is nevertheless remarkable that the semiempirical model, with no adjustment of the parameters described above, agrees relatively well with other independently derived descriptions of the latitudinal profile of mean annual $[DMS]_{SW}$.

This is not meant in any way as an attempt to test one model against another. This would require much more work, making sure, for example, that the impact of the zonal variability in the independent variables on predicted $[DMS]_{SW}$ is preserved rather than averaged out as is done here. A critical test would have to examine how different models reproduce the seasonal and geographical variability in $[DMS]_{SW}$. The divergences among models remain unacceptably large (factor of 3–4 at 20°N, for example). It would be important then to examine the sensitivity of the Lawrence (1993) predictions to its parameters. Parameter estimation might reduce the strong discrepancy between the Lawrence (1993) model and the Kettle et al. (1999) profile in the northern subtropical ocean. Again, this is beyond the scope of this review. This exercise is meant only to suggest that ecosystem-based dynamical approaches should be explored alongside empirical approaches for modelling at global scales. It is also interesting to note that models based on different assumptions about what controls $[DMS]_{SW}$, i.e., bulk production and recycling (Lawrence 1993) versus community structure (Aumont et al. 2002), may not be distinguishable when applied at global scales. Tests with more discriminatory power are needed to determine what aspect of model structure needs to be developed further for regional and global applications.

Summary and conclusions

Ecosystem-based modelling of marine sulfur dynamics is still in its infancy. The development of such models is certain

© 2004 NRC Canada

to accelerate further as more data and better understanding of sulfur dynamics become available. This will undoubtedly lead to more complex and realistic models. It is worth reminding, however, that complexity and realism are not absolutely required for better understanding and prediction (Franks 2002). Simple models, such as that of Lawrence (1993) explored here, can generate useful insights into the dynamics of the system of interest. Sometimes, complex models rediscover interactions that were already in simpler models. If only to identify real advances in modelling, simple models need to be explored along with more complicated ones. In fact, finding out when and where simple models fail to account for observations is likely to spur the development of better and more robust models.

The development of DMS ecosystem models is also intimately linked to that of ecosystem models that focus on carbon and nitrogen dynamics. Improved C/N ecosystem models are key to improved DMS ecosystem models. DMS(P) is a significant part of the labile DOC pool that cycles actively in the surface ocean. The fundamental processes, bacterial utilization and photochemical degradation, are the same. Both DMS and DOC cycling have major impacts on exchanges of radiatively active gases between the ocean and the atmosphere. There are strong links between DMS and DOC modelling that should be developed further. The longer history of C/N ecosystem modelling also suggests some avenues for further improvement of DMS ecosystem models. One is the need for accurate and detailed representation of the physical environment. Another is that formal parameter estimation techniques, coupled with adequate observations, greatly aid in the development of better models.

A critical factor limiting the development of DMS ecosystem models, however, and one that was not discussed at length in this review, is that we do not understand what is responsible for the variability in parameters such as DMS(P) quotas and microbial yield. What conditions affect the phytoplankton sulfur quota? Is it just phylogenetic or are there environmental variables involved? Recent findings point to an antioxidant function for DMSP (Sunda et al. 2002). Pinning down functional roles for DMSP would help to develop better parameterizations of the DMS(P) quota. Similarly, we need to better understand what determines whether bacteria will use $DMSP_d$ as a carbon or a sulfur source. This boils down to understanding the pathways linking carbon and sulfur flows as well as carbon (nitrogen) or sulfur flows on their own. Until we have some clear responses to these questions, DMS models will remain less robust than C/N models where at least some of the underlying processes are better understood.

Finally, empirical approaches to the extrapolation of DMS cycling and fluxes over global scales have proven to be very useful and will continue to provide insights into global climate-related issues. However, process-based ecosystem approaches to extrapolation also need to be explored and applied at regional and global scales. A simplistic attempt at this was presented here as an illustration of a possible avenue. The relative success of the semiempirical algorithm in reproducing global annual $[DMS]_{SW}$ fields shows promise for a dynamical approach to extrapolation. At the same time, it should be kept in mind that success at this global scale does not indicate that this approach or any other would be particularly successful at apprehending the impact of DMS on climate. Critical interactions between marine DMS and the atmosphere occur at the mesoscale. Therefore, much more testing at the appropriate scales is required before confidence can be gained in empirical or process-based models for extrapolation.

Acknowledgements

This work was supported by a Natural Sciences and Engineering Research Council of Canada (NSERC) discovery grant, a joint NSERC – Canadian Foundation for Climate and Atmospheric Science grant to the Canadian SOLAS Research Network, and Fisheries and Oceans Canada. I thank two anonymous referees for their helpful comments on the manuscript.

References

Anderson, T.R., Spall, S.A., Yool, A., Cipollini, P., Challenor, P.G., and Fasham, M.J.R. 2001. Global fields of sea surface dimethylsulfide predicted from chlorophyll, nutrients and light. J. Mar. Syst. **30**: 1–20.

Andreae, M., and Crutzen, P. 1997. Atmospheric aerosols: biogeochemical sources and role in atmospheric chemistry. Science (Wash., D.C.), **276**: 1052–1058.

Archer, D. 1995. Upper ocean physics as relevant to ecosystem dynamics: a tutorial. Ecol. Appl. **5**: 724–739.

Archer, S.D., Gilbert, F.J., Nightingale, P.D., Zubkov, M.V., Taylor, A.H., Smith, G.C., and Burkill, P.H. 2002. Transformation of dimethylsulphoniopropionate to dimethylsulphide during summer in the North Sea with an examination of key processes via a modelling approach. Deep-Sea Res. **49**: 3067–3101.

Aumont, O., Belviso, S., and Monfray, P. 2002. Dimethylsulfoniopropionate (DMSP) and dimethylsulfide (DMS) sea surface distributions simulated from a global three-dimensional ocean carbon cycle model. J. Geophys. Res. **107** (doi: 10.1029/1999JC000111).

Bates, T., Charlson, R., and Gammon, R. 1987. Evidence for the climatic role of marine biogenic sulphur. Nature (Lond.), **329**: 319–321.

Charlson, R.J., Lovelock, J.E., Andreae, M.O., and Warren, S.G. 1987. Oceanic phytoplankton, atmospheric sulphur, cloud albedo and climate. Nature (Lond.), **326**: 655–661.

Chen, F., and Annan, J. 2000. The influence of different turbulence schemes on modelling primary production in a 1d coupled physical–biological model. J. Mar. Syst. **26**: 259–288.

Chin, M., Rood, R., Allen, D., Andreae, M., Thompson, A., Lin, S.J., Atlas, R., and Ardizzone, J. 1998. Processes controlling dimethylsulfide over the ocean: case studies using a 3-d model driven by assimilated meteorological fields. J. Geophys. Res. **103**: 8341–8353.

Christian, J.R., and Anderson, T.R. 2002. Modeling DOM biogeochemistry. *In* Biogeochemistry of dissolved organic matter in the ocean. *Edited by* D. Hansell and C. Carlson. Academic Press, New York. pp. 717–747.

Dacey, J., Howse, F., Michaels, A., and Wakeham, S. 1999. Temporal variability of dimethylsulfide and dimethylsulfoniopropionate in the Sargasso Sea. Deep-Sea Res. **45**: 2085–2104.

Doney, S. 1999. Major challenges confronting marine biogeochemical modeling. Global Biogeochem. Cycles, **13**: 705–714.

Doney, S., Glover, D., and Najjar, R. 1996. A new coupled, one-dimensional biological–physical model for the upper ocean: ap-

© 2004 NRC Canada

plications to the JGOFS Bermuda Atlantic time-series study (BATS) site. Deep-Sea Res. **43**: 591–624.

Eigenheer, A., Kuhn, W., and Radach, G. 1996. On the sensitivity of ecosystem box model simulations on mixed-layer depth estimates. Deep-Sea Res. **43**: 1011–1027.

Eppley, R., and Peterson, B. 1979. Particulate organic matter flux and planktonic new production in the deep ocean. Nature (Lond.), **282**: 677–680.

Franks, P. 2002. Npz models of plankton dynamics: their construction, coupling to physics, and application. J. Oceanogr. **58**: 379–387.

Gabric, A., Murray, N., Stone, L., and Kohl, M. 1993. Modelling the production of dimethylsulfide during a phytoplankton bloom. J. Geophys. Res. **98**: 22 805 – 22 816.

Gabric, A., Whetton, P., Boers, R., and Ayers, G. 1998. The impact of simulated climate change on the air–sea flux of dimethylsulphide in the subantarctic Southern Ocean. Tellus Ser. B Chem. Phys. Meteorol. **50**: 388–399.

Gabric, A., Matrai, P., and Vernet, M. 1999. Modelling the production and cycling of dimethylsulphide during the vernal bloom in the Barents Sea. Tellus Ser. B Chem. Phys. Meteorol. **51**: 919–937.

Gabric, A.J., Whetton, P., and Cropp, R. 2001. Dimethylsulphide production in the subantarctic Southern Ocean under enhanced greenhouse conditions. Tellus Ser. B Chem. Phys. Meteorol. **53**: 273–287.

Hurtt, G.C., and Armstrong, R. 1999. A pelagic ecosystem model calibrated with BATS and OWSI data. Deep-Sea Res. **46**: 27–61.

Jodwalis, C.M., Benner, R.L., and Eslinger, D.L. 2000. Modeling of dimethylsulfide ocean mixing, biological production and sea-to-air flux for high latitudes. J. Geophys. Res. **105**: 14 387 – 14 399.

Karl, D., and Lucas, R. 1996. The Hawaii Ocean Time-series (HOT) Program: background, rationale and field implementation. Deep-Sea Res. II, **43**: 129–156.

Kettle, A.J., Andreae, M.O., Amouroux, D., Andreae, T.W., Bates, T.S., Berresheim, H., Bingemer, H., Boniforti, R., Curran, M.A.J., DiTullio, G.R., Helas, G., Jones, G.B., Keller, M.D., Kiene, R.P., Leck, C., Levasseur, M., Malin, G., Maspero, M., Matrai, P., McTaggart, A.R., Mihalopoulos, N., Nguyen, B.C., Novo, A., Putaud, J.P., Rapsomanikis, S., Roberts, G., Schebeske, G., Sharma, S., Simó, R., Staubes, R., Turner, S., and Uher, G. 1999. A global database of sea surface dimethyl sulfide (DMS) measurements and a procedure to predict sea surface DMS as a function of latitude, longitude, and month. Global Biogeochem. Cycles, **13**: 399–444.

Kiene, R.P., and Linn, L.J. 2000. Distribution and turnover of dissolved DMSP and its relationship with bacterial production and dimethylsulfide in the Gulf of Mexico. Limnol. Oceanogr. **45**: 849–861.

Lawrence, M. 1993. An empirical analysis of the strength of the phytoplankton–dimethylsulfide–cloud–climate feedback cycle. J. Geophys. Res. **98**: 20 663 – 20 673.

Lawson, L., Hofmann, E., and Spitz, Y. 1996. Time series sampling and data assimilation in a simple marine ecosystem model. Deep-Sea Res. **43**: 625–651.

Lefèvre, M., Vézina, A., Levasseur, M., and Dacey, J. 2002. A model of DMS production and dynamics in the subtropical North Atlantic. Deep-Sea Res. I, **49**: 2221–2239.

Levasseur, M., Sharma, S., Cantin, G., Michaud, S., Gosselin, M., and Barrie, L. 1997. Biogenic sulfur emissions from the Gulf of St. Lawrence and assessment of its impact on the Canadian East Coast. J. Geophys. Res. **102**: 28 025 – 28 039.

Malin, G., Turner, S., and Liss, P. 1992. Sulfur: the plankton/climate connection. J. Phycol. **28**: 590–597.

Martin, J., Knauer, G., Karl, D., and Broenkow, W. 1987. VERTEX: carbon cycling in the northeast Pacific. Deep-Sea Res. **34**: 267–285.

Michaels, A., and Knap, A. 1996. Overview of the U.S. JGOFS Bermuda Atlantic Time-series Study and the Hydrostation S Program. Deep-Sea Res. II, **43**: 157–198.

Moloney, C., Bergh, M., Field, J., and Newell, R. 1986. The effect of sedimentation and microbial nitrogen regeneration in a plankton community: a simulation investigation. J. Plankton Res. **8**: 427–445.

Montagnes, D., Berges, J., Harrison, P., and Taylor, F. 1994. Estimating carbon, nitrogen, protein, and chlorophyll *a* from volume in marine phytoplankton. Limnol. Oceanogr. **39**: 1044–1060.

Moore, J., Doney, S., Kleypas, J., Glover, D., and Fung, I. 2002. An intermediate complexity marine ecosystem model for the global domain. Deep-Sea Res. **49**: 403–462.

Newberger, P.A., Allen, J.S., and Spitz, Y.H. 2003. Analysis and comparison of three ecosystem models. J. Geophys. Res. **108**.

Robinson, A.R., and Lermusiaux, P.F. 2002. Chapter 12. Data assimilation for modeling and predicting coupled physical–biological interactions in the sea. *In* The sea. Vol. 12. *Edited by* A.R. Robinson, J.J. McCarthy, and B.J. Rothschild. John Wiley & Sons, Inc., New York. pp. 475–536.

Sharples, J. 1999. Investigating the seasonal vertical structure of phytoplankton in shelf seas. Mar. Models, **1**: 3–38.

Spitz, Y., and Abbott, M. 2000. Comparison of two oligotrophic environments using data assimilative modeling. *In* 2000 Ocean Sciences Meeting, San Antonio, Tex. American Geophysical Union, Washington, D.C.

Spitz, Y.H., Moisan, J.R., and Abbott, M.R. 2001. Configuring an ecosystem model using data from the Bermuda Atlantic Time Series (BATS). Deep-Sea Res. **48**: 1733–1768.

Sunda, W., Kieber, D.J., Kiene, R.P., and Huntsman, S. 2002. An antioxidant function for DMSP and DMS in marine algae. Nature (Lond.), **418**: 317–320.

Tian, R.C., Vézina, A.F., Starr, M., and Saucier, F. 2001. Seasonal dynamics of coastal ecosystems and export production at high latitudes: a modeling study. Limnol. Oceanogr. **46**: 1845–1859.

van den Berg, A., Turner, S., van Duyl, F., and Ruardij, P. 1996. Model structure and analysis of dimethylsulphide (DMS) production in the southern North Sea, considering phytoplankton dimethylsulphoniopropionate- (DMSP) lyase and eutrophication effects. Mar. Ecol. Prog. Ser. **145**: 233–244.

Watts, M., and Bigg, G. 2001. Modelling the nitrogen cycle and DMS production in Lagrangian experiments in the North Atlantic. Deep-Sea Res. **48**: 1019–1042.

Appendix A

The phytoplankton growth rate in the surface mixed layer at a coordinate $y(\mu(y))$ is the minimum of

$$\text{(A1)} \quad \mu(y)_N = \mu^T_{max}(y)N(y)/(K_N + N(y))$$

or

$$\text{(A2)} \quad \mu(y)_L = \text{Chl:C}(\alpha\,\text{PAR}_m(y) - r_B)$$

where $\mu(y)_N$ and $\mu(y)_L$ are nutrient- and light-limited growth rates, respectively, $\mu^T_{max}(y)$ is a temperature-dependent maximum growth rate, $N(y)$ is nitrate concentration, K_N is the half-saturation constant for $N(y)$ uptake (0.5 mmol·m^{-3}), Chl:C is the chlorophyll to carbon ratio (1/60 mg Chl·mg C^{-1}), α is the photosynthetic efficiency (1.4 mg C·m^{-2}·mg Chl^{-1}·W^{-1}·day^{-1}), $\text{PAR}_m(y)$ is the mean photosynthetically available radiation (PAR) in the mixed layer (watts per square metre), and r_B is a chlorophyll-specific respiration rate (3.5 mg C·mg Chl^{-1}·day^{-1}). The coordinate y refers to the midpoint of any 4° latitude bin

© 2004 NRC Canada

between 90°S and 90°N over which the independent variable data were averaged zonally (for each combination of ocean basin and season). $\mu^T_{max}(y)$ is given by

(A3) $$\mu^T_{max}(y) = \mu_{max} 2^{(T(y)-T_{opt})/10}$$

where μ_{max} is the maximum growth rate (2.0·day^{-1}), T_{opt} is the optimum temperature for growth (25 °C), and $T(y)$ is surface temperature. $PAR_m(y)$ is calculated as

(A4) $$PAR_m(y) = 0.43I_0(y)(1 - \exp(-k_t Z_M(y)))/k_t Z_M(y)$$

where $I_0(y)$ is the mean daily incident shortwave radiation (watts per square metre), k_t is the total light extinction coefficient in the water column ($k_t = k_w + k_P P(y)$, $k_w = 0.03 \cdot m^{-1}$, $k_P = 0.04$ m^2·mg Chl^{-1}, and $P(y)$ is phytoplankton biomass (milligrams chlorophyll per cubic metre)), and 0.43 is the factor used to convert shortwave radiation into PAR.

© 2004 NRC Canada

Culinary Herbs for Short-Season Gardeners

By Ernest Small and Grace Deutsch

Softcover
ISBN 0-660-17785-4
NRC 42737
$24.95 CAN. Other countries $24.95 US
Canadian customers add GST (7%)

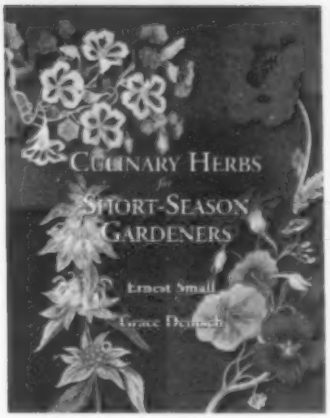

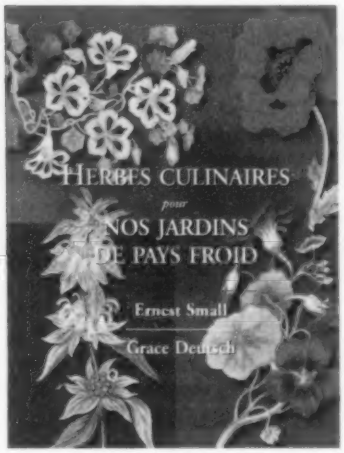

Herbes culinaires pour nos jardins de pays froid

Par Ernest Small et Grace Deutsch

Édition brochée
ISBN 0-660-96164-4
CNRC 43254
24,95 $CAN. À l'étranger 24.95 $US
Clients du Canada, ajoutez la TPS (7 %)

Orders may be submitted by mail or fax to:
Les commandes peuvent être soumises par courrier ou par télécopieur à :

Order Office / Bureau des commandes

NRC Research Press / Presses scientifique du CNRC
National Research Counci l/ Conseil national de recherches
Ottawa, ON K1A 0R6, Canada
Telephone / Téléphone : (613) 990-2254
Fax / Télécopieur :(613) 952-7656
E-mail / Courriel: pubs@nrc-cnrc.gc.ca
Website / Site web : http://pubs.nrc-cnrc.gc.ca

PLEASE PRINT/LETTRES MOULEES

☐ Payment enclosed / Paiement inclus — Charge to/ Imputer à ☐ Visa ☐ MasterCard

Account no./N° de compte — Expiry date/Date d'expiration

Name/Nom

Signature

Address/Adresse

City/Ville — Province

Postal code/Code postal — Country/Pays

Telephone/Téléphone — Fax/Télécopieur

E-mail/Courriel:

Prepayment required unless order is accompanied by a purchase order number. Cheques or money orders should be made payable to : "Receiver General for Canada, Credit NRC". All sales are final.
Les commandes doivent être payées d'avance à moins qu'elles ne soient accompagnées d'un numéro de bon de commande. Les chèques ou mandats doivent être libellés au « Receveur général du Canada, crédit du CNRC ». Toutes les ventes sont finales.

Fisheries and Aquatic Sciences
Sciences halieutiques et aquatiques

Photographic Atlas of Fish Otoliths of the Northwest Atlantic Ocean
By / Par Stephen E. Campana

$54.95 CAN. Other countries $54.95 US
54,95 $CAN. À l'étranger 54,95 $US
Softcover / Édition brochée
(*Can. Spec. Publ. Fish. Aquat. Sci. / Publ. spéc. can. sci. halieut. aquat. 133*)
284 pages ISBN 0-660-19108-3 ISSN 0706-6481 NRC / CNRC 46328

Salmonine Introductions to the Laurentian Great Lakes:
An Historical Review and Evaluation of Ecological Effects
By / Par Stephen S. Crawford

$42.95 CAN. Other countries $42.95 US
42,95 $CAN. À l'étranger 42,95 $US
Softcover / Édition brochée
(*Can. Spec. Publ. Fish. Aquat. Sci. / Publ. spéc. can. sci. halieut. aquat. 132*)
215 pages ISBN 0-660-17639-4 ISSN 0706-6481 NRC / CNRC 42734

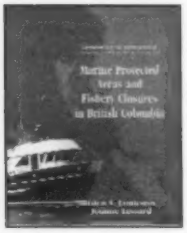

Marine Protected Areas and Fisheries Closures in British Columbia
By Glen S. Jamieson and Joanne Lessard

$69.95 CAN. Other countries $69.95 US
69,95 $CAN. À l'étranger 69,95 $US
Softcover / Édition brochée
(Can. Spec. Publ. Fish. Aquat. Sci. / Publ. spéc. can. sci. halieut. aquat. 131)
414 pages ISBN 0-660-17788-9 ISSN 0706-6481 NRC / CNRC 42846

Workshop on Rebuilding Abalone Stocks in British Columbia
By / Par Alan Campbell

$42.95 CAN. Other countries $42.95 US
42,95 $CAN. À l'étranger 42,95 $US
Softcover / Édition brochée
(*Can. Spec. Publ. Fish. Aquat. Sci. / Publ. spéc. can. sci. halieut. aquat. 130*)
158 pages ISBN 0-660-18292-0 ISSN 0706-6481 NRC / CNRC 42841

To order any of the above titles / Commandez n'importe quel titre ci-dessus à :

Telephone / Téléphone : (613) 990-2254
Fax / Télécopieur : (613) 952-7656
E-mail / Courriel : pubs@nrc-cnrc.gc.ca
Web site / Site web : http://pubs.nrc-cnrc.gc.ca

Order Office / Bureau des commandes
NRC Research Press / Presses scientifique du CNRC
National Research Council / Conseil national de recherches
Ottawa, ON K1A 0R6, Canada

Canadian customers add GST (7%). Prepayment required unless order is accompanied by a purchase order number. Cheques or money orders should be made payable to : "Receiver General for Canada, Credit NRC". For all orders outside Canada, rates are in U.S. Dollars. All sales are final.
Clients du Canada, ajoutez la TPS (7 %). Les commandes doivent être payées d'avance à moins qu'elles ne soient accompagnées d'un numéro de bon de commande. Les chèques ou mandats doivent être libellés au « Receveur général du Canada, crédit du CNRC ». Pour les commandes hors-Canada, les tarifs sont en dollars américains. Toutes les ventes sont finales.

Stephen D. Archer, Francis J. Gilbert, J. Icarus Allen, Jerry Blackford, and Philip D. Nightingale	**765–787**	Modelling of the seasonal patterns of dimethylsulphide production and fate during 1989 at a site in the North Sea
Yvonnick Le Clainche, Maurice Levasseur, Alain Vézina, John W.H. Dacey, and François J. Saucier	**788–803**	Behaviour of the ocean DMS(P) pools in the Sargasso Sea viewed in a coupled physical–biogeochemical ocean model
S. Belviso, C. Moulin, L. Bopp, and J. Stefels	**804–816**	Assessment of a global climatology of oceanic dimethylsulfide (DMS) concentrations based on SeaWiFS imagery (1998–2001)
Moire A. Wadleigh	**817–825**	Sulphur isotopic composition of aerosols over the western North Atlantic Ocean
Laurent Bopp, Olivier Boucher, Olivier Aumont, Sauveur Belviso, Jean-Louis Dufresne, Mai Pham, and Patrick Monfray	**826–835**	Will marine dimethylsulfide emissions amplify or alleviate global warming? A model study
PERSPECTIVES		PERSPECTIVES
H.J. Zemmelink, J.W.H. Dacey, and E.J. Hintsa	**836–844**	Direct measurements of biogenic dimethylsulphide fluxes from the oceans: a synthesis
Alain F. Vézina	**845–856**	Ecosystem modelling of the cycling of marine dimethylsulfide: a review of current approaches and of the potential for extrapolation to global scales

NRC Research Press 75th Anniversary

Since the publication of the first issue of the *Canadian Journal of Research* in 1929, the National Research Council has provided scientists and engineers in Canada and elsewhere with a means to communicate with their peers in the international research community through the production of high-quality journals. NRC Research Press is proud to celebrate 75 years of science and technology publishing in Canada.

Le 75e anniversaire des Presses scientifiques du CNRC

Depuis la parution du premier numéro du *Canadian Journal of Research* en 1929, le Conseil national de recherches du Canada publient des revues savantes de qualité grâce auxquelles les chercheurs et ingénieurs du Canada et d'ailleurs peuvent partager les résultats de leurs recherches avec leurs pairs de la collectivité scientifique internationale. Les Presses scientifiques du CNRC sont fières de célébrer 75 ans d'édition scientifique et technique au Canada.

National Research Council Canada
Ottawa, Canada K1A 0R6

Conseil national de recherches Canada
Ottawa, Canada K1A 0R6

Postage paid at Ottawa
Publications mail
Registration No. 40062591

Port payé à Ottawa
Poste-publication
Enregistrement n° 40062591

USPS periodical postage paid at Champlain, N.Y.

Canadian Journal of Fisheries and Aquatic Sciences

Volume 61, Number 5, May 2004

Journal canadien des sciences halieutiques et aquatiques

Volume 61, numéro 5, mai 2004

Third International Symposium on Biological and Environmental Chemistry of DMS(P) and Related Compounds

[Troisième symposium international sur la biochimie et la chimie environnementale du DMS(P) et des composés apparentés]

Maurice Levasseur	**v–vi**	Introduction / Introduction
	PERSPECTIVE	PERSPECTIVE
Rafel Simó	**673–684**	From cells to globe: approaching the dynamics of DMS(P) in the ocean at multiple scales
	ARTICLES	ARTICLES
Maureen D. Keller, Patricia A. Matrai, Ronald P. Kiene, and Wendy K. Bellows	**685–699**	Responses of coastal phytoplankton populations to nitrogen additions: dynamics of cell-associated dimethylsulfoniopropionate (DMSP), glycine betaine (GBT), and homarine
Hyakubun Harada, Mary-Anne Rouse, William Sunda, and Ronald P. Kiene	**700–711**	Latitudinal and vertical distributions of particle-associated dimethylsulfoniopropionate (DMSP) lyase activity in the western North Atlantic Ocean
Anissa Merzouk, Maurice Levasseur, Michael Scarratt, Sonia Michaud, and Michel Gosselin	**712–720**	Influence of dinoflagellate diurnal vertical migrations on dimethylsulfoniopropionate and dimethylsulfide distribution and dynamics (St. Lawrence Estuary, Canada)
S.F. Riseman and G.R. DiTullio	**721–735**	Particulate dimethylsulfoniopropionate and dimethylsulfoxide in relation to iron availability and algal community structure in the Peru Upwelling System
Nobue Kasamatsu, So Kawaguchi, Shuichi Watanabe, Tsuneo Odate, and Mitsuo Fukuchi	**736–743**	Possible impacts of zooplankton grazing on dimethylsulfide production in the Antarctic Ocean
M. Levasseur, M. Scarratt, S. Roy, D. Laroche, S. Michaud, G. Cantin, M. Gosselin, and A. Vézina	**744–757**	Vertically resolved cycling of dimethylsulfoniopropionate (DMSP) and dimethylsulfide (DMS) in the Northwest Atlantic in spring
Richard W. Hill, John W.H. Dacey, Susan D. Hill, Ahser Edward, and Wayne A. Hicks	**758–764**	Dimethylsulfoniopropionate in six species of giant clams and the evolution of dimethylsulfide after death

Continued on inside back cover / Suite au verso

Printed in Canada by / Imprimé au Canada par
NRC Reprographic Services / Service de reprographie CNRC
Page production by / Mise en page par
NRC Research Press / Presses scientifiques du CNRC

0706-652X(200405)61:5;1-7